American Association for the Advancement of Science

SCIENCE

1 December 1995
Vol. 270 • Pages 1409–1540
$7.00

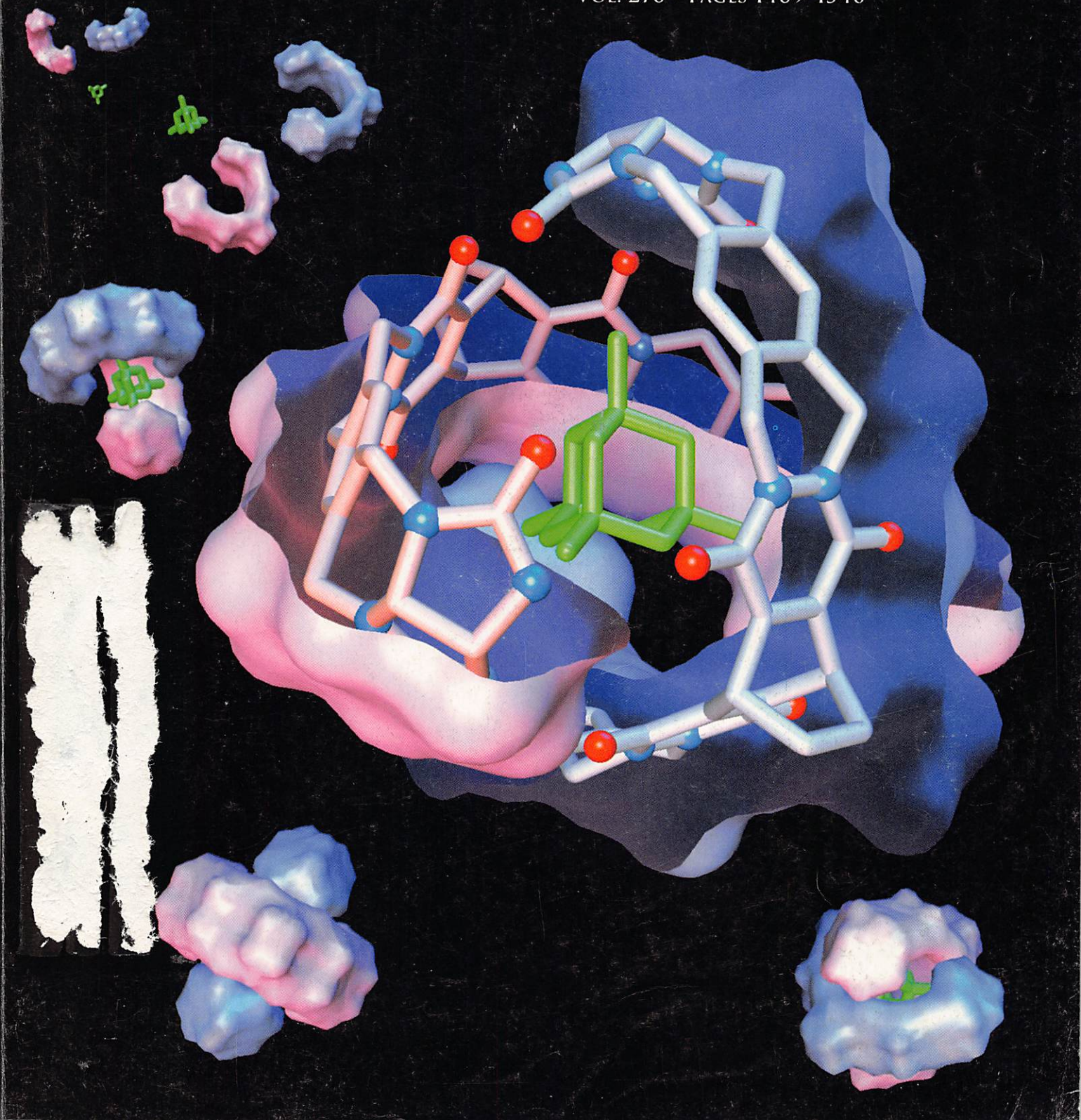

New Eagle Eye® Lineup

STRATAGENE

Microscope Camera Kit

- Avoids expense of dedicated microscopy system
- Connects microscope to Eagle Eye II system
- Ideal for fluorescence microscopy imaging

Economical Camera Stand

- For white-light imaging or darkroom use
- Perfect camera position without adjusting
- All imaging and processing capabilities of benchtop system

Light-Tight Benchtop Cabinet

- Images and analyzes at the bench
- Holds any size transilluminator
- Overhead UV and fluorescent white lights
- Detects chemiluminescence using integration of up to 55 minutes

Stratagene's Eagle Eye® still video imaging has expanded its field of vision. New innovations in the Eagle Eye lineup now allow this versatile system to be configured for the benchtop, darkroom or electronic light microscopy. The choice is yours.

All three setups let you take advantage of the Eagle Eye II system's advanced image capture and processing capabilities. So whether documenting gels, blots, autoradiographs or FISH assays, you can display, enhance, archive, retrieve, print and analyze your digital images.

For specific information about the best Eagle Eye system for you, please call 1-800-424-5444 or your nearest Stratagene distributor.

STRATAGENE

Internet Mail
techservices@stratagene.com

USA
Corporate Headquarters
(800) 424-5444
(619) 535-5400
Fax (619) 535-0045

Germany
Stratagene GmbH
Telephone (06221) 400634
Telefax (06221) 400639

United Kingdom
Stratagene Ltd.
Telephone (01223) 420955
Telefax (01223) 420234

Switzerland
Stratagene GmbH
Telephone (01) 3641106
Telefax (01) 3657707

Circle No. 36 on Readers' Service Card

The Secret of Making Ultra Pure GC Gas

H_2 Purity 99.99999 % without Caustic Solutions

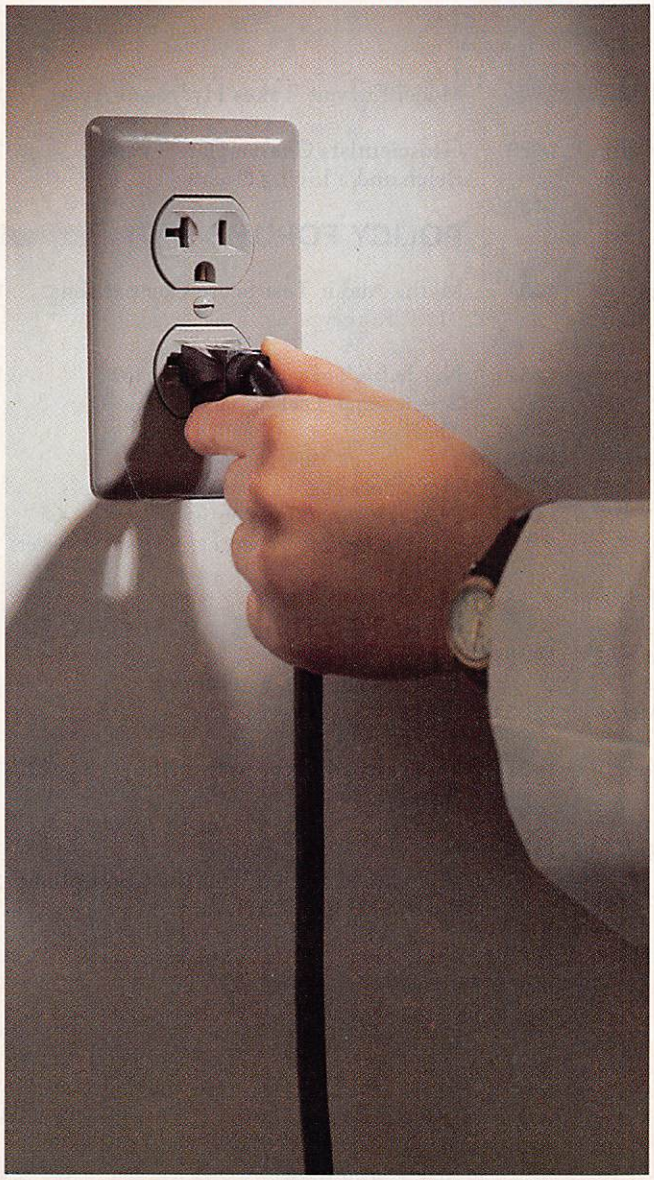

Just plug in your gas generator and get a continuous supply of ultra pure gas for predictable GC operation.

Ultra Pure Hydrogen Generator

Proven in over 10,000 installations worldwide, Packard's hydrogen generator technology has often been copied, but never matched.

Thanks to its exclusive SPE® (Solid Polymer Electrolyte) Electrolyzer, a Packard system does not require a liquid electrolyte to produce hydrogen. Simply supply deionized water and a standard electrical supply to generate continuous, pure, clean hydrogen at flow rates for carrier gas usage.

Since there is no need to replenish the system with a caustic electrolyte, there are no personal hazards involved in using a Packard hydrogen generator. It complies with all OSHA safety regulations, and it is the only system certified for laboratory use by CSA, UL and IEC 1010.

UHP Zero Air Generator

To further save you the inconvenience and costs of replacing gas cylinders, Packard introduces a new UHP Zero Air Generator.

Within minutes, you can convert your house air into a UHP zero air source. Just connect the system to a standard electrical outlet; wait a few minutes to warm up the catalyst of the convertor; and your UHP zero air generator is ready to deliver up to 2500 cc/minute of hydrocarbon-free air.

Unlike other zero air generators, Packard's system automatically compensates for ambient temperature and line voltage variations. Absolute temperature control of the convertor guarantees years of stable, maintenance-free operation. That's why this UHP zero air generator will pay for itself in just six months of operation.

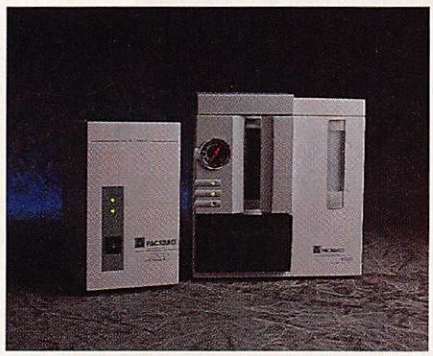

Call Packard for more information on our new hydrogen and UHP zero air gas generators.

It's no secret at all

Pure, clean, high quality gas. That's what you get when you plug your Packard Ultra High Purity (UHP) gas generator in a standard electrical outlet. No need to handle hazardous cylinders or worry about safety regulations.

PACKARD
A Canberra Company

Packard Instrument Company, 800 Research Parkway, Meriden, CT 06450 U.S.A.
Tel: 203-238-2351: 1-800-323-1891 FAX: 203-639-2172 Web Site: http://www.packardinst.com

Packard Instrument, Co. SYSTEM CERTIFIED ISO 9001

Packard International Offices:
Australia, Mt Waverley 61-3-543-4266; **Austria**, Vienna 43-1-2702504; **Belgium**, Brussels 32-2-4668210; **Canada**, Ontario 1-800-387-9559; **Central Europe**, Vienna 43-2230-3263; **Denmark**, Greve 45-42909023; **France**, Rungis (33) 1 46.86.27.75; **Germany**, Dreieich 49 6103 385-0; **Italy**, Milano 39-2-33910796/7/8; **Japan**, Tokyo 81-3-3866-5850; **Netherlands**, Groningen 31-50-5413360; Tilburg (013) 5423900; **Russia**, Moscow, 7-095-238-7335; **Switzerland**, Zurich (01) 481 69 44; **United Kingdom**, Pangbourne, Berks (44) 0734 844981.

Circle No. 35 on Readers' Service Card

ISSN 0036-8075
1 DECEMBER 1995
VOLUME 270
NUMBER 5241

SCIENCE

AMERICAN ASSOCIATION FOR THE ADVANCEMENT OF SCIENCE

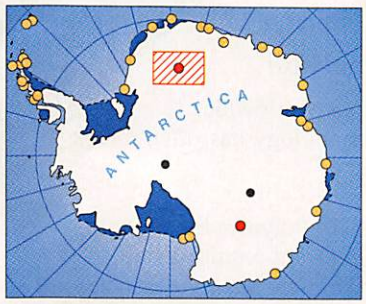

1433
Antarctic research feels the chill

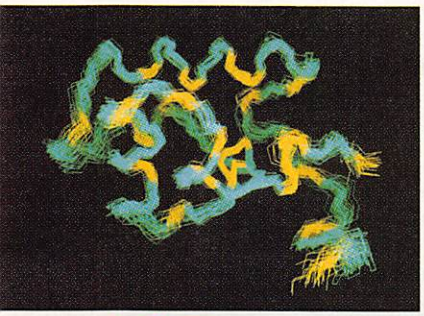

1495
Prokaryotic activation

NEWS & COMMENT

Are Wildlife Corridors the Right Path? 1428

Report Strips R&D Down to the Basics 1430

Scientific Misconduct: Panel Urges New Approach to Inquiries 1431

Japan: Consortia to Boost Efforts to Develop Genome Industry 1432

Pressure on Budget Triggers Review of Antarctic Program 1433

Europeans Make Room for Ice-Core Project 1434

RESEARCH NEWS

Found: A Star Too Small to Shine 1435

Why Mammal Ears Went on the Move 1436

Brain Researchers Speak a Common Language 1437

Measurements Are the Only Reality, Say Quantum Tests 1439

Model Enzyme Takes Hydrogen Apart 1440

Geoscientists Contemplate a Fatal Belch and a Living Ocean 1441

POLICY FORUMS

Myths About Test Score Comparisons 1446
I. C. Rotberg

Needed: Coherent Budgeting for Science and Technology 1448
F. Press

How Does the Texaco Case Affect Photocopying by Scientists? 1450
The National Conference of Lawyers and Scientists

PERSPECTIVES

An Exploding Star in Motion 1452
R. A. Chevalier

Molecular Mimicry in Protein Synthesis? 1453
P. B. Moore

The United Nations Climate Convention: Unattainable or Irrelevant 1454
P. E. Kauppi

DEPARTMENTS

THIS WEEK IN *SCIENCE* 1415

EDITORIAL 1417
Multifaceted Chemistry
G. A. Olah

LETTERS 1419
Lyme Disease Research: P. McFadden • Diet and Test Animals: R. W. Hart, A. Turturro, J. Leakey, W. T. Allaben; J. R. Bucher, G. N. Rao, K. Abdo, F. Kari, G. Lucier • Genetic Discrimination: Actuarial Aspects: A. Dicke; K. Hudson and F. Collins

SCIENCESCOPE 1427

RANDOM SAMPLES 1443
Substitute for Shock Therapy? • Biocontrol for Kiwi Mold • Subterranean Rumbling at Mount St. Helens • Tunable Sensors • Virtual Course on Protein Structure • Fuzzy Athletic Vegetarian ISO ...

BOOK REVIEWS 1511
DNA Repair and Mutagenesis, reviewed by B. S. Strauss • *Physics and Chemistry of Earth Materials*, R. Jeanloz • Books Received • Vignettes • Publishers' Addresses

PRODUCTS & MATERIALS 1515

Board of Reviewing Editors

Frederick W. Alt
Don L. Anderson
Michael Ashburner
Stephen J. Benkovic
Alan Bernstein
David E. Bloom
Piet Borst
Henry R. Bourne
Michael S. Brown
James J. Bull
Kathryn Calame
C. Thomas Caskey
Dennis W. Choi
David Clapham
Adrienne E. Clarke
John M. Coffin
F. Fleming Crim
Paul J. Crutzen
James E. Dahlberg
Robert Desimone
Paul T. Englund
G. Ertl
Richard G. Fairbanks
Douglas T. Fearon
Harry A. Fozzard
Klaus Friedrich
Roger I. M. Glass
Stephen P. Goff
Peter N. Goodfellow
Corey S. Goodman
Peter Gruss
Philip C. Hanawalt
Ira Herskowitz
Nobutaka Hirokawa
Tomas Hökfelt
Tasuku Honjo
Susan D. Iversen
Eric F. Johnson
Stephen M. Kosslyn
Michael LaBarbera
Nicole Le Douarin
Charles S. Levings III
Alexander Levitzki
Harvey F. Lodish
Richard Losick
Reinhard Lührmann
Ruth Lynden-Bell
Seth Marder
Diane Mathis
Anthony R. Means
Shigetada Nakanishi
Kim Nasmyth
Roger A. Nicoll
Staffan Normark
Stuart L. Pimm
Yeshayau Pocker
Dennis A. Powers
Ralph S. Quatrano
Martin Raff
V. Ramanathan
Douglas C. Rees
T. M. Rice
David C. Rubie
Erkki Ruoslahti
Gottfried Schatz
Jozef Schell
Ronald H. Schwartz
Terrence J. Sejnowski
Ellen Solomon
Thomas A. Steitz
Michael P. Stryker
Tomoyuki Takahashi
Masatoshi Takeichi
Keiji Tanaka
Robert T. N. Tjian
Yoshinori Tokura
Emil R. Unanue
Geerat J. Vermeij
Bert Vogelstein
Arthur Weiss
Zena Werb
George M. Whitesides
Owen N. Witte
William A. Wulf

COVER

Tetramethyladamantane (green) is encapsulated by two molecules of a self-complementary synthetic receptor. An array of weak intermolecular forces are balanced to produce the assembly in solution. (Red spheres, oxygen atoms; blue spheres, nitrogen atoms.) See page 1485. [Image: Michael Pique, The Scripps Research Institute, on a Sun Workstation with software by Michael Connolly and AVS, Inc.]

ARTICLES

The Interstellar Carbon Budget and the Role of Carbon in Dust and Large Molecules 1455
T. P. Snow and A. N. Witt

Venus Reconsidered 1460
W. M. Kaula

RESEARCH ARTICLE

Crystal Structure of the Ternary Complex of Phe-tRNA^{Phe}, EF-Tu, and a GTP Analog 1464
P. Nissen, M. Kjeldgaard, S. Thirup, G. Polekhina, L. Reshetnikova, B. F. C. Clark, J. Nyborg

REPORTS

Phase Diagram of Iron by in Situ X-ray Diffraction: Implications for Earth's Core 1473
C. S. Yoo, J. Akella, A. J. Campbell, H. K. Mao, R. J. Hemley

Expansion of SN 1993J 1475
J. M. Marcaide, A. Alberdi, E. Ros, P. Diamond, I. I. Shapiro, J. C. Guirado, D. L. Jones, T. P. Krichbaum, F. Mantovani, R. A. Preston, A. Rius, R. T. Schilizzi, C. Trigilio, A. R. Whitney, A. Witzel

Infrared Spectrum of the Cool Brown Dwarf Gl 229B 1478
B. R. Oppenheimer, S. R. Kulkarni, K. Matthews, T. Nakajima

Molecular Organization of Surfactants at Solid-Liquid Interfaces 1480
S. Manne and H. E. Gaub

Scaling Properties of Stretching Ridges in a Crumpled Elastic Sheet 1482
A. Lobkovsky, S. Gentges, H. Li, D. Morse, T. A. Witten

Autoencapsulation Through Intermolecular Forces: A Synthetic Self-Assembling Spherical Complex 1485
R. S. Meissner, J. Rebek Jr., J. de Mendoza

Yeast Checkpoint Genes in DNA Damage Processing: Implications for Repair and Arrest 1488
D. Lydall and T. Weinert

Activation of the Estrogen Receptor Through Phosphorylation by Mitogen-Activated Protein Kinase 1491
S. Kato, H. Endoh, Y. Masuhiro, T. Kitamoto, S. Uchiyama, H. Sasaki, S. Masushige, Y. Gotoh, E. Nishida, H. Kawashima, D. Metzger, P. Chambon

Solution Structure of the Activator Contact Domain of the RNA Polymerase α Subunit 1495
Y. H. Jeon, T. Negishi, M. Shirakawa, T. Yamazaki, N. Fujita, A. Ishihama, Y. Kyogoku

A Population Genetic Test of Selection at the Molecular Level 1497
M. F. J. Taylor, Y. Shen, M. E. Kreitman

Definition of Two Angiogenic Pathways by Distinct α_v Integrins 1500
M. Friedlander, P. C. Brooks, R. W. Shaffer, C. M. Kincaid, J. A. Varner, D. A. Cheresh

Essential Ca^{2+}-Binding Motif for Ca^{2+}-Sensitive Inactivation of L-Type Ca^{2+} Channels 1502
M. de Leon, Y. Wang, L. Jones, E. Perez-Reyes, X. Wei, T. W. Soong, T. P. Snutch, D. T. Yue

Coactivator and Promoter-Selective Properties of RNA Polymerase I TAFs 1506
H. Beckmann, J.-L. Chen, T. O'Brien, R. Tjian

TECHNICAL COMMENTS

The Evolution of Molecular Computation 1510
W. P. C. Stemmer

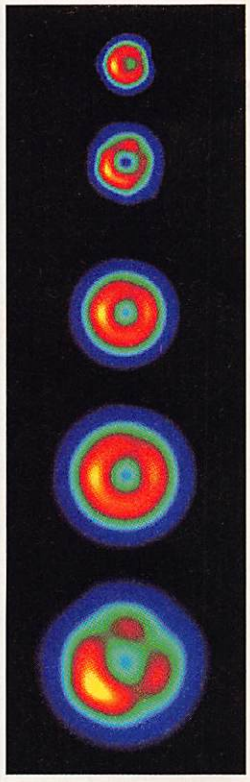

1452 & 1475
Symmetry in an expanding supernova

AAAS Board of Directors

Francisco J. Ayala
Retiring President, Chairman
Rita R. Colwell
President
Jane Lubchenco
President-elect
William A. Lester Jr.
Simon A. Levin
Michael J. Novacek
Anna C. Roosevelt
Alan Schriesheim
Jean E. Taylor
Chang-Lin Tien
Nancy S. Wexler
William T. Golden
Treasurer
Richard S. Nicholson
Executive Officer

◩ Indicates accompanying feature

■ **SCIENCE (ISSN 0036-8075) is published weekly on Friday, except the last week in December, by the American Association for the Advancement of Science, 1333 H Street, NW, Washington, DC 20005.** Second-class postage (publication No. 484460) paid at Washington, DC, and additional mailing offices.

Copyright © 1995 by the American Association for the Advancement of Science. The title SCIENCE is a registered trademark of the AAAS.

Domestic individual membership and subscription (51 issues): $97 ($50 allocated to subscription). Domestic institutional subscription (51 issues): $228. Foreign postage extra: Mexico, Caribbean (surface mail) $53; other countries (air assist delivery) $93. First class, airmail, student and emeritus rates on request. Canadian rates with GST available upon request, GST #1254 88122. **Printed in the U.S.A.**

Change of address: allow 4 weeks, giving old and new addresses and 8-digit account number. **Postmaster:** Send change of address to *Science*, P.O. Box 1811, Danbury, CT 06813–1811. **Single copy sales:** $7.00 per issue prepaid includes surface postage; bulk rates on request.

Authorization to photocopy material for internal or personal use under circumstances not falling within the fair use provisions of the Copyright Act is granted by AAAS to libraries and other users registered with the Copyright Clearance Center (CCC) Transactional Reporting Service, provided that $3.00 per article is paid directly to CCC, 27 Congress Street, Salem, MA 01970. The identification code for *Science* is 0036-8075/83 $3.00. *Science* is indexed in the *Reader's Guide to Periodical Literature* and in several specialized indexes.

FIDELITY™
DNA Sequencing System

Simply Better.

Now, You Have A Real Alternative.

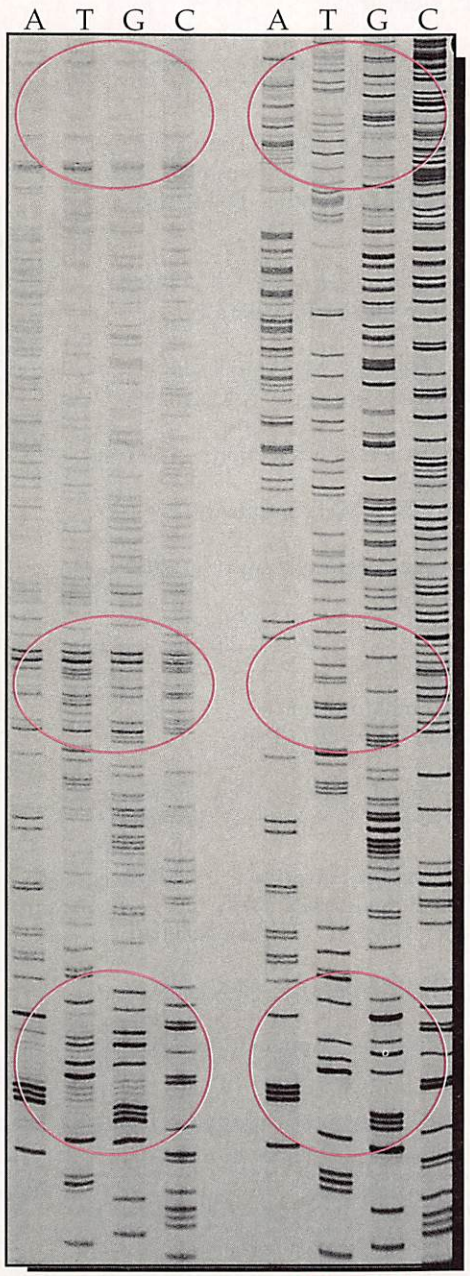

Template: pUC19 (α-^{35}S)

Introducing the Oncor **FIDELITY™** DNA Sequencing System, with better resolution on double-stranded DNA.

See how much better manual sequencing can be.

Call Oncor today at 1-800-776-6267.

GLOBAL SOURCES
PERSONAL SOLUTIONS

oncor®

209 Perry Parkway
Gaithersburg,
MD 20877

1-800-77-ONCOR
301-963-3500
Fax: 301-926-6129

http://www.oncorinc.com/home
techsvc@oncor.com
custsvc@oncor.com

For Research Use Only. Not for use in diagnostic procedures. FIDELITY is a trademark of Oncor, Inc.
Sequenase is a trademark of United States Biochemical Corporation.

edited by PHIL SZUROMI

Abundant carbon

It is often assumed that the solar system was formed from matter that is representative of the galaxy as a whole, and thus solar carbon abundances can be used to gauge the abundance of carbon in other stars and in interstellar dust. Snow and Witt (p. 1455) review evidence which shows that carbon in the sun is significantly more abundant than in other stars. This overabundance of carbon has important implications for models of nucleosynthesis in supernovae and for models of interstellar dust formation.

Nailing down the core

Knowledge of the phase diagram of iron at high pressures and temperatures is key for prediction of the temperature and composition of Earth's core. Yoo *et al.* (p. 1473) obtained in situ x-ray diffraction measurements from samples in a laser-heated diamond-anvil cell to identify phases of iron directly. The results show that hexagonal close-packed iron (ε-Fe) has a wide stability field at high pressures and temperatures and is the likely stable phase at conditions of the solid inner core.

Surfactants on surfaces

Surfactants adsorbed on atomically smooth surfaces might be expected to form simple monolayers and bilayers. Manne and Gaub (p. 1480) found instead a variety of morphologies in their atomic force microscopy studies of quaternary ammonium cationic surfactants. Half-cylinders formed on hydrophobic surfaces, full cylinders formed on mica, and spheres formed on amorphous silica. Such variations could find use in surface patterning.

A cool brown star

The nuclear reactions that light up the sun can only occur if a star's mass exceeds 0.08 solar masses; objects smaller than this are called brown dwarfs. Oppenheimer *et al.* (p. 1478; see the news story by Glanz, p. 1435) report spectroscopic measurements of an unusually low-luminosity brown dwarf, the recently discovered Gl 229B, that has a mass approximately 20 times that of Jupiter. Absorption features in the spectra indicate the presence of methane and water vapor, which implies a surface temperature below 1000 K. The spectra are quite different from those seen in stars and instead bear a greater resemblance to the spectra of Jupiter. The characterization of such objects is necessary to understand whether they could constitute a dominant species in the galaxy.

Closing the trap

Processes such as self-assembly and molecular recognition, hallmarks of many biomolecules, can also be performed by synthetic analogs. Meissner *et al.* (p. 1485; see cover) have designed and synthesized a molecule which, in the presence of suitable guest molecules, self-assembles to form a dimeric spherical complex that can encapsulate rather large guest molecules, such as derivatives of adamantane and ferrocene. Such complexes could find use as reaction vessels or drug delivery systems.

Tu complex

Elongation factor Tu (EF-Tu) is a guanosine triphosphate (GTP)–binding protein that delivers the aminoacylated transfer RNA to the empty A site on the ribosome, a key step in chain elongation during protein synthesis. Nissen *et al.* (p. 1464; see the Perspective by Moore, p. 1453) present an x-ray structure of EF-Tu in a complex with phenylalanine transfer RNA and a GTP analog. The overall shape of the complex is similar to that on the translocation factor, EF-G–GDP, suggesting a type of "molecular mimicry" between protein and

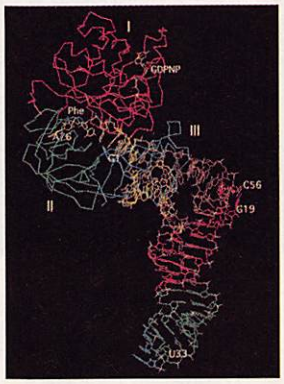

nucleic acid counterparts in the translational apparatus.

Enhancing estrogen

Efficient coordination of cellular responses to hormones requires cross-talk between various signaling pathways. Kato *et al.* (p. 1491) report that mitogen-activated protein (MAP) kinase, which is activated in cells treated with peptide growth factors such as insulin and epidermal growth factor, can phosphorylate the receptor for the steroid hormone estrogen. Activation of MAP kinase in transfected cells resulted in increased estrogen-induced transcriptional activity of the estrogen receptor. In this way, regulation of transcription by estrogen can be modulated by growth factors or other agents that influence the activity of MAP kinase.

Calcium channel feedback

Unlike other voltage-gated ion channels, the L-type calcium channel is inactivated by a high concentration of the ion it transports, Ca^{2+}. This feedback inhibition controls the Ca^{2+} flux into many types of neuronal and muscle cells and is critical, for example, in the regulation of contraction strength in heart muscles. De Leon *et al.* (p. 1502) identify the likely molecular mechanism for this inactivation. A region in one of the subunits that make up the L-type calcium channel contains a Ca-binding motif—an EF hand—that is responsible for the sensitivity of the channel to Ca concentration. Donation of this domain to another channel that is insensitive to the surrounding Ca concentration confers Ca inactivation.

Natural selection

What role does natural selection play in setting up the patterns of variation among populations? Taylor *et al.* (p. 1497) looked for selection in field populations by using a combination of molecular genetics, evolutionary biology, and agricultural entomology. They examined the heterogeneity in a known insecticide resistance locus (a voltage-gated sodium channel) in a generalist crop pest (the tobacco budworm) at four different locations in the United States exposed to different levels of pesticide. The patterns of heterogeneity at the sodium channel locus differed markedly in the different populations, but a control allele did not. The correlation between insecticide resistance and allelic diversity suggests that differential (or natural) selection does indeed occur.

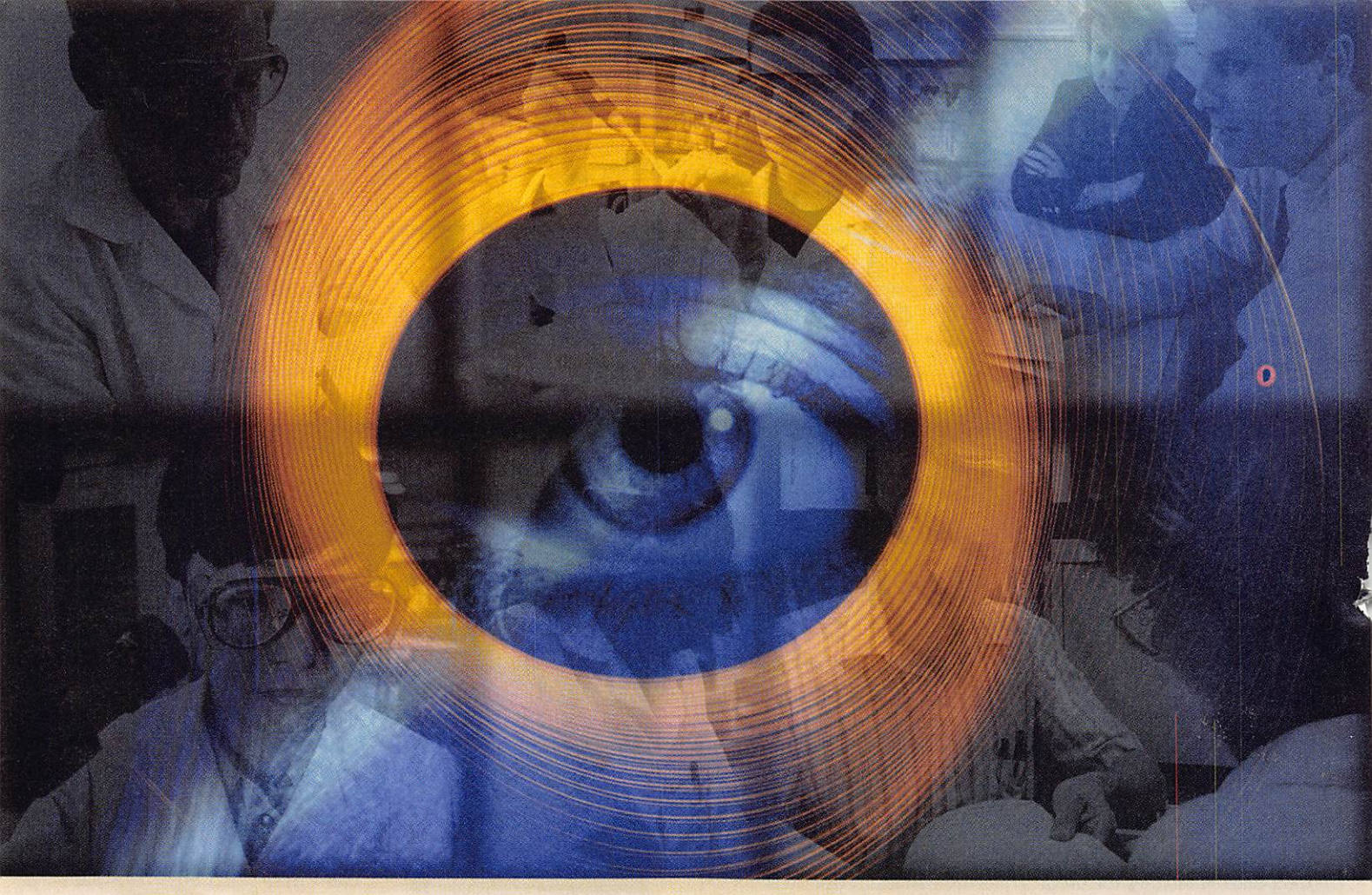

ONE VISION

MANY FACES

INTRODUCING SIGMA BIOSCIENCES™

Change... Growth... Adaptation... Our vision of serving the future needs of life sciences means transforming the way we do business.

Our vision has built Sigma BioSciences – a union of our Cell Culture, Immunochemical and Molecular Biology divisions. Sigma BioSciences combines the strengths of each division to create a balance of skills, disciplines and customer support that will set the standard into the next century.

Today, Sigma BioSciences stands as your single source for life science research and manufacturing products.

MOLECULAR SIGMA BIOLOGY

Sigma Immuno Chemicals

SIGMA CELL CULTURE

SIGMA BIOSCIENCES™

We are committed to the success of our customers through science, technology and service.

Germany-0130 5155 **France**-05 21 14 08 **UK**-0800 373731 **Italy**-1678 27018 **Belgium/Netherlands**-0800 14747/06 022 4748 **USA/Canada**-800-325-3010

Circle No. 7 on Readers' Service Card

SCIENCE
http://www.aaas.org

Publisher: Richard S. Nicholson
Editor-in-Chief: Floyd E. Bloom
Editor: Ellis Rubinstein
Managing Editor: Monica M. Bradford
Deputy Editors: Philip H. Abelson *(Engineering and Applied Sciences);* John I. Brauman *(Physical Sciences);* Thomas R. Cech *(Biological Sciences)*

Editorial Staff
Assistant Managing Editor: Dawn Bennett
Senior Editors: Eleanore Butz, R. Brooks Hanson, Pamela J. Hines, Barbara Jasny, Katrina L. Kelner, Paula A. Kiberstis, Linda J. Miller, L. Bryan Ray, Phillip D. Szuromi, David F. Voss
Associate Editors: Gilbert J. Chin, Suki Parks, Linda R. Rowan
Letters: Christine Gilbert, *Editor;* Steven S. Lapham
Book Reviews: Katherine Livingston, *Editor;* Jeffrey Hearn, *Editorial Assistant*
Editing: Valerie Jablow, *Supervisor;* Cara Tate, *Senior Copy Editor;* Jeffrey E. Cook, Harry Jach, Erik G. Morris, Christine M. Pearce
Copy Desk: Ellen E. Murphy, *Supervisor;* Sherri Byrand, Joi S. Granger, Daniel T. Helgerman, Beverly Shields, Kameaka Williams, *Assistant*
Editorial Support: Sherryf Farmer, *Supervisor;* Brent Gendleman, Carolyn Kyle, Michele Listisard, Diane Long, Patricia M. Moore, Ted Smith
Administrative Support: Sylvia Kihara, Charlene King
Computer Specialist: Roman Frillarte
Telephone: 202-326-6501; **FAX:** 202-289-7562; **TDD:** 202-408-7770

News Staff
News Editor: Colin Norman
Features Editor: John M. Benditt
Deputy News Editors: Tim Appenzeller, Joshua Fischman, Jean Marx, Jeffrey Mervis
News & Comment/Research News Writers: Linda B. Felaco (copy), Constance Holden, Jocelyn Kaiser, Richard A. Kerr, Andrew Lawler, Eliot Marshall, Rachel Nowak, Robert F. Service, Lori Wolfgang (intern)
Bureaus: Marcia Barinaga (Berkeley), Jon Cohen (San Diego), James Glanz (Chicago), Dennis Normile (Tokyo), Wade Roush (Boston)
Contributing Correspondents: Barry A. Cipra, Elizabeth Culotta, Ann Gibbons, Charles C. Mann, Anne Simon Moffat, Virginia Morell, Robert Pool, Gary Taubes
Administrative Support: Fannie Groom
Telephone: 202-326-6500; **FAX:** 202-371-9227; **Internet Address:** science_news@aaas.org

Art & Production Staff
Production: James Landry, *Director;* Wendy K. Shank, *Manager;* Lizabeth A. Harman, *Assistant Manager;* Laura A. Creveling, Scherraine B. Mack, Stephen E. Taylor, *Associates;* Leslie Blizard, *Assistant*
Art: Amy Decker Henry, *Director;* C. Faber Smith, *Associate Director;* Katharine Sutliff, *Scientific Illustrator;* Holly Bishop, *Graphics Associate;* Elizabeth Carroll, Preston Morrighan, *Graphics Assistants*

Europe Office
Editorial: Richard B. Gallagher, *Office Head and Senior Editor;* Stella M. Hurtley, Julia Uppenbrink, *Associate Editors;* Belinda Holden, *Editorial Associate*
News: Daniel Clery, *Editor;* Nigel Williams, *Correspondent;* Michael Balter *(Paris),* Patricia Kahn *(Heidelberg),* Richard Stone *(Russia), Contributing Correspondents*
Administrative Support: Janet Mumford; Anna Sewell
Address: 14 George IV Street, Cambridge, UK CB2 1HH
Telephone: (44) 1223-302067; **FAX:** (44) 1223-302068
Internet address: science@science-int.co.uk

Science Editorial Board

Charles J. Arntzen	F. Clark Howell
David Baltimore	Paul A. Marks
J. Michael Bishop	Yasutomi Nishizuka
William F. Brinkman	Helen M. Ranney
E. Margaret Burbidge	Bengt Samuelsson
Pierre-Gilles de Gennes	Robert M. Solow
Joseph L. Goldstein	Edward C. Stone
Mary L. Good	James D. Watson
Harry B. Gray	Richard N. Zare
John J. Hopfield	

EDITORIAL

Multifaceted Chemistry

Humanity's drive to uncover the secrets of life processes and to use this knowledge to improve human existence has led to spectacular advances in the biological and health sciences. Chemistry richly contributes to these advances by helping to increase our understanding of processes at the molecular level, and it provides many of the methods and techniques of biotechnology. However, chemistry is not just an adjunct of biology and biotechnology. It is and always will be a central science in its own right.

Chemists make compounds and strive to understand their reactions. Chemical synthesis, coupled with biotechnology, is well on its way to being able to reproduce many of nature's wonderful complex compounds and also to make unnatural ones. My own interest lies in the much simpler chemistry of hydrocarbons, compounds of the elements carbon and hydrogen. Although this field is considered by many to be of only limited significance, hydrocarbons are essential to our everyday life because they make up petroleum oil and natural gas. Hydrocarbon fuels generate energy and electricity, heat our houses, and propel our cars and airplanes. They are also the raw materials for most man-made substances, ranging from plastics to pharmaceuticals. What nature has given us over the eons, however, humans are rapidly using up. As our nonrenewable reserves diminish in the 21st century, it will be up to chemists to synthesize hydrocarbons on an increasingly large scale and in new and economical ways.

To better use our existing resources and to make our refineries and plants safer and more environmentally responsible, new technologies that build on the results of ongoing fundamental research are needed. Many of the chemical reactions essential to hydrocarbon transformations are catalyzed by acids and proceed through positive ion intermediates, called carbocations. To allow the preparation and direct study of these long-elusive species in stable form, acids billions of times stronger than concentrated sulfuric acid were needed (so-called superacids). Once carbocations had been prepared, their chemistry made rapid strides. It was discovered that in carbocations either three or five (in some cases even six) groups or atoms are simultaneously attached to the core carbon atom. August Kekulé's concept of the limiting tetravalency of carbon was thus extended by the discovery of higher coordinate carbon compounds and of related hypercarbon chemistry. The Swedish Academy, reflecting on the significance of these studies, was moved to say, "to understand carbocations is to understand chemistry."

Understanding of the fundamentals of hydrocarbon chemistry has also led to practical results. We can now improve widely used acid-catalyzed industrial processes as well as develop new ones. An example is the production of improved high-octane and oxygenated gasoline. Toxic and dangerous acids used in refineries, such as hydrofluoric acid, can be modified to make them substantially less volatile and thus much safer. New generations of diesel fuel additives are being developed to allow cleaner burning and less pollution. Ways are being found to convert natural gas directly to liquid hydrocarbons and their oxygenated derivatives. In the long run, we will be able to convert even carbon dioxide from the atmosphere into hydrocarbons if we can find sources of abundant cheap energy (probably safer atomic energy) that allow us to produce the needed hydrogen from seawater. We will then be able to parallel nature's photosynthetic recycling of carbon dioxide and provide for our hydrocarbon needs even after we have exhausted our fossil fuels. The relevant chemistry is already being developed in laboratories such as mine. This process will also lessen any atmospheric greenhouse effect caused by excessive production of carbon dioxide.

Chemistry does not always enjoy the best of reputations. Many plants and refineries are still potentially dangerous and pollute their surroundings. At the same time, however, our society enjoys a high standard of living that few would give up; a standard produced in no small measure by the results of chemistry. Chemistry can and will be able to bring into equilibrium the two goals of providing for our needs and responding to societal environmental concerns. The challenges are great, but I believe we will meet them.

George A. Olah

The author is director of the Loker Hydrocarbon Research Institute at the University of Southern California in Los Angeles. This editorial is adapted from his speech at the Nobel banquet in Stockholm after he was awarded the 1994 Nobel Prize for Chemistry, given in recognition of his work on carbocations.

Lasergene

SOFTWARE FOR MACINTOSH AND WINDOWS BY DNA* DNASTAR

CHOSEN PRODUCT OF THE YEAR by Biotechnology Software Journal, Sept. 1995

BIOCOMPUTING

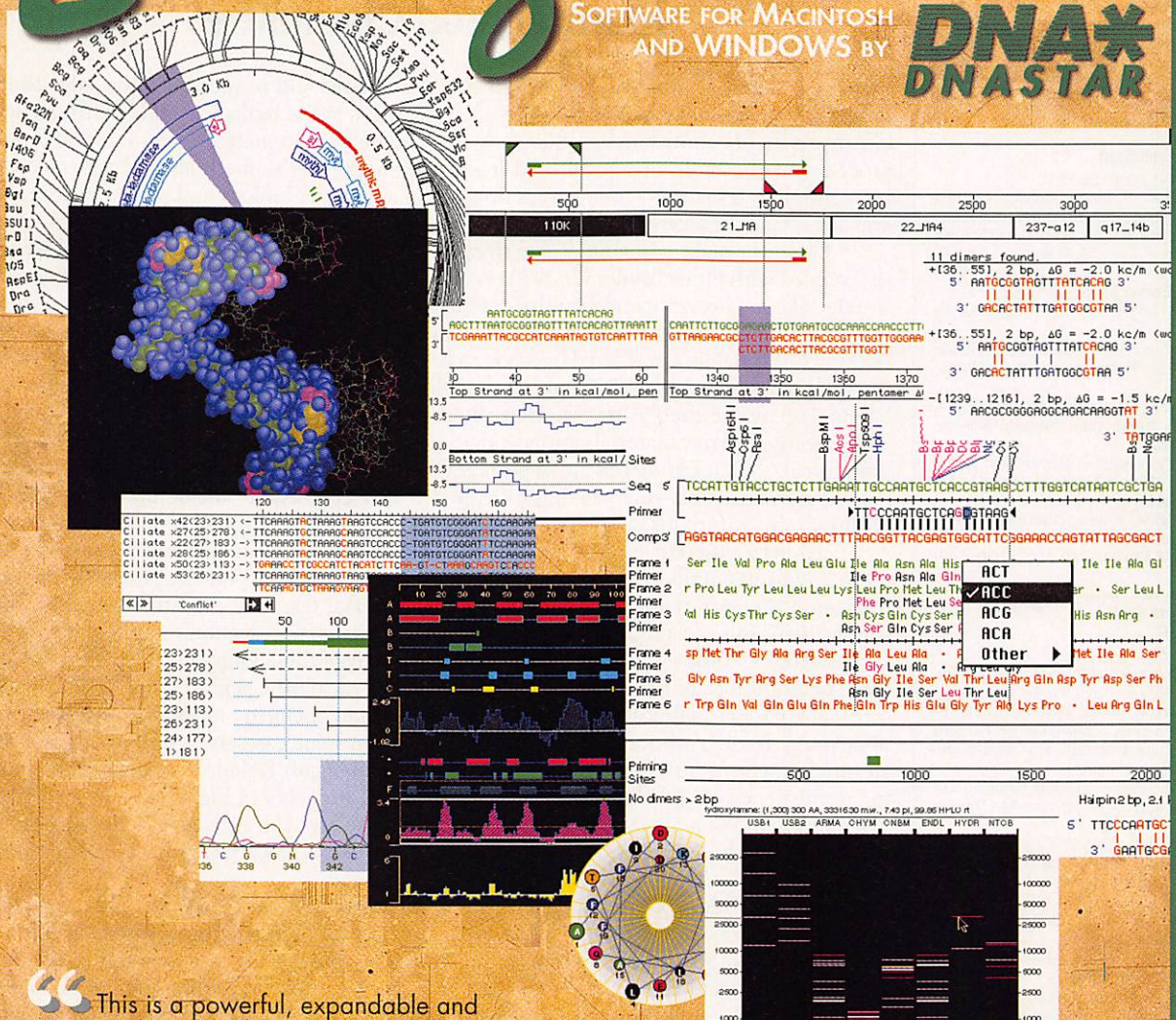

"This is a powerful, expandable and comprehensive molecular biology package with the best protein analysis and restriction mapping software available. I recommend DNASTAR to any lab requiring this level of power and expandability. DNASTAR is currently unique in its support for networking as well.

Peter Markiewicz, *UCLA*

LASERGENE is the best network system available. Easy installation and management make it an intelligent choice for every network. Simultaneous client licensing is a fair and honest method for delivering such sophisticated power.

Mitch Sogin, *Marine Biological Laboratory*"

Find out for yourself. Call DNASTAR for research consulting and evaluation software systems

In USA: (608) 258-7420 Fax (608) 258-7439 In Europe: (44)-81-566 8282 Fax (44)-81-566 9555

Visit us at **http://www.dnastar.com**

Accelerated for Power Macintosh

Circle No. 14 on Readers' Service Card

SCIENCE
http://www.aaas.org

Published by the **American Association for the Advancement of Science (AAAS),** *Science* serves its readers as a forum for the presentation and discussion of important issues related to the advancement of science, including the presentation of minority or conflicting points of view, rather than by publishing only material on which a consensus has been reached. Accordingly, all articles published in *Science*—including editorials, news and comment, and book reviews—are signed and reflect the individual views of the authors and not official points of view adopted by the AAAS or the institutions with which the authors are affiliated.

The American Association for the Advancement of Science was founded in 1848 and incorporated in 1874. Its objectives are to further the work of scientists, to facilitate cooperation among them, to foster scientific freedom and responsibility, to improve the effectiveness of science in the promotion of human welfare, to advance education in science, and to increase public understanding and appreciation of the importance and promise of the methods of science in human progress.

Membership/Circulation

Director: Michael Spinella
Deputy Director: Marlene Zendell
Member Services: Rebecca Dickerson, *Manager*; Mary Curry, *Supervisor*; Pat Butler, Helen Williams, Laurie Baker, *Representatives*
Marketing: Dee Valencia, *Manager*; Jane Pennington, *Europe Manager*; Hilary Baar, *Associate*; Angela Mumeka, *Coordinator*
Research: Renuka Chander, *Manager*
Business and Finance: Robert Smariga, *Manager*; Kevin Bullock, Nina Araujo de Kobes, *Coordinators*
Computer Specialist: Chris Hageman
***Science* Member Services**
Danbury, CT: 800-731-4939
Washington, DC: 202-326-6417
Other AAAS Programs: 202-326-6400

Advertising and Finance

Associate Publisher: Beth Rosner
Advertising Sales Manager: Susan A. Meredith
Recruitment Advertising Manager: Janis Crowley
Business Manager: Deborah Rivera-Wienhold
Finance: Randy Yi, *Senior Analyst;* Shawn Williams, *Analyst*
Marketing: John Meyers, *Manager;* Allison Pritchard, *Associate*
Traffic: Carol Maddox, *Manager*; Christine Pierpoint, *Associate*
Recruitment: Terri Seiter Azie, *Assistant Manager*; Pamela Sams, *Production Associate*; Celeste Miller, Bethany Ritchey, Rachael Wilson, *Sales*; Debbie Cummings, *European Sales*
Reprints: Corrine Harris
Permissions: Lincoln Richman
Exhibits Coordinator: Arlene Ennis
PRODUCT ADVERTISING SALES: East Coast/E. Canada: Richard Teeling, 201-904-9774, FAX 201-904-9701 • **Midwest/Southeast:** Elizabeth Mosko, 312-665-1150, FAX 312-665-2129 • **West Coast/W. Canada:** Neil Boylan, 415-673-9265, FAX 415-673-9267 • **UK, Scandinavia, France, Italy, Belgium, Netherlands:** Andrew Davies, (44) 1-457-838-519, FAX (44) 1-457-838-898 • **Germany/Switzerland/Austria:** Tracey Peers, (44) 1-270-760-108, FAX (44) 1-270-759-597 • **Japan:** Mashy Yoshikawa, (3) 3235-5961, FAX (3) 3235-5852
RECRUITMENT ADVERTISING SALES: US: 202-326-6555, FAX 202-682-0816 • **Europe:** Debbie Cummings, +44 (0) 1223-302067, FAX +44 (0) 1223-576208 • **Australia/New Zealand:** Keith Sandell, (61) 02-922-2977, FAX (61) 02-922-1100
Send materials to *Science* Advertising, 1333 H Street, NW, Washington, DC 20005.

Information for Contributors appears on pages 112–114 of the 6 January 1995 issue. Editorial correspondence, including requests for permission to reprint and reprint orders, should be sent to 1333 H Street, NW, Washington, DC 20005.
***Science* World Wide Web address:** http://www.aaas.org
Other Internet addresses: science_editors@aaas.org (for general editorial queries); science_letters@aaas.org (for letters to the editor); science_reviews@aaas.org (for returning manuscript reviews); membership@aaas.org (for member services); science_classifieds@aaas.org (for submitting classified advertisements); science_advertising@aaas.org (for product advertising)

LETTERS

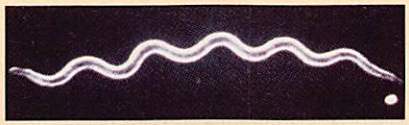

CHARLES W. STRATTON/VISUALS UNLIMITED

Serious concerns

Correspondents focus on test animals in a continuing discussion of how to assess risks from the many substances that must be tested for possible toxic effects to humans; an advocate of Lyme disease patient groups points to "mounting" evidence that the Lyme disease spirochete, *Borrelia burgdorferi* (above), can persist in some patients despite antibiotic treatment; and a representative of the American Academy of Actuaries speaks out on genetic discrimination.

Lyme Disease Research

The main focus of Eliot Marshall's article "Lyme disease: NIH gears up to test a hotly disputed theory" (News & Comment, 13 Oct., p. 228) is the controversy between patient advocacy groups and treating physicians on one side, and university-based researchers (who frequently dispute the existence of chronic Lyme disease) on the other. The article reports that the patient groups' tactics to have chronic Lyme disease studied "have angered research leaders such as Allen Steere of Tufts University." Is patient-initiated research really so bad?

Steere has been one of the most outspoken skeptics about the existence of a chronic Lyme disease epidemic (*1*) and one of the most outspoken proponents of the success of modest (10- to 30-day) courses of antibiotics (*1*). In 1993, Steere wrote (*2*) that, in Lyme disease, "Standard antibiotic treatment probably fails less often than one might think. Most apparent treatment failures actually reflect misdiagnosis."

However, evidence is mounting that the Lyme disease spirochete, *Borrelia burgdorferi*, can persist in some patients despite antibiotic therapy. The spirochete has been isolated from the skin (*3*, *4*), spinal fluid (*4*, *5*), blood (*6*), ligamentious tissue (*7*), and iris tissue (*8*) of patients after antibiotic therapy, including intravenous or long courses of supposedly curative antibiotics, or both (*9*).

It may surprise some to learn that in the first few years he was associated with Lyme disease, Steere promoted the idea that antibiotics were ineffective. In 1977 (*10*), Steere and his colleagues stated, "We remain skeptical that antibiotic therapy helps." In 1978, Steere and his colleagues wrote (*11*), "To sum up the therapy of Lyme arthritis (Lyme disease), it appears that at this point only symptomatic treatment is feasible." In a 1979 paper about the neurological abnormalities of Lyme disease (*12*), Steere and his colleagues reported that they "have noted no benefit from antibiotic treatment." However, an extensive literature search revealed 17 medical papers published before 1979 reporting the efficacy of antibiotics in treating Lyme disease. Only one (besides Steere's) reported no benefit.

The controlled studies (*12*) to see whether longer term antibiotics can help prevent chronic or relapsing Lyme disease (both successful) were performed in Europe. As Steere himself is quoted by Marshall as saying, the proposed National Institutes of Health study of chronic Lyme disease "would never have been funded" through the "normal mechanisms" of investigator-initiated research.

Peter McFadden
4611 Governor's Drive, Huntsville, AL 35805, USA

References

1. A. C. Steere *et al.*, *J. Am. Med. Assoc.* **269**, 1812 (1993).
2. ———, *Hosp. Prac.* (April 1993), p. 37.
3. D. Hassler *et al.*, *Lancet* **338**, 193 (1991).
4. V. Preac-Mursic *et al.*, *Infection* **17**, 355 (1989).
5. H. Pfister *et al.*, *J. Infect. Disease* **163**, 311 (1991).
6. E. Masters *et al.*, "Spirochetemia two weeks post cessation of six months of continuous p.o. Amoxicillin therapy" (Abstr. 65, Fifth International Conference on Lyme Borreliosis, Arlington, VA, 1992).
7. T. Haupl *et al.*, *Arthritis Rheum.* **36**, 1621 (1993).
8. V. Preac-Mursic *et al.*, *J. Neuro-ophthalmol.* **13**, 155 (1993).
9. P. Wahlberg *et al.*, *J. Infect.* **29**, 255 (1994); I. Bojic *et al.*, *Glas. Srp. Akad. Nauka Umet Od. Med. Nauka* **43**, 257 (1993).
10. A. C. Steere *et al.*, *Ann. Intern. Med.* **86**, 685 (1977).
11. A. C. Steere *et al.*, *Hosp. Pract.* (April 1978), p. 143.
12. L. Reik and A. C. Steere, *Medicine* **58**, 281 (1979).

■

Diet and Test Animals

Philip H. Abelson's editorial "Flaws in risk assessments," (13 Oct., p. 215) correctly points out the critical role that diet can play

in public health and the assessment of risk. He raises two important issues: (i) over the last two decades there has been a steady increase in variability, decrease in survival, and increase in degenerative diseases and tumor incidence, proportional to a concurrent increase in body weight, across a number of rodent species and strains used in toxicity testing; and (ii) relatively small differences in dietary intake, as reflected by body weight differences, can lead to significant changes in the way animals respond to chemical or agent exposure (*1*, *2*). We agree with these two observations, and wish to add three others based on our work in this area (*3*).

First, failure to control or stabilize body weight between and among control animals, by allowing ad libitum feeding, results in increased inter- and intra-experimental variability. Recent studies suggest that between 60 and 95% of the variability in the occurrence of liver tumors in different studies can be accounted for by differences in body weight (*3*, *4*). Other studies suggest that a similar relationship between body weight and other pathologies may also exist (*5*). Thus, the impact of body weight differences on the induction of chemical or agent toxicity can be as significant as test agent dose (*6*).

Second, according to a broad-based consensus developed over 50 years of work within the field of dietary restriction, it appears that, while individual dietary components may be of importance relative to the frequency of specific pathologies, total caloric content, rather than any one macro- or micronutrient, has the greatest overall impact on the health of the animal (*3*, *4*, *7*, *8*).

Third, dietary intake exerts its effect on a wide range of physiological, metabolic, and molecular parameters important to the toxicity of compounds (*1*, *9*). Many of these effects are observed in both sexes and across different genotypes and species, including monkeys and humans (*3*, *7*, *10*). Additionally, in certain cases, primary cell cultures in vitro can reflect the dietary history of the animal from which they were excised in their capacities for transformation, oncogene expression, or DNA repair (*3*, *10*, *11*). Failure to adjust for differences in dietary intake and the resultant differences in toxicity mechanisms will increase variability, reduce reproducibility, and possibly provide misleading information.

In the absence of malnutrition, generally, the lower the body weight, the greater is the ability of an animal to cope with chemical or agent exposure. Therefore, in optimizing the health of animals used in testing and research, one could potentially reduce body weight such that they become less sensitive or refractory to chemical- or agent-induced toxicity. It is important that the biological mechanisms involved in the initiation and expression of toxicity and carcinogenicity end points be functional and that the body weights of control and test groups be comparable. Scientists should therefore use moderate and reasonable dietary control measures in reaching the goals noted above. The Food and Drug Administration is currently preparing two documents for publication in the *Federal Register* which identify the problems associated with uncontrolled food consumption and address which levels of dietary control are appropriate to achieve standardized growth curves.

Ronald W. Hart
Angelo Turturro
Julian Leakey
William T. Allaben
National Center for Toxicological Research, Food and Drug Administration, Jefferson, AR 72079, USA

References

1. W. Allaben *et al.*, *Korean J. Toxicol.* **6**, 167 (1990).
2. R. Hart and A. Turturro, in (*3*), pp. 1–13.

3. R. W. Hart, D. A. Neumann, R. T. Robertson, Eds., *Dietary Restriction: Implications for the Design and Interpretation of Toxicity and Carcinogenicity Studies* (ILSI Press, Washington, DC, 1995).
4. A. Turturro, P. Duffy, R. Hart, *Mutat. Res.* **295**, 151 (1993).
5. ———, in (*3*), pp. 79–98; S. Seilkop, *Fund. Appl. Toxicol.* **24**, 247 (1995).
6. D. Gaylor and C. McCarty, *A Relook at the ED_{01} Study: Relationship Between Body Weight and Tumor Incidence* (Proceedings, Toxicology Forum Annual Summer Meeting, Toxicology Forum, Washington, DC, in press); F. Kari and K. Abdo, in (*3*), pp. 63–78.
7. R. Weindruch and R. Walford, *The Retardation of Aging and Disease by Dietary Restriction* (Thomas, Springfield, IL, 1988).
8. Committee on Diet, Nutrition, and Cancer, Assembly of Life Sciences, National Research Council, *Diet, Nutrition, and Cancer* (National Academy Press, Washington, DC, 1982); Committee on Chemical Toxicity and Aging, Board on Environmental Studies and Toxicology, Commission of Life Sciences, National Research Council, *Aging in Today's Environment* (National Academy Press, Washington, DC, 1987); A. Tannenbaum and H. Silverstone, in *Advances in Cancer Research*, J. P. Greenstein and A. Haddow, Eds. (Academic Press, New York, 1953), pp. 451–500.
9. R. Hart *et al.*, *Fund. Appl. Toxicol.* **25**, 184 (1995).
10. R. Walford, S. Harris, M. Gunion, *Proc. Natl. Acad. Sci. U.S.A.* **89**, 11553 (1992).
11. V. Haley-Zitlin and A. Richardson, *Mutat. Res.* **295**, 237 (1993); B. Hass, R. Hart, M. Lu, B. Lyn-Cook, *ibid.*, p. 281.

Abelson states that changes in weight gain characteristics of rodents used in chemical toxicity and carcinogenicity studies affect the outcome of numerical risk assessments derived from these studies. While there are few published data on which to base an evaluation of this issue, this assumption is likely correct. The National Toxicology Program has performed rodent cancer assays on numerous substances of potential importance to public health. We have examined this issue over the last decade (*1*) and have come to appreciate the complexities associated with dietary restriction that are only hinted at by Abelson. The ad libitum offering of food to test animals was standard practice in the 1970s and remains so today. The inadvertent selection of faster growing rodents, combined with improved animal husbandry, has paradoxically resulted in shorter lived animals. Dietary restriction is known to lessen the incidence of "spontaneous" tumors in control animals, and to dramatically increase longevity. However, the effects of marked versus moderate dietary restriction on the sensitivity of the animal model to respond to a chemical carcinogen appear to differ, and at this point insufficient data have been collected to determine exactly how the response of the assay changes in relation to the degree of restriction. Because of this, the National Toxicology Program has taken a different approach. While continuing to offer food ad libitum, we have recently changed the diet to decrease the protein and increase the fiber content. We have also ensured that the breeding bias toward selection of faster growing rodents is stopped. Preliminary results indicate that these changes have resulted in slower rates of rodent growth in 2-year studies, and will decrease the incidence of Fischer rat nephropathy, which is a dietary protein-related disease responsible for early mortality. We believe that these changes will maintain the sensitivity of the rodent models to detect carcinogens and also stabilize the quantitative response of the assays with respect to time. It is important to note that the reproducibility of the results in a qualitative sense is not at issue here, as we and others have noted good reproducibility in replicate assays with regard to target organs and tumor types. However, Abelson's goal of "time invariant" reproducible quantitative results may be unattainable as unappreciated fluctuations occur in the rodent bioassay as in any biological system. It is unlikely that simply offering a restricted amount of food will prevent these fluctuations from occurring.

John R. Bucher
G. N. Rao
Kamal Abdo

MWC 995

Automatically determine HLA types with tools from an ÅÄÖ country?

Can you say your method of determining HLA types is completely accurate? If not, a new approach to detecting HLA types offers you real accuracy.

Introducing HLA SBTyper,™ the new software for automatic sequence based typing from Pharmacia Biotech in Sweden—an ÅÄÖ country.

HLA SBTyper uses raw sequence data, generated by ALFexpress,™ to automatically generate high-resolution HLA typing for class II genes. It determines HLA types by comparing sequence results against a database of well defined and established subtypes. And it all takes just two minutes. ALFexpress and HLA SBTyper also let you access raw data—so you can always go back and verify your results.

HLA SBTyper with AutoLoad™ Solid Phase Sequencing Kit and ALFexpress—together they're the tools that present you with the most accurate way of determining HLA types, and handle every step from capture of PCR products to evaluation.

Just call us at 1 (800) 526 3593 in the United States or +46 18 16 5011 from the rest of the world. Ask for more information about what we Swedes have done for automated sequence based HLA typing. You'll find we've taken every å (pronounced ooh) ä (aah) and ö (uh) out of determining HLA types.

Pharmacia Biotech
Uppsala, Sweden. (And the rest of the world)

Circle No. 46 on Readers' Service Card

Frank Kari
George Lucier
National Institute of Environmental Health Sciences, Post Office Box 12233, Research Triangle Park, NC 27510, USA

References

1. R. W. Hart, D. A. Neumann, R. T. Robertson, Eds., *Dietary Restriction: Implications for the Design and Interpretation of Toxicity and Carcinogenicity Studies* (ILSI Press, Washington, DC, 1995), and references therein.
2. G. N. Rao and J. Huff, *Fund. Appl. Toxicol.* **16**, 617 (1991).

■

Genetic Discrimination: Actuarial Aspects

As a policy spokesman for the actuarial profession, I would like to respond to the 20 October Policy Forum "Genetic discrimination and health insurance: An urgent need for reform" by Kathy L. Hudson *et al.* (p. 391). While the Policy Forum highlights certain theoretical concerns and proposes regulatory restrictions, the impact of genetic information on insurance rates and availability is in some cases exaggerated, and the impact of the restrictions on the voluntary insurance market, and on the risk classification system that is one of its essential elements, is largely ignored.

Actuaries have found that risk classification serves three primary purposes in the design of financial security systems: it promotes fairness, it permits economic incentives to operate and encourages widespread availability of coverage, and it protects the soundness of the financial security system. As a basic principle, any sound risk classification system should reflect cost-of-insurance differences based on relevant risk characteristics.

Clearly, individuals with certain genetic traits may have risk characteristics that would result in increased claim costs. The Policy Forum refers to the risk-sharing function of insurance. The main goal of insurance risk-sharing is to allow individuals subject to an unpredictable risk to pool resources, so that the individuals who, on a random basis, may suffer the effects of the insured event will receive the benefit of the pooling mechanism, which will in turn be appropriately paid for by other members of the class. If all the insured in a class face a roughly comparable probability of loss, they will be willing to pay a premium equal to their expectation of loss.

There is a great temptation to use insurance as a means of providing subsidies. Subsidies may, in some cases, be warranted; but trying to collect them through insurance tends to create incentives on the part of both the insured and insurers that warp the insurance mechanism, reduce the availability of coverage, and in some cases even threaten the soundness of the insurance system.

The Policy Forum suggests that genetic information is "distinct from other types of medical information" and suggests that the appropriate response to the availability of genetic information is to ban its use in the determination of health insurance rates and insurability, at least. Genetic information is often costly to obtain, and the benefits of reduced claim costs may not be commensurate with the cost of obtaining the information on the numerous applicants screened every day by insurance companies. Many genetic factors are related to long-term tendencies that are likely to result in an increased, but not unaffordable, rate—if the appropriate risk factors are used. Special situations, such as the reticence of persons to become involved in certain studies because of the fear of insurance restrictions, can probably be handled by special coverages or other techniques.

Anything that's frozen is never the same again.

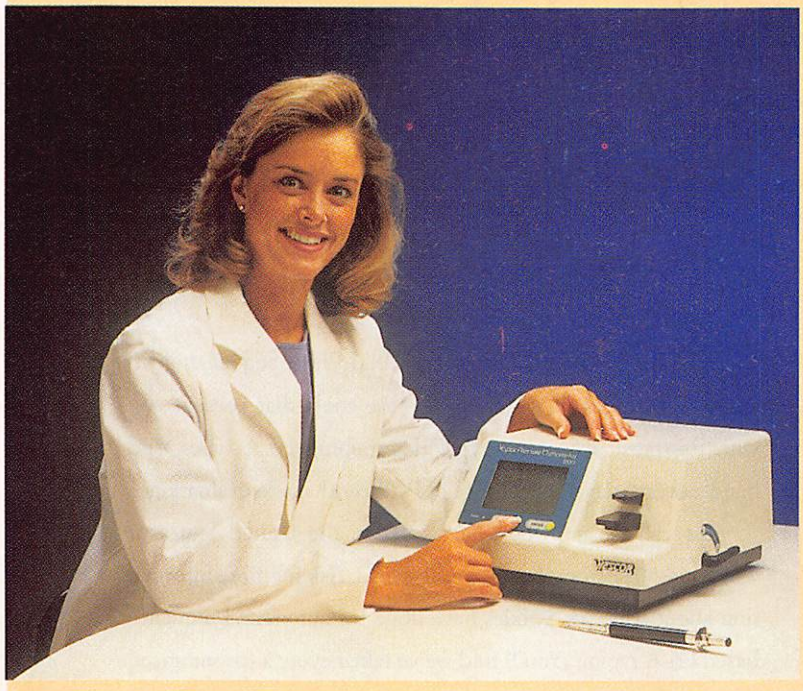

If you need to measure osmolality, basically you have two choices. You can measure osmolality using the older freezing point method, or you can use the modern-day vapor pressure osmometer from Wescor. Now available in a new, easier-to-use menu-driven version, the VAPRO™ osmometer accepts all biological samples, including the highly viscous and tissue specimens. *All without cryoscopic artifacts!* And it can be calibrated for samples as small as 2μL.

The Wescor vapor pressure osmometer is ideally suited for all areas of biological research. It's widely used in marine biology, tissue culture, soil and plant physiology, and lab animal studies. You'll also find it performing Q.C. work in the food, pharmaceutical, beverage, and ophthalmology industries.

Contact us for more details or to arrange a demonstration. Wescor, Inc., 459 South Main Street, Logan UT. 84321 USA. Phone 1-800-453-2725. FAX 801-752-4127.

WESCOR®

Circle No. 37 on Readers' Service Card

Arnold Dicke
Vice President, American Academy of Actuaries, and Executive Vice President–Product Actuary, USLIFE Corporation, New York, NY 10038–4985, USA

Response: The Policy Forum did not include specific predictions about the impact of genetic information on insurance availability and cost. It did provide data on the current impact: survey results showing 22% of individuals from families with genetic disorders have been discriminated against and case studies in which individuals have been treated unfairly by insurers on the basis of genetic information. The concern of the National Action Plan on Breast Cancer (NAPBC) and the National Institutes of Health–Department of Energy Working Group on Ethical, Legal, and Social Implications is shared by many. A majority of Americans (86%) are very or somewhat concerned that insurers or employers might use genetic test results to discriminate (Harris Poll No. 34, 1995). The U.S. Congress is also concerned about this issue. On 15 November, Senator Mark Hatfield (D–OR) introduced the "Genetic Privacy and Nondiscrimination Act of 1995" (S. 1416), which would prevent discrimination by employers and insurers on the basis of genetic information.

Dicke argues that the Policy Forum ignores the impact of the recommendations on the system of risk classification. The current system takes into account the risk of diseases whose genetic components are not yet identified—these risks are spread. Retaining a system of spreading these risks need not be detrimental to industry. In fact, a number of states have already enacted laws to prevent the use of genetic tests to restrict access or increase health insurance rates. Such a law has been in place in Wisconsin for 5 years, and we are unaware of any adverse effects on the insurance industry in that state.

*Kathy Hudson**
Francis Collins†
National Center for Human Genome Research, National Institutes of Health, Bethesda, MD 20892, USA

*Assistant Director for Policy Coordination. †Director; Co-chair, Hereditary Susceptibility Working Group, NAPBC.

Corrections and Clarifications

In note 17 (p. 805) of the report "Superior parietal cortex activation during spatial attention shifts and visual feature conjunction" by M. Corbetta *et al.* (3 Nov., p. 802), the Charles A. Dana Foundation and NIH grant NS32979 should have been credited with support.

In the Random Samples item "Scientists as managers" (3 Nov., p. 741), Alan Merten's name and e-mail address were spelled incorrectly. Merten can be reached at merten@johnson.cornell.edu.

In the report "Aberrant subcellular localization of BRCA1 in breast cancer" by Yumay Chen *et al.* (3 Nov., p. 789), the amino acid position of the putative nuclear localization signal NKLKRKRRP was given incorrectly. The correct position for the signal is amino acids 500 to 508.

Letters to the Editor

Letters may be submitted by e-mail (at science_letters@aaas.org), fax (202-289-7562), or regular mail (*Science*, 1333 H Street, NW, Washington, DC 20005). Letters will not be routinely acknowledged. Full addresses, signatures, and daytime phone numbers should be included. Letters should be brief (300 words or less) and may be edited for reasons of clarity or space. Beginning in October 1995, our previous policy of consulting with all letter authors before publication will be discontinued.

• **DNA Sequencing**
Fully Documented

• **Custom Oligo Synthesis**
$1.50 Base

Fast Turn-around
Cost Effective
Reliable

SSR

Molecular Biology Into the 21st. Century

SOUTHWEST SCIENTIFIC RESOURCES
5300 Sequoia NW, Suite 150
Albuquerque, NM 87120

Phone: (800) 343-8998
Fax: (505) 831-2635

Circle No. 24 on Readers' Service Card

It's Here!
Automated Plasmid Purification Your Lab Can Afford.

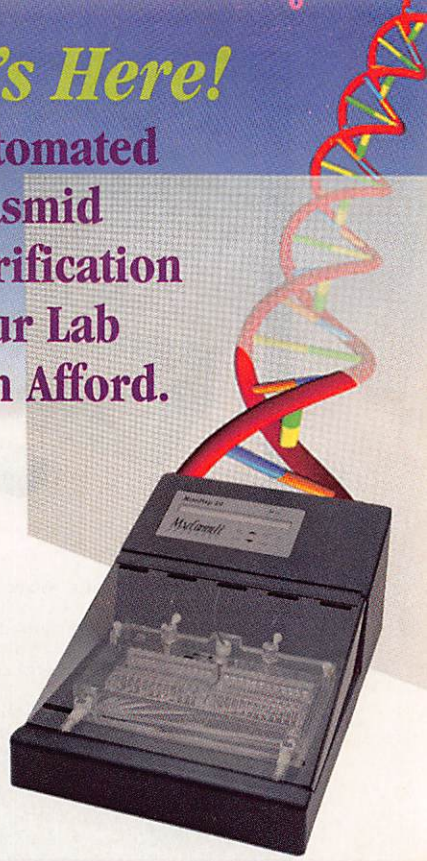

Making Manual Plasmid Mini-Preps a Thing of the Past.

- **High Purity**
  Sufficient for automated, fluorescent and manual sequencing
- **Direct Loading of Culture**
- **Up to 24 Preps in 60 Minutes**
- **Easy Operation**
  No centrifugation, no organic solvent or extractions

Step into the future of automated plasmid DNA preparation!

Call Now !
1-800-466-7949

MACCONNELL RESEARCH
11408 Sorrento Valley Road, Suite 202
San Diego, CA 92121 • 619-452-2603

FUNAKOSHI CO., LTD.
JAPAN
Tel: 81-3-5684-1622
Fax: 81-3-5684-1633

Circle No. 20 on Readers' Service Card

MICROMANIPULATORS

STABILITY

MP-185 MICROMANIPULATOR

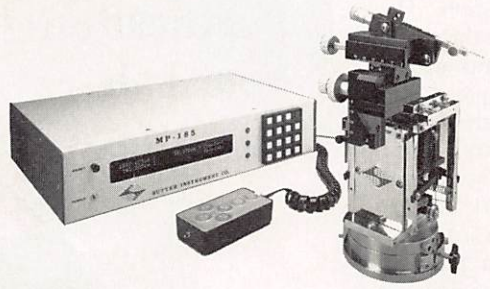

ULTRASTABLE MOTORIZED MICROMANIPULATION

PRECISION MOVEMENT WITH 25NM STEP SIZE

LOCAL HAND-HELD OR COMPUTER CONTROL

CONTINUOUS OR STEPPED MOTION

SERIAL INTERFACE FOR ROBOTIC APPLICATIONS

SUTTER INSTRUMENT COMPANY

40 LEVERONI COURT, NOVATO, CA 94949

PHONE: 415.883.0128 FAX: 415.883.0572

INFO@SUTTER.COM HTTP://WWW.SUTTER.COM

MICROELECTRODE BEVELERS

MICROPIPETTE/NEEDLE PULLERS

OPTICAL FILTERWHEELS

Circle No. 6 on Readers' Service Card

GRANT OPPORTUNITY

U.S. Civilian Research & Development Foundation
for the Independent States of the Former Soviet Union

announces the

COOPERATIVE GRANTS PROGRAM

Teams of scientists and engineers from the U.S. and the former Soviet Union may apply jointly for two-year cooperative grants ranging from $10,000 to $80,000 in any area of civilian research and development.

Applications due March 1, 1996!

For application materials, please contact:

U.S. Civilian Research & Development Foundation
1800 North Kent Street, Suite 1106
Arlington, VA 22209
USA
Tel: 703-526-9720 • Fax: 703-526-9721
E-mail: information@crdf.org
WWW: http://www.internext.com/crdf

Circle No. 41 on Readers' Service Card

Designed for 50 mL Centrifuge Tubes

You'll Flip Over The Convenience.

The Steriflip™ Filter Unit is a disposable, sterile, vacuum-driven device ideal for sterilizing tissue culture media, microbiological media and other biological solutions. To filter, just attach the unit to a 50 mL centrifuge tube and flip it over. The Steriflip device is:

- ***Convenient*** – Filter from the same tube used to mix the sample
- ***Easy*** – No transfer of filtrate. Collect in a 50 mL centrifuge tube for easy use or storage
- ***Economical*** – Less plastic waste

Best of all, the Steriflip device uses the Millipore Express (PES) membrane for fast flow and low protein binding. Filter samples in half the time without sacrificing recovery.

Call or fax for more information. U.S. and Canada, call Technical Services: 1-800-MILLIPORE (645-5476); in Japan, call: (03) 3474-9111; in Europe, fax: +33.88.38.91.95.

MILLIPORE

MILLIPORE LAB CATALOG ON **INTERNET:** ACCESS **URL** MENU AND TYPE:
http://www.millipore.com/steriflip

Circle No. 31 on Readers' Service Card

PEPROTECH

On the Leading Edge of Developing Recombinant Cytokines for Life Science Research

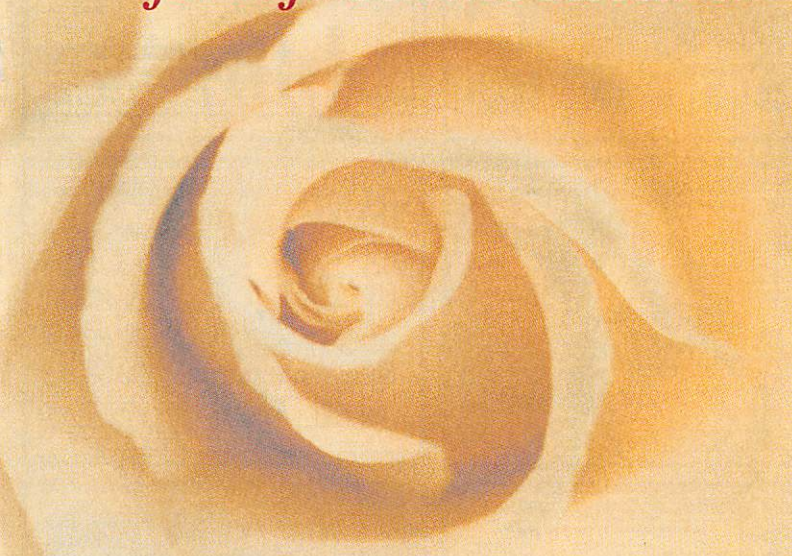

HUMAN GROWTH FACTORS & CYTOKINES

MURINE & RAT GROWTH FACTORS & CYTOKINES

HUMAN, MURINE & RAT CHEMOKINES

HUMAN & RAT NEUROTROPHIC FACTORS

MONOCLONAL & POLYCLONAL ANTIBODIES

Our Business Is Cytokines

Since 1988, PeproTech has been devoted to the development and manufacture of recombinant cytokines for life science research. We have developed cost-effective processes for the commercial production of over 70 fully biologically-active cytokines of utmost purity and have grown to become a world leader in this field.

Continuous Product Development

PeproTech continues to focus on the development of more products with an emphasis on the most recently discovered cytokines. On average, PeproTech has added ten new products per year to its growing line of recombinant cytokines and is committed to pursuing this effort for years to come. In response to customer requests, we have added a complementary line of monoclonal and polyclonal antibodies.

Together We're Better

An important aspect of PeproTech's operation has been the creation of collaborative efforts with academic research groups pioneering the field of intercellular communication. We welcome investigators to collaborate with us toward the development of exciting new cytokine products.

Affordable, Quality Products

PeproTech's products are being made available at quantities ranging from a few micrograms to several milligrams and are offered at the lowest possible price. Our standard size package is now being offered at a reduced price of $170. We guarantee quality products, technical support, and quick delivery.

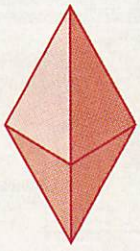

PEPROTECH INC

Developing and Manufacturing Recombinant Cytokines

Princeton Business Park
5 Crescent Ave, G2
P.O. Box 275
Rocky Hill, NJ 08553

Tel: (800) 436-9910
(609) 497-0253
Fax: (609) 497-0321

in Europe contact
PeproTech EC Ltd.
23 St. James's Square
London SW1Y 4JH
England

Tel: 0171 603 8288
Fax: 0171 603 8233

Circle No. 42 on Readers' Service Card

STATISTICA

Windows 3.1 and WINDOWS 95

STATISTICA supports multitasking.
For example, now I am typing this text in MS Word, and in the background, STATISTICA is recalculating a large model (see the red progress bar).

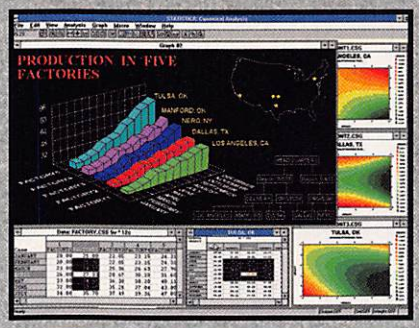

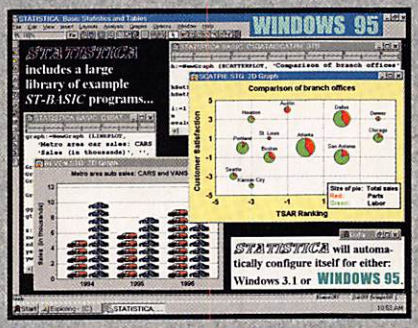
WINDOWS 95
STATISTICA includes a large library of example ST-BASIC programs...
STATISTICA will automatically configure itself for either: Windows 3.1 or WINDOWS 95.

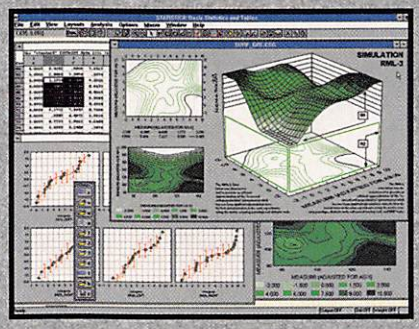

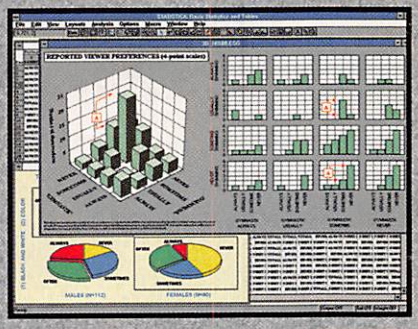

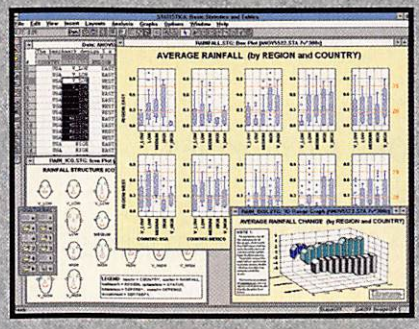

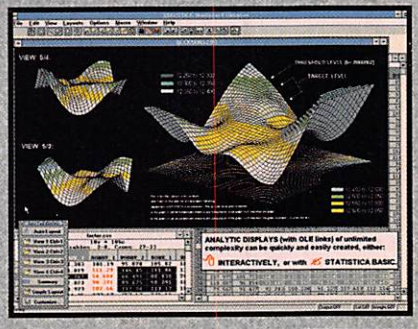
ANALYTIC DISPLAYS (with OLE links) of unlimited complexity can be quickly and easily created, either:
INTERACTIVELY, or with STATISTICA BASIC

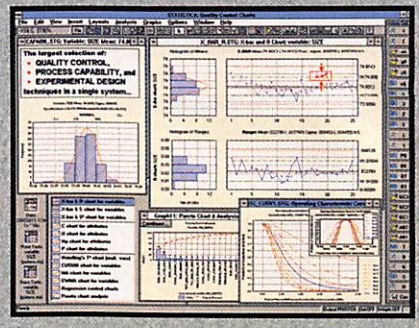

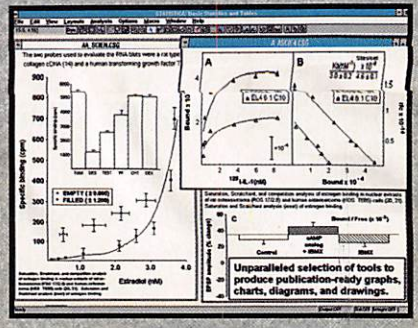

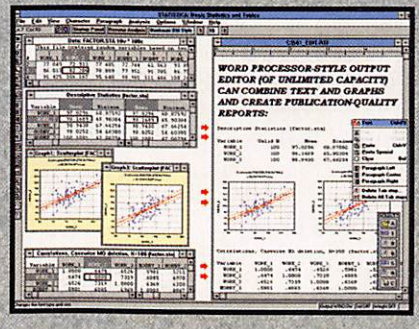
WORD PROCESSOR-STYLE OUTPUT EDITOR (OF UNLIMITED CAPACITY) CAN COMBINE TEXT AND GRAPHS AND CREATE PUBLICATION-QUALITY REPORTS:

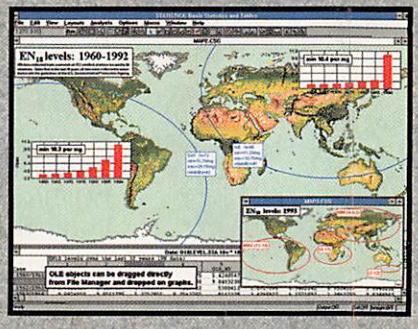

STATISTICA™ (automatically configures itself for Windows 3.1 or WINDOWS 95) ■ A complete data analysis system with thousands of on-screen customizable, presentation-quality graphs fully integrated with all procedures ■ Comprehensive *Windows*™ support, OLE (client and server), DDE, customizable *Auto Task* toolbars, pop-up menus ■ Multiple data-, results-, and graph-windows with *data-graph* links ■ The largest selection of statistics and graphs in a single system; comprehensive implementations of: Exploratory techniques with advanced brushing; multi-way tables with banners (presentation-quality reports); nonparametrics; distribution fitting; multiple regression; general nonlinear estimation; stepwise logit/probit; general ANCOVA/MANCOVA; stepwise discriminant analysis; log-linear analysis; confirmatory/ exploratory factor analysis; cluster analysis; multidimensional scaling; canonical correlation; item analysis/reliability; survival analysis; a large selection of time series modeling/forecasting techniques; structural equation modeling with *Monte Carlo* simulations; and much more ■ On-line *Electronic Manual* with comprehensive introductions to each procedure and examples ■ Hypertext-based Stats Advisor expert system ■ Workbooks with multiple *AutoOpen* documents (e.g., graphs, reports) ■ Extensive data management facilities (fast spreadsheet of unlimited capacity with long formulas, *Drag-and-Drop, AutoFill, Auto-Recalculate,* split-screen/variable-speed scrolling, advanced Clipboard support, DDE links, hot links to graphs, relational merge, data verification/cleaning) ■ Powerful *STATISTICA BASIC* language (professional development environment) with matrix operations, full graphics support, and interface to external programs (*DLLs*) ■ Batch command language and editable macros, flexible "turn-key" and automation options, custom-designed procedures can be added to floating *Auto Task* toolbars ■ All output displayed in Scrollsheets™ (dynamic, customizable, presentation-quality tables with instant 2D, 3D, and multiple graphs) or word processor-style report editor (of unlimited capacity) that combines text and graphs ■ Extremely large analysis designs (e.g., correlation matrices up to 32,000x32,000, unlimited ANOVA designs) ■ Megafile Manager with up to 32,000 variables (8 Mb) per record ■ Unlimited size of files; extended ("quadruple") precision; unmatched speed ■ Exchanges data and graphs with other applications via DDE, OLE, or an extensive selection of file import/export facilities (incl. *ODBC* access to virtually all data bases and mainframe files) ■ Hundreds of types of graphs, incl. categorized multiple 2D and 3D graphs, ternary 2D/3D graphs, matrix plots, icons, and unique multivariate (e.g., 4D) graphs ■ Facilities to custom-design new graph types and add them permanently to menus or toolbars ■ On-screen graph customization with advanced drawing tools (e.g., scrolling and editing of complex objects in 32x real zoom mode), compound (nested) OLE documents, *Multiple-Graph AutoLayout Wizard,* templates, special effects, icons, page layout control for slides and printouts; unmatched speed of graph redraw ■ Interactive rotation, perspective and cross-sections of 3D displays ■ Large selection of tools for graphical exploration of data: extensive brushing tools with animation, fitting, smoothing, overlaying, spectral planes, projections, layered compressions, marked subsets ■ Price **$995.**

Quick STATISTICA (for Windows) ■ A subset of *STATISTICA*; comprehensive selection of basic statistics and the full analytic and presentation-quality graphics capabilities of *STATISTICA* ■ Price **$495.**

STATISTICA/QC - *Industrial statistics add-on package* (requires *STATISTICA* or Quick *STATISTICA* for Windows) ■ The largest selection of industrial statistics in a single package; quality control charts (compatible with real-time data acquisition systems), process capability analysis, R&R, sampling plans, and an extremely comprehensive selection of experimental design (DOE) methods ■ Flexible tools to customize and automate all analyses and reports (incl. "turn-key" system options, and tools to add custom procedures) ■ Price **$495.**

STATISTICA/Mac (for Macintosh) ■ Price **$695** (Quick - **$395**).

Domestic sh/h $12 per product; 30-day money back guarantee.

Circle No. 4 on Readers' Service Card

StatSoft®

2325 E. 13th St. • Tulsa, OK 74104 • (918) 583-4149
Fax: (918) 583-4376

Overseas Offices: StatSoft of Europe (Hamburg, FRG), ph: 040/ 4200347, fax: 040/4911310; **StatSoft UK** (London), ph: 01462/482822/ fax: 01462/482855; **StatSoft Pacific** (Melbourne, Australia), ph: (03) 663 6580, fax: (03) 663 6117; **StatSoft France** ph: (1) 45 66 97 00, fax: (1) 45 66 06 51; Available from other Authorized Representatives worldwide: Sweden: AkademiData Scientific ph: 018-210035, fax: 018-210039; Finland: Statcon Oy ph: 24-334678, fax: 24-333867; Belgium: Texma NewTech ph: 010 61 16 28, fax 010 61 69 57; South Africa: Osiris ph: 12-663-4500, fax 12-663-6114; Japan (Macintosh): Three's Company, Inc., ph: 03-3770-7600, fax 03-3770-7784; Japan (Windows): Design Technologies, Inc., ph: 03-3667-1110, fax: 03-3668-3110; Italy: Prompt SRL ph: 49-893-3227, fax: 49-893-2897; Poland: Companion Oprogramowanie ph: 12-369680, fax: 12-360791; Taiwan: Intelligent Integration Corp. ph: 2-759-1791, fax: 2-759-1790.

StatSoft, the StatSoft logo, STATISTICA, and Scrollsheet are trademarks of StatSoft, Inc.

edited by JOCELYN KAISER

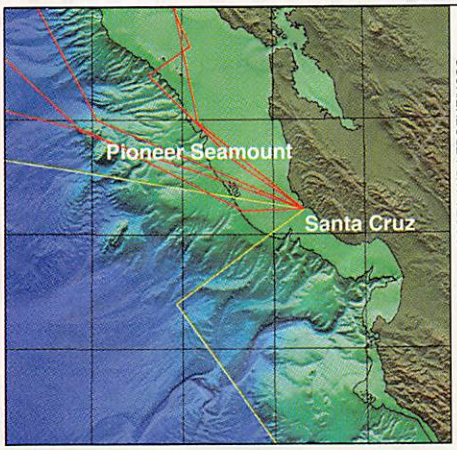

COSTA AND LEBOEUF/UCSC

Sea routes. Paths of elephant seals tracked this fall by ATOC scientists off California.

Ocean Experiment Finally on Track?

After 18 months of delays and setbacks, including a false alarm triggered by the coincidental deaths of three whales last month, a $35 million experiment to use undersea broadcasts to study global warming and the effects of noise on marine mammals was set to begin in California this week.

Bad weather forced the Acoustic Thermometry of Ocean Climate (ATOC) project to postpone its launch date of 7 November, when scientists planned to begin transmitting a 185-decibel hum from Pioneer Seamount, an undersea ridge 55 miles off San Francisco. Then three dead humpback whales turned up in the area, prompting an investigation by the National Marine Fisheries Service to see whether the cause could have been sounds emitted during testing of the ATOC loudspeaker. ATOC was cleared last week of any connection to the whale deaths, and the project was to proceed on 1 December.

The experiment differs from ATOC's original plan, which called for measuring ocean temperatures by detecting how fast the hum travels to receivers around the world. In response to protests from environmentalists, who claimed the sound could harm marine mammals, ATOC is now having its biologists run the show. They'll survey species in the area, then begin turning the hum on intermittently for 2 days and off for 4 days while watching whales, seals, and other marine mammals for changes in behavior. ATOC oceanographers will take what data they can when the sound is on.

The ATOC team hoped to establish by late next year whether the sound drives animals away from their habitat. But the latest delay could cost them critical data, because many humpbacks have headed south for the winter by now, says Dan Costa, a marine biologist at the University of California, Santa Cruz, and leader of ATOC's Marine Mammal Research Program in California. ATOC's funding runs out in September 1996.

Chief Chosen for U.K. Research Council

Oxford University biochemist George Radda will likely be tapped to head the United Kingdom's influential Medical Research Council (MRC) when Sir Dai Rees, the current head, retires next September. Sources say Radda is the favored candidate from a short list of three interviewed last month by the government's Office of Science and Technology (OST), which handles senior-level appointments. Radda, who now heads the MRC's Biochemical and Clinical Magnetic Resonance Unit, would control a budget of $415 million as chief of the MRC, Britain's largest source of public funds for biomedical research.

Radda, 59, is seen as a somewhat surprise choice, given that his career is based more firmly in research than administration. But colleagues such as David Gadion of the Institute of Child Health in London point to his scientific leadership in developing nuclear magnetic resonance for noninvasive analysis of tissue metabolism. OST officials would not comment on the appointment earlier this week, and no announcement is expected until the end of the year.

Oncomouse Patent Debate on Hold

A review of a controversial animal patent in Europe that some had hoped would reach a climax this fall now appears to have stalled. The issue arose at a hearing on objections from animal rights and other groups to a patent for a mouse engineered to be susceptible to cancer—viewed by some as a test case for patents on life forms. But the public session ended last week without resolution, and a decision by the European Patent Office (EPO) on whether or not to revoke the patent could be months away.

European patent number 0169672 was awarded to Harvard University and DuPont in 1992 by the EPO, the first the office had ever granted on an animal. The patent covers transgenic mice—and other animals yet to be developed—with an activated oncogene predisposing them to cancer. Seventeen groups have since filed petitions opposing the patent under the European Patent Convention, with some arguing that such transgenic animals experience a great deal of suffering.

At a hearing in Munich that began on 21 November, EPO officials suggested that the patent's claims may have to be reformulated, and the patent owners quickly complied. One revision would restrict the scope of the patent to onco-rodents only. Before it could reach a conclusion, EPO closed the hearing abruptly, asking parties to submit their views on the proposed new claims in writing.

Peter Stevenson of Compassion in World Farming, one of the parties, says if the patent's scope is restricted, it would send a message "that it would be hard to patent transgenic animals at the EPO." But biotech firms don't regard the case as setting a precedent, says Keith McCullagh, chair of the UK BioIndustry Association. "It's a sideshow," he says, to a debate on biotech patents in the European Parliament, which is to consider a draft directive on the matter in January.

Communists Promise to Save Russian Science

With elections for seats in the Russian Duma scheduled for 17 December, only one major party is campaigning hard for votes from the country's struggling scientific community. Who's beating the pro-science drum? The modern Communist Party.

Although Russia's scientific elite is able to do world-class research thanks to peer-reviewed grants from the government and Western sources, most scientists are floundering on the pittance they receive from the Russian Academy of Science. In the Soviet Union, scientists were members of a well-funded, prestigious community; now each earns on average $80 a month, less than a third the wage of a Moscow city bus driver.

It's this disenfranchised lot the Communists are wooing in stump speeches and appearances at research strongholds such as the Siberian science city of Novosibirsk. If the Communists win a majority in the Duma—the lower house of Parliament that drafts the majority of Russia's laws—they say they will push through legislation that would double or triple funding for science. "The position of science during the Soviet era was good; it was a stable system," says one Moscow-based scientist who plans to vote for the Communists. "Now science is not stable."

However, the Communists' agenda also calls for rolling back economic reforms and shoring up Russia's military—a strategy many scientists dislike. Says Novosibirsk physicist Semen Musher, "Modern Communists only promise to support science for military research," a relatively weak sphere of Russian science. Moscow pundits predict the Communists will make major gains in the Duma at the expense of the squabbling market-reform parties. If so, Russian scientists may gain an all-too-familiar benefactor.

Are Wildlife Corridors the Right Path?

The popular strategy of connecting patches of otherwise isolated habitat could save many endangered species—or it could be a vastly expensive failure

Not far from La Jolla, California, lies some of the last undeveloped land left along the coast of fast-growing San Diego County. Pardee Construction, the Weyerhaeuser subsidiary that owns the central portion of the land, plans to turn it into a suburban neighborhood. But local environmental activists believe it should serve a more valuable purpose: The area forms a corridor connecting the Los Peñasquitos Canyon to the Torrey Pines nature preserves, a link that they believe would let some of the area's threatened species travel between the preserves. Wanting to keep the corridor open, the activists have been campaigning to block Pardee's plans.

Their efforts, however, have run into two big problems. The cost of stopping Pardee could be as high as $40 million—the land's value, according to the company. And the ecological value of such corridors is disputed by some of the discipline's leading researchers. Indeed, wildlife corridors have quietly become one of the most important battlegrounds in conservation, with major development projects and the future of valuable nature preserves at stake.

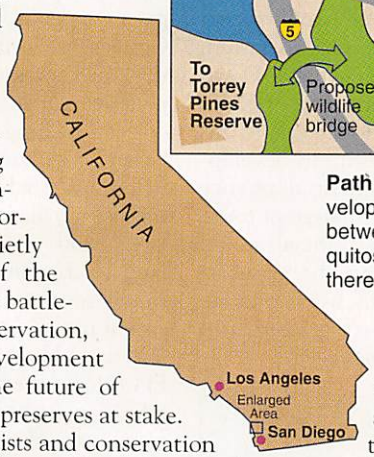

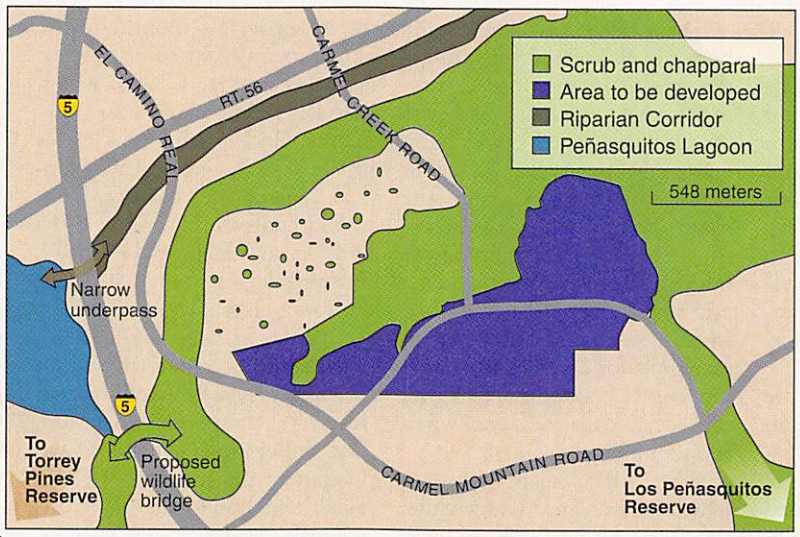

Path to salvation? Activists want to stop development *(purple)* to widen a corridor *(green)* between the Torrey Pines and Los Peñasquitos reserves. But some researchers say there's no evidence to support the plan.

Many ecologists and conservation activists argue that corridors are critical for maintaining biodiversity. "Connectivity is absolutely crucial," says Reed Noss, editor of *Conservation Biology*, "especially when you're talking about a species that doesn't have enough habitat in one place to maintain a viable population." As a result, big habitat-management efforts in ecological hot spots such as Florida, southern California, and the Pacific Northwest have focused on establishing these links between blocks of habitat. Corridors, Keith Hay of the Conservation Fund told *Defenders* magazine (May-June 1990, pp. 19–30), "hold more promise for the management of the diversity of life than any other management factor except stabilization of the human population."

But other ecologists worry that efforts to preserve linking areas like the one in La Jolla may be a shot in the dark. "People are encouraged to think there's a quick, easy answer—a technological fix—when there's no evidence that quick, easy answers are forthcoming," says ecologist Daniel Simberloff of Florida State University. Dennis Murphy, a conservation biologist at Stanford University who advocates careful use of corridors, agrees with this assessment, pointing to the inherent difficulty of studying complex ecological interactions in the field.

One reason for the popularity of corridors, according to Hartmuth Walter, an ecologist at the University of California (UC), Los Angeles, is that they seem to provide a "scientific" rationale for activists to preserve locally favored parcels of land: "It can always be described as a unique link that must be used to preserve connectivity, which sounds better to them than 'just preserve this land because we don't want it to be developed.' " But the result of this well-meaning application of science, he fears, may in the long run not be good for either conservation or science.

Although the notion of ecological connectivity has a long history, it did not appear in modern form until 1970, when Richard Levins, an ecologist at the Harvard School of Public Health, created the first mathematical model of what he called a "metapopulation": a set of linked local populations of a species, each in its own separate patch of habitat.

In Levins's formulation, the population of any given patch rises and falls over time; there is always a small chance that the population on any individual patch can vanish. But the empty habitats can be repopulated if the members of populations are able to disperse from patch to patch—if, that is, the metapopulation has sufficient "connectivity," a term coined in 1984 by ecologist Gray Merriam of Carleton University in Ontario. In Levins's theory, metapopulations can persist through time if the rate of recolonization matches the extinction rate.

A widely cited example is the pool frog *Rana lessonae*, which lives in ponds along the Baltic coast of Sweden. According to Per Sjögren-Gulvë of the Genetics Centre in Uppsala, the pools sometimes dry up, wiping out individual populations; when the pools refill, they are recolonized. The species stays in equilibrium, as long as it has enough pools and frogs can migrate among them. In a classic demonstration of the threat posed to biodiversity by human activity, Sjögren reported last year that the frog is threatened because foresters are draining and ditching these ponds [*Ecology* 75: 1357–67 (1994)].

Theory becomes policy

The intuitive clarity of such scenarios has produced a rapid flourishing of metapopulation theory. In the 1980s, modeling metapopulations became what Simberloff calls a "cottage industry—there must be hundreds of papers by now." One reason for the appeal of this work, he says, is that "the models are mathematically interesting. You get these fascinating theoretical results, like multiple stable equilibria." In such situations, the range of possible states for the metapopulation is mathematically similar to the range of

possible locations for a marble on a dented sheet of metal—it can be at rest in many locations, but cannot shift easily among them.

Theory has produced policy. As ecologist Susan Harrison of UC Davis, puts it, many habitat managers now believe that a "successful [biodiversity] strategy requires conserving numerous habitat patches and the potential for dispersal between them." Corridors thus fill conservation plans in many of America's biodiversity battlegrounds. Florida has spent millions of dollars to create them, including the construction of costly tunnels under interstate highways in an effort to link tracts of land suitable for the endangered Florida panther. In Riverside County, California, the protection of corridors linking patches of habitat for the endangered Stephens' kangaroo rat was a "very important" guideline in setting up the proposed 17,400 hectares of reserves, according to the official habitat-conservation plan. In the Pacific Northwest, the U.S. Fish and Wildlife Service approved a plan offered by the timber firm Murray-Pacific covering a 22,250-hectare tract of land that houses the endangered northern spotted owl. The company gained the right to cut trees even if an owl is harmed, as long as the land itself is maintained as "dispersal habitat." On the grandest scale, the Wildlands Project—an attempt to map out a network of corridors among all of the nation's remaining undeveloped areas backed by Noss, Michael Soulé of UC Santa Cruz, and other influential conservation biologists—is intended to maintain connectivity across huge areas (*Science*, 25 June 1993, p. 1868).

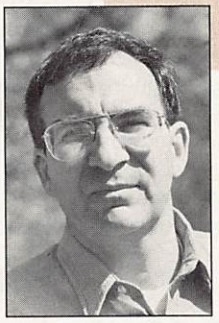

"People are encouraged to think there's a quick, easy answer ... when there's no evidence that quick, easy answers are forthcoming."
—Daniel Simberloff

Gaps in corridor research

But skeptics like Harrison and Simberloff argue that many plans to preserve corridors need closer examination. In the first place, not all species exist as metapopulations. "The phenomenon is a lot less ubiquitous than it seems," says Harrison. "Just because you see patchy habitats and blinking populations doesn't mean you have a situation where you have this balance between extinction and recolonization." And even if there are good theoretical reasons for believing the metapopulation model applies, empirical research on connectivity is extraordinarily difficult. "You have to look at an entire set of populations over the landscape over a long period of time," she says. "The amount of energy you have to have to collect the data running from patch to patch is incredible. The important processes—extinction and recolonization—are so rare that they are virtually impossible to observe."

The difficulties are illustrated in research by Ilkka Hanski and three collaborators at the University of Finland, who have conducted one of the few large-scale studies of metapopulation dynamics. The study, which took place in the Aland islands off the coast of southwest Finland, focused on the Glanville fritillary (spotted) butterfly, *Melitaea cinxia*, which breeds in small dry meadows at the end of summer. During that period, the research team repeatedly surveyed 1530 suitable butterfly meadows—some as small as 12 square meters—in an area of 3500 square kilometers. They found that neighboring populations tended to rise and fall in synchrony, suggesting that the whole area indeed held a metapopulation with many possible stable states (*Nature*, 19 October, pp. 618–621). Yet because the Finnish team has only 2 years' worth of data, Harrison cautions, the results of this "very ambitious and very exciting" study remain "compatible with other explanations" than metapopulation dynamics. The populations could be independent and the synchrony only coincidence.

"I think the burden of proof should fall on those who would deny corridors ... not on those who lobby for them."
—Dennis Murphy

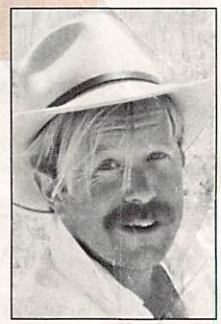

Even if a metapopulation exhibits connectivity, corridors may not be needed to provide it. "When you look at populations that are naturally fragmented, they often aren't connected by corridors," says R. J. (Rocky) Gutierrez of Humboldt University in California, a wildlife biologist who has studied bird populations in the western United States. "Yet there are populations of these species on habitat islands. That's an indication that they can reach these islands independent of corridors." He points to Manhattan's Central Park as an example. "You have a good complement of [northeastern] migratory birds there," he says, "and there's no corridor connecting it" to anyplace else.

Large mammals' need for corridors is intuitively easy to understand, because they often have large home ranges or use migratory pathways. Indeed, Paul Beier, a biologist at Northern Arizona University, tracked cougars with radio collars and found that the animals always follow the same paths between patches of habitat, even paths that are kilometers long and pass through golf courses and highway underpasses. "These animals will really use corridors if they're available—even surprisingly poor corridors," says Beier. And he has some evidence that such paths are needed: "The cats will not walk through a mile of tract homes. None of the radio-tagged animals ever did that."

But even this evidence isn't conclusive. The best way to prove that organisms use corridors, Simberloff says, is to cut them off and see what happens. But in a real landscape, this is a rather difficult proposition. Beier acknowledges, for example, that he couldn't cut off all the cougars' possible corridors to see if they could still find their way across the landscape because the corridors wind through private property and under freeways. Moreover, because corridors are not always self-evident, it would be hard to know what to cut. Ted Case, an ecologist at UC San Diego, says that ecologists usually define corridors by vegetation types—strips of forest land between the lawns of suburban developments, for instance—but species such as salamanders may follow different trails. "I'm not as sure they are responding to vegetation types, rather than microbes in the soil or fungus or ants," Case says.

Finally, Simberloff also points out that corridors can have down sides. They can allow disease, predators, and exotic species to spread through a metapopulation. And corridors, which are sometimes touted as ways to increase genetic diversity among populations, may also function to decrease it, because the migration among individual populations may end up genetically homogenizing the metapopulation as a whole. Like the evidence in favor of corridors, Simberloff admits, these possibilities are largely theoretical. But, he adds, "there are examples of predators," such as eastern diamondback rattlesnakes, that use corridors for "trap-lining"—that is, lying in wait for their prey along a corridor. He also cites a 1987 study that found corridors facilitating the spread of exotic feral pigs through forest fragments in New Zealand, menacing a

genus of tree snail (in D. A. Saunders *et al.*, *Nature Conservation: The Role of Remnants of Native Vegetation*, Chipping Norton, N.S.W. Surrey Beatty, 1987).

Making trade-offs

The land between the Los Peñasquitos Canyon and Torrey Pines nature preserve exemplifies many of these issues. The area is hardly pristine wilderness. Laced with roads and suburban neighborhoods, it is bordered on the west by the eight lanes of Interstate 5, one of the most heavily traveled roads in the country. But in the middle is a relatively undisturbed mesa covered with scrub and chaparral.

Pardee's plans call for creating a development of almost 1000 homes on 160 hectares of this mesa. In exchange, the company would set aside a number of other parcels—including a wildlife corridor that snakes around the developed areas and past I-5 by way of a tunnel and a proposed bridge, forming a 3-kilometer route between the two reserves. This corridor will keep the two reserves connected, Pardee believes, and allow large predators like coyotes, bobcats, and cougars to maintain a presence in Torrey Pines, which in turn may help prevent it from being overrun by squirrels and smaller predators like feral cats and raccoons.

But corridor advocates like Soulé and Michael Beck of the Endangered Habitats League, a southern California environmental group that is spearheading the fight to protect the mesa, argue that this skinny, winding path is not enough to assure connectivity and safeguard Torrey Pines from isolation. They want to see the development on the mesa moved to the southern portion, creating a much wider corridor through the northern part and preserving much of the mesa's scrub and chaparral. And they have vowed to fight Pardee.

This is, advocates say, the only cautious and prudent course. Noss argues that in the absence of hard evidence, it is always a good idea to maintain existing connections wherever possible. And Beck, who admits there is no definitive evidence to support the mesa's use as a corridor, agrees that the best course is to be conservative. Pardee's development proposal, in his words, "is not biologically conservative at all. It takes the heart out of the mesa." He believes Pardee's needs are sufficiently flexible to allow a wider corridor.

Skeptics think corridor boosters are going to give up a guaranteed deal that will create open space in favor of an unproven scientific concept. Studies similar to Beier's, UCLA's Walter points out, suggest large mammals need no more than the narrow path called for in Pardee's current plans. Moreover, he says, the "caution" of corridor advocates actually disguises other risks. Money does not grow on trees, the ecologist says, and tapping public coffers to buy the mesa almost certainly precludes spending funds on other conservation efforts. Noting that exotic plants and other forms of degradation plague the Torrey Pines reserve—an observation that has broad scientific support—Walter asks if the area's limited conservation resources might be better spent on restoring the reserve's ecological health.

Beck worries, however, that without the biggest possible link, the degradation in Torrey Pines will only continue. "If we write off wildlife dispersal to Torrey Pines," he says, "it won't have the dynamic mechanisms that balance wildlife activity."

The debate over the corridor through the mesa, like many others around the country, must be resolved without the evidence scientists usually rely upon to settle such disputes. To Walter, it is risky for scientists to come out strongly for a concept with such uncertain empirical backing. "How are we going to get Congress to listen to biology if they think it is being used solely as an excuse to stop development?" he asks. And he worries that the result could be a discrediting of science.

Others argue that development pressure is too intense to allow researchers to work with perfect data, no matter what they do. But they disagree about what to do in the absence of evidence. "Corridors are not bad per se," says Harrison, "but there's a range of [possible conservation strategies], and you should at least consider them before blindly rushing into things." Murphy doesn't disagree, but feels that corridors should be given the benefit of the doubt. "Given what we know about the dispersal of species and the persistence of populations," he says, "I think the burden of proof should fall on those who would deny corridors to a reserve system, not on those who lobby for them."

–Charles C. Mann and Mark L. Plummer

Charles C. Mann and Mark L. Plummer are co-authors of Noah's Choice: The Future of Endangered Species.

SCIENCE FUNDING

Report Strips R&D Down to the Basics

When it comes to federal spending on research, the National Academy of Sciences (NAS) hopes that less may be more. A report* released this week argues that the federal science budget is now defined so broadly that its ups and downs say little about the health of U.S. research. Instead, the academy argues, a tighter definition of R&D that includes only activities that generate new knowledge or technologies, and leaves out items such as developing new weapons and launching rockets, would provide a much sounder basis for federal policy-making. It would focus attention on the elements of the science budget most likely to keep the nation healthy and economically strong.

The report, written by a panel chaired by former NAS President Frank Press and discussed in a Policy Forum on page 1448, estimates that the current science and technology (S&T) budget would amount to around $37 billion under such a definition. That's a little more than half the sum the government now claims to spend on R&D. The programs not included in this total should be defended on their own terms, not for their contributions to science, the committee says.

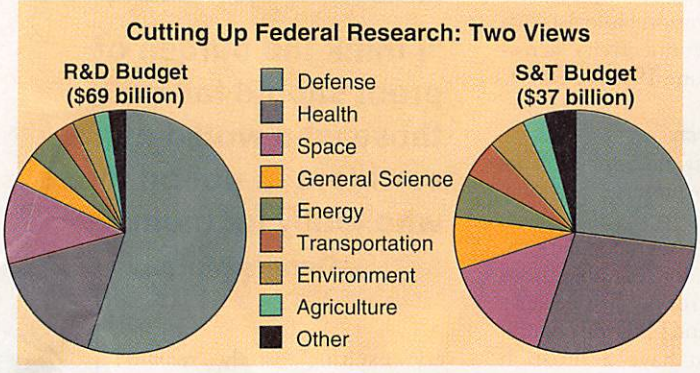

A healthy change. Biomedical research would become the largest component of the new S&T budget, surpassing defense R&D.

Committee member Barry Bloom, an immunologist at Albert Einstein College of Medicine, acknowledges that some may view this new definition as implying that the country can get by with less research—"that we've sold out." But, he says, "the fact is that budgets are going down, and we're suggesting a way to protect what's most important when you don't have enough to do everything." Bloom says the committee assumed that the federal R&D budget, as it's currently defined, might shrink by 30% by 2002, and that prospect set the tone for its deliberations. By tightening the definition of R&D, he says, you can get a better sense of how core programs are faring.

The study was requested last fall by the Senate appropriations committee to help it decide how to allocate scarce R&D dollars. Funded by the National Institutes of Health, the National Science Foundation, the De-

* "Allocating Federal Funds for Science and Technology," National Academy Press, 1995.

fense Department, and the academy itself, the report not only redefines research spending but offers tools to help policy-makers squeeze the most out of the existing system.

Among its 13 recommendations is a separate S&T budget, drawn up by the White House under the new definition and presented to Congress. Within that budget, says the committee, the focus should be on people and projects rather than research institutions. The report praises university-based research, citing its use of peer review, its role in training the next generation of scientists, its easy dissemination of new knowledge, and its flexibility in accommodating new research directions. "The committee does not presume that academic research is always of higher quality than that conducted in industry or federal laboratories," the report says, but it "supports a general preference for academic over nonacademic institutions."

Federal laboratories, the panel says, should be downsized or closed if they no longer serve the mission of the funding agency. An independent commission, similar to the panel the military used to close unneeded military bases, "will probably be needed as a last resort" if individual agencies prove incapable of taking decisive action, the report notes.

Some of the recommendations echo earlier calls from other advisory panels, including a 1993 report by the academy's Committee on Science, Engineering, and Public Policy that says the goal of federal research should be world leadership in selected fields and world-class abilities in all areas. The new report also revives a suggestion by the 1993 panel for 5-year reviews of how U.S. efforts stand up to those of the rest of the world.

Several committee members see the efforts of the National Science and Technology Council, set up by the Clinton Administration to coordinate R&D spending among 20-odd federal agencies, as a first step toward the unified approach to science that they are recommending. "Our report represents an endorsement of the current process," says Lew Allen Jr., chair of the Charles Stark Draper Lab in Pasadena, California, and former director of NASA's Jet Propulsion Lab. The next step, says the report, is a mechanism for both Congress and the White House to monitor the fate of R&D priorities as they make their way through the legislative maze, rather than simply waiting until all spending bills have passed and tallying up the results.

"It would have been easier to ask for a 10% increase" in the research budget, says Bloom about the challenge facing the NAS panel. "But we decided to focus on the process, emphasizing the S&T budget and peer review, to help Congress make the hard choices that lie ahead."

–Jeffrey Mervis

SCIENTIFIC MISCONDUCT

Panel Urges New Approach to Inquiries

In the criminal justice system, those who investigate alleged crimes—the police—are not asked to take the case to trial also, much less decide whether the defendant is guilty or what sentence to mete out. But when some biomedical researchers funded by the federal government are accused of committing scientific misconduct, the Office of Research Integrity (ORI) does it all—investigates, adjudicates, and recommends punishment. That's too many hats to wear, says an outside panel of experts who studied how ORI operates.

Last week, in an 80-page report,* the Commission on Research Integrity recommended that ORI shed some of its enforcement responsibilities. The recommendations are intended to correct flaws in how the office has operated, notes the report, including exercising poor judgment in choosing some cases and being too secretive during investigations. The 12-member commission also concluded that research institutions should take the lead in preventing as well as rooting out misconduct, and it revised a definition of misconduct that clarifies an earlier draft (*Science*, 29 September, p. 1811).

"It's an accepted standard that the investigation and prosecution are separate from the judicial [outcome]."

—Kenneth Ryan

"[ORI officials] haven't always selected or pursued their cases very well because they've gotten caught up in the chase," says one member of the commission, which was created 17 months ago after Congress asked the Department of Health and Human Services (HHS) to review its approach to alleged misconduct. The report says ORI Director Lyle Bivens "cannot be considered a disinterested party to the success of the investigative effort."

Separating adjudication and investigation at HHS—a principle that should also be applied at the institutional level—would help solve these problems, the report concludes. "It's a commonly accepted standard of law that the investigation and prosecution are separate from the judicial [outcome]," notes Kenneth Ryan, a Harvard reproductive biologist and chair of the commission.

The commission favors the approach taken by the National Science Foundation, where the inspector general performs investigations and makes recommendations to the deputy director, who then decides if the accused is guilty and sets the appropriate punishment. Ryan says the changes could involve "some new relationship" between ORI and the department's appeals board, the next step in the adjudicatory process. The report even discusses having investigations be "assisted or directed by" the HHS inspector general, leaving ORI to concentrate on education and other functions.

Despite endorsing a role for the government, the panel says that individuals, institutions, and professional societies should "have primary responsibility" for enforcing good research conduct. "Those who are closest to the work are best suited to make the decisions," explains commission member Kristina Gunsalus, associate vice chancellor for academic affairs at the University of Illinois. The report says institutions should expand programs for teaching researchers about misconduct, now required only for recipients of training grants, and should handle most investigations.

The report also recommends replacing the current Public Health Service definition of research misconduct, which begins with the words "fabrication, falsification, plagiarism," with two categories explained at length—misappropriation and misrepresentation—and a new term, interference. The panel also recommends that an interagency task force be formed to develop a common research misconduct definition and that the HHS secretary come up with a regulation to protect those who first report allegations.

The report is getting a lukewarm reception from experts in the field. The recommendations "would probably make a useful difference," says Barbara Mishkin, a misconduct attorney in Washington. However, Mishkin says the commission has gone overboard in recommending that some disputes among collaborators be treated as misconduct without defining the rights of team members to data. And Paul Friedman, a radiologist at the University of California, San Diego, says a recommendation that the government make site visits to institutions "would be an excruciating waste of time."

The next step is for the panel's recommendations to be reviewed by a group of senior HHS officials. Next year the department is expected to issue a proposed rule—including a new definition—telling how it plans to handle allegations of misconduct.

–Jocelyn Kaiser

* Integrity and Misconduct in Research; contact Henrietta Hyatt-Knorr, 301-443-3400.

JAPAN

Consortia to Boost Efforts to Develop Genome Industry

TOKYO—Two years ago, venture capitalist Yoshihiro Ohtaki was becoming increasingly alarmed that Japanese pharmaceutical companies were all but ignoring the potential commercial value of work on the human genome. While European and U.S. drug giants were pouring hundreds of millions of dollars into start-up companies, databases, and academic labs, the only major Japanese company to show any real interest in turning genome findings into new drugs was Otsuka Pharmaceutical Co., which established a small genome research unit in 1993.

Ohtaki, fearing that these overseas commercial ventures were building up an insurmountable lead in genome work and putting a proprietary lock on genetic data, took his concerns to the government. He got a receptive hearing: The Ministry of International Trade and Industry (MITI) promptly set up a joint government-industry group, of which he was made a member, to study what should be done. The first fruits of its labor are expected to be announced within the next few months: a private company, backed by MITI and 20 large corporations, that will study gene function and develop automated technologies to advance genomic research. The company, tentatively called the Helix Institute, could be followed by a second venture, co-sponsored by the Ministry of Health and Welfare and industry, that would hunt for genes responsible for hereditary diseases, especially in children. Observers consider the MITI company a sure bet, while the Health and Welfare scheme is seen as a long shot.

"Two years ago, Japan's pharmaceutical companies did not realize the importance of genome research," says Ohtaki, president of Japan Associated Finance Corp. in Tokyo. "But now they finally understand the need to have their own base of intellectual property" to develop new drugs. Yasufumi Murakami, a genome researcher at the Institute for Physical and Chemical Research who has advised the MITI panel, says the rapid accumulation of genome sequence data and moves toward identifying gene function have forced the hand of Japanese industry.

Although some preliminary information about the prospective companies has appeared in the press, there has been no public announcement, and officials at both ministries will say only that the proposals are under study. News of the ventures has been percolating through the research community, however, and researchers have generally welcomed the plans. Kenichi Matsubara, a professor at Osaka University's Institute for Molecular and Cellular Biology, says, "I think it could be a very good thing—if properly operated."

The main objectives of the ventures are to develop technologies and generate basic knowledge that can support the new ventures and be shared among members of the consortia. The new companies are also expected to create a pool of talent, including scientists borrowed from participating companies. The first plan, presented by companies and under review by MITI, would have the trade ministry contribute as much as 70% of the $60 million to be put into the company over 6 years. The second proposal asks the health ministry to contribute 50% to 60% of a 6-year budget of $40 million.

Some genome researchers worry that these efforts will be too small to have a significant impact, and that the rules governing university-industry interactions and intellectual property rights may hinder collaboration with academic efforts. "With the stated goals, the [MITI] project should really be a bit bigger, maybe double," says Murakami.

Indeed, the annual budget of the MITI affiliate is only one-fourth that of Human Genome Sciences (HGS), a Rockville, Maryland, company formed to capitalize on the work of J. Craig Venter, formerly of the National Institutes of Health. Smith-Kline Beecham has provided $125 million to HGS. Even Otsuka Pharmaceutical will be outspending the MITI consortium: The company already provides its Otsuka Gen Research Institute with $15 million a year and projects rapid growth as it adds staff.

Otsuka will not be part of the MITI consortium, because it prefers to work on its own. The institute's deputy director, Hiroumi Maekawa, says 36 scientists have turned out some 30,000 partial sequences that serve to identify genes, and that the data on 12,000 partial sequences have already been deposited in an open, international database. The next step is to focus on gene function, he says, and Otsuka plans to hire 30 more researchers to tackle the job.

Ohtaki notes that the money the government and the private sector plan to put into the ventures is considered an investment, not a subsidy, and both companies are expected to show a return. The MITI affiliate expects to generate profits through a proprietary gene function database and by developing new automated methods to do such things as screen various proteins expressed by genes. That focus, he says, explains the presence of Hitachi Ltd. and Olympus Optical Co., which manufacture analysis equipment and precision instruments.

To be successful, the new ventures will have to overcome serious obstacles. To compensate for their small budgets, says Ohtaki, the companies need to form collaborations with research groups at Japanese universities and national research institutes. But unlike in the United States, professors at Japanese national universities cannot participate in start-up ventures or work directly for private companies.

Collaborations are a possibility, although these are complicated by questions about intellectual property rights. Universities typically do not have patent offices and are generally not set up to exploit the commercial potential of research discoveries. "There is

GETTING ON BOARD THE GENOME EXPRESS

	Helix Institute	Genome Pharmaceutical Science Research Center
Funding Agency	Key Technology Center, under International Trade and Industry and Posts and Telecommunications ministries	Ministry of Health and Welfare
Investment	$60 million over 6 years, 70% from government	$40 million over 6 years, 50%–60% from the government
Industrial Participants	20 companies, including Yamanouchi, Fujisawa, and Chugai Pharmaceutical Cos.; Hitachi; Mitsubishi Chemical; and Toray Industries	10 companies, including Eisai, Yamanouchi Pharmaceutical, Kirin Brewery, Olympus Optical, and Tanabe Seiyaku
Research Goals	Gene function and automated analysis and screening	Genes responsible for hereditary diseases, especially in children

SOURCES: JAPANESE PRESS REPORTS, JAPAN ASSOCIATED FINANCE CORP., COMPANIES

no mechanism to transfer intellectual property to the private sector," Ohtaki says.

Neither is it easy to hold joint patents on collaborative work. Although such arrangements are possible, says an official at the Ministry of Education, Science, Sports, and Culture, the procedures are cumbersome and not well known. The ministry is now studying ways to help universities benefit from intellectual property and work with the private sector. In the meantime, Murakami says he hopes academics will be willing to act as unpaid advisers to the new companies.

The biggest benefit of the new ventures for existing companies may be to stimulate their own human genome research efforts. A director of research planning at one of the participating drug firms, who requested anonymity, said his company sees participation as a step in developing "an infrastructure of genome research." The company plans to assign its own researchers to the consortia temporarily and then use them as the nucleus of the firm's own genome research team when they return. The consortia will focus on very basic work, he adds, leaving drug development in the hands of individual companies.

That arrangement is fine with Murakami, who sees such collaboration as the key to success. "If the tasks are separated in a well-organized manner, the new company could produce substantial [results] in conjunction with genome labs at each participating company," he says. The joint activity, he adds, could also contribute to global efforts.

–Dennis Normile

POLAR RESEARCH

Pressure on Budget Triggers Review of Antarctic Program

This month, under the brilliant 24-hour-a-day sunlight of high summer, a team of physicists at the U.S. South Pole station is drilling half a dozen holes deep into the ice as part of an experiment to flag down elusive cosmic neutrinos. Not far away, astronomers are peering into the cosmos with newly installed infrared and millimeter-wave telescopes that take advantage of the pole's high, dry, frigid environment. Other areas around the base are also a buzz of activity, as geophysicists, atmospheric scientists, and geologists probe the workings of Earth and its climate, both ancient and modern.

All this work is supported by the U.S. Antarctic program as part of a $195-million-a-year effort run by the National Science Foundation (NSF). It's by far the largest and most productive scientific presence on the continent, accounting for 40% of the roughly 3000 people working on the continent on any given austral summer day, by NSF estimates. But size is not always a virtue during times of fiscal austerity: The program has caught the attention of Congress, which has asked for a thorough review of U.S. policy in Antarctica.

At issue is whether the country still wants—and can afford—such a dominant effort. Last week more than a dozen federal officials gathered at the Old Executive Office Building to kick off the review, which could decide not only the future of these ongoing scientific activities but also the fate of NSF's plans for a $200 million replacement for its South Pole station. The review, requested by the Senate appropriations subcommittee that oversees NSF's budget and endorsed last month by the House, could also affect research by other countries that are partners in joint activities and whose own efforts are coming under closer scrutiny (see box).

The trouble is that Antarctic research doesn't come cheap. The current program—three year-round stations, two research vessels, and the world's only fleet of planes capable of landing on the ice—eats up 9% of NSF's overall research budget and requires $5.50 in logistical support for every dollar spent on research. Both figures will increase if the government replaces the 20-year-old Amundsen-Scott Station with a new structure that NSF officials say must be built in the next 5 to 7 years to meet the scientific, health, and environmental needs of those working at the South Pole (*Science*, 24 June 1994, p. 1836).

Hot spot. NSF hopes to avoid a meltdown of its plans to rebuild South Pole station.

Congress wants federal officials to think about ways to trim costs, including making the new station an international effort and operating it for only part of the year. And it's asking the Administration to look at these issues in a broad context: "It's not [just] how much money you can save," says a congressional aide who follows the issue closely, but "the rationale behind why you're there." The White House has assigned the job to a task force of the Committee on Fundamental Science, one of nine panels that make up the president's National Science and Technology Council, which includes 20 federal agencies with an interest in science. The Senate subcommittee wants a report by 31 March, in time to review NSF's 1997 budget request, which could include a downpayment on a new station.

Polar scientists seem confident that the research portfolio can withstand scrutiny by federal officials. "I've been going there since 1959, and the science is better now than it's ever been," says Robert Rutford, a geologist at the University of Texas, Dallas, and the U.S. representative to the international Scientific Committee on Antarctic Research, which coordinates the various national programs. "NSF rolled the dice when it decided to build a new station," he says, "and now it needs to be able to defend the value of the whole program."

But the debate is not just about science. Although the 1959 Antarctic Treaty binds the 26 signatory nations to peaceful scientific activity, the U.S. government long viewed Antarctica as an important outpost in its campaign to contain Soviet expansionism—a role underscored by the use of military personnel for logistical support. In addition, seven countries continue to hold territorial claims that the treaty puts in abeyance and that a U.S. station at the South Pole serves to blunt.

Those strategic concerns have helped NSF survive past reviews, and Cornelius Sullivan, head of NSF's Office of Polar Programs, says the fundamental issues haven't changed. "Is there something wrong with our policy over the past 40 years, or is it basically sound?" he wonders. In 1982, after soaring fuel prices threatened to curtail the program, the Reagan Administration endorsed "an active and influential presence" in Antarctica with the existing complement of facilities. A review early in the Clinton Administration, part of a 1994 directive that remains classified, cited along with science the importance of protecting the environment, cooperating with other countries, and preserving the region's living resources.

R. Tucker Scully, director of the department's office of ocean affairs and a veteran of Antarctic policy debates, is convinced that the current policy is correct. "I would be quite surprised if the task force concluded that our fundamental interests in Antarctica have changed, because I don't think that they have," he says.

However, NSF may have fewer allies at a time when budgets are shrinking, national

Europeans Make Room for Ice-Core Project

The U.S. Antarctic program isn't the only national effort coming under scrutiny from budget-conscious politicians. Both France and Italy, leading members of a 10-nation European effort to drill two 3500-meter-deep ice cores on the Antarctic plateau to uncover 500,000 years of climatic history, are asking polar scientists to justify the additional expense for the $60 million project. At the same time, two other major partners, Britain and Germany, have reshuffled their Antarctic programs to make room for the new project in a tight budget.

The two-core European drilling project, known as the European Program for Ice Coring in Antarctica (EPICA), hopes to test whether the findings from Europe's recently completed Greenland Icecore Project apply on a global scale. Drilling will begin in December 1997, in a region influenced by the Pacific and Indian Ocean, while the second phase will drill in an area affected by the South Atlantic Ocean.

In France, the debate is focused on plans for a $28 million year-round national station, Dome Concordia, at one of the two drilling sites. "Of course other scientists are interested in the money we will be spending at Dome C," says Roger Gendrin, director of the French Institute for Polar Research and Technology in Brest. "The criticism is based on people asking if it is really necessary to maintain a winter presence there and carry out continuous measurements at the site. We think the answer is yes."

When completed in 2000, Dome Concordia will host research in astrophysics, medicine, meteorology, seismology, and other disciplines. It is likely to be only the second year-round station, after the U.S. South Pole station, operating on the Antarctic plateau. (Winter operations at the inland Russian station at Vostok were suspended after the 1993–94 austral summer to save money, and the station, although it stayed open last year, is scheduled to close again at the end of the current summer season.) France currently operates one year-round coastal station, Dumont d'Urville.

In Italy, legislators are debating whether funds from Antarctic research would be better spent closer to home, on studies of the Mediterranean Sea. "Fortunately," says Mario Lucchelli, manager of Italy's National Program for Antarctic Research, "the program has lots of friends who know how important it is for Italy to be part of high-quality international research." Italy's only station, at Terra Nova Bay, is highly automated and is staffed only during the austral summer.

The EPICA project is already spurring some changes in Britain's and Germany's programs. Among other things, the British Antarctic Survey (BAS) is cutting two of its four year-round stations. Signy Station in the South Shetland Islands will close its winter operations next year, says BAS Director Peter Heywood, and in February Ukraine will take over operations at Faraday Station, on the Antarctic Peninsula. "We decided we wanted to put our money elsewhere, and we had to make some hard-nosed decisions," says Heywood.

Germany is also shifting resources to accommodate the drilling project in a tight budget. "We're trying to cut down on the number of winter-over people at Neumayer Station [Germany's sole year-round facility] by seeing how much of the work we can automate," says Max Tilzer, director of the Alfred Wegener Institute in Bremerhaven, which runs the country's Antarctic research program. The institute has shifted some money into Arctic programs to fund joint expeditions with Russia, and it is also in the process of dismantling a 10-year-old Atlantic station, Georg Forster, inherited from the former East Germany.

–J.D.M.

SOURCE: SCIENTIFIC COMMITTEE ON ANTARCTIC RESEARCH

Spreading out. EPICA's inland sites will double the number of year-round stations not located along the Antarctic coast.

security is being redefined as economic competitiveness, and environmentalism is under attack. Although one important player, the National Security Council, has so far remained neutral in the debate, it has never been a big booster of the research program. And a few influential senators, led by defense appropriations panel chair Ted Stevens (R–AK), believe that a slimmed-down Defense Department should focus on areas of greater strategic importance than Antarctica. Last summer, for example, Stevens proposed that no military units be allowed to provide logistical support to the region, even though NSF reimburses the Pentagon for its use of military personnel and equipment. The language was modified by House-Senate conferees, but it spurred NSF to step up its effort to reduce its historic reliance on the military.

NSF's environmental research agenda may also be a harder sell. "If Congress doesn't believe in ozone depletion and global warming, then it's hard to get them to understand the importance of the work going on there," says Beth Marks, head of the Antarctica Project, a Washington, D.C.–based environmental group that closely follows U.S. activities in Antarctica.

But even if the review reaffirms the program's value, NSF's supporters also wonder if the agency is savvy enough to avoid getting hit in the crossfire in upcoming budget battles. "The problem with the South Pole station, for example, is that there were several options, and they picked the most expensive one," says Marks. "I don't think they realize what could happen to them. If Congress says cut [the overall NSF budget] and they don't have a fallback position, then they are out of luck."

In response, NSF's Sullivan says there is a plan to carry out the South Pole renovation in phases, putting safety and preservation of the environment first and delaying an upgrade of research facilities if money is tight. But he says that wholesale trade-offs involving the rest of NSF's budget would violate language in the 1982 review declaring that other NSF programs should not be taxed to pay for U.S. activity in Antarctica.

For Antarctic researchers, the unique science they are doing is ample justification for the program. Still, they will be anxiously watching Washington in the months ahead for clues to whether the sun will continue to shine on their projects.

–Jeffrey Mervis

Found: A Star Too Small to Shine

The discovery of methane in the atmosphere of a dim, starlike object marks it as a brown dwarf—a failed star—and fills a gap in theorists' picture of star formation

Steelworkers tell the temperature of a glowing ingot by its color. For astronomers who sift the galaxy in search of the dimly glowing objects called brown dwarfs, however, life is not so simple. A faint glow in the infrared region of the spectrum is a good marker for one of these "failed stars"—objects too small for hydrogen fusion to heat their cores. But it's not a foolproof one: Great distance can dim the light of a normal star, and very old stars, cooling toward extinction, could mimic the dull red glow of a dwarf that has never caught fire. As a result, the existence of brown dwarfs, long suspected on theoretical grounds, has remained controversial despite several reported detections. But a team of astronomers from the California Institute of Technology reports on page 1478 that they have finally taken the measure of one of these elusive beasts.

Instead of relying on indirect indicators of cool temperature, Benjamin Oppenheimer, Shrinivas Kulkarni, Keith Matthews, and Tadashi Nakajima did the equivalent of finding dew on a steel girder, a sure sign that it is cool. In light from the outer layers of a brown-dwarf candidate called Gl 229B, they found the signature of methane, a compound that has been seen in the chilly atmosphere of Jupiter, but never before in any star. Says atmospheric modeler Takashi Tsuji of the University of Tokyo, "Methane could never be so strong as was observed in Gl 229B unless the temperature is near 1000 kelvin"—compared to 6000 K for the surface of the sun and roughly 2000 K for the coolest brown-dwarf candidates found earlier. There's no arguing about this one, says Adam Burrows of the University of Arizona: "The thing is a brown dwarf."

The detection, say Tsuji and other astronomers, could have wide-ranging implications for theories of how stars form and the structure of stellar and planetary atmospheres. It may also suggest efficient new search strategies for future brown-dwarf hunters. Among other things, it might help them determine whether much of the universe's "missing mass," which seems to influence the motions of galaxies, could be locked away in these obscure objects.

Stellar theory leaves little doubt that brown dwarfs should exist. They are simply the smallest offspring of star formation, which takes place as huge clouds of gas called nebulas coalesce. When a star forms with more than about 8% the mass of the sun—or 80 Jupiter masses—gravity compresses and heats the core of the young star enough to ignite fusion reactions, which can provide energy for billions of years. Below 80 Jupiter masses, a star will still heat up and glow but will do no more than flirt with fusion. After some early signs of life, such a star gradually cools, growing dimmer with time. "The luminosity comes only from the release of gravitational energy" as the gas contracts, says Nakajima.

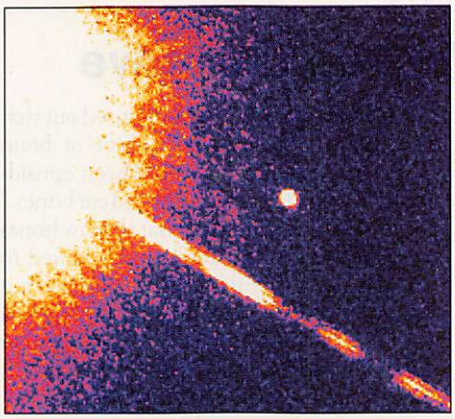

S. KULKARNI, D. GOLIMOWSKI, AND NASA

Dark star. An image from the Space Telescope shows the brown dwarf Gl 229B next to the glare of its companion star.

In trying to confirm this theoretical picture, astronomers have tended to focus on nearby star clusters, searching for especially dim, red members—a strategy designed to ensure that an unusually dim star really is a brown dwarf and not a normal star at a great distance. They have netted a handful of candidates in recent years, many of them in the Pleiades cluster, 400 light-years away. And for one of the dimmest Pleiads, there's an extra piece of evidence that it may be a brown dwarf. In a paper to appear in the *Astrophysical Journal*, Geoff Marcy of San Francisco State University and the University of California, Berkeley, and his Berkeley colleagues Gibor Basri and James Graham report that the object's spectrum bears the signature of lithium—an element that should be consumed by the evanescent fusion reactions in the most massive brown dwarfs, let alone in hydrogen-burning "main sequence" stars.

Still, Marcy notes that the color of this object's light, like that of all of the other potential brown dwarfs detected in the Pleiades, implies a temperature above 2000 K. To some researchers, that puts these candidates uncomfortably close to the smallest and coolest main-sequence stars. Also worrisome is the slight chance that an unmixed "pristine layer" of the material from which a star formed could persist at the object's surface, masking a lithium depletion below, says Saul Rappaport, a theorist at the Massachusetts Institute of Technology.

To get around such objections, the Caltech team, along with Sam Durrance and David Golimowski of Johns Hopkins University, came up with a way to search much closer to home, where they might be able to detect even dimmer and cooler brown dwarf candidates. Instead of relying on clusters of stars to yield candidates at a known distance, they looked for dim companions of nearby stars. Working with the Mount Palomar 60-inch telescope, Durrance and Golimowski designed a stellar coronagraph to block out the bright main star, creating an artificial "eclipse" that would open any cool, dim companion stars to detection. Because the coronagraph used so-called adaptive optics to follow the star's flickering image and maintain a steady eclipse, the method yielded a "very powerful" way to pan for companions, says Kulkarni.

After screening about 100 nearby stars, the team struck pay dirt just 18.6 light-years away from Earth. In October 1994, the coronagraph revealed for the first time a possible dim companion to a known star that moves across the sky. Taking another look this year, "we saw [the object] again," says Kulkarni, "and then we realized, 'Wow, it's the same distance from the star.'" That meant that the two objects must be companions, separated by something like the distance between the sun and Pluto.

First spotted at near-infrared wavelengths, as the team reports in yesterday's *Nature*, the companion is so cool that it emits 100,000 times less radiation than the sun and can't be seen at all in visible light, at least with Earth-based telescopes. Working with Chris Burrows of the Space Telescope Science Institute, however, the team has made images with the Hubble Space Telescope that do show its dim red glow. And with the Palomar 200-inch telescope, the team was able to collect enough near-infrared radiation to form a spectrum.

When that spectrum was paired with Jupiter's at a conference on cool stars in Florence, Italy, in October, says James Liebert of the University of Arizona, "there was an audible gasp" as the audience recognized the

signature of methane. Adds Liebert, who chaired the session, "The methane spectrum proves beyond a shadow of a doubt that this object is way below the mass of a [main-sequence] star."

Yet it's not a planet, say researchers. The older and smaller a brown dwarf is, the dimmer its light. By assuming that the age estimated for the main star also applies to the smaller companion, Oppenheimer and his colleagues were able to come up with an estimate of its mass: at least 20 times that of Jupiter. At that size, says Peter Bodenheimer of Lick Observatory at the University of California, Santa Cruz, "it's extremely unlikely that it formed in a planet mode"—as a rock and ice core that grew as it swept up gases from a protoplanetary disk around the main star. Such a process is thought to be self-limiting: By the time the planet reaches a size somewhat larger than Jupiter, it has swept out a big enough gap in the disk to shut down the growth process.

Bodenheimer says the object is more likely to have formed as a star does, at the center of a collapsing nebula. Either a fragment of the main stellar nebula or a new nebula spawned when a gravitational instability ripped away part of the circumstellar disk could have given birth to it, he says. Such possibilities should give theorists who model star formation plenty of work as they try to reproduce the object's mass and orbit around the companion star.

The detection of methane, along with other features of the spectrum such as a hint of water, should also provide a new reality test for theorists trying to explain the structure and composition of atmospheres in objects as different as Jupiter and brown dwarfs. And for brown-dwarf hunters, Kulkarni says, the methane could mean an end to having to limit their searches to companion stars or dim members of clusters; instead, they can simply screen dim objects for the gas's signature.

But unless such searches boost the brown dwarf population dramatically, everyone agrees that they won't account for the universe's dark matter. "We looked at 100 stars and we found one interesting guy," says Kulkarni. "That doesn't add much to the dark-matter problem."

–James Glanz

PALEONTOLOGY

Why Mammal Ears Went on the Move

The mark of a mammal is a migrating ear. About 160 million years ago, a chain of small bones that formed the hinge attaching jaw and skull in mammal ancestors moved back along the skull. The journey spanned just a few centimeters, but it sets true mammals apart from every other vertebrate. Freed of their hinge function, these bones teamed up with the inner ear to form a delicate sound-amplifying system known as the modern middle ear, and no nonmammal has it. Yet researchers have not been sure why this unique trip took place.

At last month's meeting of the Society of Vertebrate Paleontology in Pittsburgh, however, Timothy Rowe of the University of Texas, Austin, argued that bigger brains made these jaw bones jump. Based on the skull anatomy of mammal ancestors, Rowe reported that the migration of the ears coincided with the emergence of the neocortex and a prolonged period of brain growth. In a process replayed in the development of living mammals, he said, these bones were torn away from the jaw by the skull as it expanded to hold the bigger brain, freeing them to become optimized for hearing.

His colleagues seemed taken by the idea. "That was a fantastic talk," says Zhexi Luo, a biologist at the College of Charleston in South Carolina who studies ear evolution. "Rowe pointed out that detachment is a secondary effect of brain evolution. In the past it's only been considered in terms of jaw and associated ear bones." Researchers had theorized that the jaw bones in question were already being modified to enhance their role in hearing, he says, but the brain change helps explain the actual move. Says paleontologist William Clemens of the University of California, Berkeley: "It comes together as a neat hypothesis."

Ear migration actually occurs in every developing mammal. Three tiny pieces of bone begin developing along the lower jaw soon after conception. After several weeks, however, they are torn loose from their moorings and resettle at the entrance to the inner ear. One piece becomes the incus, or anvil, another becomes the malleus, or hammer, and the third becomes a bony ring called the ectotympanic, which holds the eardrum. Sound waves strike the eardrum, and the vibrations are then transmitted along the other bones to the inner ear.

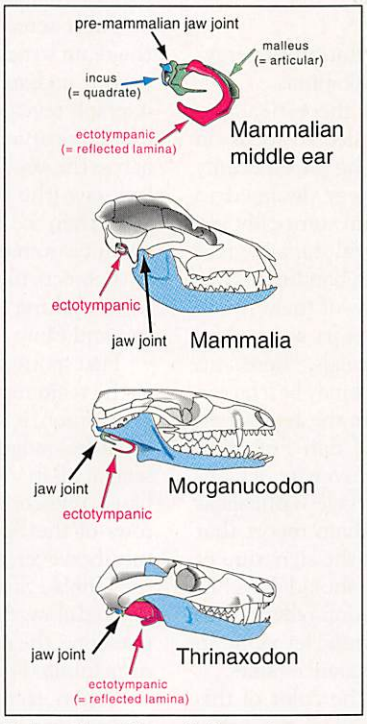

Relocation. The middle ear began as part of the jaw in mammal ancestors such as *Thrinaxodon* and gradually traveled back on the skull.

Researchers, notably Edgar Allin of Midwestern University in Chicago, have argued that in evolutionary terms, this transformation began in mammal ancestors known as synapsids. Over 200 million years ago, synapsids began shrinking, going from dog-sized to shrew-sized, becoming nocturnal, and adopting a diet of insects. Allin noted that the smaller jaw bones, called auditory ossicles, already formed a chain that contacted the inner ear as well as the jaw joint. These bones were shrinking and becoming lighter as well, and Allin suggested they had begun to do double duty: picking up higher frequency sounds made by insects as well as hinging the jaw.

The question, says Rowe, is why they didn't go on bridging the gap between jaw and inner ear. The answer, he says, is that they could no longer reach. Rowe's examination of the skulls of mammal precursors revealed marks of a burgeoning neocortex. By the time of the first true mammals, this new structure had nearly doubled brain volume. This bigger brain, he suggests, keeps growing after the ossicles have stopped. Rowe's CT scans of a developing *Monodelphis*, a primitive, opossumlike mammal, show the auditory ossicles reach their maximum size 3 weeks after conception. But the brain and skull keep growing for another 9 weeks. The expanding arc between the jaw joint and the inner ear tears the ossicles away from the jaw, carrying them backward.

Allin agrees that brain growth in early mammals could have triggered the migration, although he emphasizes that his scenario is a prerequisite: First, the ossicles had to have become specialized for hearing, or in the tug of war between jaw and ear, evolutionary pressure would have kept them with the jaw joint. Removal from the jaw was a further sign of this evolutionary selection for hearing ability—it's hard to hear when you're chewing. Rowe and Clemens agree. "You could have a series of stepwise interactions between development and selection," Clemens says. The next step for understanding mammals, the paleontologists say, is to figure out what drove the development of the brain.

–Joshua Fischman

NEUROSCIENCE MEETING

Brain Researchers Speak a Common Language

SAN DIEGO—This year's 25th annual meeting of the Society for Neuroscience was the largest ever, as nearly 23,000 neuroscientists crowded into the convention center here to sample more than 12,000 talks and poster presentations. Just one of the countless areas covered at this year's meeting was how the brain processes language. Imaging studies of the human brain, as well as studies of songbirds, whose learning of song has some parallels with our learning of language, are shedding light on this uniquely human trait.

Vive la Différence

Anyone who has tried to master a second language in adult life knows the mental effort it takes. Struggling adult learners may envy those who became fluent in a second language while they were still young. But at the San Diego meeting, neuropsychologist Brenda Milner of McGill University in Montreal reported evidence suggesting that even people who have been fluent speakers of a second language since childhood still use a little extra brain power to speak their nonnative tongue. The result has piqued the interest of neuroscientists because the apparent site of that extra brain power is a deep brain region called the putamen, an area not previously thought to play a special role in the memory of learned language.

Milner and postdoc Denise Klein made the discovery while studying how language tasks activate various regions of the brain. Because they work in the predominantly French-speaking province of Quebec, it seemed natural to add an extra twist to their experimental design and compare the brain activation patterns generated in bilingual individuals speaking French with those generated while they were speaking English.

As subjects for their study, Klein and Milner chose native English speakers who had learned French when they were about 7 years old and spoke both languages fluently and daily. The researchers imaged the subjects' brains with positron emission tomography, which measures cerebral blood flow (an indicator of brain activation), while they were doing one of several spoken tasks that included repeating a French or English word or speaking its synonym in the same language, and translating words from English to French and vice versa.

When the researchers compared the brain activation patterns of subjects performing the tasks in English versus French, they found equivalent activation in all brain areas, with one striking exception. "Whenever the [spoken] response was in French, we saw the left putamen lighting up," says Milner. The putamen was silent, however, when the subjects answered in their native English. The fact that the putamen was activated when the subjects were speaking French suggests, Milner says, that even though these people are fluent, "there is some sort of extra control of articulation" required for them to speak their second language.

This was a bit of a surprise, because the putamen had not previously been linked to language learning. It is part of the basal ganglia, a collection of brain structures sitting underneath the cortex in the front of the brain, whose main role was thought to be the production of rote movements.

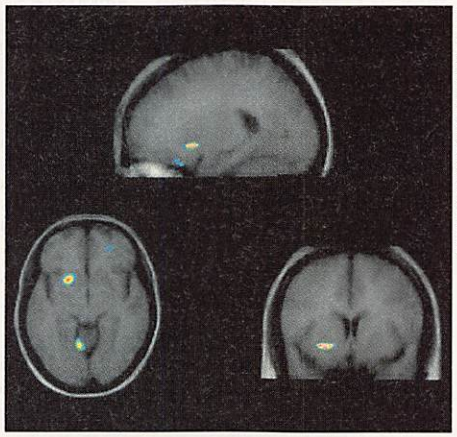

BRENDA MILNER/MCGILL UNIVERSITY

Non-native. In these three brain views, the putamen is activated differentially when a native English speaker speaks French.

Still, Milner and Klein's result does fit with recent work suggesting that the brain area may have a role in the learning and memory of tasks involving movement, says Ann Graybiel, a neurobiologist who studies the basal ganglia at the Massachusetts Institute of Technology: "If we interpret [Milner and Klein's result] in a straightforward way, then it seems that something you have had to put your mind to, to learn, has a special trace in the basal ganglia, reflective of a role of basal ganglia in learning and memory." The finding is also consistent with other evidence that learning and memory are distributed in many brain regions rather than being isolated in specific structures.

Milner plans to follow up the finding, first of all by making sure that it is not specific to English speakers who have learned French. She intends to do the reverse experiment with native French speakers who learned English at an early age and also hopes to check the effects on the brain of learning other languages that are even more different from English, such as Chinese. If those findings support the first results, then late language learners can find solace in knowing that even facile multilinguists who learned their second language at an early age need an extra boost from their putamens.

Baby Sparrows Thrive on Word Salad

To understand the human brain, neuroscientists often turn to the brains of mammals, such as rats or monkeys. Language, however, is a uniquely human trait, into which rats or monkeys provide little insight. But our more distant relatives, the songbirds, do have something akin to language: For their mating songs, they learn a complex vocabulary of whistles, buzzes, and trills. Some researchers believe the way their brains do this may provide insights into how our brains learn language. Those researchers will take heart from new results presented in San Diego by Carol Whaling, a postdoc with behavioral neurobiologist Peter Marler at the University of California (UC), Davis, and neurophysiologists Allison Doupe and Michele Solis of UC San Francisco.

The group found that baby birds distinguish the song of their species by responding to individual sounds making up the song. That process seems to parallel the one seen in human infants, who recognize individual vowels and consonants common in their language before they learn words, phrases, and sentences. And it's reflected in a change in the selectivity of the birds' neurons—a change that suggests parallels with how human infants learn language.

Until recently, most bird-song research has focused on exploring the neuronal changes that occur as adolescent birds learn to sing. That work has shown that, while the learning is going on, neurons in the brain's song-production center, known as HVC, show increasingly selective responses to song. Early in learning, individual neurons respond to multisyllabic phrases of song from any bird of the same species, even if these phrases are presented out of order. Later the neurons become more specific, requiring the song to be in the right order, ignoring most species members and responding best to the bird's own song or that of its tutor. Finally the HVC neurons respond only to the bird's own song.

Whaling and her colleagues, however, decided to take a close look at the HVC neurons in naive baby birds, to see how much

selectivity these neurons start out with. Because baby birds have an innate ability to recognize their own species' song, some researchers suspected that the neurons might be innately programmed to recognize whole multisyllabic sequences of that song.

The new work shows that isn't quite the case. The team found that both baby birds and their neurons start with a more general kind of selectivity for the individual words or syllables of which that song is made. This, says Doupe, is reminiscent of what University of Washington psycholinguist Patricia Kuhl has shown to occur in human babies, who recognize the vowel and consonant sounds of their language before they learn words.

The team came to this conclusion by first playing parts of white crowned sparrow song, as well as parts of the songs of other sparrow species, to baby white crowned sparrows that had never before heard song. As previously shown in Marler's lab, baby birds peep when they hear their species' song, and the researchers found that the baby sparrows responded not just to the complete song of their species, but to individual whistles, buzzes, and trills, played forward or backward or jumbled together in random ways.

When the group recorded the activity of the birds' HVC neurons, they found that they parallel the birds' behavior, responding to syllables rather than multisyllabic phrases. Some neurons specialized in recognizing whistles; others liked buzzes or trills, either played forward or backward. "These neurons are all tuned to individual features of a song," says Whaling.

Now, says UCSF's Doupe, "we can go in and find what's changing neurally" as a bird learns to sing and its HVC neurons go "from initially responding to all species syllables backward and forward, later to syllables, but only forward, and finally only to the right syllables in the right order." That's an exciting prospect, says bird-song researcher Daniel Margoliash of the University of Chicago: "It allows us in very quantitative terms to explore this issue of innate versus environmental [learned] influences ... and how it interacts with the [neurological] process that eventually results in the adult song." And it might just shed some light on how language transforms our own brains.

Stuttering Comes Into Focus

To an onlooker, a stutterer struggling to get out a sentence appears to be having trouble with the motor control of his lips and tongue. And in fact that has been what some neurobiologists who study stuttering have suspected. But a new brain imaging study implies that movement control is unlikely to be the whole stuttering story. The results, reported in San Diego, suggest that the origins of stuttering may lie deep in multiple language centers of the brain.

Performed by Peter Fox of the University of Texas Health Science Center in San Antonio, Roger Ingham of the University of California, Santa Barbara, and their colleagues, the study doesn't pin down a single cause in the brain; researchers who have linked stuttering to defects in motor control, auditory feedback, and overall language development will all find support in the group's findings. But the work does suggest that brain imaging could eventually bring stuttering into sharper focus, and may even help illuminate which interventions, if any, can reduce stuttering by making stutterers' brains more normal.

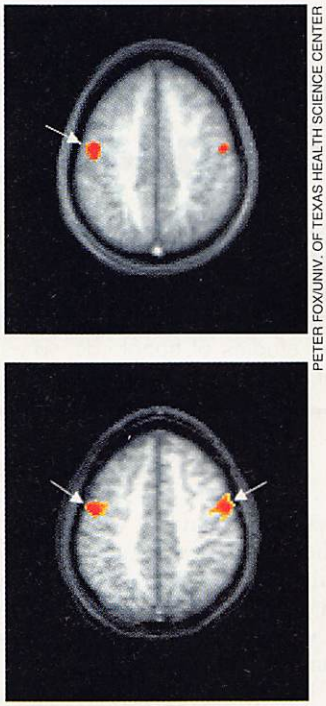

PETER FOX/UNIV. OF TEXAS HEALTH SCIENCE CENTER

Skewed. The motor cortex activation in a stutterer's brain *(bottom)* lacks the left dominance seen in normal controls *(top)*.

The team used positron emission tomography scanning to compare the overall brain activation of 10 normal right-handed men to that of 10 right-handed male stutterers. Each subject was scanned while reading a paragraph aloud on his own, and again while reading aloud in unison with a recording. That condition, called "chorus reading," is known to suppress stuttering, and did so in the stutterer subjects.

The researchers found significant differences between activation levels in the brains of stutterers and normal subjects during solo reading. In normal right-handed men, brain activation was higher on the left side of the brain than on the right in the areas that control the movements necessary for speech, and also in the auditory areas that process incoming language information. That makes sense, as language is normally controlled almost exclusively from the left half of the brain. But the stutterers were far less left-dominant; activation in their brains was shifted toward the right in both the motor and auditory language areas, revealing an inherent difference in the way the two groups process language.

And that difference persisted, even during chorus reading, when the men weren't stuttering, suggesting that it reflects a fundamental difference in brain organization. During chorus reading the differences in the motor areas were less pronounced, but didn't go away. And in the auditory areas the difference between the stutterers and normal subjects was the same during chorus and solo reading: The stutterers' left auditory speech areas were nearly silent, while those of the controls were highly active.

The chorus reading results point to what might be a key flaw in handling auditory information. During chorus reading, the stutterers, like the controls, showed activation of their right auditory cortex in response to the recorded reading, which was piped into their left ears. But the lack of response in the left auditory region suggests, says Fox, that "they're not moving [the information] over to the left hemisphere," where speech-related auditory processing normally occurs.

Taken together, Fox says, the findings support three different theories of stuttering. The exaggerated brain activation in the stutterers' right motor control areas agrees with the idea that stuttering is a motor problem, while the silence of the left auditory language area supports a second theory that stutterers don't get proper auditory feedback when they are speaking. A third theory, that the stuttering arises from the failure of the brain to develop normal left-hemisphere dominance for language, is bolstered by the general shift of language activity away from the left hemisphere in stutterers' brains. And that, says speech pathologist Christy Ludlow, of the National Institute on Deafness and Other Communication Disorders (NIDCD), is the most striking result of all, because it occurs in all of the language areas studied, making the last theory the winner in her view.

Ludlow and her NIDCD colleague Allan Braun have unpublished findings that are similar to Fox and Ingham's. She and Braun found that when stutterers speak, "the left-hemisphere language areas seem to be reduced in activation compared to normals," even if stuttering is suppressed. That, she adds, means "that we can't look on [stuttering] simply as a motor-control disorder, that it has much more to do with the system interface between language and speech."

Will this idea bring new treatments for stuttering? Not directly, says Ludlow. But if stuttering results from a general flaw in language development, that lends support to a new view that speech therapy should begin as soon as a child shows signs of stuttering or other lack of fluency, often as early as age 4. Treating the problem early, when the language system is still malleable, should offer the best chance of actually influencing language development.

–Marcia Barinaga

PHYSICS

Measurements Are the Only Reality, Say Quantum Tests

Hamlet would run a few lines short in a quantum-mechanical theater, where "to be or not to be" is not the question at all. The usual interpretation of quantum mechanics holds that a physical quantity—such as an electron's position or a photon's polarization direction—has no reality, or "being," until an experimenter measures its value. "To measure or not to measure," that is the question.

That script didn't sit well with Einstein, who insisted that unmeasured quantities must exist in some definite state, even though we might not know what that state is. And Einstein's view "makes so much common sense," says Anton Zeilinger of the University of Innsbruck, that even now, some physicists hold out for it. They pin their hopes on the absence of a clear-cut experimental contradiction of Einstein's attempt to inject common sense into quantum mechanics. But two new experiments are coming closer than ever before to showing that quantum "reality" is every bit as bizarre as Einstein feared.

One experiment, led by Leonard Mandel at the University of Rochester in New York, has provided the most intuitively direct test yet of the "local realism" hypothesis put forth by Einstein, Boris Podolsky, and Nathan Rosen (EPR) in 1935. Einstein and his colleagues argued that physical quantities whose value can be predicted with certainty before they are measured must have an "element of reality." By creating photons with polarizations that are correlated—making one photon predictable once another is measured—the Rochester group has trapped EPR in a contradiction. They showed that if the polarizations have any reality apart from the properties that are directly measured, the observed correlations imply yet another correlation—one that is never, ever observed. "The weirdness of quantum mechanics jumps out at you" in the work, says Paul Kwiat of Los Alamos National Laboratory.

Another new experiment, led by Zeilinger, is less intuitively comprehensible but demonstrates the strongest violation of local realism ever, in mathematical terms. Neither experiment closes all loopholes, however. "A devoted advocate of the EPR world view can squirm through," says Michael Horne of Stonehill College in North Easton, Massachusetts, because the detectors capture only a small and possibly unrepresentative fraction of the photons. But several planned experiments, designed to build on the new results, could soon close the loopholes once and for all.

JAMES MONTANUS/ UNIV. OF ROCHESTER

Quantum interrogator. Rochester's David Branning at a laser table used to probe the nature of quantum reality.

These disagreements over the nature of existence date back to the titanic debates between Einstein and physicist Niels Bohr in the 1930s. By then, the majority school of thought, led by Bohr, had concluded that unmeasured physical quantities have only a "potential" existence, with their ranges of possible values described by a haze of probability that drifts about according to the equations of quantum mechanics. Only when a measurement is made does this "wavefunction" collapse to just one value.

The EPR paper was meant to discredit this scenario by showing what strange situations it could lead to, as when two particles fly apart in such a way that their total momentum must add up to zero. In quantum mechanics, such particles are said to be "entangled." If the momentum of each individual particle has no reality before it's measured, then measuring one particle's momentum must instantly collapse the other's wavefunction down to the equal and opposite value, no matter how far apart the particles have traveled. Somehow, a distant particle instantly "knows" what value to adopt.

More reasonable than that bizarre picture, Einstein thought, was the idea that the particles had opposite, although perhaps unknown, values from the moment they flew apart. But tests of this proposal stayed in the realm of philosophical Gedanken experiments for decades, both because practical tests didn't exist and "we inherited from the '30s the feeling that ordinary physicists should keep out [of the debate] or they'll get stung," says Daniel Greenberger of the City College of New York.

Then in the mid-1960s physicist John Bell of CERN, the European particle physics laboratory in Geneva, "took everybody by surprise," says Greenberger, by formulating a method of testing local realism experimentally. Bell's test relied on two particles with entangled "spins"—a quantum concept somewhat analogous to a planet's rotation. In a difficult, abstract argument, Bell showed that if the spins had objective, although unknown, angles from the moment they flew apart, then later measurements of the two angles would show weaker correlations than quantum mechanics predicts.

Early experiments based on Bell's proposal, using photon polarizations instead of particle spins, seemed to support orthodox quantum mechanics. But inefficiencies in the apparatus meant that only a tiny fraction of the available light could be captured, and Bell's argument—although agreed to be correct—is involved enough that "the first couple times through [it] ... you wonder if somewhere the rabbit has gone into the hat," says Los Alamos's Kwiat. Since then, experimental physicists have developed better methods for producing entangled photons and more efficient detectors. And, in 1992, theorists came up with a more direct and vivid test of local re-

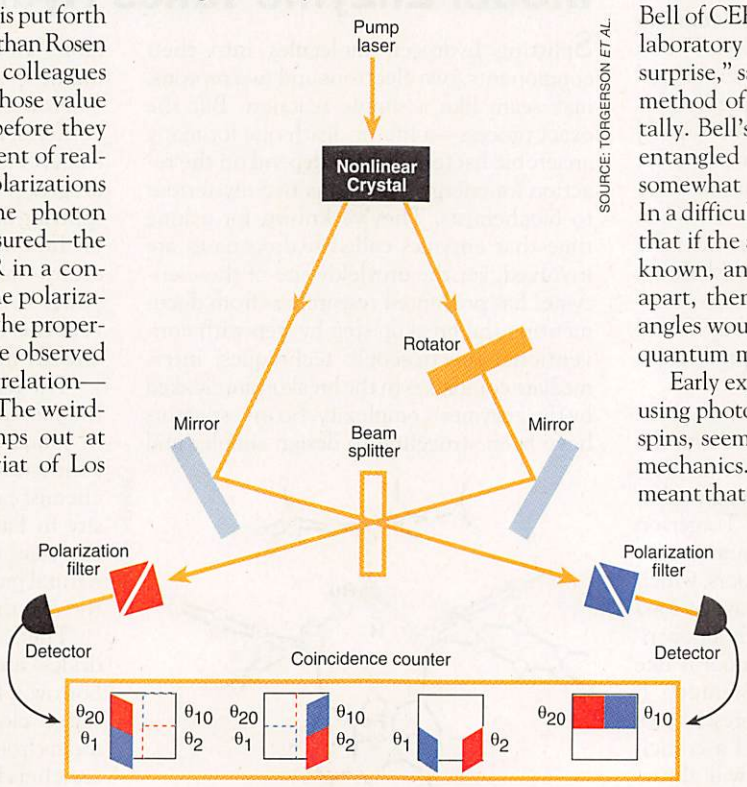

SOURCE: TORGERSON *ET AL.*

A trap for local realism. Two photons with different polarizations are mixed at a beam splitter, entangling them. Correlated photon detections (open doors) at different settings of the two polarization filters *(colors)* predict yet another correlation that is not observed (closed doors).

alism. Building on theoretical work by Greenberger, Horne, and Zeilinger, Lucien Hardy at the University of Durham in the United Kingdom constructed a test that, says Kwiat, is "brilliant in terms of being able to explain the whole thing to your grandmother."

That's the scheme that Mandel and his colleagues, Justin Torgerson and David Branning at Rochester and Carlos Monken at the Universidade Federal de Minas Gerais in Brazil, describe in the 28 August issue of *Physics Letters A*. The group sent ultraviolet laser light through a crystal of lithium iodate, a nonlinear material that can split a photon into a longer wavelength pair with identical polarizations. They then passed one photon in an occasional pair through a polarization rotator, which turned its polarization by 90 degrees, then mixed it back together with its mate at a beam splitter—a step that entangled the quantum-mechanical wavefunctions of the rotated and unrotated photons. The result was two photons composed of mixed-up pieces of the original two.

The beam splitter then sent the mixed wavefunctions down two separate arms of the apparatus. At the end of each arm lay an adjustable polarization filter and a light detector. The filter served as a measuring device by letting a photon reach the detector or blocking it, depending on its polarization.

Because each photon is a mixture of two orthogonal polarizations, it can exhibit any polarization when measured. And because the two photons are entangled, their polarization angles have a statistical correlation. When quantum theory is applied to the entangled wavefunctions, it makes specific predictions about how often the two detectors should record photons simultaneously for particular polarizer angles in the setup's two arms. If, for example, detector 1 records a photon when its polarizer is set to 74.3 degrees, then the theory predicts that detector 2 should always record a photon when its polarizer is set to −33.2 degrees. The Rochester group found that these quantum mechanical predictions hold up nicely, says Mandel.

That result doesn't create a serious problem for local-reality holdouts. For them, the real trouble comes when the experimenters look for other pairs of polarizer angles that also yield perfect coincidences. Torgerson and Branning liken the measurements to watching the opening of Dutch doors, which are split in the middle so that trays of food can be served through the top without opening the entire door. "Opening a door is like making a photodetection," says Branning. If the sections of a Dutch door represent two polarizer angles that always yield a coincidence, the top half of the door will always open along with the bottom.

Having found two pairs of polarizer angles corresponding to two doors that must swing open in this way, the researchers started checking the coincidences when one angle was chosen from each door. For certain sets of angles, they found, the bottom halves of both doors sometimes opened together. And here's the rub: The top halves never did. Yet the top and bottom of each door had swung open together in the earlier set of measurements. If the polarizations exist irrespective of measurement, detecting the bottom polarizations in both arms implies that the top polarizations should also be present, unmeasured, in the opposite arms. But in quantum mechanics, which makes no assertion at all about one set of polarizations while others are being measured, there's no contradiction at all.

"These experiments remind us not to fall into [a] comfortable, local-realistic picture," says John Rarity of the Defense Research Agency in the United Kingdom. Rarity and others point out, however, that such work rigorously eliminates local realism only under the "fair sampling" assumption, which takes the photons captured in the still-inefficient detectors to be representative of all photons present. That sends up a red flag to EPR advocates like Augusto Garuccio of the University of Bari in Italy, who collaborated for a time on the Mandel experiment. The fair-sampling assumption, if incorrect, "could be the cause of the claimed violation of the locality," says Garuccio.

That criticism is almost—but not quite—put to rest by a paper in press at *Physical Review Letters* by Kwiat along with Klaus Mattle, Harald Weinfurter, and Zeilinger at Innsbruck, and Alexander Sergienko and Yanhua Shih at the University of Maryland, Baltimore County. Using related techniques in an experiment based on Bell inequalities, these authors have observed the most extreme statistical violation of local realism ever reported. The overall detection efficiency is also the highest on record, and members of this group, along with Philippe Eberhard of the Lawrence Berkeley National Laboratory, believe this may be a step toward a loophole-free experiment within the next few years. And in independent work, Edward Fry of Texas A & M University is now building what he hopes will be a loophole-free experiment based on atomic spins rather than photons.

The success of these experiments may finally prove Einstein's "common sense" view to be wrong. But they won't ease discomfort with quantum mechanics. Einstein "was driven [to his conclusions] because he realized how strange quantum mechanics is," says Zeilinger. Experiments like Zeilinger's insist that the strangeness is a fact of life.

–James Glanz

BIOCHEMISTRY

Model Enzyme Takes Hydrogen Apart

Splitting hydrogen molecules into their components, two electrons and two protons, may seem like a simple reaction. But the exact process—a life-or-death one for many anaerobic bacteria, which depend on the reaction for energy—has remained mysterious to biochemists. They've known for a long time that enzymes called hydrogenases are involved, yet the unwieldy size of these enzymes has prevented researchers from documenting the breakup step by step with conventional spectroscopic techniques; intermediate complexes in the breakup are cloaked by the enzymes' complexity. So investigators have been struggling to design simpler and more easily observable compounds that mimic this hydrogen-splitting ability.

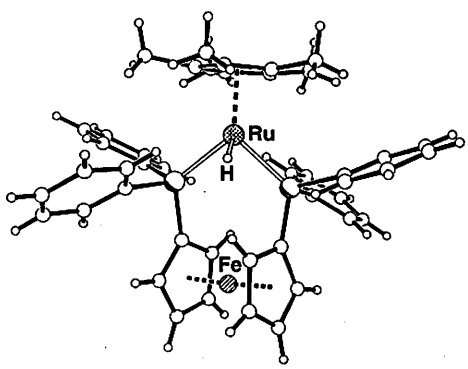

SOURCE: R. HEMBRE

New metal, new model. Substituting ruthenium (Ru) for nickel made this molecule a hydrogenase mimic.

Now a group of researchers from the University of Nebraska, Lincoln, led by chemist Robert Hembre, report creating the first hydrogenase model that performs hydrogen-splitting duties. In addition to shedding light on how the enzymes work, the new molecules may be inexpensive catalysts for power systems, known as fuel cells, that convert the chemical energy in hydrogen gas directly into electricity.

The research, which will be published in the *Journal of the American Chemical Society* in January, is already drawing praise from colleagues. "It's really dynamite work," says chemist James Collman of Stanford University in Palo Alto, California. Even though the new structures are different from the natural protein, "they imitate the function of the real thing," says Collman.

The compounds, known as metal hydrides, are such good mimics because they borrow a key element from hydrogenase itself: a closely knit pair of electron-hungry atoms from a so-called transition metal. Researchers have long thought that an atom of nickel, a transition metal that's part of the hydrogenase molecule, steals electrons from hydrogen. But hydrogenases also carry an iron atom located near the nickel, which

may also play a role in the theft. So researchers have been trying to make model compounds with both nickel and iron, but the task is "extremely difficult," says Hembre. The reason, in part, is that nickel and iron have similar chemical reactivities, causing them to form clusters during synthesis and yield a variety of different compounds.

So Hembre and his colleagues J. Scott McQueen and Victor Day opted to use ruthenium, another transition metal, instead of nickel, because its chemical reactivity differs from that of iron. To better control the synthesis, they made their ruthenium-iron model compound by attaching each transition-metal atom to ring-shaped groups known as cyclopentadienes. These groups help stabilize the reactivity of the transition metals, making them easier to bring together. And because these models only have a pair of transition-metal atoms, while hydrogenase has many, it's much easier for researchers to use electrochemistry and spectroscopy to track changes in electronic behavior: The signal doesn't get lost in the noise.

First, the researchers determined how closely the models mimic hydrogenase. When placed in solution with hydrogen, both the enzymes and the new models grab electrons from H_2 and parcel them out one at a time to electron acceptors, such as methyl viologen, causing the viologens to change color from yellow to bright blue. The researchers were then able to get a closer look at the process using electrochemistry and nuclear magnetic resonance spectroscopy. The studies show that H_2 releases a proton after it binds to ruthenium. Next, the metal steals H_2's electron pair, and finally the remaining proton falls away.

"The final question is, does the real thing work that way?" asks Collman. To find the answer, Hembre and his colleagues are currently working to create new model compounds that contain nickel and iron in the core, hoping to see those compounds split H_2 in the same fashion as the real protein. They hope the stabilizing effects of the cyclopentadiene groups will make this synthesis easier.

Even if the strategy fails, some ruthenium-based compounds themselves may still prove useful. The hydrogen-splitting reaction is crucial in some fuel cells, which power things such as hospital generators. The cells strip the electrons from hydrogen to generate an electric current. At present, however, fuel cells typically perform this reaction with the help of a costly, but efficient, platinum catalyst. If Hembre's compounds based on ruthenium—a much less expensive metal—convert hydrogen to electricity just as efficiently, their relatively low cost may make these model compounds part of a model power source.

–Robert F. Service

MEETING BRIEFS

Geoscientists Contemplate a Fatal Belch and a Living Ocean

NEW ORLEANS—Paleontologists may deal with dusty fossils, but they also ponder some of the planet's greatest catastrophes. At last month's annual meeting of the Geological Society of America in New Orleans, one eye-opening presentation argued that the extinctions at the end of Permian period might have been triggered by a belch of deep-sea carbon dioxide. Another suggested that the scope of the Cretaceous-Tertiary catastrophe at the end of the age of the dinosaurs needs to be scaled back, at least in the oceans.

Another Killer Charged With Mass Extinction

No wonder life took a beating—its worst ever—250 million years ago at the end of the Permian period. Just months ago, researchers determined that the largest known volcanic eruption on land took place in present-day Siberia at the same geological moment as the extinctions, which wiped out 90% of all genera in the oceans. Now they've stumbled on evidence of another assault—a sudden surge of carbon dioxide from the deep sea that allegedly poisoned marine life.

Paleontologists studying the extinctions don't yet know how much to blame the eruptions or the gas belch—assuming it happened. And researchers in other fields aren't fully convinced by the scenario that paleontologists Andrew Knoll of Harvard University and Richard Bambach of Virginia Polytechnic Institute and State University and sedimentologist John Grotzinger of the Massachusetts Institute of Technology (MIT) have sketched out as the driving force behind their postulated carbon dioxide surge. But the idea, and the circumstantial evidence that Knoll and his colleagues are marshaling, is capturing imaginations. "It isn't as yet backed up by a tremendous amount of data," says paleontologist Douglas Erwin of the National Museum of Natural History, a leader in studies of the extinction, but "I think it's an interesting, even fascinating, hypothesis."

Knoll and his colleagues were drawn into the fray when a paleontologist colleague showed a slide of a layered rock from late in the Permian. The paleontologist assumed it was a fossil stromatolite, a mound of sediments glued together by primitive blue-green algae. But Knoll and Grotzinger immediately recognized it as an inorganic carbonate precipitate, a rock type that rarely formed in the past 500 million years but was common in earlier times. Carbonates are usually formed from the remains of once-living animals, but during five cycles of glaciation in the late Precambrian between 600 million and 800 million years ago, carbonates precipitated directly from seawater without any help from living things, presumably when the concentration of dissolved carbonate—that is, dissolved carbon dioxide—became exceedingly high. As it turned out, these anomalous carbonates are also relatively common at the time of the mass extinction, and Knoll and Grotzinger saw them as a sign of climate and geochemistry gone awry.

DOUGLAS ERWIN/NMNH

Trace of a killer? Did the high seawater carbon dioxide that precipitated this carbonate also trigger a mass extinction?

The ultimate cause, they propose, was a shutdown in the circulation of the deep ocean. Toward the end of the Permian, all the continents were huddled in a single supercontinent, Pangaea. That would have left a globe-girdling ocean with some narrow seas within the supercontinent. With no continental ice sheets to chill surface waters and send them diving into the deep sea, as they do today around Antarctica, the group argues, deep waters grew sluggish and even stagnant. As phytoplankton in surface waters continued to extract carbon dioxide from the atmosphere, converting it to organic matter that sank and oxidized to carbon dioxide, the deep sea's carbon dioxide content would have soared.

The deep ocean's gain was the atmosphere's loss, according to the Harvard-MIT scenario. As the "biological pump" of phytoplankton kept driving atmospheric carbon

dioxide into deeper waters, the greenhouse effect weakened, sending Earth into a new ice age. Glaciation, in turn, would eventually have reinvigorated the circulation of the deep sea, churning the carbon dioxide–laden waters to the surface in an event something like the disastrous turnover of Lake Nyos in 1986 in Cameroon (*Science*, 1 April 1994, p. 26). The influx of carbon dioxide to shallow Permian waters could have precipitated the anomalous carbonates. And it could also have triggered the mass extinction by poisoning or smothering organisms in surface waters, where most marine species live.

Aside from the anomalous carbonates, Knoll and his colleagues point to other evidence supporting their scenario. Geologists have recently recognized signs of glaciation in the late Permian in northern Siberia. And the isotopic composition of the carbon locked in some of the carbonates hints at an oceanic turnover, say Knoll and his colleagues. Fluctuations in the ratio of heavy and light carbon isotopes imply that carbon was first stashed away in deep water, then swept up into the shallows.

The hand of carbon dioxide can also be recognized in the pattern of extinction at the end of the Permian, the group says. Those marine organisms that were already tolerant of higher concentrations of carbon dioxide—because their higher metabolic rates produced the gas in abundance or because they were accustomed to burrowing into bottom sediments, where carbon dioxide would accumulate—did relatively well in the mass extinction, losing less than 50% of their genera. But organisms having lower metabolic rates, like corals, or those that would have difficulty forming carbonate skeletons when high carbon dioxide levels boosted the acidity of ocean waters, like planktonic foraminifera, suffered greatly, losing 80% to 100% of their genera.

It will take more than circumstantial evidence to convince paleontologists like Erwin, however. "What we need is a much more precise idea of exactly when the extinctions occurred and how rapidly they occurred," he says. That would help distinguish the oceanic kill mechanism, which would have operated in the few million years leading up to the end of the Permian, from the effect of the eruption, which began only at the end of the Permian and was over within a million years or so (*Science*, 6 October, p. 27). Experts in other fields encompassed by the hypothesis also have their doubts. Says Steven D'Hondt of the University of Rhode Island, a paleoceanographer who heard Knoll's talk: "I have a hard time believing the ocean can be stagnant long enough or can hold enough carbon dioxide to do what I think he needs it to do."

But Knoll is optimistic for now: The death-by-carbon dioxide scenario "can stand or fall on things you can actually observe by careful field work. The best part of this it that it suggests about 10 years' worth of further research."

A Strangelove Ocean Comes Back to Life

The more researchers have speculated about conditions on Earth after a huge meteorite smashed into the Yucatán Peninsula 65 million years ago, the grimmer they have looked. Some proposed that debris hurled into space would have became red-hot as it re-entered the atmosphere, turning the surface into an oven for hours. Others said that the heat would have given way to months of cold as dust hurled into the stratosphere by the impact's blast shut out the sun. Acid rain, tidal waves, and global forest fires have all been included in the litany of destruction. But now one element of the scenario is actually looking less dire. Reports of the ocean's death, it seems, have been much exaggerated.

Geochemists analyzing microfossils from sea-floor muds had thought they saw evidence that the ocean was nearly devoid of life for tens of thousands of years after the impact—a Strangelove ocean, it was called, after the fictional movie character who builds a doomsday machine. Now Steven D'Hondt of the University of Rhode Island (URI) and his colleagues have traced the Strangelove signal a full 2 million years in a core of sediment from the southeastern South Atlantic. That's far too long for the ocean to have remained sterile, says D'Hondt, even in the direst scenarios. For all that time, he thinks, the ocean was not dead, only disturbed. "There's no reason to hypothesize a Strangelove ocean," he says. "The data don't require it."

D'Hondt and URI colleagues Danielle Luttenberg and Percy Donaghay monitored the ocean after the impact by analyzing the difference between the carbon isotopic compositions of surface and deep waters. In a normal, healthy ocean like today's, the carbonate dissolved in deep waters has more of the lighter isotope of carbon—carbon-12—than the heavier carbon-13. This difference is sustained by the so-called biological pump. Phytoplankton in surface waters preferentially extract the lighter carbon from carbon dioxide dissolved in seawater and incorporate it into their organic matter. When the plankton die, the carbon-12–rich organic matter can settle into the deep sea where it returns to dissolved carbon dioxide.

For an ancient ocean, these ratios have to be inferred by analyzing the carbonate fossils of microscopic animals that lived at shallow depths, forming their skeletons exclusively from surface-water carbonate, or those that lived on the ocean floor, drawing on deep waters. Earlier researchers had found that the isotope difference between surface and deep waters nearly vanished at the time of the impact and did not recover for tens of thousands of years. Together with the fossil evidence that nearly 50% of marine species went extinct at the Cretaceous-Tertiary boundary, the shift seemed to signal the worst sort of catastrophe, in which the oceans themselves became nearly lifeless under a pall of dust. In the mid-1980s, Kenneth Hsü of the Swiss Federal Institute of Technology in Zurich dubbed this bleak period the Strangelove ocean. Hsü imagined it lasting at most a few thousand years, says D'Hondt, but longer isotopic records deciphered later seemed to stretch it to 50,000 years and then to 500,000 years.

But now that the URI analysis extends the reduced carbon isotopic gradient to 2 million years, D'Hondt doesn't think a Strangelove ocean could be responsible. There's no plausible way to depress biological productivity for that long, he says. A Strangelove ocean, he says, "is okay as long as darkness persists following the impact, but once light returns, if you have any phytoplankton out there at all, it should be extraordinarily abundant very rapidly." Unconstrained phytoplankton populations can double once or twice a day, he notes, and he argues that nothing about the impact, including the acid rain it produced, could have held back the phytoplankton for more than a few decades.

Rather than invoking a dead ocean, D'Hondt and his colleagues explain the prolonged isotopic shift as a result of an ecological change due to the extinction of larger organisms. The amount of organic matter reaching the deep sea depends not only on phytoplankton productivity but also on how efficiently that organic matter is transported down from the surface. Large chunks sink fastest and are the least likely to be broken down in surface waters. As a result, the extinction of most larger phytoplankton as well as animals of all sizes, which package organic matter into pellets of feces as well as dead tissues, could have short-circuited the supply of isotopically light carbon to the deep sea, says D'Hondt. After a few million years, however, evolution reconstructed an efficient web of plankton grazers, and the system recovered.

The URI analysis "is moving in the right direction," says paleoceanographer James Zachos of the University of California, Santa Cruz. To test it, though, "we need some way to see what's happening higher in the food chain." Therein lies a challenge for paleontologists: Larger zooplankton leave no fossil record, and fossil fish are few and far between. Now that the Strangelove ocean has been pronounced alive, the problem is gauging the state of its health.

–Richard A. Kerr

edited by CONSTANCE HOLDEN

Substitute for Shock Therapy?

For serious, drug-resistant cases of depression, electroconvulsive therapy (ECT) has been the only effective treatment. But ECT entails general anesthesia, the inducement of seizures, and some memory loss. Now some researchers think there's a potential alternative: transcranial magnetic stimulation (TMS).

TMS entails holding a metal coil against a patient's left temple—imaging studies have shown metabolism in the left prefrontal cortex to be low in depressed people—and sending a series of short electromagnetic pulses into the brain. Clinical studies on the technique are just starting to come out. A team headed by psychiatrist Mark George, now at the Medical University of South Carolina in Charleston, reports in the 2 October issue of *Neuroreport* giving daily doses of TMS to 6 patients for a week. One went into "remission," and one showed "significant" but temporary improvement. An unpublished study just completed by neurobiologist Pasqual Leone of the University of Valencia, Spain, involved 17 badly depressed patients. Leone says TMS and a sham procedure were administered in a "crossover" design, using patients as their own controls. TMS alleviated the symptoms in 11 of them, he says, while the sham was ineffective.

"If this turns out to be something that really works, it would be a major advance," says psychiatrist Frank Guerra of the University of Colorado Health Sciences Center. It might also lead psychiatrists to rethink the notion that a generalized brain seizure is essential for ECT to work. Researchers surmise that TMS is changing the chemistry in deep brain structures—just as ECT apparently does—but that because magnetism, unlike electricity, easily passes through body tissues, it can do the job without the need to trigger a seizure.

Some psychiatrists are still skeptical. Longtime ECT researcher Max Fink of the State University of New York, Stony Brook, is not impressed with the George study and says optimism about TMS is at best premature. People have tried both electricity and magnetism throughout this century to try to treat depression without inducing seizures, he says, and it never works. But TMS researchers are optimistic. "Our feeling is that ECT responders will respond to [TMS] and that this could potentially replace ECT," says neurologist Eric Wassermann of the National Institute of Neurological Disorders and Stroke. And the hope is that further research will cast more light on how both ECT and TMS actually work.

Biocontrol for Kiwi Mold

Consumers who delight in the kiwifruit have a serious competitor—a fungus called *Botrytis*, which preys on the fruit while it is in storage. Last year, according to Robert Hill of the Horticulture and Food Research Institute of New Zealand, *Botrytis* destroyed about $10 million of New Zealand's $400 million kiwi crop, and it takes only a slightly lesser toll in dry California. But scientists in New Zealand have now found something that can keep the greedy fungus at bay: a dab of 6-pentyl-alpha-pyrone (6-PAP)—an aromatic extract of another fungus.

After the success of a pilot experiment in which 3000 kiwifruits treated with the extract survived 12 months of refrigerated storage, scientists are monitoring the fate of 26,000 kiwis stored in sites around New Zealand. After 5 months they are still free of *Botrytis*, says Hill. The 6-PAP, which smells like a combination of coconut and celery, apparently acts as a natural fungicide, stopping the *Botrytis* at its entry point: the wound created when the fruit is picked.

6-PAP has waited a long time to be put to work. The active ingredient of a mold called *Trichoderma*, it was isolated in the 1970s by chemist Hank Cutler of the U.S. Department of Agriculture's Agricultural Research Service (ARS), who found that it could destroy other fungi. But according to ARS spokesperson Jim DeQuattro, 6-PAP lay on the shelf until 1991, when kiwifruit orchards in New Zealand were being destroyed by the fungus *Armillaria*. Hill observed that vines harboring *Trichoderma* seemed resistant to *Armillaria*, and he sought out Cutler. The two developed a treatment that proved successful in fighting the fungus.

HANK CUTLER

Storage rot. This doesn't happen when picking wounds are treated with 6-PAP.

Now that 6-PAP is showing promise at protecting kiwis in storage as well as on the vine, it may permit growers to sell the fruit year-round. Growers in the Northern and Southern hemispheres have opposite growing seasons. To break into each others' markets, they would have to provide fruit that could keep its fresh flavor even in long storage, as the 6-PAP–treated kiwis seem to do.

Mark Houston of the California Kiwifruit Commission says he hadn't heard about 6-PAP. But if it is a natural fungicide, he adds, "we're very interested in it. We don't really have anything to fight *Botrytis* right now."

EDWARD WOLFE

Trouble brewing? Mountain's dome and crater during last series of outbursts in February 1991.

Subterranean Rumbling At Mount St. Helens

After 4 years of calm, Mount St. Helens is getting indigestion again. Since the giant eruption in 1980, the mountain has periodically given off explosive bursts of gas, the last of them in 1991. Now a gradual resurgence of tiny earthquakes deep under the volcano is hinting to researchers that the mountain could be on the verge of belching again. The National Forest Service has closed the likely blast zone indefinitely, keeping tourists and scientists out of the crater. Similar explosions at two South American volcanoes have killed 10 volcanologists and tourists in recent years (*Science*, 16 April 1993, p. 289).

Since last January, volcanologists at the U.S. Geological Survey's Cascades Volcano Observatory (CVO) in Vancouver, Washington, have recorded a steady increase in the frequency of small, deep earthquakes—to 100 in September. The crescendo suggests a pressure buildup of gas as magma lingering from the big eruptions of the 1980s continues to crystallize and force gases out of solution, like a warming bottle of soda.

The result could be a gas explosion like the six that ripped the 280-meter-high lava dome within the crater between 1989 and 1991, tossing soccer-ball–size blocks almost a kilometer and sending ash-laden plumes as high as 6 kilometers. Those explosions struck without warning, so, says Daniel Dzurisin, CVO's scientist-

(continued on page 1445)

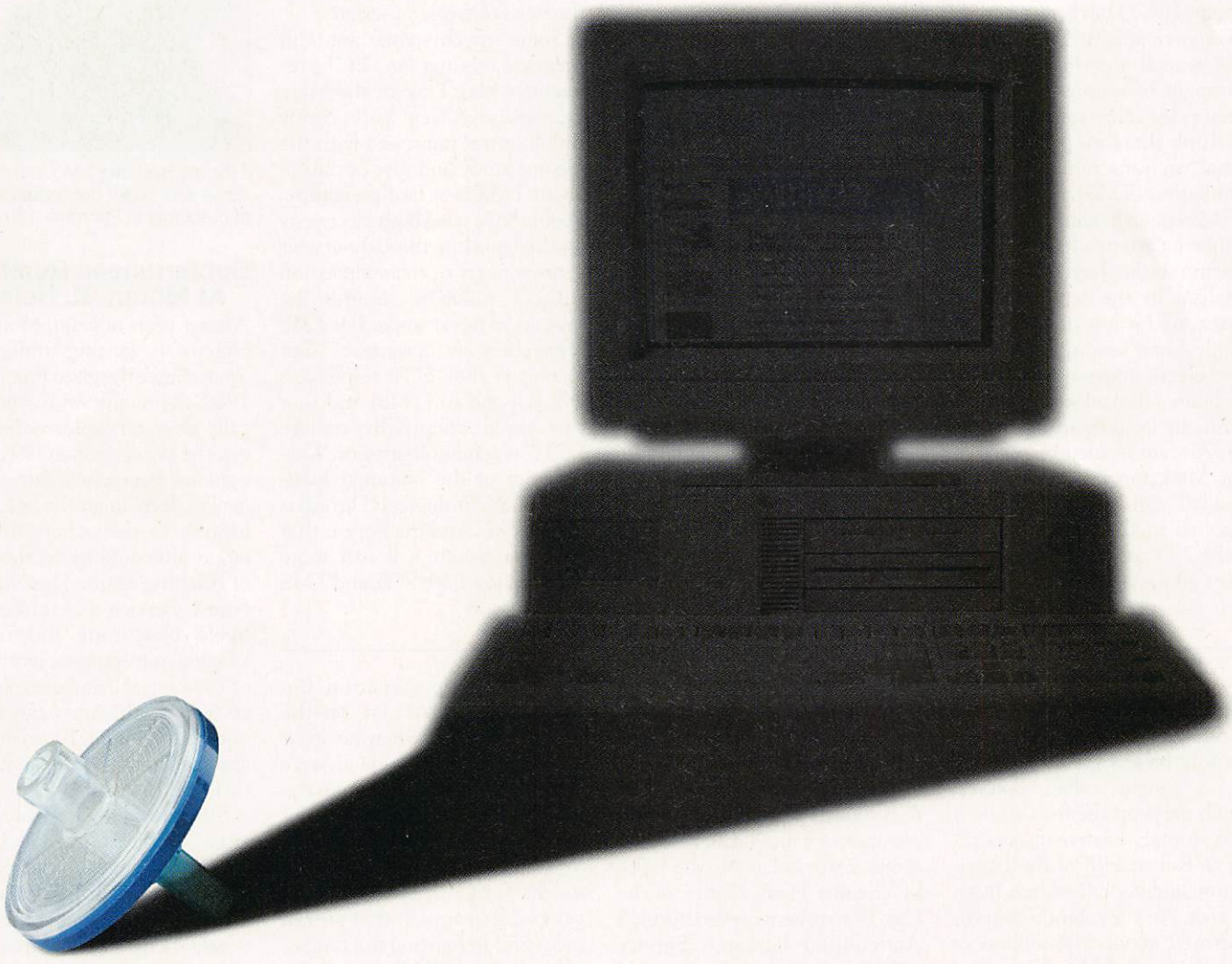

What appears to be a simple filter is actually an on-line gateway to laboratory filtration techniques. Looks can be deceiving. This unassuming filter actually links you to our Internet site (URL: http://www.millipore.com), expert phone support and volumes of research and references. For laboratory analysis help, log on or call 1-800-MILLIPORE in the U.S. In Europe, fax to +33-88.38.91.95. In Japan, call (03)3474-9111. And use the filter with more behind it.

MILLIPORE

© 1995 Millipore Corporation

Circle No. 17 on Readers' Service Card

(continued from page 1443)

in-charge, the earthquake build-up may be the only sign that another outburst is coming.

Even if that happens, though, says Dzurisin, it's all probably part of the hangover from the big blowout. There is nothing, he says, "that indicates the mountain is doing anything but continuing to go to sleep."

Tunable Sensors

People known for their precision usually aren't very flexible, and the same goes for industrial sensors. Sensor arrays that could measure tiny changes in concentrations of many different gases at once, including ethanol, carbon monoxide, and water vapor, would be a boon to industry. The precision sensors available today are not nearly versatile enough to do the job, however. But tomorrow's may be. Researchers at Purdue University have figured out how to make "tunable" sensors that can be adjusted to detect an array of different molecules.

In the 11 October issue of the *Journal of the American Chemical Society*, Purdue chemist Thomas Bein and his colleague Yongan Yan report that they have developed a way to tailor the sensitivity of devices that rely on porous crystalline compounds known as zeolites. The zeolites, which have molecule-size holes, act as filters that allow only one kind of molecule to reach a detector. Currently, if researchers wanted to make an array of zeolite-based sensors for different compounds, they would have to cast thin films of zeolites with different pore sizes—a tricky task. But Bein and Yan have devised a way to alter pore sizes in a single type of zeolite film.

The technique uses what Bein calls "embarrassingly simple" chemistry. Zeolites are made up of a negatively charged framework of atoms (such as silicon, aluminum, and oxygen) to which positively charged atoms, or ions, (such as sodium) are added to create an overall neutral charge. The positive ions occupy sites in and around the crystal's openings, thereby helping to determine the size of the pores. To change this pore size, the researchers replaced one set of positively charged ions with another by dipping a sodium-containing zeolite film in a bath containing potassium, calcium, or rubidium ions. When the other, different-sized ions diffused into the zeolite crystal, they took the place of the sodium ions, changing the zeolite's pore size. Switching from sodium to potassium, for example, narrowed the pore size from about 4 to 3 angstroms and made the potassium zeolite porous only to water vapor.

"It's beautiful work," says Geoffrey Ozin, an inorganic chemist at the University of Toronto, and he thinks manufacturers of everything from semiconductors to food may end up agreeing.

Virtual Course on Protein Structure

NEWS FROM THE NET

Cyberspace pioneers have chalked up another one: a course on protein structure that its creators, a multinational team of scientists, call "the first international multimedia science education course to be taught entirely via the Internet."

The course, "Principles of Protein Structure," was conceived by Peter Murray-Rust, a crystallographer at Glaxo-Wellcome and honorary professor at Birkbeck College, University of London, which is the physical headquarters for the course. Murray-Rust says he got the idea from a course on the programming language C++, which he says was the first totally Internet-based course.

This is "not a Mickey Mouse course," says Murray-Rust. Rather, it's been "created by volunteers from some of the world's top-class laboratories." Seventy graduate students and researchers from around the world have already "graduated" from a pilot course. Each student is assigned a particular protein to study. Students get weekly assignments, participate in tutorials, do dissertations, and display their work and hold real-time discussions in virtual meeting spaces or "MOOs" (*Science*, 13 May 1994, p. 900).

The next course—which the college credits as an advanced-level course—starts in January and will cover three 11-week terms ending next October. The cost is £163 for citizens of the European Union; £500 for others. The URL is **http://www.cryst.bbk.ac.uk/PPS2/**. A "complete mirroring of much of the [course] material," which obviates time-consuming waits to download graphics and animation from across the Atlantic, is available from Brookhaven National Laboratory (**http://www.pdb.bnl.gov/**).

FIVE BIGGEST FOREIGN R&D INVESTORS IN THE UNITED STATES, 1993

Country	Expenditures ($billions)	R&D employees	No. of companies
Switzerland	2.524	14,700	16
Germany	2.321	19,200	32
United Kingdom	2.295	20,000	61
Japan	1.781	11,800	107
France	1.204	9,300	22

Fertile U.S. soil. R&D expenditures by foreign companies in the United States have quadrupled in the past decade and now amount to about 15% of U.S. industrial R&D spending, according to a new report from the Department of Commerce.* Major acquisitions by foreign pharmaceutical companies of U.S. corporations such as Genentech, Chiron, and Smith-Kline have helped swell the numbers, which grew from $3.7 billion in 1982 to $14.6 billion in 1993. Foreign biotechnology companies set up R&D shops in the United States to acquire technology and take advantage of a favorable research environment, notes the report, while electronics and automotive companies do so to help their parent companies increase sales and, for automakers, to meet U.S. environmental regulations. The report also includes data on R&D spending abroad by U.S. companies, which has tripled since 1982 to $9.8 billion in 1993. The most popular site for U.S. R&D investment is Germany, followed by the United Kingdom, Canada, France, and Japan.

* Globalizing Industrial R&D, Office of Technology Policy, U.S. Department of Commerce, October 1995.

Fuzzy Athletic Vegetarian ISO ...

For Romeo, a diademed sifaka—a member of the lemur family—finding that special someone is a little more complicated than placing a singles ad. He's the only such animal in captivity, residing at the Duke Primate Center. Now Duke wants him to have a family, with the ultimate hope of repopulating the wild community in Madagascar. Fund raising is under way for an expedition to Madagascar next spring, led by center director Kenneth Glander, where scientists hope to locate the already-named Juliet. Because of rapid depletion of Madagascar habitat, "this is a salvage operation" as much as a mating foray, says Glander. Interestingly, while the diademed sifakas (which the locals eat) are almost extinct, a close relative, the indri, is still common. That's because they have an "eerie, almost human-like call," says Glander, so Malagasies regard them as sacred and don't kill them.

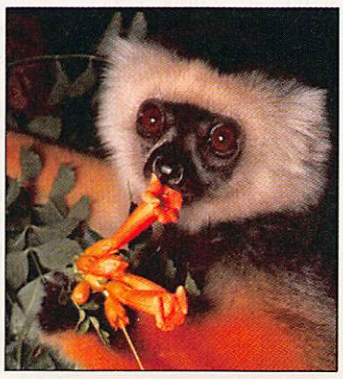

DAVID HARING

Myths About Test Score Comparisons

Iris C. Rotberg

In recent years, our expectations about what we can learn from testing students have become increasingly unrealistic. We use tests for inappropriate purposes and draw inaccurate conclusions from the results. To fix the perceived problem—low test scores—we administer more tests. In the process, we ignore real problems.

Testing has become an integral part of the public policy dialogue about major national issues. Scores on standardized tests are blamed for perceived failures in our economy and in international competition. They drive the debate on school reform. When educators express concern about the focus on standardized tests, we create new and, inevitably, more time-consuming tests that do not address the basic problem: Test score comparisons are highly misleading indicators of the quality of education and are irrelevant to decisions about the wisdom of any particular school reform.

I will address here a set of myths that surround standardized testing. Let me acknowledge at the outset, however, that tests can be valuable for some purposes. They have been used effectively to measure student progress, predict future performance, diagnose learning problems, encourage changes in curriculum and teaching methods, and describe national trends. However, the current use of tests has gone well beyond the reality of what they can accomplish.

Myth 1: Test score comparisons between nations, states, or schools provide valid measures of the quality of education. The international science and mathematics comparisons demonstrate the fallacy of equating test scores with school quality. These comparisons are methodologically flawed and have little to do with the quality of education. The basic problem is student selectivity: The fewer the students who take the test, the higher the average score. That score is not a valid measure of the overall quality of the education system. It simply reflects the fact that the students represented in the test comparisons have been much more highly selected in some countries than in others.

In addition, the test results reflect differences among nations in the proportion of low-income children in the test-taking population. The United States, for example, has a large proportion of low-income students as compared with many other industrialized countries. There is a strong association between poverty and low test scores. We tend to hold the education system responsible for test results reflecting broad societal problems.

Test score rankings also reflect differences in curriculum emphases among nations; for example, the proportion of 12th-grade students who study calculus, the degree of subject-matter specialization after age 16, and the amount of time devoted to cram courses in addition to regular schooling. The decision about whether or not to adopt a particular educational practice should be based on a careful consideration of the merits of the proposed change, not on rankings on standardized tests that compare quite different systems (*1*).

Sampling problems found in international studies also apply to state rankings on the Scholastic Aptitude Test (SAT). The states with the highest proportions of students taking the SAT tend to have the lowest average SAT scores (*2*).

Comparisons of schools within a school system are similarly biased by sampling problems. The fewer and more highly selected the students who take the test, the higher the average score. That score has little to do with the quality of the school.

Schools can raise their scores by excluding low-performing students. After an elementary school was put on probation for low test scores, the third graders made major gains within a single school year because the "officials simply stopped testing most of the third graders. . . .'[Four years later], only 28 percent of the class took the standardized test. . ." (*3*).

Schools also inflate their scores by encouraging students to drop out of school before the examination or by retaining them in their grade. An educator put it this way: "I'm concerned because we have fewer students after grade 9 and it looks like it's to a school's advantage to get a kid to drop out rather than to keep him on the rolls and have poor test scores at grade 12" (*4*).

This technique is not limited to the United States. A World Bank study described primary schools in Kenya that increased test scores by encouraging low-achieving students to drop out before the test was administered. And as many as 20% of Chinese students may be retained in grade in upper-middle school in order to increase that school's scores—and, therefore, its reputation—on university entrance examinations (*5*).

Myth 2: The quality of our schools has declined; that is why we are no longer competitive. We incorrectly conclude from the flawed test comparisons that our schools or our parents or our students have failed. We overestimate the quality and rigor of education in previous generations. We ignore the strides that have been made in educating a large proportion of the population. In 1940, 38.1% of 25- to 29-year-olds in the United States had graduated from high school. By 1993, that percentage had risen to 88.2%. In the same time period, graduation rates from 4-year colleges rose from 5.9% to 23.7% (*6*). Moreover, our educational accomplishments equal and in many cases surpass those of previous years. A recent study by the RAND Corporation found that students' reading and mathematics performance improved for all racial and ethnic groups between 1970 and 1990 (*7*).

Clearly, the United States faces serious educational problems, but they are not the problems identified by the public rhetoric. In the 1950s, we responded to Sputnik by blaming the schools for a perceived inferiority to the Soviet Union in science and technology. Later, we predicted a shortage of scientists and engineers in the 1990s—again due to the failures of our education system. Both concerns were unjustified.

We continue, however, to hear about problems in international competitiveness. The conventional wisdom is that U.S. economic competitiveness has declined because our schools produce a poorly trained work force. Yet, the evidence shows that the problems are caused by quite different factors, such as the realities of the global economy, business practices, and government policies—for example, financial incentives that encourage offshore manufacturing; differential wage rates, profit margins, and government subsidies; licensing practices; exchange rates; and trade policy.

Myth 3: We can fix our schools by administering more tests. Or, if we hold teachers accountable for students' standardized test scores our schools will improve. The evidence shows the opposite.

Testimony before the U.S. House of Representatives put it this way: "[Test-based accountability] has been tried many times over a period of centuries in numerous countries, and its track record is unimpressive. . . . It was the linchpin of the educational reform movement of the 1980s, the failure of which provides much of the impetus for the current wave of reform. . . . Holding people accountable for performance on tests tends to narrow the curriculum. It inflates test scores, leading to phony accountability. It can have pernicious effects on instruction, such as substitution of cramming for teaching. . . . It can adversely affect students already at risk—for example, increasing the dropout rate and

The author is at 7211 Brickyard Road, Potomac, MD 20854, USA.

producing more egregious cramming for the tests in schools with large minority enrollments" (8).

Test comparisons do not provide a valid basis for an accountability system. The results do not control for changes in student population, for incentives to encourage certain students to take or not take the test, or for consistency between the test and the instructional program. We can raise test scores if we teach to the test or if we exclude low-achieving students from taking the test, but the higher scores gained under those circumstances do not reflect improved education.

The RAND study referred to above concluded: "Comparisons of simple, unadjusted test scores from one year to the next or across different schools or districts do not provide a valid indicator of the performance of the teachers, schools, or school districts unless the differences in scores are very large compared to what might be accounted for by changing demographic or family characteristics. This is rarely the case; so, any use of unadjusted test scores to judge or reward teachers or schools will inevitably misjudge which teachers and schools are performing better" (9).

A key question is whether we can alleviate the problem by using alternative measures, such as attendance rates, graduation rates, or the proportion of students going to college. Clearly, these measures provide communities with valuable information about educational accomplishments and problems. However, they do not provide an equitable basis for measuring teacher accountability. The basic problem remains: The effects of teacher quality cannot be separated from the wide range of other factors that influence school outcomes.

Myth 4: The problems in current standardized testing programs can be solved by development of new and improved tests. It is argued that innovative tests, called performance tests or portfolio assessments, will take care of flaws in current testing programs. However, little attention is paid to how long such tests take to develop, how much they cost, whether they can be administered on a large scale, the amount of instructional time they displace, and the validity of the resulting comparisons.

Studies of state testing programs show that the new tests do not reduce methodological problems, they increase them. The scoring is unreliable and measures of validity (for example, whether the tests predict students' future academic performance) are lacking (*10*, *11*). Some state testing programs have tried to use complex statistical formulas to control for student background variables that might affect scores. The attempt has not worked. Indeed, it has resulted in a scoring system that is incomprehensible even to educators working within the system (*12*).

Although the new tests may draw teachers' attention toward writing and problem-solving skills and away from rote learning, this benefit could be obtained by incorporating performance tests or portfolio assessments into a school's instructional program without attempting to make comparisons that provide spurious information.

Moreover, the testing programs are extremely costly and time consuming. Researchers estimate the potential cost of national testing in five subject areas in only three grades to be more than $3 billion per year (*13*). In Kentucky's testing program, fourth-grade teachers were "overwhelmed" by the administration and grading of writing and mathematics portfolios (*14*). In Vermont, teachers spent an average of 30 hours per month, excluding training, working on mathematics portfolios—time taken from instruction children otherwise would receive (*10*).

Perhaps the best example of what happens to testing programs comes from England. In 1988, Parliament mandated national curricula and assessments. The assessments of 7-year-olds took 2 to 4 weeks out of the school year. The marking and reporting form for 14-year-olds in mathematics was 112 pages long. As a result, teachers, with strong parental support, boycotted administration of the tests and reporting of test scores. They cited a range of concerns similar to those emerging from testing programs in the United States—overwork, bureaucracy, disruption of regular schooling, flawed tests, invalid comparisons of schools, and opposition to a national curriculum (*15*). The program has been abandoned.

Myth 5: We can compensate for the inadequate resources spent on poor children by increasing testing requirements. Or, put another way, money does not matter. Research shows, however, that per pupil expenditure, teacher expertise, and class size do make a difference in student achievement (*16*). Increasing testing requirements does not buy better teachers or the attention children can receive in small schools or classes. Tests do not provide low-income inner city or rural students with science laboratories, computers, or decent facilities, amenities that affluent students take for granted.

Nor will tests reduce school finance inequities that relegate low-income children to the most poorly funded schools. For example, the 100 poorest districts in Texas spend an average of just under $3000 per student. The 100 wealthiest districts spend about $7200 per student. In Illinois, school districts spend between $2400 and $8300 per student (*17*).

We cannot improve our schools by giving more tests. The danger is that myths about testing will lead to policies that are irrelevant and counterproductive in addressing the nation's most pressing educational problems: the large proportion of children who live in poverty and the vast differences in educational resources between rich and poor schools. My greatest concern is that a focus on test scores takes attention away from our most troubled schools, the work that needs to be done to resolve the problems, and the resources needed to do it.

REFERENCES AND NOTES

1. The first set of international comparisons, conducted 25 years ago, did not take into account the percentage of the age group actually enrolled in upper secondary school. At the time the tests were administered, only about 20% of the age group in Europe attended upper secondary school—the highest achieving 20%—compared with 80% of the age group in the United States (*18*). More recent studies have tried to deal with the sampling problem by testing only those 12th-grade students who are in an academic track and taking mathematics or advanced science (*19*). These changes do not address the problem. Consider, for example, a recent assessment of mathematics students in Hungary and England. Hungary ranks near the top in the eighth-grade comparison. By the 12th grade, when Hungary retains more students in mathematics than any other country, Hungary ranks among the bottom countries. England, by contrast, scores in the bottom half in most of the eighth-grade comparisons, but ranks among the top countries by the 12th grade, when only a highly select group of students there takes the test, students who have studied science and mathematics almost exclusively since the age of 16. When a country's rank can change so dramatically between the eighth and 12th grades, it simply shows that the test comparisons are meaningless as a measure of school quality (*20*). Another example of the methodological problems comes from a comparison of 11th-grade students at several different sites: Minneapolis, MN; Fairfax County, VA; the province of Alberta in Canada; Beijing, China; Taipei, Taiwan; and Sendai, Japan (*21*). Clearly, these sites are not representative of their nations as a whole, nor were the students selected within each site representative of the age group in their communities. The comparison between China and Japan shows how biases in the sample lead to misleading findings. China ranked first even though we know that Japan educates a much higher proportion of its young people, and Japanese students often spend up to 20 hours a week in cram courses in addition to their regular schooling. The reality is that the test score rankings reflected student selectivity, not the overall performance of the education system. Like many other developing countries with scarce resources, China has an elitist education system that provides upper secondary education to only a small proportion of its young people. Although most Japanese students complete high school, a majority of Chinese students already have left school by the 11th grade. As a result, only a small proportion of the age group in China is represented in the test results. They are the highest achieving students, in the capital city, in a country with particularly wide disparities between urban and rural education. A recent study showed no significant difference between U.S. and Chinese ninth-grade scores when students were selected from both urban and rural areas. Although these samples are more representative than those in the study described above, selectivity remains a problem because a large number of Chinese students have already left school by the ninth grade and therefore are not tested (*22*).
2. *College-Bound Seniors: The Class of 1990* (College Board, New York, August 1990); I. C. Rotberg, *Phi*

Delta Kappan **65**, 10 (1984).
3. B. Ziatos, "Scores That Don't Add Up," *New York Times*, 11 November 1994, p. 28.
4. R. F. Elmore, C. H. Abelmann, S. H. Fuhrman, paper presented at the Brookings Institution conference on Performance-Based Approaches to School Reform, Washington, DC, 6 and 7 April 1995, p. 34.
5. V. Greaney and T. Kellaghan, *Equity Issues in Public Examinations in Developing Countries*, Technical Paper No. 272 (World Bank, Washington, DC, 1995).
6. *Digest of Education Statistics: 1994*, National Center for Education Statistics 94-115 (U.S. Department of Education, Washington, DC, 1994), p. 17.
7. D. W. Grissmer, S. N. Kirby, M. Berends, S. Williamson, *Student Achievement and the Changing American Family*, MR-488-LE (RAND Institute on Education and Training, Santa Monica, CA, 1994).
8. D. M. Koretz, G. F. Madaus, E. Haertel, A. E. Beaton, *National Educational Standards and Testing: A Response to the Recommendations of the National Council on Education Standards and Testing*, CT-100 (RAND Corp., Santa Monica, CA, 1992), p. 9.
9. D. W. Grissmer, *ibid.*, p. XXXV.
10. See, for example, D. Koretz, B. Stecher, S. Klein, D. McCaffrey, *The Vermont Portfolio Assessment Program*, RP-366 (RAND Corp., Santa Monica, CA, 1995).
11. See, for example, R. K. Hambleton *et al.*, *Review of the Measurement Quality of the Kentucky Instructional Results Information System, 1991–1994* (Office of Educational Accountability, Kentucky General Assembly, Frankfort, KY, June 1995).
12. R. F. Elmore, C. H. Abelmann, S. H. Fuhrman, paper presented at the Brookings Institution conference on Performance-Based Approaches to School Reform, Washington, DC, 6 and 7 April 1995.
13. D. M. Koretz, G. F. Madaus, E. Haertel, A. E. Beaton, *National Educational Standards and Testing: A Response to the Recommendations of the National Council on Education Standards and Testing*, CT-100 (RAND Corp., Santa Monica, CA, 1992).
14. R. F. Elmore, in (*11*), p. 43.
15. "Massive Teacher Boycott Derails British National Tests," reprinted from *FairTest Examiner* (Summer 1993).
16. See, for example, R. F. Ferguson, *Harvard J. Legis.* **28**, 465 (1991); L. V. Hedges, R. D. Laine, R. Greenwald, *Educ. Res.* **23**, 3 (1994); R. J. Murnane, *Harvard J. Legis.* **28**, 457 (1991).
17. I. C. Rotberg and J. J. Harvey, *Federal Policy Options for Improving the Education of Low-Income Students, Volume I: Findings and Recommendations*, MR-209-LE (RAND Corp., Santa Monica, CA, 1993).
18. T. Husen, *Phi Delta Kappan* **64**, 7 (1983).
19. *The Underachieving Curriculum: Assessing U.S. School Mathematics from an International Perspective* (International Association for the Evaluation of Educational Achievement, University of Illinois, Champaign, IL, 1987).
20. Adapted from a more detailed analysis by I. C. Rotberg in *Phi Delta Kappan* **72**, 4 (1990).
21. *Stevenson Study of Mathematics Achievement in Alberta Schools*, Summary Report based on a presentation by Harold Stevenson, Alberta Education Department, Edmonton, Alberta, Canada, 24 October 1993.
22. J. Wang, paper presented at the 76th Annual Meeting of the American Educational Research Association, San Francisco, CA, 18 to 22 April 1995.
23. This paper is based on remarks presented at the North Central Alberta Teachers' Convention, Edmonton, Alberta, Canada, 8 to 10 February 1995, and the American Youth Policy Forum, Institute for Educational Leadership, Washington, DC, 2 June 1995.

Needed: Coherent Budgeting for Science and Technology

Frank Press

The intellectual function of trouble is to lead men [and women] to think.

—JOHN DEWEY

All of those concerned with science and technology in the United States—politicians who allocate federal funds, working scientists and engineers, and users of science and technology throughout the public and private sectors—are troubled about the future. Almost all affirm publicly that maintaining a leadership role for U.S. science and technology is vital to the future, but there are divergent views on how to achieve this goal. The basic science and technology policy question for the next few years is how to fit this goal into the framework of a changing world, where security has a new and broader definition than superpower confrontation, where deficit reduction is a top priority of both the Democratic and Republican parties, and where science and technology are poised for more advances than ever before.

This was the backdrop for a task from the Senate Appropriations Committee, set before the National Academy of Sciences, the National Academy of Engineering, and the Institute of Medicine, to address "the criteria that should be used in judging the appropriate allocation of funds to research and development activities, the appropriate balance among different types of institutions that conduct such research, and the means of assuring continued objectivity in the allocation process" (*1*). To respond, the academies assembled a panel drawn from those with extensive experience in how the government works, how science and technology progresses in universities, federal laboratories, and industry, and what nurtures successful innovation (*2*). Our report makes specific recommendations on management, budgeting, and allocation of federal funds that will maintain our nation's tradition of excellence in science and technology in times of severe budgetary pressure. It compares the different institutions that perform research and development, discusses the balance between accountability and regulation, and provides practical examples of how our suggestions could be implemented without new legislation or reorganization of the congressional committee structure. Our recommendations are supported by supplements that provide historical background and analyses of current budgets and practices. As the report (*3*) is available on the World Wide Web (*4*) and is covered elsewhere in this issue, I will highlight here some major policy questions and the principles that guided our recommendations.

The author is senior fellow at the Carnegie Institution of Washington, 5241 Broad Branch Road, Washington, DC 20015, and former president of the National Academy of Sciences.

Guiding Principles

U.S. success in science and technology did not happen by chance. To their credit, our political leaders and their advisers of previous decades introduced policies, the best of which will work in the future as they have in the past. Building science and technology competency in federal departments by supporting federal laboratories and awarding grants to universities for research and training improved government performance in its missions of health, defense, economic growth, agriculture, science, space, training, and other tasks. Concomitantly, these policies created a pluralistic system of support that survived the clash of personalities and the rise and fall of budgets.

The distinctly U.S. tradition of drawing on the private sector for advice, testimony, review, and evaluation has worked particularly well for science and technology. It has resulted in healthy competition and identified the best people and projects to support. Government agencies have benefited, as has the national science and technology enterprise. Competitive merit review, especially that involving external reviewers, is key. At a time of fiscal stringency, it is even more important that it continue to be the preferred way to make science and technology allocations to universities, federal laboratories, and in general to all those involved in research and development. Naturally, special conditions do exist in highly specific mission areas where other modes of allocation are more appropriate.

The combination of training and research in U.S. universities has been a major factor in creating scientific and technical preeminence as well as in providing competent professionals to staff industries and federal laboratories. It is one of the most effective means of technology transfer, and government allocation criteria in the future should recognize this record of achievement.

Many federal laboratories have unmatched facilities and capabilities and con-

tribute in unique ways to national goals. As a result, it would be unwise to weaken them. The reasons for supporting other federal laboratories, however, are less compelling than they were in the past. Where mission requirements have diminished or when external reviewers find them less useful, then alternative resources should be redirected.

Parsing the Budget

There is no more powerful statement of government policy than budget decisions. The annual federal research and development budget is usually reported to be more than $70 billion. A substantial part of these funds is awarded by the Department of Defense to private industry for such things as testing and evaluation, setting up production lines for aircraft, and upgrading and modernization of weapons components and systems. These contracts are driven primarily by national security considerations and the interplay between military requirements and the political system. Despite their inclusion in the research and development budget, such projects do not constitute research and development as generally understood in this country or abroad. It is misleading to include them, and we set them aside from our consideration. Indeed, the Department of Defense itself considers them outside its "science and technology base." Instead, we focused on those items whose justification rests on the national need for science and technology.

Thus, our report deals with the remaining $35 to $40 billion of the federal research and development budget, the fraction that expands fundamental knowledge and creates new technologies. We defined this as the Federal Science and Technology (FS&T) budget and proposed that in the future, government support for basic and applied science and fundamental technology be presented and evaluated in terms of an FS&T budget. Just about every federal department and agency contributes to the FS&T pool either by extramural contracts and grants or by support of intramural laboratories.

The concept of an FS&T budget is not simply an alternate aggregation of numbers. It is the core of a new budgeting process that should encourage selective reductions and increases within and across agencies to reflect changing missions and performance evaluations. We need a system that continually frees funds from poorly performing or less needed projects and allocates them to better and more important ones, channeling resources to high-quality people and projects in universities, federal laboratories, or other institutions.

As science has progressed, a complex relationship has evolved between basic and applied science and technology to the point that it is more appropriate to treat them as one interrelated FS&T enterprise. Such an enterprise can be represented by the research and training programs of the science and engineering departments of our research universities and many of the activities of federally supported laboratories (the national laboratories and other intramural and extramural research and development centers). Federal laboratories (both in-house and contractor-run) account for the largest share (39%) of the FS&T budget, followed by academic institutions (31%), industry (21%), and nonprofit and other institutions (9%). With a total pool of some $35 to $40 billion, this breakdown shows that the flexibility of transfers across agencies and among performers, inherent in the FS&T budget, is a powerful tool for maintaining science and technology excellence in the United States.

Budget deficits and fiscal stringency are powerful incentives to introduce reform in the government and, in the case of science and technology, to search for a process that will maintain a leadership role for the United States. The FS&T budget represents a process for coherent decision-making at the macroallocation level. In a climate of fiscal stringency, it is the only way to fund new initiatives, pursue excellence, and maintain the overall strength of U.S. science and technology. At the microallocation level, our recommendations preserve the advantages of pluralism and the decentralized, competitive, reviewed allocation process.

Congress is zealous in guarding decisions about how it organizes itself, and members have responsibilities to constituents that go well beyond science and technology. The introduction of an FS&T budget will be just one determinant in how the committee structure of the Congress evolves. However, given efforts in the current Congress to authorize science programs more broadly rather than piece by piece, it is not at all fanciful to argue that if the president submits an FS&T budget that shows coherence and integration across agencies and sensitivity to maintaining a strong science and technology enterprise, the congressional budget, authorization, and appropriation committees would work together to review the overall budget, then disaggregate it and send it with guidance to separate subcommittees.

Most importantly, an FS&T budget should command attention in both the executive and legislative branches. In the executive branch, this would entail active management of FS&T by the Office of Management and Budget and the Office of Science and Technology Policy, working with departments and agencies that support research and development. In Congress, it will require monitoring by the Congressional Budget Office and a more coherent process within the existing committee structure of both houses. The intent is ultimately to inform the appropriation subcommittees, where most of the critical funding decisions are made, of the rationale for the overall FS&T budget, including the reasons for proposed reductions and increases. In this way, the subcommittees would act with knowledge of the impact of their separate decisions on the whole enterprise, and their individual actions would be monitored collectively throughout the budgetary process.

The Politics of Science and Technology in a Democracy

In a democracy, it is the prerogative of elected officials to promulgate policies and allocate budgets with outcomes that can weaken or strengthen U.S. science and technology. The demands on public officials for public funds are enormous. In our system, scientists and engineers enjoy an unusual degree of autonomy and provide advice on many levels, but elected officials make critical decisions. As scientists and engineers, we can and should point out the importance of science and technology to the nation's future on the basis of their contributions to about every sector of American life. If we are to be heard, our advice must be professional, credible, balanced, and not self-serving. We are proposing guidelines for management and resource allocation that, with disciplined and informed implementation, can maintain U.S. leadership in the face of severe fiscal constraints. Some would counsel us not to show where reductions can be made, because of the real possibility that the cuts will be taken though the savings would not be reallocated within the FS&T pool. This may be so, but we see no alternative but to speak truthfully about optimal allocations if the preeminent position of U.S. science and technology is to be maintained. The call for a process of budget discipline does not derive from naïve or wishful thinking but is made with full understanding of the political system and the tenor of the times.

REFERENCES AND NOTES

1. Report language accompanying Public Law 103-733, Appropriations for the Department of Labor, Health and Human Services, and Related Agencies for fiscal year 1995.
2. Panel members include the following: Frank Press, chair, senior fellow, Carnegie Institution of Washington; Lew Allen Jr., chairman, Charles Stark Draper Laboratory; David H. Auston, provost, Rice University; Forest Baskett, senior vice president, Silicon Graphics Computer Systems; Barry R. Bloom, professor of microbiology and immunology, Albert Einstein College of Medicine; Daniel J. Evans, chairman, Daniel J. Evans & Associates; Baruch Fischhoff, professor of social and decision sciences, Carnegie Mel-

Ion University; Marye Anne Fox, vice president for research, University of Texas; Richard J. Mahoney, chairman and CEO (retired), Monsanto Company; Steven L. McKnight, research director, Tularik; Marcia K. McNutt, Griswold Professor of Geophysics, Massachusetts Institute of Technology; Paul M. Romer, professor of economics, University of California at Berkeley; Luis Sequeira, professor of plant pathology, University of Wisconsin; Harold T. Shapiro, president, Princeton University; and H. Guyford Stever, Trustee and Science Advisor.

3. *Allocating Federal Funds for Science and Technology* (National Academy Press, Washington, DC, 1995).
4. The report is available on the World Wide Web at http://www.nas.edu

How Does the Texaco Case Affect Photocopying by Scientists?

The National Conference of Lawyers and Scientists*

Most people who read professional journals occasionally copy articles of special interest or significance. Does this common, everyday practice break the law? A recent case from the U.S. Court of Appeals for the Second Circuit tells us that the answer is sometimes yes and sometimes no. In this case—*American Geophysical Union* v. *Texaco, Inc.*—the court held that the photocopying of eight scholarly articles from separate issues of the same scientific journal by a research scientist was not a "fair use" under the Copyright Act (*1*). The parties politely agreed to stipulated facts describing the activities of one researcher (Chickering) chosen at random as an example through which to determine the question of fair use.

The case highlights the tension between the interests of author-scientists who want their ideas to reach the largest possible audience and their editor-publishers who profit more directly from the dissemination of those ideas. The court ruled that a commercial institution may not encourage photocopying by purchasing a small number of journals to circulate among a large number of scientists. It also held that photocopying by corporate researchers for their files is an archival use rather than a fair use, and thus it violates copyright law.

The court revised the text of its opinion twice, apparently to clarify certain points that may have been missed or misunderstood by readers of the original version (*2*). In restating its decision, the court identified two kinds of copying it explicitly did not intend to address. In the final text, the court specified that it was not deciding "the case that would arise if [the researcher] were a professor or an independent scientist engaged in copying and creating files for independent research, as opposed to being employed by an institution in the pursuit of his research on the institution's behalf" (*3*). It also noted that "[O]ur ruling does not consider photocopying for personal use by an individual. Our ruling is confined to the institutional, systematic, archival multiplication of copies revealed by the record. . ." (*4*).

Before the issuance of the last amended decision, Texaco and a steering committee of publishers agreed to settle the dispute (*5*). Under the settlement, Texaco admitted to no wrongdoing but agreed to pay a large settlement amount that includes retroactive license fees for the period 1985 through 1994. In addition, Texaco agreed to a standard licensing agreement with the Copyright Clearance Center, which collects fees from corporate entities for the right to photocopy articles from those journals whose publishers use the service (*6*).

The decision appears to affect photocopying practices that have long been accepted as a reasonable and customary practice in scientific research (*7*). Because of the particular circumstances of the case, however, many issues remain unresolved; nevertheless, the decision should cause all institutions to review their photocopy and licensing policies. Meanwhile, the victorious publishers praise the outcome as an affirmation of their intellectual property rights, and scientists fear the chilling effect the decision may have on research.

Armed with this decision, publishers may press for stricter enforcement, particularly as to corporate entities. An aggressive campaign to license large research institutions through the Copyright Clearance Center or similar mechanisms can be expected, despite the court's clear denial that it was deciding whether photocopying of articles by anyone in any setting is a fair use.

Based on *Texaco*, how should various types of for-profit, nonprofit and scholarly institutions deal with photocopying and licensing? At what point does individual copying cross the line from fair use to copyright infringement? Which institutions should be paying license fees? A few answers are found in the text of the decision. For the most part, however, the *Texaco* decision leaves many questions unresolved.

The Limited Reach of the Decision

To understand the limited reach of *Texaco*, it is important to keep in mind the narrow question the Second Circuit addressed. In the final version of its opinion, the court expressly limited its decision to (*8*):

> Whether Texaco's photocopying by 400 to 500 scientists as represented by Chickering's example, is fair use. This includes the question whether such institutional, systematic copying increases the number of copies available to scientists while avoiding the necessity of paying for license fees or for additional subscriptions. We do not deal with the question of copying by an individual, for personal use in research or otherwise (not for resale) . . . .

The *Texaco* decision strongly suggests that any large, for-profit corporation in which employees systematically make copies of journal articles for archival purposes probably violates copyright. Thus, the U.S. Court of Appeals appears to have lowered the threshold at which other courts may find copyright violations, at least within the context of for-profit entities. Any for-profit institution whose copying practices resemble those of Texaco would be well advised to pay license fees or make other arrangements with journal publishers. But what if the copies are made for convenience and not archival purposes? What if the copying is isolated and not systematic? What if the institution is nonprofit? In discussing an important factor for determining fair use—the purpose and character of the use—the court characterized Chickering's use as archival because the copying was "done for the primary purpose of providing numerous Texaco scientists (for whom Chickering served as an example) each with his or her own personal copy of each article without Texaco's having to purchase another original journal" (*9*). The court noted, however (*10*):

> [W]e do not mean to suggest that no instance of archival copying would be fair use, but [this] factor tilts against Texaco in this case because the making of copies to be placed on the shelf in

*This essay was prepared for the National Conference of Lawyers and Scientists (NCLS), a joint committee of the AAAS and the American Bar Association Science and Technology Section, under the direction of Barbara Mishkin and Joseph M. Potenza, with the assistance of Victor Marton. A working draft was circulated to all NCLS members and the final text reflects comments received.

Barbara Mishkin, Hogan and Hartson, Washington, DC; Alan I. Leshner, National Institute on Drug Abuse; R. Stephen Berry, University of Chicago; Linda M. Distlerath, Merck Research Laboratories; Alicia K. Dustira, Office of Research Integrity; William P. Gardner, University of Pittsburgh; Paul Goldstein, University of Texas; Rebecca Klemm, Klemm Analysis Group, Washington, DC; Bert Black, Weinberg & Green, Baltimore, MD; Alice H. Fraenkel, Columbus, OH; Françoise Gilbert, Altheimer & Gray, Chicago, IL; Joseph M. Potenza, Banner and Allegretti, Ltd., Washington, DC; Joseph I. Rosenbaum, New York, NY; Oliver R. Smoot, Information Technology Industry Council, Washington, DC; Lee Loevinger, Hogan and Harston, Washington, DC

Chickering's office is part of a systematic process of encouraging employee researchers to copy articles so as to multiply available copies while avoiding payment.

To avoid liability and license fees, an institution might establish a policy that discourages photocopying. Even with such a policy, however, if an institution knowingly permits noncompliance, it might still be held accountable. Is archival copying fair use if it is not systematic? What does "systematic" mean? The answers will have to come from future cases.

Important Issues Remain Unresolved

Many questions of immediate concern to research scientists and engineers remain unresolved. For example, may an individual make photocopies for subsequent research from a journal received as an incident of membership in a scientific society? The *Texaco* decision suggests that such copying is a fair use because the photocopy is made for research purposes, from an individual's own copy of the journal, and likely does not substitute for additional subscriptions. May the researcher also make a second copy for a collaborator? Possibly, but at some point, making multiple copies for a group of collaborators presumably would be more akin to systematic copying than personal use.

Policy-makers currently considering revisions to the copyright law apparently are focusing more on issues surrounding cyberspace than the question of photocopying (*11*). But important questions about fair use also need to be addressed, bearing in mind the context in which scientific research is conducted today. Distinctions between scientists working in industry and those employed by the government or an academic institution may no longer be valid, because scientists in all settings conduct research of potential commercial value. Although the for-profit or nonprofit status of the scientist's employer, or the institutional setting, has been a factor in the traditional fair use analysis, its continued applicability is questionable. As Judge Jacobs observed in his dissent in *Texaco* (*12*):

> Research is largely an institutional endeavor nowadays, conducted by employees pursuing the overall goals of corporations, university laboratories, courts and law firms, governments and their agencies, think-tanks, publishers of newspapers and magazines, and other kinds of institutions. The majority's limitation of its holding to institutional environments may give comfort to inventors in bicycle shops, scientists in garage laboratories, freelance book reviewers, and solo conspiracy theorists, but it is not otherwise meaningful.

Drawing the line instead between individual and institutional subscriptions may be equally inappropriate. There is a common perception that the higher subscription rate paid by institutions anticipates the kind of copying at issue in *Texaco* (*13*). The publishers reply that the higher price anticipates a broader readership, not a photocopy license. There is some irony in the result that under *Texaco*, an individual with his own (less expensive) subscription apparently may engage in at least some archival copying, whereas an employee using an institutional subscription (for which the publisher charges more) must pay additional fees to make a photocopy.

We have heard research scientists and engineers express dismay that they risk being sued by their own societies for engaging in a common practice. Their primary goal in publishing is to have their work disseminated to the widest possible audience. They receive little, if any, financial compensation for their contribution to a scientific journal. The editors, on the other hand, are concerned with the bottom line and typically do not share royalties or copying fees with individual authors. In fact, the authors sometimes must pay the journal a fee (per page) to be published.

As a legal matter, publishers may establish their own rules. For example, the AAAS allows individuals to photocopy from the printed journal of *Science* as permitted by the Copyright Act or by paying a fee to the Copyright Clearance Center, including printing a copy from pages posted on the Internet. How can an individual scientist know what the Copyright Act permits? How may a scientist lawfully obtain a copy of a research report? As the *Texaco* court acknowledges, it is not easy to obtain a copy of a single journal article (other than by photocopying) because publishers typically provide reprints "only in bulk and with some delay" (*14*). The traditional method of requesting a reprint from the author merely increases the author's cost, requiring advance purchase of hundreds of reprints to distribute in response to requests. One might legitimately ask why the author, rather than the consumer, should bear the cost of the reprints. What is the best policy for science (*15*)?

REFERENCES AND NOTES

1. 60 F.3d 913 (2nd Cir. 1995).
2. *Ibid.* The opinion was first issued on 28 October 1994. It was amended on 23 December 1994, and further amended on 17 July 1995.
3. *Ibid.* at 916.
4. *Ibid.* at 931.
5. See A. Lawler, *Science* **268**, 1127 (1995).
6. The CCC is described at 60 F.3d at 929, n. 16; *see also ibid.* at 936-939 (Jacobs, J., dissenting).
7. *Ibid.* at 924.
8. *Ibid.* at 916.
9. *Ibid.* at 919.
10. *Ibid.* at 920.
11. "A Facelift for Copyright" (editorial), *The Washington Post*, 7 September 1995 at A-18; E. Corcoran, "A Digital duel: Whose party is this?" *ibid.*, 3 September 1995 at H-1.
12. 60 F.3d at 935 (Jacobs, J., dissenting).
13. An individual subscription to *Science* (51 issues) costs $50, whereas an institutional subscription costs $228 for the same number of issues. *See*, for example *Science* **269**, 1647 (1995).
14. 60 F.3d at 927.
15. The NCLS plans to study copyright issues during the coming year and would like to know your thoughts. You need not identify yourself, but please include the date of your most recent (earned) degree, your discipline, and the setting in which you work (for example, for-profit, nonprofit, or government). Address your comments to NCLS Copyright Project, 1333 H Street, NW, Washington, DC 20005; FAX (202) 289-4950; e-mail: ncls@aaas.org

If you are interested in participating in an electronic forum on the topic of copyright law and its relation to scholarly publishing, see the "Beyond the Printed Page" section of *Science* On-Line (http://sciencemag.aaas.org/science/).

An Exploding Star in Motion

Roger A. Chevalier

Stars in other galaxies are normally far too small to be resolved at Earth, but as Marcaide *et al.* report on page 1475 of this issue, a sensitive array of radio telescopes in a worldwide network has now produced a time sequence of images of an exploding star (*1*). The supernova, designated SN 1993J, was discovered in the galaxy M81 by a Spanish amateur astronomer on 28 March 1993 (*2*). With an estimated distance from Earth of 12 million light years, it is relatively close for a supernova. Observations of the progenitor object imply that it is an extended star with a radius approximately equal to the Earth-sun distance. The explosion accelerated the outer stellar layers to a speed of more than 10,000 km s^{-1}, so that the star had expanded by a factor of more than 1000 at the time of the radio imaging. Despite the rapid expansion, the radio imaging could begin only 6 months after the initial explosion because of the great distance. The results directly show the expansion of a circular shell with some persistent structure.

Not all supernovae are strong radio emitters. The fact that the progenitor star was highly extended is a crucial aspect of the radio emission. Massive, extended stars in the late phases of evolution have slow, dense stellar winds; it is the collision of the supernova with this dense wind that gives conditions suitable for radio emission. The supernova sweeps up a shell of the wind gas (see figure), with a shock front at the leading edge. The shell tends to slow down with time, so that the cool, expanding supernova gas catches up with the shell and creates another shock front, the reverse shock. Shock fronts are sites of relativistic electron acceleration, and in the presence of the magnetic field in the swept-up shell, the high-energy electrons emit radio synchrotron radiation. This is the basis for the wind-interaction model of radio supernovae (*3*). Supernova SN 1987A was the first naked-eye supernova in nearly 400 years and was by a factor of 70 closer than SN 1993J, but it was a faint radio emitter. The reason is that its progenitor star was compact, by a factor of 10 smaller than that of SN 1993J, and it had a fast, low-density stellar wind. In that case, the observed radiative phenomena were powered by radioactivity and there was little evidence of the wind interaction.

The wind-interaction model predicted that the radio emission from SN 1993J would be in a fast shell, and the radio imaging has confirmed that this is the case. This would not be so for a central power source such as a pulsar. In more detail, the interaction model predicts that the inner boundary of the radio shell should be the reverse shock front. This shock front can initially heat the gas to a temperature of 10 million kelvin, hotter than the solar corona, and the gas radiates x-rays. If the density is sufficiently high, the radiation cools the gas to the point at which optical line radiation is emitted. Spectra of SN 1993J at optical and ultraviolet wavelengths show the broad-line emission expected from the cooling shock wave, and the breadth of the lines gives the velocity of gas at the reverse shock front. Combining the velocity with the age yields the radius of the reverse shock front. The angular size measured from the radio image, combined with the distance to M81, also yields a physical size, which agrees within the errors with the first measurement.

For more distant supernovae with poorly determined distances, this technique has the promise of determining distances to galaxies and yielding a value of the Hubble constant, as has already been attempted for SN 1979C (*4*). The problem is that imaging is difficult for distant supernovae and the radio observations can give only a crude size. The structure of the emitting shell is then important. The observations of Marcaide *et al.* (*1*) show a ratio of inner shell radius to outer of 0.7 and self-similar evolution; that is, the structure relative to the outer radius remains time invariant even though the outer radius is expanding. The interaction theory predicts self-similar evolution, but with a narrower emitting region. The ratio of inner to outer shock radius is about 0.8, and instabilities that can build up the magnetic field occur in only the inner half of the shell. The broader emitting region may be associated with clumping in the wind. Detailed calculations are necessary to investigate this association. Unfortunately, different supernovae may have different shell structures, which will introduce an uncertainty in Hubble constant estimates.

The radio images show the shell to be surprisingly circular, especially in view of detectable polarization at optical wavelengths (*5*). The wind and outer supernova

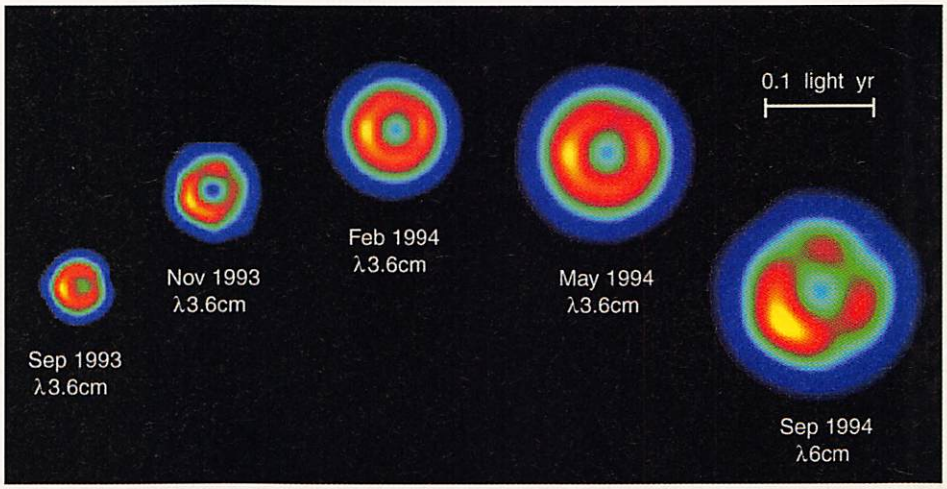

Shocking images. A sequence of SN 1993J radio images, produced by Marcaide *et al.*, reveals a year in the life of a supernova—and a symmetrical shock front development. [From (*1*)]

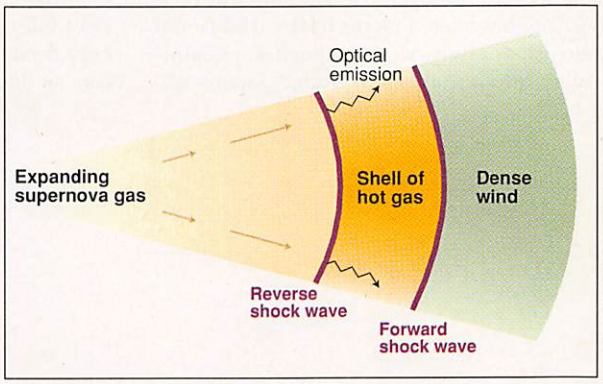

Detonation aftermath. The collision of the exploding star with the surrounding wind creates a shell of hot gas that is bounded by forward and reverse shock waves. The observed radio emission is likely to be associated with the hot shell.

The author is in the Department of Astronomy, University of Virginia, Charlottesville, VA 22903, USA. E-mail: rac5x@virginia.edu

matter appear to be symmetric, and any asymmetry is more centrally located. Despite the symmetric shape, there are brightness variations around the shell that persist with time (*1*). One possible reason for this behavior is that the efficiency of particle acceleration at the outer shock front depends on the magnetic-field orientation. The magnetic field in a stellar wind should have a spiral pattern aligned about the stellar rotation axis. The magnetic field is too weak to affect the shock-wave dynamics, but it could imprint a pattern on the radio synchrotron emission.

The observations thus confirm the basic wind-interaction model but raise issues that will require more detailed modeling and computer simulation. The combination of high densities and high velocities creates extreme conditions that are comparable with those in quasars, but here we have a clear picture of the physical situation. When the radio observations are combined with observations at optical, ultraviolet, and x-ray wavelengths, we have a chance to follow and understand the initial expansion phases of the most extreme explosive events in nearby galaxies—supernovae.

References and Notes

1. J. M. Marcaide *et al.*, *Science* **270**, 1475 (1995).
2. J. Ripero, *IAU Circ. 5731* (1993).
3. R. A. Chevalier, *Astrophys. J.* **259**, 302 (1982).
4. N. Bartel *et al.*, *Nature* **318**, 25 (1985).
5. S. R. Trammell, D. C. Hines, J. C. Wheeler, *Astrophys. J.* **414**, L21 (1993).

6. My research on supernovae is supported in part by NSF grant AST-9314724.

Molecular Mimicry in Protein Synthesis?

Peter B. Moore

This week's issue of *Science* includes the first report by the Aarhus group of the crystal structure of elongation factor Tu (EF-Tu) complexed with aminoacylated phenylalanyl transfer RNA (tRNA) and guanosine triphosphate (GTP)—the EF-Tu ternary complex (*1*). EF-Tu and its eukaryotic homolog EF-1α deliver aminoacyl tRNAs to the ribosome during the elongation phase of protein synthesis (see figure). In addition to providing insights into the way aminoacyl tRNAs get to the ribosome, this structure addresses a long-standing, mechanistic question: Why does EF-Tu deliver only aminoacylated elongator tRNAs to the ribosome, never uncharged tRNAs or initiator tRNAs? Both because of the biological importance of protein synthesis and because of the long scientific history of this complex, the publication of its structure is a landmark.

The article by the Aarhus group does more than present an important structure, however. Nissen and co-workers have discovered that the overall shape of the ternary complex resembles that of the guanosine diphosphate (GDP) form of elongation factor G (EF-G; EF-2 in eukaryotes), the protein that catalyzes the translocation step of elongation (see figure). During translocation, the ribosome moves down its messenger RNA (mRNA) by three bases, and the tRNAs bound to it are rearranged so that the ternary complex called for by the next codon can be accepted.

That EF-G and EF-Tu are structurally related was already known. Their amino-terminal domains bind guanine nucleotides and are conformationally similar, as are their second domains (*2*–*5*). The new observation is that three domains at the carboxyl-terminal end of EF-G, which have no homologs in EF-Tu, together resemble tRNA and, relative to EF-G's nucleotide binding site, are positioned the same way as tRNA in the ternary complex. It seems that we have just been given a huge—albeit Delphic—hint about the mechanism of protein synthesis.

It was also known that EF-G and EF-Tu are functionally related (*6*, *7*). EF-G and EF-Tu compete for a single factor binding site on the ribosome. Both bind to the ribosome when complexed with GTP and have guanosine triphosphatase (GTPase) activities that are activated by binding. Furthermore, both adopt conformations that have a low affinity for ribosomes after GTP hydrolysis. Nevertheless, the discovery that EF-G resembles the ternary complex suggests that the mechanism of EF-G–catalyzed translocation resembles the mechanism of EF-Tu–catalyzed tRNA binding at a far deeper level.

EF-G's function is easier to understand than EF-Tu's (*6*, *7*). Translocation results when an elongating ribosome switches from its pretranslocational state to its posttranslocational state. EF-G–GTP binding

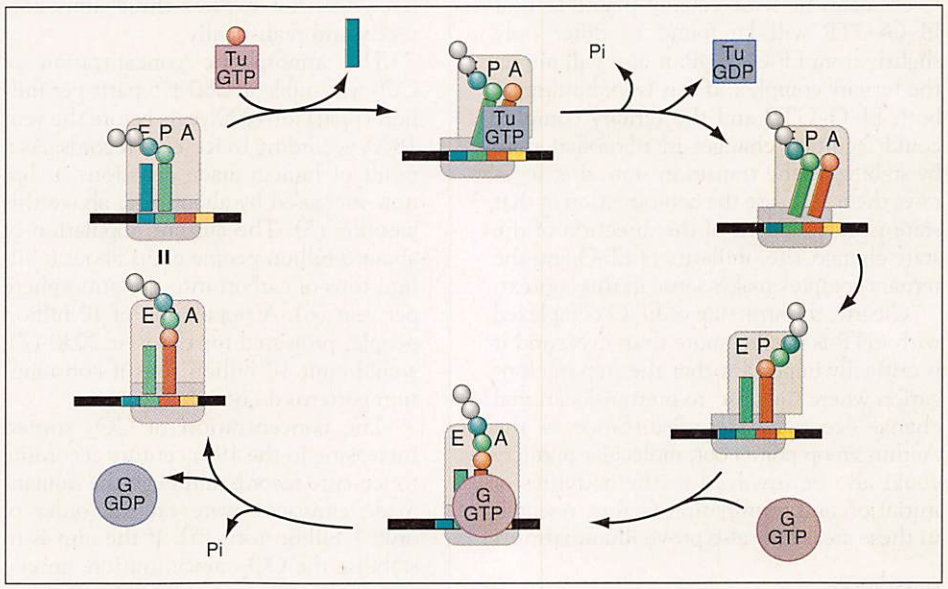

Elongation cycle of protein synthesis. The cycle starts with the binding of ternary complex to the ribosome (upper left), which results in the discharge of deacylated tRNA from the E site, placement of a new aminoacyl tRNA in the A site, and conversion of the ribosome from the post- to the pretranslocational state. Peptide transfer follows (right, middle). The binding of EF-G–GTP to the ribosome (lower right) restores the ribosome to the posttranslocational state, the mRNA advances by one codon, and its tRNAs are rearranged so that another cycle of elongation can ensue (*8*). Ribosomes are shown as rectangles; the upper third is the large subunit and the lower third is the small subunit. When the subunits are aligned, the ribosome is in its posttranslocational state. When they are misaligned, ribosomes are in the pretranslocational state. Transfer RNAs appear as colored bars, and their amino acids as small circles of the same color. Square, EF-Tu; large circle, EF-G. Messenger RNA is shown as a horizontal line that crosses the small subunit. Its colored segments represent specific codons, whose colors match those of the corresponding amino acids.

The author is in the Departments of Chemistry and Molecular Biophysics and Biochemistry, Yale University, New Haven, CT 05620-8107, USA. E-mail: moore@proton.chem.yale.edu

reduces the activation energy required for this change. EF-G leaves the ribosome after translocation because its GTPase is activated in the posttranslocational complex. The return of the ribosome to the pretranslocational state occurs at some point between the stage when the ternary complex binds to the ribosome and the formation of the next peptide bond. If the ternary complex is like EF-G, shouldn't its binding to the ribosome trigger that conformational change? Otherwise, what is the common function that calls for a common structure?

GTP cleavage has a huge effect on the arrangement of domains in EF-Tu (*2*, *3*, *8*). Furthermore, in the placement of its first two domains, EF-G–GDP resembles the ternary complex, not EF-Tu–GDP (*4*, *5*). Nissen *et al.* argue that the reason EF-G–GDP resembles the ternary complex is because it is associated with the ribosomal state to which ternary complexes bind. This is not convincing. Because neither EF-G–GDP nor EF-Tu–GDP bind to the ribosome, their conformations do not necessarily tell us anything about the ribosome. Only the structures of EF-G–GTP—which is unknown—and of the ternary complex are relevant; they both bind. Furthermore, Nissen *et al.* suggest that EF-G–GTP ought to resemble EF-Tu–GDP, and if EF-G–GTP is as different from EF-G–GDP as EF-Tu–GTP is from EF-Tu–GDP, the case for molecular mimicry could disappear entirely.

It seems at least equally plausible that EF-G–GTP will be found to differ only slightly from EF-G–GDP; it also will mimic the ternary complex. If this is so, binding of both EF-G–GTP and the ternary complex could facilitate changes in ribosomal state by stabilizing the transition state that separates them. Because the conformation of that state is independent of the direction of the state change, the similarity of EF-G and the ternary complex makes sense in this context.

Clearly, the structure of EF-G complexed with GTP is needed more than ever, and it is critically important that the step in elongation where the post- to pretranslocational change occurs be identified. Since, as the Aarhus group points out, molecular mimicry could also be involved in the activities of initiation and termination factors, research in these areas may also prove illuminating.

References

1. P. Nissen *et al.*, *Science* **270**, 1464 (1995).
2. M. Kjeldgaard, P. Nissen, S. Thirup, J. Nyborg, *Structure* **1**, 35 (1993).
3. H. Berchtold *et al.*, *Nature* **365**, 126 (1993).
4. A. Aevarsson *et al.*, *EMBO J.* **13**, 3669 (1994).
5. J. Czworkowski, J. Wang, T. A. Steitz, P. B. Moore, *ibid.*, p. 3661.
6. Y. Kaziro, *Biochim. Biophys. Acta* **505**, 95 (1978).
7. A. S. Spirin, *Prog. Nucleic Acids Res. Mol. Biol.* **32**, 75 (1985).
8. M. Kjeldgaard and J. Nyborg, *J. Mol. Biol.* **223**, 721 (1992).
9. H. F. Noller, *Annu. Rev. Biochem.* **60**, 191 (1991).

The United Nations Climate Convention: Unattainable or Irrelevant

Pekka E. Kauppi

"The ultimate objective of this Convention and any related legal instruments that the Conference of the Parties may adopt is to achieve, in accordance with the relevant provisions of the Convention, stabilization of greenhouse gas concentrations in the atmosphere at a level that would prevent dangerous anthropogenic interference with the climate system (1)."

According to general circulation models (GCMs), a doubling of atmospheric CO_2 concentration would increase the global mean temperature by 1.5° to 4.5°C (*2–4*). This change would be dangerous in drought-prone regions and low coastal areas. Although other regions might benefit and the net global effect could be positive, some would suffer.

The United Nations Convention as quoted above tries to maintain the status quo by protecting the losers and minimizing the immense risks of global climate change. Although laudable, the specific wording of the "ultimate objective" does not express these aims correctly and realistically.

The atmospheric concentration of CO_2 was stable at 280 ± 5 parts per million (ppm) for 1000 years before the year 1800, according to ice-core records. As a result of human-made emissions, it has now increased by about 30% above this baseline (*5*). The current population of about 6 billion people emits about 6 billion tons of carbon into the atmosphere per year (*6*). A population of 10 billion people, projected for the year 2030 (*7*), would emit 10 billion tons if consumption patterns do not change.

The concentration of CO_2 started increasing in the 19th century according to ice-core records, although the human-made emissions were on the order of only 1 billion tons (*5*). If the aim is to stabilize the CO_2 concentration, annual emissions of less than 1 billion tons are therefore probably required; emissions must certainly be less than 2 billion tons per year.

With the current pattern of fossil fuel use, the population trend, and the trends in per capita emissions of CO_2 (*6*), a level of emissions as low as 1 to 2 billion tons annually will not be reached in the next 50 years. A mere stabilization of emissions at the current level of 6 billion tons would be an achievement (*8*).

To avoid danger, greenhouse gas concentrations would need to be stabilized at a level less than double the preindustrial value. However, reasonable emission scenarios indicate that a doubling of the greenhouse gas concentrations is inevitable in the 21st century. If the GCM projections are right, the climate will change, there will be dangerous effects, and the Convention objective will be unattainable.

Although the latest analyses suggest otherwise (*4*), let us assume that the GCM projections are wrong. If the climate dynamics are such that strong negative feedback prevents the doubling of greenhouse gas concentrations from inducing significant changes in climate, there will be no dangerous impacts. In that case, there is no need to control the greenhouse gas emissions, and the Climate Convention is irrelevant.

As phrased, the "ultimate objective" is either unattainable or irrelevant. We can all wish that it were irrelevant. More likely, however, it is relevant but unattainable.

The author is in the Finnish Forest Research Institute, Unioninkatu 40A, Fin-00170 Helsinki, Finland.

References and Notes

1. *U. N. Framework Convention on Climate Change* (United Nations, New York, 1992).
2. J. F. B. Mitchell, S. Manabe, V. Maleshko, T. Tokiota, in *Report Prepared for IPCC by Working Group I*, J. T. Houghton, G. J. Jenkins, J. J. Ephraums, Eds. (IPCC, Cambridge Univ. Press, Cambridge, 1990), pp. 131–172.
3. J. F. B. Mitchell, T. C. Johns, J. M. Gregory, S. F. B. Tett, *Nature* **376**, 501 (1995).
4. T. M. L. Wigley, *ibid.*, p. 463.
5. U. Siegenthaler and J. L. Sarmiento, *ibid.* **356**, 119 (1993); U. Siegenthaler and H. Oeschger, *Tellus* **39**, 140 (1987).
6. G. Marland, R. J. Andres, T. A. Boden, in "Trends '93: A Compendium of Data on Global Change," *ORNL/CDIC-65*, T. A. Boden, D. P. Kaiser, R. J. Sepanski, F. W. Stoss, Eds. (Carbon Dioxide Information Center, Oak Ridge National Laboratory, Oak Ridge, TN, 1994), pp. 505–584.
7. World Resources Institute, *World Resources, 1994–1995: A Guide to the Global Environment* (Oxford Univ. Press, New York, 1994).
8. J. Alcamo *et al.*, in *Climate Change* 1994, J. T. Houghton *et al.*, Eds. (IPCC, Cambridge Univ. Press, Cambridge, 1995), pp. 247–304.

The Interstellar Carbon Budget and the Role of Carbon in Dust and Large Molecules

Theodore P. Snow* and Adolf N. Witt

Published data on stellar composition show that carbon in the sun is substantially more abundant than in other stars. A carbon abundance of 225 carbon atoms per 10^6 hydrogen atoms is representative of galactic stars, whereas published values for the sun range from 350 to 470 carbon atoms per 10^6 hydrogen atoms. Other elements are also present in enhanced quantities in the solar system, consistent with suggestions that a supernova event was closely associated with the formation of the solar system. The overabundance of carbon in the solar system has many important implications, including new constraints on nucleosynthesis models for supernovae and substantial modification of the so-called "cosmic" composition normally adopted in discussions of galactic and interstellar abundances. A reduction in the galactic carbon budget, as suggested by the stellar composition data, strongly constrains the quantity of carbon that is available for the formation of interstellar dust, and some dust models now appear implausible because they require more carbon than is available.

Carbon is essential to many physical and chemical phenomena on Earth and in the universe. It dominated the chemistry of our early atmosphere and is still the major atmospheric constituent on the other terrestrial planets; it forms the basis for biology on Earth; and in stars and interstellar space it is one of the most abundant and important elements. In stars carbon is a stepping stone to the formation of heavy elements, and in space carbon governs physical and chemical processes and probably forms the basis for interstellar dust, itself the precursor to newly forming solar systems. Therefore, it is important for us to know how much carbon there is in the universe.

The quantity of carbon available in the diffuse interstellar medium (ISM) for the formation of dust and large molecules is constrained by the quantity that is depleted from the interstellar gas. The amount depleted is inferred from a combination of measured gas-phase column densities and an assumed standard or "cosmic" carbon abundance. Recent developments have improved the accuracy of measured atomic carbon column densities while at the same time calling into question the cosmic carbon budget. Here, we analyze these recent developments, offer a recommendation for the values that should be accepted, and examine the impact on current models and hypotheses for the content of the dust and large molecules in the diffuse ISM.

T. P. Snow is at the Center for Astrophysics and Space Astronomy, University of Colorado, Boulder, CO 80309, USA. A. N. Witt is at the Ritter Observatory, University of Toledo, Toledo, OH 43606, USA.

*To whom correspondence should be addressed.

The Cosmic Carbon Budget

Astronomers tend to assume that the solar system was formed from material that is representative of the galaxy in general, and therefore we generally use solar abundances of the elements in establishing the standards for other stars and the ISM; that is, we assume that the sun represents cosmic abundances of the elements. However, doing so involves underlying assumptions that are rarely questioned, and the material in the sun's atmosphere and elsewhere in the solar system may not be representative of other nearby stars or of the diffuse ISM.

The solar abundance of carbon. It has been common usage to refer to solar elemental abundances and cosmic relative abundances interchangeably, even though solar abundances appear to be anomalous in several respects. Lambert (*1*) reported a solar carbon abundance of 468 C atoms per 10^6 H atoms; this early reference was used as an underpinning for models of interstellar dust containing substantial carbon or graphite components. A frequently used recent reference for the solar carbon abundance is Grevesse *et al.* (*2*), who reported 400 C atoms per 10^6 H atoms, with an uncertainty of ~50 C atoms per 10^6 H atoms. This value was found very consistently in a series of independent studies of lines from various carbon-bearing systems: CH (104 lines), C_2 Swan (20 lines), C_2 Phillips (20 lines), CH (A-X) (9 lines), C I (19 lines), and [C I] (1 line). The common feature in these analyses was a solar photospheric model by Holweger and Mueller (*3*). This solar model has recently been updated because of a reduction in the photospheric abundance of iron (from 47 to 32 Fe atoms per 10^6 H atoms) as a consequence of improved atomic data, particularly the oscillator strengths (f values) of the lines. For the same reason, the abundance of carbon calculated from C I lines has been revised to 355 C atoms per 10^6 H atoms (*4*). Studies of the other carbon systems confirm this number (*5*). Table 1 lists various determinations of the solar carbon abundance.

Carbon abundances in young stars. The sun formed about 4.6 billion years ago (Ga). Simple models for galactic chemical evolution suggest that the relative abundance of carbon in the sun might be indicative of conditions in the galactic ISM at 4.6 Ga, and that today, as a result of ongoing chemical evolution, the carbon abundance in the ISM might well exceed the solar value. According to these models, the current ISM should have heavy element abundances 30% greater than the solar value. However, observational evidence does not support this notion; rather, the opposite seems to be true.

Recently formed stars might be more meaningful sources of information about the true cosmic carbon abundance, provided several conditions are met: (i) Mass loss has been insignificant, so that photospheric abundances still reflect the original composition. (ii) The results of internal nuclear processing have not contaminated the surface layers. (iii) The photospheric physics is well represented by current local and nonlocal thermodynamic equilibrium (LTE and NLTE) models. Main-sequence B stars generally satisfy these conditions. A study of early-B main-sequence stars by Gies and Lambert (*6*) yielded a mean NLTE abundance of $160 \pm {}^{70}_{50}$ C atoms per 10^6 H atoms (*7*). Cunha and Lambert's more recent investigation of 18 early-B main-sequence stars in the Orion association (*8*) produced a carbon abundance of 229 ± 34 C atoms per 10^6 H atoms, which is marginally consistent with the Gies and Lambert results, although both are substantially below even the most recently revised solar value of 355 ± 50. Other studies of field B stars also revealed reduced carbon abundances relative to the sun; Kilian (*9*) and Adelman *et al.* (*10*), in studies including some 30 stars in all, found an average carbon abundance of 195 C atoms per 10^6 H atoms. Analyses of B stars in clusters show similar results. The galactic cluster NGC 6231 has been particularly well studied (*11*) and shows a carbon abundance of 234 C atoms per 10^6 H atoms. Similarly, the clusters NGC 6611, S 285, and S 289 have values of 195, 120,

and 380 C atoms per 10^6 H atoms (*12*). The average for all studies of these clusters is 232 C atoms per 10^6 H atoms.

An analysis of young, later-type stars might be a useful way to determine whether systematic errors arise from the differences in physics between the B-star atmosphere models and the solar photospheric model. Luck (*13*) derived elemental abundances in 40 late-type stars, ranging in age from 0.012 to 1.4 Ga, in eight open clusters within 1 kpc of the sun. These stars included main-sequence stars, giants, and supergiants of spectral types F through K. The carbon abundances were derived from six indicators: four lines of C I (5052, 5380, 7110, and 8335 Å), one line of [C] (8727 Å), and one line of C_2 (5135 Å). The mean carbon abundance for the entire sample was $214 \pm \frac{150}{100}$ C atoms per 10^6 H atoms. The relatively large uncertainty makes this result consistent with both the B-star results and the solar abundance, but when CNO abundances are combined, the late-type stars in these young clusters appear to be deficient in CNO relative to the sun; their CNO abundances are much more consistent with those of the B stars.

Another check on the consistency of the solar carbon abundance with respect to that of other stars of similar type and history was recently provided by Tomkin *et al.* (*14*), who dealt with the carbon abundance in 107 field F and G disk dwarfs. The metallicity range in these stars, $-0.8 \leq$ [Fe/H] ≤ 0.2, reflects a range of ages or chemical environments. One interesting result of Tomkin *et al.* is that for stars within a given range of galactocentric distance, the increase in carbon abundance with decreasing stellar age (as measured by comparing the stars' positions in the magnitude–effective temperature diagram with theoretical isochrones) is either marginal or nonexistent. The mean carbon abundance among these 107 F and G dwarfs is 202 C atoms per 10^6 H atoms.

The uncertainties in the derivations of stellar abundances can be quite large (the errors quoted in the papers cited here are sometimes as large as ± 0.3 log units, but uncertainties on the order of ± 0.1 log units are more common). Thus, individual measures of the carbon abundance can be incorrect by as much as a factor of 2, whereas the more typical errors are 25% or so. Combining these uncertainties with the range of values (hence uncertainties) in the measured solar carbon abundance might allow for consistency between the sun and other stars. However, when the overall trend is considered or when averages of all the various measurements are calculated, there is no escaping the conclusion that the carbon abundance in the sun is much greater than in other stars.

The comparison of values for the solar carbon abundance with values for stars that should have similar or greater carbon abundances leads to a consistent and very interesting result: The sun appears to have an exceptionally large carbon abundance for a star of its age and position in the galaxy. There is no indication that the solar carbon abundance is in any way typical of the interstellar environment from which a large number of comparison objects have formed.

Carbon abundances in nebulae. Gaseous nebulae, especially the Orion nebula, afford yet another way to assess the carbon abundance in the current ISM near the solar neighborhood. However, several problems are inherent in this approach. We know that H II regions, and especially the Orion nebula, contain dust. Depending on whether the dust/gas ratio is normal or subnormal, a substantial fraction of the heavy elements—possibly including carbon—might be depleted and reside in the dust grains. On the other hand, regions of massive star formation such as the Orion region may have experienced fairly recent supernova explosions. The resulting enrichment with heavy elements (*15*, *16*) could therefore distort the relative abundances of these elements. Several recent studies have provided values for the carbon abundance in the Orion nebula (Table 1). These values resulted from analysis processes that were affected by particular assumptions about temperature fluctuations in the ionized gas. The range of these values probably reflects the status of the certainty of such assumptions more than it reflects observational uncertainties. With these reservations, we conclude that the Orion nebula abundances are probably consistent with the abundances found in the Orion B stars (*8*); however, with respect to CNO abundances, the Orion nebula seems to be deficient in these elements relative to the sun.

Galactic chemical evolution and the cosmic carbon abundance. The various indicators discussed above suggest a local cosmic carbon abundance of $\sim 225 \pm 50$ C atoms per 10^6 H atoms, which is some 63% of the most recently determined carbon abundance in the sun. How can we reconcile this finding with current theories and observations relating to galactic chemical evolution? The "simple" model of galactic chemical evolution, which assumes a closed box, instantaneous mixing, and instantaneous recycling (*17*), would predict an opposite result; that is, the carbon abundance should increase monotonically with time. This simple model is not only inconsistent with solar data but also with the two principal observational constraints for chemical evolution models: the age-metallicity relation (*18–20*) and the abundance distribution function of long-lived stars formed in the vicinity of the solar annulus (*21*). The spread in metallicities in a given age bracket in the F-star data (*19*) is well in excess of observational uncertainties, and so is the spread in the age-metallicity relation for nearby clusters (*22*). A study of 189 field F and G dwarfs shows that considerable variation exists in the metallicities of stars formed in a given time in the disk (*23*). The abundance distribution function of G dwarfs in the solar neighborhood exhibits a deficiency of low-metallicity stars that deviates from the predictions of the simple model by nearly two orders of magnitude (*24*).

We are thus forced to consider inhomogeneous chemical evolution models that incorporate the effects of self-enrichment of star-forming regions (*15*, *16*, *25*), realistic time scales for the dispersal of nuclear evolution products, infall of metal-poor gas from the galactic halo, and temporary removal of enriched gas from the star-forming state. Such models have been developed (*24*, *26*, *27*). The time scales for various mixing mechanisms in the ISM depend on the length scale considered (*27*). On intermediate galactic scales of 10^2 to 10^3 pc, efficient mixing can be expected only after $\sim 10^8$ years. This period is long compared to the time scale of triggered star formation in giant molecular clouds, which can then lead to localized enrichment with heavy elements; this enrichment is not communicated to other regions until much later, and then only in a severely diluted form.

Considerable evidence for such processes has emerged. Rolleston *et al.* (*28*), who investigated the metal abundance of several open clusters at a galactocentric distance of 13 kpc but situated within 1 kpc of each other, found abundance differences of as much as a factor of five. The CNO abundances in the Orion OB association show that the substantially greater scatter in the oxygen abundance among the stars of the Orion OB association, relative to the distributions of the carbon and nitrogen abundances, is to be interpreted as the result of local inhomogeneities in the oxygen abundance caused by supernovae among the massive stars in the association (*8*). The stars with the greatest oxygen abundances are tightly clustered at one end of the association and are spatially distinct from the other stars.

The age-metallicity relation for stars in the solar circle shows that the sun has one of the highest ratios of Fe/H among these stars, some of which are only half the solar age [figure 31 of (*23*)]. All the evidence discussed so far suggests that the sun was formed in a chemically enriched environment of limited spatial extent, possibly as a result of a triggered star formation process. As a result, the sun inherited a greater heavy element abundance than normal for stars forming at that time. The local ISM

may have undergone an evolutionary history that could well have included infall of metal-poor gas from the galactic halo, and the currently observed abundance differences between the sun and stars formed from the local ISM more recently (*29*) may be one result.

Adopted carbon abundance. The wide variation in values for the C/H ratio creates substantial uncertainty in deciding what cosmic value to adopt. The data in Table 1 strongly suggest that the preferred value should be smaller than the canonical 400 C atoms per 10^6 H atoms, and probably also considerably smaller than the solar value of 355 C atoms per 10^6 H atoms adopted by Grevesse *et al.* (*5*). We believe the evidence points toward a value in the range of 200 to 250 C atoms per 10^6 H atoms, and we adopt a value of 225 ± 50 C atoms per 10^6 H atoms. On the logarithmic scale (relative to 10^{12} H atoms) that is often used, this corresponds to a value of 8.35 ± 0.10. The value we infer for the C/H ratio implies that interstellar carbon depletions have been overestimated; that is, there is not as much carbon missing from the gas phase as is commonly supposed. The data also offer the unsettling suggestion that the cosmic carbon abundance may, in fact, be locally variable on distance scales that are comparable to or less than typical lines of sight to reddened stars.

Implications for the Solar System and for Other Planetary Systems

The enhanced carbon abundance in the solar system may have resulted from a particular event. It has long been suggested that the formation of the solar system was associated with a nearby type II supernova, the collapse and explosion of a massive star (*16*, *25*). This suggestion originally was based on an enhanced oxygen abundance in the solar system and was supported by high values for other elements such as iron. However, these suggestions did not necessarily include carbon among the elements that would have been enhanced, because nucleosynthesis theory indicates that most of the carbon formed in the interior of a massive star during its lifetime would be destroyed in the supernova explosion. The destruction mechanism is the α-capture reaction $^{12}C + \alpha \rightarrow {}^{16}O$, which is thought to consume nearly all the ^{12}C; however, the cross section for this process is poorly known, and the uncertainties in its value allow for a substantial quantity of ^{12}C to survive. Although recent experimental evaluations of the cross section (*30*) have refined its value, it is still imprecisely known because only one of the two major contributing terms to the cross section could be measured in the experiments. However, the carbon produced in type II supernovae is expected to be in the isotopic form ^{12}C, whereas carbon produced from less massive stars through the CNO cycle and expelled into the ISM by stellar winds should be dominated by ^{13}C. The solar system has a higher $^{12}C/^{13}C$ ratio than does the general ISM, which supports the notion that a supernova event contributed to the carbon budget in the solar system.

Supporting evidence for this view comes from the study of isotopic ratios in carbonaceous inclusions in meteorites. In recent reviews, Ott (*31*) and Anders and Zinner (*32*) have shown that the $^{12}C/^{13}C$ ratio ranges from ~2 to several thousand for small (~1 μm) graphitic inclusions in meteorites. A very recent analysis (*33*) confirms these results for the carbon isotopic ratio and extends them to isotopes of nitrogen and oxygen, all of which show anomalies in meteoritic inclusions that are consistent with an origin in massive stars. The high values for the $^{12}C/^{13}C$ ratio presumably represent carbon that has come directly from supernovae, with virtually no contribution from stellar winds. Therefore, the presence of particles with such isotopic ratios in the solar system specifically suggests that a supernova event may have played a role in the formation of the system.

If the solar system formed in a carbon-rich environment, we may expect that other planetary systems had lower carbon budgets available to them during their formation. Thus, the role of carbon in planetary atmospheres might be substantially different in other systems and could have an effect on planetary surface conditions. Although carbon dominates the atmospheres of Venus and Mars and played a strong role in the early evolution of Earth's atmosphere, on the terrestrial planets of other stars we may find carbon to have been less important. However, if the hypothesis that the carbon on Earth came primarily from cometary accretion (*34*) is correct, such a process might have the effect of concentrating carbon on the terrestrial planets of other stars even if the initial system carbon abundance was lower than in the solar system. Thus, it is not clear that the formation of carbon-based organisms in other planetary systems would be adversely affected by a lower overall carbon budget. The evolution of planetary atmospheres and of life in the context of a reduced carbon abundance is an area that deserves further attention.

The Abundance and Depletion of Gas-Phase Carbon

Before the Hubble Space Telescope (HST) was operational, most measures of carbon abundance in the diffuse ISM came from observations of C II lines with the Copernicus satellite (*35*, *36*). Two strong lines were available to Copernicus, at 1036.3367 and 1334.5323 Å. Both lines were always highly saturated, even in lightly reddened stars, and this seriously compromised the accuracy of the results. The 1036 Å feature has a large damping constant and displays damping wings in many cases, but because of confusion with the (5,0) Lyman band of H_2, few accurate column densities were derived from this line. The 1334 Å feature has no redeeming characteristics. However, there is a very weak, spin-forbidden line at 2325.403 Å, which should almost never be saturated in diffuse-cloud lines of sight. Hobbs *et al.* (*37*) were the first to take advantage of this phenomenon; they used a special observing technique with the noisy V1 phototube on Copernicus to marginally detect the line toward δ Sco. Later, Welty *et al.* (*38*) added further upper limits toward other stars with the use of data from the International Ultraviolet Explorer, but those limits were not restrictive and shed little light on the interstellar carbon budget.

The Goddard High Resolution Spectrograph on the HST has superior sensitivity, resolution, and signal-to-noise characteristics and has proven to be capable of detecting the C II] line. It was first detected in ξ Per (*39*) and then in ζ Oph (*40*) but has been pursued in only a few other cases (*41*). Column densities derived from this line are sensitive to uncertainties in its *f* value, but recent laboratory measurements of the lifetime of the upper state (*42*) and the relative line transition probabilities within the multiplet (*43*) have reduced the uncertainties. Only two definite and accurate detections

Table 1. Estimates of the cosmic carbon abundance.

Environment	Carbon abundance (C atoms per 10^6 H atoms)	Reference
Sun	370	(*65*)
	370	(*66*)
	468	(*1*)
	363	(*67*)
	400	(*2*)
	355	(*5*)
	355	(*4*)
Main-sequence B stars	160	(*6*)
Orion B stars	229	(*8*)
Field B stars	157	(*9*)
	218	(*10*)
B stars in NGC 6231	234	(*11*)
B stars in other clusters	213	(*12*)
Young late-type stars	214	(*13*)
F and G disk dwarfs	202	(*14*)
Orion nebula	214	(*68*)
	339	(*69*)
	282	(*70*)
	332	(*71*)
Recommended interstellar value	225 ± 50	

of the weak C II] line on the basis of HST data have been published to date, bringing to only three the total number of sight lines that have reasonably accurate gas-phase carbon abundances. A fourth line of sight, toward the distant O9.5Ib supergiant HD 154368, has been analyzed with the use of HST data, but the weak 2325 Å line was not clearly detected, and the derived column density was augmented by the analysis of damping wings on the strong 1334 Å line (*41*). The result, though less certain than in the cases where the weak line was cleanly detected, is consistent with those cases.

The best values for interstellar gas-phase carbon are shown in Table 2, which also includes the number of C atoms per 10^6 H atoms in the interstellar gas and the number available for the formation of dust or large molecules (on the basis of our adopted value of 225 ± 50 C atoms per 10^6 H atoms). The implied depletions are indeed smaller than previously assumed, although in their depletion study Sofia *et al.* (*7*) did include calculations on the basis of the lower cosmic carbon abundance implied by B stars. With the exception of ξ Per, the numbers show that only about one-third of the cosmic carbon is missing from the gas; that is, less than ~100 C atoms per 10^6 H atoms are available for dust and molecules. Oddly enough, for ξ Per, the carbon abundance is actually slightly greater than the cosmic value, indicating virtually no depletion for this line of sight. This anomaly was discussed in some depth by Cardelli *et al.* (*40*), who attempted possible explanations on the basis of the partial destruction of the dust grains toward ξ Per. However, they omitted from their discussion the possibility that this star lies behind a carbon-enriched region as a result of the evolution of massive stars, as may be implied by its association with a well-known supernova shell (*44*). The case of ξ Per suggests again that cosmic carbon abundances may vary with location. The H I data on ξ Per should be reexamined to double-check the column density from Bohlin *et al.* (*45*) for any possibility that the inferred low depletion of carbon is the result of an error in the hydrogen column density. Despite the difficulty in assessing accurate carbon depletions in individual cases, we argue that the low depletions implied by the carbon abundance in young stars are a realistic indication of the general state of the diffuse ISM, and that this must be taken into account by models of dust and large molecules that depend on carbon.

Carbon in Dust and Molecules: Constraining the Models

Whittet (*46*) attempted to constrain dust models on the basis of what was then known about the cosmic carbon abundance and the depletion of carbon from the interstellar gas onto the dust. His database came from Copernicus satellite observations of neutral atomic carbon (*47*), which can be accurately measured but requires a large correction for ionization to derive the quantity of ionized carbon, which is far more abundant. Whittet was ultimately unable to limit the allowed models for the dust because of the large uncertainties in the observed quantity of gaseous carbon. The HST has now provided more accurate measurements of ionized carbon, and we used these new values, along with our revised value for the cosmic carbon abundance, to reexplore the dust models.

Published models of specific spectral features are summarized in Table 3, which shows the quantity of carbon (relative to 10^6 H atoms) required to reproduce the observed features. A number of interesting conclusions can be reached. Most of the spectral features considered [the unidentified infrared emission features (UIRs), the 3.4-μm absorption attributed to hydrocarbons on dust grains, the 2175 Å extinction bump, and the optical diffuse interstellar bands (DIBs)] can be produced by the available carbon, even with the low value we have adopted for the cosmic carbon abundance. Only models for the 3.4-μm hydrocarbon absorption become implausible; for example, the amorphous carbon model of Adamson *et al.* (*48*) and possibly the coal model of Papoular *et al.* (*49*) apparently demand more carbon than is available. Thus, our revised value for the cosmic carbon abundance may rule out this class of models.

The 3.4-μm feature has been studied both in dense clouds and in the diffuse ISM (*50–52*), and it shows somewhat different behavior in dense and diffuse regions. In the diffuse-cloud lines of sight that have been studied, clear signatures of aliphatic structures (containing subgroups of $-CH_2$ and $-CH_3$) are seen in the band profile, whereas the dense clouds show featureless profiles thought to be caused by more amorphous hydrocarbons. The column density estimates are more secure for the diffuse clouds, and they show that a rather small fraction of the cosmic carbon is needed, even with our revised value.

Table 2. Measurements of the C II] 2325 Å line. Values for the number of C atoms per 10^6 H atoms that are available for dust and molecules are for conditions where the cosmic abundance of carbon is 175 to 275 C atoms per 10^6 H atoms.

Star	C (atoms cm^{-2})	H (atoms cm^{-2})	Carbon abundance (C atoms per 10^6 H atoms)		Reference
			As atomic gas	Available for dust and molecules	
ξ Per	5.1×10^{17}	2.0×10^{21}	262	−87 to 13	(*39*)
δ Sco	2.2×10^{17}	1.5×10^{21}	149	26 to 126	(*35*)
ζ Oph	1.9×10^{17}	1.4×10^{21}	134	41 to 141	(*40*)

Table 3. Carbon required for observed spectral features.

Feature	Assumed carrier	Carbon abundance (C atoms per 10^6 H atoms)	Reference
UIR emission	Hot gas-phase PAH ions	4	(*72*)
		4 to 15	(*73*)
		65	(*74*)
	Hot solid PAH (anthracene)	26	(*75*)
3.4-μm absorption	Amorphous carbon on grains	290	(*48*)
	Aliphatic hydrocarbon on grains	96	(*76*)
		11 to 154	(*50*)
3.3-μm absorption	Cold PAHs in diffuse ISM	15 to 20	(*51*)
4.67-μm absorption	Solid CO	9	(*77*)
DIBs (all)	PAHs in HAC; $f = 10^{-2}$	$0.3m$*	(*78*)
DIB λ4430	Ionized pyrene	<1	(*79*)
DIB λ7141	Ionized naphthalene	<2	(*80*)
DIB λ4430	Ionized methyl pyrene	<1	(*81*)
DIBs λλ9577, 9632	C_{60}^+	<1	(*82*)
2175 Å bump	Amorphous carbon	70	(*83*)
	Small graphite grains	60	(*84*)
	Anthracite (coal)	106	(*49*)

*In this model, m represents the average number of carbon atoms per DIB carrier. For moderate-sized PAHs, m would be in the vicinity of 20.

The DIBs are of some interest because of the recent consensus that they must be formed by large carbonaceous molecules (*53*). There are now nearly 200 recognized bands throughout the optical and near-infrared, and they certainly do not all arise from a single carrier. Among the popular current suggestions are ionized polycyclic aromatic hydrocarbons (PAHs), ionized fullerenes, and carbon chain molecules, all of which are dominated by carbon. Even with our revised value for the cosmic carbon abundance, there appears to be no difficulty in producing the observed spectrum of bands. All of the models for spectral features that invoke PAH molecules require only modest fractions of the overall carbon budget, although this becomes potentially problematic when the enormous number of possible PAH forms is summed. However, spectroscopic considerations suggest that by some mechanism a limited number of PAHs must be selected in the ISM; if so, then there appears to be no abundance problem with invoking PAHs as the carriers of the UIRs and the DIBs, nor is the possible detection of cold gas-phase PAH absorption (*51*) ruled out.

The question of explaining the general extinction curve by various models presents more difficulties. Table 4 shows that several such models can be ruled out, or at least cast into doubt, by the revised cosmic carbon abundance value. All of the models that invoke hydrogenated amorphous carbon (HAC) to explain the general extinction lose credibility; this is potentially very important because HAC has been suggested as the explanation for other phenomena, such as the extended red emission (ERE) (*54*). These models generally postulate core-mantle dust grains, with HAC (or any icy mantle including hydrocarbons) overlying silicate cores, and they have a long heritage (*55*). However, there is just enough uncertainty in both the required quantity of carbon in HAC and the cosmic carbon abundance to leave some room for these models to fit, and therefore further scrutiny is warranted.

It also appears difficult to attribute the general extinction to the presence of graphite. Graphite can produce the 2175 Å bump without encountering abundance constraints (Table 3), but in light of our revised cosmic carbon abundance value, it does not seem to be responsible for the general extinction. This implication contradicts the graphite-plus-silicate scenario of Draine and Lee (*56*) [which is based on the earlier Mathis *et al.* (*57*) model] as well as the recent work of Aanestad (*58*), who was able to reproduce observed extinction curves very accurately with a mixture of large and small graphite grains, large and small silicate grains, and gas-phase PAHs. Our results suggest that graphite may well be the carrier of the 2175 Å bump but that it probably does not also produce the general extinction.

The composite "fluffy grain" model of Mathis and Whiffen (*59*) also appears to be untenable with respect to the revised cosmic carbon abundance value. This model calls for dust grains made of small particles stuck together in an amorphous matrix, with a large fraction of the volume in vacuum, and it has many attractive features. It uses graphite to form the 2175 Å bump and amorphous carbon for the general ultraviolet (UV) extinction. The models that do appear to fit into our revised carbon budget are those that call for a combination of graphite and amorphous carbon grains (*60*, *61*) or a combination of PAH and graphite grains (*62*), but substantial questions remain, particularly concerning the absorption efficiency of the amorphous forms of carbon.

Table 4. Carbon required for selected general extinction models.

Model	Carbon abundance (C atoms per 10^6 H atoms)	Reference
Graphite + silicates	≥240	(*57*)
Small carbon grains + carbon in mantles	280	(*55*)
HAC	130	(*85*)
HAC + graphite	185	(*86*)
HAC + solid PAH	185	(*87*)
PAH + graphite	101	(*62*)
HAC coatings on silicates	75 to 300*	(*86*)
Very small amorphous carbon grains + PAH	45†	(*60*)
Graphite + amorphous carbon grains	110	(*61*)
Composite grains	265	(*59*)
Graphite + silicates	300	(*56*)
Graphite, PAH, and silicate grains	180 to 295	(*58*)

*The range in values represents the contrasting requirement for carbon in HACs for low far-UV extinction and high far-UV extinction. †This model fits far-UV extinction and the 2175 Å bump only; additional carbon in the form of large grains may be needed to reproduce the visual extinction.

Discussion and Outlook

It is interesting that many of the same conclusions that we have reached concerning the carbon abundance may also be true of oxygen. One difficulty faced by interstellar dust models is that they fall far short of accounting for the large amounts of oxygen thought to be depleted from the interstellar gas; silicates are the major form suspected to be present in the dust, and the dust models generally do not require all of the available oxygen if the solar oxygen abundance is assumed. The quantity of oxygen tied up in water ice and in solid CO is also known, and it also falls short (*63*). Meyer *et al.* (*64*) recently noted that gas-phase absorption measurements of oxygen in the Orion region revealed abundances that were lower than the solar oxygen abundance; they attributed this finding to infall from the galactic halo of gas that is not enriched. An alternative explanation would be that Orion has "normal" oxygen whereas the sun is enriched, as was suggested more than a decade ago by Olive and Schramm (*16*).

With respect to the measurement of interstellar carbon, it is clear that further observations of the C II] line at 2325 Å are required, in view of the small number of sight lines for which data now exist and the apparent variation in the carbon depletion. A larger data set will help to establish the uniformity of the relatively small carbon depletion as a general diffuse ISM characteristic, to demonstrate whether the carbon depletion is in fact variable, and to explore whether and how the carbon depletion varies with the shape of the UV extinction curve, as some models predict.

Note added in proof: Cardelli *et al.* (*64a*) have measured the CII] line in a few additional lines of sight, with results similar to those reported here.

REFERENCES AND NOTES

1. D. L. Lambert, *Mon. Not. R. Astron. Soc.* **182**, 249 (1978).
2. N. Grevesse *et al.*, *Astron. Astrophys.* **242**, 488 (1991).
3. H. Holweger and E. A. Mueller, *Sol. Phys.* **39**, 19 (1974).
4. N. Grevesse and A. Noels, in *Origin and Evolution of the Elements*, N. Prantzos *et al.*, Eds. (Cambridge Univ. Press, Cambridge, 1993), pp. 15–25.
5. N. Grevesse, A. J. Sauval, R. Blomme, in *Infrared Solar Physics*, D. Rabin and T. J. Jeffries, Eds. (Kluwer Academic, Dordrecht, Netherlands, 1992), pp. 539–542.
6. D. R. Gies and D. L. Lambert, *Astrophys. J.* **387**, 673 (1992).
7. U. J. Sofia, J. A. Cardelli, B. D. Savage, *ibid.* **430**, 650 (1994).
8. K. Cunha and D. L. Lambert, *ibid.* **426**, 170 (1994).
9. J. Kilian, *Astron. Astrophys.* **262**, 171 (1992).
10. S. J. Adelman, R. D. Robinson, G. M. Wahlgren, *Publ. Astron. Soc. Pac.* **105**, 327 (1993).
11. J. Kilian, O. Montenbruck, P. E. Nissen, *Astron. Astrophys.* **284**, 437 (1994).
12. J. Kilian-Montenbruck, T. Gehren, P. E. Nissen, *ibid.* **291**, 757 (1994).
13. R. E. Luck, *Astrophys. J. Suppl. Ser.* **91**, 309 (1994).
14. J. Tomkin, V. M. Woolf, D. L. Lambert, M. Lemke, *Astron. J.* **109**, 2204 (1995).
15. H. Reeves, in *Protostars and Planets*, T. Gehrels, Ed. (Univ. of Arizona Press, Tucson, 1978), pp. 399–423.
16. K. A. Olive and D. N. Schramm, *Astrophys. J.* **257**, 276 (1982).
17. L. Searle and W. L. W. Sargent, *ibid.* **173**, 25 (1972); B. M. Tinsley, *Fundam. Cosmic Phys.* **5**, 587 (1980).
18. B. Twarog, *Astrophys. J.* **242**, 242 (1980); ——— and J. C. Wheeler, *ibid.* **261**, 636 (1982).
19. R. G. Carlberg, P. Dawson, T. Hsu, D. A. Vanden Berg, *ibid.* **294**, 674 (1985).
20. W. J. Schuster and P. E. Nissen, *Astron. Astrophys.* **222**, 69 (1989).
21. B. E. J. Pagel and B. E. Patchett, *Mon. Not. R. Astron. Soc.* **172**, 13 (1975); B. E. J. Pagel, in *Evo-*

lutionary Phenomena in Galaxies, J. E. Beckmann and B. E. J. Pagel, Eds. (Cambridge Univ. Press, Cambridge, 1989), pp. 201–223.
22. A. M. Boesgaard, *Astrophys. J.* **336**, 798 (1989).
23. B. Edvardsson *et al.*, *Astron. Astrophys.* **275**, 101 (1993).
24. G. Malinie, D. H. Hartmann, D. D. Clayton, G. J. Mathews, *Astrophys. J.* **413**, 633 (1993).
25. A. G. W. Cameron, P. Höflich, P. C. Meyers, *ibid.* **447**, L53 (1995).
26. L. Carigi, *ibid.* **424**, 181 (1994).
27. J.-R. Roy and D. Kunth, *Astron. Astrophys.* **294**, 432 (1995).
28. W. R. J. Rolleston, P. L. Dufton, A. Fitzsimmons, *ibid.* **284**, 72 (1994).
29. F. Matteuci and C. Chiosi, *ibid.* **123**, 121 (1983).
30. L. Buchmann *et al.*, *Phys. Rev. Lett.* **70**, 726 (1993); Z. Zhao *et al.*, *ibid.*, p. 2066.
31. U. Ott, *Nature* **364**, 25 (1993).
32. E. Anders and E. Zinner, *Meteoritics* **28**, 490 (1993).
33. S. Amari, E. Zinner, R. S. Lewis, *Astrophys. J.* **447**, L147 (1995).
34. C. Chyba and C. Sagan, *Nature* **355**, 125 (1992).
35. D. C. Morton, *Astrophys. J.* **197**, 85 (1975).
36. T. P. Snow, *ibid.* **204**, 759 (1976).
37. L. M. Hobbs, D. G. York, W. R. Oegerle, *ibid.* **252**, L21 (1982).
38. D. E. Welty, D. G. York, L. M. Hobbs, *Publ. Astron. Soc. Pac.* **98**, 857 (1986).
39. J. A. Cardelli *et al.*, *Astrophys. J.* **377**, L57 (1991).
40. J. A. Cardelli, J. S. Mathis, D. C. Ebbets, B. D. Savage, *ibid.* **402**, L17 (1993).
41. T. P. Snow *et al.*, *Astrophys. J.*, in press.
42. Z. Fang, V. H. S. Kwong, J. Wang, W. H. Parkinson, *Phys. Rev. A* **48**, 1114 (1993).
43. D. J. Lennon, P. L. Dufton, A. Hibbert, A. E. Kingston, *Astrophys. J.* **294**, 200 (1985).
44. R. Sancisi, in *Galactic Radio Astronomy*, F. J. Kerr and S. C. Simonson, Eds. (Reidel, Dordrecht, Netherlands, 1974), pp. 115–128.
45. R. C. Bohlin, B. D. Savage, J. F. Drake, *Astrophys. J.* **224**, 132 (1978).
46. D. C. B. Whittet, *Mon. Not. R. Astron. Soc.* **210**, 479 (1984).
47. E. B. Jenkins and E. J. Shaya, *Astrophys. J.* **231**, 55 (1979); E. B. Jenkins, M. Jura, M. Lowenstein, *ibid.* **270**, 88 (1983).
48. A. J. Adamson, D. C. B. Whittet, W. W. Duley, *Mon. Not. R. Astron. Soc.* **243**, 400 (1990).
49. R. Papoular, J. Breton, G. Gensterblum, I. Nenner, J.-J. Pireaux, *Astron. Astrophys.* **270**, L5 (1993).
50. S. A. Sandford *et al.*, *Astrophys. J.* **371**, 607 (1991).
51. Y. J. Pendleton, S. A. Sandford, L. J. Allamandola, A. G. G. M. Tielens, K. Sellgren, *ibid.* **437**, 683 (1994).
52. T. P. Snow, Y. Pendleton, T. R. Geballe, P. Jenniskens, A. G. G. M. Tielens, in preparation.
53. A. G. G. M. Tielens and T. P. Snow, Eds., *The Diffuse Interstellar Bands* (Kluwer, Dordrecht, Netherlands, 1995).
54. W. W. Duley, *Mon. Not. R. Astron. Soc.* **215**, 259 (1985); D. G. Furton and A. N. Witt, *Astrophys. J.* **415**, L51 (1993).
55. S. S. Hong and J. M. Greenberg, *Astron. Astrophys.* **88**, 194 (1980) and references therein.
56. B. T. Draine and H. M. Lee, *Astrophys. J.* **285**, 89 (1984).
57. J. S. Mathis, W. Rumpl, K. H. Nordsieck, *ibid.* **217**, 425 (1977).
58. P. A. Aannestad, *ibid.* **443**, 653 (1995).
59. J. S. Mathis and G. Whiffen, *ibid.* **341**, 808 (1989).
60. F.-X. Désert, F. Boulanger, J. L. Puget, *Astron. Astrophys.* **237**, 215 (1990).
61. W. H. Sorrell, *Mon. Not. R. Astron. Soc.* **243**, 570 (1990).
62. J. Puget and A. Léger, *Annu. Rev. Astron. Astrophys.* **27**, 161 (1989).
63. D. C. B. Whittet, in *Dust and Chemistry in Astronomy*, T. J. Millar and D. A. Williams, Eds. (Institute of Physics, Bristol, UK, 1993), pp. 9–35.
64. D. M. Meyer, M. Jura, I. Hawkins, J. A. Cardelli, *Astrophys. J.* **437**, L59 (1994).
64a. J. Cardelli, D. M. Meyer, M. Jura, B. D. Savage, *Astrophys. J.*, in press.
65. G. L. Withbroe, in *NBS SP-353*, K. B. Gebbie, Ed. (Government Printing Office, Washington, DC, 1971), p. 127.
66. A. G. W. Cameron, *Space Sci. Rev.* **15**, 121 (1973).
67. E. Anders and N. Grevesse, *Geochim. Cosmochim. Acta* **53**, 197 (1989).
68. J. A. Baldwin *et al.*, *Astrophys. J.* **374**, 580 (1991).
69. R. H. Rubin, J. P. Simpson, M. R. Haas, E. F. Erickson, *ibid.*, p. 564.
70. R. H. Rubin, R. J. Dufour, D. K. Walter, *ibid.* **413**, 242 (1993).
71. R. H. Peimbert, P. J. Storey, S. Torres-Peimbert, *ibid.* **414**, 626 (1993).
72. L. J. Allamandola, A. G. G. M. Tielens, J. R. Barker, *Astrophys. J.* **290**, L25 (1985).
73. ———, *Astrophys. J. Suppl. Ser.* **71**, 733 (1989).
74. C. Joblin, A. Léger, P. G. Martin, *Astrophys. J.* **393**, L79 (1992).
75. W. W. Duley and A. P. Jones, *ibid.* **351**, L49 (1990).
76. A. G. G. M. Tielens and L. J. Allamandola, in *Interstellar Processes*, D. J. Hollenbach and H. A. Thronson, Eds. (Reidel, Dordrecht, Netherlands, 1987), pp. 397–469.
77. D. C. B. Whittet, A. J. Adamson, W. W. Duley, T. R. Geballe, A. D. McFadzean, *Mon. Not. R. Astron. Soc.* **241**, 707 (1989).
78. W. W. Duley, in (*53*), pp. 359–362.
79. F. Salama and L. J. Allamandola, *Astrophys. J.* **395**, 301 (1992).
80. ———, *Nature* **358**, 42 (1992).
81. A. Léger, L. d'Hendecourt, D. Défourneau, *Astron. Astrophys.* **293**, L53 (1995).
82. B. Foing and P. Ehrenfreund, *Nature* **369**, 296 (1994).
83. E. Busoletti, L. Colangeli, V. Orofino, *Astrophys. J.* **321**, L87 (1987).
84. B. T. Draine, in *Interstellar Dust*, L. J. Allamandola and A. G. G. M. Tielens, Eds. (Kluwer, Dordrecht, Netherlands, 1989), pp. 313–32.
85. W. W. Duley, *Mon. Not. R. Astron. Soc.* **229**, 203 (1987).
86. W. W. Duley, A. P. Jones, D. A. Williams, *ibid.* **236**, 709 (1989).
87. A. P. Jones, *ibid.* **247**, 305 (1990).
88. We thank D. N. Schramm for helpful comments. Supported by NASA grants NAGW-3600 (to the University of Colorado) and NAGW-3168 (to the University of Toledo).

Venus Reconsidered

William M. Kaula

The Magellan imagery shows that Venus has a crater abundance equivalent to a surface age of 300 million to 500 million years and a crater distribution close to random. Hence, the tectonics of Venus must be quiescent compared to those of Earth in the last few 100 million years. The main debate is whether the decline in tectonic activity on Venus is closer to monotonic or episodic, with enhanced tectonism and volcanism yet to come. The former hypothesis implies that most radioactive heat sources have been differentiated upward; the latter, that they have remained at depth. The low level of activity in the last few 100 million years inferred from imagery favors the monotonic hypothesis; some chemical evidence, particularly the low abundance of radiogenic argon, favors the episodic. A problem for both hypotheses is the rapid decline of thermal and tectonic activity some 300 million to 500 million years ago. The nature of the convective instabilities that caused the decline, and their propagation, are unclear.

Perceptions of Venus have changed significantly in the last 5 years, not only because of results returned by the Magellan spacecraft but also because of better experiments on the rheology of dry crustal rocks. As of 1990, it was generally but not universally agreed that plate tectonics was negligible on Venus, that Venus must have a stiff upper mantle, and that at least the northernmost 25% of the surface (the part observed by Venera orbiters) must average several 100 million years in age. The surface compositions measured at most Venera landing sites were considered to be consistent with a primitive basaltic crust, and two of the sites indicated further differentiations. The strength indicated by high depth/diameter ratios of craters was interpreted to limit the mean thickness of the crust to less than 20 km. Leading inferences in 1990 were (i) that Venus lacks water in its outer few hundreds of kilometers; (ii) that the energy delivery from the mantle must be less than Earth's, perhaps half as much; and (iii) that some appreciable energy sources persist at great depths to sustain the few great mountain complexes. The problem identified as the greatest was reconciling a voluminous crust with the indications of considerable strength at shallow depths of 20 to 100 km (*1*).

The most important data from Magellan radar imagery are the impact craters, of which 915 have been identified. They have an abundance indicating an average surface age of 300 million to 500 million years and a geographic distribution consistent with randomness on a global scale (*2*). Furthermore, the lack of clusters of older craters implies a rapid decline in the resurfacing of Venus, perhaps within a few tens of millions of years. Although more detailed examinations infer that Venus is not entirely dead (*3*), they generally confirm inferences from Pioneer Venus altimetry (*4*) that recent tectonic activity on Venus is slight compared to Earth's. An important general characteristic inferred from Magellan imagery is that deformation on Venus is distrib-

The author is in the Department of Earth and Space Sciences, University of California, Los Angeles, CA 90095, USA.

Table 1. Abundances of radioactive elements on Venus. The numbers are based on gamma ray spectrometry, except for Venera 13 and 14, for which x-ray fluorescence was used to measure K_2O and K/U = 9000; K/Th = 3000 has been assumed. N-MORB, normal midocean ridge basalt.

Landing site	K_2O (%)	K/U	K/Th	Heat generation (10^{-12} W kg^{-1})
Venera 8 (*12*)	5.0	18,000	6000	531
Venera 9 (*12*)	0.8	7800	1300	172
Venera 10 (*12*)	0.3	6500	4300	74
Venera 13 (*12*)	4.0			768
Venera 14 (*12*)	0.2			107
Vega 1 (*12*)	0.6	7000	3000	118
Vega 2 (*12*)	0.5	5900	2000	134
N-MORB (*13*)	0.09	15,000	5600	14

uted, with strain patterns extending hundreds of kilometers, rather than concentrated in relatively narrow zones, as on Earth (*5*). The Magellan imagery also raised some compositional problems, such as the nature and source of lavas creating long sinuous rills (*6*), which may relate to the mechanisms of the resurfacing, and the cause of the high radar reflectivity of upland regions (*7*), which constrains the subsequent rate of change in the surface of Venus.

Important new experimental data on the rheology of dry diabase (*8*) showed it to have a viscosity as high as that of dry olivine (*9*), although at strain rates 10 orders of magnitude greater than those inferred for Venus (*10*). This finding removed the constraint on crustal thickness from the high depth/diameter ratios of craters (*11*), which was based on earlier rheological experiments that apparently failed to dry out the specimens. It may also remove the need for deep convective sources to support the highland regions.

Several problems remain. Those that appear most important to the long-term evolution of Venus are as follows: (i) Can the quiescent tectonics of Venus be attributed to the differentiation of most of its radioactive heat sources up into the crust, thus reducing temperature gradients? (ii) Are the apparent stiffness of the venusian upper mantle and the slow time scale of its tectonics explicable by the lack of water? (iii) What mechanisms caused the apparent rapid decline in resurfacing at 300 million to 500 million years ago?

Evolution of the Venus Crust

A quiescent Venus could be explained by upward differentiation of the radiogenic elements K, U, Th, which are the principal heat sources, to the crust. The abundances of the radiogenic elements were measured at seven Venera and Vega landing sites (Table 1). The five sites with K_2O concentrations of less than 1% (*12*) are often dismissed as resembling terrestrial tholeiites. However, they are actually high in K, U, and Th content, not only in measured values compared to the most comparable Earth rocks (*13*) but also with respect to their formation and circumstances of measurement. Most of Venus appears to be resurfaced by lavas. The area-dominant lavas should be those of the lowest viscosity. Low viscosity basalts have basic compositions and thus low contents of the radiogenic elements, which are all large ion lithophiles. It is likely that the lander sites were selected to minimize the chance that the lander would tip over; thus, they would have been smooth areas, indicated by radar darkness. Such selection would cause a bias in favor of low viscosity basic lavas. All the lander sites, as analyzed on Magellan imagery, are indeed in radar dark areas (*14*). The most radioactive rocks on Venus, as on Earth, were probably produced by remeltings of crust, which, normally being smaller scale events, are more often plutonic than volcanic (*15*). The ratio of plutonism to volcanism plausibly increases with the decline in the level of activity and hence could be higher on quiescent Venus than on active Earth (*16*). Finally, Venus lacks the dominant process, erosion, that brings highly radioactive plutonic rocks to the surface of Earth; Venus exhibits only tectonism, which characterizes a minor fraction of the surface.

Turcotte (*17*) argued that packing radioactive elements into the crust would cause it to melt. This process would have been even more likely when the rate of heat generation was much higher—twice as much at 2.7 billion years ago. The resulting intracrustal differentiation would have been an effective mechanism for moving radioactive elements upward, leaving ample time for the crust to cool. The high surface temperature of Venus would have helped to reduce temperature gradients at depth, because of the strong positive temperature dependence of thermal conductivity above 500 K (*18*).

Thus, it is plausible for a Venus crust to evolve to a strong upward concentration of radioactive elements, with a maximum concentration a few kilometers below the surface because of the absence of erosion. This would have kept crustal temperatures low enough, and hence viscosities high enough (*8*), to ensure strong coupling of the dry crust to the dry lithosphere and hence to dry mantle. This coupling would inhibit broad-scale plate tectonics (*19*) and hence Earth-like subduction as a mechanism of crustal recycling. The evident mechanism of crustal recycling on Venus thus becomes the gabbro-to-eclogite transition (*20*), dependent on the phase transformation of low density feldspars to garnet. The resulting rock eclogite has a density higher than that of ferromagnesian silicates, which constitute the bulk of the mantle. Hence, this mechanism would cause detachment, and thus recycling, of crust. This transition occurs at depths of 50 to 70 km under Venus conditions, thus requiring a thick crust to be effective.

The main evidence contrary to this scenario of a high content of radiogenic elements in Venus's crust is the low abundance of radiogenic Ar, ^{40}Ar, in the Venus atmosphere, about one-third that of Earth (*21*). Although Venus does not exhibit erosion, which would release Ar from rocks, the temperatures of 740 K or more should cause Ar to diffuse easily. There are some explanations, such as intracrustal differentiations and nonrepresentativeness of the lander measurements, but none are fully persuasive (*22*).

Another consequence of intracrustal differentiation would be a reduction in the density of shallow crustal rocks compared to that of deep rocks, as occurs in Earth's continents, where shallow igneous layers are estimated to be less dense by at least 300 kg m^{-3} than typical oceanic crustal rocks. This mechanism appears essential to explain the highest region on Venus, Maxwell Montes. The radar imagery strongly indicates that Maxwell Montes was created by convergent flow (*23*). The revised diabase rheology (*8*) now predicts that the topographic height would take several 100 million years to slump away (*24*). Models that assume a crust of uniform lateral density cannot posit sufficient crust to compensate for the 10 km of topography by purely Airy isostasy within the gabbro-to-eclogite transition (*20*). But a model of convergent flow, followed by intracrustal differentiation to create a Pratt compensation, in which the more mafic component sinks below the position of the gabbro-to-eclogite transition, satisfies the topography and gravity quite well (*25*). The parallel ridge belts of about 20-km spacing, indicating instability of a competent layer over a weaker substratum (*26*), would have to be frozen in from the terminal phase of such an evolution. This crustal differentiation pertains to the support of regional features that are less than 1000 km in extent. Ishtar Terra as a whole

(as well as the edifices of Beta Regio and Atla Regio) must be supported by mantle mechanisms, thermal or compositional, because the apparent depths of compensation inferred from the long wavelengths of gravity and topography exceed 100 km (*25*).

Effects of Dryness on Tectonics and Mantle Convection in Venus

The high ratio of correlated gravity to topography on Venus, implying apparent depths of compensation of greater than 100 km in the long wavelengths, requires a strong coupling of the mantle to the lithosphere and hence no Earth-like asthenosphere (*19*). It was conjectured that this characteristic of Venus arose from a lack of water in its outer parts (*1*). Turcotte (*17*) has criticized this conjecture on the grounds that if Venus's mantle lacked water but still had a comparable amount of heat to lose, then it would merely heat up enough to lower the viscosity so as to ensure the necessary rate of convection. This is true to the zeroth order but is not applicable to the first-order problem of an asthenosphere, which is a quite distinct layer under Earth's oceans, being less viscous than both the material above it and the material below it. This property is sometimes ascribed to pressure release melting. But if all else were equal except surface temperature, as in the Turcotte conjecture, then this explanation indicates that Venus should have an asthenosphere as well.

Packing most of the heat sources in the crust, as suggested above, would help to prevent an asthenosphere on Venus. But this would be a circular argument, because the inability to recycle crust underlying the crust depends on the strong rheological coupling between lithosphere and mantle. Hence, in principle, the absence of an asthenosphere on Venus should occur even though there was significant heat delivery from the mantle. If the dryness of Venus is the explanation, it must affect the gradient of viscosity with respect to depth.

The solidus of wet mantle rock on Venus is markedly lower than that of dry rock at pressures corresponding to the depth of Earth's asthenosphere (*27*). If there were an analogous effect on viscosity, then dryness might explain the absence of an asthenosphere on Venus, even if heat sources remained at depth; the important thing is not the temperature dependence of viscosity per se, but the gradient of this dependence with respect to pressure. It is desirable that this conjecture be verified experimentally, but sufficient pressures have not been attained in the laboratory. Meanwhile, there is ample room for theoretical speculation. The effect of water on the solidus arises from the breakdown of hydrated phases (mainly hornblende) at asthenospheric pressures, whereas its effect on viscosity probably arises from intergranular flow plus intragranular diffusion at large grain sizes (*9*). These effects are rather different, but a connection cannot be summarily ruled out; in particular, lowered viscosity in Earth's asthenosphere may be in part caused by, as well as correlated with, small degrees of partial melting.

The most important consequence of the stiff upper mantle on Venus is the inhibition of crustal recycling. On Earth, this process is dominated by the subduction of tectonic plates (*28*). On Venus, the distributed deformation arising from the tight coupling of lithosphere to mantle (*19*) could prevent the concentration necessary for such an instability. There are asymmetric chasms on Venus suggestive of subduction trenches, but they are limited in extent (*29*). The lack of water may make the lithosphere more difficult to break; marginal zones on Earth are characterized by a high abundance of hydrated rocks (*30*). In the past, the mechanism of crustal recycling by the gabbro-to-eclogite phase transition may have been quite effective, but the present high subcrustal viscosity must slow any sinkings substantially. Another consequence of the prevention of subduction is that the mantle convective pattern is more influenced by internal, rather than by upper boundary layer, instabilities. This would lead to more regional flow patterns, characterized by plumes or internal avalanches associated with phase transitions, as occur in three-dimensional computer experiments (*31*). But the effect of internal flow patterns on thermal evolution should be less than the inhibition of crustal recycling, which leads to the concentration of radioactive energy sources in the crust.

Models of Venus Evolution Satisfying the Evidence of Rapid Decline

The crater distribution on Venus is consistent with randomness (*2*). However, to infer therefrom that the distribution is random (*32*) is a misapplication of Ockham's razor. The actual distribution of craters per unit area has a lower peak and higher extremes than the centroid of a Poisson distribution (*33*). The question then becomes what is the range of models consistent with the observed distribution. This is difficult to define systematically, because volcanism and tectonism on Venus are obviously nonrandom, as they are on any planet. The evident reference frame, the topography, is quite non-Gaussian, with positive skewness and excess (*34*). Relatively recent volcanic occurrences do have fewer than average craters (*3*), whereas old-appearing tesserae have an abundance of larger craters 40% higher than average but a deficiency of small craters (*35*).

Hence, the time scale of the shutdown of tectonic activity in Venus could be several times 10 million years, perhaps more than 100 million years. This is still difficult to reconcile with a decrease in average strain rate by at least a factor of 100 (*10*). Clearly, the decline cannot be due solely to the interaction of nonlinear rheology with a global, nearly uniform thermal state; it must entail nonlinearities of the flow system, compositional as well as thermal. The significant tectonic activity probably was widespread but involved only a minor, tectonically active part of the globe (analogous to contemporary Earth); however, the lavas produced thereby must have been voluminous and fluid enough to resurface the entire planet within 100 million years or so. Factors that have been suggested to affect evolution and the rapid decline include the following: (i) upward concentration of radioactive heat sources in the crust; (ii) a lithosphere hotter than Earth's, leading to a more free top boundary (*36*); (iii) the accumulation of a high Mg-Fe residuum in the upper mantle (*37*); (iv) a transition of the lithosphere to positive buoyancy with cooling (*38*); (v) increased rigidity of the lithosphere with cooling (*39*); (vi) nonlinear dependence of viscosity on temperature and strain rate (*11*, *39*); and (vii) the absence of water (*1*).

A transition of dominance from factors i and ii, which promote the escape of heat from the mantle, to factors iii through v, which act to shut off heat escape, is characteristic of most scenarios, implicitly if not explicitly. Dominance of factors ii through vi, coupled with retention of heat sources at depth, would have caused a temperature rise leading to massive melting, rupturing the lithosphere. The nonlinearity of factor vi enhances instabilities that propagate rupture, whereas factor vii acts to strengthen the lithosphere, thus increasing the temperature buildup required for rupture.

The lack of water may also have acted to prevent plate tectonics, which depends on weak lithospheric margins (*30*), throughout Venus's history. This idea is contrary to the hypothesis of Herrick (*38*) but is consistent with the more distributed deformation implied by the models of Arkani-Hamed (*39*). But factor i, the removal of heat sources from the interior, still seems essential.

Instabilities require density inhomogeneities, thermal or compositional, which in turn are normally associated with interfaces. The more pronounced the density differential at the interface, the more likely it is that an instability can occur. Possible locations include (i) the surface, from development of a thick, dense lithosphere, which breaks and sinks, as in Earth's subduction

(abetted by lateral variations in crustal density and thickness); (ii) the base of a crust thick enough to reach the basalt-to-eclogite transition; (iii) the upper mantle, after accumulation of a Mg-rich layer residual to crustal differentiation (*37*); as the convective vigor slowed, such a layer may not have been swept aside so quickly (as it is on Earth); (iv) the zone, 400 to 700 km deep, of olivine-spinel-perovskite phase transitions, which in three-dimensional computer experiments trigger avalanche downflows (*31*); and (v) the core mantle interface, about 2800 km deep in Venus, which has the largest density change and is often conjectured to originate plumes in both Earth and Venus. A combination of mechanisms associated with locations i and iii seems most plausible. Both mechanisms depend on crustal differentiation, but not on the growth of crust to a thickness of more than 50 km or more, as do mechanisms associated with location ii. Mechanisms associated with location iv depend on the smallest density difference, whereas the development of a density excess sufficient to penetrate the core mantle boundary seems impossible.

Probably the greater difficulty is the propagation of instability, a problem somewhat analogous to that of earthquake occurrence: relief of an instability in one place enhances instabilities elsewhere. It is particularly a problem if the upper mantle were already stiff. Propagation would be greatly aided by the presence of an asthenosphere, as in Turcotte's episodic model (*17*), to which the main objection is that if heat sources remained at depth, their effects should be seen within a time much less than 300 million years after the resurfacing event (as with secondary convection under Earth's oceans). Any monotonic model (*40*) would require that the instabilities not return too many heat sources to the interior and hence would be facilitated by intracrustal differentiations and the stripping off of the upper crust in downflows.

Constraints on the nature of activity more than 500 million years ago are slight. The occurrence of contorted tessera terrain in many areas is generally thought to indicate a regime of more vigorous distributed tectonics. The thoroughness of the latest resurfacing and the decline of radioactivity indicate that convection was more vigorous in the past, and hence the tendency for oscillatory behavior was greater, as is characteristic of convection at higher Rayleigh numbers. Arkani-Hamed (*39*) suggested that the high temperatures on Venus led to a surface condition closer to stress-free, and hence a greater cooling of the mantle, than has occurred in Earth. This makes the radiogenic Ar deficiency a greater problem; if the Arkani-Hamed model is correct, then on Venus there must have been an initial deficiency of K, relative to that on Earth.

A consequence of the greater cooling of the mantle on Venus could be to freeze the core, thus accounting for the absence of a magnetic field (*39*). Another hypothesis is that the core is entirely fluid, thus lacking the solidification of the inner core generally thought to be the energy source for Earth's magnetic field (*41*). This question is accessible to observational testing, by inference of Venus's Love number k_2, a measure of its nonrigid yielding to tides. Early estimates from Magellan orbiter tracking obtained a relatively high Love number, 0.28 ± 0.07, tending to favor a fluid core (*42*).

Conclusions

The striking differences between Venus and Earth stimulate hypotheses that may seem contrived, even though they depend on effects that are known to exist but are of secondary significance on Earth. Insight would be aided by computer experiments, but such experiments are time-consuming if nonlinear rheology and compositional differentiations in three dimensions are included, and there is a danger of wish fulfillment in the macroscale simulation of magmatism.

Describing the debate as monotonic versus episodic is an oversimplification; the question is more the magnitude of the oscillations about an inevitably declining trend. But certainly Venus's activity in the last 300 million years has been slight compared to Earth's. During this period, the magnitude of sea-floor spreading on Earth has varied by a factor of ~2 (*43*). It is hard to believe that the oscillations could be much greater for a Venus that is now so quiescent. Perhaps a requisite condition for catastrophic episodicity is the dryness, by making the lithosphere more difficult to break. It is also difficult to adjust Earth-conditioned intuitions to the long time scales indicated by the stiff dry rheology on Venus.

The greatest observational constraint on packing radioactive elements in the crust of Venus is the low abundance of radiogenic Ar in the atmosphere, which requires either a K/U ratio much lower than that on Earth or a much lower average level of activity in Venus's entire thermal and compositional evolution. If the K/U ratio on Venus is as high as Earth's, the material could not have been brought close to Venus's surface at a rate comparable to that by Earth's mantle convection (*44*), in view of the transparency to Ar diffusion of rocks at Venus's temperatures. The observations we would most like to have of Venus are chemical samplings to depths of at least 10 cm, preferably 30 cm, to avoid atmospheric effects that concentrate volatiles (including K) in the upper few centimeters. These appear to be unlikely within the near future. In laboratory experiments, it would be desirable to extend rheological experiments on wet and dry olivine or peridotite to pressures of 6.0 GPa or more, a procedure that is of considerable technical difficulty, to verify the extent to which water makes a difference at depths up to 200 km in the mantle.

REFERENCES AND NOTES

1. W. M. Kaula, *Science* **247**, 1191 (1990).
2. G. G. Schaber *et al.*, *J. Geophys. Res.* **97**, 13257 (1992); R. J. Phillips *et al.*, *ibid.*, p. 15923.
3. N. Namiki and S. C. Solomon, *Science* **265**, 929 (1994); M. Price and J. Suppe, *Nature* **372**, 756 (1994); R. J. Phillips and N. R. Izenberg, *Geophys. Res. Lett.* **22**, 1517 (1995).
4. W. M. Kaula and R. J. Phillips, *Geophys. Res. Lett.* **8**, 1187 (1981).
5. R. J. Phillips and V. L. Hansen, *Annu. Rev. Earth Planet. Sci.* **22**, 597 (1994).
6. V. R. Baker *et al.*, *J. Geophys. Res.* **97**, 13421 (1992).
7. K. B. Klose, J. A. Wood, A. Hashimoto, *ibid.*, p. 16353; R. A. Brackett, B. Fegley, R. E. Arvidson, *ibid.* **100**, 1553 (1995).
8. S. J. Mackwell, M. E. Zimmerman, D. L. Kohlstedt, D. S. Scherber, in *Rock Mechanics*, J. J. K. Daemen and R. A. Schultz, Eds. (Balkema, Rotterdam, 1995), p. 207.
9. S.-I. Karato, M. S. Paterson, J. D. FitzGerald, *J. Geophys. Res.* **91**, 8151 (1986).
10. R. E. Grimm, *ibid.* **99**, 23163 (1994).
11. ——— and S. C. Solomon, *ibid.* **93**, 11911 (1988).
12. Y. A. Surkov, V. L. Barsukov, L. P. Moskalyeva, V. P. Kharyukova, A. L. Kemurd-zhian, *ibid.* **89**, B383 (1984); Y. A. Surkov *et al.*, *ibid.* **92**, E537 (1987).
13. O. V. Nikolayeva, *Lunar Planet. Sci. Conf.* **26**, 1049 (1995).
14. J. S. Kargel, G. Komatgsu, V. R. Baker, R. G. Strom, *Icarus* **103**, 253 (1993).
15. A. H. Lachenbruch, *J. Geophys. Res.* **75**, 3291 (1970).
16. But an opposite hypothesis is that Earth would have the higher ratio of plutonism to volcanism because water-saturated magmas are more likely to freeze upon ascent, as a result of the negative slope of the phase transition [C. W. Burnham, in *The Evolution of Igneous Rocks*, H. S. Yoder, Ed. (Princeton Univ. Press, Princeton, NJ, 1979), p. 439].
17. D. L. Turcotte, *J. Geophys. Res.* **98**, 17061 (1993).
18. If we use the formula for thermal conductivity of J. F. Schatz and G. Simmons [*J. Geophys. Res.* **77**, 6966 (1972)] and assume a heat flow from the mantle of 0.03 W m^{-2}, plus a surface heat source density of 275×10^{-12} W kg^{-1} with a decay depth of 40 km, a numerical integration of the thermal conduction equation gives, at a depth of 60 km, a temperature of 1550 K and a thermal conductivity of 4.0 m^{-1} per degree Celsius. If we assume a strain rate of 10^{-17} s^{-1} (*9*), the effective viscosity for dry diabase (*17*) is 10^{23} Pa-s.
19. R. J. Phillips, *J. Geophys. Res.* **95**, 1301 (1990); ———, R. E. Grimm, M. C. Malin, *Science* **252**, 651 (1991); W. S. Kiefer, M. A. Richards, B. H. Hager, B. G. Bills, *Geophys. Res. Lett.* **13**, 14 (1986).
20. N. Namiki and S. C. Solomon, *J. Geophys. Res.* **98**, 15025 (1993); S. G. Herzog, P. C. Hess, E. M. Parmentier, *Lunar Planet. Sci. Conf.* **26**, 591 (1995); M. G. Jull and J. Arkani-Hamed, *Phys. Earth Planet. Inter.* **89**, 163 (1995).
21. J. B. Pollack and D. C. Black, *Icarus* **51**, 169 (1992); N. Namiki and S. C. Solomon, *Lunar Planet. Sci. Conf.* **26**, 1029 (1995).
22. W. M. Kaula and T. M. Harrison, in preparation.
23. W. M. Kaula *et al.*, *J. Geophys. Res.* **97**, 16085 (1992).
24. A. M. Freed and H. J. Melosh, *Lunar Planet. Sci. Conf.* **26**, 421 (1995).
25. Using the model of D. W. Forsyth [*J. Geophys. Res.* **90**, 12623 (1985)] plus the assumption of a deep

positive load, one obtains from the gravimetry and altimetry of the Maxwell Montes region a crust to a depth of 50 km with a negative density anomaly of about 500 kg m^{-3}.
26. M. T. Zuber, *J. Geophys. Res.* **92**, E541 (1987).
27. D. H. Green, *Earth Planet. Sci. Lett.* **19**, 37 (1973).
28. R. W. Carlson, *Rev. Geophys.* **32**, 337 (1994).
29. D. T. Sandwell and G. Schubert, *Science* **257**, 766 (1992).
30. G. P. Bird, *Rev. Geophys.* **33**, Suppl. (*U.S. Natl. Rep. 1991–1994*), 379 (1995).
31. P. J. Tackley, D. J. Stevenson, G. A. Glatzmaier, G. Schubert, *Nature* **361**, 699 (1993).
32. R. G. Strom, G. G. Schaber, D. D. Dawson, *J. Geophys. Res.* **99**, 10899 (1994).
33. W. M. Kaula, *Lunar Planet. Sci. Conf.* **24**, 767 (1993).
34. Both the third and the fourth moments are higher than those of a Gaussian distribution of the same mean square σ^2: >0 and >3(σ^2)^2 [W. M. Kaula, *Geophys. Res. Lett.* **20**, 2583 (1993)].
35. M. A. Ivanov and A. T. Basilevsky, *Geophys. Res. Lett.* **20**, 2579 (1993).
36. J. Arkani-Hamed, G. G. Schaber, R. G. Strom, *J. Geophys. Res.* **98**, 5309 (1993).
37. R. J. Phillips and R. E. Grimm, *Lunar Planet. Sci. Conf.* **21**, 1065 (1990); E. M. Parmentier and P. C. Hess, *Geophys. Res. Lett.* **19**, 2015 (1992).
38. R. R. Herrick, *Geology* **22**, 703 (1994).
39. J. Arkani-Hamed, *Phys. Earth Planet Inter.* **76**, 75 (1993); *J. Geophys. Res.* **99**, 2019 (1994).
40. S. C. Solomon, *Lunar Planet. Sci. Conf.* **24**, 1331 (1993).
41. D. J. Stevenson, T. Spohn, G. Schubert, *Icarus* **54**, 466 (1983).
42. A. S. Konopliv and C. M. Yoder, unpublished results.
43. C. Lithgow-Bertelloni, M. A. Richards, Y. Ricard, R. J. O'Connell, D. C. Engebretson, *Geophys. Res. Lett.* **20**, 375 (1993).
44. Currently, about 20 km^3 of crust, averaging about 6 km thick, is differentiated per year in Earth. This crust is the product of multiple differentiations extending 60 km deep, and so the volume rate of material associated with magmatism, which would release Ar, is about 200 km^3 $year^{-1}$. The volume of the mantle is 9 × 10^{11} km^3. Hence, if it were uniformly sampled, the entire mantle would have been cycled through the near surface layer in 4.5 × 10^9 years. However, convection, and hence magmatism, was much more vigorous in the past, whereas the sources of comtemporary basalts are clearly recycled. But, regardless of the numbers, the comment in the text applies.
45. This paper has been significantly improved by discussions with A. Lenardic and T. M. Harrison and by reviews by R. J. Phillips and M. T. Zuber. This work was supported in part by National Aeronautics and Space Administration grant NAGW-2085 from the Planetary Geology and Geophysics Program.

RESEARCH ARTICLE

Crystal Structure of the Ternary Complex of Phe-tRNA^{Phe}, EF-Tu, and a GTP Analog

Poul Nissen, Morten Kjeldgaard, Søren Thirup, Galina Polekhina, Ludmila Reshetnikova, Brian F. C. Clark, Jens Nyborg*

The structure of the ternary complex consisting of yeast phenylalanyl–transfer RNA (Phe-tRNA^{Phe}), *Thermus aquaticus* elongation factor Tu (EF-Tu), and the guanosine triphosphate (GTP) analog GDPNP was determined by x-ray crystallography at 2.7 angstrom resolution. The ternary complex participates in placing the amino acids in their correct order when messenger RNA is translated into a protein sequence on the ribosome. The EF-Tu–GDPNP component binds to one side of the acceptor helix of Phe-tRNA^{Phe} involving all three domains of EF-Tu. Binding sites for the phenylalanylated CCA end and the phosphorylated 5′ end are located at domain interfaces, whereas the T stem interacts with the surface of the β-barrel domain 3. The binding involves many conserved residues in EF-Tu. The overall shape of the ternary complex is similar to that of the translocation factor, EF-G–GDP, and this suggests a novel mechanism involving "molecular mimicry" in the translational apparatus.

Protein biosynthesis is a central process in every organism. It provides the link between the genetic information encoded in DNA and functional proteins. Understanding the steps of protein biosynthesis should have an impact on our overall perception of the process of translation. An essential participant in protein biosynthesis is the ternary complex of aminoacyl transfer RNA (aa-tRNA), elongation factor Tu (EF-Tu or EF-1α), and guanosine triphosphate (GTP), yet its three-dimensional structure has hitherto been unknown. The determination of this structure allows a much more precise and testable description of the molecular mechanism of protein biosynthesis.

The process of synthesizing proteins on the ribosome can be divided into initiation, elongation, and termination. Initiation and termination are punctuation events in that they deal with starting and stopping synthesis as a response to specific start and stop codons on messenger RNA (mRNA). These steps are assisted by initiation and release factors, respectively.

The central step in protein biosynthesis is elongation, in which amino acids are added one at a time to the growing polypeptide chain according to the sequence of codons present on mRNA. In prokaryotes, three elongation factors are involved as catalysts in this process: EF-Tu, the EF-Tu specific nucleotide exchange factor EF-Ts, and the translocation factor EF-G. Both EF-Tu and EF-G are members of the G protein superfamily, which consists of proteins with a conserved, common structural design (*1*). Thus EF-Tu exists in one of two states, either bound to guanosine diphosphate (GDP) as the inactive complex EF-Tu–GDP, or in the active form EF-Tu–GTP. The active EF-Tu–GTP binds aa-tRNA to form the ternary complex aa-tRNA–EF-Tu–GTP. The exposed anticodon of aa-tRNA is recognized on the ribosome by interaction with a codon on mRNA. This is part of the overall interaction between the ternary complex and the so-called A site of the ribosome. The ribosome induces hydrolysis of EF-Tu–GTP to EF-Tu–GDP, which is released from the ribosome (*2*). This inactive form of EF-Tu is recycled by the exchange of GDP for GTP, a process catalyzed by EF-Ts. The third elongation factor, EF-G, catalyzes the translocation reaction whereby the ribosome advances to the next codon on mRNA and translocates the peptidyl tRNA from the A site to the P site.

Both EF-Tu and aa-tRNA synthetases (aaRS) are proteins that can bind tRNA. However, in contrast to an aaRS, EF-Tu forms complexes with all aa-tRNAs. It is therefore expected that EF-Tu recognizes common features of all aa-tRNAs. Some structural information on how an aaRS binds to its cognate tRNA is available (*3*). A survey of features of tRNAs believed to be involved in ternary complex formation has been presented by Faulhammer and Joshi (*4*). Investigations of the specific parts or residues of aa-tRNA or EF-Tu participating in ternary complex formation have led to the formulation of possible models for the ternary complex (*5–7*). However, none of these models is in agreement with the x-ray model described in this article.

The crystal structure of yeast tRNA^{Phe} revealed the structural organization of tRNA as two double-helical segments almost perpendicular to each other (*8*, *9*). Each helical segment contains two base-

P. Nissen, M. Kjeldgaard, S. Thirup, G. Polekhina, B. F. C. Clark, and J. Nyborg are in the Department of Biostructural Chemistry, Institute of Chemistry, Aarhus University, Langelandsgade 140, DK-8000 Aarhus C, Denmark. L. Reshetnikova is at the Engelhardt Institute of Molecular Biology, Russian Academy of Sciences, 32 Vavilov str., 117984 Moscow, Russia.

*To whom correspondence should be addressed.

paired stems of the classical cloverleaf structure (Fig. 1). The acceptor helix is composed of the T stem and the acceptor stem and ends in the common 3′ CCA sequence, where the amino acid is coupled by an ester linkage to a hydroxyl group of the terminal ribose ring. The anticodon helix is composed of the D stem and the anticodon stem. The loop containing the anticodon is at the end of this helix.

EF-Tu is composed of an NH_2-terminal G domain, which binds the nucleotide cofactor, and two β-barrel domains (Fig. 1). The crystal structure of trypsin-modified EF-Tu–GDP from *Escherichia coli* is known (*10*). Crystal structures of active EF-Tu from *T. thermophilus* and *T. aquaticus* with the GTP analog GDPNP have been determined (*11*, *12*). When the structures of EF-Tu–GDP and EF-Tu–GDPNP are compared, an unexpectedly large movement of domains 2 and 3 relative to domain 1 is observed. This domain rearrangement creates in EF-Tu–GDPNP a narrow cleft between domains 1 and 2, which has been predicted to bind part of the tRNA molecule (*11*, *12*). *Thermus aquaticus* EF-Tu consists of 405 amino acid residues with a total molecular mass of 44.6 kilodaltons (kD).

A substantial amount of structural information on G proteins is now available. The structures of the closely related translocation factor EF-G in the GDP-bound (*13*) and in the nucleotide-free state (*14*) have been determined. Structures of the *ras* proto-oncogene product p21 and the similar proteins *Ran* and ARF are also now known (*15*–*18*). Structures of the much larger heterotrimeric G proteins, $G_{t\alpha}$ and $G_{i\alpha 1}$, have been reported (*19*–*21*).

We have already reported the purification and crystallization of the ternary complex (*22*). We now describe the results of the successful determination of the crystal structure at 2.7 Å resolution of the ternary complex of yeast Phe-tRNA^{Phe} with EF-Tu–GDPNP from *T. aquaticus*. Although the Phe-tRNA and the EF-Tu are not from the same species we believe that this structure represents a canonical model for all ternary complexes because EF-Tu–GTP has a general aa-tRNA binding capability and EF-Tu and tRNA structures are expected to be generally conserved.

Structure determination. Two data sets were collected from two different crystals at 100 K (Table 1). The structure was determined by molecular replacement with data from crystal 1 (Table 2). Models were based on the known structures of EF-Tu–GDPNP (*12*) and tRNA^{Phe} (*23*). Parts that were expected to undergo some structural alterations during complex formation were removed from the search models. Different deletion models of tRNA^{Phe} were tested, and a model with the acceptor stem and anticodon loop excluded gave the best solutions. As a control, GDPNP and Mg^{2+} were omitted from the EF-Tu model in order to see whether molecular replacement phases would reproduce electron density for the bound nucleotide. The search models for EF-Tu and tRNA represented 20 and 7.7 percent, respectively, of the total macromolecular mass of the asymmetric unit. A self-rotation function indicated pseudo three-

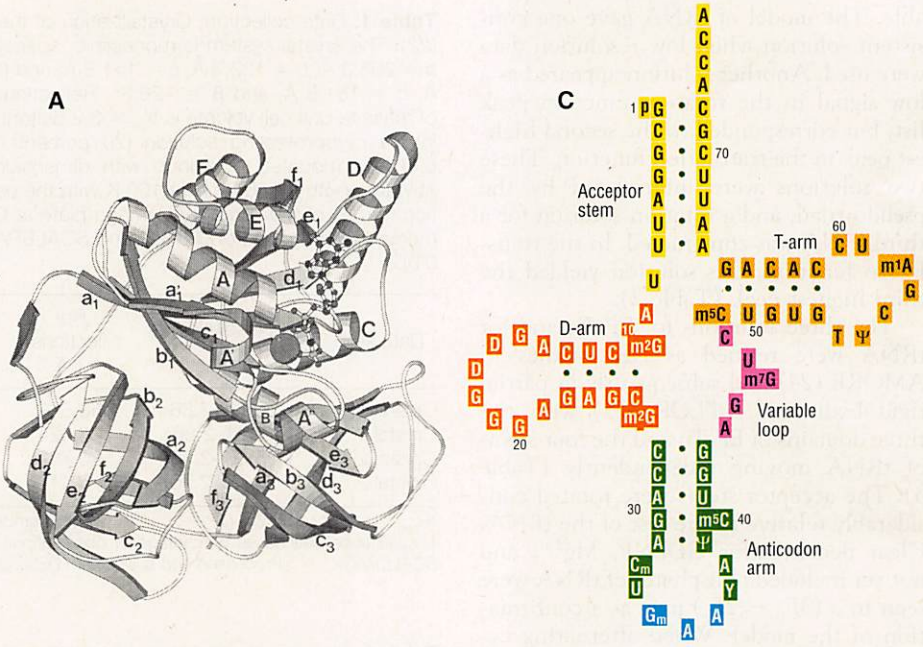

B

```
sec.s      1 ___bbbb__bbbbbbbbb_____aaaaaaaaaaaaaaa--------------____bbbb
T.aqua     1 AKGEFIRTKPHVNVGTIGHVDHGKTTLTAALTYVAAAE--------------NPNVEVKD
E.coli     1 SKEKFERTKPHVNVGTIGHVDHGKTTLTAAITTVLAKT--------------YGGAARA
Yeast      0 ---MGKE-KSHINVVVIGHVDSGKSTTTGHLIYKCGGIDKRTIEKFEKEAAELGKGSFKY

sec.s     47 aaaaa__aaaaa_____bbbbbbbb___bbbbbbb_____aaaaaaaaaaa__bbbbbb
T.aqua    47 YGDIDKAPEERARGITINTAHVEYETAKRHYSHVDCPGHADYIKNMITGAAQMDGAILVV
E.coli    46 FDQIDNAPEEKARGITINTSHVEYDTPTRHYAHVDCPGHADYVKNMITGAAQMDGAILVV
Yeast     57 AWVLDKLKAERERGITIDIALWKFETPKYQVTVIDAPGHRDFIKNMITGTSQADCAILII

sec.s    107 _______-------aaaaaaaaaaaaa___bbbbbbb_____--aaaaaaaaaaaaaa
T.aqua   107 SAADGPM-------PQTREHILLARQVGVPYIVVFMNKVDMVDD--PELLDLVEMEVRDL
E.coli   106 AATDGPM-------PQTREHILLGRQVGVPYIIVFLNKCDMVDD--EELLELVEMEVREL
Yeast    117 AGGVGEFEAGISKDGQTREHALLAFTLGVRQLIVAVNKMDSVK-WDESRFQEIVKETSNF

sec.s    158 aaaa_______bbbb__aaaaaaaaaa_____------____aaaaaaaaaaaaa____
T.aqua   158 LNQYEFPGDEVPVIRGSALLALEEMHKNPKTK------RGENEWVDKIWELLDAIDEYIP
E.coli   157 LSQYDFPGDDTPIVRGSALKALEGDAE--------------WEAKILELAGFLDSYIP
Yeast    176 IKKVGYNPKTVPFVPISGWNGDNMIEATTNAPWYKGWEKETKAGVVKGKTLLEAIDAIEQ

sec.s    212 _________bbbbbbbbb_____bbbbbb____bbbb__bbbbbb____bbbbbbbbbbb
T.aqua   212 TPVRDVDKPFLMPVEDVFTITGRGTVATGRIERGKVKVGDEVEIVGLAPETRKTVVTGVE
E.coli   201 EPERAIDKPFLLPIEDVFSISGRGTVVTGRVERGIIKVGEEVEIVGIK-ETQKSTCTGVE
Yeast    235 -PSRPTDKPLRLPLQDVYKIGGIGTVPVGRVETGVIKPGMVVTFAPAG---VTTEVKSVE

sec.s    272 b____________bbbbbb_____________bbb_----_____________bbbbbbbb_____
T.aqua   272 MHRKTLQEGIAGDNVGLLLRGVSREEVERGQVLA----KPGSITPHTKFEASVYILKKEE
E.coli   260 MFRKLLDEGRAGENVGVLLRGIKREEIERGQVLA----KPGTIKPHTKFESEVYILSKDE
Yeast    292 MHHEQLEQGVPGDNVGFNVKNVSVKEIRRGNVCGDAKNDPPKG--CASFNATVIVL----

sec.s    328 _________bbbbbbb___bbbbbbbbb-------------_____________bbbbbbbb
T.aqua   328 GGRHTGFFTGYRPQFYFRTTDVTGVVRL--------------PQGVEMVMPGDNVTFTVE
E.coli   316 GGRHTPFFKGYRPQFYFRTTDVTGTIEL--------------PEGVEMVMPGDNIKMVVT
Yeast    345 -NHPGQISAGYSPVLDCHTAHIACRFDELLEKNDRRSGKKLE-DHPKFLKSGDAALVKFV

sec.s    374 ___________------bbbbbbb____bbbbbbbbb_
T.aqua   374 LIKPVALEEGL------RFAIREGGRTVGAGVVTKILE
E.coli   362 LIHPIAMDDGL------RFAIREGGRTVGAGVVAKVLS
Yeast    404 PSKPMCVEAFSEYPPLGRFAVRDMRQTVAVGVIKSVDKTEKAAKVTKAAQKAAKK
```

Fig. 1. The components of the ternary complex. (**A**) Structural cartoon (*72*) of *T. aquaticus* EF-Tu–GDPNP (*12*) with labels on the secondary structure elements. (**B**) Sequence alignment of *T. aquaticus* EF-Tu (*73*), *E. coli* EF-Tu (*74*), and yeast EF-1α (*75*) extracted from an alignment of the 94 complete EF-Tu and EF-1α sequences found in release 31 of the SwissProt database (*76*). Conservations observed in more than 98 percent of the sequences are shown in reverse print. The secondary structure as it appears in (A) is indicated by "sec. s." The alignment and the figure were made with the alignment editor ALMA (*77*). (**C**) The cloverleaf structure of yeast tRNA^{Phe}. The two helical segments of the tRNA structure are the acceptor helix (acceptor stem and T stem in yellow and orange) and the anticodon helix (D stem and anticodon stem in red and green). The variable loop is in violet and the anticodon is in blue.

fold symmetry, and the EF-Tu model gave three significant solutions to both the rotation and translation functions (Table 2), which were interrelated by the pseudo triad. Electron density maps were calculated on this preliminary EF-Tu structure alone, but the traces of tRNA were not interpretable. The model of tRNA gave one consistent solution when low resolution data were used. Another solution appeared as a low signal in the rotation function peak list, but corresponded to the second highest peak in the translation function. These two solutions were interrelated by the pseudo-triad, and a rotation solution for a third tRNA was constructed. In the translation function, this solution yielded the third highest peak (Table 2).

The three solutions for EF-Tu and for tRNA were refined as rigid bodies in AMORE (*24*) and subsequently as partial rigid bodies in X-PLOR (*25*) with the three domains of EF-Tu and the four stems of tRNA moving independently (Table 3). The acceptor stems were rotated considerably relative to the rest of the tRNA. Clear densities for GDPNP, Mg^{2+}, and not yet included phosphates of tRNA were seen in a $(3F_o - 2F_c)$ map as a confirmation of the model. When alternating cycles of simulated annealing refinement in X-PLOR and model building in program O (*26*) were performed, the effector loop and the CCA end could be traced in $(3F_o - 2F_c)$ maps (Table 3). Noncrystallographic symmetry (NCS) was restrained for EF-Tu molecules and tRNA molecules, and the resolution was increased to 2.8 Å. Strong densities were observed at the expected positions of the terminal adenine and phenylalanine, but an assignment could not be made with confidence. Furthermore, several parts of the anticodon helix were still badly defined in the electron density as were a few loops of the EF-Tu structure. At this stage the data from crystal 2 (Table 1) were introduced. After partial rigid body refinement and one cycle of simulated annealing with the 5.0 to 2.7 Å data, the densities for the 3′ ends became clear, and the aminoacyl group and the adenine could be assigned (Table 3).

When the anticodon helices were omitted and the NCS restraints on the tRNA molecules were released, the densities of the anticodon arm became interpretable. The NCS of the anticodon helices appeared to be imperfect and therefore the NCS restraints on the tRNA structure was split into two clusters with the three acceptor helices as one and only two of the three anticodon helices (E and F) as the other (Table 3). The simulated annealing protocol did not improve the model any further and positional refinement was continued in TNT (*27*). After one batch of TNT refinement, the map and the refinement statistics improved considerably. Subsequent cycles of refitting in O and TNT refinement with high weights on geometry and the split NCS improved the refinement statistics further.

The model includes all residues of the three Phe-tRNA–EF-Tu–GDPNP complexes and three well-defined Mg^{2+} ions found in the T stems, a total of 14,523 non-hydrogen atoms. The EF-Tu main

Table 1. Data collection. Crystallization of the purified ternary complex has been described earlier (*22*). The crystal system is monoclinic, spacegroup *C*2. For crystal 1, the unit cell parameters are a = 208.3 Å, b = 122.3 Å, c = 151.8 Å, and β = 126.7°; and for crystal 2, a = 206.8 Å, b = 122.3 Å, c = 151.6 Å, and β = 126.3°. Reflections were observed beyond 2.6 Å resolution. The ratio of mass to unit cell volume is V_m = 3.2 daltons per cubic angström. Crystals were gradually soaked into a cryoprotecting solution [20 percent (w/v) sucrose in 65 percent $(NH_4)_2SO_4$ buffer, pH 6.8] and mounted in a loop with dimensions matching the crystal. Data sets were collected at wavelength λ = 0.87 Å at 100 K with the use of an Oxford Cryostream cooling system in oscillation frames of 2.0° on a MAR image-plate at Daresbury, station 9.6. The data were processed and merged with the use of DENZO and SCALEPACK (*69*) or ROTAVATA-AGROVATA and TRUNCATE (*70*).

Data set	Resolution (Å)	Reflections (*N*)	R_{sym}* (%)	Redundancy† (*N*)	Completeness (%)	Significance‡ (%)
Crystal 1§	20.00–2.86	58,529	5.6	2.4	78.3	85.9
Crystal 1	2.91–2.86	3,024	31.3	2.4	77.5	63.8
Crystal 2‖	25.00–2.70	80,769	5.2	2.8	96.8	79.3
Crystal 2	2.79–2.70	5,417	37.6	2.4	82.7	51.6

*$R_{sym} = \Sigma|I - \langle I \rangle|/\Sigma\langle I \rangle$. †Average number of observations per reflection after rejection analysis. ‡Significance defined as percentage of observations with $I > 3\sigma$. §Processed and scaled with DENZO and SCALEPACK. ‖Processed and scaled with DENZO and ROTAVATA-AGROVATA.

Table 2. Structure determination. Rotation search and translation search. The structure was solved by molecular replacement (*24*). Normalized structure factors were calculated with ECALC (*70*). The search models used were derived from EF-Tu–GDPNP from *T. aquaticus* (*12*) (with residues 1 to 9, 43 to 64, GDPNP, and Mg^{2+} removed) and yeast $tRNA^{Phe}$ (*23*) (with nucleotides 1 to 7, 32 to 38, and 64, to 76 removed). Three solutions from the EF-Tu model and two solutions using the tRNA model were found by crossrotational and "fixed solution" translational searches. A third solution from the tRNA search model (E) was identified by a translational search based on rotational solutions generated by NCS and spanning the possible degeneration of the pseudo triad.

Search model	Fraction* (%)	Resolution (Å)	Search radius (Å)	Angles α	Angles β	Angles γ	Rank† (*N*)	Peak height‡ (%)
EF-Tu								
A	20	10.0–3.0	35	296.1	82.9	304.6	2	10.4
B				44.4	95.2	305.7	1	10.8
C				161.9	82.7	314.9	3	5.8
tRNA								
D	7.7	15.0–6.2	45	96.1	53.7	66.8	1	10.2
E				219.0	45.0	70.0		
F				335.2	57.3	56.4	85	5.7

	Resolution (Å)	Fractional coordinates x	Fractional coordinates y§	Fractional coordinates z	Rank (*N*)	Peak height‖ (%)	*R* factor¶ (%)
EF-Tu							
A	10.0–4.0	0.491	0.0	0.186	2	10.9	53.7
B		0.264	−0.308	0.199	1	13.9	52.9
C		0.245	0.234	0.122	3	8.2	54.2
tRNA							
D	15.0–5.0	0.744	0.864	0.460	1	28.2	49.2
E		0.904	0.986	0.425	3	25.8	50.0
F		0.241	0.696	0.424	2	26.2	49.5

*Percentage (in mass) of search model relative to total macromolecular content of asymmetric unit. †Rank of solution in rotation peak list. ‡Patterson correlation coefficient. §Relative y coordinates were determined by fixing solution A. ‖Patterson correlation coefficient. EF-Tu solutions alone, tRNA solutions with all three EF-Tu solutions fixed. ¶*R* factor $= \Sigma|F_o - F_c|/\Sigma F_o$, where F_o and F_c are observed and calculated structure factor amplitudes of reflections used in the translation function. *R* factors for solutions of tRNA are calculated with all three EF-Tu's fixed.

chain and most parts of tRNA, except for the D arm, appear in continuous electron density contoured at 1.25σ in all three complexes (Fig. 2).

Structure of the ternary complex. The asymmetric unit consists of three ternary complexes forming a trimer related by a pseudo-threefold axis (Fig. 3). The trimer is the basic element of the crystal lattice and the crystal contacts between trimers involve only protein-protein and RNA-RNA interactions. No protein-protein contacts are found within the trimer.

The ternary complex is elongated (115 Å by 40 Å by 64 Å) and has an overall shape resembling a corkscrew. EF-Tu and the acceptor helix form a knob-like handle and the anticodon helix forms the screw (Fig. 4). Small angle x-ray scattering studies have been performed on the complex (28), resulting in an overall description of the ternary complex in excellent agreement with our model. However, the results of similar experiments suggested a compact model (29).

All three domains of EF-Tu–GDPNP take part in the Phe-tRNA binding and interact with the CCA-Phe end and the acceptor helix on one side (Fig. 4), but only minor parts of both protein and RNA make real contacts. The binding of Phe-tRNA to EF-Tu–GDPNP can thus be described as having three main components: (i) binding of 3′ CCA-Phe (Fig. 5A), (ii) binding of the 5′ end (Fig. 5B), and (iii) binding of the T stem (Fig. 2).

The binding site for the CCA-Phe end on EF-Tu–GDPNP is formed by a narrow cleft between domains 1 and 2. The single-stranded CCA-Phe end enters this cleft below helix A″ (Figs. 4 and 5A) and docks the amino acid Phe into a pocket with the phenyl ring stacked on the side chain of His^{67}. This pocket is lined with side chains of Phe^{229}, Asp^{227}, Glu^{226}, and Thr^{239}. There is space to accommodate any of the 20 naturally ocurring amino acids. The amino ester is recognized by main chain atoms of EF-Tu. The amino group can form hydrogen bonds to the main chain CO of Asn^{285} and the main chain NH of His^{273}. The carbonyl oxygen of the amino ester can form a hydrogen bond with the main chain NH of residue Arg^{274}, the side chain of which interacts with the phosphate of A76. The ester bond is made to the 3′-OH of the terminal ribose while the 2′-OH can make a hydrogen bond with the side chain of the conserved Glu^{271}.

The electron density does not support a 2′,3′-orthoester structure, as proposed on the basis of ^{13}C-NMR (nuclear magnetic resonance) experiments on the ternary complex (30). Furthermore, the ester bond is 26 Å away from Arg^{59}, which fails to support the suggestion that Arg^{59} stabilizes the orthoester anion (30). Other ^{13}C-NMR experiments have not detected the existence of an orthoester (31). Residue His^{66} in *Escherichia coli* EF-Tu has been crosslinked to ε-bromo-Lys-tRNA and the same modified tRNA gave crosslinks to His^{296} of rabbit EF-1α (7). These residues correspond to *T. aquaticus* residues His^{67} and Arg^{274} that are both participating in the binding of the aminoacyl group (Fig. 5A).

Two protruding loops of domain 2 (12), which are found between the β strands a_2 and b_2 (residues 229 to 236) and d_2 and e_2 (residues 272 to 277) form a pocket for the 3′ terminal adenine. The conserved residue Glu^{271} stacks to the adenine on one side and the conserved residues Val^{237} and Ile^{231} make a hydrophobic platform for the adenine on the other side together with Leu^{289}. The phosphates at positions 74 and 75 form contacts with Lys^{52} and the three bases of A73, C74, and C75 stack in continuation of the acceptor helix and point away from the protein, which is in agreement with several observations that various substitutions of these bases do not prevent the formation of a ternary complex (4).

The 5′ end of the tRNA chain is bound tightly at the junction of the three EF-Tu domains (Figs. 4 and 5B). A pocket is formed by helix A″, the COOH-terminal part of helix B, and the two loops between β-strands e_2 and f_2 (residues 300 to 303), and b_3 and c_3 (residues 346 to 348). The phosphate forms a salt bridge to the conserved residue Arg^{300}, and the ribose interacts with the conserved residues Lys^{90} and

Table 3. Refinement and model building. Stages are (A) Partial rigid body refinement; (B) six alternating batches of simulated annealing and model building; (C) anisotropic *B*-factor refinement; (D) one batch of partial rigid body refinement and three cycles of simulated annealing and model building with data of crystal 2; (E) one batch of simulated annealing with anticodon helices omitted; (F) three batches of simulated annealing with split NCS and model building of anticodon helices; (G) individual *B*-factor refinement; (H) one batch of TNT refinement; (I) extensive rebuilding in O followed by six alternating batches of TNT refinement and model building. Crystallographic contacts were excluded in the NCS restraints. Simulated annealing in X-PLOR (25) was performed with fast or slow cooling from 1000 or 2000 K. Higher temperatures resulted in destruction rather than improvement of the tRNA structure. The parameters for the protein structure were derived by Engh and Huber (71), and the parameters for the tRNA structure were part of X-PLOR. TNT refinement (27) was performed in batches of 20 cycles of conjugate gradient refinement with *B*-factor correlation. A preliminary parameter set for tRNA, equal to the Engh and Huber set for protein, was used (71). The $(3F_o - 2F_c)$ electron density maps were calculated in X-PLOR and TNT. The protein structure was built with the `lego` and `manip` options of O and regularly checked against a structural database with `pep_flip`. Outliers from `pep_flip` were carefully inspected. The tRNA structure was built with the manip options of O.

Stage	Resolution (Å)	Reflections* (*N*)	*R* factor (%)		
			Initial†	Final†	Free‡
A	15.0–4.0	19,741	45.9	43.0	
B	7.0–2.8	51,941	43.0	34.8	41.6
C	7.0–2.8	51,940	34.8	30.3	38.3
D	5.0–2.7	75,629	44.6	34.0	38.9
E	5.0–2.7	75,629	35.0	33.9	38.8
F	5.0–2.7	75,629	34.3	31.2	37.3
G	5.0–2.7	75,629	31.2	30.8	36.2
H	25.0–2.7	76,349	32.5	19.9	33.5
I	25.0–2.7	76,349	32.7	22.8	30.7

Scatterers	14,523
Amino acid residues	1,215
Nucleotide residues	228
Macromolecules	6
Special chemical groups	3 amino-ester bonded phenylalanines 39 modified nucleotides
Cofactors	3 GDPNP nucleotides
Ions	3 Mg^{2+} in EF-Tu, 3 Mg^{2+} in Phe-tRNA
⟨Protein B⟩ (Å²)§	23.8
⟨RNA B⟩ (Å²)§	31.2
Rmsd bonded atoms B (Å²)‖	4.54
Rmsd EF-Tu NCS (Å)¶	0.19
Rmsd tRNA NCS1 (Å)#	0.16
Rmsd tRNA NCS2 (Å)**	0.29
Rmsd bonds (Å)	0.009
Rmsd angles (°)	1.60
Rmsd planar groups (°)	0.009

*Reflections with $F > 2.0\ \sigma$ after initial random removal of 5 percent of reflections for use in *R*-free calculations. †*R* factor = $\Sigma|F_o - F_c|/\Sigma F_o$ where F_o and F_c are observed and calculated structure factor amplitudes of reflections used for refinement. ‡*R* free = *R* factor of 5 percent random set of reflections removed before model refinement. §From stage G. ‖From stage I. ¶Excluding crystal contacts. #Acceptor helix cluster, excluding crystal contacts. **Anticodon helix cluster of tRNA E and F.

Asn[91]. The ribose of C2 and the phosphate of G3 are in contact with Tyr[88] and Glu[55], which interact with the conserved Arg[59]. Residue His[85] is in contact with Asp[87], which coordinates the phosphates of G3 and A64 in a regular triangle.

Two short stretches of the backbone on one side of the T stem make contacts with main and side chains exposed on domain 3 of EF-Tu (Figs. 2 and 4). Residue Arg[330] interacts with the ribose of U52 and the phosphate group of G53. The phosphate of T54 is close to His[331]. The main chain of Gly[391] makes contacts to the ribose of C63 and A64. The ribose groups of A64 and G65 interact with Gln[341] and Thr[350], respectively. The phosphate of U67 is in contact with Lys[376].

The side of the acceptor helix that interacts with EF-Tu has previously been identified by footprinting studies with analysis of RNase digestion. The positions 74, 72, 68, 64, 63, and 44 to 51 of tRNA were observed to be protected in the ternary complex (*32*) which is in good agreement with the structure (Fig. 4). The lysine residues of *E. coli* EF-Tu–GTP have been subjected to reaction with ethyl acetimidate (*33*). Three of those, Lys[2], Lys[4], and Lys[263] (corresponding to Lys[2], Lys[4], and Lys[275] in *T. aquaticus*) were reported to have a very reduced reactivity in the ternary complex. This is not in agreement with the structure where they are found in regions of EF-Tu that are not in contact with Phe-tRNA. Strikingly, the environments of these lysines are highly altered upon the conformational change in EF-Tu which take place during nucleotide exchange (*10–12*).

Structures of the components of the ternary complex. The structures of the two macromolecular components of the ternary complex are generally similar to the structures of free EF-Tu–GDPNP and tRNA^{Phe}. By alignment of all Cα atoms (*26*) of free and Phe-tRNA–bound EF-Tu–GDPNP, the greatest deviation is a 2.5 Å shift of helix A″ (residues Pro[54] to Ile[61]). Furthermore, the Cα position of Arg[274] differs by 1.9 Å. A few other differences are in the order of 1 to 2 Å and are caused by the crystal packing.

The single-stranded 3′ end of the complexed tRNA has a helical curvature induced by the binding of CCA-Phe to EF-Tu as it is observed in tRNA complexes of class II aaRS (*3*). When superimposing the T stems of the EF-Tu–bound tRNA molecules with that of free tRNA^{Phe}, some differences are observed. The tRNA in the complex exhibits a small alteration in the angle and twist between the acceptor stem and the T stem, which expands into a 16 Å shift in the position of the 3′ end. The anticodon helix is bent, though most prominently in two of the three tRNA molecules, denoted E and F (Table 2), which differ by 12 Å in the position of the anti- codon region relative to D, which again is shifted by 3 Å relative to free tRNA^{Phe}. Interestingly, tRNA molecules E and F were the most difficult to detect in the molecular replacement procedure and this explains the advantage of splitting the NCS restraints on the tRNA molecules in the model refinement. The bending is imposed by the continued stacking of the 3′-stacked anticodon onto G20 in the D loop of the neighboring tRNA in the trimer. G20 is exposed next to the conserved G19 · C56 base pair.

Discrimination in ternary complex formation. Dissociation constants for various ternary complexes are in the nanomolar range (*34, 35*). However, affinities of individual aa-tRNAs towards EF-Tu–GTP vary within one order of magnitude (*34*). The dissociation constants of uncharged tRNA in complex with EF-Tu–GTP are several orders of magnitude higher (*36*). This large difference has been a puzzle since it is difficult to explain by the finite number of possible interactions with the amino ester group.

The binding of the T stem and the 5′ end of Phe-tRNA on the surface of EF-Tu must be independent of the presence of the aminoacyl group. A possible explanation for the specificity for aa-tRNA is that the 5′ end binding to EF-Tu and the length of the overhang of the four 3′ end

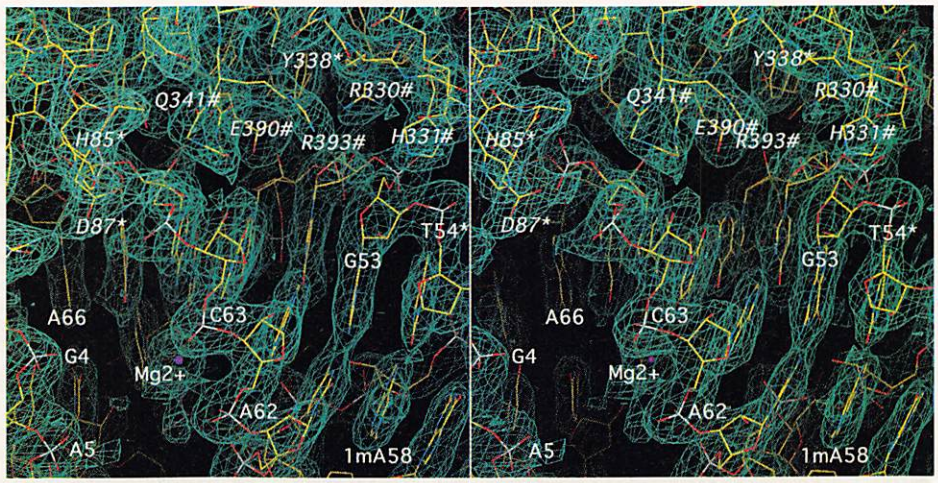

Fig. 2. Stereo diagram of the electron density of the EF-Tu–tRNA contact between domain 3 and the T stem (complex B+E). The electron density is a ($3F_o - 2F_c$) map contoured at 1.25 σ with a cutoff radius of 2.0 Å. The Mg^{2+} ion included in the T stem of the tRNA molecules is seen. Residue labels are marked with respect to the sequence alignment, thus * represents conserved residues in all sequences and # represents conservation in prokaryotes. Amino acid labels are in italic.

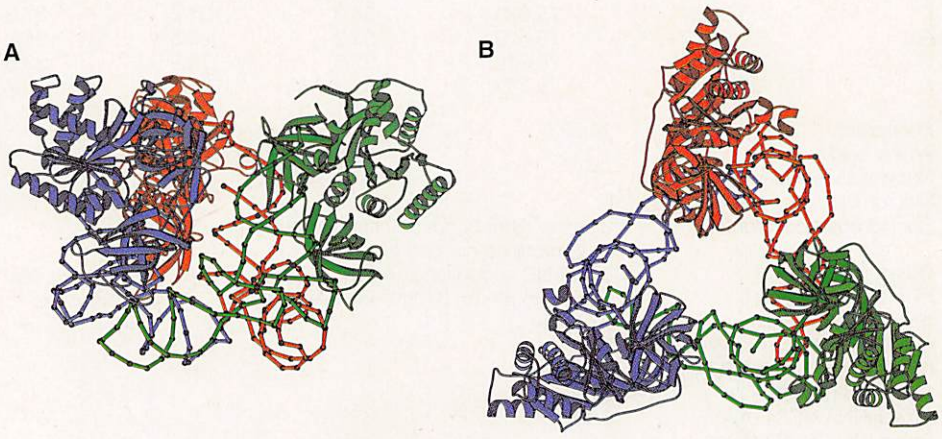

Fig. 3. Schematic representations (*72*) of the trimer forming the asymmetric unit. The EF-Tu–GTP molecules are represented as structural cartoons, and the tRNA molecules are shown as ball-and-stick connected C3′ atoms. The complexes of A+D, B+E, and C+F (table 2) are colored green, blue, and red, respectively. (**A**) Side view of the trimer, in the shape of a triangular frustum with EF-Tu flanking the top and the tRNA-tRNA contacts forming the bottom. (**B**) View along the pseudo threefold axis, with the EF-Tu molecules closest to the viewer, perpendicular to the first view. The lack of EF-Tu–EF-Tu contacts in the trimer can be seen as well as the tRNA-tRNA contacts forming corners of the trimer. See text and following figures for further detail.

nucleotides exactly allows the binding of the amino acid and the terminal adenine in their respective binding pockets between domains 1 and 2. Aminoacylation of the 3′ end regulates a "lock-and-key" match between EF-Tu–GTP and the CCA end. The additional binding energy comes from the protective binding of the amino ester, interactions with the aminoacyl side chain, and from induced interactions with the adenine and the rest of the CCA-end. The T stem and the 5′ end of uncharged tRNA can probably bind to EF-Tu–GTP, but the absence of the aminoacylation disfavors the binding of any part of the 3′ end. In prokaryotic initiator tRNA the last base pair is mismatched giving an overhang of five nucleotides. Furthermore, a formylation prevents the binding of the amino ester. Eukaryotic initiator tRNA is not formylated, but has a phosphoribosylation of nucleotide 64 which would prevent an interaction with domain 3 (*37*, *38*).

In the GDP form of EF-Tu, the tRNA binding site does not exist. Domains 2 and 3 are rotated by 90° relative to domain 1 (*11*, *12*), and the two GTPase switch regions of domain 1 adopt new conformations. Thus, all features of the aa-tRNA binding site have been moved apart. However, EF-Tu–GDP does protect the aminoacyl bond against spontaneous hydrolysis, albeit very weakly (*39*). We propose that aa-tRNA can induce an EF-Tu–GTP–like conformation of EF-Tu–GDP in an equilibrium that is shifted towards free EF-Tu–GDP and aa-tRNA.

His^{119} and aa-tRNA binding. Several studies of *E. coli* EF-Tu indicate that not only His^{66} but also His^{118} is involved in the ternary complex formation (His^{67} and His^{119} in *T. aquaticus*). Crosslinks of *trans*-diaminedichloro-platinum(II) to His^{66} and His^{118} in the ternary complex has been reported (*40*). The same two residues have been shown to be protected against photo-oxidation in the ternary complex (*41*). Finally, mutational analysis has indicated that they both participate in aa-tRNA binding (*42*, *43*). In the present structure, His^{67} interacts directly with the side chain of the aminoacyl group of Phe-tRNA. However, the structure cannot account for the apparent involvement of His^{119} in tRNA binding. This residue is buried in an interface between domains 1 and 3 in all of the structures of EF-Tu yet known, and the minimal distance to aa-tRNA is 16 Å. We suggest that part of the explanation could be the dynamic properties of EF-Tu.

When EF-Tu is transformed from the GDP form to the GTP form, or vice versa, the interface between domains 1 and 3 most likely dissociates temporarily and subsequently reassembles in the new conformation (*12*). This transformation will expose His^{119} transiently. The dynamics of this transformation must be affected by the presence of aa-tRNA that will stabilize the GTP-bound form of EF-Tu.

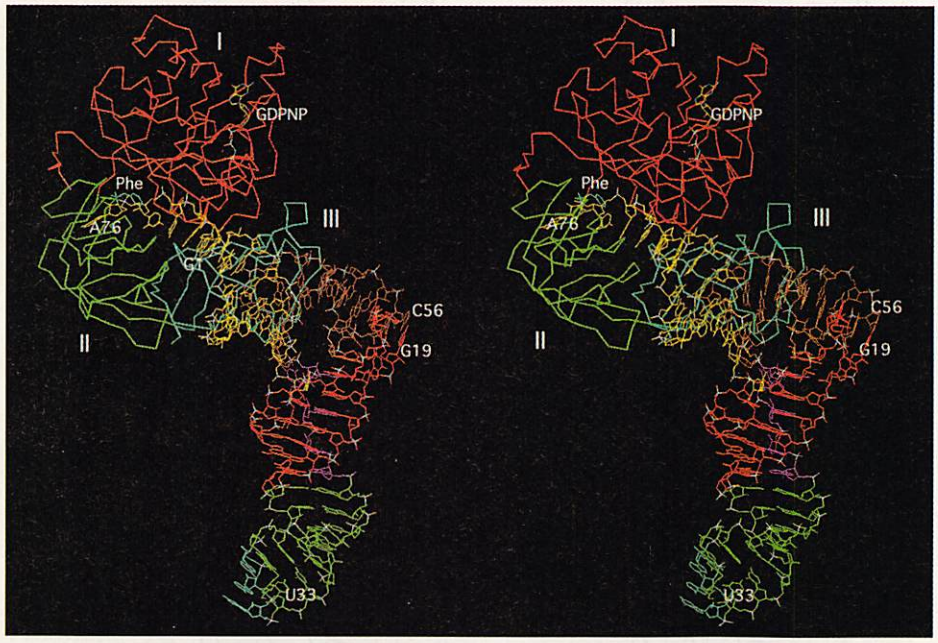

Fig. 4. Stereo diagram of the "corkscrew" structure of the ternary complex (complex C+F). EF-Tu–GDPNP is represented as a Cα trace, with domain 1 (1 to 213) in red, domain 2 (214 to 313) in green, domain 3 (314 to 405) in blue, and the GDPNP cofactor as a stick model. Phe-tRNA is colored with respect to the cloverleaf structure: acceptor stem in yellow (1 to 8 and 66 to 76), D arm in red (9 to 26), anticodon arm in green (27 to 43), variable loop in violet (44 to 48), T arm in orange (49 to 65), and the phenylalanyl group and the anticodon in blue. Phosphorus atoms are colored white.

Effector binding in G proteins. The G proteins have a common design of the G domain and a common mechanism of function has been suggested (*44*). However, the molecular design of the switch I and II regions determining the "on" and "off" state of the G proteins as a response to GDP and GTP binding may vary. This is most obvious in the response of the switch I region, which can be part of a loop in some proteins and part of a large insert in others (*1*). The response of the switch II region, where a helix changes its spatial orientation, varies in more subtle ways (*11*, *12*, *20*). The structure of the complex between Rap1A-GDPNP and a domain of an effector, c-Raf1, reveals an expected interaction between the effector and the effector loop (*45*). The functional effector of EF-Tu–GTP is aa-tRNA and the ribosome acting in cooperation. As such, the structure of the ternary complex is another example of a G protein in complex with an effector.

In EF-Tu, the switch I region is the "effector loop" between helix A and strand b_1 (residues 39 to 65) and the switch II region consists of helix B and connecting loops (residues 83 to 100). These switch regions are involved critically in the aa-tRNA binding (Figs. 4 and 5), and their conformations have not been greatly altered by the complex formation. This suggests that the switch regions of G proteins in the GTP-bound state may participate specifically in the formation of the binding site for the effector. Consequently, the switch would be unique to the target effector.

Stoichiometry of the ternary complex. We have speculated whether the quaternary structure of three ternary complexes in a trimer has a physiological role (Fig. 3). It is primarily formed through unspecific contacts. Trimers constituted of randomly selected aa-tRNAs could be advantageous with respect to the speed and fidelity of the selection process on the ribosome. The high concentration of ternary complexes in the cytosol (exceeding 100 μM) could also favor a trimeric assembly.

This is not the first proposal for a stoichiometry different from that of the classical ternary complex. A 3′-oxidized tRNA in complex with *E. coli* EF-Tu–GTP (*46*) was shown to cross-link to Lys^{208} and Lys^{237} (Lys^{219} and Lys^{248} in *T. aquaticus*), and a complex of two tRNAs per EF-Tu–GTP on the ribosome was suggested (*47*). These observations do not agree with our structure. None of these lysines is close enough to the 3′ end of tRNA to allow cross-linking without a major prior change in the conformation of the ternary complex.

A more persistent model of two EF-Tu's

per tRNA in a quinternary ("pentameric") complex (*48–50*) is based on the observation that two GTPs are hydrolyzed for each elongation cycle. Although the exact interpretation has been questioned (*51, 52*) the consumption of two GTP equivalents was also reported from studies on an XTP binding EF-Tu mutant (*53*). Two EF-Tu's are indeed in contact with one tRNA in the trimeric structure, but it seems unlikely that this could be the scaffold for a quinternary complex. However, the real question is not so much whether a quinternary complex exists as why two GTPs are consumed per peptide bond formed.

As mentioned earlier, footprinting studies identified interactions between tRNA and EF-Tu in the ternary complex monomer (*32*). Protections were observed at positions 44 to 51 and less obviously in the anticodon loop, where enhancements of nuclease digestion were also observed. This fits surprisingly well with the trimer structure, in which positions 44 to 51 are close to the anticodon loop of a neighboring tRNA and forms a corner of the trimer by the continuous stacking of the anticodon to G20. As these observations are in agreement with the RNA-RNA contacts in the trimer and originates from experiments using ternary complexes from *E. coli*, we take them as independent experimental evidence supporting our speculation that ternary complexes can exist as trimers in solution.

Comparison with elongation factor EF-G. The translocation factor EF-G exhibits a vigorous GTPase activity which is dependent on the presence of ribosomes and on the mRNA-directed binding of tRNA. In vivo, EF-G promotes fast translocation in pretranslocational ribosomes and converts them to the posttranslocational form (*54*). The crystal structures of EF-G from *T. thermophilus* in the nucleotide-free (*14*) and in the GDP form (*13*) are largely isomorphous. The molecule consists of five domains and has an overall shape resembling a tadpole, with a large head and a cylindrical tail. Domains 1 (the G domain) and 2 are structurally analogous to domains 1 and 2 of EF-Tu. Domains 3 and 5 of EF-G have topologies similar to that of the ribosomal protein S6 (*14*). Domain 4, forming the tip of the tail, reveals an unusual βαβ topology, with a left-handed crossover connection of two central β-strands. This topology is also found in the ribosomal protein S5 and in a domain of DNA gyrase (*55*).

In Fig. 6 we have aligned the Phe-tRNA–EF-Tu–GDPNP structure with EF-G, using the Cα coordinates from the G domains and the domains 2. The complete superposition of the two structures is almost perfect. Domains 3, 4, and 5 of EF-G appear to mimic the shape of the tRNA moiety of the ternary complex, with domain 3 acting as the acceptor stem, domain 5 as the T stem (and part of EF-Tu domain 3), and domain 4 as the anticodon helix. The position of the tRNA mimic of EF-G differs slightly from that of tRNA in the ternary complex. This overall resemblance of the ternary complex and EF-G represents a structural example of similarity between protein and nucleic acids counterparts. Functional mimicry of a major autoantigenic epitope of human insulin receptor by RNA has been reported (*56*) and the structure of an inhibitor of uracil-DNA glycosylase has been described as a DNA mimic (*57, 58*), which suggests that molecular mimicry is likely to be a new concept of general importance.

Translation factor interaction with the ribosome. The implication of the molecular mimicry of EF-G–GDP and the ternary complex is that they must have a common binding site on the ribosome. Most probably, this site is physically close to the ribosomal A site. This proposal is supported by the observations that both factors protect the α-sarcin loop of 23S RNA from reaction with chemical probes (*59*) and that the interaction of both factors with the ribosome is abolished if the α-sarcin loop is cleaved (*60*). In addition, the factors have been mapped on the ribosomal surface by electron microscopy with immunostaining (*61–63*), and there is a substantial correspondence between their locations.

EF-G interacts with the ribosome in its pretranslocational state, catalyzing the transition of the ribosome to its posttranslocational state (*54*). The ternary complex catalyzes the transition in the opposite direction. The overall structural similarity supports an explanation for the puzzling observation that the organization of domains 1 and 2 in the GDP form of EF-G resembles that of the GTP form of EF-Tu (*14*). Both species interact with the ribosome in its posttranslocational state.

The overall resemblance between EF-G–GDP and the ternary complex (Fig. 6) raises questions concerning the structure and function of these two elongation factors on the ribosome. Three inferences can be drawn. First, EF-G catalyzed translocation transforms the ribosome into a state with a binding pocket for a ternary complex. This pocket could be formed by the shape of EF-G–GDP after GTP hydrolysis on the ribosome. Hence, before translocation EF-G–GTP must bind to a pocket with a somewhat

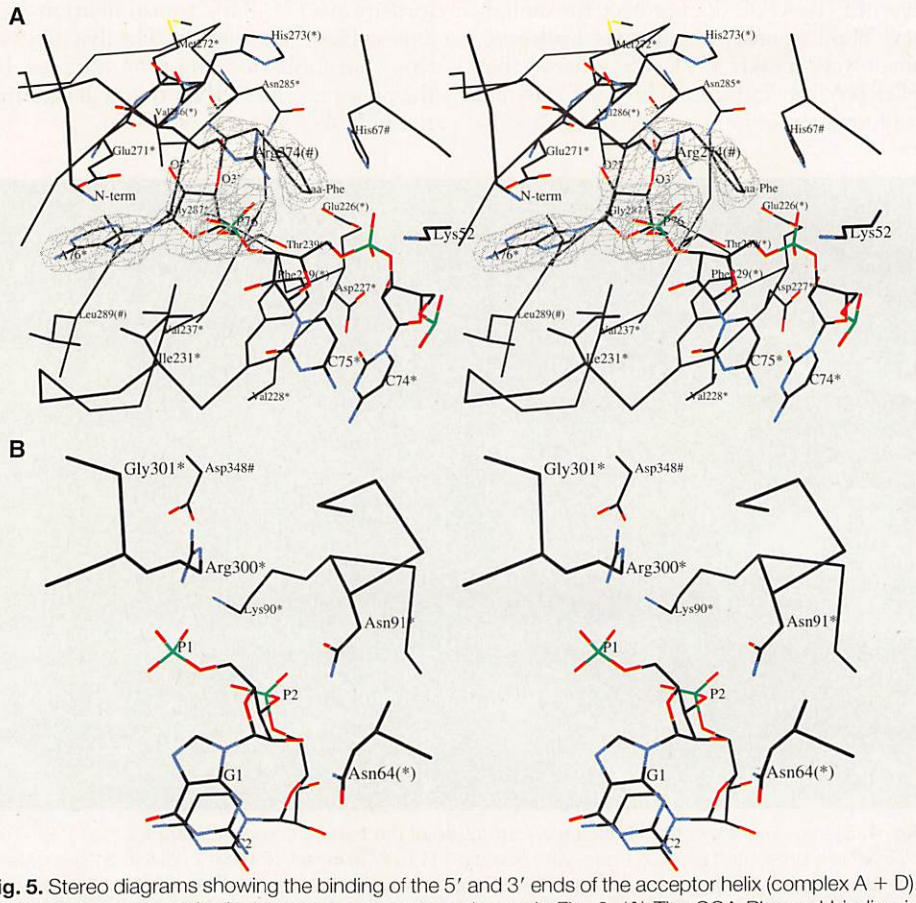

Fig. 5. Stereo diagrams showing the binding of the 5′ and 3′ ends of the acceptor helix (complex A + D). Residue labels are marked with respect to conservation as in Fig. 2. (**A**) The CCA-Phe end binding in EF-Tu–GDPNP. The electron density around the 3′ aminoacyl group has been contoured at 1.0 σ with a cutoff of 1.0 Å. (**B**) Binding of the 5′ end to EF-Tu–GDPNP.

different shape. Second, the GTPase activities of EF-G and EF-Tu must be stimulated by the same center on the ribosome. This makes it likely that all G proteins in protein biosynthesis will have their guanosine triphosphatase (GTPase) activities stimulated by this center and by the same mechanism at the same time. Third, the structural similarity suggests that the anticodon stem mimicking domain 4 of EF-G during the translocation process competes with peptidyl-tRNA for a translocation center near the codon-anticodon recognition site on the 30S subunit (2).

How these correlated binding pockets for EF-G and the ternary complex relate to the classical A-site on the ribosome is not clear at the moment. Nevertheless, the catalytic effect of the translation factors could be the modulation of the ribosome structure in a mechanical manner closely correlated with the GTPase induced switch of the structures of the factors.

There has been some debate on the configuration of the two tRNAs in the A and P sites on the ribosome (*64*, *65*). The two configurations, designated the R and S forms (after "Rich" and "Sundaralingam"), are based on the assumption that during peptidyl transfer the anticodons and the CCA ends must be close together. The two configurations place the A site tRNA on either side of a P site tRNA (*64*). From the present structure the binding of EF-Tu–GDPNP on one side of tRNA would exclude this side for interaction with the P site tRNA. This makes the S form the most probable configuration.

Possibility of other translation factors with tRNA-like components. It is tempting to predict some features of tRNA mimicry in the structures of the initiation and release factors. IF-2–GTP stimulates the binding of fMet-tRNA directly into the P site of the 70S (*66*), and we predict that IF-2, in analogy to EF-G, will be found to have tRNA-mimicking domains, which would occupy part of the A site during the initiation reaction and thus mediate the binding of fMet-tRNA to the P site. We find it most probable that the G domain of IF-2 is bound close to the GTPase center of the ribosome. The relative orientations of fMet-tRNA and the putative tRNA-mimicking domain of IF-2 could then provide a model for the spatial organization of the GTPase center and tRNAs in the A and P sites of the ribosome.

The release factors catalyze the final hydrolysis of the peptidyl-tRNA ester bond and the dissociation of the ribsomal subunits. In prokaryotes, three release factors, RF-1, RF-2 and RF-3, are known. Both RF-1 and RF-2 induce peptidyl-tRNA hydrolysis as a response to the stop codons on mRNA and it is further stimulated by RF-3, which is a G protein. The primary structure of RF-3 from *E. coli* shows an overall similarity with EF-G (*67*), and thus a similar structure and function can be expected. The factors RF-1 and RF-2 have been postulated to be protein analogs of tRNAs, which is very probable in light of their codon specific function and their size (*68*). Furthermore, it has long been a puzzle that a nucleic acid in the form of suppressor tRNA could compete with release factor activity. We propose that termination is a final "elongation cycle" with release factors interacting with the ribosome instead of a ternary complex and EF-G. Binding of RF-1 or RF-2 to the ribosome leads to the hydrolysis of peptidyl-tRNA. The RF-3–GTP–mediated "translocation" of RF-1 or RF-2 into the P site and of the empty tRNA into the E site results in the dissociation of the ribosome.

Following the concept of tRNA mimicry, the ancestor of all GTPases in translation must be EF-Tu which acts in conjunction with tRNA itself. In fact, this makes EF-Tu the most likely candidate for an ancestor of all G proteins since the development of a translational apparatus must have been an early event in evolution. We suggest that molecular mimicry is an important property of protein-RNA interactions involved in the process of translation and that the appearance of similarity between protein and RNA structure has been an important event in evolution.

Fig. 6. Ternary complex (A+D) to the left and EF-G (*14*) to the right shown side by side in a schematic representation (*72*). EF-Tu and EF-G are shown as structural cartoons and tRNA as a ball-and-stick model of the C3′ atoms. The two molecules are shown in almost the same orientation as in Fig. 4.

REFERENCES AND NOTES

1. H. R. Bourne, D. A. Sanders, F. McCormick, *Nature* **349**, 117 (1991).
2. D. Moazed and H. F. Noller, *ibid.* **342**, 142 (1989).
3. M. Delarue and D. Moras, *BioEssays* **15**, 675 (1993).
4. H. G. Faulhammer and R. L. Joshi, *FEBS Lett.* **217**, 203 (1987).
5. C. Förster, S. Limmer, S. Ribeiro, R. Hilgenfeld, M. Sprinzl, *Biochimie* **75**, 1159 (1993).
6. B. F. C. Clark, M. Kjeldgaard, J. Barciszewski, M. Sprinzl, in *tRNA: Structure, Biosynthesis and Function*, S. Söll and U. RajBhandary, Eds. (American Society for Microbiology, Washington, DC, 1995), pp. 423–442.
7. T. G. Kinzy, J. P. Freeman, A. E. Johnson, W. C. Merrick, *J. Biol. Chem.* **267**, 1623 (1992).
8. J. D. Robertus *et al.*, *Nature* **250**, 546 (1974).
9. S.-H. Kim *et al.*, *Science* **185**, 435 (1974).
10. M. Kjeldgaard and J. Nyborg, *J. Mol. Biol.* **223**, 721 (1992).
11. H. Berchtold *et al.*, *Nature* **365**, 126 (1993).
12. M. Kjeldgaard, P. Nissen, S. Thirup, J. Nyborg, *Structure* **1**, 35 (1993).
13. J. Czworkowski, J. Wang, T. A. Steitz, P. B. Moore, *EMBO J.* **13**, 3661 (1994).
14. A. Ævarsson *et al.*, *ibid.*, p. 3669.
15. E. Pai *et al.*, *ibid.* **9**, 2351 (1990).
16. L. Tong, A. M. de Vos, M. V. Milburn, S.-H. Kim, *J. Mol. Biol.* **217**, 503 (1991).
17. K. Scheffzek, C. Klebe, K. Fritz-Wolf, W. Kabsch, A. Wittinghofer, *Nature* **374**, 378 (1995).
18. J. C. Amor, D. H. Harrison, R. A. Kahn, D. Ringe, *ibid.* **372**, 704 (1994).
19. D. G. Lambright, J. P. Noel, H. E. Hamm, P. B. Sigler, *ibid.* **369**, 621 (1994).
20. J. P. Noel, H. E. Hamm, P. B. Sigler, *ibid.* **366**, 654 (1993).
21. D. E. Coleman *et al.*, *Science* **265**, 1405 (1994).
22. P. Nissen *et al.*, *FEBS Lett.* **356**, 165 (1994).
23. A. Jack, J. E. Ladner, A. Klug, *J. Mol. Biol.* **108**, 619 (1976).
24. J. Navaza, *Acta Crystallogr.* **A50**, 157 (1994).
25. A. T. Brünger, M. Karplus, G. A. Petsko, *ibid.* **A45**, 50 (1989).
26. T. A. Jones, S. Cowan, J.-Y. Zou, M. Kjeldgaard, *ibid.* **A47**, 110 (1991).
27. D. E. Tronrud, *ibid.* **A48**, 912 (1992).
28. R. Österberg, B. Sjöberg, R. Ligaarden, P. Elias, *Eur. J. Biochem.* **117**, 155 (1981).
29. B. Antonsson, R. Leberman, B. Jacrot, G. Zaccai, *Biochemistry* **25**, 3655 (1986).
30. C. Förster, S. Limmer, W. Zeidler, M. Sprinzl, *Proc. Natl. Acad. Sci. U.S.A.* **91**, 4254 (1994).
31. J. P. Abrahams *et al.*, *Spectroscopy* **10**, 1 (1992).
32. F. P. Wikman, G. E. Siboska, H. U. Petersen, B. F. Clark, *EMBO J.* **1**, 1095 (1982).
33. B. Antonsson and R. Leberman, *Eur. J. Biochem.* **141**, 483 (1984).
34. A. Louie, N. S. Ribeiro, B. R. Reid, F. Jurnak, *J. Biol. Chem.* **259**, 5010 (1984).
35. G. Ott *et al.*, *Biochim. Biophys. Acta* **1050**, 222 (1990).
36. R. G. Shulman, C. W. Hilbers, D. L. Miller, *J. Mol. Biol.* **90**, 601 (1974).
37. S. Kiesewetter, G. Ott, M. Sprinzl, *Nucleic Acids Res.*

18, 4677 (1990).
38. R. Basavappa and P. B. Sigler, *EMBO J.* **10**, 3105 (1991).
39. A. Pingoud, W. Block, A. Wittinghofer, H. Wolf, E. Fischer, *J. Biol. Chem.* **257**, 11261 (1982).
40. M. H. Metz-Boutigue, J. Reinbolt, J. P. Ebel, C. Ehresmann, B. Ehresmann, *FEBS Lett.* **245**, 194 (1989).
41. J. Jonak, T. E. Petersen, B. Meloun, I. Rychlik, *Eur. J. Biochem.* **144**, 295 (1984).
42. J. Jonák, P. H. Anborgh, A. Parmeggianni, *FEBS Lett.* **343**, 94 (1994).
43. C. Andersen and O. Wiborg, *Eur. J. Biochem.* **220**, 739 (1994).
44. P. F. W. Stouten, C. Sander, A. Wittinghofer, A. Valencia, *FEBS Lett.* **320**, 1 (1993).
45. N. Nassar *et al.*, *Nature* **375**, 554 (1995).
46. J. M. van Noort *et al.*, *Proc. Natl. Acad. Sci. U.S.A.* **81**, 3969 (1984).
47. J. M. van Noort, B. Kraal, L. Bosch, *ibid.* **82**, 3212 (1985).
48. M. Ehrenberg, A. M. Rojas, J. Weiser, C. G. Kurland, *J. Mol. Biol.* **211**, 739 (1990).
49. J. Scoble, N. Bilgin, M. Ehrenberg, *Biochimie* **76**, 59 (1994).
50. V. Dinçbas, N. Bilgin, J. Scoble, M. Ehrenberg, *FEBS Lett.* **357**, 19 (1995).
51. M. V. Rodnina and W. Wintermeyer, *Proc. Natl. Acad. Sci. U.S.A.* **92**, 1945 (1995).
52. R. Leberman, *FEBS Lett.* **358**, 71 (1995).
53. A. Weijland and A. Parmeggiani, *Trends Biochem. Sci.* **19**, 188 (1994).
54. K. H. Nierhaus *et al.*, in *The Translational Apparatus*, K. H. Nierhaus, F. Franceschi, A. R. Subramanian, V. A. Erdmann, B. Wittmann-Liebold, Eds. (Plenum, New York, 1993), pp. 263–272.
55. A. G. Murzin, *Nature Struct. Biol.* **2**, 25 (1995).
56. J. A. Doudna, T. R. Cech, B. A. Sullenger, *Proc. Natl. Acad. Sci. U.S.A.* **92**, 2355 (1995).
57. R. Savva and L. H. Pearl, *Nature Struct. Biol.* **2**, 752 (1995).
58. C. D. Mol *et al.*, *Cell* **82**, 701 (1995).
59. D. Moazed, J. M. Robertson, H. F. Noller, *Nature* **334**, 362 (1988).
60. T.-P. Hausner, J. Atmadja, K. H. Nierhaus, *Biochimie* **69**, 911 (1987).
61. A. S. Girshovich, T. V. Kurtskhalia, T. A. Avchinnikov, V. D. Vasiliev, *FEBS Lett.* **130**, 54 (1981).
62. A. S. Girshovich, E. S. Bochkareva, V. D. Vasiliev, *ibid.* **197**, 911 (1986).
63. J. A. Langer and J. A. Lake, *J. Mol. Biol.* **187**, 617 (1986).
64. M. Yarus and D. Smith, in *tRNA: Structure, Biosynthesis, and Function*, D. Söll and U. Rajbhandary, Eds. (American Society for Microbiology, Washington, DC, 1995), pp. 443–469.
65. V. Lim *et al.*, *Nucleic Acids Res.* **20**, 2627 (1992).
66. R. Spurio *et al.*, in *The Translational Apparatus. Structure, Function, Regulation, Evolution*, K. H. Nierhaus, F. Franceschi, A. R. Subramanian, Eds. (Plenum, New York, 1993), pp. 241–252.
67. G. Grentzmann, D. Brechemier-Baey, V. Heurgué, L. Mora, R. H. Buckingham, *Proc. Natl. Acad. Sci. U.S.A.* **91**, 5848 (1994).
68. C. R. Cantor, in *Transfer RNA: Structure, Properties, and Recognition*, P. R. Schimmel, D. Söll, J. N. Abelson, Eds. (Cold Spring Harbor Laboratory, Cold Spring Harbor, NY, 1979), pp. 363–392.
69. Z. Otwinowski, Oscillation data reduction program, L. Sawyer, N. Isaacs, S. Bailey, Eds., *CCP4 Study Weekend: Data Collection and Processing* (Daresbury Laboratory, Warrington, UK, 1993).
70. CCP4 (Daresbury Laboratory, Warrington, UK, 1979).
71. R. A. Engh and R. Huber, *Acta Crystallogr.* **A47**, 392 (1991).
72. P. J. Kraulis, *J. Appl. Crystallogr.* **24**, 946 (1991).
73. R. H. Voss *et al.*, *Eur. J. Biochem.* **207**, 839 (1992).
74. M. D. Jones *et al.*, *ibid.* **108**, 507 (1980).
75. P. Cottrelle *et al.*, *J. Biol. Chem.* **260**, 3090 (1985).
76. A. Bairoch and B. Boeckmann, *Nucleic Acids Res.* **22**, 3578 (1994).
77. S. Thirup and N. E. Larsen, *Proteins* **7**, 291 (1990).
78. We thank P. B. Moore, J. Czworkowski, A. Ærsson, S. Al-Karadaghi, and A. Liljas for supplying their coordinates of EF-G, and for stimulating discussions; W. C. Merrick and J. Jonak for continued interest and fruitful discussions; L. Clowney and H. Berman for supplying updated nucleic acid geometric parameters prior to their public release, and G. Siboska and L. B. Van for technical assistance. Supported by the Protein Engineering Research Centre and the Synchrotron Radiation Committee of the Natural Science Research Council in Denmark, and by a stipend from Aarhus University (P.N.). Coordinates have been deposited in the Protein Data Bank, Brookhaven, NY, with accession number 1TTT.

11 August 1995; accepted 15 October 1995

AAAS–Newcomb Cleveland Prize

To Be Awarded for a Report, Research Article, or an Article Published in *Science*

The AAAS–Newcomb Cleveland Prize is awarded to the author of an outstanding paper published in *Science*. The value of the prize is $5000; the winner also receives a bronze medal. The current competition period began with the 2 June 1995 issue and ends with the issue of 31 May 1996.

Reports, Research Articles, and Articles that include original research data, theories, or syntheses and are fundamental contributions to basic knowledge or technical achievements of far-reaching consequence are eligible for consideration for the prize. The paper must be a first-time publication of the author's own work. Reference to pertinent earlier work by the author may be included to give perspective.

Throughout the competition period, readers are invited to nominate papers appearing in the Reports, Research Articles, or Articles sections. Nominations must be typed, and the following information provided: the title of the paper, issue in which it was published, author's name, and a brief statement of justification for nomination. Nominations should be submitted to the AAAS–Newcomb Cleveland Prize, AAAS, Room 924, 1333 H Street, NW, Washington, DC 20005, and **must be received on or before 30 June 1996**. Final selection will rest with a panel of distinguished scientists appointed by the editor-in-chief of *Science*.

The award will be presented at the 1997 AAAS annual meeting. In cases of multiple authorship, the prize will be divided equally between or among the authors.

Phase Diagram of Iron by in Situ X-ray Diffraction: Implications for Earth's Core

C. S. Yoo,* J. Akella, A. J. Campbell,† H. K. Mao, R. J. Hemley

The phase diagram of iron has been studied to 130 gigapascals (1 gigapascal = 10^4 atmospheres) and 3500 kelvin by a combined laser-heated diamond-anvil cell and x-ray diffraction technique that provides direct identification of the solid phases. Iron in the hexagonal close-packed (hcp) phase (ε-Fe) is stable from 50 to at least 110 gigapascals at high temperatures. The wide stability field of ε-Fe indicates that this polymorph should currently be considered the most relevant solid phase for Earth's core. The triple point between the γ, ε, and liquid phases is located at 2500 ± 200 kelvin and 50 ± 10 gigapascals. There is evidence for a phase with a double hcp structure below 40 gigapascals and for another transition above 110 gigapascals and 3000 kelvin.

Because iron is the dominant component of Earth's core, information on the behavior of iron at high pressures and temperatures is fundamental to Earth science. In particular, determination of the phase diagram of iron is central to understanding a number of properties and processes of the planet's deep interior, including the temperature profile, chemical composition, energy balance, dynamics, and geomagnetism (*1–4*). High-pressure diamond-anvil cell (*5–7*) and shock-wave experiments (*7–10*) are providing important constraints on the phase relations over a growing range of pressure and temperature. However, the accurate determination of the phase diagram of this crucial element under Earth-core conditions is still a formidable experimental problem because of the extreme pressure and temperature (*P-T*) conditions involved.

Five phases of iron, namely α [body-centered cubic (bcc)], γ [face-centered cubic (fcc)], δ (bcc), ε (hcp), and β (no structural information), have been reported. Crystal structures and phase boundaries of α-, γ-, δ-, and ε-Fe are well determined at low pressures (below 20 GPa). As indicated by x-ray diffraction measured to 300 GPa at ambient temperature, ε-Fe is the stable phase of iron at 300 K to pressures of Earth's core (*11*). Phase boundaries at high temperatures and pressures, however, have been determined primarily by indirect methods. Because these do not provide unequivocal identification of solid phases, several key aspects of the phase diagram are uncertain. First, the location of the ε-γ-liquid triple point is not well established (*1, 5, 12, 13*). Second, various determinations of the melting temperature above 50 GPa are discrepant; this includes differences among the static measurements (*5–7*) and between static and shock-wave results (*7–10*). Third, the structure and stability field of the β phase remain to be clarified. Fourth, the nature of the 200-GPa transition suggested by shock-wave experiments is unknown (*10*). A reentrant α′ (bcc) phase (*2*) or the β phase (*5, 6*) was proposed to explain the transition; however, subsequent theoretical calculations indicated that the bcc structure is mechanically unstable under these conditions (*3, 14*).

We developed an integrated diamond-anvil cell, x-ray, and laser-heating technique to examine the iron phase diagram by directly probing the crystal structure of the phases in situ at high temperatures and pressures. This system consists of three components (*15*): (i) a Nd–yttrium-aluminum-garnet laser-heating system to heat the sample in a diamond-anvil cell, (ii) a microscope system to measure temperature and view the sample for alignment and direct observation, and (iii) a synchrotron x-ray and energy-dispersive diffraction system. A small piece of thin iron foil is loaded in a diamond cell, together with a pressure medium such as argon, Al_2O_3, or LiF. Polychromatic (white) x-ray radiation from the synchrotron source is coaxially aligned to the center of laser heating spot, and the diffraction from the sample is recorded at a fixed scattering angle 2Θ as a function of energy. The temperature of the sample is simultaneously determined from the thermal emission from the laser-heated area. The pressure of the sample is determined either by the equation of state of the sample or from the ruby luminescence method (*16*).

There was a distinct change in the x-ray diffraction pattern of iron upon melting during laser heating. For example, at 50 GPa (Fig. 1) at least four strong features from ε-Fe and several weak bands from Al_2O_3 were observed at 300 K. During laser heating to 2280 K, all of the diffraction lines of ε-Fe shifted to lower energies or higher *d* spacings, indicating thermal expansion of the iron. There was little change in the relative intensity of the iron diffraction pattern in comparison to that of Al_2O_3, and thermal broadening of the diffraction bands was negligible. Near 2580 K, however, the diffraction lines of ε-Fe weakened and disappeared, indicating that the sample in the laser-heated spot had melted. Upon cooling, each of the diffraction lines of ε-Fe reappeared (Fig. 1, top curve). The quenched ε-Fe crystallized with preferred orientation of the (100) plane in the diffraction direction. After heating, a small circular trace was evident visually in the laser-heated area, providing further indication of melting. These measurements also bracketed the melting temperature at this pressure between 2280 and 2580 K.

At 50 GPa, we observed ε-Fe up to 2480 K and conclude that the melting temperature is 2530 ± 50 K. This value is consistent with results reported in (*5*). The ε-Fe is the only solid phase observed up to at least 110 GPa. We noticed during laser heating at 96 GPa (Fig. 2) that the diffraction peaks shifted and changed in intensity, particularly the 101, 110, and 112 reflections. All of the features can be understood in terms of ε-Fe and Al_2O_3, and no new features developed at high temperatures. The above measurements indicate that between 50 to 110 GPa, ε-Fe is the stable solid phase at least to the melting curve proposed in (*5*).

There were indications of a transition at higher pressures (above 110 GPa) and higher temperatures. Diffraction peaks charac-

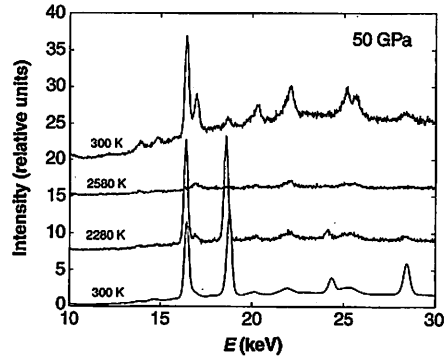

Fig. 1. The x-ray diffraction patterns of the laser-heated iron at 50 GPa, showing the melting of iron at 2580 K. Starting at 300 K (bottom curve; divided by 50 for clarity), the sample was heated through 2280 K to 2580 K, and then cooled back to 300 K (top curve; multiplied by 3). The ε phase is evident from four strong features—the 100 diffraction peak at 16.44 keV, 101 at 18.78 keV, 102 at 24.36 keV, and 110 at 28.48 keV—and a weaker feature of the 200 peak at 17.80 keV (Ed = 33.94 keV Å, where E is energy and d is the d spacing). The iron melted from the ε phase, suggesting that the γ-ε-liquid triple point is located in the vicinity of this pressure.

C. S. Yoo and J. Akella, Lawrence Livermore National Laboratory, University of California, Livermore, CA 94551, USA.
A. J. Campbell, H. K. Mao, R. J. Hemley, Geophysical Laboratory and Center for High Pressure Research, Carnegie Institute, Washington, DC 20015, USA.

*To whom correspondence should be addressed.
†Present address: G.E. Superabrasives, 6325 Huntley Road, P.O. Box 568, Worthington, OH 43085, USA.

teristic of the ε phase were observed below 2500 K at 125 GPa (Fig. 3), but these diffraction lines weakened significantly above 2500 K and eventually disappeared above 3300 K. Moreover, a new line developed at 15.22 keV (d = 2.229 Å) above 2920 K, where the diffraction lines of ε-Fe disappeared. The new band was not associated with Al_2O_3 but arose from the iron portion of the sample. In addition, the 104 and 110 lines of Al_2O_3 should have been located at 14.62 keV (d = 2.321 Å) and 15.68 keV (d = 2.164 Å), respectively, at this pressure (*17*). We were able to quench the new diffraction band at ambient temperature after heating. The iron sample quenched from 3300 K showed no relation to the ε phase; in addition, there was little change in visual appearance of the sample.

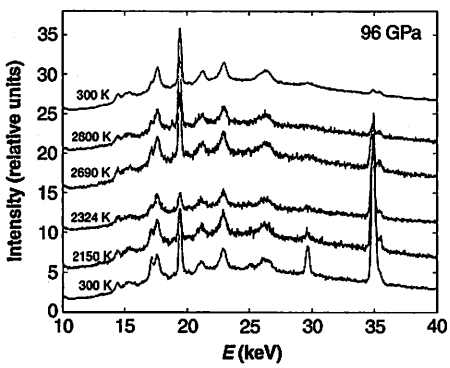

Fig. 2. The x-ray diffraction patterns of the laser-heated iron at 96 GPa, showing that β-Fe is not evident to 2800 K at this pressure. The heating cycle starts with the bottom curve and moves upward. The ε phase is evident at all of the temperatures by the 100, 101, 102, 110, and 112 bands at, respectively, 17.15, 19.46, 25.10, 29.64, and 34.97 keV (Ed = 33.94 keV Å). Other, weaker broad features are from Al_2O_3. Also noticed is the recrystallization of ε-Fe above 2300 K.

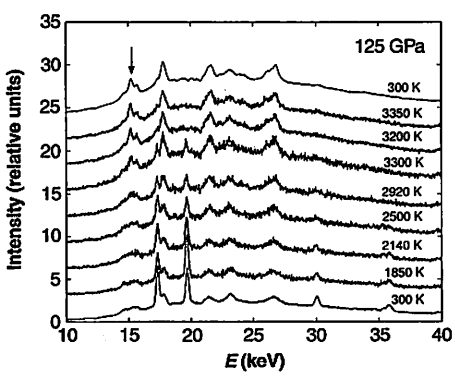

Fig. 3. The x-ray diffraction patterns of the laser-heated iron at 125 GPa, showing that a new diffraction line (arrow) develops as the diffraction lines from ε-Fe disappear above 3000 K. The 100, 101, 110, and 112 reflections of ε-Fe are located at 17.33, 19.71, 30.07, and 35.81 keV, respectively (Ed = 33.94 keV Å). The heating cycle starts with the bottom curve and moves upward.

We conclude that the loss of the diffraction intensity of ε-Fe was not a result of melting but instead arose either from a previously undisclosed high P-T solid-solid transition or from a reaction between Fe and Al_2O_3 (*18*). The transition temperature was close to that previously reported for melting at this pressure (*5*). It is therefore possible that these observations refer to the same transition, although our current understanding of the transition is too premature to completely rule out alternative hypotheses.

The P-T conditions of the present measurements are compared in Fig. 4 with phase boundaries taken from the literature. Between 50 and 110 GPa, only the hcp diffraction pattern is observed. These results contrast with the previously suggested stability field of β-Fe. The β phase was originally suggested on the basis of an abrupt change in either the laser power or the reflected light intensity as a function of the sample temperature during laser heating (*5*, *6*). Such change does not necessarily reflect a structural phase transition; it could also be caused by electronic transitions or even by mechanisms unrelated to phase transitions (*19*).

Our results also provide information on the phase diagram at lower pressures. Between 15 and 40 GPa at moderate temperatures, we found a phase of iron that yields a diffraction pattern that can be indexed as a double hcp (dhcp) structure, that is, with an ABAC stacking sequence (*20*). The dhcp phase has also been observed in a recent study below 40 GPa (*21*). Our measurements indicate that from 40 GPa to between 110 and 150 GPa, the dhcp phase is not observed

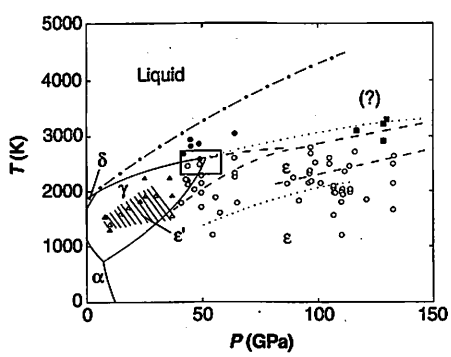

Fig. 4. Constraints for the phase diagram of iron. Various symbols indicate the phases of iron as determined by in situ x-ray diffraction at high pressures and temperatures: liquid iron (●), ε-Fe (○), ε′-Fe (△), γ-Fe (▲), and new crystalline (■). The area indicated by the large rectangle constrains the location of the ε-γ-liquid triple point. The hatched area indicates the P-T region of which the ε′ phase forms between 15 and 40 GPa. Previously reported phase boundaries are also reproduced for comparison: melting lines are reproduced from (*5*) (upper dashed lines), from (*6*) (upper dotted line), and from (*7*) (dashed-dotted line), and ε-β boundaries are shown from (*5*) (lower dashed line) and from (*6*) (lower dotted line).

in most of the previously suggested β-Fe field (*5*, *6*). This phase, which we tentatively called ε′-Fe, was observed mostly in a portion of stability field previously assigned for γ-Fe, and a small corner of the field for β-Fe. The γ-phase was observed at higher temperatures than the ε′-phase to 50 GPa, but not at higher pressures. These results indicate that γ-Fe and ε′-Fe are lower pressure phases and thus are not relevant to the core (135 to 363 GPa).

In summary (Fig. 4), our results indicate that the line between the γ or ε′ phases and the ε phase should be either straight or concave up (*22*). Considering that the melting temperature determined here agrees with values reported earlier (*5*, *6*), one can extrapolate the γ(ε′)-ε phase line to the melting line in Fig 4. This indicates that the ε-γ-liquid triple point is at 2500 ± 200 K and 50 ± 10 GPa, substantially lower than 100 GPa. Above 50 GPa, we observed neither the ε′ phase nor any diffraction lines that could be indicative of other new phases (for example, β- or α-Fe). Only the ε phase is evident between 50 and 110 GPa, in a wide range of temperatures at least to the melting line reported in (*5*). Above 100 to 120 GPa, however, the nature of the iron phase diagram is not well established (Fig. 3). We conjecture that either a new solid-solid transition or more likely a chemical reaction occurs above 110 GPa and 3000 K in Fig. 4. In this case, the actual melting temperatures of iron at these pressures could be substantially higher than those reported in (*5*).

REFERENCES AND NOTES

1. O. L. Anderson, *J. Geophys. Res.* **95**, 21697 (1990).
2. M. Ross, D. A. Young, R. Grover, *ibid.*, p. 21713.
3. J. Moriarty, in *High Pressure Science and Technology–1993*, S. C. Schmidt *et al.*, Eds. (American Institute of Physics, New York, 1994), p. 233; R. E. Cohen *et al.*, *ibid.*, p. 891.
4. L. Stixrude and R. E. Cohen, *Science* **267**, 1972 (1995).
5. R. Boehler, *Nature* **363**, 534 (1993); ———, N. von Bargen, A. Chopelas, *J. Geophys. Res.* **95**, 21731 (1990).
6. S. K. Saxena, G. Shen, P. Lazor, *Science* **260**, 1312 (1993); *ibid.* **264**, 405 (1994).
7. Q. Williams *et al.*, *ibid.* **236**, 181 (1987).
8. C. S. Yoo, N. C. Holmes, M. Ross, D. J. Webb, C. Pike, *Phys. Rev. Lett.* **70**, 3931 (1993).
9. K. G. Gallagher and T. J. Ahrens, *Eos* **75** (fall suppl.), 653 (1994).
10. J. M. Brown and R. G. McQueen, *J. Geophys. Res.* **91**, 7485 (1986). Two transitions of iron were reported in this work: a solid-solid transition at 200 GPa and melting at 240 GPa. The transition temperatures were calculated to be 4400 ± 400 K at 200 GPa and 5300 ± 400 K at 240 GPa.
11. H. K. Mao, Y. Wu, L. C. Chen, J. F. Shu, A. P. Jephcoat, *J. Geophys. Res.* **95**, 21737 (1990).
12. R. Boehler *et al.*, *J. Appl. Phys.* **65**, 1795 (1989).
13. H. K. Mao, P. M. Bell, C. Hadidiacos, in *High Pressure Research in Mineral Physics*, M. H. Manghnani and Y. Syono, Eds. (American Geophysical Union, Washington, DC, 1987), p. 135.
14. W. A. Bassett and M. S. Weathers, *J. Geophys. Res.* **95**, 21709 (1990).
15. The technique used synchrotron x-ray radiation from beamline X17C of the National Synchrotron Light

Source and a laser-heating system similar to one reported previously [C. S. Yoo *et al.*, *Phys. Rev. B* **48**, 15529 (1993)]. The x-ray beam size, 20 μm by 20 μm, was comparable to the size of laser-heating spot, which varied from 30 to 100 μm, depending on the temperature. (For the later part of this study, we reduced the size of x-ray beam to 5 μm by 20 μm by focusing the 75 μm by 20 μm beam in the vertical direction with an x-ray focusing reflector.) Therefore, the temperature gradients could be large in both the radial and axial directions of the sample being x-rayed; we estimated that this could be as much as 10% of the value reported here. The x-ray diffraction of iron was collected at $2\Theta = 19°$ or 21° for 1 to 10 min to obtain the spectra presented here. The microscope system contains an achromatic objective lens that can cause some chromatic abberation and, thereby, the uncertainty in temperature. This uncertainty could be significant in the case where the temperature is measured from a heating spot smaller than a few to several micrometers. However, considering the relatively large heating spot used in this study, we estimate that it is a minor effect. The details regarding the setup will be presented elsewhere [C. S. Yoo *et al.*, in preparation].

16. H. K. Mao *et al.*, *J. Appl. Phys.* **49**, 3276 (1978).
17. A. P. Jephcoat, R. J. Hemley, H. K. Mao, *Physica B* **150**, 115 (1988).
18. The *d* spacing of the new diffraction line, 2.229 Å, is close to the 100 peak of the NiAs structure of FeO found at 96 GPa and 800 K [Y. Fei and H.-K. Mao, *Science* **266**, 1678 (1994)], which could suggest that a new chemical reaction occurs at megabar pressures.
19. For example, the observed recrystallization of ε-Fe at 2320 K (Fig. 2) is close to the previously reported ε-β boundary (*5*, *6*). The change of texture could conceivably alter the nature of light reflection or absorption and give rise to the previously observed effect.
20. The ε′-Fe phase was found at temperatures below those of γ-Fe and at pressures between 15 and 40 GPa. At 30 GPa, the volume of ε′-Fe is about 6.111 cm³/mol, which lies between those of ε-Fe (5.976 cm³/mol) and γ-Fe (6.298 cm³/mol) (C. S. Yoo *et al.*, in preparation).
21. S. K. Saxena *et al.*, *Science* **269**, 1703 (1995).
22. For convenience, we refer to the γ-ε phase line as the γ(ε′)-ε line. There are two constraints for the γ(ε′)-ε phase line. First, the resistivity measurements of iron at low pressures constrain the γ-ε phase line below 20 GPa (*13*). Second, the present study shows that the ε-γ-liquid triple point is located at the vicinity of 50 GPa. To satisfy these two conditions, the ε-γ phase line cannot be concave down as presented in (*5*) and should be either concave up or at least straight. However, considering the existence of ε′-Fe and the magnetic properties of γ-Fe and ε′-Fe (*20*), the exact nature of the γ-ε phase line could be substantially more complicated.
23. We thank C. Ruddle and J. Hu for experimental assistance, B. Goodwin and C. Mailhiot for support, and C. Meade, N. C. Holmes, W. J. Nellis, and M. Ross for discussions. Work at Lawrence Livermore National Laboratory (LLNL) was supported by the Laboratory Directed Research and Development Program grant LDRD 94-SR-042 and a Defense Program and was performed under the auspices of the U.S. Department of Energy (DOE) by LLNL under contract W-7405-ENG-48. Research at the Geophysical Lab and the National Synchrotron Light Source (NSLS) was supported by the National Science Foundation; NSLS is supported by DOE.

20 June 1995; accepted 25 August 1995

Expansion of SN 1993J

J. M. Marcaide,* A. Alberdi, E. Ros, P. Diamond, I. I. Shapiro, J. C. Guirado, D. L. Jones, T. P. Krichbaum, F. Mantovani, R. A. Preston, A. Rius, R. T. Schilizzi, C. Trigilio, A. R. Whitney, A. Witzel

A sequence of images from very long baseline interferometry shows that the young radio supernova SN 1993J is expanding with circular symmetry. However, the circularly symmetric images show emission asymmetries. A scenario in which freely expanding supernova ejecta shock mostly isotropic circumstellar material is strongly favored. The sequence of images constitutes the first "movie" of a radio supernova.

The recent discovery (*1*) by very long baseline interferometry (VLBI) of a shell-like radio structure in SN 1993J in the galaxy M81 offers the opportunity to monitor a supernova expansion in a manner that is free from modeling uncertainties (*2*, *3*). Indeed, the angular resolution limit of VLBI, imposed by the size of the Earth, and the angular size of a supernova, determined by its distance from Earth, have generally not permitted a model-free determination of expansion in a young supernova. The relative proximity of SN 1993J, however, together with its strong centimeter emission, permit a reliable determination of the details of the expansion.

Our observations were carried out from September 1993 through September 1994 (Table 1). Images were obtained at 3.6 cm and 6 cm (Fig. 1). The image from November 1993 is from the discovery of the shell-like structure (*1*). The image from May 1994 was obtained with a large and well-calibrated array; therefore, all details in it are reliable. However, to obtain the images from September 1993 and February 1994, we used circularly symmetric models of sizes extrapolated and interpolated from the images from November 1993 and May 1994, respectively, as initial models in the mapping process. For the September 1993 image, extrapolation was needed because there was insufficient interferometric resolution to resolve the shell; and for the February 1994 image, interpolation was needed because there were insufficient data (UV coverage) to reconstruct the image unambiguously without a priori information. The procedure we followed allowed us to reliably compare the sizes of the images obtained from the data at each epoch and thus to obtain the angular size growth rate and to learn how the emission enhancement in the southeastern part of the images evolved with time. The latter question is important in distinguishing which features of the emission correspond to traces of the initial explosion and which are induced by the dynamics of the evolution. In spite of the wavelength difference, the image at 6 cm (Fig. 1) from September 1994 shows a remarkably similar structure to those shown in images obtained at 3.6 cm at earlier epochs. However, comparison of the size of the image from this epoch with those from previous epochs is done with caution, because relevant opacity effects may not be accounted for.

Although the interferometric phases for September 1993 contain key information about the emission asymmetry, the source was not large enough then for us to distinguish shell emission from disk emission even when we used the largest available Earth-sized array: A range of limb-brightened disk-like images, each with a characteristic size, are compatible with these data (image degeneracy) (*4*). Therefore, to determine the expansion rate without bias, we used the backward-extrapolated image from our November 1993 and May 1994 images in Fig. 1 in the mapping process to break this degeneracy and thus to estimate a size (*4*).

From observation in February 1994 we have high-quality data, but from only a three-antenna array. The interferometric amplitude data require a shell-like structure, and the interferometric phase data require an emission asymmetry in the shell. Use of a point-like source as an initial model made

J. M. Marcaide and E. Ros, Departamento de Astronomía, Universitat de València, E-46100 Burjassot, València, Spain.
A. Alberdi, Laboratorio de Astrofísica Espacial y Física Fundamental, Instituto Nacional de Técnica Aeroespacial (INTA), E-28080 Madrid, Spain, and Instituto de Astrofísica de Andalucía–Consejo Superior de Investigaciones Cientificas (CSIC), Apdo. Correos 3004, E-18080 Granada, Spain.
P. Diamond, National Radio Astronomy Observatory, Socorro, NM 87801, USA.
I. I. Shapiro, Harvard-Smithsonian Center for Astrophysics, Cambridge, MA 02138, USA.
J. C. Guirado, D. L. Jones, R. A. Preston, Jet Propulsion Laboratory, California Institute of Technology, Pasadena, CA 91109, USA.
T. P. Krichbaum and A. Witzel, Max-Planck Institut für Radioastronomie, Auf dem Hügel 69, D-50131 Bonn, Germany.
F. Mantovani, Istituto di Radioastronomia, Consiglio Nazionale delle Ricerche (CNR), I-Bologna 40129, Italy.
A. Rius, Laboratorio de Astrofísica Espacial y Física Fundamental, INTA, E-28080 Madrid, Spain, and Centre d'Estudis Avançats-C.S.I.C., Camí de Santa Barbara s/n, E-17300 Blanes, Girona, Spain.
R. T. Schilizzi, Joint Institute for VLBI in Europe, Postbus 2, 7990 AA Dwingeloo, Netherlands, and Leiden Observatory, Postbus 9513, 2300 RA Leiden, Netherlands.
C. Trigilio, Istituto di Radioastronomia, CNR, Noto, Italy.
A. R. Whitney, Massachusetts Institute of Technology–Haystack Observatory, Westford, MA 01886, USA.
*To whom correspondence should be addressed.

the imaging difficult. Instead, as an initial model we used a radio source that was similar to a map interpolated from those from November 1993 and May 1994 but was totally circularly symmetric. After only two mapping iterations, the image displayed the slight southeast emission enhancement characteristic of all the images.

The sequence of maps in Fig. 1 shows that the supernova expanded with circular symmetry. Hence, the asymmetry of the medium surrounding the progenitor and its reaction to the shock induced by the supernova ejecta must be small. In addition, the enhanced emission in the southeast survived but declined with time.

If we assume a free expansion similar to that indicated by older supernovae (5) and fit a straight line to the sizes measured at 3.6 cm and given in Table 1, with the constraint that the size is zero at the explosion date, we find an angular expansion rate of 2.39 ± 0.03 μarcsec day^{-1} (Fig. 2), which is very similar to our earlier estimate (*1*). Such an angular expansion rate corresponds, at the distance to SN 1993J of 3.6 Mpc (6), to an expansion speed of 14,900 ± 200 km s^{-1}. If we fit to the 3.6-cm results a power law of the form $\theta \propto t^m$, where θ is the angular radius, t the time after explosion, and m a deceleration parameter, we obtain $m = 0.93 \pm 0.14$. Size estimates reported even earlier (*2*, *3*) appear to be biased toward higher values. Only if the radio supernova looked like a disk of uniform brightness at those earlier epochs rather than like a shell would those higher values correspond to true larger source sizes (*4*) and hence to higher early expansion speeds. If earlier estimates from Bartel *et al.* (*3*) were taken at face value, we would obtain a deceleration with $m = 0.82 \pm 0.03$. In any case, the size estimate at 6 cm from the September 1994 data appears smaller than that expected from the 3.6-cm data only. Further images from later epochs at 6 cm are needed to help understand this surprising result.

All our maps show that the ratio of the shell thickness to the supernova shell outer radius is about 0.3 (*7*). Such a ratio and its (near) constancy are typical of self-similar models (*8*, *9*) of emission generated in regions of circumstellar material shocked by supernova ejecta. To explain the slow rise of the early radio emission (*10*, *11*), it has been argued that the density profile of the ionized circumstellar medium must be proportional to $r^{-1.5}$, where r is the distance from the supernova explosion center (*11*–*14*). Such a density profile is compatible with a disk-shaped density distribution seen edge-on (*13*, *14*). From analyses of other aspects of the radio data it has also been argued that the circumstellar medium must have two mixed isotropic components, one smooth and one clumpy (*11*). The remarkable circular symmetry of all the images and the equally remarkable similarity of the 3.6- and 6-cm images imply a rather isotropic density distribution of the circumstellar medium.

In spite of our improved estimate of the expansion rate, based on the 3.6-cm data, the result does not imply a more accurate determination of the distance to M81 than

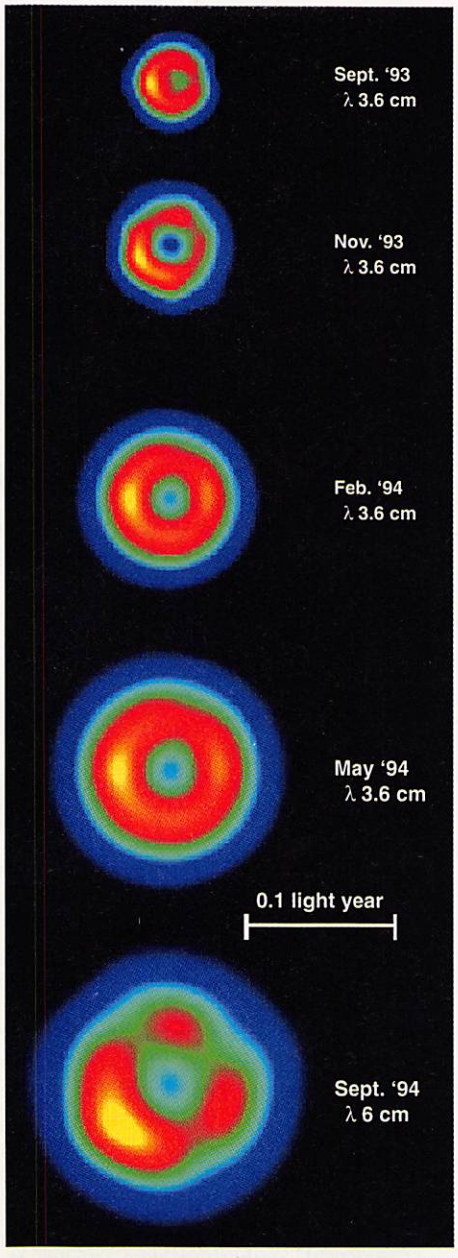

Fig. 1. Sequence of images of supernova SN 1993J made at the wavelengths (λ) of 3.6 and 6 cm and placed at vertical positions proportional to days elapsed after explosion, clearly showing a uniform expansion. The images have been convolved by circular beams whose radii are proportional to the days elapsed after explosion, such that the two tangents to the images should converge to a point at explosion time. The sizes of the beams have been chosen to be within a factor of 2 of the interferometric beam of each observation. In the sequence of images, the extreme circular (spherical) symmetry of the expansion and the consistency of the emission enhancement in the southeast part of the shell-like emission are clearly apparent.

Table 1. SN 1993J observations and source parameters (*30*).

Date of observation	Age* (days)	Wavelength (cm)	Antenna symbols†	Total flux density used for mapping‡ (mJy)	Shell outer radius§ (μarcsec)
26 September 1993	182	3.6	BdLMY	78	467 ± 90
22 November 1993	239	3.6	BDLMY	58	581 ± 40
20 February 1994	330	3.6	DMY	51	790 ± 90
29 May 1994	427	3.6	BDHLMNVY	42	1000 ± 60
20 September 1994	541	6	BFHLNOTY	52	1110 ± 50

*Age of the supernova with respect to estimated explosion date of 28 March 1993. †See (*30*) for definitions. ‡Compact core of the galaxy M81 and compact source 0917 + 624 (*31*) used as calibrators. §Estimate from direct measurements on the images given in Fig. 1. See text and caption to Fig. 2.

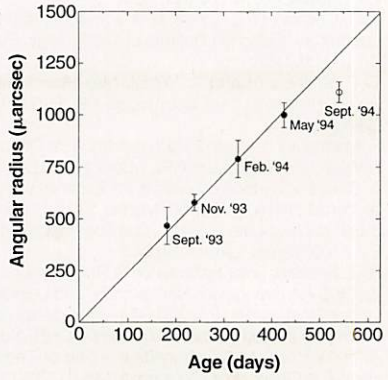

Fig. 2. Measured angular size (external radius of the shell) versus age of SN 1993J for observations made at 3.6 (solid circles) and 6 cm (open circle). The errors correspond to the root mean square (rms) of the radii measured along 24 cuts across the image equally spaced in azimuth. For February 1994 (day 330 after explosion), the error has been enlarged by a factor of 3 to account for the deficiency in the mapping as explained in the text; for a similar reason, the error for September 1993 (day 182) was arbitrarily made equal to that of February 1994, although this error corresponds for day 182 to 18 times the rms of the measured radii. The straight line through the origin is a weighted least-squares linear fit to the 3.6-cm data only, with the restriction that it must pass through the origin. It corresponds to an expansion rate of the outer shell radius of 2.39 μarcsec day^{-1} (14,900 ± 200 km s^{-1} at an assumed distance of 3.6 Mpc).

obtained in earlier VLBI work (*1*) (3.8 ± 0.8 Mpc), because the uncertainty in the estimate of the maximum supernova ejecta speed by optical spectroscopy dominates. Recent spectra (*15–17*) show broad, flat-topped Hα emission from material moving at up to ~11,000 km s^{-1}. These speeds are much lower than those reported from early spectra (*1, 3, 15, 18*) and are about 30% lower than those we estimated for the outer shell radius if we assume a distance of 3.6 Mpc to M81 (*6*). However, because our estimate of the shell width is about 30% of the outer shell radius for every epoch of observation, the inner shell radius expands at ~70% the rate of the outer radius. Such a coincidence is likely not accidental. Thus, the various estimates of the gas speeds are compatible, and there is no need to invoke any deceleration, if the highest speed Hα emission comes from around the reverse-shocked region just inside the innermost part of the radio shell (*9, 12, 16, 19*).

Chevalier and Blondin (*20*) have recently shown that the hydrodynamic instabilities generated by radiative cooling from the shocked region are not capable of producing the protrusions that have been observed in radio supernovae (*21, 22*). However, these authors also suggested that cases such as SN 1993J might have cooling reverse shocks capable of producing such protrusions, because the high level of radio emission is indicative of strong radiative cooling and of a dense circumstellar medium. Our images in Fig. 1, especially the one corresponding to May 1994, which is shown in Fig. 3 convolved with the full interferometric beam, clearly show that SN 1993J does not yet have any protrusions. There is no evidence of instabilities having developed in any region of the source. The region of enhanced emission and the rest of the shell emission appear to evolve smoothly. Small changes in the position angle of emission features in the shell are not significant. These small differences are possibly due to imperfections in the imaging. Also, there is no clear evidence yet of deceleration of the supernova due to interaction with the circumstellar medium, and hence it may be too early to expect instabilities in the source due to convective or Rayleigh-Taylor instabilities (*20*).

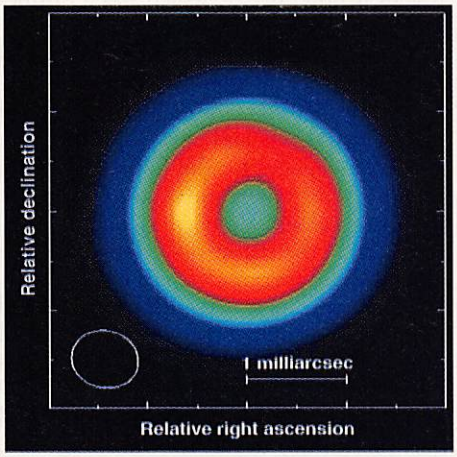

Fig. 3. Image at 3.6 cm (8.4 GHz) of SN 1993J from 29 May 1994, 427 days after explosion. The maximum brightness is 5.7 millijansky (mJy) per beam (1 Jy = 10^{-26} W m^{-2} Hz^{-1}). The elliptical gaussian beam used in the convolution to obtain this CLEAN map is shown in the lower left and has full widths at half maxima of 0.68 × 0.58 milliarcsec, with the major axis along position angle 77°. One milliarcsecond is equivalent to 5.4 × 10^{16} cm (0.05 light year) for a distance to the supernova of 3.6 Mpc.

The mechanism responsible for the enhanced emission in the southeast part of every image has to be capable of maintaining the enhancement over at least the 1-year period for which we have images. The region of enhanced emission appears in September 1994 as the region of steepest spectral index ($\alpha \leq -1.5$, $S \propto \nu^{\alpha}$, where S denotes the flux density and ν the frequency) of the source (average spectral index $\alpha \sim -1.1$), which is perhaps indicative of a region with large energetic losses. From September 1993 to May 1994, the maximum brightness temperature in this region decreased from ~1.8 × 10^9 K to ~2.6 × 10^8 K (in the rest of the radio shell, such temperature decreased from ~1.1 × 10^9 K to ~2.0 × 10^8 K). It has been suggested (*23, 24*) that the progenitor was part of a binary system. The expansion rate of the supernova is such that the ejecta travel about 8 astronomical units per day. Hence, the ejecta would sweep past a putative close companion on a time scale of a day (*24*). It is perhaps conceivable that generation of local turbulence could in turn intensify the local energetics. The radio emission was first detected from SN 1993J 5 days after explosion (*10*). Until then, the radio emission was heavily absorbed at centimeter wavelengths, a condition persisting to a lesser degree at 3.6 cm through day 100 after explosion (*11*). Thus, although the interaction with a possible close companion would have taken place in the first days, its effects could not have been detectable for perhaps 2 or 3 months. Indeed, Bartel *et al.* (*3*) do not report any asymmetry in the emission from their VLBI observations during the first 60 days after explosion. What seems difficult to reconcile with the hypothesis that a companion star was the cause of the enhancement of emission is the large extent of the enhancement in November 1993, 8 months after explosion, and the survival of such an enhancement 12 months later.

There are other mechanisms that could enhance the emission (*21*) but would also produce a departure from circular symmetry, which has not been observed. Although the circumstellar medium appears to be isotropic at the distances from the explosion point represented by the shell shown in our maps, it is conceivable that in the early stages of expansion the supernova ejecta encountered a circumstellar medium that was not quite isotropic, and hence radiation from the densest regions of the circumstellar medium could have increased. An anisotropic circumstellar medium close to the progenitor that was ionized by the initial supernova flash could also have given rise to the reported optical polarization (*25*). For this scenario to be plausible, a mechanism is needed to inhibit the alteration of the circular symmetry of the radio map by such a denser region. However, given that a variable stellar presupernova wind rate (*11–14*) has produced a circumstellar medium that has not detectably modified either the expansion rate or the circular symmetry, perhaps it is possible that a denser region of the circumstellar material had no other effect on the shock than to enhance the emission. Even the hypotheses of large-scale slightly anisotropic distribution of circumstellar material and of magnetic field density, with the relatively denser regions in the southeast directions being responsible for the enhanced radiation, are plausible.

REFERENCES AND NOTES

1. J. M. Marcaide *et al.*, *Nature* **373**, 44 (1995).
2. J. M. Marcaide *et al.*, *Astrophys. J.* **424**, L25 (1994).
3. N. Bartel *et al.*, *Nature* **368**, 610 (1994).
4. A. P. Marscher, in *Supernovae as Distance Indicators*, N. Bartel, Ed. (Springer, Berlin, 1985), pp. 130–137. The phase information from our September 1993 data requires an emission asymmetry in the image. This asymmetry is seen at later epochs as an emission enhancement in the southeast part of the otherwise circularly symmetric image.
5. T. W. B. Muxlow *et al.*, *Mon. Not. R. Astron. Soc.* **266**, 455 (1994).
6. W. L. Freedman *et al.*, *Astrophys. J.* **427**, 628 (1994).
7. We estimated this ratio by creating synthetic interferometric data corresponding to various shell models (*4*) and comparing the synthetic data with the data from the observations. Although the maps in Fig. 1 contain this information, it is not straightforward to obtain it from them only.
8. R. Chevalier, *Astrophys. J.* **259**, 302 (1982); *ibid.*, p. L85; *ibid.* **285**, L63 (1984); P. L. Biermann, in *Cosmic Winds and the Heliosphere*, J. R. Jopikii *et al.*, Eds. (Univ. of Arizona Press, Tucson, AZ, in press).
9. R. A. Chevalier and C. Fransson, *Astrophys. J.* **420**, 268 (1994). These authors have suggested a smaller extent for such a region, perhaps up to 15%, but Fransson (private communication) considers that widths of 30% are not ruled out by their models.
10. G. G. Pooley and D. A. Green, *Mon. Not. R. Astron. Soc.* **264**, L17 (1993); K. W. Weiler, S. D. Van Dyk, R. A. Sramek, N. Panagia, M. P. Rupen, in *Circumstellar Media in the Late Stages of Stellar Evolution*, R. E. S. Clegg, I. R. Stevens, W. P. S. Meikle, Eds. (Cambridge Univ. Press, Cambridge, 1994), pp. 207–212.
11. S. D. Van Dyk, K. W. Weiler, R. A. Sramek, M. P. Rupen, N. Panagia, *Astrophys. J.* **432**, L115 (1994).
12. C. Fransson, in *Circumstellar Media in the Late Stages of Stellar Evolution*, R. E. S. Clegg, I. R. Stevens, W. P. S. Meikle, Eds. (Cambridge Univ. Press, Cambridge, 1994), pp. 120–138.
13. P. Lundqvist, in *Circumstellar Media in the Late Stag-*

es of Stellar Evolution, R. E. S. Clegg, I. R. Stevens, W. P. S. Meikle, Eds. (Cambridge Univ. Press, Cambridge, 1994), pp. 213–220.
14. C. Fransson, P. Lundqvist, R. A. Chevalier, *Astrophys. J.*, in press.
15. A. V. Filippenko, T. Matheson, A. J. Barth, *Astron. J.* **108**, 2220 (1994).
16. F. Patat, N. Chugai, P. A. Mazzali, *Astron. Astrophys.* **299**, 715 (1995).
17. The maximum velocity estimate was obtained from the red side of the Hα emission because the blue side appears blended with emission from neutral oxygen [OI]. Even more recent spectra (*29*) that are free of [OI] emission also show a symmetrical flat-topped Hα emission centered at 6560 Å, with gas speeds also having maxima with similar values.
18. J. R. Lewis *et al.*, *Mon. Not. R. Astron. Soc.* **266**, L27 (1994).
19. R. Terlevich, G. Tenorio-Tagle, J. Franco, J. Melnick, *ibid.* **255**, 713 (1992). The highest speed Hα emission would originate at the cool shell outward of the reverse-shocked region and at the outermost part of the ejecta close to the reverse shock.
20. R. A. Chevalier and J. M. Blondin, *Astrophys. J.* **444**, 312 (1995).
21. N. Bartel *et al.*, *ibid.* **323**, 505 (1987).
22. N. Bartel *et al.*, *Nature* **350**, 212 (1991).
23. K. Nomoto *et al.*, *ibid.* **364**, 507 (1993); Ph. Podsiadlowski *et al.*, *ibid.*, p. 509.
24. S. E. Woosley *et al.*, *Astrophys. J.* **429**, 300 (1994).
25. S. R. Trammell *et al.*, *ibid.* **414**, L21 (1993).
26. A. E. E. Rogers *et al.*, *Science* **219**, 51 (1983).
27. J. D. Romney, in *The Impact of VLBI on Astrophysics and Geophysics*, M. Reid and J. M. Moran, Eds. (Kluwer, Dordrecht, Netherlands, 1988), pp. 461–468.
28. T. J. Pearson, *Bull. Am. Astron. Soc.* **23**, 991 (1991).
29. C. Fransson, private communication; A. V. Filippenko, private communication.
30. The observations were made with the following antennas (symbols, diameters, affiliations, and locations are given in parentheses): Effelsberg [B, 100 m, Max-Planck Institut für Radioastronomie (MPIfR), Effelsberg, Germany]; DSS15 (d, 34 m, NASA, Goldstone, CA); DSS14 (D, 70 m, NASA, Goldstone, CA); Fort Davis (F, 25 m, Fort Davis, TX); Hancock (H, 25 m, Hancock, NH); Medicina (L, 32 m, CNR, Medicina, Italy); DSS63 (M, 70 m, NASA, Robledo, Spain); Noto (N, 32 m, CNR, Noto, Italy); Owens Valley (O, 25 m, Big Pine, CA); Kitt Peak (T, 25 m, Kitt Peak, AZ); Saint Croix (V, 25 m, U.S. Virgin Islands); VLA [Y, equivalent diameter 130 m, National Radio Astronomy Observatory (NRAO), near Socorro, NM]. At each station, a hydrogen maser frequency standard was used to govern the local oscillator chain and the "time tagging" of the recorded data. The data were recorded with the Mark IIIA (*26*) or compatible very long baseline array (VLBA) instrumentation (*27*), in mode B double speed, yielding bandwidths of 56 MHz. Right-hand circular polarization (IEEE convention) was recorded at the wavelength of 3.6 cm, and left-hand circular polarization was recorded at 6 cm. The data were correlated at MPIfR, Bonn, Germany and were further analyzed with the Caltech VLBI Package (*28*).
31. K. J. Standke *et al.*, *Astron. Astrophys.*, in press.
32. We thank the many people that made this research possible: B. Clark, R. Schwartz, P. Wolken, and the staffs at the participating observatories, at NASA-JPL, and at the MPIfR, where all the data were correlated. We also thank K. W. Weiler for useful comments on our manuscript. This research was partly supported by the Dirección General de Investigación Científica y Tecnológica in Spain and by NSF in the United States. NRAO is a facility of NSF operated under cooperative agreement by Associated Universities, Inc. DSS14, DSS15, and DSS63 are operated by NASA-JPL. This work was carried out in part by JPL, California Institute of Technology, under contract to NASA. E.R. acknowledges receipt of a scholarship of the Generalitat-Valenciana. Partial support for the correlator operation from the European Union Access to Large Scale Facilities Programme is acknowledged.

2 August 1995; accepted 10 October 1995

Infrared Spectrum of the Cool Brown Dwarf Gl 229B

B. R. Oppenheimer, S. R. Kulkarni,* K. Matthews, T. Nakajima

Spectroscopic measurements of a cool brown dwarf, Gl 229B, reveal absorption features attributable to methane in the near infrared much like those of Jupiter. These features are not seen in any star. The presence of methane indicates that the surface temperature of Gl 229B is below 1000 kelvin. Features attributed to water vapor also indicate that Gl 229B is much cooler than any known star.

Stars like our sun fuse hydrogen into helium and in the process produce energy, most of which appears as light. Current stellar models agree that objects less massive than $0.08M_\odot$ cannot sustain hydrogen fusion (*1*, *2*) (the sun is denoted by the symbol ⊙, and $M_\odot$ is the mass of the sun). Such objects are called brown dwarfs. When young ($\lesssim 10^8$ years), they contract relatively rapidly, and the gravitational binding energy released makes these objects quite luminous. As they age, they rapidly cool, and grow dim, becoming increasingly harder to detect. At even lower masses, there exist giant planets, the only examples of which are the giant outer planets of our solar system, including Jupiter (mass $M_J \sim 10^{-3} M_\odot$). According to theory, the objects in the mass range $1M_J$ to $100M_J$ have similar characteristics. All of them have fully convective interiors and thin radiative atmospheres that radiate mostly between bands of molecular absorption. In addition, they all have about the same radius, $R \sim 0.1R_\odot$. Despite these similarities, brown dwarfs and giant planets are thought to form differently. It is believed that planets condense within a protoplanetary disk. In contrast, brown dwarfs are thought to form like stars through direct condensations of interstellar gas.

There are at least two reasons why the study of brown dwarfs, especially cool brown dwarfs, excites considerable attention. First, astronomers would like to investigate these objects because they lie in the unexplored mass range between stars and planets. Although these objects were predicted some 30 years ago (*1*), the lack of unambiguous specimens has been a major stumbling block in this field. Second, planetary scientists would like to study the atmospheres of cool brown dwarfs to understand how they are related to the atmospheres of planets. Such understanding is critical in the search for other planetary systems.

The emergent spectrum of radiation from a condensed object depends on the chemical composition, the surface gravity, and the effective surface temperature T_{eff}, which is defined here by the relation $\sigma T_{eff}^4 = L/4\pi R^2$, where L is the luminosity of the object and σ is the Stefan-Boltzmann constant. The minimum luminosity of hydrogen-fusing stars (main-sequence stars) is $10^{-4}\ L_\odot$ (*2*). Thus, for these stars, $T_{eff} \gtrsim 1800$ K. This is about equal to the temperature of GD 165B (*3*), the coolest condensed object known until the discovery of Gl 229B (*4*). As discussed above, old brown dwarfs do not generate nuclear power and thus can have very low T_{eff}.

At the low temperatures characteristic of planets and old brown dwarfs, molecules and possibly dust are readily formed. Molecules have a large number of energy levels, which drastically complicates detailed modeling of their atmospheres. To date, there exist no detailed models for T_{eff} below 2000 K (*5*, *6*). However, predictions do exist. For example, below T_{eff} of 1000 K, most of the carbon is predicted (*7*) to reside in methane (CH_4). In contrast, the cool, late-type stars (with $T_{eff} > 1800$ K) have no CH_4. Their carbon resides mainly in CO, which has a distinctive appearance in spectra of these stars.

Observations of cool objects are crucial to any further progress in this field. As Stevenson (*8*) remarked in a review of high-mass planets and brown dwarfs, "The biggest challenges for the future lie not in theory but in observations: we need more than two colors. We need spectra. . . . Refinement of the theory does not seem to be a compelling task until this happens."

Here we report the first near-infrared (IR) spectroscopic observation of a cool brown dwarf, Gl 229B (*4*). This object has the same proper motion as that of Gl 229 and is thus most likely a companion of Gl 229 (hereafter Gl 229A). Nakajima *et al.* (*4*) obtained broadband photometric measurements from which they deduced $L \lesssim 10^{-5}\ L_\odot$. This is 1/10 of the minimum luminosity of any main-sequence star. Nakajima *et al.* concluded that Gl 229B is a cool ($T_{eff} \lesssim 1200$ K) condensed object. At the present time, we are unable to determine the origin of this object. For simplicity, we will refer to Gl 229B as a brown dwarf.

Palomar Observatory 105-24, California Institute of Technology, Pasadena, CA 91125, USA.

*To whom correspondence should be addressed.

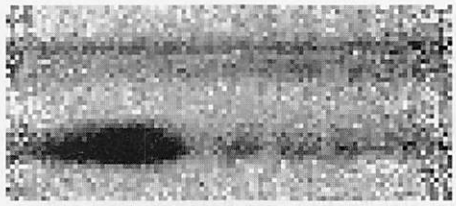

Fig. 1. Typical spectral image of Gl 229B in the H band. The vertical dimension covers 5.4 arc sec west along the slit. The upper dark stripe is the spectrum of the light from Gl 229A diffracted by the telescope spider, and the lower dark stripe is the spectrum of Gl 229B. These two stripes do not overlap; thus, the one-dimensional spectra must in fact be correct extractions from these spectral images. The wavelength coverage is from 1.5 μm (left) to 1.8 μm (right). The diffracted light from Gl 229A is separated from the light of Gl 229B by 2.4 arc sec. The spectrum of Gl 229A, a cool star of spectral type M1, is almost flat through the H band, whereas that of Gl 229B strongly peaks just below 1.6 μm. This spectral feature of Gl 229B distinguishes it from any previously known hydrogen-burning star.

Our IR spectra were obtained at the *f*/70 Cassegrain focus of the Hale 200-inch telescope with a grism spectrograph and an IR camera consisting of reimaging optics and a 256 pixel by 256 pixel InSb detector (Santa Barbara Research). For all of the observations reported here, a focal slit of 0.5 arc sec by 32 arc sec was used. The appropriate orders of the spectrum dispersed by the grism were selected with interference filters: Z (0.95 to 1.11 μm), J (1.15 to 1.40 μm), H (1.49 to 1.81 μm), and K (1.95 to 2.55 μm). For each of the spectra, the resolution was $\lambda/\Delta\lambda \sim 150$ (λ, wavelength). The detector pixel size was 0.125 arc sec in the spatial dimension and one-quarter of the resolution in the spectral dimension.

Spectra of Gl 229B were obtained in the K and H bands on the night of 14 September 1995, and in the Z, J, H, and K bands on the following night. We also obtained spectra of Jupiter for comparison. For atmospheric transmission calibration, G dwarf stars were observed at air masses similar to those of Gl 229B and Jupiter. For wavelength calibration, we observed the bright planetary nebula NGC 7027.

When obtaining the spectrum of Gl 229B, we oriented the long axis of the slit east-west to minimize the contamination of light from Gl 229A diffracted by the secondary mirror support. Data obtained with the star at three different positions on the slit allowed us to remove time-varying sky contributions by subtracting consecutive images. The data were then divided by the spectral image of the G star HR 683, which we uniformly scanned along the slit by tilting the secondary; for Jupiter, we used HR 6269. In addition, we subtracted the adjacent sky for Gl 229A, in order to remove atmospheric emission features, and obtained a spectral image (Fig. 1). This image demonstrates that the spectra of Gl 229A and Gl 229B are well separated and cannot be a combination of the two. By summing the data along the spatial dimension, we created one-dimensional spectra. Next, we removed the blackbody shape of the G star. The absolute flux calibration of the Gl 229B spectrum involved (i) the removal of the blackbody shape of the G star used, (ii) the normalization of the flux density to the photometry of Nakajima *et al.* (*4*), and (iii) the assumptions that Gl 229B has a radius of $0.1R_{\odot}$ and is 5.7 pc distant. The result, then, is the flux density at the surface of Gl 229B. The assumptions in step (iii) have no effect on the shape of the spectrum (Fig. 2).

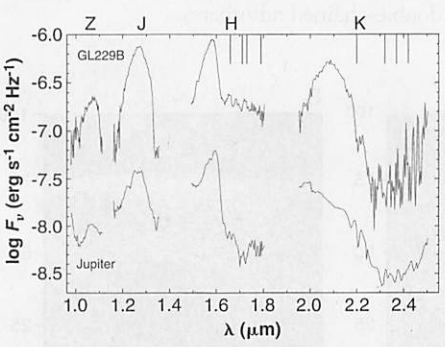

Fig. 2. Near-IR spectra of Gl 229B and Jupiter (in flux per unit frequency, wavelength, F_ν, plotted versus λ). The spectra of Jupiter are shifted vertically for ease of comparison. The spectral resolution is 150. The vertical bars at the top of the plot indicate the locations of CH_4 absorption features at 1.66, 1.71, 1.79, 2.20, 2.32, 2.37, and 2.4 μm.

The spectrum of Gl 229B is different from the spectra of late M stars, including that of GD 165B [figure 1 of (*9*)], but is similar to that of Jupiter. The striking features in the Gl 229B spectrum are the absence of any signal in one-half (1.62 to 1.80 μm) of the H band and one-half (2.25 to 2.40 μm) of the K band. However, these features are seen in Jupiter's spectrum (Fig. 2). In Jupiter, the H-band absorption is primarily attributed (*10*) to strong CH_4 bands, and the K-band depression is attributable to CH_4 and also collisionally induced absorption by molecular hydrogen. The similarity of the H-band spectra of Gl 229B to that of Jupiter is a clear indication that CH_4 is present in Gl 229B. Some similar features are observed in the dusty envelopes surrounding the bright asymptotic giant branch (AGB) stars. However, Gl 229B has a large proper motion (*4*). If it were an AGB star, with an intrinsic luminosity typical of such stars, Gl 229B would lie outside the galaxy and would be moving at a relativistic speed.

A deep absorption feature at 1.34 μm is seen in the spectrum of Gl 229B. Such a feature is also seen in all cool stars and GD 165B and is attributed to an H_2O absorption band. Jones *et al.* (*9*) argued that the depth of this absorption feature—defined as R_{H_2O}, the ratio of flux in the band 1.286 to 1.303 μm to the flux in the band 1.338 to 1.356 μm—is inversely related to T_{eff}. The absorption of GD 165B is much deeper than that of any of the M stars, and thus, the largest value of $R_{H_2O} \sim 1.9$. For Gl 229B, $R_{H_2O} \sim 10$. Jones *et al.* (*9*) also pointed out that the slope of the spectrum in the range 2.05 to 2.15 μm is inversely proportional to T_{eff}. The slope for Gl 229B is more than an order of magnitude larger than that for GD 165B.

Tsuji (*7*), on the basis of chemical equilibrium considerations, has argued that for atmospheres with T_{eff} less than 1000 K, almost all of the carbon is in the form of CH_4, rather than in CO. This explains why CH_4 is seen in Jupiter but not in any main-sequence star. The presence of CH_4 in Gl 229B is an independent indication that T_{eff} for Gl 229B is less than 1000 K. Further support for this conclusion comes from the extreme values of the two spectral diagnostics described above. These imply that Gl 229B is indeed a cool brown dwarf, with $T_{eff} \lesssim 1000$ K.

Our upper limit on T_{eff} is based purely on chemical thermodynamics and molecular excitation physics. In contrast, Nakajima *et al.* (*4*) used broadband photometric data and the assumption that Gl 229B is at the distance of Gl 229A to estimate that $T_{eff} \lesssim 1200$ K. Our upper limit on T_{eff} lends strong credence to the idea that Gl 229A and Gl 229B constitute a binary system at a distance of 5.7 pc.

REFERENCES AND NOTES

1. S. S. Kumar, *Astrophys. J.* **137**, 1121 (1963).
2. D. J. Stevenson, *Annu. Rev. Astron. Astrophys.* **29**, 163 (1991); A. Burrows and J. Liebert, *Rev. Mod. Phys.* **65**, 301 (1993).
3. B. Zuckerman and E. E. Becklin, *Astrophys. J.* **386**, 260 (1992).
4. T. Nakajima *et al.*, *Nature*, in press.
5. T. Tsuji, K. Ohnaka, W. Aoki, in *The Bottom of the Main Sequence—and Beyond*, C. G. Tinney, Ed. (Springer, Berlin, 1995), p. 45.
6. F. Allard and H. P. Hauschildt, *ibid.*, p. 32.
7. T. Tsuji, *Ann. Tokyo Astron. Obs. Ser. II* **9**, 1 (1964).
8. D. J. Stevenson, in *Astrophysics of Brown Dwarfs*, M. C. Kafatos, R. S. Harrington, S. P. Maran, Eds. (Cambridge Univ. Press, Cambridge, 1986), p. 218.
9. H. R. A. Jones *et al.*, *Mon. Not. R. Astron. Soc.* **267**, 413 (1994).
10. R. E. Danielson, *Astrophys. J.* **143**, 949 (1966).

11. Much of the research activity reported here is supported by the Packard Foundation, the National Science Foundation (NSF), and the National Aeronautics and Space Administration. B.R.O. is supported by an NSF Graduate Research Fellowship. Infrared astronomy at Palomar is supported by a grant from the NSF. We thank M. van Kerkwijk and T. Tsuji for discussion and comments.

12 October 1995; accepted 6 November 1995

Molecular Organization of Surfactants at Solid-Liquid Interfaces

Srinivas Manne* and Hermann E. Gaub†

Interactions between surfactant solutions and solid surfaces play a key role in technologically important processes such as colloidal stabilization, ore flotation, and soil removal; however, the interfacial aggregation of surfactant molecules is not yet well understood. Direct images of surfactant aggregates at solid surfaces in aqueous solutions were obtained with atomic force microscopy. The resulting structures for quaternary ammonium surfactants (above the critical micelle concentration) are consistent with half-cylinders on crystalline hydrophobic substrates, full cylinders on mica, and spheres on amorphous silica. These structures—surprisingly different from earlier models—appear to result from a compromise between the natural free curvature as defined by intermolecular interactions and the constraints imposed by specific surfactant-surface interactions. Such interfacial aggregates can potentially be used to pattern surfaces at nanometer-length scales.

The self-assembly of amphiphilic molecules into spheres, cylinders, bilayers, and bicontinuous phases in free solution is fairly well understood (*1–3*), but it is not clear how these aggregates are affected by the presence of a solid boundary surface. Pioneering research into interfacial aggregation with adsorption isotherms (*4*) and the surface force apparatus (SFA) (*5*) has provided quantitative measures of adsorption but little information on aggregate structure. Recent efforts to probe this structure have used fluorescence decay (*6*) and neutron reflection (*7*). Here we report direct images of surfactant aggregates at a variety of hydrophilic and hydrophobic substrates with the use of atomic force microscopy (AFM) (*8*). We restrict this study to (i) atomically flat substrates, where surface corrugation is less than the surfactant dimensions; (ii) cationic surfactants with quaternary ammonium headgroups [typically tetradecyl trimethylammonium bromide (C_{14}TAB)], whose aggregation properties have been characterized (*9*); and (iii) surfactant concentrations above (typically twice) the critical micelle concentration (CMC). In general, the AFM images show interfacial aggregates with a high degree of curvature and periodic structure, in contrast to previously assumed models of flat monolayers and bilayers (see below).

AFM imaging of surface aggregates was performed not in the usual contact mode but by means of precontact repulsive forces as described (*10*, *11*). The imaging tip and sample surface were immersed in surfactant solution in the AFM fluid cell and consequently became charged through adsorption of the cationic surfactant ion. Force curves showed repulsion between the tip and sample, due to electric double-layer forces at long range and probably additional steric forces at short range. The adsorbate layer was imaged by setting the force setpoint in the precontact region, thus "flying" the tip at a few nanometers above the plane of hard contact while scanning (*12*, *13*).

For quaternary ammonium surfactants (above the CMC) on silica, a variety of aggregate structures have been proposed, ranging from uniform bilayers (*14–16*) to patchy bilayers (*7*, *17*) to spherical aggregates resembling bulk micelles (*18*). AFM images of the adsorbate layer (Fig. 1, A and B) revealed roughly symmetrical dots consistent with previously proposed spherical aggregates (*18*). Fourier transforms (Fig. 1A, inset) typically showed a bright ring, indicating a well-defined nearest neighbor distance between aggregates but little orientation on a large scale (resembling a glassy or random close-packed structure). Neighboring micelles often appeared to be connected by a thin neck, giving rise to two-dimensional networks similar to bicontinuous surfactant phases in bulk solution (*3*). The observed nearest neighbor distance varied inversely with solution pH (compare Fig. 1A with 1B), ranging from 5.6 ± 0.6 nm at pH 9.9 to 9.0 ± 1.2 nm at pH 2.6 (*19*). This result is in agreement with previous studies (*14*, *16*, *20*) showing that the adsorbate density decreases with decreasing solution pH, because of a reduction in the surface charge by protonation of SiO^- groups.

For quaternary ammonium surfactants on mica, the generally held view is that surfactant molecules above the CMC adsorb in the form of a uniform bilayer (*5*). Such systems have been used as model bilayers in the investigation of double-layer forces (*21*), bilayer fusion (*22*), and micellar depletion forces (*23*). Surprisingly, AFM images showed an adsorbate structure consisting of meandering stripes (Fig. 2, A and B), which were separated by 5.3 ± 0.3 nm and showed no consistent orientation relative to the underlying lattice. Considering these images together with previous SFA measurements (*5*) of the adsorbate layer thickness (roughly twice the molecular length), we propose interfacial aggregates in the form of full cylinders (Fig. 2C) (*24*). The stripe spacing on mica did not vary with solution pH (in the pH range from 2.6 to 11.4) and was always less than or equal to the interaggregate spacing on silica, probably reflecting a difference in the adsorption mechanism between the two substrates (see below).

Aggregate curvature in free solution can be altered markedly by changing the geometry of the surfactant ion (*1*). Specifically, low curvature can be attained by increasing the tail-group cross-sectional area. Accordingly, the double-chained surfactant didodecyl dimethylammonium bromide [$(C_{12})_2$DAB] gave rise to uniform and featureless images (Fig. 2D) indicative of a flat bilayer on mica, in agreement with previous interpretations (*22*) of double-chained adsorbates.

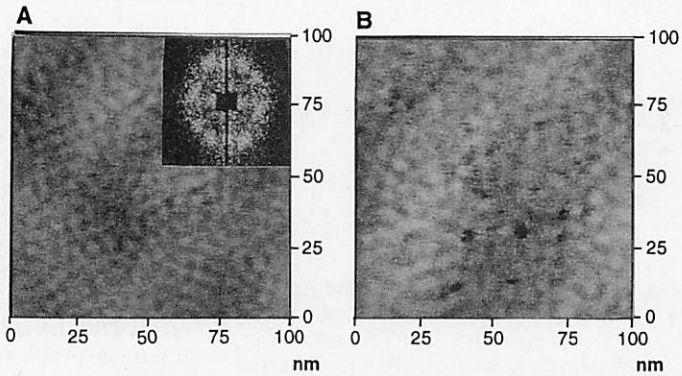

Fig. 1. Aggregation of the cationic surfactant C_{14}TAB on silica from 7 mM aqueous solution (twice the CMC). (**A**) A 100 nm by 100 nm AFM image of surfactant aggregates on silica at pH 6.3. The observed dots suggest roughly spherical micelles. The Fourier transform of a larger image (**inset**) shows a ring with a few bright spots, indicating a well-defined nearest neighbor distance (5.7 ± 0.7 nm in real space) but little crystalline symmetry. (**B**) A 100 nm by 100 nm image of the same sample at pH 2.9. The micelles are now spaced farther apart, at 7.0 ± 0.9 nm.

Department of Physics E22, Technische Universität München, 85748 Garching, Germany.

*To whom correspondence should be addressed. Present address: Princeton Materials Institute, 70 Prospect Avenue, Princeton University, Princeton, NJ 08540, USA. E-mail: smanne@phoenix.princeton.edu

†Present address: Ludwig Maximilian Universität, Lehrstuhl für Angewandte Physik, Amalienstrasse 54, 80799 Munich, Germany.

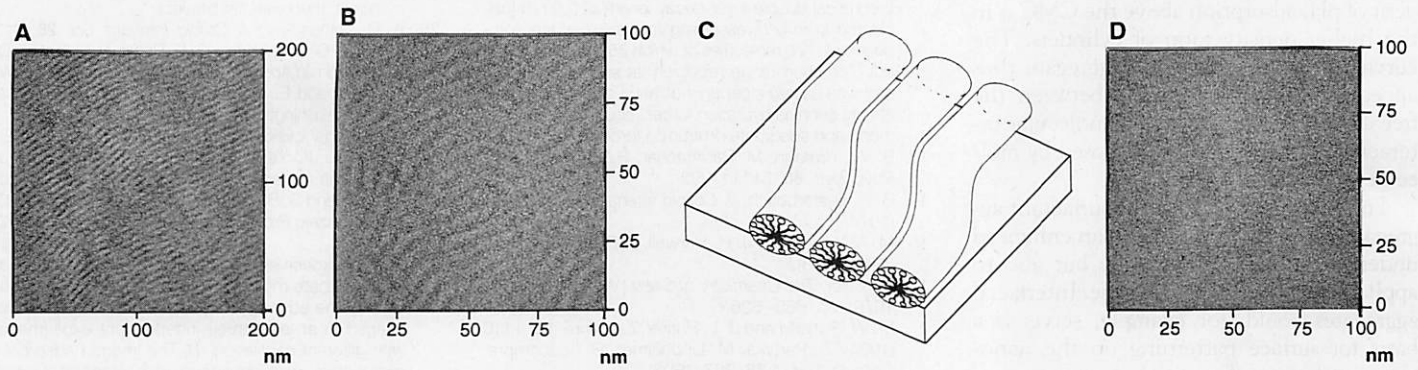

Fig. 2. Cationic surfactant aggregates on mica. (**A**) A 200 nm by 200 nm AFM image of C_{14}TAB aggregates from 7.0 mM solution, showing meandering stripes spaced 5.3 ± 0.3 nm apart. (**B**) A 100 nm by 100 nm image of C_{14}TAB aggregates, showing that the stripes have variable orientations over the sample surface. (**C**) Proposed schematic of cylindrical surfactant aggregates, consistent with AFM images and previous SFA data (*5*). (Cylinders may be flattened at the bottom to allow greater contact area between headgroups and surface.) (**D**) A 100 nm by 100 nm image of the double-chained $(C_{12})_2$DAB adsorbate layer from 0.30 mM solution (twice the CMC). Although force curves indicate electrical double-layer forces as for C_{14}TAB, the images of the double-chained adsorbate are featureless and indicate a flat bilayer.

Unlike silica and mica, hydrophobic substrates interact primarily with surfactant tailgroups through hydrophobic and van der Waals interactions. Adsorption isotherms for ionic surfactants on graphite have indicated a coverage roughly consistent with a vertical monolayer above the CMC (*25*), although hemispherical aggregates have also been suggested (*26*). However, AFM images (Fig. 3, A and B) of C_{14}TAB aggregates on graphite and MoS_2 revealed straight, parallel stripes, separated by roughly twice the length of the surfactant molecule and oriented perpendicular to a substrate symmetry axis. These results are consistent with half-cylindrical aggregates (Fig. 3C) (*11*), in which the tailgroups adjacent to the surface lie parallel to a line connecting nearest neighbor surface atoms.

It has been suggested that epitaxy is responsible for surfactant tailgroups and alkane chains adsorbing parallel to a graphite symmetry axis (*11*, *27*), because the positions of carbon atoms in an alkane chain closely match those of the graphite surface (*27*). Yet we observed similar surfactant aggregates at the same relative orientation on the cleavage plane of MoS_2, which consists of sulfur atoms in a symmetry and periodicity different from that of graphite. The common mechanism might be a crystalline anisotropy in van der Waals interactions (analogous to bulk anisotropy in polarizability, refractive index, and so forth) rather than a specific correspondence between adsorbate and substrate atoms. Although the effect of such an anisotropy may be insignificant on small symmetrical adsorbates, the linearity of the surfactant molecule should enhance the direction sensitivity of its adsorption.

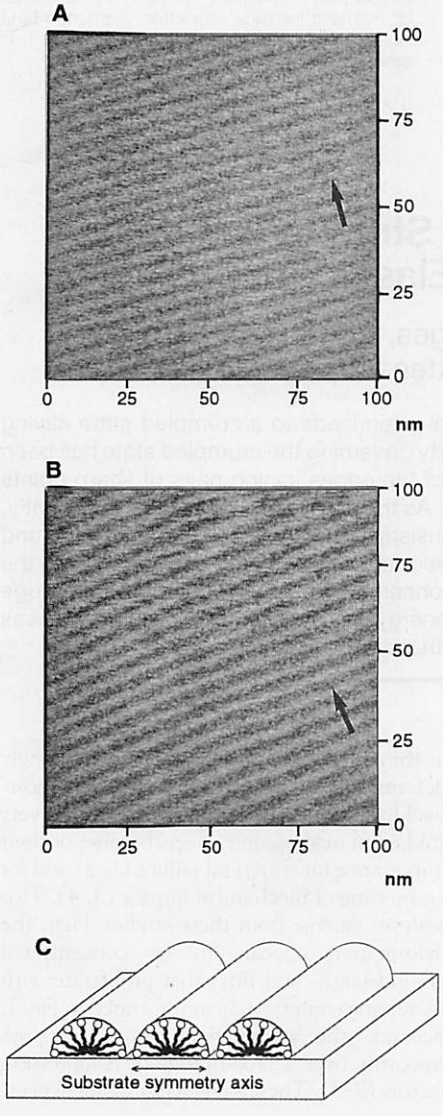

Fig. 3. Aggregates of C_{14}TAB from 7.0 mM solution on hydrophobic substrates. (**A**) A 100 nm by 100 nm image on graphite, showing parallel stripes spaced at 4.7 ± 0.3 nm. The arrow indicates a symmetry direction of the underlying lattice as determined by lattice scans. (**B**) A 100 nm by 100 nm image on MoS_2, showing parallel stripes spaced at 5.1 ± 0.4 nm. Arrow indicates a symmetry direction of the underlying lattice. (**C**) Proposed model of half-cylindrical aggregates, consistent with AFM images and with adsorption isotherms (*25*) indicating coverage roughly equivalent to a monolayer. The bottom plane of molecules is oriented with tails parallel to a substrate symmetry axis.

Comparison of observed adsorption morphologies (*28*) for the above four substrates provides some general insight into surfactant aggregation at interfaces. Single-chain quaternary ammonium surfactants do not adsorb in uniform layers—neither uniform monolayers on hydrophobic substrates nor uniform bilayers on hydrophilic ones—evidently because of a spontaneous curvature that results from interheadgroup repulsion (*1*). The same geometric packing considerations that determine aggregate shapes in bulk solution also affect aggregate shapes at interfaces. A double-chained surfactant, which is capable of forming bilayers in solution, is capable of doing so at interfaces as well.

Although surfactant geometry is important, the substrate also plays a role in determining the adsorbate structure. Hydrophobic surfaces interact primarily with tailgroups, causing them to orient along directions of crystalline symmetry; the resulting molecular strips or ribbons adjacent to the surface serve as a foundation for half-cylindrical aggregates above the CMC. In contrast, oppositely charged hydrophilic substrates interact primarily with surfactant headgroups, giving rise to aggregate structures that depend on the density of the electrostatically bound headgroups. On silica, the solution pH can be used to vary the surface charge, thus varying the nearest neighbor spacing of the roughly spherical aggregates. On mica, where ion exchange between the surface K^+ ions and headgroups can give rise to a greater density of electrostatically bound surfactants indepen-

dent of pH, adsorption above the CMC is in the higher density form of cylinders. The curvature of the interfacial aggregate thus appears to be a compromise between the free curvature defined by intermolecular interactions and constraints imposed by molecule-surface interactions.

Further study of interfacial surfactant aggregation may lead not only to an enhanced understanding of self-assembly but also to applications in materials science. Interfacial aggregates could, for example, serve as a basis for surface patterning on the nanometer scale, complementing recent patterning strategies on the submicrometer scale (*29*). "Fixing" the liquid-crystalline aggregates could be accomplished by ultraviolet polymerization of modified tailgroups, electroless metal deposition (*30*), or polymerization of certain inorganic counterions (*31*) such as silicates.

REFERENCES AND NOTES

1. J. N. Israelachvili, *Intermolecular and Surface Forces* (Academic Press, London, ed. 2, 1992), pp. 341–385.
2. W. Helfrich, *J. Phys. Condensed Matter* **6**, A79 (1994).
3. S. M. Gruner, *J. Phys. Chem.* **93**, 7562 (1989).
4. A. M. Gaudin and D. W. Fuerstenau, *Trans. Am. Inst. Min. Metall. Pet. Eng.* **202**, 958 (1955); D. W. Fuerstenau, *J. Phys. Chem.* **60**, 981 (1956); J. J. Kipling, *Adsorption from Solution of Non-Electrolytes* (Academic Press, London, 1965).
5. R. M. Pashley and J. N. Israelachvili, *Colloids Surf.* **2**, 169 (1981); R. M. Pashley, P. M. McGuiggan, R. G. Horn, B. W. Ninham, *J. Colloid Interface Sci.* **126**, 569 (1988); P. Kekicheff, H. K. Christenson, B. W. Ninham, *Colloids Surf.* **40**, 31 (1989); J. L. Parker, *Prog. Surf. Sci.* **47**, 205 (1994).
6. P. Levitz, H. Van Damme, D. Keravis, *J. Phys. Chem.* **88**, 2228 (1984).
7. D. C. McDermott, J. McCarney, R. K. Thomas, A. R. Rennie, *J. Colloid Interface Sci.* **162**, 304 (1994).
8. G. Binnig, C. F. Quate, Ch. Gerber, *Phys. Rev. Lett.* **56**, 930 (1986).
9. F. Reiss-Husson and V. Luzzati, *J. Phys. Chem.* **68**, 3504 (1964).
10. T. J. Senden, C. J. Drummond, P. Kekicheff, *Langmuir* **10**, 358 (1994).
11. S. Manne, J. P. Cleveland, H. E. Gaub, G. D. Stucky, P. K. Hansma, *ibid.*, p. 4409.
12. We used a commercial atomic force microscope (Digital Instruments, Santa Barbara, CA) and cantilevers (Ultralevers; Park Scientific Instruments, Sunnyvale, CA) cleaned by exposure to ultraviolet light for 15 to 60 min. Typical imaging times were 30 to 60 s, and imaging forces were ~1 nN. Samples were immersed in surfactant solution long enough to minimize thermal drift of the cantilever (15 to 120 min); mica immersed for several days showed no difference in the aggregate structure, indicating that the adsorbate reaches equilibrium configuration within a few minutes. Surfactants were purchased from Fluka (Buchs, Switzerland) (>98% pure), and solutions were prepared in Millipore water. Highly oriented pyrolytic graphite (Digital Instruments), mica, and the MoS_2 crystal were exposed to surfactant solution within 3 min of cleavage. Silica samples [thermally grown oxide on a Si (100) wafer (Wacker, Burghausen, Germany)] were cleaned and stored as described (*13*) and were mounted and exposed to surfactant solution within 20 min of removal from the storage oven. All images shown are unfiltered except for slope removal along scan lines. Typical force versus distance curves in 7 mM C_{14}TAB solution showed a long-range repulsion that varied exponentially (*32*) with a measured decay length of 2.8 ± 0.3 nm, comparing favorably to a theoretical double-layer decay length of 2.9 nm [calculated from (*21*), assuming that micelles are composed of ~70 molecules of which 25% are dissociated]. The short-range repulsion (at separations <~6 nm) was usually steeper, indicating steric or entropic effects such as hydration forces, counterion confinement, and adsorbate protrusion forces.
13. R. W. Tillmann, M. Radmacher, H. E. Gaub, *Appl. Phys. Lett.* **60**, 3111 (1992).
14. B. H. Bijsterbosch, *J. Colloid Interface Sci.* **47**, 186 (1974).
15. M. A. Yeskie and J. H. Harwell, *J. Phys. Chem.* **92**, 2346 (1988).
16. R. K. Iler, *The Chemistry of Silica* (Wiley, New York, 1979), pp. 680–686.
17. M. W. Rutland and J. L. Parker, *Langmuir* **10**, 1110 (1994); S. Partyka, M. Lindheimer, B. Faucompre, *Colloids Surf. A* **76**, 267 (1993).
18. J. Leimbach, J. Sigg, H. Rupprecht, *Colloids Surf. A* **94**, 1 (1995); T. Gu and Z. Huang, *ibid.* **40**, 71 (1989).
19. These spacings varied somewhat from sample to sample, probably due to surface variations as reported (*7*).
20. T. Gu, B.-Y. Zhu, H. Rupprecht, *Prog. Colloid Polym. Sci.* **88**, 74 (1992).
21. R. M. Pashley and B. W. Ninham, *J. Phys. Chem.* **91**, 2902 (1987).
22. C. A. Helm, J. N. Israelachvili, P. M. McGuiggan, *Science* **246**, 919 (1989).
23. P. Richetti and P. Kekicheff, *Phys. Rev. Lett.* **68**, 1951 (1992).
24. Previous SFA measurements (*21*) with quaternary ammonium surfactants have found that aggregate layers on mica have dissociation constants (20 to 25%) similar to those of spherical micelles. Given that any aggregate curvature should be a function of the dissociation constant (because the degree of charge neutralization affects the interheadgroup spacing), the above measurement is more consistent with curved surface aggregates (such as the proposed cylinders) than with flat bilayers.
25. A. C. Zettlemoyer, *J. Colloid Interface Sci.* **28**, 343 (1968); F. G. Greenwood, G. D. Parfitt, N. H. Picton, D. G. Wharton, in *Adsorption from Aqueous Solutions*, W. J. Weber and E. Matijevic, Eds. (American Chemical Society, Washington, DC, 1968), pp. 135–144.
26. A. M. Koganovskii, *Colloid J. USSR* **24**, 702 (1962).
27. Y. H. Yeo, K. Yackoboski, G. C. McGonigal, D. J. Thompson, *J. Vac. Sci. Technol. A* **10**, 600 (1992); J. P. Rabe and S. Buchholz, *Science* **253**, 424 (1991); A. J. Groszek, *Proc. R. Soc. London Ser. A* **314**, 473 (1970).
28. Control experiments were performed to ensure that the adsorbate morphology was not an imaging artifact: (i) The adsorbate layer on each substrate was imaged in at least three independent experiments with different cantilevers. (ii) The imaged adsorbate morphology was confirmed to be repeatable and independent of scan size, speed, and direction. (iii) In many cases, a single cantilever was used to image two or more different aggregate structures (such as stripes and spheres) on different substrates.
29. A. Kumar, H. A. Biebuyck, G. M. Whitesides, *Langmuir* **10**, 1498 (1994); J. J. McClelland, R. E. Scholten, E. C. Palm, R. J. Celotta, *Science* **262**, 877 (1993).
30. J. M. Schnur, *Science* **262**, 1669 (1993).
31. Q. Huo, R. Leon, P. M. Petroff, G. D. Stucky, *ibid.* **268**, 1324 (1995).
32. W. A. Ducker, T. J. Senden, R. M. Pashley, *Nature* **353**, 239 (1991); H.-J. Butt, *Biophys. J.* **60**, 1438 (1991).

33. We thank H. Rupprecht, S. M. Gruner, V. A. Parsegian, D. E. Walters, and J. P. Cleveland for helpful discussions; W. Heckl for the MoS_2 crystal; and U. G. Hofmann for silica substrates. Supported by a Humboldt Fellowship (S.M.) and the Deutsche Forschungsgemeinschaft (H.E.G.).

6 July 1995; accepted 4 October 1995

Scaling Properties of Stretching Ridges in a Crumpled Elastic Sheet

Alex Lobkovsky, Sharon Gentges, Hao Li,* David Morse, T. A. Witten†

Strong deformation of a sheet of solid material often leads to a crumpled state having sharp points of high curvature. A scaling property governing the crumpled state has been numerically demonstrated by an examination of the ridges joining pairs of sharp points in a range of simple geometries of variable size. As the linear size X increases sufficiently, the deformation energy grows as $X^{1/3}$ and consists of similar amounts of bending and stretching energy. The deformation energy becomes concentrated in a fraction of the sheet that decreases as $X^{-1/3}$. Despite this concentration, the local strain in the ridge decreases as $X^{-2/3}$. Nearly all the deformation energy in thin, crumpled elastic sheets was found to be concentrated in ridges that obey these scaling laws.

Buckled sheets such as a crumpled piece of paper, a collapsed storage tank, or a shriveled raisin represent a ubiquitous form of material deformation. These objects may be considered as thin, elastic sheets that have been strongly deformed by some external force. Such "post-buckling" phenomena have been extensively studied in macroscopic sheets because of their importance for structural failure (*1*, *2*) and for cushioning of mechanical impact (*3*, *4*). Two features emerge from these studies. First, the deformation appears to be concentrated around points and lines that proliferate with increasing compression, as illustrated in Fig. 1. Second, the compressive force increases smoothly over a broad range of compression factors (*3*, *5*). These same features are expect-

A. Lobkovsky, S. Gentges, H. Li, T. A. Witten, James Franck Institute, University of Chicago, Chicago, IL 60637, USA. World Wide Web: http://arnold.uchicago.edu/MRSEC

D. Morse, Institute for Theoretical Physics, University of California, Santa Barbara, CA 93106, USA.

*Present address: NEC Research Institute, Incorporated, 4 Independence Way, Princeton, NJ 08540, USA.

†To whom correspondence should be addressed. E-mail: t-witten@uchicago.edu

ed for microscopic elastic membranes, such as layered compounds (6) (Fig. 1C) and solidlike surfactant vesicles (7).

Current understanding of the strongly buckled state remains primitive. Some scaling properties of this state have been explored empirically (8–10). Still, it is not even known how the energy of a crumpled sheet ought to scale with compression. With such scaling laws one could predict, for instance, the energy of a large crumpled sheet given that of a smaller one. Mathematical treatment of strong buckling has been confined to isolated cases (11–13) in which the buckling behavior is different from that of a crumpled sheet. The bulk of analytical work concerns sheets weakly deformed by thermal fluctuations (14, 15) or by incipient buckling (16, 17). Here, we demonstrate a structural element responsible for the deformation energy of strongly buckled thin sheets: the stretching ridge.

To define this strong buckling, we consider a thin, flat elastic disk confined in an impenetrable sphere. The thickness h of the disk is taken to be much smaller than its radius R_0 so as to accentuate the contrast with an ordinary three-dimensional solid. The confining sphere is gradually contracted to a radius $R < R_0$, so that the elastic sheet within it must deform. A point originally at spatial position $\mathbf{s} \equiv (s_1, s_2, 0)$ moves to the point $\mathbf{r}(\mathbf{s})$. The deformation energy is the sum of the strain energy S and bending energy B. The sheet takes on a conformation $\mathbf{r}(\mathbf{s})$ that minimizes the energy $S + B$.

We expect the confined sheet to bend in preference to stretching when $R \gg h$. Accordingly, we first consider an unstretchable sheet. Every point on such a sheet must have vanishing curvature in some direction (18). If the confining sphere is contracted to two-thirds of the radius R_0, for example, the sheet can distort into a conical shape (Fig. 2A) with a singular curvature at the vertex. At each point of the cone there is no curvature in the direction toward the vertex. The radius of curvature $1/C$ grows linearly with distance from the vertex. The resulting energy $B = \kappa \int^{R_0} d^2s C^2$ grows logarithmically with the size R_0. Here κ is the cylindrical bending modulus, d^2s denotes the surface integration element, and the integration is taken over the surface (16). As the confining sphere is contracted further, a single cone can no longer fit inside it. An increasing number of singular vertices is necessary; hence, we investigated the shape of a surface with two such vertices (Fig. 2B).

The addition of a second vertex alters the curvature qualitatively. A generic point P must now have zero curvature in the direction of both the first vertex and the second. Thus, the surface must be flat except along the line joining the vertices. This line must form a sharp ridge, whose energy is propor-

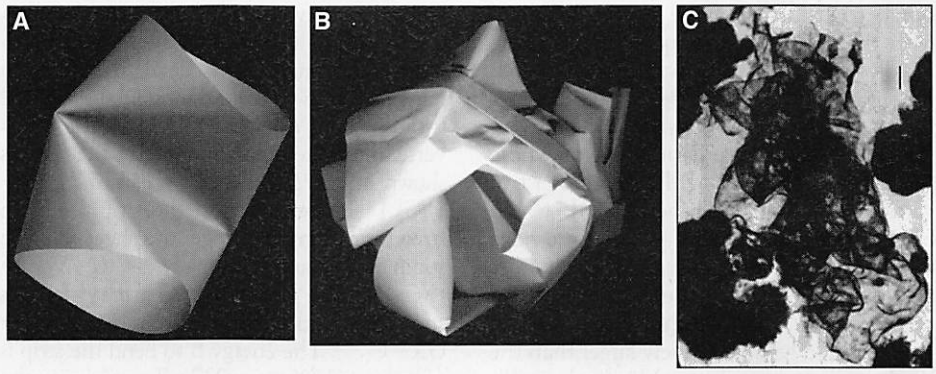

Fig. 1. Examples of buckled and crumpled sheets. (**A**) Simulated buckled thin cylinder [courtesy of the authors of (27)]. (**B**) A piece of paper lightly crumpled between the hands. (**C**) Rag phase of molybdenum disulfide [courtesy of the authors of (28)]. The calibration bar is 20 nm.

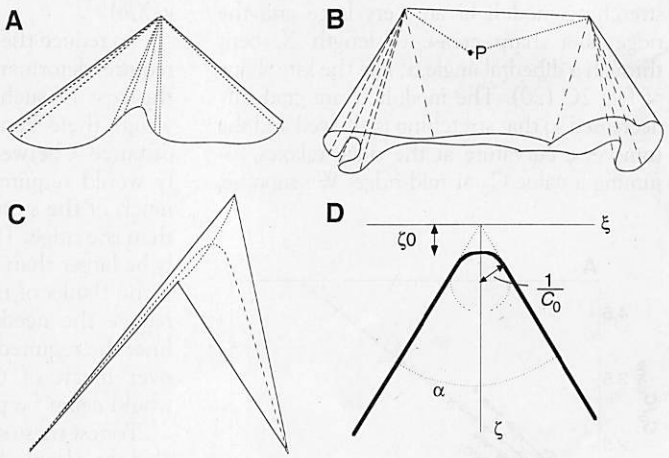

Fig. 2. Deformations of a thin elastic sheet with increasing confinement. (**A**) Cone shape resulting from moderate confinement. (**B**) Double-cone shape resulting from further confinement. A generic point P is indicated. (**C**) Kite shape which exhibits a ridge [such as the one in (B)] being bent through a dihedral angle. (**D**) Approximate shape of the transverse diagonal in (C). Axes for the normal coordinate ζ and the transverse coordinate ξ are shown. Deflection ζ_0 from the unstretchable ridge and dihedral angle α are indicated.

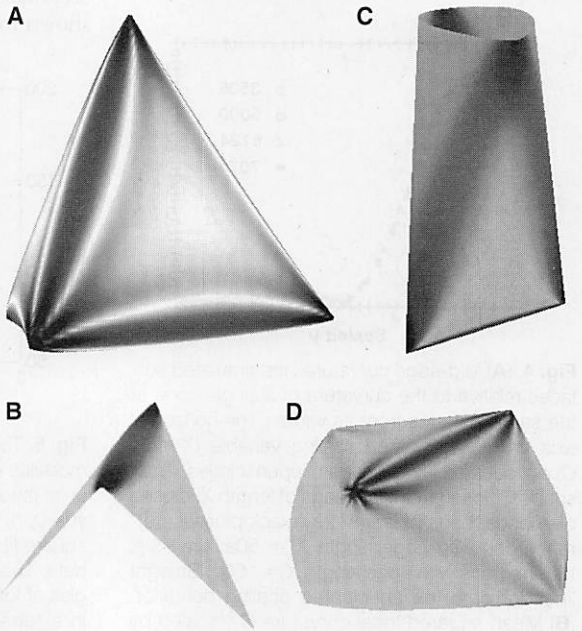

Fig. 3. Sample shapes simulated with a triangular lattice of springs of unstretched length a and spring constant K. Shading is proportional to the local stretching energy. Bending rigidity is imparted by an additional energy $J(1 - \hat{n}_i \cdot \hat{n}_j)$ for each pair of adjacent triangles (i, j) with unit normals $\hat{n}_i$ and $\hat{n}_j$ (13), where J is proportional to the bending modulus. This lattice is equivalent to a sheet of isotropic elastic material of thickness $h = 2\sqrt{2}\sqrt{J/K}$ and bending modulus $\kappa = J\sqrt{3}/2$. (**A**) Regular tetrahedron. The distance X between vertices is 100 times the lattice spacing a. Elastic thickness $h = a/27.4$. (**B**) Kite shape made from a flat, rhombus-shaped surface by exerting normal forces on the perimeter sites. The forces constrain the perimeter to follow a rectilinear frame with a dihedral angle α equal to that of the tetrahedron, namely $\cos^{-1}(1/3)$. Ridge length $X = 100a$ and thickness $h = a/13.7$. (**C**) Two-vertex bag shape with $X = 50a$, $h = a/27.4$, and length of $2X$. The "sharpness" of the vertices (integrated Gaussian curvature or disclination charge) is π, as in a regular tetrahedron. (**D**) Two-vertex boat shape with $X = 67.48a$ and $h = a/20.4$. The two vertices have sharpness $\pi/3$.

tional to its length. The energy increases with the system size R_0 qualitatively more rapidly with two vertices than with one. If the surface is allowed to stretch, the effect on the single cone is minor: the singularity at the vertex spreads over a finite region whose size is independent of R_0. In the case of two vertices [discussed elsewhere (*19*)], it has been argued that stretching allows the ridge to soften to a radius of curvature 1/C of order $h^{1/3} R_0^{1/3}$. The associated energy was argued to grow as $R_0^{1/3}$. For very thin sheets, such an energy would be qualitatively larger than the single-vertex energy, yet qualitatively smaller than the energy of an unstretchable sheet.

We may extend the energy-balance reasoning (*19*) to treat the ridge joining two vertices, as in the double-cone shape of Fig. 2B. We consider an initial state in which the stretching moduli G are very large and the ridge is a sharp crease of length X, bent through a dihedral angle α, like the kite shape of Fig. 2C (*20*). The moduli G are gradually decreased so that stretching is allowed and the transverse curvature at the ridge relaxes, assuming a value C_0 at mid-ridge. We suppose, and later justify, that the bulk of the deformation occurs in a strip along the ridge of width $w \simeq 1/C_0$. Then, as C_0 decreases, the strip must deflect away from the original ridge line by an amount ζ_0 of order $1/C_0$. (If the transverse lines were simply rounded at the apex as shown in Fig. 2D, then $\zeta_0 = \{[\sin(\alpha/2)]^{-1} - 1\}/C_0$.) The deflection of the strip results in stretching along the ridge: the sheet must be strained by an amount $\gamma \simeq (\zeta_0/X)^2 \simeq (XC_0)^{-2}$. The energy $S = G \int d^2s\gamma^2$ for this stretching of the strip is of order $G\gamma^2 Xw \simeq GX^{-3}C_0^{-5}$. The energy B to bend the strip is of order $\kappa C_0^2 Xw \simeq \kappa XC_0$. To minimize the sum of these two energies requires $C_0 \simeq (1/X)\,[X/(\kappa/G)^{1/2}]^{1/3}$. For sheets made of isotropic material, the length $(\kappa/G)^{1/2}$ is approximately equal to the thickness h (*16*). The optimal energy achieved is of order $S \simeq B \simeq \kappa(X/h)^{1/3}$.

To reduce the ridge energy further would require deformation in other regions, but the cost of such deformations would outweigh their benefit. Thus, to reduce the distance X between the vertices substantially would require a strain of order γ over much of the surface—a region much larger than the ridge. The energy cost would clearly be larger than the ridge energy. Likewise, if the flanks of the ridge stretched so as to reduce the needed deflection of the ridge line, the required strain would be of order γ over much of the surface, and the cost would again be prohibitive.

To test these scaling predictions, we modeled the elastic sheet numerically as a triangular lattice of springs, following, for example, Seung and Nelson (*13*, *21*, *22*). Some minimum-energy surfaces having a variety of secondary structures near each ridge are shown in Fig. 3. The stretching energy oscillates as one moves away from the ridge line of the tetrahedron rather than going monotonically to zero. For the shapes with a free edge (Fig. 3, C and D), there are regions of large curvature at the free edge opposite to the vertices. Faint induced ridges appear between the vertices and the induced "vertices" at the edges. These induced features become stronger as the effective size X/h increases.

We plotted the transverse curvature at mid-ridge versus the reduced size X/h for the four different shapes (Fig. 4). The curvature is expressed relative to the curvature at the same point if only one vertex were present. We note first that the curvatures follow the anticipated $(X/h)^{1/3}$ scaling. The tetrahedron has a reduced curvature of $0.22(X/h)^{1/3}$, as determined from fitting all the data. The uncertainty in this coefficient derived from the scatter of the data is less than 0.001. Second, the curves for different shapes have similar slopes. This indicates that the shape of the ridge does not depend strongly on the sharpness of the vertices or on the shape of the surface far from the ridge. Third, the dihedral angle α affects the slope more than the sharpness of the vertices does. For the bag shapes (Fig. 3C) with fixed sharpness, the slope increases with the bag length (that is, with decreasing α), but for different shapes with equal dihedral angles (Fig. 3, A and B), there is no discernable difference in slope. Fourth, in all cases, the ridge begins to dominate the curvature (doubling the reduced curvature) for X/h in the range of 350 to 1000.

We analyzed the tetrahedral shape in greater detail. We first verified that the shapes were independent of lattice size for fixed X/h. The curvature at mid-ridge differs from the extrapolation to an infinitely fine lattice by no more than 2%. The entire profile shrinks inward with increasing X/h; the shrinkage is consistent with the anticipated $(X/h)^{-1/3}$ scaling. This can be seen by plotting the mean squared curvature across the ridge as shown in Fig. 4B for four different values of X/h. The ridge profiles collapse onto a single scaling curve. Because our results are insensitive to the lattice spacing for a given X/h, they are not sensitive to the lattice spring model used, but they would hold quantitatively for any elastic material.

The total energy of the tetrahedron is expected to scale as $\kappa(X/h)^{1/3}$. The measured total energy S + B in units of κ is plotted in Fig. 5. The energy is consistent with the asymptotic formula $S + B = 6\kappa(1.55 \pm 0.002)\,(X/h)^{1/3}$. The indicated uncertainty reflects only the scatter in the data used. For comparison the combined energy of the four disconnected cones making up the tetrahedron is shown; namely,

$$4\kappa[4.081 \log(X/a) + \text{constant}] \quad (1)$$

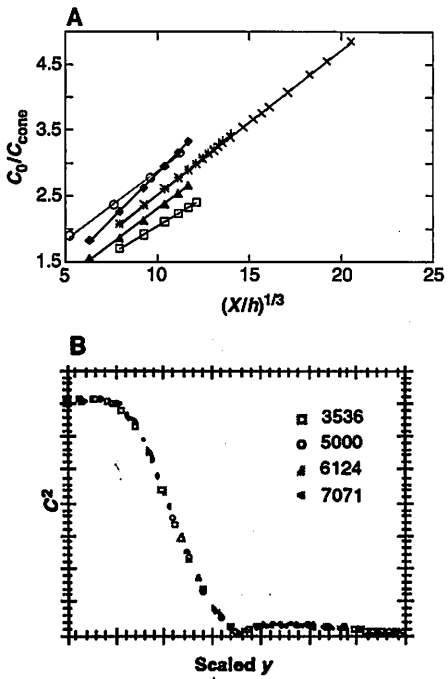

Fig. 4. (**A**) Mid-ridge curvatures for simulated surfaces relative to the curvature of a single cone at the same distance from its vertex. The horizontal axis is the anticipated scaling variable $(X/h)^{1/3}$. Open squares, kite shapes; open circles, boat shapes; closed triangles, bags of length X; closed diamonds, bags of length 2X; black plusses, tetrahedrons with ridge length $X = 50a$; gray x's, tetrahedrons with ridge length $X = 100a$. Straight lines indicate the anticipated scaling behavior. (**B**) Mean squared local curvature C^2 scaled by $X^{-2}(X/h)^{2/3}$ along the perpendicular bisector of the ridge. The distance y from the ridge is scaled by $X(X/h)^{-1/3}$ for tetrahedron ridges with different X/h as indicated. The strain profile $\gamma(y)$ is similar.

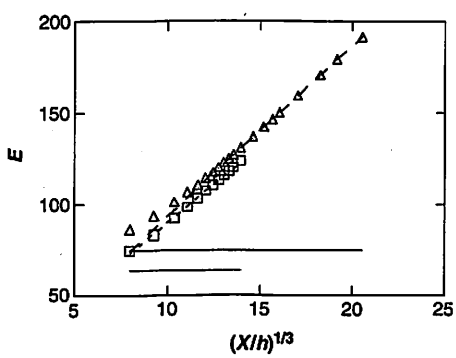

Fig. 5. Total energy $E = S + B$ in units of bending modulus κ for lattice tetrahedra with $X = 50$ lattice units (squares) or 100 lattice units (triangles), versus $(X/h)^{1/3}$. The dashed lines indicate the least square fits through the upper seven points of the data. The solid lines indicate the continuum energies of four separated cones with sharpness π as in a tetrahedron and with length X, determined from Eq. 1 without the additive constant: lower line, $X = 50$ lattice units; upper line, $X = 100$ lattice units (numerically determined cone energies fall close to these lines).

The cone energy is independent of the moduli G and thus independent of the elastic thickness h (23). The cone energy remains a significant fraction of the tetrahedron energy for all tetrahedra studied. Nevertheless, the asymptotic scaling gives less than 10% error for tetrahedra larger than about 10^3 times their thickness (for example, a 10-cm tetrahedron made of standard 0.1-mm-thick office paper). The simulated sheets of Tersoff (24) and of Kroll (22) did not approach these size-to-thickness ratios; thus, it is not surprising that they saw no evidence for the energy scaling predicted here.

The ridges suggest an approach for describing a strongly crumpled sheet. From common observation, crumpled sheets contain a large number of vertices. We may suppose that pairs of adjacent vertices give rise to ridges like the ones seen in our simple shapes. The neighboring ridges can be expected to influence one another. Still, this mutual influence cannot be too great. Our study has shown that well-developed ridges are but little influenced by the surface at distances of order X from the ridge line. This is natural, because the ridge energy is concentrated at distances much smaller than X from this line. We are led to treat the ridges as independent, at least as a first approximation. Thus, we may find the approximate energy of a given crumpled sheet from its ridge lengths X_i by simply adding the individual energies to obtain a total energy $E \approx \kappa \Sigma_i (X_i/h)^{1/3}$.

We expect the stretching-ridge concept to contribute to future understanding of the crumpled materials like those in Fig. 1. When the ridges are a few hundred times longer than the membrane thickness, they give a quantitative account of the deformation energy. The ridge concept should aid in the design of macroscopic energy-absorbing materials such as packing material (4) and protective vehicle structures (3), for example, by placing defects to control where ridges form. Knowledge about ridges may aid the understanding of microscopic phenomena such as the collapse of graphite membranes (6) and the passage of blood cells through capillaries (25), and it may elucidate large-scale phenomena such as the buckling of the Earth's crust (26).

REFERENCES AND NOTES

1. *Post-Buckling of Elastic Structures*, proceedings of the *Euromech Colloquium*, no. 200, Matrafured, Hungary, 5 to 7 October 1985 (Elsevier, Amsterdam, 1986).
2. N. Yamaki, *Elastic Stability of Circular Cylindrical Shells* (North-Holland, New York, 1984).
3. P. Stutenkemper and R. Brasche, in *International Technical Conference on Experimental Safety Vehicles*, sponsored by the Government of France, Paris, 5 to 8 June 1979 (Government Printing Office, Washington, DC, 1980), pp. 321–329.
4. C. E. Crede, in *Symposium on Simulated Service Testing of Packaging*, Sponsored by the Administrative Committee on Simulated Service Testing, New York, NY, 1962 (American Society for Testing and Materials, Philadelphia, PA, 1963), pp. 1–49.
5. R. E. Newton, in *Shock and Vibration Handbook*, C. M. Harris and C. E. Crede, Eds. (McGraw-Hill, New York, 1988), p. 31-1; P. E. Franklin and M. T. Hatae, *ibid.*, p. 41-1.
6. M. S. Spector, E. Naranjo, S. Chiruvolu, J. A. Zasadzinski, *Phys. Rev. Lett.* **73**, 2867 (1994).
7. E. Sackmann *et al.*, *Ber. Bunsen-ges. Phys. Chem.* **89**, 1198 (1985).
8. J. B. C. García, M. A. F. Gomes, T. I. Jyh, T. I. Ren, *J. Phys. A. Gen. Phys.* **25**, L353 (1992).
9. F. Abraham, paper presented at the Workshop on Biomaterials, University of California, Santa Barbara, CA, 31 August 1994.
10. Y. Kantor, M. Kardar, D. R. Nelson, *Phys. Rev. Lett.* **57**, 791 (1986).
11. R. Scheidl and H. Troger, in (1), p. 293.
12. M. Ortiz and G. Giola, *J. Mech. Phys. Solids* **41**, 531 (1994).
13. H. S. Seung and D. R. Nelson, *Phys. Rev. A* **38**, 1005 (1988).
14. D. Nelson, T. Piran, S. Weinberg, Eds., *Statistical Mechanics of Membranes and Surfaces* (World Scientific, Singapore, 1989).
15. D. R. Nelson and L. Peliti, *J. Phys. (Paris)* **48**, 1085 (1987); F. David and E. Guitter, *Europhys. Lett.* **5**, 709 (1988).
16. L. D. Landau and E. M. Lifshitz, *Theory of Elasticity* (Pergamon, Oxford, 1986), sections 14 and 15. Our cylindrical bending modulus κ is denoted there as D.
17. See, for example, G. Gerard, *Handbook of Structural Stability* (New York University, New York, NY, 1956).
18. In (14), p. 143.
19. T. A. Witten and H. Li, *Europhys. Lett.* **23**, 51 (1993).
20. A full description requires two stretching and two bending moduli; however, these details are not important for our scaling argument.
21. D. C. Morse and T. C. Lubensky, *J. Phys. II* **3**, 531 (1993).
22. Z. Zhang, H. T. Davis, D. M. Kroll, *Z. Phys. B* **97**, 337 (1995).
23. More precisely, the cone energy is independent of h in the limit that h is much smaller than the lattice spacing a. In our numerical studies h varied from a to a few percent of a. Accordingly, we observed a few-percent dependence of the cone energy on h.
24. J. Tersoff, *Phys. Rev. B* **46**, 15546 (1992).
25. W. H. Reinhart *et al.*, *Biorheology* **28**, 537 (1991).
26. See, for example, R. J. Chorley, S. A. Schumm, D. E. Sugden, *Geomorphology* (Methuen, London, 1984), chap. 7.
27. Y. L. Kergosien, H. Gotoda, T. L. Kunii, *IEEE Comput. Graphics Appl.* **14**, 40 (1994).

28. R. R. Chianelli, E. B. Prestridge, T. A. Pecoraro, J. P. DeNeufville, *Science* **203**, 1105 (1979).
29. We are grateful to J. Gao, N. Lebovitz, S. Antman, and S. Nagel for assistance and discussions. Supported by NSF under award number DMR-9205827 and through its Materials Research Science and Engineering Center Program under award number DMR-9400379. S.G. was supported as a summer intern by the NSF Research Experiences for Undergraduate Program under NSF Research Experience for Undergraduates site grant Phy-9212351. We thank the authors of (27) for providing the image for Fig. 1A.

3 July 1995; accepted 29 September 1995

Autoencapsulation Through Intermolecular Forces: A Synthetic Self-Assembling Spherical Complex

Robert S. Meissner, Julius Rebek Jr.,* Javier de Mendoza

The synthesis and characterization of a system for the study of molecular recognition phenomena are described. The system involves a tetraurea molecule that is capable of assembly into various associated states through hydrogen bonding. In organic solvents, the dynamic transition between a low-ordered (aggregate) state and a highly ordered dimeric assembly can be induced by the introduction of smaller molecules of appropriate size and shape. These smaller molecules, such as benzene, adamantanes, and ferrocenes, act as guests that occupy the pseudospherical capsule formed by the dimeric host. Among various guests, those that best fill the cavity and offer chemical complementarity to the host are preferentially encapsulated.

How molecules fit together—molecular recognition—can be explored with biological macromolecules and with synthetic structures of low molecular weight. Recognition expresses structural information and takes the form of complementarity in size, shape, and chemical surfaces. A subtle expression of information is possible with self-complementary molecules. Multiple copies of such molecules can give rise to ordered superstructures—assemblies—with functions that are unique to their assembled states. In molecular assembly formation, favorable binding forces (enthalpy) compete with energy loss due to the decreased freedom of the individual subunits (entropy). Guest molecules that match a host assembly in size and shape interact to produce an increased van der Waals attraction, and those guests with functional groups capable of forming hydrogen bonds with the host produce increased electrostatic attraction. Guests that maximize the attractive forces are preferred (1). Here we describe a molecule that assembles to provide a host for the reversible encapsulation of sizable, complementary guests (2).

Molecule 1 consists of 13 fused rings that

R. S. Meissner and J. Rebek Jr., Massachusetts Institute of Technology, Department of Chemistry, Cambridge, MA 02139, USA.
J. de Mendoza, Universidad Autonoma de Madrid, Departamento de Quimica, Cantoblanco, 28049 Madrid, Spain.

*To whom correspondence should be addressed.

give it an extended, rigid structure (Fig. 1A). The stereoisomer shown presents the R groups on the same face of the molecule as the central ethylene bridge. This feature permits the structure to assume low-energy conformations of an overall C-shape, with all R groups positioned on its convex surface. As in other cases of molecular assembly formation (*3*), hydrogen bonds provide the attractive forces. The hydrogen bond acceptors on the ends of the structure (the four N–H bonds) are complementary to the hydrogen bond donors near its center (the four carbonyl oxygens). When two molecules of **1** come together with their concave surfaces opposed, a structure of roughly spherical shape can result. The assembly is modeled (*4*) in Fig. 1B, where the hydrogen bonding sites and the gentle curvature of the units are highlighted.

In the synthesis of compound **1a** (Fig. 2), we took advantage of its symmetry and modular nature. The urea-containing termini of the target were made by sequential treatment of tetrabromodurene (**2**) with *tert*-butyl hydrazodiformate (**3**) and diphenylglycoluril (**5**). Although only modest yields of **6** were obtained, this procedure avoids the use of protecting groups at the remaining reactive sites of **2** and **5** (*5*). Compound **6** was then deprotected with acid to produce the hydrazine salt **7**. The central unit **8** was prepared by a multiple-step process that relied on the Diels-Alder cylcloaddition of the acetylene **9** and the diene **10** as the key reaction (Fig. 3) (*6*). The final assembly fused the tetraacid-chloride **8** to two molecules of hydrazine **7** (Fig. 2). The reaction produced a mixture of the three possible stereoisomers. Isolation of the desired C-shaped isomer was achieved by a combination of extraction and silica gel chromatography. A parallel synthesis, in which each phenyl group was replaced with an isopentyl ester, gave a derivative (**1b**) with greater solubility in organic solvents.

In the solvent benzene-d_6, proton nuclear magnetic resonance (NMR) signals of molecule **1a** are sharp, and downfield shifts were observed for the N–H resonances, characteristic of an ordered, extensively hydrogen-bonded system (Fig. 4A). However, in $CDCl_3$, the molecule dissolved with difficulty and formed a gel-like phase after a few minutes. The spectrum showed broad unresolved peaks (Fig. 4B), and the suspension in the NMR tube could be turned upside down without loss of its contents. Evidently, in this solvent an aggregate of relatively low order was formed.

The more soluble derivative **1b** showed

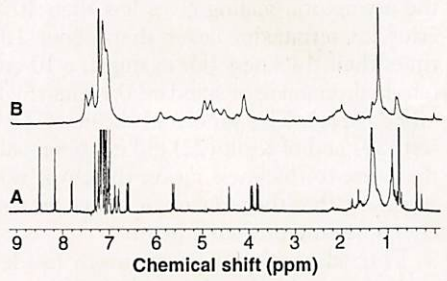

Fig. 4. ^{1}H NMR spectra of **1a**. (**A**) Benzene-d_6 solvent. The signals between 7.2 and 7.0 ppm, and between 2.2 and 0 ppm, are from the solvent and its impurities. (**B**) Chloroform-*d* solvent. The single peak at 7.26 ppm is from the solvent.

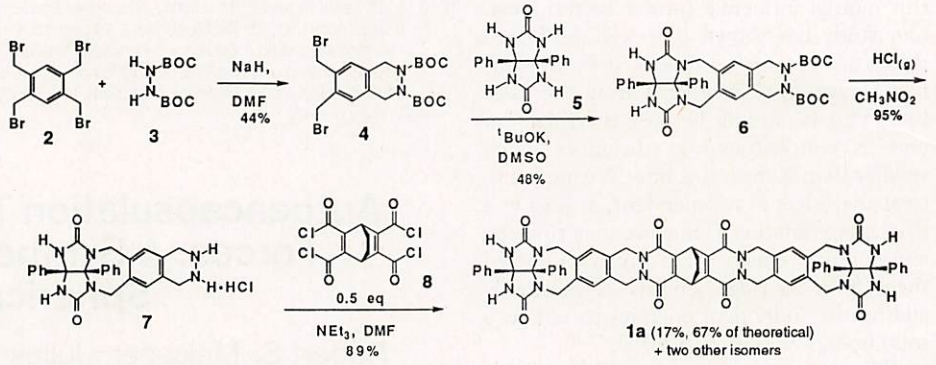

Fig. 2. Synthesis of monomer **1a**. Abbreviations: BOC, *tert*-butoxycarbonyl; DMF, *N,N*-dimethyl formamide; ^{t}BuOK, potassium *tert*-butoxide; Ph, phenyl; DMSO, dimethyl sulfoxide; Net_3, triethyl amine; and eq, equivalents.

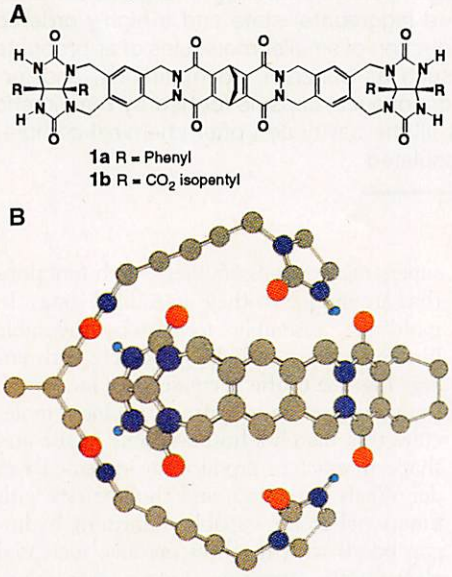

Fig. 1. (**A**) Structural depiction of monomer **1**. (**B**) Energy-minimized (*4*) dimeric depiction of the self-assembled structure **1**. The R groups and some hydrogens have been omitted for clarity. Carbon atoms are gray, nitrogen are dark blue, oxygen are red, and hydrogen are light blue.

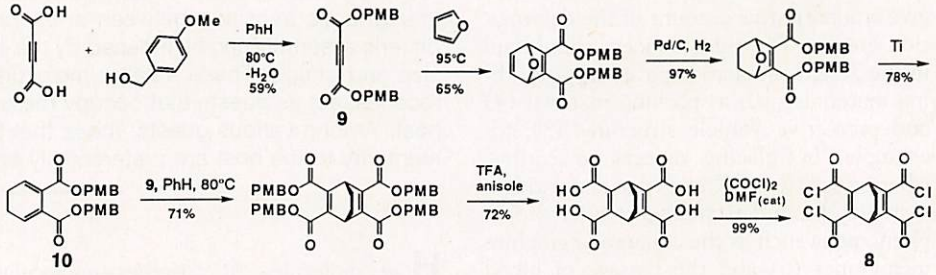

Fig. 3. Synthesis of the central tetraacylchloride. Abbreviations: Me, methyl; PMB, *para*-methoxy benzyl; and TFA, triflouroacetic acid.

Table 1. Stoichiometric and kinetic data. Abbreviations: $[\mathbf{1b}]_{tot}$, total concentration of **1b**; $[guest]_{tot}$, total guest concentration; K_a(app), apparent association constants; and M, molar.

Guest	Stoichiometry*	$[\mathbf{1b}]_{tot}$ (mM)	$[guest]_{tot}$ (mM)	K_a(app) (M^{-1})†
1,3,5,7-tetramethyladamantane	0.9	8.15	40.8	6.7
1-adamantaneamine	1.0	6.70	3.35	190
1-adamantanecarboxamide	0.9	6.70	2.65	310
1-adamantanecarboxylic acid	1.0	6.70	2.65	780
1,3-adamantanedicarboxlic acid	1.0	6.70	–‡	–‡
1-ferrocenecarboxylic acid	1.1	6.40	3.20	280

*Equivalents of guest per equivalent host dimer (±10%). †Calculated with Eq. 1 (*10*). ‡Value was not calculated because of the insolubility of the free guest.

a spectrum similar to that of **1a** in benzene-d_6, but in *para*-xylene-d_{10} it produced broad signals in the NMR spectrum (Fig. 5A). Addition of 1-adamantanecarboxylic acid to the xylene solution led to a significant sharpening of the signals, and a set of upfield signals emerged between –0.1 and –1.0 parts per million (ppm) (Fig. 5B). These can be attributed to an inclusion complex in which two molecules of **1b** surround the 1-adamantanecarboxylic acid; the four benzene rings of the host provide the anisotropic environment that leads to the shielding of the NMR signals of the guest. Similarly, 1,3-adamantanedicarboxylic acid (Fig. 5C), 1-adamantanecarboxamide (Fig. 5D), 1-ferrocenecarboxylic acid (Fig. 5E), 1,3,5,7-tetramethyladamantane (Fig. 5F), 1-adamantaneamine, and ferrocene can also be encapsulated by the dimeric host. In the case of 1,3-adamantanedicarboxylic acid, the guest alone was completely insoluble in the *para*-xylene-d_{10} solvent but was rapidly drawn into solution by encapsulation (*7*).

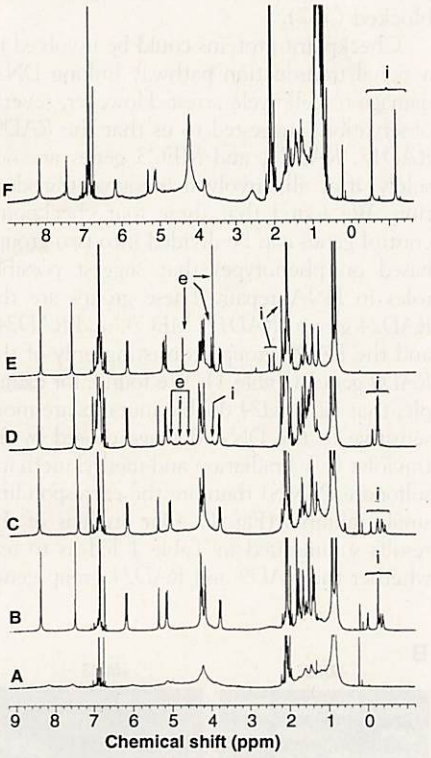

Fig. 5. ^{1}H NMR spectra of **1b** in *para*-xylene-d_{10} solvent with various guests. The signals of the included guest are labeled with an "i," and the excluded guest signals, when resolved, are labeled with an "e." (**A**) Compound **1b** (6.70 mM) in *para*-xylene-d_{10} solvent. The signals between 7.0 and 6.6 ppm, 2.2 and 1.8 ppm, and at 0.17 ppm are from the solvent and its impurities; the residual water signal is at 0.22 ppm. (**B**) Compound **1b** (6.70 mM) in *para*-xylene-d_{10} solvent with 2 equivalents of 1-adamantanecarboxylic acid added. (**C**) Compound **1b** (6.70 mM) in *para*-xylene-d_{10} solvent with 2 equivalents of 1,3-adamantanedicarboxylic acid added. (**D**) Compound **1b** (6.70 mM) in *para*-xylene-d_{10} solvent with 2 equivalents of 1-adamantanecarboxamide added. The labeled guest peaks between 3.6 and 5.0 ppm are the amide N–H signals. (**E**) Compound **1b** (6.40 mM) in *para*-xylene-d_{10} solvent with 2 equivalents of 1-ferrocenecarboxylic acid added. (**F**) Compound **1b** (8.15 mM) in *para*-xylene-d_{10} solvent with 10 equivalents of 1,3,5,7-tetramethyladamantane added.

The spectroscopic observations can be interpreted as follows. In the presence of a solvent ill-suited for encapsulation (the small chloroform or the elongated *p*-xylene), intermolecular hydrogen bonding led to low-order aggregation of the monomer. With the addition of a guest of complementary size and shape, such as benzene or 1,3,5,7-tetramethyladamantane, the spherical dimeric form is favored, because attractive van der Waals interactions between host and guest are maximized within the inclusion complex. The equilibrium is further displaced toward the dimeric capsule when guests such as the functionalized adamantane derivatives or 1-ferrocenecarboxylic acid fill the space and provide hydrogen bonds to the interior surface of the host (Fig. 6).

Integration of the ^{1}H NMR signals provides the stoichiometry of the host-guest complex, and in each case, one guest per host dimer is clearly indicated (Table 1). The widely separated signals for free and bound guests in the NMR spectra indicate that exchange of guests in and out of the cavity is slow on the NMR time scale.

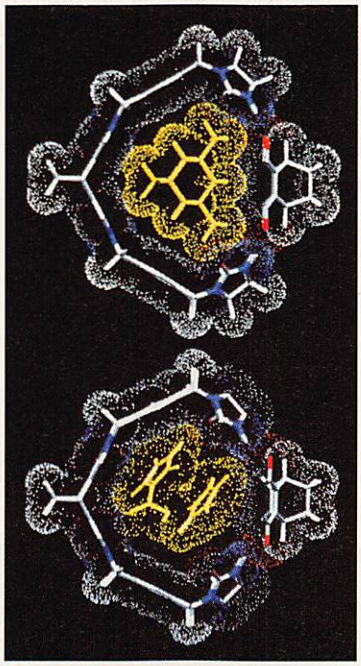

Fig. 6. Host-guest complexes. Energy-minimized models with cutaway views showing the van der Waals radii of the complex with tetramethyladamantane (top) and 1-ferrocenecarboxylic acid (bottom) encapsulated in dimer **1b**. The R groups have been omitted and the guests colored yellow for clarity.

The inclusion studies indicate that the functionality of the guest can be most important in organizing the assembly. The addition of only 1 equivalent of the functionalized adamantane derivatives to the solution of **1b** produced the sharp spectrum indicative of a well-ordered dimeric assembly, whereas even 10 equivalents of 1,3,5,7-tetramethyladamantane was insufficient to produce such order. Similarly, the proportion of encapsulated-to-free guest was much greater for the functionalized adamantanes (*8*), a result consistent with larger contributions of electrostatic versus van der Waals interactions (*9*).

The analysis of quantitative data obtained from the ^{1}H NMR spectra can be used to calculate equilibrium association constants for various guests. These values are here denoted as apparent association constants, K_a(app), because of the simplification of the several dynamic processes present into one process in by Eq. 1 (*10*).

$$\mathbf{1b}_{(\text{aggregate})} + \text{guest} \rightleftarrows \mathbf{1b} \cdot \text{guest} \cdot \mathbf{1b} \quad (1)$$

$$K_a(\text{app}) = \frac{[\mathbf{1b} \cdot \text{guest} \cdot \mathbf{1b}]}{[\mathbf{1b}_{(\text{aggregate})}][\text{guest}]}$$

The apparent association constants listed in Table 1 allow comparison of the relative affinities of the dimeric assembly for these guests.

In summary, the behavior and functions of molecule **1** can, to some extent, be controlled, either by solvation or encapsulation of guests. The considerations of host-guest complementarity and the sizable cavity of the dimeric capsule suggest that catalysis of reactions that feature transition states of the appropriate size, shape, and functionality may be possible within the assembly.

REFERENCES AND NOTES

1. J. Israelachvili, *Intermolecular and Surface Forces* (Academic Press, London, ed. 2, 1992); F. Diederich, *Angew. Chem.* **100**, 372 (1988).
2. For a sampling of three-dimensional supramolecular aggregates, see C. Seto and G. M. Whitesides, *J. Am. Chem. Soc.* **113**, 712 (1991); M. Simard, D. Su, J. D. Wuest, *ibid.*, p. 4696; P. Baxter, J.-M. Lehn, A. DeCian, J. Fisher, *Angew. Chem. Int. Ed. Engl.* **32**, 69 (1993); R. P. Bonar-Law and J. K. M. Sanders, *Tetrahedron Lett.* **34**, 1677 (1993); M. R. Ghadiri, J. R. Granja, R. A. Milligan, D. E. McRee, N. Khazanovich, *Nature* **366**, 324 (1993); J. Yang, E. Fan, S. J. Geib, A. D. Hamilton, *J. Am. Chem. Soc.* **115**, 5314 (1993); M. R. Ghadiri, K. Kobayashi, J. R. Granja, R. K. Chadha, D. E. McRee, *Angew. Chem. Int. Ed. Engl.* **34**, 93 (1995); J. P. Mattias, C. T. Seto, E. E. Simanek, G. M. Whitesides, *J. Am. Chem. Soc.* **116**, 1725 (1994); J. P. Mathias, E. E. Simanek, J. A. Zerkowski, C. T. Seto, G. M. Whitesides, *ibid.*, p. 4316; J. P. Mathias, E. E. Simanek, G. M. Whitesides, *ibid.*, p. 4326.
3. N. Branda, R. Wyler, J. Rebek Jr., *Science* **263**, 1267 (1994); R. Wyler, J. de Mendoza, J. Rebek Jr., *Angew. Chem. Int. Ed. Engl.* **32**, 1699 (1993); D. J.

Cram, R. Jaeger, K. Deshayes, *J. Am. Chem. Soc.* **115**, 10111 (1993); D. J. Cram, *Nature* **356**, 29 (1992); M. Fujita, N. Satoshi, K. Ogura, *J. Am. Chem. Soc.* **117**, 1649 (1995).
4. The assembly was modeled on a Silicon Graphics Personal Iris with Macromodel V3.5X, MM2 force field with the GB/SA model [F. Mohamadi *et al.*, *J. Comput. Chem.* **11**, 440 (1990)].
5. For similar reactions of *tert*-butyl hydrazodiformate, see L. A. Carpino, *J. Am. Chem. Soc.* **85**, 2144 (1963).
6. The synthesis follows that of a related tetramethyl ester [R. Beerli and J. Rebek Jr., *Tetrahedron Lett.* **36**, 1813 (1995)].
7. Introduction of the 1,3-adamantanedicarboxylic acid to the NMR tube followed by vigorous shaking for 10 s is all that is necessary to cause dissolution.
8. In the cases of the 1-adamantaneamine and 1-adamantanecarboxylic acid (Fig. 5B), the proton resonances of nonencapsulated guests are discernable in the region between 1 and 2 ppm and can be estimated to be about equal in intensity to the resonances of the included guest. For 1,3,5,7-tetramethyladamantane (Fig. 5E), the proton resonances of the nonencapsulated guest are the very large peaks whose bases are visible at 0.8 ppm; at full scale, these resonances are about 60 times as intense as the resonances of the included guest. This guest can be displaced by the addition of 20 equivalents of benzene for each equivalent of 1,3,5,7-tetramethyladamantane, indicating that benzene, by comparison, is a much less favored guest.
9. H. Dugas, *Bioorganic Chemistry* (Springer-Verlag, New York, ed. 2, 1989), pp. 20–21.
10. The value for the complex term [**1b** · guest · **1b**] was measured from the NMR spectra by using an internal standard, and the [$\mathbf{1b}_{(aggregate)}$] and [guest] values were calculated by subtracting the complex amount from the total amounts. Several assumptions were made: (i) the amount of dimer (unfilled or filled with solvent) present before addition of the guest is negligible, (ii) after addition of the guest, all the host material not assembled into the complex is in the aggregate state, and (iii) the association of the guest with itself is negligible.
11. R.S.M. thanks NIH for a fellowship, and we thank NIH for support of this research.

2 June 1995; accepted 22 August 1995

Yeast Checkpoint Genes in DNA Damage Processing: Implications for Repair and Arrest

David Lydall and Ted Weinert

Yeast checkpoint control genes were found to affect processing of DNA damage as well as cell cycle arrest. An assay that measures DNA damage processing in vivo showed that the checkpoint genes *RAD17, RAD24*, and *MEC3* activated an exonuclease that degrades DNA. The degradation is probably a direct consequence of checkpoint protein function, because *RAD17* encodes a putative 3′-5′ DNA exonuclease. Another checkpoint gene, *RAD9*, had a different role: It inhibited the degradation by *RAD17*, *RAD24*, and *MEC3*. A model of how processing of DNA damage may be linked to both DNA repair and cell cycle arrest is proposed.

Checkpoint controls recognize DNA damage and halt cell division until DNA repair is complete. They are thought to play an important role in tumor prevention, because human checkpoint genes, such as *p53* and *ATM*, are often compromised in tumor cells (*1*). How eukaryotic checkpoint controls work to sense DNA damage and to signal arrest is unclear. Studies in yeasts have identified genes that are essential for arrest in G_2 after DNA damage, at the G_2 checkpoint. Here we examine the role of the G_2 checkpoint genes *RAD9*, *RAD17*, *RAD24*, and *MEC3* (*2–5*) in yeast. Other genes, *MEC1*, *RAD53*, and *POLε*, are also required for checkpoint control at the S-phase checkpoint when DNA replication is blocked (*5–7*).

Department of Molecular and Cellular Biology, University of Arizona, Tucson AZ 85721, USA.

Checkpoint proteins could be involved in a signal transduction pathway linking DNA damage to cell cycle arrest. However, several observations suggested to us that the *RAD9*, *RAD17*, *RAD24*, and *MEC3* genes are not solely, if at all, involved in signal transduction. We found that these four checkpoint control genes can be divided into two groups based on phenotypes that suggest possible roles in DNA repair. These groups are the *RAD24* group (*RAD17*, *MEC3*, and *RAD24*) and the *RAD9* group (consisting only of the *RAD9* gene) (Table 1). We found, for example, that *rad9 rad24* double mutants are more sensitive to the DNA damage caused by ultraviolet (UV) radiation and methyl methane sulfonate (MMS) than are the corresponding single mutants (Fig. 1). Our analysis of the results summarized in Table 1 led us to test whether the *RAD9* and *RAD24* group genes

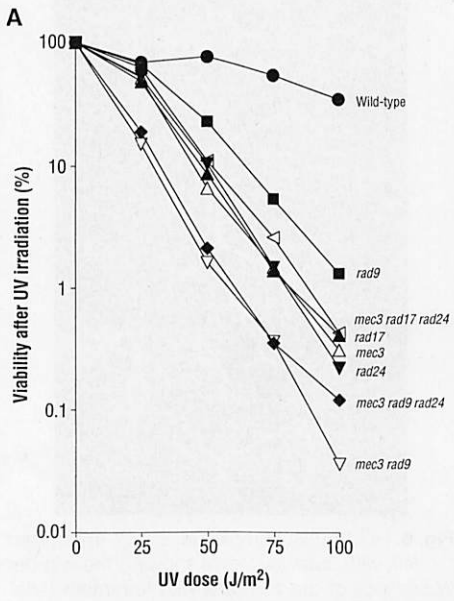

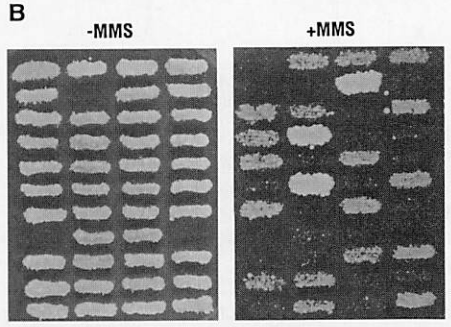

Tetrad number	a	b	c	d
1	9, 17	9	3, 17, 24	3, 24
2	3, 9	–	WT	3, 9, 17, 24
3	3, 17, 24	9	3, 9, 24	17
4	24	WT	3, 9, 17	3, 9, 17, 24
5	24	9, 17, 24	3, 17	3, 9
6	3, 9, 24	WT	9, 17, 24	3, 17
7	17, 24	3, 9	3, 17	9, 24
8	–	9, 17, 24	9, 24	–
9	3, 9, 24	9, 17	3, 24	17
10	3	3, 17, 24	9, 17	9, 24
11	3, 9, 24	3	9, 17, 24	17

Fig 1. Assignment of *rad9* mutants to a different epistasis group than *rad17*, *rad24*, and *mec3* mutants. (**A**) Sensitivity of checkpoint mutant strains to UV irradiation. A series of A364a strains in which combinations of the *RAD9, RAD17, RAD24*, and *MEC3* genes had been deleted were tested for their sensitivity to UV irradiation. All the survival curves shown were obtained on the same day. There was slight day-to-day variation in cell viability, but whenever a *rad9* mutation was combined with any other checkpoint mutation the cells were more sensitive to UV irradiation. Experiments in the W303 background produced a similar pattern (*16*). (**B**) Sensitivity of checkpoint mutant strains to the alkylating agent MMS. Strain DLY 217 (A364a background, *Mat**a** rad9::HIS3 rad17::LEU2 rad24::TRP1 mec3::URA3*) was crossed to strain DLY221 (A364a background, *Matα his3 leu2 trp1 ura3*). The diploid was sporulated, and all possible combinations of mutations were found in the haploid progeny. Strains were replica-plated to YEPD-rich plates (containing yeast extract, peptone, and dextrose) with (+) or without (−) 0.01% MMS. In addition, the progeny from each tetrad (labeled a, b, c, or d in table) were replica-plated to −URA, −HIS, −LEU, and −TRP plates to determine which checkpoint mutations were present. Abbreviations in table are as follows: 3, *mec3::URA3*; 9, *rad9::HIS3*; 17, *rad17::LEU2*; 24, *rad24::TRP1*; and WT, wild type. A dash indicates that this particular spore did not grow. Three levels of growth were observed in the presence of MMS: Wild-type cells were MMS-resistant, *rad9* or *rad24* group mutants were sensitive, and *rad9 rad24* group double mutants were supersensitive. Consistent results were found in the W303 genetic background (*16*).

have different roles in DNA repair. In addition, *rad9* and *rad24* group mutants had different viabilities after meiosis and after the *CDC13* DNA replication gene was inactivated (Table 1 and Fig. 2).

To study the role of checkpoint genes in DNA repair we needed a way to measure DNA repair in vivo. Garvik *et al.* have recently characterized the type of damage formed in temperature-sensitive *cdc13* mutants (*8*). They have shown that *cdc13* strains generate telomere-proximal DNA damage at 36°C in which the TG strand becomes single-stranded (ss) because the AC strand is lost. Centromere-proximal DNA sequences remain intact. *CDC13* is therefore thought to have a specific role in the replication of the ends of chromosomes. We were encouraged to assay *cdc13*-induced DNA damage because both *RAD9* and *RAD24* are needed for cell cycle arrest of *cdc13* mutants. We suspected that *rad9* and *rad24* mutants might process *cdc13*-induced damage differently because, although both strains are equally checkpoint-defective, *cdc13 rad9* strains lose viability more rapidly than do *cdc13 rad24* mutants (Table 1 and Fig. 2E). We thought that the differences in viability might reflect differences in damage processing.

To assay DNA damage processing in *cdc13* mutants, we measured the amount of ss DNA that accumulated at a single copy sequence near the telomere of chromosome V during a single cell cycle (Fig. 2A). Cells began in G_1 and proceeded synchronously through S and G_2 before arresting in late mitosis (Fig. 2, B and C). We harvested cells during the experiment to analyze their DNA. We found that *RAD*$^+$, *rad24*, and *rad9* cells processed *cdc13*-induced DNA damage with very different kinetics (Fig. 2D). In the checkpoint-proficient *RAD*$^+$ cells, ss DNA first appeared after cells had completed DNA replication and while they were arrested in G_2. In contrast, *rad24* mutants failed to accumulate ss DNA until long after they had passed the G_2-M checkpoint. *rad9* mutants had yet another phenotype and accumulated ss DNA damage even earlier than did *RAD*$^+$ cells. This experiment allowed us to draw several conclusions. First, the ss DNA observed in *cdc13 RAD*$^+$cells is not due to incomplete DNA replication per se, but rather is largely a consequence of *RAD24*-mediated DNA degradation. Second, *RAD9* seems to be able to inhibit the *RAD24*-dependent degradation. The idea that *RAD9* inhibits a *RAD24*-dependent

Table 1. Mutants of the *rad9* and *rad24* groups show different phenotypes. Double mutants of the *rad9 rad24* group were more sensitive to UV- and MMS-induced DNA damage than was either single mutant (Fig. 1). R, resistant; S, sensitive; SS, supersensitive. The *rad9* diploids produced viable spores, but *rad24* group diploids showed low spore viabilities. The *cdc13 rad9* mutants died more rapidly than did the *cdc13 rad24* mutants (cell viabilities after 4 hours at 36°C in the type of experiment shown in Fig. 2 are given). Previously published results show that *cdc13 rad17* and *cdc13 mec3* mutants behave like *cdc13 rad24* mutants (*3*, *5*). All experiments used checkpoint gene disruptions (*2*). ND, not determined.

Mutants	UV or MMS damage	Spore viability (%)	Viability with *cdc13* (%)
RAD+	R	90	93 ± 18.1
rad9	S	92	0.6 ± 0.33
rad24	S	9	43 ± 13.3
rad17	S	22	ND
mec3	S	20	ND
rad9 rad24	SS	ND	25 ± 2.9

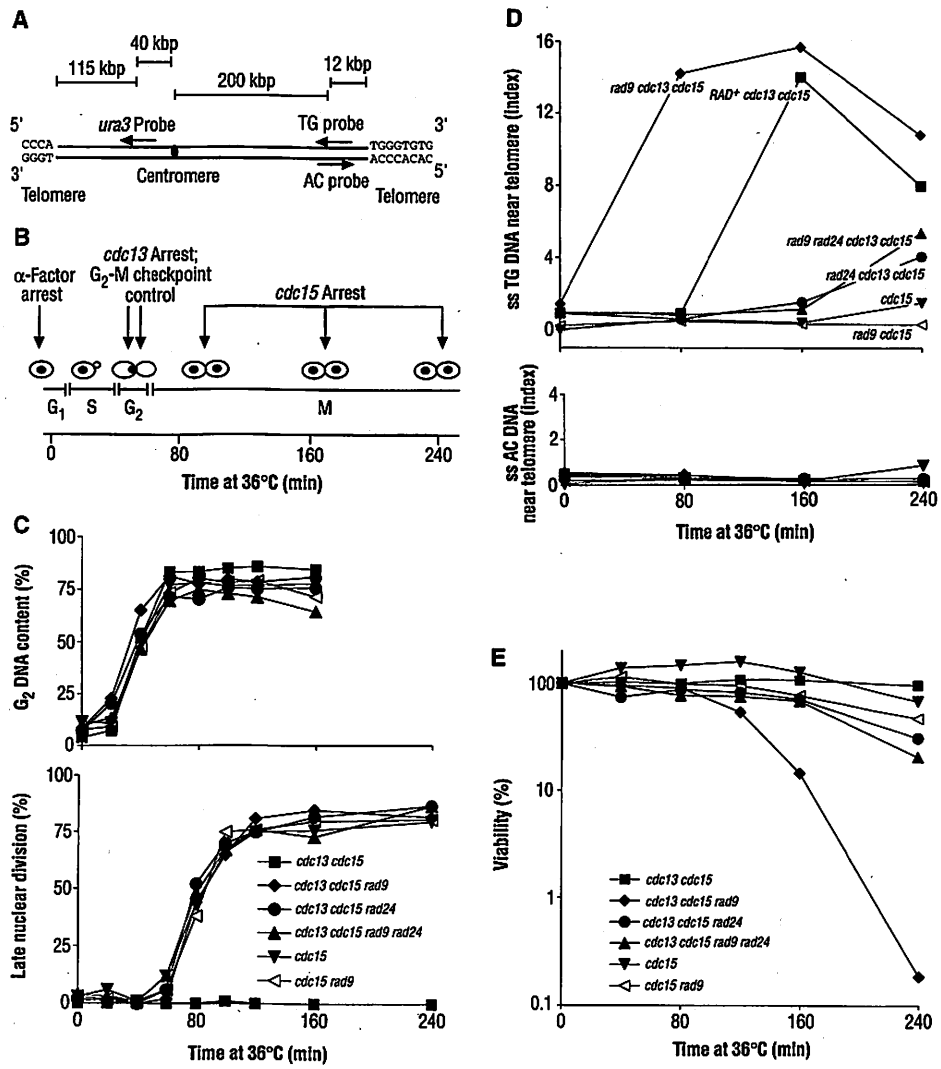

Fig. 2. Effect of checkpoint genes on DNA metabolism in *cdc13* mutants. (**A**) Physical map of chromosome V (*17*). (**B**) Strategy used to synchronize *cdc13* cultures. Strains were arrested in G_1 by the addition of α-factor (20 nM for 2.5 hours at 23°C). The α-factor was removed by centrifugation, and the temperature of the cultures was changed to 36°C to inactivate *cdc13* and *cdc15*. Thereafter, samples were removed to determine the DNA content (by flow cytometry), cell cycle position (by 4′,6′-diamidino-2-phenylindole staining of DNA and fluorescence microscopy), and cell viability (by counting of colonies after 3 days of growth at 23°C). The bulk of the culture was harvested and frozen for subsequent DNA extraction. (**C**) Top panel shows the percentage of cells that contained G_2 DNA. Bottom panel shows the percentage of cells in late nuclear division. The relevant genotypes for strains were as follows: DLY408, squares (*cdc13-1 cdc15-2*); DLY409, diamonds (*cdc13-1 cdc15-2 rad9::HIS3*); DLY410, circles (*cdc13-1 cdc15-2 rad24::TRP1*); DLY411, solid upward-pointing triangles (*cdc13-1 cdc15-2 rad9:HIS3 rad24::TRP1*); DLY418, solid downward-pointing triangles (*cdc15-2*); and DLY419, open triangles (*cdc15-2 rad9::HIS3*). (**D**) Single-stranded DNA accumulation in *cdc13* strains. Symbols are the same as in (C). We determined the ss index by measuring the amount of ss DNA present in nondenatured DNA samples in comparison with a denatured loading control (at the URA3 locus) (*18*). The data shown are the mean of four experiments. Analysis of a DNA sequence 30 kbp closer to the centromere than the locus shown in Fig. 2D revealed similar trends; the ss DNA that accumulated was strand-specific, and *rad9* mutants accumulated it more quickly than did *rad24* mutants (*16*). (**E**) Cell viability.

function is supported by the behavior of *rad9 rad24* double mutants; they degrade DNA as slowly as do *rad24* single mutants (Fig. 2D).

These results also suggest that the death of *rad9 cdc13* mutants is not due to the checkpoint defect, as we had previously supposed (*5*). Rather, death is a consequence of DNA degradation controlled by *RAD24*, because the viability of *cdc13 rad9 rad24* mutants is high, whereas that of *cdc13 rad9 RAD24* mutants is low (Fig. 2E). Therefore, in *cdc13 rad9* cells, *RAD24* induces cell death, or suicide, rather than cell cycle arrest.

Our analyses of damage processing suggest that *RAD24* controls an exonuclease that degrades DNA and that *RAD9* counteracts or inhibits this degradation (Fig. 3). The effects of checkpoint proteins on DNA damage processing are probably direct, because we found that *RAD17*, a member of the *RAD24* group, encodes a putative 3′-5′ DNA exonuclease (Fig. 4). Rad17p is similar to the evolutionarily conserved checkpoint and repair proteins Rec1p (*Ustilago maydis*) and Rad1p (*Schizosaccharomyces pombe*) (Fig. 4).

The idea that *RAD9* and *RAD24* have different roles in processing DNA damage may explain the enhanced sensitivity of double mutants to UV- and MMS-induced DNA damage (Fig. 1). The precise roles of *RAD9* and *RAD24* in the repair of different types of DNA damage are, however, unclear. The two genes act in opposition in one pathway of repair after *cdc13*-induced damage, whereas after UV- and MMS-induced damage they appear to act in different pathways of repair (Fig. 1). In addition, we have yet to understand the problem of why the Rad17p 3′-5′ putative exonuclease is required for cell cycle arrest after DNA damage that leaves a 3′ overhang (*9*).

How is processing of DNA damage linked to cell cycle arrest? We suggest that DNA degradation by Rad17p and Rad24p could generate an intermediate in recombinational repair. We suggest two possible causes of cell cycle arrest: Either the processing of damage by checkpoint control proteins sends the signal for arrest [for example, as a result of an allosteric effect caused by DNA binding (Fig. 3, large box)], or the processing of damage generates a DNA structure that sends the signal for arrest (Fig. 3, small box). In either model, other checkpoint proteins (such as Mec1p and Rad53p) may mediate arrest. We must also consider a third possibility, that processing and arrest may be entirely separate activities of checkpoint control proteins, as appears to be the case for the cyclin-dependent kinase inhibitor p21 (*10*).

The bacterial SOS response to DNA damage provides precedence for the link between DNA damage processing and cell cycle arrest. In *Escherichia coli*, ss DNA generated by damage processing activates RecA to signal the SOS response (*11*). For example, double-stranded breaks must be processed by the recBC helicase-exonuclease and pyrimi-

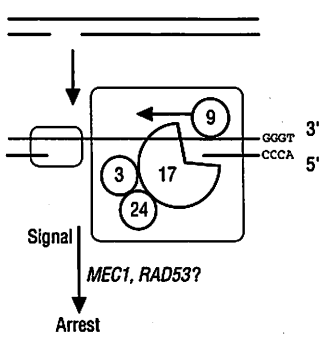

Fig. 3. Model of the role of checkpoint control proteins in *cdc13*-induced DNA damage processing. According to this model, *cdc13* mutants accumulate a small amount of DNA damage during DNA replication at 36°C. Checkpoint control proteins recognize the DNA damage and initiate DNA damage processing. Rad17p (17), Rad24p (24), and Mec3p (3) activate an exonuclease that degrades the AC strand of DNA near telomeres. Rad9p (9) might act as a direct inhibitor of the exonuclease or counteract the exonuclease, for example, by activating a polymerase. *MEC1* and *RAD53* are also required for cell cycle arrest after *cdc13*-induced DNA damage (see text for further details).

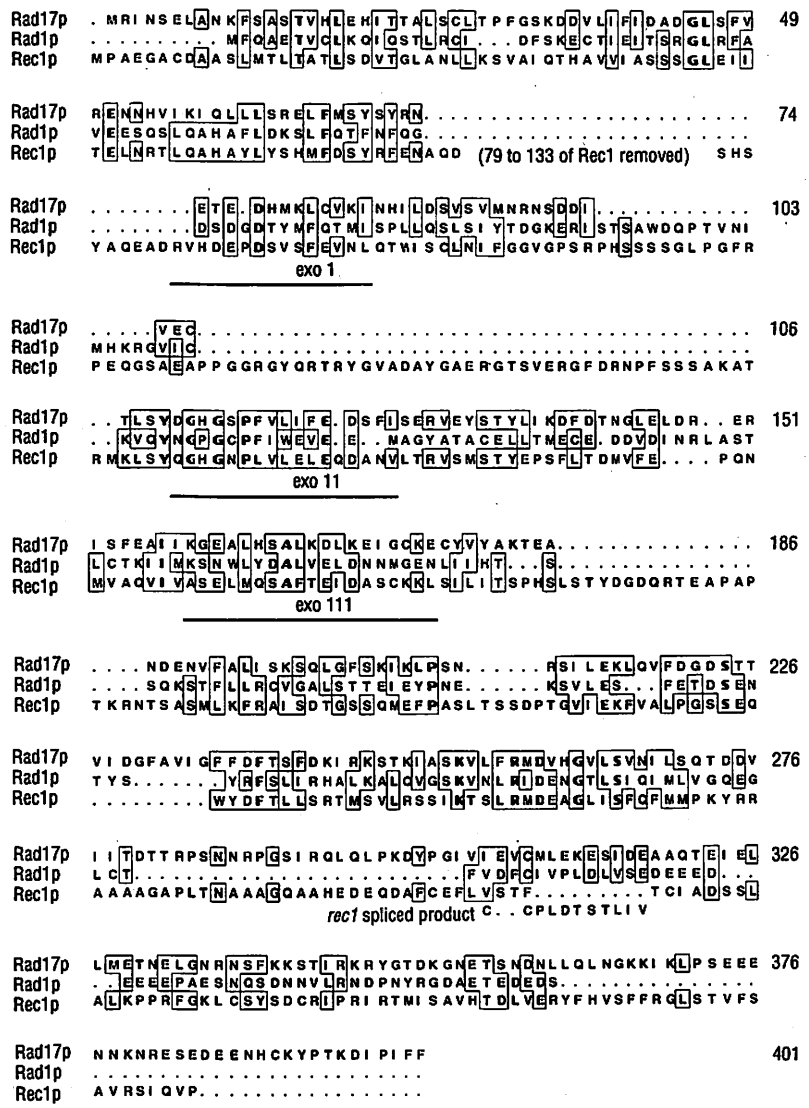

Fig. 4. Comparison of Rad17p, Rad1p, and Rec1p (*19*). *Schizosaccharomyces pombe* Rad1p is 23.2% identical and 50.3% similar to Rad17p. *Ustilago maydis* Rec1p is 21.1% identical and 44.2% similar, and the spliced version is 16.2% identical and 38.2% similar to Rad17p. The three exonuclease domains of 3′-5′ exonucleases, as previously defined (*20*, *21*) and aligned to Rec1p (*22*), are highlighted. These domains are well conserved among Rad17p, Rad1p, and Rec1p, which suggests that all three are 3′-5′ exonucleases (*20–22*). *rad1*$^+$ and *rec1* are each checkpoint control genes, which suggests that evolutionarily conserved proteins link DNA repair to cell cycle arrest (*13*, *23–26*). Dots indicate gaps in the sequence. Amino acids 79 to 113 of Rec1 were deleted in the alignment shown because they did not align to either Rad17p or Rad1p. The numbers on the right refer to the Rad17p sequence. The *rec1* transcript is spliced to make the cDNA product (*24*).

dine dimers must be replicated so that they may generate the ss DNA to activate recA (*12*).

We suggest that other eukaryotic checkpoint control proteins may also participate in DNA damage processing. For example, S-phase checkpoint control may require different proteins to process the type of DNA damage that is induced after DNA replication is inhibited. *POLε* is required for S but not for G_2 checkpoint control (*7*); perhaps this is because *POLε* is specifically required for processing after DNA replication is disturbed. Differences in processing may explain the perplexing patterns of checkpoint gene requirements among species. For example, *rad1*$^+$ and *RAD17* in fission and budding yeasts encode putative 3′-5′ exonucleases and both are required for the G_2 checkpoint in their respective cell types (Fig. 4). However, *rad1*$^+$, yet not *RAD17*, is also required at the S-phase checkpoint (*13*). Similarly, *cdc2*$^+$ and *CDC28* in fission and budding yeasts encode conserved protein kinases. *cdc2*$^+$, yet not *CDC28*, is needed for S-phase checkpoint control (*14*). Perhaps *rad1*$^+$ and *cdc2*$^+$ in fission yeast are required for DNA damage processing after S-phase inhibition, but their homologs in budding yeast are not.

REFERENCES AND NOTES

1. R. Nowak, *Science* **268**, 1700 (1995); K. Savitsky *et al.*, *ibid.*, p. 1749; M. B. Kastan, O. Onyekwere, D. Sidransky, B. Vogelstein, R. W. Craig, *Cancer Res.* **51**, 6304 (1991); S. J. Kuerbitz, B. S. Plunkett, W. V. Walsh, M. B. Kastan, *Proc. Natl. Acad. Sci. U.S.A.* **89**, 7491 (1992).
2. D. Lydall and T. Weinert, in preparation.
3. T. A. Weinert and L. H. Hartwell, *Genetics* **134**, 63 (1993).
4. ———, *Science* **241**, 317 (1988).
5. T. A. Weinert, G. L. Kiser, L. H. Hartwell, *Genes Dev.* **8**, 652 (1994).
6. J. B. Allen, Z. Zhou, W. Siede, E. C. Friedberg, S. J. Elledge, *ibid.*, p. 2401.
7. T. A. Navas, Z. Zhou, S. J. Elledge, *Cell* **80**, 29 (1995).
8. B. Garvik, M. Carson, L. Hartwell, *Mol. Cell. Biol.* **15**, 6128 (1995).
9. Two breaks that cause checkpoint-mediated arrest—an HO endonuclease–induced break during mitosis (*15*) (S. Kim and T. Weinert, unpublished data) and double strand breaks produced during meiosis (D. Lydall and T. Weinert, unpublished data)—both become processed to give a 3′ overhang (implying degradation by a 5′-3′ exonuclease). How a putative 3′-5′ exonuclease (Rad17p) mediates arrest, and perhaps processing, at these two breaks is unclear.
10. R. Li, S. Waga, G. J. Hannon, D. Beach, B. Stillman, *Nature* **371**, 534 (1994).
11. E. M. Witkin, *Biochimie* **73**, 133 (1991).
12. M. Sassanfar and J. W. Roberts, *J. Mol. Biol.* **212**, 79 (1990).
13. T. Enoch, A. M. Carr, P. Nurse, *Genes Dev.* **6**, 2035 (1992); F. Al-Khodairy and A. M. Carr, *EMBO J.* **11**, 1343 (1992); R. Rowley, S. Subramani, P. G. Young, *ibid.*, p. 1335.
14. T. Enoch and P. Nurse, *Cell* **60**, 665 (1990); P. K. Sorger and A. W. Murray, *Nature* **355**, 365 (1992); A. Amon, U. Surana, I. Muroff, K. Nasmyth, *ibid.*, p. 368.
15. L. L. Sandell and V. A. Zakian, *Cell* **75**, 729 (1993).
16. D. Lydall and T. Weinert, data not shown.
17. L. Riles *et al.*, *Genetics* **134**, 81 (1993).
18. Yeast strains used were *MATa bar1::hisG ade2-1 can1-100 cdc15-2 ura3 leu2-3,112 his3-11 trp1-1* and contained various combinations of *cdc13-1*, *rad9::HIS3*, and *rad24::TRP1*. The *bar1* mutation was present to ensure that G_1 arrest was efficient. The *cdc15-2* mutation was present to ensure that checkpoint control mutants replicated their DNA only once. At 36°C, *cdc15* mutants initiate anaphase but are unable to complete nuclear division. We modified the method of Garvik *et al.* and cut purified yeast DNA with Eco RI before applying the DNA to a slot blot apparatus (*8*). Different filters were probed with GT, AC (from pHR85-31), and *URA3* ss RNA probes. Eco RI was necessary because in some experiments ss DNA was present in a non–strand- and non–locus-specific fashion. This ss DNA did not depend on the presence or absence of *CDC13*. Our interpretation is that it represented replication forks moving through the chromosome. This inconsistent *cdc13*-independent signal disappeared after cutting of the DNA with Eco RI, presumably because the chance that a replication fork was attached to the locus we were probing was reduced. After cutting with Eco RI, most (>95%) of the DNA did not bind to the filter, even after it was denatured. We assume this was because smaller fragments of DNA bind the filter less efficiently. The ss DNA index increased for two reasons. First, ss DNA is created in vivo. Second, as ss DNA is created, Eco RI sites are destroyed, so that the size of the ss DNA increased and it bound the nylon membrane more efficiently. Therefore we cannot make quantitative deductions about the amount of ss DNA produced.
19. Single-letter abbreviations for the amino acid residues are as follows: A, Ala; C, Cys; D, Asp; E, Glu; F, Phe; G, Gly; H, His; I, Ile; K, Lys; L, Leu; M, Met; N, Asn; P, Pro; Q, Gln; R, Arg; S, Ser; T, Thr; V, Val; W, Trp; and Y, Tyr.
20. L. Blanco, A. Bernad, M. Salas, *Gene* **112**, 139 (1992).
21. A. Bernad, L. Blanco, J. M. Lazaro, G. Martin, M. Salas, *Cell* **59**, 219 (1989).
22. M. P. Thelen, K. Onel, W. K. Holloman, *J. Biol. Chem.* **269**, 747 (1994).
23. R. Holliday, R. E. Halliwell, M. W. Evans, V. Rowell, *Genet. Res.* **27**, 413 (1976).
24. K. Onel, M. P. Thelen, D. O. Ferguson, R. L. Bennett, W. K. Holloman, *Mol. Cell. Biol.* **15**, 5329 (1995).
25. K. Onel, R. L. Bennett, P. Unrau, A. Koff, W. K. Holloman, in preparation.
26. A. Nasim and B. P. Smith, *Genetics* **79**, 573 (1975).

27. We thank B. Garvik and L. Hartwell for invaluable discussions and advice about the *cdc13* defect; N. Seaver for help with flow cytometry; A. Adams, L. Hatfield, and M. Ramaswami for criticizing the manuscript; and all the yeasty boys and girls in Tucson for input. D.L. thanks E. Ayres for encouragement. Supported by grants to T.W. from NIH (GM 45276-01), the American Cancer Society, and the March of Dimes foundation.

27 June 1995; accepted 27 September 1995

Activation of the Estrogen Receptor Through Phosphorylation by Mitogen-Activated Protein Kinase

Shigeaki Kato, Hideki Endoh, Yoshikazu Masuhiro, Takuya Kitamoto, Shimami Uchiyama, Haruna Sasaki, Shoichi Masushige, Yukiko Gotoh, Eisuke Nishida, Hiroyuki Kawashima, Daniel Metzger, Pierre Chambon*

The phosphorylation of the human estrogen receptor (ER) serine residue at position 118 is required for full activity of the ER activation function 1 (AF-1). This Ser^{118} is phosphorylated by mitogen-activated protein kinase (MAPK) in vitro and in cells treated with epidermal growth factor (EGF) and insulin-like growth factor (IGF) in vivo. Overexpression of MAPK kinase (MAPKK) or of the guanine nucleotide binding protein Ras, both of which activate MAPK, enhanced estrogen-induced and antiestrogen (tamoxifen)-induced transcriptional activity of wild-type ER, but not that of a mutant ER with an alanine in place of Ser^{118}. Thus, the activity of the amino-terminal AF-1 of the ER is modulated by the phosphorylation of Ser^{118} through the Ras-MAPK cascade of the growth factor signaling pathways.

The ER belongs to a superfamily of ligand-inducible transcription factors that includes receptors for steroid hormones, thyroid hormones, vitamin D_3, and retinoic acid, as well as peroxisome proliferator–activated receptors and orphan receptors (*1*). The ER has two transcriptional activation functions, AF-1 and AF-2, which are located in the NH_2-terminal A/B region and in the ligand-binding domain (region E), respectively (*2–6*). Like other steroid hormone receptors, the ER is phosphorylated (*7–9*). The ER becomes phosphorylated at several sites when transfected COS-1 cells are treated with estradiol (E_2), and Ser^{118}—the main residue in the A/B region to be phosphorylated (*7, 8*)—is required for full activity of AF-1 (*7*). The five amino acids located around Ser^{118} (PQLSP) (Fig. 1) (*7, 10*) are conserved among vertebrate species

S. Kato, Y. Masuhiro, T. Kitamoto, S. Uchiyama, H. Sasaki, S. Masushige, Department of Agricultural Chemistry, Tokyo University of Agriculture, Setagayaku, Tokyo 156, Japan.
H. Endoh and H. Kawashima, Molecular Medicine Research Laboratory II, Yamanouchi Institute for Drug Discovery Research Co. Ltd., Tsukuba, Ibaraki 305, Japan.
Y. Gotoh and E. Nishida, Institute for Virus Research, Kyoto University, Sakyo-ku, Kyoto 606, Japan.
D. Metzger and P. Chambon, Institut de Génétique et de Biologie Moléculaire et Cellulaire, Centre National de la Recherche Scientifique (CNRS)/Institut National de la Santé et de la Recherche Médicale (INSERM)/Université Louis Pasteur/Collège de France, BP163-67404 Illkirch Cedex, Communauté Urbaine de Strasbourg, France.

*To whom correspondence should be addressed.

(human, mouse, rat, chick, *Xenopus*, and trout) and correspond to the consensus phosphorylation site [PX_n(S or T)P] (where X is a neutral or basic amino acid and n = 1 or 2) for MAPK (*11*). The finding that the ligand-induced transcriptional activity of ER can be further enhanced by growth factors such as EGF and IGF (*12*) suggests a possible cross talk between the E_2 signaling pathway and growth factor signaling pathways. MAPK is activated by growth factors such as EGF, insulin, and IGF, through membrane-associated receptor tyrosine kinases, which in turn activate Ras followed by activation of the protein kinase Raf. Activated Raf then mediates signal transduction to MAPK through the MAPKK or extracellular signal–regulated protein kinase (ERK) kinases (MEKs) (*13*). Taken together, these observations suggested that phosphorylation of the ER Ser^{118} residue through the growth factor–Ras-Raf-MAPK cascade may modulate the activity of AF-1.

To determine whether Ser^{118} was phosphorylated by MAPK in vitro, we expressed the human ER (hER) truncated mutant HE15, which contains regions A through C (*2*), and its Ser^{118} mutants HE15/457 and HE15/458 (Fig. 1) (*7*) as glutathione-S-transferase (GST) fusion proteins in *Escherichia coli* (Fig. 2A). Purified recombinant HE15 (Fig. 2A) was phosphorylated by MAPK purified from *Xenopus* oocytes (*14*), under conditions in which myelin basic protein (MBP) was a good substrate for MAPK (Fig. 2B). Mutation of Ser^{118} to Ala^{118} (HE15/457) or to Glu^{118} (HE15/458) abolished phosphorylation (Fig. 2B). MAPK purified from either human cervix epithelioid carcinoma HeLa cells, African green monkey kidney COS-1 cells, or rat osteosarcoma Ros cells, with a polyclonal antibody directed against *Xenopus* MAPK, gave similar results (*15*). In contrast, purified recombinant HE15, HE15/457, and HE15/458 proteins were not phosphorylated by adenosine 3′,5′-monophosphate (cAMP)–dependent protein kinase (PKA), although PKA did phosphorylate histones (Fig. 2B). We used an electrophoretic mobility-shift assay to show that *E. coli*–produced or in vitro translated HE15 and HE15/457 efficiently bound to an estrogen response element (ERE) and that their binding was not affected by MAPK phosphorylation (*15*). The mutation of Ser^{118} did not affect ERE binding by ER produced in cultured cells (*7*), and our findings are in agreement with this result.

To examine the ability of growth factors to induce phosphorylation of hER Ser^{118}, we transfected COS-1 cells with HE15 or HE15/457 (Fig. 1) and incubated them with [^{32}P]orthophosphate in the presence or absence of EGF or IGF. Immunoprecipitation of cell extracts showed that phosphorylation of HE15 was enhanced in cells treated with EGF or IGF (Fig. 2, C and D), whereas no enhancement was observed when Ser^{118} was mutated (HE15/457). Similarly, expression of a dominant active form of MAPKK (*16*) induced phosphorylation of HE15, but not of HE15/457, in transfected COS-1 cells (Fig. 2C).

To investigate whether MAPK could be involved in ER-mediated transcriptional activation, we transiently transfected COS-1 cells with the wild-type hER expression vector HEG0 (Fig. 3A) and with an expression vector for either c-Ki-Ras (k-Ras) or the dominant active mutant c-Ki-Ras^{Val12} (k-Ras^{Val12}) (*17*), together with the ERE-G-CAT or ERE-TATA-CAT reporter genes, which contain promoter elements of the rab-

Mutant	99 PLNSVSPSPLMLLHPPPQLSPF 120 (102 104 106 118)	Induction by k-Ras^{Val12}
HE15	.....	3.1 ± 0.1
HE15/451	.....P.A.....	2.9 ± 0.2
HE15/452	...N.P.A.....	2.8 ± 0.1
HE15/453	.....A.....	2.9 ± 0.2
HE15/454	.....P.E.....	2.7 ± 0.1
HE15/455	...N.P.E.....	2.9 ± 0.1
HE15/456	.....E.....	3.1 ± 0.2
HE15/457	.....A..	1.1 ± 0.1
HE15/458	.....E..	1.2 ± 0.1

Fig. 1. Abrogation of k-Ras–induced activation of AF-1 by mutation of Ser^{118}, but not of Ser^{102}, Ser^{104}, and Ser^{106} (*10*). Amino acids 99 to 120 of the hER and the point mutations that were created in the A/B region (*7*) are shown. COS-1 cells were cotransfected with ERE-G-CAT and each of the HE15 mutants (*7*) in the absence or presence of the expression vector for k-Ras^{Val12}, and the relative amounts of chloramphenicol acetyltransferase (CAT) activity were determined as in Fig. 3. Values for induction by k-Ras^{Val12} (average ± SEM) for six independent experiments are given.

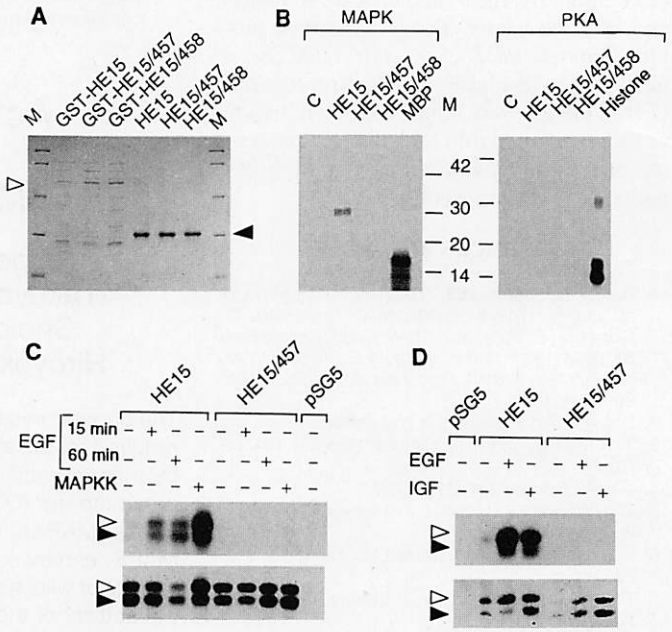

Fig. 2. Phosphorylation of the COOH-terminal truncated human ER mutant (HE15) at Ser^{118} by EGF, IGF, MAPKK, and MAPK. (**A**) Analysis of purified bacterially produced GST fusion proteins and purified HE15, HE15/457, and HE15/458 recombinant proteins. Purified GST fusion proteins (500 ng) and purified HE15 and derivatives (500 ng) (*28*) were analyzed by electrophoresis on an SDS gel (12% polyacrylamide) and stained with Coomassie blue. Positions of GST fusion proteins and recombinant proteins after cleavage are indicated by open and solid arrowheads, respectively. The molecular size markers (M) were rabbit phosphorylase (97 kD), bovine serum albumin (66 kD), rabbit aldolase (42 kD), bovine carbonic anhydrolase (30 kD), and soybean trypsin inhibitor (20 kD). (**B**) In vitro phosphorylation of hER Ser^{118} by MAPK. Purified bacterially produced HE15, HE15/457, or HE15/458 (1 μg) was incubated for 30 min at 30°C with MAPK (0.5 U/μl) [purified from nonfertilized *Xenopus* eggs (*14*)], in 50 mM tris-HCl (pH 8.0), 0.5 mM EDTA, 25 mM $MgCl_2$, 1 mM dithiothreitol, 20 μM adenosine triphosphate (ATP) (0.05 μCi of [γ-^{32}P]ATP), and 10% glycerol or with PKA (0.5 U/μl) [from bovine heart (Sigma)], in 20 mM tris-HCl (pH 6.8), 10 mM magnesium acetate, 1 μM cAMP, and 20 μM ATP (0.05 μCi of [γ-^{32}P]ATP). MBP (Sigma; 1.25 μg) and histones (type II-S, Sigma; 2 μg) were phosphorylated by MAPK and PKA, respectively. Phosphorylation of substrates was analyzed by SDS-PAGE (10 to 20% gradient gel) and autoradiography. C, control lacking HE15. (**C** and **D**) EGF-, IGF-, and MAPKK-induced phosphorylation of hER Ser^{118} in vivo. COS-1 cells were transfected with HE15, HE15/457, or the parental expression vector pSG5 (*7*). In (C), the expression vector for a dominant active form of MAPKK (400 ng) (*15, 16*) was cotransfected as indicated. Starvation with phosphate- and serum-free Dulbecco's modified Eagle's medium (DMEM) was done 40 hours after transfection. After 5 hours of starvation, in vivo labeling was done for 4 hours in phosphate- and serum-free DMEM containing 50 μM vanadate, 50 nM okadaic acid, and 1 mCi of [^{32}P]orthophosphate. In (C) and (D), EGF (100 ng/ml) was added as indicated; in (D), EGF and IGF (100 ng/ml) were added 15 min before harvesting. ^{32}P-labeled extracts of HE15 and HE15/457 were immunoprecipitated with the monoclonal antibody (mAb) B10, followed by SDS-PAGE analysis and immunoblotting, as described (*7*). Upper lanes, autoradiograph signal from the nitrocellulose membrane; lower lanes, HE15 and HE15/457 protein revealed by chemiluminescence after the membrane was probed with mAb B10. Open and closed arrowheads denote the positions of HE15 and a proteolysed form, respectively.

bit β-globin promoter (−119 to +10) and the minimal promoter region (−34 to +33) of the adenovirus-2 major late promoter, respectively. Coexpression of k-Ras or k-Ras^{Val12} led to increases in E_2-induced transactivation by HEG0 (by 1.8 and 2.1 times, respectively, with ERE-G-CAT; by 1.8 and 2.3 times, respectively, with ERE-TATA-CAT) (Fig. 3, B and C). Similar results were obtained in HeLa cells (*15*).

Because there are two transcriptional activation functions (AF-1 and AF-2) in the ER, we investigated whether k-Ras could activate AF-1 or AF-2 with the hER truncated mutants HE15 and HEG19, respectively (Fig. 3A). Transactivation by AF-2 (HEG19) was not enhanced by cotransfection of k-Ras or k-Ras^{Val12}, whereas the activity of AF-1 (HE15) was clearly enhanced, as measured with either of the two reporter genes in COS-1 cells (Fig. 3, B and C). These observations indicate that enhancement by k-Ras of E_2-induced transactivation by hER is essentially mediated through AF-1.

An S118A substitution in HEG0 (HE457) (Fig. 3A) not only decreased the transcriptional activity of the hER, but also abolished k-Ras–mediated enhancement of transcription from both the ERE-TATA-CAT and ERE-G-CAT reporter genes (Fig. 3, B and C). In the absence of AF-2 (HE15) (Fig. 3A), the S118A mutation also abolished k-Ras–mediated transcriptional activation of both reporter genes (Fig. 4A). In sharp contrast, mutations of Ser^{102}, Ser^{104}, or Ser^{106} to nonphosphorylatable residues did not affect k-Ras–induced transactivation (Fig. 1), which indicated a specific role for Ser^{118} in this induction.

We used chimeric proteins in which the A/B region was linked to the GAL4 DNA binding domain (AB-GAL) (Fig. 4B) to confirm that MAPK-induced activation of hER was the result of enhanced AF-1 activity. In cells transfected with the 17M$_2$-G-CAT reporter gene, which contains two GAL4 17M binding sites located upstream of the globin promoter region (*3*), expression of k-Ras or of a dominant active form of MAPKK (*16*) enhanced the activation of transcription by AB-GAL (Fig. 4B), and the S118A mutation (AB/457-GAL) abolished these effects. In contrast, expression of CL100, a MAPK-specific phosphatase (*18*), decreased the activation of transcription by AB-GAL (Fig. 4B). Thus, it appears that MAPK increases the activity of AF-1 by inducing the phosphorylation of Ser^{118}. To determine whether PKA also affects the activity of AF-1, we transfected COS-1 cells with the AB-GAL expression vector and then either cotransfected these cells with a PKA expression vector or

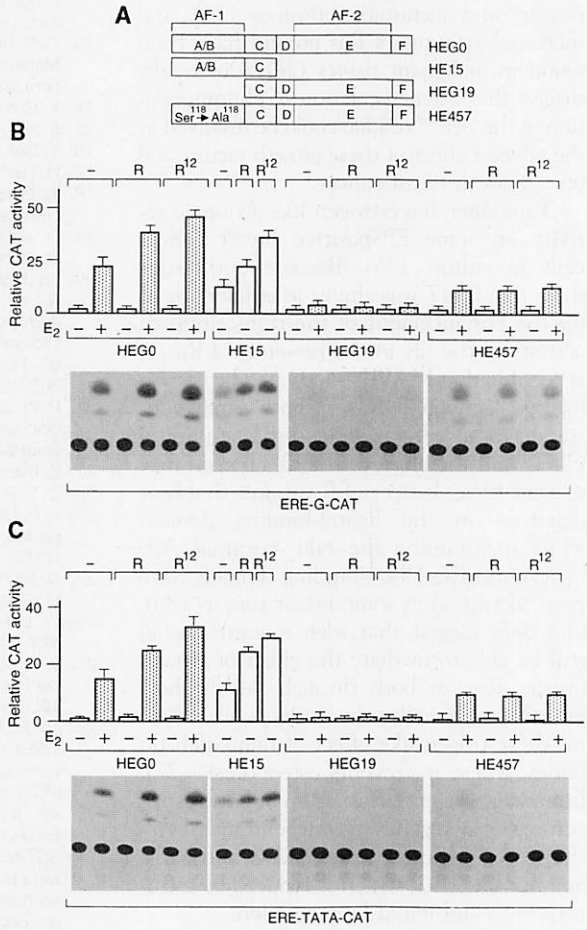

Fig. 3. Enhancement of the transcriptional activity of the hER by overexpressed k-Ras. (**A**) Representations of the hER (with regions A through F shown) and of the mutants used in (B) and (C). (**B** and **C**) Enhanced estrogen-induced transcriptional activity of the hER through AF-1 in cells overexpressing k-Ras. ERE-G-CAT was constructed by inserting a synthetic oligonucleotide containing a perfect palindromic ERE into pG-CAT (*29*). Transient transfections and CAT assays were done as described (*7, 29*). COS-1 cells were cotransfected with either 1 μg of ERE-G-CAT (B) or 2 μg of ERE-TATA-CAT (C) and 0.5 μg of receptor expression vector HEG0, HE15, HEG19, or HE457, in the presence and absence of 10 nM E_2, as indicated. Expression vectors (0.5 μg) for k-Ras (R) and k-Ras^{Val12} (R^{12}) (*17*) were also cotransfected as indicated. Representative CAT assays and graphs corresponding to means and SEM for three independent experiments are shown.

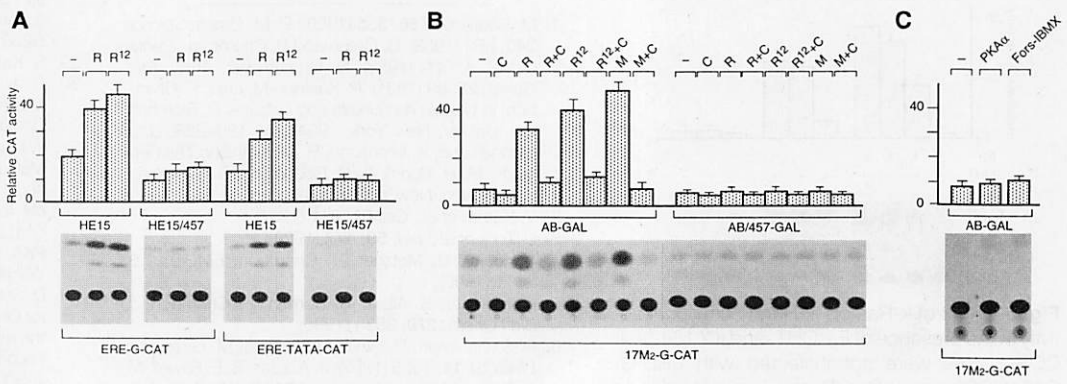

Fig. 4. Requirement of Ser^{118} for k-Ras–induced transactivation. (**A**) Transcriptional activity of HE15, but not of HE15/457, is enhanced by k-Ras overexpression. COS-1 cells were cotransfected with either ERE-G-CAT or ERE-TATA-CAT and either HE15 or HE15/457 (*7*). The expression vectors for k-Ras (R) or k-Ras^{Val12} (R^{12}) were cotransfected as in Fig. 3, as indicated. Representative CAT assays and graphs corresponding to means and SEM for three independent experiments are shown. (**B**) Transcriptional activity of AB-GAL, but not of AB/457-GAL, is enhanced in cells overexpressing k-Ras or MAPKK. AB/457-GAL was constructed by replacing the A/B region of AB-GAL (*5*) with the A/B region of HE15/457 (*7*). COS-1 cells were cotransfected with 17M$_2$-G-CAT (*3*) and with AB-GAL or AB/457-GAL expression vectors. The expression vectors for k-Ras (R), k-Ras^{Val12} (R^{12}), MAPKK (M) (400 ng), or CL100 (C) (20 ng) (*15, 18*) were cotransfected as indicated. (**C**) Lack of effect of PKA on the activity of AF-1. COS-1 cells were cotransfected with 17M$_2$-G-CAT and with AB-GAL or AB/457-GAL expression vectors, as in (B). An expression vector for the cAMP-dependent protein kinase catalytic subunit isoform α (PKAα; 0.5 μg) (*30*) was also cotransfected; alternatively, the cells were treated with 50 μM forskolin and 500 nM IBMX (Fors-IBMX), as indicated.

treated them with forskolin and isobutylmethylxanthine (IBMX) to induce accumulation of cAMP. In both instances, there was no effect on transcription of the $17M_2$-G-CAT reporter (Fig. 4C), in agreement with the absence of phosphorylation of purified HE15 protein by PKA in vitro (Fig. 2B).

The antiestrogen 4-hydroxytamoxifen (OHT) has mixed agonistic and antagonistic activities, whereas ICI 164,384 acts as a pure antiestrogen (*4*, *7*, *19*). Although OHT and ICI 164,384 do not appear to inhibit the DNA binding of the receptor, OHT blocks the activity of AF-2 but not of AF-1, whereas ICI 164,384 blocks the activities of both AF-1 and AF-2 (*4*, *19*). We investigated the effect of k-Ras on transcriptional activation by HEG0 in COS-1 cells with the use of the ERE-G-CAT reporter gene in the presence of E_2, OHT, or ICI 164,384. The partial agonistic activity of OHT was enhanced in cells transfected with k-Ras, whereas k-Ras had no effect in the presence of ICI 164,384 (Fig. 5).

Taken together, our results indicate that transcriptional activation by a member of the nuclear receptor superfamily (ER) can be induced by growth factors (EGF and IGF). This effect is mediated through the membrane-associated receptor tyrosine kinase–Ras-Raf-MAPK cascade, which enhances the activity of ER AF-1 by stimulating phosphorylation of the Ser^{118} residue located in the NH_2-terminal A/B region. Although only the Ras-mediated pathway of MAPK activation was examined here, other MAPK activation pathways (*13*) may also lead to enhanced activity of ER AF-1. Also, MAPK may phosphorylate and regulate other members of the nuclear receptor superfamily.

EGF, TGFα, and IGF-I, which promote the growth of several breast cancer–derived cell lines in culture, are produced by some breast tumors in vivo (*20*). The c-ErbB2 protein (also called HER2-Neu, a proto-oncogene product related to the EGF receptor) is overexpressed in ~20% of human breast cancers, which leads to amplification of the Ras signaling pathway and may cause an aggressive tumor phenotype (*21*). Overexpression of c-ErbB3, another member of the same family, has also been observed in 13 to 29% of breast cancers (*22*). Activating Ras mutations are found at a low frequency in primary breast cancers and metastatic effusions (*23*), and increased amounts of Ras protein have been found in malignant tissues (*24*). Our results suggest that the deregulation of phosphorylation of the Ser^{118} residue could be involved in the adverse effect of these growth factors and oncogenes in breast cancer.

Tamoxifen has estrogen-like agonistic activity on some ER-positive breast cancer cells in culture (*25*). Because our results show that OHT was almost as efficient as E_2 for the enhancement of the transcriptional activity of the ER in the presence of Ras, it is possible that MAPK—activated by growth factors, "activated" Ras, or both—may contribute to an enhanced agonistic activity of OHT, and therefore to the OHT resistance of some breast cancers. ER variants that bear deletions in the ligand-binding domain while maintaining the NH_2-terminal A/B region and the DNA-binding domain have been identified in some breast tumors (*26*). Our data suggest that such mutants would still be able to mediate the effect of growth factors, Ras, or both through Ser^{118} phosphorylation. Finally, our results may account for the estrogen-like effect of tamoxifen on bones, where it prevents osteoporosis (*27*). Enhancement of transcription of bone estrogen-responsive genes may depend mainly on the growth factor–activated AF-1 of the ER, and not on AF-2, which is induced by estrogens but is inhibited by tamoxifen.

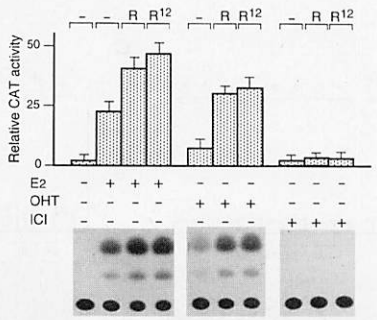

Fig. 5. Effect of k-Ras on hER transcriptional activity in the presence of E_2, OHT, and ICI 164,384. COS-1 cells were cotransfected with ERE-G-CAT, HEG0, and k-Ras (R) or $k\text{-}Ras^{Val12}$ (R^{12}), as indicated, and were grown in the presence or absence of 10 nM E_2, 100 nM OHT, or 100 nM ICI 164,384 (ICI). CAT activities were determined as in Fig. 3. Representative CAT assays and graphs corresponding to means and SEM for three independent experiments are shown.

REFERENCES AND NOTES

1. M. Beato, *Cell* **56**, 335 (1989); R. M. Evans, *Science* **240**, 889 (1988); S. Green and P. Chambon, *Trends Genet.* **4**, 309 (1988); H. Gronemeyer, *Annu. Rev. Genet.* **25**, 89 (1991); P. Kastner, M. Leid, P. Chambon, in *Vitamin A in Health and Disease*, R. Blomhoff, Ed. (Dekker, New York, 1994), pp. 189–238; D. J. Mangelsdorf, K. Umesono, R. M. Evans, in *The Retinoids*, M. B. Sporn, A. B. Roberts, D. S. Goodman, Eds. (Raven, New York, 1994), chap. 8.
2. V. Kumar *et al.*, *Cell* **51**, 941 (1987).
3. L. Tora *et al.*, *ibid.* **59**, 477 (1989).
4. M. Berry, D. Metzger, P. Chambon, *EMBO J.* **9**, 2811 (1990).
5. D. Metzger, S. Ali, J.-M. Bornert, P. Chambon, *J. Biol. Chem.* **270**, 9535 (1995).
6. P. S. Danielian, R. White, J. A. Lees, M. G. Parker, *EMBO J.* **11**, 1025 (1992); J. A. Lees, S. E. Fawell, M. G. Parker, *J. Steroid Biochem.* **34**, 33 (1989); N. J. G. Webster, S. Green, J. R. Jin, P. Chambon, *Cell* **54**, 199 (1988).
7. S. Ali, D. Metzger, J.-M. Bornert, P. Chambon, *EMBO J.* **12**, 1153 (1993).
8. P. B. Joel, A. M. Traish, D. A. Lannigan, *Mol. Endocrinol.* **9**, 1041 (1995).
9. S. F. Arnold, J. D. Obourn, M. R. Yudt, T. H. Carter, A. C. Notides, *J. Steroid. Biochem. Mol. Biol.* **52**, 159 (1995); R. R. Denton, N. J. Koszewski, A. C. Notides, *J. Biol. Chem.* **267**, 7263 (1992); P. Le Goff, M. M. Montano, D. J. Schodin, B. S. Katzenellenbogen, *ibid.* **269**, 4458 (1994); M.-T. Tsai and B. W. O'Malley, *Annu. Rev. Biochem.* **63**, 451 (1994); T. Wasburn, A. Hocutt, D. L. Brautigan, K. S. Korach, *Mol. Endocrinol.* **5**, 235 (1991).
10. Abbreviations for the amino acid residues are: A, Ala; E, Glu; F, Phe; H, His; L, Leu; M, Met; N, Asn; P, Pro; Q, Gln; S, Ser; T, Thr; and V, Val.
11. F. A. Gonzalez, D. L. Raden, R. J. Davis, *J. Biol. Chem.* **266**, 22159 (1991).
12. S. Aronica and B. S. Katzenellenbogen, *Mol. Endocrinol.* **7**, 743 (1993); D. M. Ignar-Trowbridge *et al.*, *ibid.*, p. 992.
13. C. S. Hill and R. Treisman, *Cell* **80**, 199 (1995); J. C. Marshall, *ibid.*, p. 179; S. L. Pelech and J. S. Sanghera, *Science* **257**, 1355 (1992).
14. Y. Gotoh *et al.*, *Nature* **349**, 251 (1991).
15. S. Kato *et al.*, unpublished data.
16. Y. Gotoh *et al.*, *Oncogene* **9**, 1891 (1994).
17. H. Fujioka *et al.*, *J. Biol. Chem.* **267**, 926 (1992).
18. Y. Gotoh, N. Masuyama, A. Suzuki, N. Ueno, E. Nishida, *EMBO J.* **14**, 2491 (1995).
19. D. Metzger, M. Berry, S. Ali, P. Chambon, *Mol. Endocrinol.* **9**, 579 (1995).
20. W. J. Gullick, *Prog. Growth Factor Res.* **2**, 1 (1990); A. Harris and S. Nicholson, in *Breast Cancer: Cellular and Molecular Biology*, M. E. Lippman and R. B. Dickson, Eds. (Kluwer Academic, Boston, 1988), pp. 93–118; L. C. Murphy *et al.*, *Semin. Cancer Biol.* **1**, 305 (1990).
21. P. W. Janes, R. J. Daly, A. deFazio, R. L. Sutherland, *Oncogene* **9**, 3601 (1994); D. J. Slamon *et al.*, *Science* **244**, 707 (1989).
22. S. Mason and W. J. Gullick, *Breast* **4**, 11 (1995).
23. C. F. Rochlitz *et al.*, *Cancer Res.* **49**, 357 (1989).
24. A. P. Efremidis, N. J. Agnantis, F. Patra, C. Papadopoulou, D. A. Spandidos, *Cancer Journal* **2**, 288 (1989).
25. N. Brünner *et al.*, *Cancer Res.* **53**, 3229 (1993); M. M. Gottardis and V. C. Jordan, *ibid.* **48**, 5183 (1988).
26. W. L. McGuire, G. C. Chamness, S. A. W. Fuqua, *Mol. Endocrinol.* **5**, 157 (1991).
27. V. C. Jordan, E. Phelps, J. U. Lindgren, *Breast Cancer Res. Treat.* **10**, 31 (1984); R. R. Love *et al.*, *ibid.* **12**, 297 (1988).
28. The bacterial expression vectors for GST fusion proteins (pGEX-HE15, pGEX-HE15/457, and pGEX-HE15/458) were constructed by cloning polymerase chain reaction (PCR)–amplified fragments derived from HE15, HE15/457, and HE15/458 (*7*), respectively, into the Bam HI–Eco RI sites of pGEX-2T (Pharmacia). The GST-HE15, GST-HE15/457, and GST-HE15/458 fusion proteins were purified from *E. coli* transfected with the corresponding expression vectors, with the use of glutathione Sepharose 4B (Pharmacia) according to the manufacturer's specifications. Each GST-fused protein (500 μg) was digested with thrombin (5 U) and then sequentially passed through the glutathione Sepharose column (to remove thrombin and GST) and through a Sephadex G200 column.
29. S. Kato *et al.*, *Cell* **68**, 731 (1992).
30. P. L. Mellon, C. H. Clegg, L. A. Correll, G. S. McKnight, *Proc. Natl. Acad. Sci. U.S.A.* **86**, 4887 (1989).

31. We thank Y. Matumura, K. Takeyama, Y. Handa, and K. Matsuda for technical assistance; M. Suzawa, C. Werlé, and J. M. Lafontaine for preparing the figures; K. Kaibuchi for the k-Ras expression vectors; S. Keyse for CL100 complementary DNA; G. S. McKnight for the PKA expression vector; S. Ali for hER mutants; A. Wakeling and Zeneca Pharmaceuticals for ICI 164,384; D. Salin-Drouin and the Laboratoires Besins Iscovesco for OHT; and J. Clifford and M. Tini for critical reading of the manuscript. Supported by a grant from Hayashida Foundation of Tokyo University of Agriculture, a grant-in-aid for priority areas from the Minister of Education, Science, and Culture of Japan (S.K.), and funds from CNRS/INSERM/Collège de France, Centre Hospitalier Universitaire Régional, Association pour la Recherche sur le Cancer, and Fondation pour la Recherche Médicale (FRM). D.M. was supported by a fellowship from the FRM.

20 July 1995; accepted 10 October 1995

Solution Structure of the Activator Contact Domain of the RNA Polymerase α Subunit

Young Ho Jeon, Tomofumi Negishi, Masahiro Shirakawa, Toshio Yamazaki, Nobuyuki Fujita, Akira Ishihama,* Yoshimasa Kyogoku*

The structure of the carboxyl-terminal domain of the *Escherichia coli* RNA polymerase α subunit (αCTD), which is regarded as the contact site for transcription activator proteins and for the promoter UP element, was determined by nuclear magnetic resonance spectroscopy. Its compact structure of four helices and two long arms enclosing its hydrophobic core shows a folding topology distinct from those of other DNA-binding proteins. The UP element binding site was found on the surface comprising helix 1, the amino-terminal end of helix 4, and the preceding loop. Mutation experiments indicated that the contact sites for transcription activator proteins are also on the same surface.

Activation of gene transcription in a prokaryote system is triggered by several kinds of transcription activators (*1*). In the *E. coli* RNA polymerase holoenzyme—composed of a core enzyme, $\alpha_2\beta\beta'$, and one of several σ subunit species (*2*)—one of the regions responsible for transcription activation has been localized to the COOH-terminal third of the α subunit. Deletion of this region does not interfere with the assembly of the core or the holoenzyme, but reconstituted RNA polymerase containing COOH-terminal truncated α subunits cannot be activated by a group of transcription activator proteins (*3*). This group of proteins contains the class I transcription factors, and their contact sites have been placed at various positions in the COOH-terminal domain (*4*). In contrast, the so-called UP element in the *rrnB* P1 promoter is required for the transcription activation of the target ribosomal RNA gene. The isolated α subunit and its COOH-terminal domain protect the UP element region from deoxyribonuclease I (DNase I) digestion (*5*), which indicates that the COOH-terminal portion of the α subunit is responsible for the contact with *cis*-acting UP elements as well as with *trans*-acting transcription factors (*6*). Proteolytic cleavage experiments indicated that the COOH-terminal portion that is essential for the activation of polymerase forms independent structural domains (*7*). We isolated αCTD, a 98–amino acid COOH-terminal fragment of the α subunit (residues 233 to 329 plus methionine at the NH_2-terminus), and we determined its solution structure by multidimensional heteronuclear magnetic resonance spectroscopy (*8*). The secondary structure elements and the calculated three-dimensional (3D) structures are shown in Fig. 1.

Y. H. Jeon, T. Yamazaki, Y. Kyogoku, Institute for Protein Research, Osaka University, Suita, Osaka 565, Japan.
T. Negishi, N. Fujita, A. Ishihama, Department of Molecular Genetics, National Institute of Genetics, Mishima, Shizuoka 411, Japan.
M. Shirakawa, Graduate School of Bioscience, Nara Institute of Science and Technology, Takayama, Ikoma, Nara 630-01, Japan.
*To whom correspondence should be addressed.

The structure of αCTD is compactly folded and comprises four helices and two long loops at the terminals of the domain (Fig. 1B). Helix 1 (residues 264 to 273), helix 2 (residues 278 to 283), and helix 4 (residues 297 to 309) are almost perpendicular to each other. Helix 2 is short but is essential for the formation of the hydrophobic core; the H-D exchange rates of amide protons in this helix were found to be very slow. Helix 3 (residues 286 to 292) is roughly antiparallel to helix 4. Helix 4 is the longest helix and shows the most typical amphipathic character. The two loops that extend from helices 1 and 4 like arms enclose the hydrophobic core and meet each other through contact between Phe^{249} in the NH_2-terminal arm and Trp^{321} and Ile^{326} in the COOH-terminal arm. The NH_2-terminal arm makes a turn at Pro^{256}, and the four residues before Arg^{255} and the four residues after Pro^{256} form α-helical turns. The COOH-terminal region from Trp^{321} to Ile^{326}, which contains two proline residues, also shows a sharp turn in which Pro^{322} takes on the *cis* configuration at the peptide bond. The root-mean-square deviation (RMSD) for the backbone heavy atoms of 50 structures from Phe^{249} to Ile^{326} (Fig. 1A) is 0.67 Å. Although this core region is rich in arms or loops, loop regions as well as helical regions are well determined (the RMSD for the region from Val^{264} to Ser^{309} is 0.57 Å). When the data were checked with Eisenberg's 3D profile analysis (*9*), this folding was found to be reasonable. Because the NH_2-terminal 16 residues preceding Phe^{249} and the COOH-terminal three residues did not show any long-range nuclear Overhauser effect (NOE), this region apparently does not form a single definite structure.

αCTD is known to interact with the *rrnB* P1 promoter UP element in DNase I

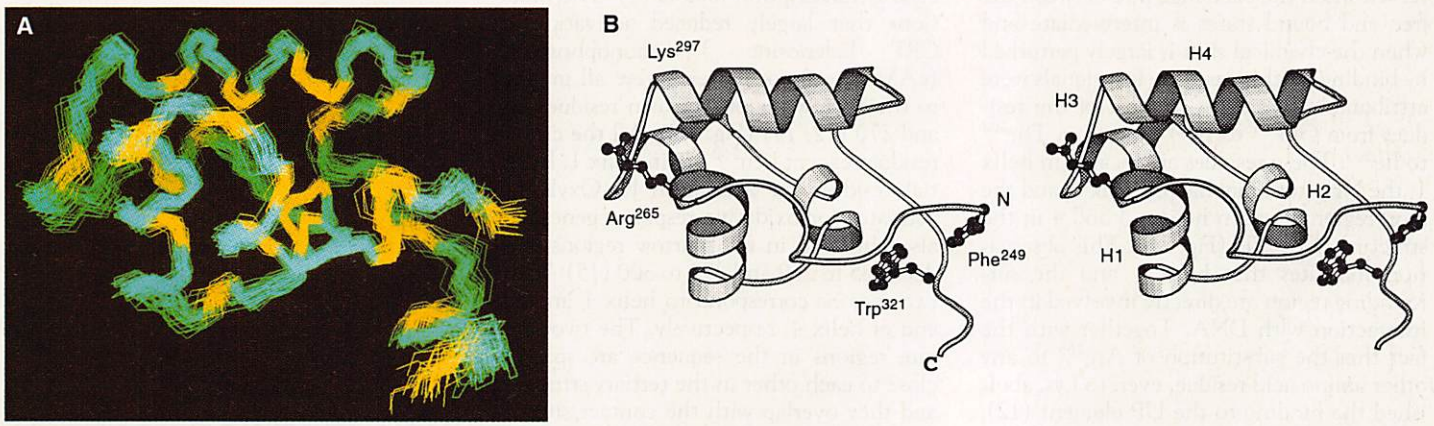

Fig. 1. (**A**) Peptide backbone traces (N, Cα, C′) of 50 simulated annealing structures of αCTD superimposed for residues Phe^{249} to Ile^{326}. Hydrophobic residues (Phe, Trp, Val, Ile, and Leu) are shown in yellow. (**B**) Stereo view of a ribbon diagram representing the calculated mean structure folding of αCTD, produced with the program Molscript (*16*). The side chains of Phe^{249}, Arg^{265}, and Trp^{321} are shown; H, helix. The atomic coordinates of the mean structure were deposited at the Brookhaven Protein Data Bank (accession number 1COO).

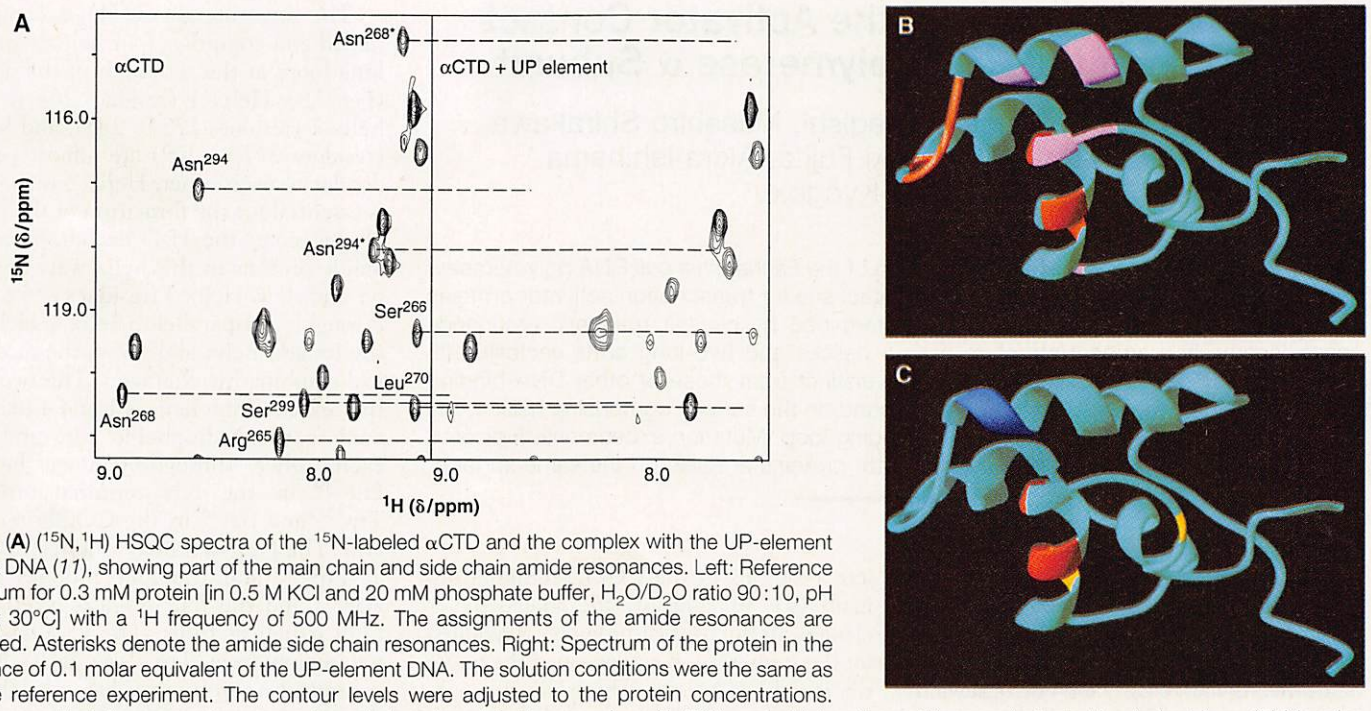

Fig. 2. (**A**) (^{15}N,^{1}H) HSQC spectra of the ^{15}N-labeled αCTD and the complex with the UP-element duplex DNA (*11*), showing part of the main chain and side chain amide resonances. Left: Reference spectrum for 0.3 mM protein [in 0.5 M KCl and 20 mM phosphate buffer, H_2O/D_2O ratio 90:10, pH 6.0, at 30°C] with a ^{1}H frequency of 500 MHz. The assignments of the amide resonances are indicated. Asterisks denote the amide side chain resonances. Right: Spectrum of the protein in the presence of 0.1 molar equivalent of the UP-element DNA. The solution conditions were the same as for the reference experiment. The contour levels were adjusted to the protein concentrations. Resonances that disappeared or were extremely broadened for the complex with DNA under high-salt conditions are indicated by dashed lines. (**B**) Mapping of the residues with a broadening effect in (^{15}N,^{1}H) HSQC spectra. The residues whose resonances completely disappeared under high salt conditions are indicated in red (Arg^{265}, Asn^{268}, Leu^{270}, Thr^{292}, Asn^{294}, Leu^{295}, and Gly^{296}), and those with an intermediate broadening effect are colored magenta (Thr^{263}, Val^{264}, Ala^{274}, Ser^{299}, and Glu^{302}). (**C**) Mapping of the proposed contact sites for CRP and OxyR in the structure of αCTD, produced with the program Ribbons (*17*). The residues whose replacement renders RNA polymerase insensitive to activation by CRP are colored yellow and red (Leu^{260}, Arg^{265}, Asn^{268}, Cys^{269}, and Leu^{270}), and those in the case of OxyR are colored dark blue and red (Arg^{265}, Asn^{268}, Cys^{269}, Lys^{298}, and Ser^{299}); the residues in red are common to both factors. Mutations in the region from Pro^{293} to Leu^{300} also give weak reduction for CRP activation (*15*).

footprinting experiments. However, it is not known which residues of αCTD are involved in the interaction. To probe the binding site, we performed chemical shift perturbation experiments (*10*). Selective signal losses were observed in the (^{15}N, ^{1}H) heteronuclear single quantum correlation (HSQC) spectrum on mixing with a small amount of a 25–base pair (bp) DNA duplex with a sequence [d(TCAGAAAATTAT-TTTAAATTTCCTC)] that corresponded to the *rrnB* P1 UP element (from −61 to −37) (*11*) (Fig. 2A). Signal losses are observed when the exchange rate between the free and bound states is intermediate and when the chemical shift is largely perturbed by binding; in this case, the lost signals were attributable to amides of most of the residues from Glu^{261} to Ile^{275} and from Thr^{292} to Ile^{303}. These residues are located in helix 1, the NH_2-terminal half of helix 4, and the loop region between helices 3 and 4 in the structure of αCTD (Fig. 2B). This observation indicates that helix 1 and the surrounding region are directly involved in the interaction with DNA. Together with the fact that the substitution of Arg^{265} to any other amino acid residue, even to Lys, abolished the binding to the UP element (*12*), our results strongly support the idea that helix 1 recognizes the base sequence of the UP element. Asn^{268} on the same side of helix 1 should also be involved in the recognition. Because one helix and the NH_2-terminal of another perpendicular helix make a binding surface to DNA, this feature may seem reminiscent of the helix-turn-helix (HTH) motif found in DNA-binding proteins. However, helices 1 and 4 of αCTD are distinct from the canonical or extended HTH (*13*); not only is there no direct connection between the two helices, but also the direction of one of the helices is opposite to that of HTH.

The COOH-terminal region of the α subunit is claimed to be the contact site for class I transcription factors (*4*). The mutations that largely reduced activation by CRP [adenosine 3′,5′-monophosphate (cAMP) receptor protein] were all mapped to the narrow region between residues 260 and 270 (*12*, *14*) (Fig. 2C). All the critical residues except Leu^{260} are in helix 1. Essential residues for activation by OxyR (an activator for oxidative response genes) are also clustered in two narrow regions, residues 265 to 269 and 293 to 300 (*15*). These two regions correspond to helix 1 and the end of helix 4, respectively. The two separate regions in the sequence are spatially close to each other in the tertiary structure, and they overlap with the contact sites for the UP element of the *rrnB* P1 promoter.

αCTD is one of the focal points in the control of transcription. Mutations in αCTD that affect the activation of many transcription activator proteins have been reported, and these mutations have been mapped at various positions of the domain. Our results may lead to the determination of interaction surfaces for activator proteins through a better understanding of whether such mutations affect the structure or interaction of the domain.

REFERENCES AND NOTES

1. A. Ishihama, *Trends Genet.* **4**, 282 (1988).
2. R. R. Burgess, in *RNA Polymerase*, R. Losick and M. Chamberlin, Eds. (Cold Spring Harbor Laboratory, Cold Spring Harbor, NY, 1976), pp. 69–100; J. D. Hellman and M. J. Chamberlin, *Annu. Rev. Biochem.* **57**, 839 (1988).
3. K. Igarashi and A. Ishihama, *Cell* **65**, 1015 (1991); K. Igarashi *et al.*, *Proc. Natl. Acad. Sci. U.S.A.* **88**, 8958 (1991); A. Ishihama, *Mol. Microbiol.* **6**, 3283 (1992).
4. A. Ishihama, *J. Bacteriol.* **175**, 2483 (1993).
5. W. Ross *et al.*, *Science* **262**, 1407 (1993); E. E. Blatter *et al.*, *Cell* **78**, 889 (1994).
6. S. Busby and R. H. Ebright, *Cell* **79**, 743 (1994); R. H. Ebright and S. Busby, *Curr. Opin. Genet. Dev.* **5**, 197 (1995).
7. T. Negishi, N. Fujita, A. Ishihama, *J. Mol. Biol.* **248**, 723 (1995).
8. αCTD was overexpressed under the control of the T7 promoter. Uniformly ^{15}N,^{13}C-doubly labeled αCTD was produced in M9 medium with [^{15}N]NH_4Cl (0.5 g/liter) and [$^{13}C_6$]D-glucose (1 g/liter) as the nitrogen and carbon sources. αCTD was collected from the supernatant fraction of the sonicated cell suspension. After salting out and dialysis, the supernatant was applied to a DEAE-Sepharose column (Pharmacia). The peak fractions of αCTD were applied to a gel-filtration column and then to a Protein-pak G-DEAE column (Waters); purity was >99%. Sequence analysis of the NH_2-terminal end showed

that methionine was retained. A sedimentation equilibrium experiment on a 0.1 mM protein solution revealed a molecular weight of 11,800, which indicates that most of the protein molecules exist as monomers. Size exclusion chromatography also showed a monomeric molecular size. Nuclear magnetic resonance measurements of 2 mM solutions of the protein [in 30 mM KCl, 20 mM phosphate buffer, and 1 mM dithiothreitol (pH 6.0) at 30°C] were performed with Bruker AMX500 and DMX500 spectrometers. Most of the observable ^{1}H, ^{15}N, and ^{13}C nuclei were given resonance assignments by means of the following 3D experiments: ^{15}N-edited total correlation spectroscopy (TOCSY)–HSQC, CBCA(CO)NH, CBCANH, HBHA(CBCACO)NH, HBHA(CBCA)NH, HNCO, and HN(CA)CO for the backbone nuclei [A. Bax and S. Grzesiek, in *NMR of Proteins*, G. M. Clore and A. M. Gronenborn, Eds. (Macmillan, London, 1993), pp. 33–52], and HEHOHEHAHA [A. Majumdar, H. Wang, R. C. Morshauser, E. R. P. Zuiderweg, *J. Biomol. NMR* **3**, 387 (1993)] for the side chain nuclei. Distance information was collected using two-dimensional homonuclear nuclear Overhauser effect spectroscopy (NOESY) with a 100-ms mixing time, and 3D (^{1}H,^{13}C) and (^{1}H,^{15}N) NOESY-HSQC spectra with a 100-ms mixing time. For torsion angle constraints, the backbone vicinal coupling constants ($^{3}J_{HN,H\alpha}$) were estimated from a two-dimensional heteronuclear multiple quantum coherence J (HMQC-J) spectrum [L. E. Kay and A. Bax, *J. Magn. Reson.* **86**, 110 (1990)] of uniformly ^{15}N-labeled αCTD. The NOE connectivities from strong, medium, and weak cross-peaks were assumed to correspond to the upper limits for proton-proton distances of 3.0, 4.0, and 5.0 Å, respectively. Because stereospecific assignments for the methyl and methylene protons have not yet been performed, appropriate corrections were added for constraints including the pseudoatoms. The hydrogen bond constraints were added for slowly exchanging amides as upper and lower limits of 3.0 and 2.7 Å for N–O, respectively, and 2.0 and 1.8 Å for H–O, respectively. For torsion angle constraints, residues that gave $^{3}J_{HN,H\alpha}$ values of <5.5 Hz, 8.0 to 10 Hz, and >10 Hz were estimated to have torsion angles φ of −90° to −40°, −160° to −80°, and −140° to −100°, respectively, except for the cases of very strong intraresidue HN-Hα NOEs. In total, 822 NOE constraints, 52 dihedral angle constraints, and 19 sets of hydrogen bond constraints were used. Simulated annealing calculations [M. Nilges, G. M. Clore, A. M. Gronenborn, *FEBS Lett.* **229**, 317 (1988)] were performed on Silicon Graphics workstations with X-PLOR [A. T. Brünger, version 3.1 (Yale Univ. Press, New Haven, CT, 1992)]. Three hundred structures were calculated, and 50 structures with distance violations of <0.3 Å and angle violations of <5° were obtained.

9. J. U. Bowie, R. Lüthy, D. Eisenberg, *Science* **253**, 164 (1991); Y. Matsuo and K. Nishikawa, *Protein Sci.* **3**, 2055 (1994).
10. N. Dekker *et al.*, *Nature* **362**, 852 (1993); Y. Kyogoku *et al.*, *Methods Enzymol.* **261**, 524 (1995).
11. A DNA titration experiment was done by adding 0.05, 0.1, 1.0, and 1.2 molar equivalents of DNA to the protein at 30 mM KCl. However, signal broadening was so severe that most peaks were barely observed. We extended the experiment by increasing the KCl concentration to 800 mM in the presence of 0.1 molar equivalent of DNA. Almost every peak reappeared at the 800 mM salt condition. No precipitation occurred throughout these experiments. The solution condition of 500 mM KCl for Fig. 2A was chosen as the best for observation of strongly perturbed peaks separately from others. To determine whether the signal losses were specifically caused by the UP-element DNA, we performed a similar experiment in the presence of a 22-bp DNA duplex [d(TAATGTGAGTTAACTCACATTA)] that corresponded to the consensus binding sequence of CRP. We observed only slight shifts of peak positions for two or three residues, but we could not see any disappearance of peaks because of broadening. Thus, the drastic change in the spectrum in the presence of the UP element was clearly distinguished from the control experiment.
12. K. Murakami, N. Fujita, A. Ishihama, unpublished data.
13. S. C. Harrison and A. K. Aggarwal, *Annu. Rev. Biochem.* **59**, 933 (1990); N. Assa-Munt, R. J. Mortishire-Smith, R. Aurora, W. Herr, P. E. Wright, *Cell* **73**, 193 (1993).
14. C. Zou, N. Fujita, K. Igarashi, A. Ishihama, *Mol. Microbiol.* **6**, 2599 (1992); M. Tang *et al.*, *Genes Dev.* **8**, 3058 (1994).
15. K. Tao, C. Zou, N. Fujita, A. Ishihama, *J. Bacteriol.*, in press.
16. P. Kraulis, *J. Appl. Crystallogr.* **24**, 946 (1991).
17. M. Carson, *ibid.*, p. 958.

18. We thank B. J. Lee of Seoul National University for CRP binding site DNA, and K. Nishikawa of the Protein Engineering Research Institute and K. Shimizu of the Nara Institute of Science and Technology for the use of the 3D-1D profile program COMPASS. Supported by a Grant-in-Aid for Scientific Research on Priority Areas from the Ministry of Education, Science and Culture of Japan, and by Human Frontier Science Program grant RG-401/95M.

4 August 1995; accepted 19 October 1995

A Population Genetic Test of Selection at the Molecular Level

M. F. J. Taylor,* Y. Shen, M. E. Kreitman

The role of natural selection in molecular evolution has been inferred primarily by rejection of null hypotheses based on neutral theory, rather than by acceptance of specific predictions based on selection. In this report, a population genetic test of a specific prediction for selection on DNA polymorphism is presented. Pyrethroid insecticide use constitutes an experiment for which form of selection and molecular target (voltage-gated sodium channels) are both known. As predicted, differential pyrethroid selection on tobacco budworm populations generated significant geographic heterogeneity in sodium channel marker allele frequencies, compared with arbitrary loci.

Many studies have sought to test the null hypothesis of neutral evolution of DNA sequence variation in populations. However, the lack of specific prior predictions based on selection has weakened such tests. Even for the most well-studied case of the high-to-low latitudinal clines in the *Adh* fast-slow polymorphism in *Drosophila melanogaster*, the form of selection presumed to maintain this polymorphism remains elusive, although patterns of polymorphism are consistent with a model of balancing selection (*1*).

If a specific form of selection is expected at a particular locus, then a prediction may be developed on the basis of selection rather than neutrality, which may be tested with the use of appropriate statistics. Differentiation in allele frequencies among populations can be estimated by F_{st}, the between population component of standardized genetic variance. Population structure and historical contingencies (range expansions or contractions) have genome-wide effects on gene frequency variation between populations, whereas selection affects variation only at target loci. Differentiation in the form of clines of allele frequency for some allozyme loci, and not for others, has been taken as evidence that spatially variable selection has been acting at such loci, whereas gene flow has homogenized frequencies at other unselected loci (*2*). However, clinal patterns for some loci may result from historical patterns of colonization and subsequent admixture, whereas nonclinal loci are homogenized by selection, acting uniformly in space and causing convergence of frequencies over a wide area (*3*). The study of nucleotide variation has permitted some resolution of this dilemma for the *Adh* cline in *D. melanogaster* (*4*). Such studies highlight the difficulties of testing for selection at the molecular level in natural populations, in the absence of prior expectations about the strength, duration, or loci of action of selection.

The widespread use of insecticides in agriculture has resulted in the rapid evolution of resistance for many pest species. Such natural "experiments" can enable explicit prediction of the outcome of selection at the molecular level. Pyrethroid insecticides act on voltage-gated sodium channels in nerve membranes (*5*). Resistance to the pyrethroid permethrin in a field-derived strain of the tobacco budworm (*Heliothis virescens*), a major cotton pest, is linked to a DNA marker for a sodium channel locus *hscp*, homologous to the *para* locus of *D. melanogaster* (*6*). Levels of resistance are known to vary considerably among populations, and resistance has arisen in response to selection in just the last 10 years (*7*). Population genetic surveys in North America, ranging from Texas to Georgia for 13 allozyme loci (*8*), and from Sonora, Mexico, to Georgia for mitochondrial DNA markers (*9*), have shown that tobacco budworm populations are little differentiated, which

M. F. J. Taylor and Y. Shen, Department of Entomology, Center for Insect Science, University of Arizona, Tucson, AZ 85721, USA.
M. E. Kreitman, Department of Ecology and Evolution, University of Chicago, 1103 East 57th Street, Chicago, IL 60637, USA.

*To whom correspondence should be addressed. E-mail: Taylor@biosci.arizona.edu

is consistent with high rates of gene flow across large distances.

We predicted that tobacco budworm populations would be highly differentiated at the target sodium channel locus as a result of geographically varying levels of selection by pyrethroids, while remaining essentially undifferentiated at other arbitrarily chosen loci as a result of gene flow. To test this hypothesis, we collected 660 adult male tobacco budworms in five samples from four widely separated U.S. locations [Georgia, Texas, Arizona, and Louisiana (two different times)]. Individuals were tested for a phenotype of "knockdown" at one of two doses of the pyrethroid cypermethrin (*10*). Resistance to the paralytic knockdown effect of these insecticides, rather than survival, was the phenotype definition chosen for comparison to other field studies (*7*).

We then examined variation in a small DNA marker *Hpy* for the sodium channel locus *hscp* (*11*) and another similar sized marker *Hejs* in the juvenile hormone (JH) esterase locus, which is unlinked to *hscp* and has no known role in pyrethroid resistance (*12*). Variation was scored by denaturing gradient gel electrophoresis that, under suitable conditions, can detect nearly all nucleotide polymorphisms in a region of interest (*13*). We assumed that the uniformly low F_{st} estimates observed for allozyme loci (ranging from near zero to 0.005) at all scales of spatial sampling reliably reflect high gene flow between tobacco budworm populations (*8*). There is no evidence that any of these allozyme loci are involved in insecticide resistance in insect species. Thus, we could make a specific prediction for the relative magnitudes of the F_{st} estimates for the marker loci in this study.

The value of F_{st} for the arbitrary *Hejs* marker was predicted to be small and not significantly different from the allozyme F_{st} estimates. The F_{st} for the sodium channel *Hpy* marker was predicted to be significantly greater than either allozyme or *Hejs* F_{st} estimates as a result of close genetic linkage to one or more unknown mutations in the sodium channel that had been favored by recent, intense pyrethroid selection in some populations. We decided, in advance, to accept the hypothesis that selection had been acting at the sodium channel locus only for this outcome of the study. Outcomes in which F_{st} for *Hpy* was indistinguishable from that for *Hejs*, or in which F_{st} for *Hejs* was significantly greater than allozyme F_{st} estimates, both entailed rejection of this hypothesis.

The five samples varied significantly in cypermethrin knockdown, showing that pyrethroid selection had been geographically variable, resulting in heterogeneous levels of resistance (Fig. 1A). It would be desirable to be able to reconstruct treatment histories to give some estimate of selection intensity in each of the regions sampled, as has been done for more restricted populations (*14*). Although the local abundance and rate of insecticide treatment for both bollworms and budworms on cotton had been similar in Georgia and Louisiana before this collection, the incidence of pyrethroid resistance was consistently much lower in Georgia (*15*). This may be attributed to a much larger untreated reservoir population on alternative wild host plants in the southeastern United States, and thus a much lower net selection intensity averaged over the local population (*16*).

A total of 50 alleles for *Hpy* and 41 alleles for *Hejs* were distinguishable on the basis of gel-mobility differences. The *Hpy* allelic diversities of samples were significantly correlated with knockdown at pesticide concentrations of 5 μg (Fig. 1B). However, no such correlation was observed for *Hejs* allelic diversities (Fig. 1B). This pattern is consistent with a process of selective removal of uncommon *Hpy* alleles in the more heavily selected populations, especially in Louisiana.

Analysis of the F_{st} statistics for the two marker loci confirmed our prediction exact-

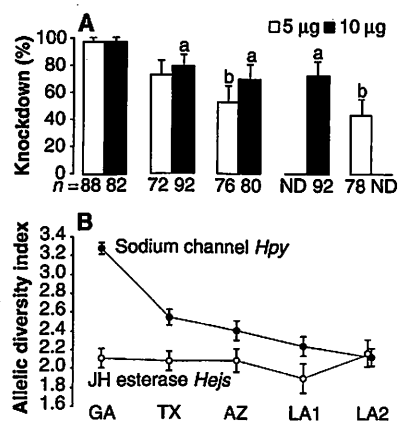

Fig. 1. (**A**) Proportion of adult male tobacco budworms dead or knocked-down ("knockdown"), with 95% confidence intervals, in bioassays with 5 or 10 μg of cypermethrin per vial for each sample (*10*). The samples, ordered by *Hpy* allelic diversities, were as follows: GA, Sparks, Georgia, August 1990; LA1, Winnsboro, Louisiana, August 1990, and LA2, same location, October 1990; TX, College Station, Texas, September 1990; AZ, Yuma, Arizona, October 1990. The numbers below the bars are sample sizes; ND, no data. Within each dose, knockdown proportions for samples with the same letters were not significantly different at the 5% level in χ^2 tests. (**B**) Means and standard errors of *H*, allelic diversity indices, for sodium channel *Hpy* and JH esterase *Hejs* markers, for each sample (*20*). Means and standard errors were estimated by the jackknife over individuals (*21*). Kendall's rank correlation coefficient between *Hpy* diversity and knockdown with 5 μg of pesticide was significant at the 5% level. Correlations between *Hpy* diversity and knockdown with 10 μg of pesticide, and between *Hejs* diversity and knockdown in either bioassay, were not significant at the 5% level.

Table 1. Differentiation among samples as measured by F_{st} and allelic diversities *H* for sodium channel *Hpy* and JH esterase *Hejs* marker loci and for allozyme loci. Values for F_{st} were calculated with the sample size correction of Nei and Chesser (*19*). Mean and standard errors were estimated by the jackknife over individuals (*21*). Hypothesis tests were performed by deriving a null sampling distribution for F_{st} by repeatedly (1000 times) reallocating genes randomly among all individuals and recalculating F_{st}. The "tail" proportion of such resampled null F_{st} estimates that equaled or exceeded the observed value of F_{st} is an estimate of the probability (Pr.) of obtaining the observed value of F_{st} under the null hypothesis ($F_{st} = 0$). For values of *H*, see Fig. 1B.

Locus	$F_{st} \pm$ SE	Pr. ($F_{st} = 0$)	$H \pm$ SE
Sodium channel *Hpy* marker, 50 alleles	0.041 ± 0.005	<0.001	2.86 ± 0.04
Hpy, pooling alleles 1 to 4	0.031 ± 0.006	<0.001	2.07 ± 0.06
JH esterase *Hejs* marker, 41 alleles	0.001 ± 0.003	0.16	2.09 ± 0.06
Thirteen allozyme loci*	0.002 ± 0.001	<0.0001	

*Date are from a larger collection at 60 pheromone trap locations between Georgia and east Texas in 1989 (*8*). Only total F_{st} is shown. The F_{st} for between traps, within sites, and within regions had the largest contribution to total F_{st}. Between regions F_{st} was very low. Mean and standard errors were estimated by the jackknife over loci. Allelic diversity is not shown, as no comparison was needed.

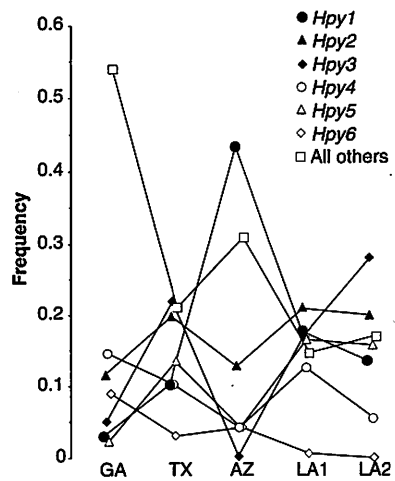

Fig. 2. Frequencies of sodium channel *Hpy* marker alleles 1 through 6, and all other alleles pooled, in each sample (each of the alleles that went into the pool was less than 5% of the total sample: 43 for GA, 33 for TX, 34 for AZ, 19 for LA1, and 15 for LA2).

ly. The value of F_{st} estimated for the sodium channel *Hpy* marker was an order of magnitude greater than for that of *Hejs* or the allozyme loci (Table 1). This was evident in the heterogeneity among samples in *Hpy* allele frequencies (Fig. 2). The *Hpy1* allele, which previously had been linked to permethrin resistance in a field-derived strain (*6*), was the most common in the entire collection and was generally more frequent in the more resistant samples (Fig. 2). Some *Hpy* marker alleles are expected to "hitchhike" along with linked resistance-conferring mutations in or near the sodium channel locus. However, this linkage disequilibrium is continually broken down by recombination, and no single *Hpy* allele is necessarily expected to be uniquely associated with resistant phenotypes.

Also as predicted, the estimated value of F_{st} for the arbitrary marker *Hejs* was low and not significantly different from zero or from the low F_{st} estimates for the allozyme loci (Table 1). *Hejs* allele frequencies were markedly homogeneous across samples, which is consistent with the low value of F_{st} (Fig. 3). It is possible that *Hejs* was in fact as heterogeneous among samples as was *Hpy* but that this was undetectable because of the skewed allelic distribution of *Hejs*, with one very common allele (Fig. 3). To test this possibility, we pooled the four most common *Hpy* alleles to construct an allelic distribution for *Hpy* with an allelic diversity index similar to that of *Hejs* for the entire collection (Table 1). The pooled F_{st} estimate for *Hpy* was only slightly different, which indicates that the difference in F_{st} estimates was not an artifact of different allelic distributions nor attributable to a single allele (Table 1). The F_{st} estimate for the *Hpy* marker was therefore quite robust.

Any contrast among loci in estimates of F_{st}, as a test of the null hypothesis of neutral molecular evolution, is weak because many outcomes are as consistent with neutral theory as with any number of unspecified models of selection (*17*). In this case, however, only one outcome was predicted for pyrethroid selection, and this therefore formed a null hypothesis of selection. The expectation from neutral theory, in the absence of evident population subdivision, was that F_{st} estimates for any allozyme and DNA markers should all be small and statistically indistinguishable. Outcomes in which one or more loci have unusually large values of F_{st} could arise from stochastic neutral processes, but should be uncommon (*17*). A neutral outcome in which precisely the locus of interest, and no other locus, has a large value of F_{st} must, correspondingly, be rare.

Here, we have attempted to bring together two scientific programs that historically have been isolated: the study of molecular evolution and the study of insecticide resistance in pest populations. In our test for selection at the molecular level, the specific outcome of selection could be predicted for a particular locus and then tested. Despite much evidence for the involvement of particular mutations in insecticide resistance and for persistence or spread of these mutations in populations (*18*), we have shown that molecular mutations at the known target locus are under strong, recent selection in field populations.

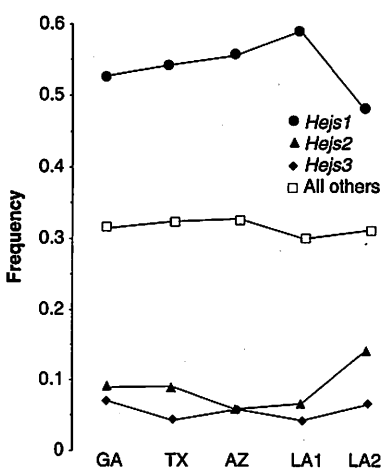

Fig. 3. Frequencies of JH esterase *Hejs* marker alleles 1 to 3, and all other alleles pooled, in each sample (each of the alleles that went into the pool was less than 5% of the total sample: 30 for GA, 31 for TX, 32 for AZ, 23 for LA1, and 24 for LA2).

REFERENCES AND NOTES

1. M. Kreitman and R. R. Hudson, *Genetics* **127**, 565 (1991).
2. F. B. Christiansen and O. Frydenberg, *ibid.* **77**, 765 (1974).
3. S. A. Karl and J. C. Avise, *Science* **256**, 100 (1992).
4. A. Berry and M. Kreitman, *Genetics* **134**, 869 (1993).
5. T. Narahashi, in *Neuropharmacology and Pesticide Action*, M. G. Ford, G. G. Lunt, R. C. Reay, P. N. R. Usherwood, Eds. (Horwood, Weinheim, Germany, 1986), pp. 37–60; D. B. Sattelle and D. Yamamoto, *Adv. Insect Physiol.* **20**, 145 (1988).
6. M. F. J. Taylor, D. G. Heckel, T. M. Brown, M. E. Kreitman, B. Black, *Insect Biochem. Mol. Biol.* **23**, 763 (1993).
7. C. A. Staetz, *J. Econ. Entomol.* **78**, 505 (1985); F. W. J. Plapp *et al.*, *ibid.* **83**, 335 (1990); A. R. McCaffery *et al.*, *Southwest. Entomol. Suppl.* **15**, 143 (1991).
8. A. Korman *et al.*, *Ann. Entomol. Soc. Am.* **86**, 182 (1993).
9. R. L. Roehrdanz, J. D. Lopez, J. Loera, D. E. Hendricks, *ibid.* **87**, 856 (1994).
10. Inner surfaces of 20-ml glass scintillation vials were coated with either 5 μg or 10 μg of cypermethrin in acetone and allowed to dry by rolling. Adult male tobacco budworms were captured in pheromone bait traps and placed individually in vials and held at ~25°C. After 24 hours, they were scored as dead or knocked down, or alive and active, and all were frozen at −80°C for genotype analysis. Knockdown was defined as the inability to turn upright after being turned upside-down.
11. Genomic DNA was prepared by homogenizing moths in 750 μl of grinding buffer [0.1 M tris-HCl (pH 8.0), 0.1 M NaCl, 50 mM EDTA, 6.8% w/v sucrose, and 0.5% w/v SDS]. The aqueous phase was extracted three times with 750 μl of phenol (pH 8) and once with 750 μl of chloroform. Nucleic acids were recovered after a 30-min incubation with 1 M potassium acetate and 50% isopropanol by centrifugation at 12,000*g* for 15 min. Pellets were washed with 70% ethanol, dried, and resuspended in 20 μl of TE [10 mM tris-HCl (pH 8) and 100 μM EDTA]. Polymerase chain reactions consisted of 0.1 to 0.5 μg of genomic DNA, 30 mM tricine-HCl (pH 8.4), 5 mM β-mercaptoethanol, 0.01% gelatin, 0.2 mM for each of the four deoxynucleotide triphosphates, 4.5 mM $MgCl_2$, 0.4 U of Taq DNA polymerase, 0.2 μM primer *CL/Hp4399-* (5′-GCCCGCCGCCGCGCCCCGCCGCCACCGCGCCGCCCGCCCCCGCGTCGTTCATGATCTGTATCCA), and 0.2 μM primer *Hp4211+* (5′-CTGATCTTCGCCATCATGGG), with a final volume of 20 μl. Reactions were incubated for 20 cycles of 94°C for 35 s, 56°C for 1 min 30 s, and 72°C for 30 s; then for 14 cycles of 94°C for 35 s, 56°C for 1 min 30 s, and 72°C for 1 min; and finally for one cycle of 94°C for 35 s, 56°C for 15 min, and 72°C for 1 min. Reactions were precipitated, resuspended in 5 μl of dye-loading buffer, and separated on a vertical polyacrylamide gel (25 cm by 15 cm by 0.5 mm) ranging from 35 to 45% denaturant concentration, at 73 V for 14 hours at 60°C. DNA was detected by ultraviolet fluorescence after a 15-min staining in ethidium bromide (0.5 μg/ml). Gel, buffer, and denaturant solutions were as described [R. M. Myers, T. Maniatis, L. S. Lerman, *Methods Enzymol.* **155**, 501 (1987)]. Primers were based on the published sequence (*6*).
12. T. N. Hanzlik, A. I. Yehia, L. G. Harshman, B. D. Hammock, *J. Biol. Chem.* **264**, 12419 (1989); L. G. Harshman *et al.*, *Insect Biochem. Mol. Biol.* **24**, 671 (1994). *Hejs* matches the published sequence between bases 487 and 553 exclusive of primers and includes a ~225-bp intron previously unreported. Primers were as follows: *CL/Hej486+* (5′-GCCCGCCGCCCCCGCCGCCTCCGCGCCGCCCGCCCCGGACCTACACGGACCAGAATA-3′) and *Hej554-* (5′-GGGATTTTTGTTGTGTTCAT-3′). Reaction conditions were the same as those for *Hpy* except that gels had 20 to 50% denaturant.
13. E. P. Lessa and G. Applebaum, *Mol. Ecol.* **2**, 119 (1993).
14. J. A. Rosenheim and M. A. Hoy, *J. Econ. Entomol.* **79**,1161 (1986); B. E. Tabashnik, N. L. Cushing, M. W. Johnson, *ibid.* **80**, 1091 (1987).
15. E. G. King and G. A. Herzog, *Proc. Beltwide Cotton Prod. Res. Conf.* (1990), p. 140; R. B. Head, *ibid.*, p.157.
16. H. H. Neunzig, *J. Econ. Entomol.* **56**, 135 (1963); E. A. Stadelbacher, M. L. Laster, T. R. Pfrimmer, *Environ. Entomol.* **1**, 318 (1972).
17. R. C. Lewontin and J. Krakauer, *Genetics* **74**, 175 (1973); M. Nei and T. Maruyama, *ibid.* **80**, 395 (1975); A. Robertson, *ibid.*, p. 396.
18. R. H. ffrench-Constant, J. C. Steichen, T. A. Rocheleau, K. Aronstein, R. T. Roush, *Proc. Natl. Acad. Sci. U.S.A.* **90**, 1957 (1993); M. Raymond, A. Callaghan, P. Fort, N. Pasteur, *Nature* **350**, 151 (1991).
19. M. Nei and R. K. Chesser, *Ann. Hum. Genet.* **47**, 253 (1983).
20. The allelic diversity index, *H*, is represented by

$$H = -\sum_{i=1}^{k} p_i \log(p_i)$$

where p_i is the frequency of allele $i = 1$ to k.
21. R. R. Sokal and F. J. Rohlf, *Biometry* (Freeman, New York, ed. 2, 1981), chap. 18.

22. This study would not have been possible without the generosity of those who made the collections and tested knockdown: C. Staetz and D. Pitts, FMC Corporation; J. Graves, Louisiana State University; B. Plapp, Texas A&M University; and T. Watson and T. Tellez, University of Arizona. The advice of B. Ballard, A. Berry, R. Feyereisen, R. C. Lewontin, B. Tabashnik, and anonymous reviewers and the assistance of K. Vick, S. Messmer, J. Tison, and G. Sword are gratefully acknowledged. This work was funded by competitive grant 9301875 from the U.S. Department of Agriculture Cooperative State Research Service.

13 July 1995; accepted 5 October 1995

Definition of Two Angiogenic Pathways by Distinct α_v Integrins

Martin Friedlander, Peter C. Brooks, Robert W. Shaffer, Christine M. Kincaid, Judith A. Varner, David A. Cheresh

Angiogenesis depends on cytokines and vascular cell adhesion events. Two cytokine-dependent pathways of angiogenesis were shown to exist and were defined by their dependency on distinct vascular cell integrins. In vivo angiogenesis in corneal or chorioallantoic membrane models induced by basic fibroblast growth factor or by tumor necrosis factor–α depended on $\alpha_v\beta_3$, whereas angiogenesis initiated by vascular endothelial growth factor, transforming growth factor–α, or phorbol ester depended on $\alpha_v\beta_5$. Antibody to each integrin selectively blocked one of these pathways, and a cyclic peptide antagonist of both integrins blocked angiogenesis stimulated by each cytokine tested. These pathways are further distinguished by their sensitivity to calphostin C, an inhibitor of protein kinase C that blocked angiogenesis potentiated by $\alpha_v\beta_5$ but not by $\alpha_v\beta_3$.

Angiogenesis, the growth of new blood vessels, occurs in most tissues and can be induced by a variety of cytokines (*1*). However, vascular cells proliferate in an anchorage-dependent manner, which suggests that adhesion-mediated signals may be important in the growth of new blood vessels (*2*). The dependence of angiogenesis on vascular cell adhesive events in vivo (*3*, *4*) is evidenced by the fact that antagonists of $\alpha_v\beta_3$ integrin block angiogenesis on chick chorioallantoic membrane (CAM) induced by basic fibroblast growth factor (bFGF) and fragments of human tumors. In this model, $\alpha_v\beta_3$ promoted a survival signal that facilitated blood vessel growth and differentiation (*4*). In addition, this integrin also potentiated blood vessel maturation in developing quail (*5*). Therefore, it is likely that signaling events potentiated by both cytokines and adhesion receptors are critical to the growth of new blood vessels.

Although vascular cells respond to multiple cytokines, they also express a variety of integrin adhesion receptors (*6*–*9*). In fact, a number of the vascular cell integrins are functionally and structurally homologous, suggesting some level of biologic redundancy. Therefore, we compared the roles of the functionally homologous integrins $\alpha_v\beta_3$ and $\alpha_v\beta_5$ in ocular angiogenesis stimulated by the distinct cytokines bFGF and vascular endothelial cell growth factor (VEGF). These cytokines are associated with ocular neovascularization (*10*–*12*). To examine the role of these integrins in ocular angiogenesis, we implanted pellets containing either bFGF or VEGF into rabbit corneas. A series of eight animals was used for paired eye experiments, and each animal received a Hydron [poly(hydroxyethyl) methacrylate; Interferon Sciences, New Brunswick, New Jersey] implant containing cytokine and monoclonal antibody (mAb) LM609 (anti-$\alpha_v\beta_3$) in one cornea, and cytokine and mAb P1F6 (anti-$\alpha_v\beta_5$) or nonimmune immunoglobulin in the other cornea (Fig. 1) (*13*). The mAb LM609 inhibited bFGF-induced angiogenesis by 86% ($P < 0.005$, Student's t test) compared with eyes treated with mAb P1F6, and by 72% compared with immunoglobulin G controls ($P < 0.005$). However, when VEGF was used to induce angiogenesis, P1F6 reduced angiogenesis by 60% compared with LM609 ($P < 0.03$; Fig. 1). Preexisting perilimbal vessels were unaffected by either antibody, suggesting that the effects observed were restricted to newly forming blood vessels in the cornea. That $\alpha_v\beta_5$ functions in VEGF-induced angiogenesis may be clinically relevant, because VEGF is reported to be temporally and spatially associated with ischemia-induced ocular angiogenesis (*11*) and is increased in intraocular fluids obtained from patients with active neovascular eye disease (*12*).

To confirm these results, we examined another model of angiogenesis, the chick CAM (Fig. 2, A and B). The mAb LM609 (anti-$\alpha_v\beta_3$) disrupted angiogenesis induced by bFGF, whereas mAb P1F6 (anti-$\alpha_v\beta_5$) had no effect. However, as shown in the preceding corneal model, LM609 had only a slight effect on angiogenesis on the CAM stimulated by VEGF (Fig. 2, A and B), whereas P1F6 blocked this event. As predicted, a cyclic peptide antagonist (RGDfV) specific for both $\alpha_v\beta_3$ and $\alpha_v\beta_5$ (*14*) abolished angiogenesis induced by either cytokine (Fig. 2, C and D). These results, together with those from the cornea, suggest that bFGF- and VEGF-induced angiogenesis depend on distinct α_v integrins.

To extend these findings, we examined

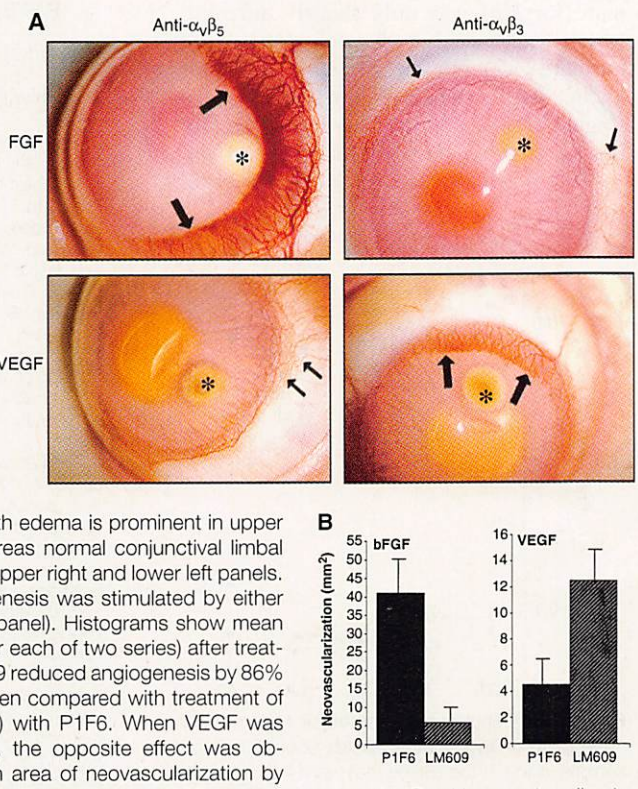

Fig. 1. Inhibition of cytokine-induced rabbit corneal angiogenesis by antibody antagonists of α_v integrins. (**A**) Hydron pellets (asterisks) containing Carafate-stabilized cytokine (750 μg; bFGF, top, or VEGF, bottom) and mAb to α_v integrin antibody (40 μg; P1F6 mAb to $\alpha_v\beta_5$, left, or LM609 mAb to $\alpha_v\beta_3$, right) were surgically implanted into paired rabbit corneas (left eye, left; right eye, right) and observed daily for 12 days. Photographs were taken on day 10 after implantation, the time at which neovascularization is maximal. Corneal angiogenesis (large arrows) with edema is prominent in upper left and lower right panels, whereas normal conjunctival limbal vessels (small arrows) appear in upper right and lower left panels. Magnification, ×2.2. (**B**) Angiogenesis was stimulated by either bFGF (left panel) or VEGF (right panel). Histograms show mean neovascular area ± SE ($n = 8$ for each of two series) after treatment with P1F6 or LM609. LM609 reduced angiogenesis by 86% ($P < 0.005$, Student's t test) when compared with treatment of the paired cornea (same animal) with P1F6. When VEGF was used to stimulate angiogenesis, the opposite effect was observed; P1F6 reduced the mean area of neovascularization by 60% ($P < 0.03$, paired t test) compared with LM609-treated paired eyes. Cytokine- and antibody-containing Hydron pellets were prepared and surgically implanted as described (*13*).

M. Friedlander, R. W. Shaffer, C. M. Kincaid, Robert Mealey Laboratory for the Study of Macular Degenerations, Department of Cell Biology, Scripps Research Institute, La Jolla, CA 92037, USA.
P. C. Brooks and D. A. Cheresh, Departments of Immunology and Vascular Biology, Scripps Research Institute, La Jolla, CA 92037, USA.
J. A. Varner, Department of Medicine, University of California, San Diego, La Jolla, CA 92093, USA.

angiogenesis on the chick CAM induced with a series of cytokines in the presence of anti-$\alpha_v\beta_3$ or anti-$\alpha_v\beta_5$. Angiogenesis was induced with bFGF, VEGF, tumor necrosis factor–α (TNF-α), transforming growth factor–α (TGF-α), or phorbol 12-myristate 13-acetate (PMA). One day later, embryos were injected with a single dose of mAb LM609 or mAb P1F6 (Fig. 3). LM609 blocked angiogenesis in response to bFGF and TNF-α, yet had minimal effect on angiogenesis induced by VEGF, TGF-α, or PMA. In contrast, P1F6 blocked angiogenesis induced by VEGF, TGF-α, and PMA, but had minimal effects on that induced by bFGF or TNF-α.

The phorbol ester PMA, a potent inducer of angiogenesis, is capable of activating protein kinase C (PKC), an intracellular family of serine-threonine kinases. Therefore, we also examined the effects of calphostin C, a PKC inhibitor, on angiogenesis on the chick CAM (Fig. 3). Calphostin C blocked angiogenesis induced by PMA, VEGF, and TGF-α, but had only a small effect on bFGF- or TNF-α–mediated angiogenesis. These results suggest the presence of two pathways of angiogenesis: one that depends on $\alpha_v\beta_3$ and that is largely independent of PKC, and a second that is potentiated by $\alpha_v\beta_5$ but also critically depends on PKC activation. These data are consistent with our previous observations that cell motility mediated by $\alpha_v\beta_5$, but not by $\alpha_v\beta_3$, depends on prior activation of a PKC-dependent signaling pathway (*15*).

Angiogenesis is associated with an array of pathologic processes, including cancer, blindness, and inflammatory disease (*1*, *3*). Our results suggest that antagonists of $\alpha_v\beta_3$ and $\alpha_v\beta_5$ may be effective in treating such processes. The LM609 mAb to $\alpha_v\beta_3$ causes variable regression of four types of human tumors grown on chick CAM (*4*). It is conceivable that tumors showing less susceptibility to LM609 might secrete several cytokines, including one such as VEGF that promotes angiogenesis in an $\alpha_v\beta_5$-dependent manner. This contention is supported by the finding that the cyclic peptide RGDfV (Fig.

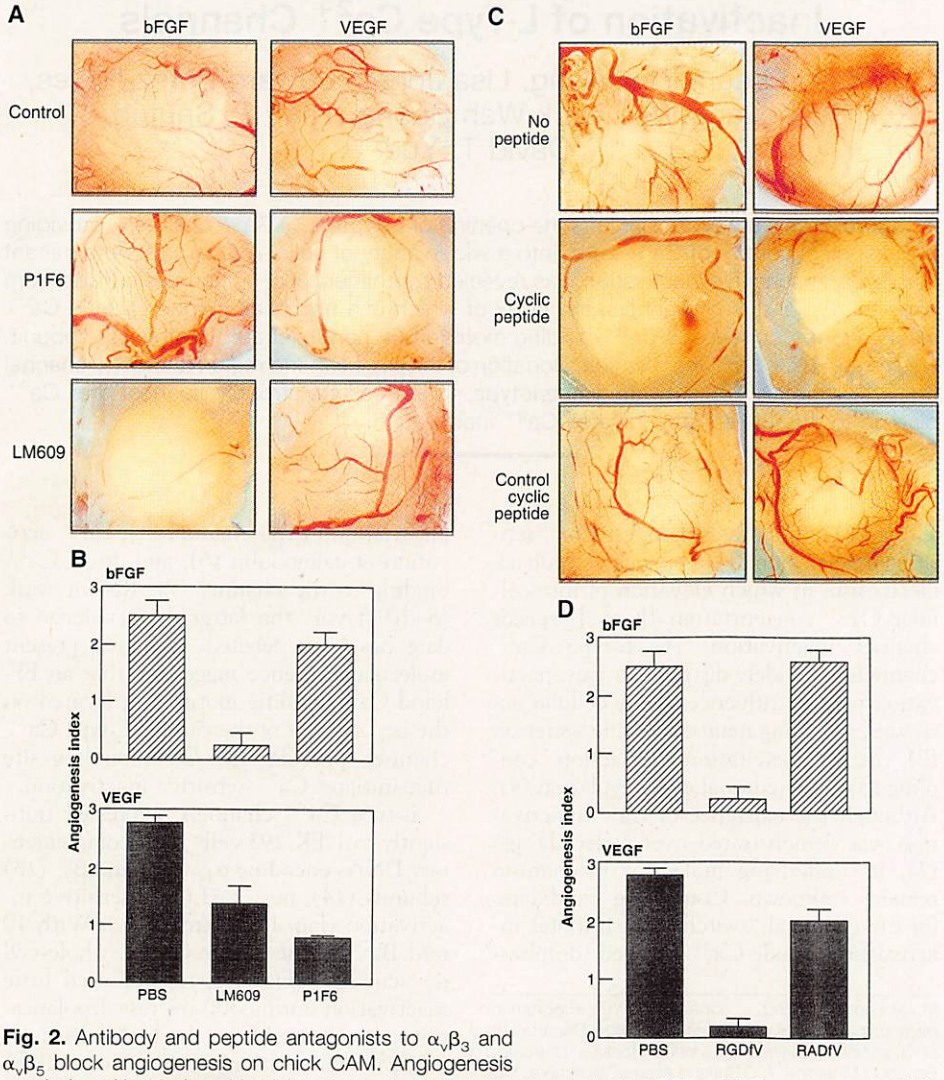

Fig. 2. Antibody and peptide antagonists to $\alpha_v\beta_3$ and $\alpha_v\beta_5$ block angiogenesis on chick CAM. Angiogenesis was induced in 10-day-old chick embryos by filter disks saturated with bFGF or TNF-α as described (*3*). (**A** and **B**) Twenty-four hours later, embryos were injected intravascularly with phosphate-buffered saline (PBS), or with LM609 (300 μg), or with P1F6 (300 μg). (**C** and **D**) Alternatively, embryos were either injected or topically treated with PBS alone or with PBS containing 300 μg of cyclic peptide RGDfV, active against $\alpha_v\beta_3$ and $\alpha_v\beta_5$ (*14*, *16*), or with the control cyclic peptide RADfV, as described (*4*). Representative CAMs were photographed through a stereomicroscope (A and C), and the mean angiogenic index (±SE) was determined for 6 to 12 CAMs per condition (B and D). Angiogenesis was scored for each embryo in a double-blind procedure that analyzed the number and extent of branching of blood vessels within the area of each disk. The scores ranged from 1+ (low) to 4+ (high), and the angiogenesis index was determined by subtracting a background score of 1 from all data. Magnification in (A) and (C), ×1.5.

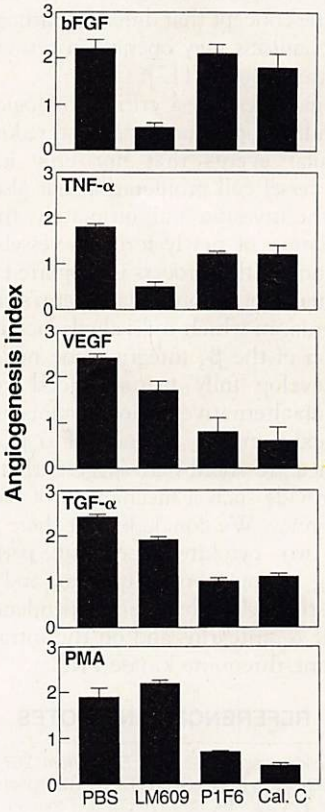

Fig. 3. Effect of anti-$\alpha_v\beta_3$, anti-$\alpha_v\beta_5$, and calphostin C (Cal. C) on CAM angiogenesis induced by multiple cytokines. CAM tissue from 10-day-old chick embryos was stimulated by filter disks saturated with 1.0 μg/ml of bFGF, TNF-α, VEGF, or TGF-α, or with 20 ng/ml of PMA. Embryos were then injected intravascularly with 300 μg per 0.1 ml per embryo of mAbs LM609 (anti-$\alpha_v\beta_3$) or P1F6 (anti-$\alpha_v\beta_5$) or topically treated with 100 nM calphostin C (0.1 ml) daily for 3 days. On day 13, filter disks and associated CAM tissue were dissected and analyzed for angiogenesis with a stereomicroscope. Angiogenesis was scored in a double-blind procedure that analyzed the number and extent of branching of blood vessels within the area of each disk. The scores for angiogenesis ranged from 1+ (low) to 4+ (high). The angiogenesis index was determined by subtracting a background score of 1 from all data. Experiments were repeated two to four times with five to six embryos per condition.

2), which blocks both α_v integrins (*16*), showed the greatest antiangiogenic and antitumoral activity when compared with either anti-$\alpha_v\beta_3$ alone or anti-$\alpha_v\beta_5$ alone (*16*).

Most ocular diseases that cause catastrophic loss of vision have as a common pathologic feature the growth of new blood vessels. Although ischemia-associated retinal neovascular diseases such as proliferative diabetic retinopathy are associated with increased VEGF (*12*), nonischemic subretinal neovascular diseases such as age-related macular degeneration have no such clear association. Our observation that VEGF-stimulated angiogenesis proceeds by an integrin-mediated angiogenic pathway distinct from that stimulated by FGF supports the concept that different pathogenetic mechanisms may operate in retinal and subretinal diseases (*17*).

Angiogenesis is a critical biologic process and, as such, may depend on redundant molecular events that not only initiate blood vessel cell proliferation but also regulate the invasion and, ultimately, the differentiation of newly forming vessels. Redundancy in this process is supported by an experiment of nature, Glanzmann's thrombasthenia, in which individuals lacking expression of the β_3 integrin gene nevertheless develop fully mature blood vessels. Thus, an alternative angiogenic mechanism must exist in the absence of $\alpha_v\beta_3$. The evidence presented here suggests that $\alpha_v\beta_5$ can provide such a mechanism of biologic redundancy. We conclude that there are at least two cytokine-dependent pathways leading to angiogenesis in vivo, and these are distinguished by their dependency on specific α_v integrins and on the intracellular serine-threonine kinase PKC.

REFERENCES AND NOTES

1. J. Folkman and Y. Shing, *J. Biol. Chem.* **267**, 10931 (1992); P. A. D'Amore and R. W. Thompson, *Annu. Rev. Physiol.* **49**, 453 (1987); J. Folkman, *Nature Med.* **1**, 27 (1995); D. Ingber and J. Folkman, *Cell Biol.* **109**, 317 (1989); D. Weinstat-Saslow and P. Steeg, *FASEB J.* **8**, 401 (1994).
2. J. E. Meredith, B. Fazeli, M. A. Schwartz, *Mol. Biol. Cell.* **4**, 953 (1993).
3. P. C. Brooks, R. A. F. Clark, D. A. Cheresh, *Science* **264**, 569 (1994).
4. P. C. Brooks *et al.*, *Cell* **79**, 1157 (1994).
5. C. J. Drake, D. A. Cheresh, C. D. Little, *J. Cell Sci.* **108**, 2655 (1995).
6. D. A. Cheresh, *Proc. Natl. Acad. Sci. U.S.A.* **84**, 6471 (1987).
7. D. I. Leavesley, M. A. Schwartz, M. Rosenfeld, D. A. Cheresh, *J. Cell Biol.* **121**, 163 (1993).
8. J. Enenstein and R. H. Kramer, *J. Invest. Dermatol.* **103**, 381 (1994).
9. D. A. Cheresh, S. A. Berliner, V. Vicente, V. Z. Ruggeri, *Cell* **58**, 945 (1989).
10. P. A. D'Amore, *Invest. Ophthalmol. Vis. Sci.* **35**, 3974 (1994).
11. J. W. Miller *et al.*, *Am. J. Pathol.* **145**, 574 (1994).
12. L. P. Aiello *et al.*, *N. Engl. J. Med.* **331**, 1480 (1994).
13. R. J. D'Amato, M. S. Loughnan, E. Flynn, J. Folkman, *Proc. Natl. Acad. Sci. U.S.A.* **91**, 4082 (1994); R. Shaffer and M. Friedlander, in *NATO ASI on Molecular, Cellular, and Clinical Aspects of Angiogenesis*, M. E. Maragoudakis, Ed. (Plenum, New York, in press). We modified the Hydron pellets so that endotoxin-free antibody was incorporated directly into the pellet. Eyes were examined and photographed daily through a Wild operating microscope. Photographs were recorded on Kodak Ektachrome 64T slide film, and images were converted for computer-assisted quantitation with Molecular Analyst 1.1 software (Bio-Rad) after acquisition through a Model GS670 imaging densitometer.
14. M. Pfaff *et al.*, *J. Biol. Chem.* **269**, 20233 (1994).
15. R. L. Klemke, M. Yebra, E. M. Bayna, D. A. Cheresh, *J. Cell Biol.* **127**, 859 (1994).
16. P. C. Brooks and D. A. Cheresh, unpublished data.
17. M. Friedlander, paper presented at the Retina Society Meeting, Santa Fe, NM, 8 September 1995.

18. Supported by grants to M.F. from the Lions Sightfirst Diabetic Retinopathy Research Program of the American Diabetes Association, the Scripps Clinic Department of Academic Affairs Clinical Research Program, and the Ralwhbnbg Fund, and by grants to D.A.C. from the National Cancer Institute and the Heart, Lung, and Blood Institute at the National Institutes of Health. D.A.C. is a recipient of an American Cancer Society Faculty Research Award. We thank S. Fallon, M. Sugita, and M. Toth for helpful comments and suggestions. We also thank S. Goodman and A. Jonczyk (E. Merck, KGaA, Darmstadt) for providing peptides and supporting evidence that cyclic peptide RGDfV (EP 0578 083 A2) blocks both $\alpha_v\beta_3$ and $\alpha_v\beta_5$. Sucralfate (Carafate) was a gift of Marion–Merrell Dow Pharmaceuticals (Cincinnati, OH).

2 June 1995; accepted 26 September 1995

Essential Ca^{2+}-Binding Motif for Ca^{2+}-Sensitive Inactivation of L-Type Ca^{2+} Channels

Marita de Leon, Yan Wang, Lisa Jones, Edward Perez-Reyes, Xiangyang Wei, Tuck Wah Soong, Terry P. Snutch, David T. Yue*

Intracellular calcium (Ca^{2+}) inhibits the opening of L-type (α_{1C}) Ca^{2+} channels, providing physiological control of Ca^{2+} entry into a wide variety of cells. A structural determinant of this Ca^{2+}-sensitive inactivation was revealed by chimeric Ca^{2+} channels derived from parental α_{1C} and α_{1E} channels, the latter of which is a neuronal channel lacking Ca^{2+} inactivation. A consensus Ca^{2+}-binding motif (an EF hand), located on the α_{1C} subunit, was required for Ca^{2+} inactivation. Donation of the α_{1C} EF-hand region to the α_{1E} channel conferred the Ca^{2+}-inactivating phenotype. These results strongly suggest that Ca^{2+} binding to the α_{1C} subunit initiates Ca^{2+} inactivation.

L-type Ca^{2+} channels manifest Ca^{2+}-sensitive inactivation (*1*), a biological feedback mechanism in which elevation of intracellular Ca^{2+} concentration ($[Ca^{2+}]$) speeds channel inactivation. As L-type Ca^{2+} channels are widely distributed, this inactivation process influences many cellular activities, including neuroendocrine secretion (*2*), cardiac excitation-contraction coupling (*3*), and neuronal gene regulation (*4*). Although the existence of Ca^{2+} inactivation was demonstrated over a decade ago (*1*), its underlying molecular mechanism remains unknown. Competing candidates for the chemical "switch" that initiates inactivation include Ca^{2+}-induced (de)phosphorylation of the channel (*5*), Ca^{2+} activation of calmodulin (*6*), and direct Ca^{2+} binding to the channel (*7*). Recent work (*8–10*) favors the latter, but evidence to date has been debated. Here, we present molecular evidence suggesting that an EF-hand Ca^{2+}-binding motif (*11*), located on the α_{1C} subunit of the cardiac L-type Ca^{2+} channel, provides the Ca^{2+} binding site that initiates Ca^{2+}-sensitive inactivation.

L-type Ca^{2+} channels, expressed transiently in HEK 293 cells from complementary DNAs encoding α_{1C} (*12*) and β_{2a} (*13*) subunits (*14*), possessed Ca^{2+}-sensitive inactivation (Fig. 1, A through C). With 10 mM Ba^{2+} as the charge carrier, whole-cell α_{1C} currents (Fig. 1A, top) showed little inactivation during 300-ms test depolarizations, as expected from the high selectivity of Ca^{2+} inactivation for Ca^{2+} over Ba^{2+} (*1*). Average data confirmed that Ba^{2+} currents decayed only slightly over the entire range of test depolarizations; peak currents were just larger than residual currents (Fig. 1A, bottom). By contrast, specimen current records decayed much more with 10 mM external Ca^{2+} as charge carrier (Fig. 1B, top), which suggests the onset of Ca^{2+} inactivation. Averages of peak and residual

M. de Leon, Y. Wang, L. Jones, D. T. Yue, Program in Molecular and Cellular Systems Physiology, Department of Biomedical Engineering, Johns Hopkins University School of Medicine, 720 Rutland Avenue, Baltimore, MD 21205, USA.
E. Perez-Reyes, Department of Physiology, Loyola University Chicago, 2160 South First Avenue, Maywood, IL 60153, USA.
X. Wei, Institute for Molecular Medicine and Genetics, Medical College of Georgia, 1120 15th Street, Augusta, GA 30912, USA.
T. W. Soong and T. P. Snutch, Biotechnology Laboratory, University of British Columbia, Vancouver, British Columbia V6T 1Z3, Canada.

*To whom correspondence should be addressed.

current confirmed the enhancement of inactivation by Ca^{2+} (Fig. 1B, bottom).

To quantitate inactivation, we plotted r_{300}, the fraction of peak current remaining at the end of a 300-ms depolarization, as a function of voltage (Fig. 1C). The r_{300} relation with Ca^{2+} defined a U-shaped plot, providing a hallmark of Ca^{2+} inactivation (*10*). The low point of the curve coincided with maximal Ca^{2+} entry (compare Fig. 1B), and r_{300} turned upward with further depolarization as the driving force for Ca^{2+} entry dropped. The small, monotonic decline of r_{300} with Ba^{2+} (Fig. 1C) reflected a separate, voltage-sensitive inactivation (*10*). Because voltage- and Ca^{2+}-sensitive inactivation are approximately independent processes (*10*), the difference between Ca^{2+} and Ba^{2+} r_{300} values provided a direct measure of Ca^{2+} inactivation, as exemplified by the parameter f (*15*) (Fig. 1C).

In contrast, a homologous Ca^{2+} channel, expressed from α_{1E} (*16*) and β_{2a} (*13*) subunits, lacked Ca^{2+} inactivation (Fig. 1, D through F), thereby establishing the feasibility of chimeric channel analysis (*17, 18*). The α_{1E} subunit is the pore-forming constituent of a medium-threshold Ca^{2+} channel in neurons (*16*). The α_{1E} Ba^{2+} currents (Fig. 1D) appeared to inactivate at the same rate as Ca^{2+} currents (Fig. 1E), despite larger current amplitudes with Ca^{2+}. The absence of Ca^{2+} inactivation was confirmed quantitatively by identical r_{300} relations with Ca^{2+} and Ba^{2+} (Fig. 1F). Because inactivation was unchanged by reduction of external [Ba^{2+}] or [Ca^{2+}] to 3 mM (*19*), the shallow U shape of the r_{300} relation did not indicate a current-sensitive inactivation with equal selectivity for Ca^{2+} and Ba^{2+}.

We tested whether differences in the COOH-termini of α_{1C} and α_{1E} account for their distinct inactivation properties, because this region contains an EF-hand motif with a possible role in Ca^{2+} activation (*20*). The entire COOH-terminus of α_{1E} was substituted into α_{1C} (*21*), and the resulting $\alpha_{1CE\text{-}1}$ chimera (Fig. 2A) completely lacked Ca^{2+} inactivation. Its Ca^{2+} inactivation parameter f was ≈0 (Fig. 2A), clearly lower than the α_{1C} value (0.44) and indistinguishable from the α_{1E} value (≈0). Thus, the α_{1C} COOH-terminus appeared to be essential for Ca^{2+} inactivation.

To refine localization of the essential region, we deleted two-thirds of the COOH-terminus of α_{1C} from amino acid 1733 to the stop codon. The resulting construct, α_{1Cdel}, manifested the same degree of Ca^{2+} inactivation as α_{1C}, with nearly identical f values (Fig. 2A). Substituting only the proximal fourth of the α_{1C} COOH-terminus (amino acids 1510 to 1690) with the corresponding α_{1E} locus produced a chimeric Ca^{2+} channel ($\alpha_{1CE\text{-}2}$; Fig. 2A) that completely lacked Ca^{2+} inactivation ($f \approx 0$). These two results suggest that the proximal fourth of the α_{1C} COOH-terminus contained a necessary region for Ca^{2+} inactivation.

When only the EF-hand region of α_{1C} (amino acids 1510 to 1560) was replaced by the homologous α_{1E} sequence, Ca^{2+} inactivation was also absent ($f \approx 0$ for $\alpha_{1CE\text{-}3}$; Fig. 2A). Comparison of whole-cell Ca^{2+} and Ba^{2+} records emphasized the complete ablation of Ca^{2+} inactivation in $\alpha_{1CE\text{-}3}$ (Fig. 2B). Both sets of records were nearly flat; the Ca^{2+} records have been scaled to illustrate the similarity of kinetics. The r_{300} plots confirmed that inactivation was consistently small and identical for Ca^{2+} and Ba^{2+} (Fig. 2B) over a wide range of potentials. The results with $\alpha_{1CE\text{-}3}$ showed that the EF-hand motif of α_{1C} is necessary for Ca^{2+} inactivation, as long as the functional knockout did not arise from higher order conformational derangement of the chimeric channel.

The chimeric channel was not likely to have serious conformational problems for several reasons. First, nonspecific distortion would change other whole-cell properties; but the average current-voltage relation of $\alpha_{1CE\text{-}3}$ (Fig. 2B) was very similar to that of α_{1C} (Fig. 1, A and B), suggesting that activation was unaffected. In fact, activation and steady-state voltage inactivation of all chimeras with an α_{1C} backbone were closely similar to those of α_{1C}.

Second, substitution of portions (including the EF hand) of the α_{1C} COOH-terminus into α_{1E} conferred the Ca^{2+}-inactivating phenotype. In particular, donation of the entire α_{1C} COOH-terminus to the α_{1E} backbone yielded a chimeric $\alpha_{1EC\text{-}1}$ channel with a Ca^{2+} inactivation parameter (f) of 0.28 (Fig. 2C). Simple deletion of up to two-thirds of the distal COOH-terminus of $\alpha_{1EC\text{-}1}$ preserved the same degree of Ca^{2+} sensitivity ($\alpha_{1EC\text{-}1\Delta4}$ and $\alpha_{1EC\text{-}1\Delta3}$) (Fig. 2C). Currents from $\alpha_{1EC\text{-}1}$ illustrated the extent to which inactivation has been conferred to these constructs (Fig. 2D). Of particular relevance is the selective enhancement of Ca^{2+} current inactivation with larger currents, a distinctive property of Ca^{2+} inactivation (compare Fig. 1C and Fig. 2D). Further COOH-terminal truncation of more than ≈50 amino acids produced nonfunctional channels ($\alpha_{1EC\text{-}1\Delta2}$) (Fig. 2C), as would be expected from previous studies (*12*).

To determine whether smaller portions of the α_{1C} COOH-terminus sufficed to impart Ca^{2+} inactivation to the α_{1E} backbone, we substituted narrow stretches of α_{1C} containing the EF hand into full-length α_{1E}, yielding $\alpha_{1EC\text{-}2}$ and $\alpha_{1EC\text{-}3}$ (Fig. 2C). Donation of smaller α_{1C} segments failed to confer Ca^{2+} inactivation ($f \approx 0$ for $\alpha_{1EC\text{-}2}$ and $\alpha_{1EC\text{-}3}$) (Fig. 2C) (*22*). To retain native

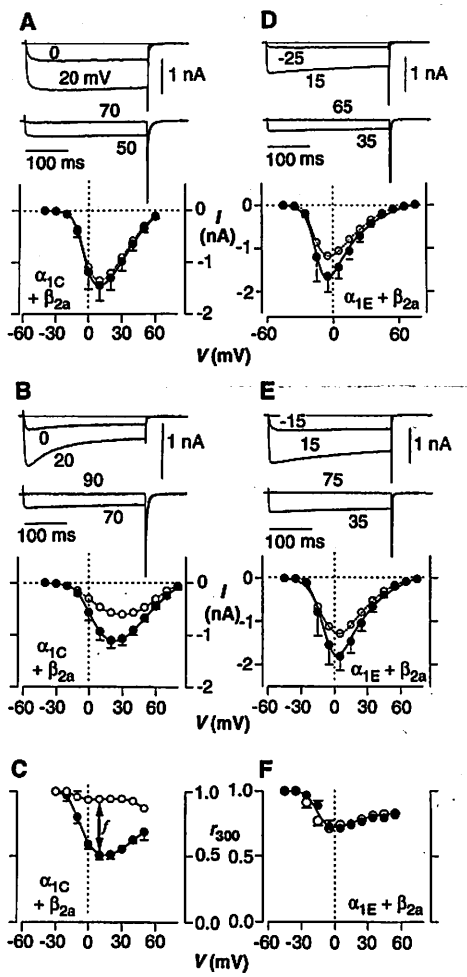

Fig. 1. Comparison of inactivation in α_{1C} and α_{1E}. **(A)** α_{1C} Ba^{2+} currents. Top, whole-cell records elicited by 300-ms depolarizations to the indicated potentials (0, 20, 70, and 50 mV). Holding potential was −60 mV; tail potential, −50 mV in a Cs-aspartate internal solution (*14*). Bottom, peak (filled) and residual (open) current at the end of 300-ms depolarizations; means of seven cells. Error bars, plotted when larger than symbols, show SEM here and throughout. **(B)** α_{1C} Ca^{2+} currents; the format is identical to that in (A). Records are from the same cell as that in (A) (top); n = 6 cells. **(C)** Residual fraction of peak current, r_{300}, for α_{1C}. The concentration of charge carrier was 10 mM throughout for six cells. The parameter f, subsequently used as a concise descriptor of Ca^{2+} inactivation, is the difference between r_{300} relations at +5 to +10 mV. Isolation of Ca^{2+} channel current, indicated by flat traces near reversal potential [for example, +70 mV in (A), and throughout], is required for quantitative interpretation of r_{300}. Ca^{2+}, solid symbols; Ba^{2+}, open symbols. **(D)** α_{1E} Ba^{2+} currents; the format is identical to that in (A). Top, holding potential, −90 mV; tail potential, −80 mV, with NMG-$MeSO_3$ internal solution (*14*) and 10 mM external Ba^{2+}. Bottom, means of n = 6 cells. **(E)** α_{1E} Ca^{2+} currents; the format is identical to that in (D), with 10 mM external Ca^{2+}. The records are from the same cell as that at the top of (D). The bottom represents results from six cells. **(F)** r_{300} for α_{1E}. The format was identical to that in (C), with 10 mM charge carrier throughout in six cells; symbols are as in (C). The small difference of r_{300} (−30 to 0 mV range) arises from differential screening of surface charge by Ba^{2+} and Ca^{2+}.

Ca^{2+} binding, an EF hand must reside within its own "globular domain" (*22*), which is made of a continuous sequence of amino acids containing the EF hand. The margin between the COOH-termini of α_{1EC-3} and $\alpha_{1EC-1\Delta3}$, amino acids 1650 to 1732 in α_{1C}, may well define a border of such a domain region.

Third, single-channel recordings (*23*) offered a further test of the specificity with which Ca^{2+} inactivation has been removed in the series of α_{1CE} chimeras (collectively denoted as α_{1CE-*}). Work with native L-type Ca^{2+} channels demonstrates that Ca^{2+} inactivation reflects a Ca^{2+}-induced shift in the overall pattern of gating (*10*) from a mode with rapidly activating, high-frequency opening (mode 1), to a mode with slowly activating, infrequent opening (mode Ca). With Ba^{2+}, there is no shift from mode 1 to mode Ca, and mode 1 often predominates. Voltage inactivation renders the channel incapable of opening, yielding depolarizations without activity ("blanks"). Selective knockout of Ca^{2+} inactivation should therefore remove Ca^{2+}-induced shifts to mode Ca but spare the induction of blanks by prolonged depolarization.

Single-channel properties of α_{1C} were compared with those of α_{1CE-1} (Fig. 3), the α_{1CE-*} chimera with the largest change from α_{1C}. Either 10 mM Ba^{2+} or 10 mM Ca^{2+} was used as the charge carrier to enable direct comparison with whole-cell results. The same prepulse protocol (top) was used throughout: depolarizations to +0 mV were alternately preceded by a 0.5-s prepulse to +20 mV or by no prepulse. α_{1C} behaved just as predicted from native L-type Ca^{2+} channels. With Ba^{2+} (Fig. 3A), unitary currents illustrated the predominance of mode 1 gating during test depolarizations with or without prepulse. Ensemble average currents hardly decayed, which is consistent with the absence of Ca^{2+} inactivation. The first latency distribution (F) and conditional open probability (P_{oo}) functions served as quantitative descriptors of these trends (*10*). Values of F plot the probability that a channel first opens by time t after the onset of test depolarization. The rapid rise of F, with and without prepulse, demonstrated the dominance of mode 1 gating throughout. The small depression of the plateau by the prepulse reflected the induction of blank sweeps, which is indicative of voltage inactivation. P_{oo}, the probability of a channel being open at time t after first opening, provided a kinetic fingerprint of gating after first opening. The similarity of values of P_{oo}, with and without prepulse, confirmed the lack of mode shifts. With Ca^{2+} (Fig. 3C), control α_{1C} traces activated rapidly in a bursting pattern, but traces following a prepulse activated slowly in a sparsely opening pattern. Thus, Ca^{2+} entry during the prepulse caused a shift from mode 1 to mode Ca^{2+}, synonymous with Ca^{2+} inactivation. Induction of a slow component in F after the prepulse, as well as depression of P_{oo}, quantitated the shift to mode Ca.

In α_{1CE-1} (Fig. 3, B and D), single-channel properties indicated a selective knockout of Ca^{2+} inactivation. With Ba^{2+} (Fig. 3B), α_{1CE-1} behaved like α_{1C} (compare Fig. 3A); with Ca^{2+} (Fig. 3D), however, there was no shift to mode Ca. The lack of Ca^{2+} inactivation in unitary Ca^{2+} currents excluded differential expression levels as a trivial mechanism for altered inactivation. A final argument against global conformational change came with the similarity of α_{1C} and α_{1CE-1} unitary current amplitudes (≈0.6 and ≈0.25 pA with Ba^{2+} and Ca^{2+}, respectively, for both). This similarity excluded appreciable alteration of permeation.

These results establish the EF-hand motif of α_{1C} as an essential structural determinant of Ca^{2+} inactivation, whereby Ca^{2+} binding to the EF-hand motif initiates Ca^{2+} inactivation. By analogy to other EF hands, the transduction of binding to inactivation might occur by Ca^{2+}-induced exposure of hydrophobic residues on the E and F helices, which could then interact with a complementary hydrophobic surface (*24*) so as to inhibit opening (*10*). "Donation" of the Ca^{2+} inactivation phenotype to $\alpha_{1EC-1\Delta3}$ suggests that the receptor is intact on α_{1E} and that only the binding domain may be defective, as supported by the alignment of the EF-hand regions from the major classes of Ca^{2+} channels (Fig. 4A). For α_{1C} and α_{1D} [which probably has Ca^{2+} inactivation (*25*)], the region is almost identical and these channels score highest (14 out of 16) on a modified Tufty-Kretsinger EF-hand test (*20*). For α_{1E}, α_{1B}, and α_{1A}, which all lack Ca^{2+} inactivation (*26*), divergence is substantial and scores are lower. However, only ≈70% of EF-hand motifs (*27*) actually bind Ca^{2+}; our proposal remains to be confirmed by in vitro methods (*22*).

The location of the EF-hand motif helps explain paradoxical features of the α_{1C} channel. Proximity of the EF hand to the inner lip of the permeation pathway (*28*) predicts insensitivity of Ca^{2+} inactivation to intracellular Ca^{2+} chelators (*29*); diffusion calculations indicate that $[Ca^{2+}]$ in the channel pore would be little affected by such agents (*29*). Conversely, because the EF hand is not

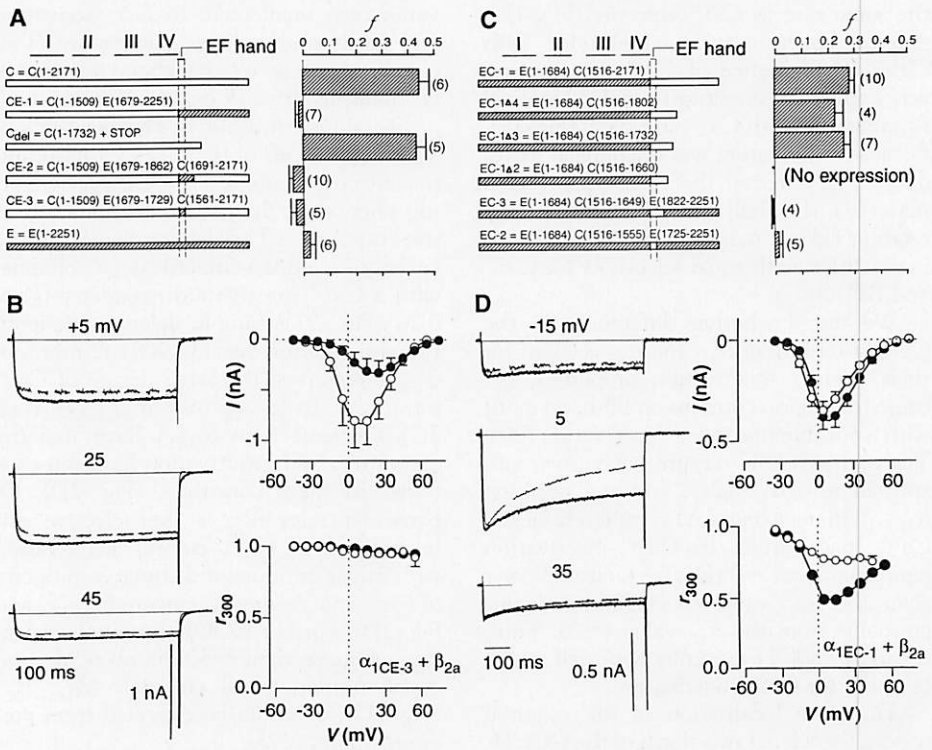

Fig. 2. Molecular determinants of Ca^{2+} inactivation. All α_1 constructs were co-expressed with the β_{2a} subunit to ensure robust expression. (**A**) Left, schematic representation of α_{1C}, α_{1E}, and chimeric constructs (not to scale). Values in parentheses indicate amino acid numbers. Right, corresponding f values (mean ± SEM from the number of cells in parentheses). (**B**) Inactivation of α_{1CE-3}. Left, Ba^{2+} (solid) and Ca^{2+} currents (dashed) during steps to various potentials. Holding potential, −90 mV; tail potential, −80 mV. Ca^{2+} currents were scaled by (from top) 4.38, 2.07, and 0.94 times to facilitate comparison of kinetics. Right, peak current and r_{300} from n = 5 cells. Symbols are as in Fig. 1C. (**C**) Schematic representation of α_{1EC-*} chimeric constructs (left) and associated f values (right). The format was identical to that in (A). (**D**) Inactivation of α_{1EC-1}. The format was identical to that in (B). Data are from 10 cells. NMG-$MeSO_3$ internal solution (*14*) was used in (A) through (D); 10 mM charge carrier was used throughout.

quite in the conduction pore, Ca^{2+} inactivation can be accelerated by extra-channel factors, like Ca^{2+} flux through adjacent Ca^{2+} channels (9) or ryanodine receptors (3). The contiguity of the EF hand to consensus protein kinase A (PKA) phosphorylation sites on the α_{1C} COOH-terminus, regarded as probable loci for channel up-regulation by PKA (30), may explain parallels in the mode-shift behavior underlying Ca^{2+} channel regulation by Ca^{2+} and phosphorylation (Fig. 4B). Phosphorylation favors a shift from mode 0_a to mode 1 (31), where mode 0_a resembles mode Ca, although L-type Ca^{2+} channels do not require dephosphorylation to inactivate (10).

Our findings may have implications for many biological systems, given the wide distribution of L-type Ca^{2+} channels. For example, in heart where the duration of action potentials is highly sensitive to Ca^{2+} inactivation (32), the EF-hand region of L-type Ca^{2+} channels is a potential locus for inherited electrical disorders like long QT syndrome (33); it also may be a molecular target for new cardiac inotropic and anti-arrhythmic drugs.

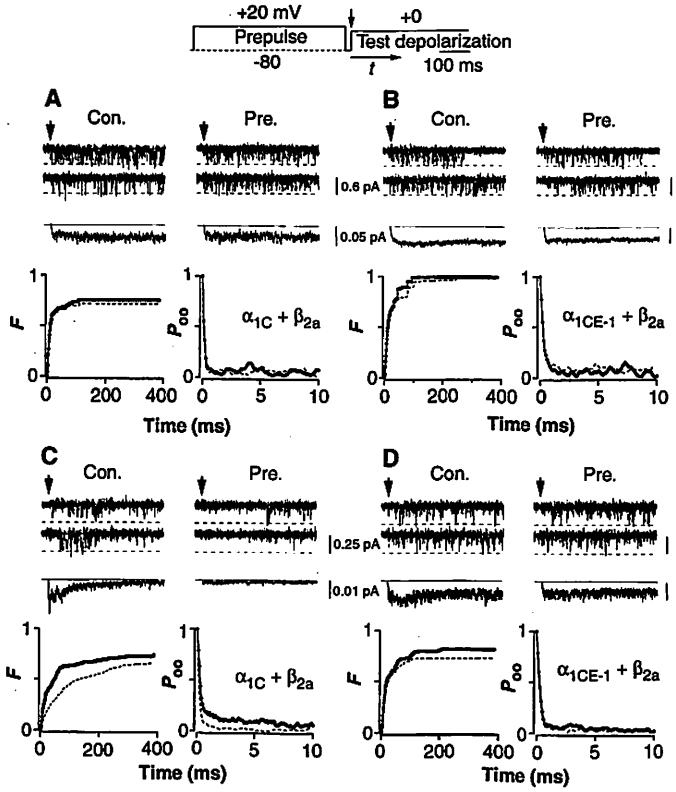

Fig. 3. Single-channel comparison of inactivation in α_{1C} and α_{1CE-1}, both co-transfected with β_{2a}. Top, Voltage-pulse protocol for all panels. Test depolarization lasts 386 ms. **(A)** α_{1C} unitary Ba^{2+} currents. Top, unitary current records from a single patch with two channels filtered at 1400 Hz. Pre., with prepulse; Con., without prepulse control. Dashed lines indicate the open-channel current level. Arrows indicate instant of test depolarization, as indicated by protocol at the top. Middle, ensemble average currents after normalization by the number of channels (here, and in all panels), derived from the same patch. Bottom, first latency distribution (left) and conditional open probability (right), derived from same patch. Solid line, without prepulse; dashed line, with prepulse. **(B)** α_{1CE-1} unitary Ba^{2+} currents. The format is identical to that in (A), with scale bar values as in (A). Shown are exemplar records from a patch with three channels, filtered at 1400 Hz. Ensemble averages, F, and P_{oo} were averaged from four patches. **(C)** α_{1C} unitary Ca^{2+} currents. The format is identical to that in (A). Shown are unitary records from a patch with three channels, filtered at 1000 Hz. Ensemble averages, F, and P_{oo} were averaged from three patches. **(D)** α_{1CE-1} unitary Ca^{2+} currents. The format was identical to that in (A), with scale bar values as in (C). Shown are records from a patch with two channels, filtered at 700 Hz. Ensemble averages, F, and P_{oo} are averaged from four patches.

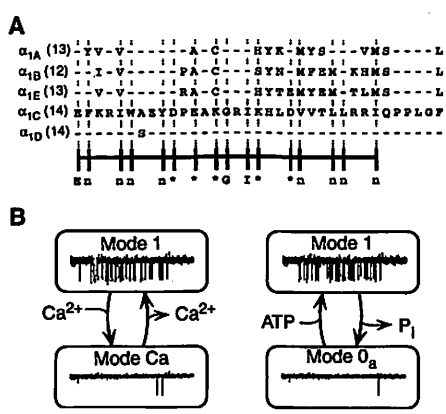

Fig. 4. Mechanistic features of Ca^{2+}-sensitive inactivation. **(A)** Alignment of EF-hand regions from five major classes of voltage-gated Ca^{2+} channels (35). Shown are amino acids 1782 to 1816 of α_{1A} (36), 1728 to 1762 of α_{1B} (37), 1695 to 1729 of α_{1E} (16), 1526 to 1560 of α_{1C} (12), and 1495 to 1529 of α_{1D} (38). Dashes show positions of identity to α_{1C} (39). For reference, the modified Tufty-Kretsinger scoring template (20) is shown at the bottom, with scoring numbers in parentheses above. Residues E, G, and I are the anticipated amino acids in this position of an EF hand. "n" denotes a hydrophobic amino acid (L, I, V, F, M, W, and Y), and the asterisk denotes a ligand vertex for Ca^{2+} (D, N, E, Q, S, and T). Each such criterion that is satisfied contributes one point; the score of each channel appears in parentheses. **(B)** Parallels in the gating modes underlying Ca^{2+} channel regulation by Ca^{2+} and PKA phosphorylation. Simulated traces are for illustration only. P_i, inorganic phosphate.

REFERENCES AND NOTES

1. P. Brehm and R. Eckert, *Science* **202**, 1203 (1978).
2. H. Scherubl *et al.*, *Am. J. Physiol.* **264**, E354 (1993).
3. J. Sham and M. Morad, *Proc. Natl. Acad. Sci. U.S.A.* **92**, 121 (1995).
4. M. Sheng, G. McFadden, M. E. Greenberg, *Neuron* **4**, 571 (1990).
5. J. E. Chad and R. Eckert, *J. Physiol. (London)* **378**, 31 (1986).
6. D. L. Armstrong, *Trends Neurosci.* **12**, 117 (1989).
7. A. Sherman, J. Keizer, J. Rinzel, *Biophys. J.* **58**, 985 (1990).
8. D. T. Yue, P. H. Backx, J. P. Imredy, *Science* **250**, 1735 (1990); J. A. Haack and R. L. Rosenberg, *Biophys. J.* **66**, 1051 (1994).
9. J. P. Imredy and D. T. Yue, *Neuron* **9**, 197 (1992).
10. ———, *ibid.* **12**, 1301 (1994).
11. R. H. Kretsinger, *Nature* **240**, 85 (1972).
12. X. Wei *et al.*, *J. Biol. Chem.* **266**, 21943 (1991); X. Wei *et al.*, *ibid.* **269**, 1635 (1994).
13. E. Perez-Reyes *et al.*, *ibid.* **267**, 1792 (1992).
14. Complementary DNAs encoding α_{1C} (12), α_{1E} (34), and β_{2a} (13) were subcloned into pGW1H (British Biotechnologies, Oxford), an expression plasmid with a cytomegalovirus promotor. HEK 293 cells were transiently transfected as described (34), with the use of α_1 and β_{2a} constructs (10 mg each per 100-mm plate). Whole-cell currents were recorded at room temperature by patch-clamp techniques with the use of an Axopatch 200A (Axon Instruments, Foster City, CA). The bath solution contained 130 mM *N*-methyl-d-glucamine (NMG) aspartate, 1 mM $MgCl_2$, 10 mM glucose, 10 mM 4-aminopyridine, 10 mM Hepes, and 10 mM $BaCl_2$ or $CaCl_2$ (pH 7.3), adjusted with NMG. The internal solution was based on either Cs-aspartate or NMG-methanesulfonate ($MeSO_3$). The Cs-aspartate solution contained 135 mM Cs-aspartate, 5 mM CsCl, 5 mM EGTA, 1 mM $MgCl_2$, 4 mM Mg adenosine triphosphate (ATP), and 10 mM Hepes (pH 7.3), adjusted with CsOH. NMG-$MeSO_3$ solution contained 140 mM NMG-$MeSO_3$, 5 mM EGTA, 1 mM $MgCl_2$, 4 mM MgATP, and 10 mM Hepes (pH 7.3), adjusted with NMG. Results with NMG-$MeSO_3$ internal solution were adjusted by +15 mV to account for the junction potential difference with Cs-aspartate internal solution. Series resistance was typically <10 megohms and was compensated by 70%. Leak and capacitance currents were subtracted by a P/8 protocol [C. M. Armstrong and F. Bezanilla, *J. Gen. Physiol.* **63**, 533 (1974)]. Voltage pulses were delivered every 15 to 20 s, and data were sampled at 10 kHz and filtered at 2 kHz (−3 dB, 4-pole Bessel). Smooth curves were fitted by eye here and throughout.
15. H. Reuter, *Prog. Biophys. Mol. Biol.* **26**, 1 (1973).
16. T. W. Soong *et al.*, *Science* **260**, 1133 (1993).
17. α_{1C} expressed alone yielded Ca^{2+} currents with Ca^{2+} inactivation properties similar to those of $\alpha_{1C} + \beta_{2a}$ (Fig. 1C), although expression levels were considerably smaller.
18. A. Welling *et al.*, *Circ. Res.* **73**, 974 (1993).
19. r_{300} relations were no different with 3 mM and 10 mM Ba^{2+} or Ca^{2+} as the charge carrier.
20. J. Babitch, *Nature* **346**, 321 (1990).
21. Chimeric Ca^{2+} channels were constructed by ligating polymerase chain reaction (PCR) products, derived from a "donor" channel, into selected restriction endonuclease sites on a "recipient" channel. PCR primers contained corresponding restriction endonuclease sites. All chimeras were subcloned into pGW1H. Methods are as follows. The chimera α_{1CE-1} contains nucleotides 1 to 4492 from α_{1C} (α_{1C}:

1 to 4492) and nucleotides 5000 to 6756 from α_{1E} (α_{1E}: 5000 to 6756), with position 1 at the start codon; the α_{1E} fragment was ligated into α_{1C} that had been cut at nucleotide position 4487 with Bcl I, and in the polylinker with Xba I. For α_{1Cdel} (α_{1C}: base pairs 1 to 5196 + TAG), the Bst EII (α_{1C}: 4641) and Xba I (polylinker) region of α_{1C} was replaced with a shorter fragment, including a premature stop codon after the codon for amino acid 1732. For α_{1CE-2} (α_{1C}: 1 to 4492 and α_{1E}: 5000 to 5586 and α_{1C}: 5071 to 6516), the α_{1C} fragment (α_{1C}: 5071 to 6516) was ligated into Sau I (α_{1CE-1}: 5071) and Xba I (polylinker) of α_{1CE-1}. For α_{1CE-3} (α_{1C}: 1 to 4492 and α_{1E}: 5000 to 5187 and α_{1C}: 4681 to 6516), the α_{1C} fragment (α_{1C}: 4681 to 6516) was ligated into Stu I (α_{1CE-1}: 4674) and Xba I (polylinker) of α_{1CE-1}. For α_{1EC-1} (α_{1E}: 1 to 5050 and α_{1C}: 4544 to 6516), the α_{1C} fragment (α_{1C}: 4544 to 6516) was ligated into the Xho I (α_{1E}: 5045) and Sal I (polylinker) sites of α_{1E}. For $\alpha_{1EC-1\Delta4}$ (α_{1E}: 1 to 5050 and α_{1C}: 4544 to 5406 + TAG), the α_{1EC-1} fragment (α_{1EC-1}: 4299 to 5913 + TAG) was ligated into the Bst 1107I (α_{1EC-1}: 4299) and Sal I (polylinker) sites of α_{1EC-1}. For $\alpha_{1EC-1\Delta3}$ (α_{1E}: 1 to 5050 and α_{1C}: 4544 to 5196 + TAG), the α_{1EC-1} fragment (α_{1EC-1}: 4299 to 5703 + TAG) was ligated into the Bst 1107I (α_{1EC-1}: 4299) and Sal I (polylinker) sites of α_{1EC-1}. For $\alpha_{1EC-1\Delta2}$ (α_{1E}: 1 to 5050 and α_{1C}: 4544 to 4980 + TAG), the α_{1EC-1} fragment (α_{1EC-1}: 4299 to 5487 + TAG) was ligated into the Bst 1107I (α_{1EC-1}: 4299) and Sal I (polylinker) sites of α_{1EC-1}. For α_{1EC-3} (α_{1E}: 1 to 5050 and α_{1C}: 4544 to 4947 and α_{1E}: 5464 to 6756), the α_{1E} fragment (α_{1E}: 5464 to 6756) was ligated into Bgl II (α_{1EC-1}: 5369) to Sal I (polylinker) of α_{1EC-1}. For α_{1EC-2} (α_{1E}: 1 to 5050 and α_{1C}: 4544 to 4667 and α_{1E}: 5175 to 6756), the α_{1E} fragment (α_{1E}: 5175 to 6756) was ligated into Bst EII (α_{1EC-1}: 5148) and Sal I (polylinker) of α_{1EC-1}. Portions of chimeric channel constructs derived from PCR were verified in their entirety with the use of the fluorescent dideoxy terminator method of thermocycle sequencing on an automated DNA sequencer (Perkin-Elmer, Applied Biosystems Division 373a).

22. P. Brodin, C. Johanson, S. Forsén, T. Drakenberg, T. Grundstrom, *J. Biol. Chem.* **265**, 11125 (1990); S. Linse, A. Helmersson, S. Forsén, *ibid.* **266**, 8050 (1991); S. Linse and S. Forsén, *Adv. Second Messenger Phosphoprotein Res.* **30**, 89 (1995).
23. Single-channel currents were recorded at room temperature by on-cell patch-clamp (*10*). Bath solution consisted of 132 mM potassium glutamate, 5 mM KCl, 5 mM NaCl, 3 mM $MgCl_2$, 2 mM EGTA, 1 mM CaATP, 10 mM glucose, and 10 mM Hepes (pH 7.3), adjusted with KOH. Pipette solution consisted of 10 mM $BaCl_2$ or 10 mM $CaCl_2$, 100 mM tetraethylammonium (TEA) chloride, and 10 mM Hepes (pH 7.4), adjusted with TEA-OH. Voltage pulses were delivered every 5 to 8 s. The integrating headstage of Axopatch 200A was used. Data were sampled at 10 kHz and filtered at 1 to 2 kHz (for Ba^{2+} data) and at 0.7 to 1 kHz (for Ca^{2+} data) (−3 dB, 4-pole Bessel). The average current, F, and P_{oo} were analyzed as described (*10*).
24. N. C. J. Strynadka and M. N. G. James, *Annu. Rev. Biochem.* **58**, 951 (1989).
25. S. Seino *et al.*, *Proc. Natl. Acad. Sci. U.S.A.* **89**, 584 (1992); T. D. Plant, *J. Physiol. (London)* **404**, 731 (1988).
26. $\alpha_{1B} + \beta_{2a}$ showed identical r_{300} curves with 10 mM Ba^{2+} or 10 mM Ca^{2+} as the charge carrier; W. A. Sather *et al.*, *Neuron* **11**, 291 (1993).
27. H. Kawasaki and R. Kretsinger, *Protein Profile* **1**, 343 (1994).
28. D. S. Ragsdale, J. C. McPhee, T. Scheuer, W. A. Catterall, *Science* **265**, 1724 (1994).
29. M. J. Gutnick, H. D. Lux, D. Swandulla, H. Zucker, *J. Physiol. (London)* **412**, 197 (1989).
30. A. Yoshida, M. Takahashi, S. Nishimura, H. Takeshima, S. Kokubun, *FEBS Lett.* **309**, 343 (1992).
31. D. T. Yue, S. W. Herzig, E. Marban, *Proc. Natl. Acad. Sci. U.S.A.* **87**, 753 (1990).
32. D. Noble, *The Initiation of the Heartbeat* (Clarendon, Oxford, 1979), pp. 1–186.
33. Q. Wang *et al.*, *Cell* **80**, 1 (1995).
34. R. S. Dhallan, K.-W. Yau, K. A. Schrader, R. R. Reed, *Nature* **347**, 184 (1990).
35. Abbreviations for the amino acid residues are as follows: A, Ala; C, Cys; D, Asp; E, Glu; F, Phe; G, Gly; H, His; I, Ile; K, Lys; L, Leu; M, Met; N, Asn; P, Pro; Q, Gln; R, Arg; S, Ser; T, Thr; V, Val; W, Trp; and Y, Tyr.
36. T. V. B. Starr, P. Ward, T. P. Snutch, *Proc. Natl. Acad. Sci. U.S.A.* **88**, 5621 (1991).
37. S. J. Dubel *et al.*, *ibid.* **89**, 5058 (1992).
38. M. E. Williams *et al.*, *Science* **257**, 389 (1992).
39. α_{1CE-3} differs from α_{1C} by two other amino acids not included in the alignment in Fig. 4A. Both are located just NH_2-terminal to the EF hand: E for D in α_{1C} (*35*), and S for W in α_{1C}, at positions 1510 and 1516, respectively, of α_{1CE-3}. Neither of these differences would be expected to alter Ca^{2+} binding to the EF hand. In fact, α_{1EC-1}, $\alpha_{1EC-1\Delta3}$, and $\alpha_{1EC-1\Delta4}$ reconstitute Ca^{2+} inactivation but maintain the E at position 1510.

40. We thank J. P. Imredy, P. G. Patil, D. L. Brody, B. A. Lewis, and K. W. Yau for discussion and comments; S. Sisodia and M. Schlissel for molecular biological advice; and the DNA Analysis Facility of Johns Hopkins for sequencing. Supported by grants from NIH (D.T.Y. and E.P.-R.) and the Medical Research Council of Canada and the Howard Hughes Medical Institute (T.P.S.); an Established Investigatorship of the American Heart Association (D.T.Y.); a Medical Scientist Training Program award (L.J.); and a National University of Sing- apore fellowship (T.W.S.).

23 March 1995; accepted 13 October 1995

Coactivator and Promoter-Selective Properties of RNA Polymerase I TAFs

Holger Beckmann, Jin-Long Chen, Thomas O'Brien, Robert Tjian*

Human ribosomal RNA synthesis by RNA polymerase I requires the activator UBF and the promoter selectivity factor SL1, which consists of the TATA binding protein (TBP) and three associated subunits, TAF_I110, TAF_I63, and TAF_I48. Here it is shown that both TAF_I110 and TAF_I63 contact the promoter, whereas TAF_I48 serves as a target for interaction with UBF and is required to form a transcriptionally active SL1 complex responsive to UBF in vitro. TAF_I48 also alters the ability of TBP to interact with TATA box elements, and the resulting complex fails to support transcription by RNA polymerase II. Thus, TAF_I48 may function both as a target to mediate UBF activation and as a class-specific promoter selectivity factor.

Enhancement of transcription initiation by sequence-specific DNA binding proteins is a principal mechanism for regulating gene expression in animal cells (*1*). Promoter-selective transcriptional activators bind DNA and interact with specific components of the basal transcriptional apparatus in order to modulate gene expression (*2*). For example, some site-specific enhancer binding proteins directly target subunits of the basal transcription factor TFIID, which consists of TBP and at least eight TBP-associated factors called TAF_{II}s (*3–8*). Transcription of the human 18*S* and 28*S* ribosomal RNA genes by RNA polymerase I (RNA Pol I) also requires a TBP-TAF complex called selectivity factor 1 (SL1). All four subunits (TBP, TAF_I48, -63, and -110) are necessary to form an SL1 complex that supports transcription in vitro with purified RNA Pol I and the upstream binding factor, UBF (*9–11*). Consequently, one or more TAFs in the SL1 complex are expected to recognize and bind core promoter DNA, whereas other subunits may be targets for activation by UBF.

To test the activator binding properties of individual TAFs in the SL1 complex, we performed protein-protein binding assays with an affinity resin containing human recombinant UBF (rUBF) (Fig. 1) (*12*). As reported previously, UBF interacts with TBP (*13*). However, TBP alone is unable to support UBF-dependent activation of transcription by RNA Pol I (*11*). We therefore tested each of the TAFs associated with

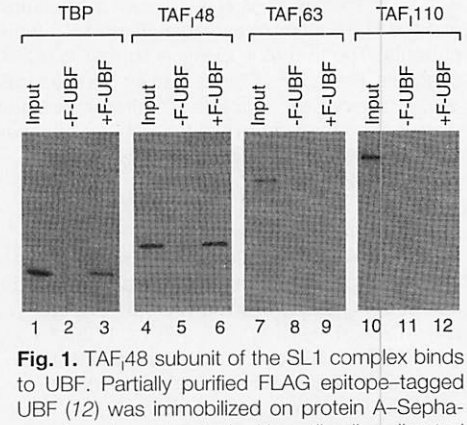

Fig. 1. TAF_I48 subunit of the SL1 complex binds to UBF. Partially purified FLAG epitope–tagged UBF (*12*) was immobilized on protein A–Sepharose beads conjugated with antibodies directed against the FLAG epitope (*10*). This resin (lanes 3, 6, 9, and 12) and resins containing the antibodies but lacking UBF (lanes 2, 5, 8, and 11) were incubated with in vitro ^{35}S-methionine–labeled TBP (lanes 2 and 3), TAF_I48 (lanes 5 and 6), TAF_I63 (lanes 8 and 9), and TAF_I110 (lanes 11 and 12). Bound proteins were resolved by SDS-PAGE and visualized by autoradiography (*10*). Lanes 1, 4, 7, and 10 show 10% of the individual TAFs used in the binding assay.

Howard Hughes Medical Institute, Department of Molecular and Cell Biology, University of California, Berkeley, CA 94720–3204, USA.

*To whom correspondence should be addressed.

SL1 and found that the smallest subunit, TAF_I48, bound efficiently and selectively to the UBF affinity resin (Fig. 1). In contrast, neither TAF_I63 nor TAF_I110 was retained on the UBF resin to a level above background. Thus, TAF_I48 and TBP are potential targets for interaction with UBF.

To test the relevance of the UBF–TAF_I48 interactions, we assembled various TBP-TAF complexes and assessed their ability to mediate UBF-dependent activation (Fig. 2). Transcription reactions supplemented with RNA Pol I and rUBF but no SL1, or reactions containing RNA Pol I and SL1 but no rUBF, produced very low levels of transcription from the human ribosomal promoter (Fig. 2). When either endogenous immunopurified holo SL1 or recombinant SL1 (rSL1) (Fig. 2) was added to these reactions, high levels of transcription were observed. However, when a partial SL1 complex containing TBP-TAF_I63-TAF_I110 but lacking TAF_I48 [rSL1(-48)] (Fig. 2) was added, the level of transcription observed was similar to that found in the absence of endogenous SL1. A triple complex of the three TAF subunits without TBP was also unable to support UBF-dependent transcription (*11*). These results, taken together with the observation that UBF can bind directly to TAF_I48 and TBP, suggest that both TBP and TAF_I48 are required to assemble an active SL1 complex able to mediate UBF-dependent transcriptional activation.

Although human SL1 on its own binds poorly to DNA, it interacts efficiently with the ribosomal RNA (rRNA) promoter in the presence of UBF (*14*). Upon UBF binding to the upstream control element (UCE) of the rRNA promoter, SL1 is recruited to the template DNA and interacts selectively with an upstream region, which produces an extended footprint pattern (*14*) (Fig. 3A). To test the DNA binding properties of a rSL1(−48) complex, we carried out deoxyribonuclease I (DNase I) protection experiments. In the absence of SL1, binding of UBF to the UCE resulted in a defined protected region (−97 to −115), as well as

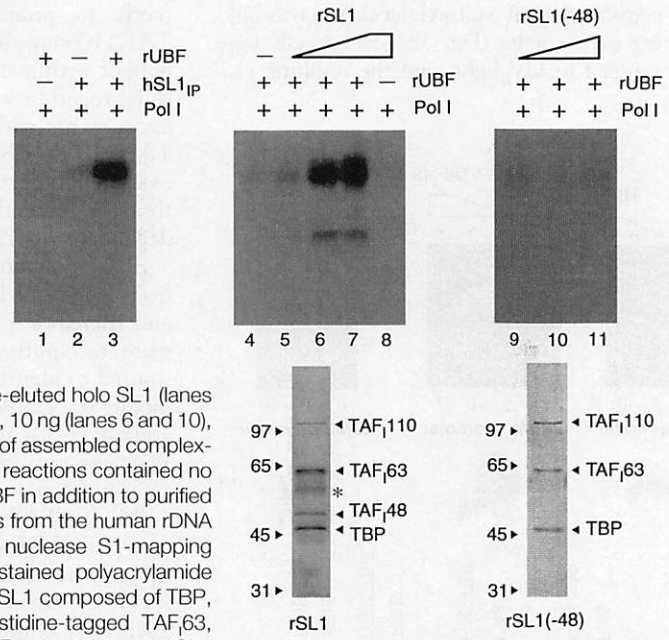

Fig. 2. TAF_I48 is required for transcriptional activation. (**Upper panels**) In vitro transcription reactions used immunopurified and peptide-eluted holo SL1 ($hSL1_{IP}$) derived from HeLa cells (lanes 2 and 3) (*12*), an in vitro assembled quadruple SL1 complex (lanes 5 to 8), or a triple complex lacking TAF_I48 but containing all three SL1 subunits (lanes 9 to 11). Assays contained either ~3 ng of peptide-eluted holo SL1 (lanes 2 and 3) or 5 ng (lanes 5 and 9), 10 ng (lanes 6 and 10), and 20 ng (lanes 7, 8, and 11) of assembled complexes, respectively. Furthermore, reactions contained no (−) or 10 ng (+) of human rUBF in addition to purified RNA Pol I (*12, 26*). Transcripts from the human rDNA promoter were analyzed by nuclease S1-mapping (*11*). (**Lower panels**) Silver-stained polyacrylamide gel of in vitro assembled holo SL1 composed of TBP, FLAG-tagged TAF_I48, polyhistidine-tagged TAF_I63, haemaglutinin (HA)-tagged TAF_I110, and a partial SL1 complex [rSL1(-48)] composed of TBP, polyhistidine-tagged TAF_I63, and HA-tagged TAF_I110. Complexes were built and purified on antibody affinity resin and subsequently eluted with peptides corresponding to the epitopes (*10, 11*). Molecular size standards (in kilodaltons) are indicated on the left. Proteins and traces of immunoglobulin heavy chain (asterisk) are indicated on the right.

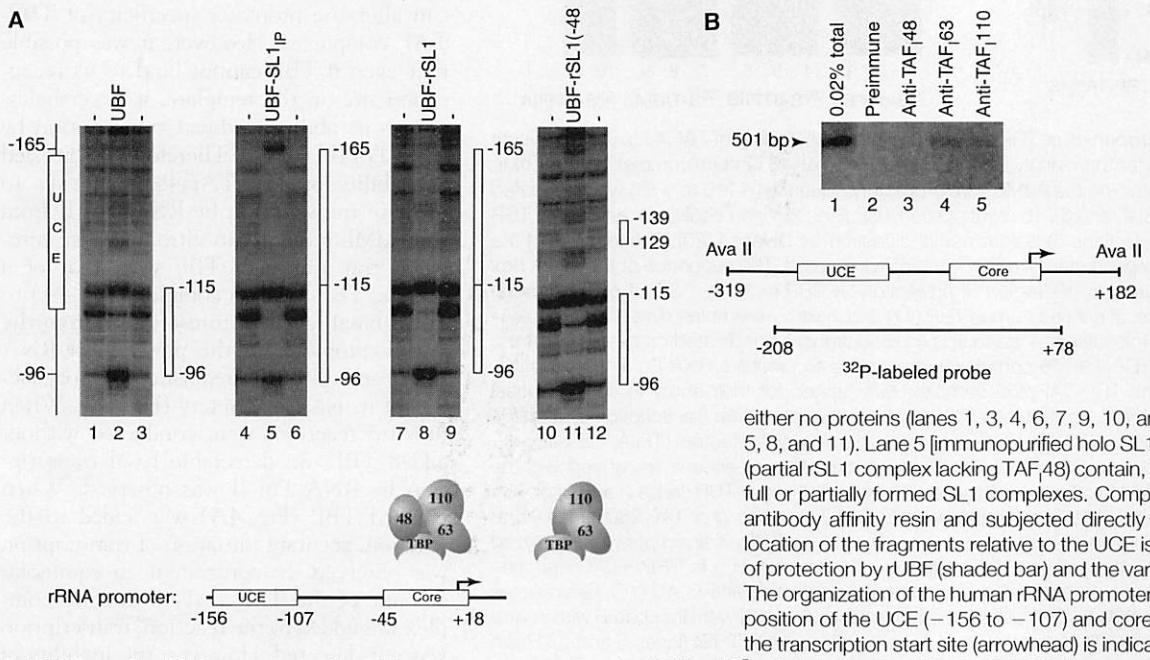

Fig. 3. DNA binding properties of TAF_Is. (**A**) A partial rSL1 lacking TAF_I48 interacts with the human rRNA promoter. DNase I footprint analysis of rUBF, endogenous immunopurified holo SL1 ($SL1_{IP}$), assembled rSL1, and an assembled rSL1(−48) complex on the human rRNA promoter. A DNA fragment containing the ribosomal core promoter sequence [−500 to +78; (*14*)] was incubated with either no proteins (lanes 1, 3, 4, 6, 7, 9, 10, and 12) or purified rUBF (lanes 2, 5, 8, and 11). Lane 5 [immunopurified holo SL1 (*12*)], lane 8 (rSL1), and lane 11 (partial rSL1 complex lacking TAF_I48) contain, in addition to UBF, the indicated full or partially formed SL1 complexes. Complexes were built and purified on antibody affinity resin and subjected directly to footprint reactions (*27*). The location of the fragments relative to the UCE is indicated in addition to regions of protection by rUBF (shaded bar) and the various SL1 complexes (white bar). The organization of the human rRNA promoter is shown schematically and the position of the UCE (−156 to −107) and core region (−45 to +18) relative to the transcription start site (arrowhead) is indicated (*14*). (**B**) Distribution of RNA Pol I TAFs on the rDNA promoter in vivo. HeLa cells, grown to a density of 7.5×10^5 cells/ml, were irradiated with UV light to covalently cross-link protein to DNA. These protein-DNA complexes were purified as described (*28*), restriction digested with endonuclease Ava II, and fragments immunoprecipitated with antibodies directed against each TAF_I (lanes 3 to 5) or preimmune serum (lane 2). The immunoprecipitated DNA fragment was visualized by DNA blot hybridization with a ^{32}P-labeled DNA probe that spans the rDNA promoter. A percentage of the total amount of DNA that was present in the immunoprecipitation reaction is included (0.02%, lane 1). Each immunoprecipitation contains ~150 μg of DNA.

an enhanced cleavage site at position −96 (Fig. 3A). However, when endogenous holo SL1 was present in the reaction with UBF, protected regions covered the entire UCE and extended to position −165 (Fig. 3A). A similar extended footprint was seen with rSL1 (Fig. 3A). In contrast, a rSL1 complex lacking TAF_I48 produced a smaller and weaker pattern of protection (−129 to −139; Fig. 3A). A similar restricted weak footprint was also seen with UBF and a dimeric complex consisting of TBP and TAF_I63 (*12*), suggesting that TAF_I63 can bind directly to promoter DNA sequences. Thus, although complexes lacking TAF_I48 retain some ability to interact with the rRNA promoter, they do so in an altered fashion and are not active transcriptionally.

To determine whether TAF_Is other than TAF_I63 contact promoter DNA directly in the context of a native SL1 complex, we performed in vivo ultraviolet (UV) cross-linking experiments (Fig. 3B). HeLa cells were exposed to UV light, and the resulting protein-DNA adducts were immunoprecipitated with antibodies to TAF_I. After immunoprecipitation with antibodies specific for TAF_I63 (anti-TAF_I63) and TAF_I110 (anti-TAF_I110), a DNA fragment of the expected size was observed. In contrast, no promoter fragments were immunoprecipitated by control serum or anti-TAF_I48. These experiments support our in vitro finding that TAF_I63 can bind directly to promoter DNA. In addition, TAF_I110 may also be a DNA binding component within the SL1 complex. These results, together with our DNase I footprint experiments with rSL1(−48), suggest that TAF_I110 may be responsible for the fully extended footprint pattern of holo SL1 and that this extended DNA binding may be dependent on TAF_I48 as well as UBF.

RNA Pol I core promoter elements differ from RNA Pol II core promoters (*15*, *16*), and therefore TAFs may control the template recognition properties of TBP. We wanted to identify TAFs in SL1 that could modify the DNA binding properties of TBP and target SL1 to the RNA Pol I promoter. Whereas purified TBP alone produced a clear protected region centered around the AdML TATA box, TBP in a dimeric complex with TAF_I48 was unable to bind and protect the TATA box (Fig. 4A). In contrast, TBP in a complex with TAF_I63 or TAF_I110 can interact with TATA sequences (*12*). These results suggest that binding of TAF_I48 to TBP alters the ability of TBP to either recognize or bind to cognate TATA box sites.

On the basis of these binding studies, one might hypothesize that class-specific TAFs can alter the promoter specificity of TBP-TAF complexes. However, it was possible that even if TBP cannot bind to its recognition site on the template, it nevertheless retains its ability to direct transcription by RNA Pol II (*16*, *17*). Therefore, we assessed the ability of TBP-TAF_I48 complexes to mediate transcription by RNA Pol II from the AdML promoter in vitro. First, we compared the ability of TBP with that of a dimeric TBP-TAF_I48 complex (Fig. 4A) to direct basal levels of transcription from the AdML promoter in the presence of RNA Pol II and all of the requisite accessory factors of its basal machinery (Fig. 4B). When in vitro reactions were conducted without added TBP, no detectable basal transcription by RNA Pol II was observed. When purified TBP (Fig. 4A) was added to the reaction, accurate initiation of transcription was observed. In contrast, if an equimolar amount of the TBP-TAF_I48 dimeric complex was added to the reaction, transcription was not detected. However, the inability of a TBP-TAF_I48 dimeric complex to direct transcription was restored by addition of an excess of free TBP to reactions containing these dimeric complexes (Fig. 4B). As a

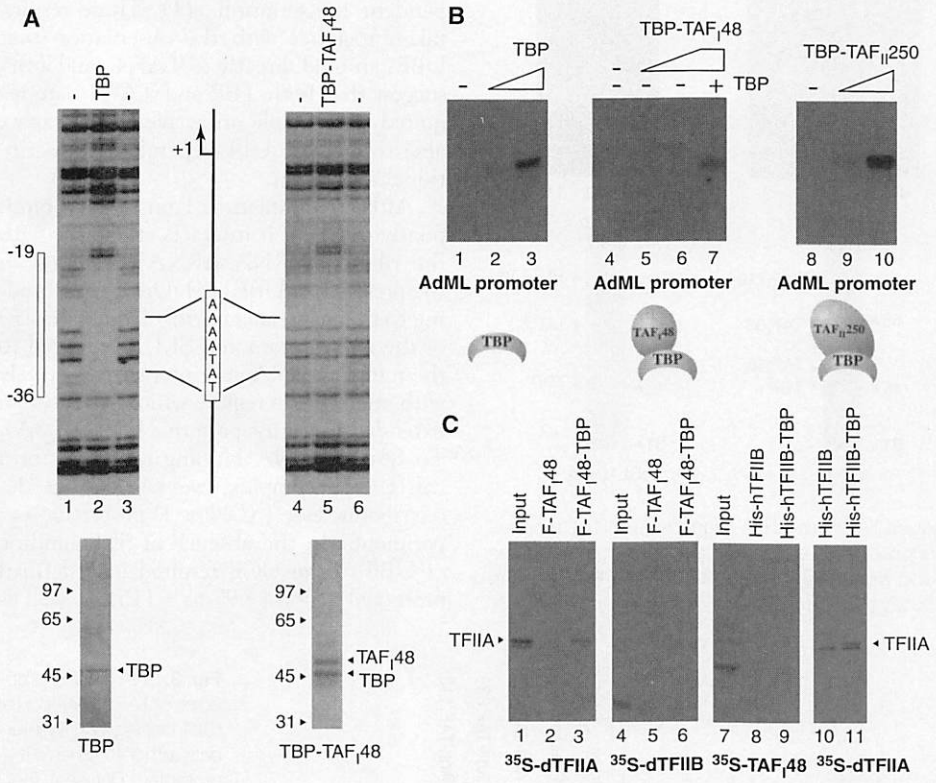

Fig. 4. TAF_I48 modulates the properties of TBP. (**A**) (**Upper panels**) Binding of TAF_I48 to TBP prevents TATA-box recognition. DNase I footprint analysis of TBP and TBP-TAF_I48 dimeric complex on the AdML promoter. A DNA fragment containing the AdML core promoter sequence (−116 to +61) was incubated with either no protein (lanes 1, 3, 4, and 6), 15 ng of purified TBP (lane 2), or an equivalent amount of TBP in a dimeric complex with TAF_I48 (lane 5) before partial digestion by DNase I (*20*). The location of the fragments relative to the transcription start site (arrowhead) is indicated. The sequence of the TATA box (−25 to −30) is shown in addition to the region of protection by TBP (−19 to −36). (**Lower panels**) Silver-stained polyacrylamide gel of purified human TBP (*11*) and in vitro assembled dimeric TBP-FLAG–tagged TAF_I48 (*10*) complex. Molecular size standards (in kilodaltons) are indicated on the left. Proteins are indicated on the right. (**B**) TBP-TAF_I48 complexes are unable to promote RNA Pol II transcription. TBP, TBP-TAF_I48 complex, and TBP-$TAF_{II}250$ complex were tested for their ability to support basal levels of transcription from the AdML promoter by RNA Pol II in a human in vitro transcription system (*5*). Each reaction contains, in addition to RNA Pol II, all of the requisite accessory factors (TFIIA, -IIB, -IIE, -IIF, and -IIH) essential for transcription by RNA Pol II. Reactions were performed either in the absence of the indicated proteins (lanes 1, 4, and 8) or in the presence of 3 ng and 20 ng of TBP (lanes 2 and 3) or with approximately equimolar amounts of TBP in complex with TAF_I48 (lanes 5 to 7) or $TAF_{II}250$ (lanes 9 and 10). Reactions in lanes 4 to 7 contain in addition no (−) or 20 ng (+) of TBP. Transcripts were analyzed by primer extension (*5*). (**C**) TAF_I48 excludes TFIIB but not TFIIA from binding to TBP. FLAG epitope–tagged TAF_I48 was immobilized on protein A–Sepharose beads containing anti-FLAG (*10*). Resin (lanes 2 and 5) and resins containing a TAF_I48-TBP dimeric complex (lanes 3 and 6) were incubated with in vitro ^{35}S-methionine–labeled *Drosophila* TFIIA (lanes 2 and 3) (*23*) or *Drosophila* TFIIB (lanes 5 and 6). Resin containing polyhistidine-tagged human TFIIB (*25*) (lanes 8 and 10) or a human TFIIB-TBP complex (lanes 9 and 11) (*12*) were incubated with in vitro ^{35}S-methionine–labeled TAF_I48 (lanes 8 and 9) or dTFIIA (lanes 10 and 11). Proteins were resolved by SDS-PAGE and analyzed by autoradiography (*10*). Lanes 1 (dTFIIA), 4 (dTFIIB), and 7 (TAF_I48 show 10% of the individual ^{35}S-methionine–labeled proteins used in the binding assays. The correct size of large dTFIIA subunit is indicated.

control, we assembled a partial TFIID complex containing TBP and $TAF_{II}250$ (*5*, *12*). This dimeric complex, unlike the TBP-TAF_I48 dimer, fully supported basal transcription by RNA Pol II (Fig. 4B). Consistent with these results is the inability of SL1 to substitute for TFIID on RNA Pol II promoters and vice versa (*12*). Taken together, these results establish that TAF_I48 can alter the DNA binding properties of TBP so that it can no longer recognize RNA Pol II core promoter elements.

Our results strongly suggest that the lack of DNA binding of a TBP-TAF_I48 dimer is sufficient to abolish transcriptional activation. However, TBP interacts directly with class II basal factors, TFIIA and TFIIB, and the recruitment of these factors by TBP or TFIID is required to assemble an active RNA Pol II initiation complex (*18*). Therefore, TAF_I48 may also disrupt such class-specific interactions. As a test of this idea, TAF_I48 or TBP-TAF_I48 complexes were tethered to an affinity resin by way of a FLAG-epitope tag on TAF_I48. Radiolabeled TFIIA or TFIIB was incubated with these complexes, and the proteins bound to the resin were analyzed by SDS–polyacrylamide gel electrophoresis (SDS-PAGE) and autoradiography (Fig. 4C). TFIIA does not interact directly with TAF_I48, but bound efficiently to the TBP-TAF_I48 resin. By contrast, TFIIB failed to bind either TAF_I48 or the TAF_I48-TBP complex. We also performed binding assays in which TBP-TFIIB complexes tethered to a resin were mixed with radiolabeled TAF_I48. Under these conditions, TAF_I48 did not bind efficiently to the TBP-TFIIB resin. In contrast, radiolabeled TFIIA bound efficiently to the TFIIB-TBP dimeric complex although it did not interact with TFIIB alone (Fig. 4C). Thus, the interaction of TAF_I48 with TBP precludes TFIIB from binding to TBP. It is possible that TAF_I48 and TFIIB interact with overlapping surfaces on TBP (*19*). Because TFIIA can bind the TBP-TAF_I48 complex, only a subset of interactions between TBP and class II factors appears to be affected.

Here we have studied both the promoter selectivity and UBF binding properties of TAFs associated with the RNA Pol I factor, SL1. We have shown that the presence of TAF_I48 in the SL1 complex is required to mediate transcriptional activation by UBF. Strictly speaking, TAF_I48 should be considered as a slightly different kind of coactivator because it is also required for transcription even in the absence of the activator UBF. For example, TAF_I48 may help position TAF_I110 within the SL1 complex in order to produce an active initiation complex. It is also likely that the TAF_I48 interaction with UBF will further stabilize the weak binding of TAF_I110 to elements of the promoter. Our experiments suggest that both TAF_I63 and TAF_I110 can make DNA contacts when in the SL1 complex. However, unlike a previous in vitro study, our in vivo studies failed to detect any direct DNA binding or contact with TAF_I48 (*20*).

Our results also indicate that a TBP-TAF_I48 complex is unable to bind to TATA boxes. The binding of TAF_I48 to TBP appears to be sufficient to block or conformationally alter the DNA binding surface of TBP in a manner that prevents recognition of the TATA-box element, consistent with the finding that SL1 fails to bind DNA containing TATA sequences (*12*, *21*). Therefore, different TBP-TAF complexes may mediate class-specific protein-protein interactions essential for the formation of active initiation complexes. For example, the inability of SL1 to transcribe RNA Pol II promoters may be due, in part, to the incompatibility between subunits of SL1 and interactions with other class-specific components of the transcription machinery (*22*, *23*). Thus, the promoter-selective and class-specific properties of different TBP-TAF complexes are reminiscent of bacterial σ-factors (*24*). Distinct TBP-TAF complexes can be viewed as multisubunit σ-factors that bind class-specific core promoter elements and interact with the transcriptional initiation complex to direct promoter-specific transcription. Future studies of TAFs, in both the SL1 and the TFIID complexes, should provide more detailed mechanisms responsible for promoter specificity and gene regulation.

REFERENCES AND NOTES

1. P. J. Mitchell and R. Tjian, *Science* **245**, 371 (1989); M. Ptashne, *Nature* **335**, 683 (1988).
2. R. Tjian and T. Maniatis, *Cell* **77**, 5 (1994).
3. T. Hoey *et al.*, *ibid.* **72**, 247 (1993).
4. J. A. Goodrich, T. Hoey, C. J. Thut, A. Admon, R. Tjian, *ibid.* **75**, 519 (1993).
5. J.-L. Chen, L. Attardi, C. P. Verrijzer, K. Yokomori, R. Tjian, *ibid.* **79**, 93 (1994).
6. C. J. Thut, J.-L. Chen, R. Klemm, R. Tjian, *Science* **267**, 100 (1995).
7. C.-M. Chiang and R. G. Roeder, *ibid.*, p. 531.
8. X. Jacq *et al.*, *Cell* **79**, 107 (1994).
9. L. Comai, N. Tanese, R. Tjian, *ibid.* **68**, 965 (1992).
10. L. Comai *et al.*, *Science* **266**, 1966 (1994).
11. J. C. B. M. Zomerdijk, H. Beckmann, L. Comai, R. Tjian, *ibid.*, p. 2015.
12. H. Beckmann and R. Tjian, unpublished results.
13. H. Kwon and M. R. Green, *J. Biol. Chem* **269**, 30140 (1994).
14. R. M. Learned, T. K. Learned, M. M. Haltiner, R. Tjian, *Cell* **45**, 847 (1986); S. P. Bell, R. M. Learned, H.-M. Jantzen, R. Tjian, *Science* **241**, 1192 (1988); S. P. Bell, H.-M. Jantzen, R. Tjian, *Genes Dev.* **4**, 943 (1990).
15. J. A. Goodrich and R. Tjian, *Curr. Opin. Cell Biol.* **6**, 403 (1994); N. Hernandez, *Genes Dev.* **7**, 1291 (1993).
16. S. T. Smale, in *Transcription: Mechanism and Regulation*, R. C. Conaway and J. W. Conaway, Eds. (Raven, New York, 1994), pp. 63–81.
17. B. Tansey, S. Ruppert, R. Tjian, W. Herr, *Genes Dev.* **8**, 2756 (1994).
18. L. Zawel and D. Reinberg, in *Progress in Nucleic Acid Research and Molecular Biology*, W. E. Cohn and K. Moldave, Eds. (Academic Press, San Diego, 1993), pp. 67–108; S. Buratowski, *Cell* **77**, 1 (1994).
19. I. Ha *et al.*, *Genes Dev.* **7**, 1021 (1993).
20. U. Rudloff, D. Eberhard, L. Tora, H. Stunnenberg, I. Grummt, *EMBO J.* **13**, 2611 (1994).
21. C. A. Radebaugh *et al.*, *Mol. Cell. Biol.* **14**, 597 (1994).
22. S. Ruppert and R. Tjian, *Genes Dev.*, in press.
23. K. Yokomori, A. Admon, J. A. Goodrich, J.-L. Chen, R. Tjian, *ibid.* **7**, 2235 (1993).
24. C. A. Gross, M. Lonetto, R. Losick, in *Transcriptional Regulation*, S. L. McKnight and K. R. Yamamoto, Eds. (Cold Spring Harbor Laboratory Press, Cold Spring Harbor, NY, 1992), pp. 129–176.
25. C. P. Verrijzer, J.-L Chen, K. Yokomori, R. Tjian, *Cell* **81**, 1115 (1995).
26. RNA Pol I was purified from HeLa nuclear extract with the following modifications (*9*). Briefly, after heparin agarose chromatography, RNA polymerase fractions (100 mM NaCl) were applied to a DEAE-CL6B ion-exchange column. RNA Pol I activity, eluted at 200 mM NaCl, was size fractionated on an S-300 gel filtration column before chromatography on a MonoS column. RNA Pol I activity elutes at 250 mM NaCl.
27. SL1 complexes were assembled as described with the following modifications (*11*). The triple SL1 complex lacking TAF_I48 was built on hemaglutinin (HA)–tagged TAF_I110 immobilized on protein A–Sepharose resin conjugated with anti-HA. After assembly, stable complexes were eluted with peptides (10 mg/ml) corresponding to the HA epitope. For footprint analysis, polyhistidine-tagged TAF_I63 (*11*) was renatured while still bound to Ni^{2+}-resin. The resin was then incubated with TBP (*11*). After the free TBP was washed away, the dimeric complexes were eluted with 500 mM imidazol [in TM buffer [25 mM tris(hydroxylmethyl)-aminomethane, pH 8; 12.5 mM $MgCl_2$, 100 mM NaCl, 10% (v/v) glycerol]]. After dialysis, the complexes were incubated with HA-110 immobilized on protein A–Sepharose cross-linked to anti-HA in the absence or presence of FLAG-tagged TAF_I48 [which was purified under native conditions from baculovirus-infected SF9 cell extracts and subsequently eluted with peptide (*10*)] to form a triple SL1 complex or complete rSL1 complex, respectively. The immobilized complexes were incubated for 1 hour at room temperature with the labeled promoter fragments that had been preincubated for 30 min with rUBF (*12*). After the unbound DNA was washed away, protein-DNA complexes were subjected directly to DNase I digestion (*15*, *25*). Reactions using endogenous, immunopurified holo SL1 from HeLa nuclear extract (*9*) were performed similarly.
28. T. O'Brien, R. C. Wilkens, C. Giardina, J. T. Lis, *Genes Dev.* **9**, 1098 (1995).

29. We thank J. Goodrich, F. Sauer, C. P. Verrijzer, K. Yokomori for providing reagents; M. Dunaway, J. Goodrich, T. Hoey, D. Rio, F. Sauer, U. Schindler, G. Peterson, C. P. Verrijzer, E. Wang, and J. Zomerdijk for valuable discussions; and D. Barnes for preparing the manuscript. Supported by a Jane Coffin Childs Memorial Fund for Medical Research (H.B.) and in part by an NIH grant (R.T.).

5 June 1995; accepted 11 October 1995

The Evolution of Molecular Computation

Leonard M. Adleman (*1*) and Richard J. Lipton (*2*) describe how molecular computing could be used to solve complex problems by physical selection of the correct sequence string from a single huge library of DNA sequences. However, others (*3*) point out that even a simple 23-node Hamiltonian path problem requires kilogram amounts of DNA. The size of the DNA library needed to solve a 100-node Hamiltonian would approximate the number of particles in the universe (10^{70}).

Does this mean that molecular computing is impractical for solving very complex problems? To answer this question, it is useful to compare molecular computing to natural biological evolution and its experimental derivative, in vitro evolution (*4*, *5*): The process of physical selection of the best sequences from large pools of sequences is similar in both settings. In natural as well as in in vitro evolution, these pools of sequences are relatively small (5×10^9 people on Earth; 10^{15} for aptamers). Yet, selection from such modest populations has yielded the vast complexity of biological DNA sequences. The explanation is that multiple, recursive cycles of selection from small pools can "compute" complex answers that far exceed the capacity of any single library of sequences.

Whereas the published examples of molecular computing focus on selection of a complex answer by screening all of the individuals in a single huge pool of sequences, evolution uses many recursive cycles of selection from pools of modest size. Recursive means that the best (partial) solutions selected from one pool are amplified and mutated to form the next pool. The natural mutation process consists of sexual, homologous recombination, with a low frequency of point mutation. For in vitro evolution, the recombination can be obtained by sexual polymerase chain reaction (*6*). Recursive selection and recombination was shown to be sufficient to "compute" a sharply improved enzyme (*4*).

Consider the difficulty of designing sequences such as the human genome. The human genome codes for approximately 100,000 proteins. Even a small protein of 300 amino acids has a sequence space of 20^{300} or 10^{390} (a "sequence space" being the number of possible sequences of a particular length). How complex would a random library need to be to contain a functional copy of, for example, β-lactamase? It appears that no library can be made large enough to allow one-step selection of an average, functional gene. For example, the size of a library of random sequence DNA needed to obtain a specific 8-bp restriction site, using the naïve algorithm given by Adleman (*1*), is 64,000. To obtain five different 8-bp restriction sites in specific locations would require a library of $(64{,}000)^5$ or 10^{24}, which is too large to be obtained from a single library. But the five sites could efficiently be obtained in five recursive selection cycles from a library of 10^5 to 10^6 bp, selecting for a different restriction site at each of five cycles.

The recursive approach allows one to move rapidly through a vast sequence space, sampling only a small fraction of all the sequences that need to be accessed with a single pool approach (five cycles of 10^6 versus 10^{24}). Only the most promising sequences are selected and used as the basis for further mutagenesis and selection.

Parallel access to a larger number of sequences was regarded as the main advantage of molecular computation over traditional computing (*1*–*3*). For those complex problems where smaller, recursive pools of sequences can be equally or more effective, molecular computation (with evolution) may be less promising than improved genetic algorithms, which simulate the same recursive process of selection and recombination of pools of sequences, but run on existing computers (Fig. 1). In the end, the advantages of the different approaches depend on the ruggedness of the sequence space landscape of each particular problem (*7*).

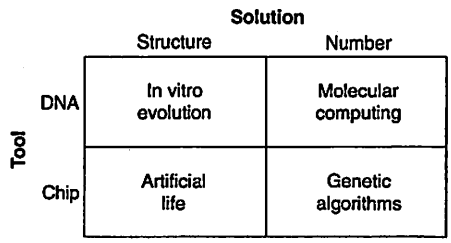

Fig. 1. Applications of evolutionary engineering.

Although DNA sequencing of the selected solutions poses a practical problem for molecular computation, this drawback does not exist for computation with genetic algorithms or for in vitro evolution or computer simulations of natural evolution, called artificial life (Fig. 1).

In summary, sequence evolution appears to be a useful general tool for solving many complex problems, whether the solution is a number, sequence, program, or structure.

Willem P. C. Stemmer
Affymax Research Institute,
4001 Mirando Avenue,
Palo Alto, CA 94304, USA
E-mail: pim_stemmer@qmgates.affymax.com

REFERENCES

1. L. M. Adleman *Science* **266**, 1021 (1994).
2. R. J. Lipton, *ibid.* **268**, 542 (1995).
3. M. Linial and N. Linial, *ibid*, p. 481; Y.-M. D. Lo, K. F. C. Yiu, S. L. Wong, *ibid.*, p. 481; B. Bunow, *ibid.*, p. 482.
4. W. P. C. Stemmer, *Nature* **370**, 389 (1994).
5. D. P. Bartel and J. W. Szostak, *Science* **261**, 1411 (1993).
6. W. P. C. Stemmer, *Proc. Natl. Acad. Sci. U.S.A.* **91**, 10747 (1994).
7. S. A. Kaufmann, *The Origins of Order* (Oxford Univ. Press, New York, 1993).

7 June 1995; accepted 14 September 1995

BOOK REVIEWS

Molecular Pathologies

DNA Repair and Mutagenesis. ERROL C. FRIEDBERG, GRAHAM C. WALKER, and WOLFRAM SIEDE. ASM Press, Washington, DC, 1995. xviii, 698 pp., illus., + plates. $79. New edition of *DNA Repair*.

Living organisms have multiple ways by which they respond to, and mitigate the effects of, damage to their DNA. This revision of a 1985 book by Errol Friedberg details these mechanisms in a manner accessible to students who wish to understand how the system works. The volume also includes an astounding amount of detail, both textual and bibliographic, for the professional who needs to ascertain the current status of an unfamiliar subspecialty. We are indebted to Friedberg and the coauthors of this edition for their careful assembling and evaluation of a vast amount of information.

The text is written from the viewpoint of comparative biochemistry and celebrates a central belief that what is true of *Escherichia coli* is true of elephants. In fact, and as the authors illustrate, elephants are also more complicated than *E. coli*. An already complex mechanism of excision repair in bacteria is made even more so in eukaryotes by the attachment of essential vital functions to some of the repair proteins. But the basic plans remain homologous, and often so do the proteins involved. Human mismatch repair genes were identified because of their homology to yeast and to bacteria.

A description of the known details of the metabolic process made up the 1985 edition of this volume. The discovery that the genic material did not stand permanently aloof from cellular metabolism was a major surprise of the 1950s and '60s. In 1946, when D. E. Lea published his book *Actions of Radiations on Living Cells*, the most productive paradigm was that the genetic material of cells was a target which when hit by a radiation "bullet" immediately, and irreversibly, suffered damage leading to death (or mutation). Insofar as biologists thought that anything as complicated as the properties of a gene could be ascribed to a single chemical structure, that structure was thought to be protein. In the next decade it gradually became clear that genes could be chemically defined as well as modified by mutagens such as mustard gas. The genic material was identified as deoxyribonucleic acid but at first was considered to be exceptionally stable in contrast to the proteins, which isotope studies showed "turned over" at an extraordinary rate. The observation that it was possible to modify physiologically the genetic effects of treatment of cells, as well as to isolate mutants that gave vastly different responses to the absorption of equal amounts of energy, implied that metabolic events intervened between the absorption of radiation and its end effects. Rather than being stable, the DNA was an active participant in the events of cellular biochemistry! By 1985, the major metabolic pathways of DNA repair had been discovered, first in the bacteria and then in mammalian cells.

This new edition details the major discoveries made since 1985 that repair genes in eukaryotes are involved in transcription and that damage in transcribed genes is repaired more efficiently. Also new is the discovery that organisms can sense when their DNA is damaged and delay replication until repair processes have had time to act. The existence of these "checkpoints" as part of control of the cell cycle is a still-developing aspect of the study of DNA repair, hardly mentioned in the text of a decade ago. Throughout the present work we see the insights gained through our ability to look for sequence homologies by comparison of the DNA of different species. Studies on yeast are remarkable predictors of the human system! The current revision has been expanded to include a detailed discussion of the phenomenon of mutation, which has always been thought of as the reverse side of the phenomenon of repair. As with all aspects of molecular biology, the study of mutation has been vastly altered by the ability of investigators to determine the exact sequence of the changes produced, and large sections of this new work are devoted to an attempt to integrate the new information into an understandable framework.

The authors point out that the new findings challenge one of the most cherished ideas in cancer research: the assumption of a necessary connection between DNA damage, DNA repair, mutation, and carcinogenesis. For years the incidence of skin cancer in excision-repair–deficient xeroderma patients has been used as an example of the importance of excision in preventing the mutation that occurs during replication by cells with damaged DNA, and this in turn has been used to connect mutagenesis and carcinogenesis. Consider the surprise of the repair community in discovering a syndrome in which individuals may have low excision repair activities owing to a defect in the same gene producing xeroderma but without the susceptibility to tumors. We may have been misled. Perhaps it is not the excision repair activities of the xeroderma gene that are important but the transcription regulation—or some other factor. This uncertainty is exacerbated by other recent findings. One of the major discoveries of the past few years has been the identification of a colon-cancer susceptibility gene as controlling one of the mismatch repair genes. But studies too recent to be included in this book (R. Parsons *et al.*, *Science* **268**, 738 [1995]) point up the mysterious finding that individuals with almost no mismatch repair activity, whose cells have high mutation rates, do not have the tremendously high cancer incidence that these findings would predict, a fact noted in a recent letter to *Science* by Bryn Bridges (*Science* **269**, 909 [1995]).

Understanding of repair mechanisms comes as a result of studies with different organisms. This truism presents a problem for these authors (or any authors). Is the discussion to be organized by organism or by type of phenomenon? Friedberg *et al.* separate the discussion of prokaryotes and eukaryotes, but properly decide to introduce the best model for double strand break repair when the phenomena that require it are first encountered in a discussion of damage responses in prokaryotes, even though this particular model was developed in yeast. Repair diseases are interesting subjects by themselves, but the analysis of these diseases reflects on the normal condition. The authors seem not quite sure how to deal with this problem. They compromise in a final chapter discussing diseases with defective repair. Much of the material of this chapter is alluded to earlier: for example, data on xeroderma are necessarily included in the discussion of mammalian excision repair genes and proteins in chapter 8. Data on ataxia are included in the section on checkpoints and cell cycle arrest. Most likely this material will be better integrated in the next edition as the molecular biology of the pathology is clarified.

At the end of the book, the authors ignore their own prefatory statement that "in very recent times, progress in the DNA repair and mutagenesis fields has been particularly rapid" and in discussing ataxia telangiectasia imprudently suggest that "progress toward the cloning of the AT gene(s) has been slow and holds no promise for immediate reward at the time of this writing." It may

The Alfred P. Sloan Foundation Technology Series

begins with *Dark Sun, Dream Reaper* and *Turbulent Skies*

Technology. Some people loathe and fear it. Some people love it too much. No matter: the 5.5 billion human beings who inhabit the earth today cannot live without it. To help us understand it, make wise use of it, employ it in ways that enrich, rather than mar, our lives and our planet, the Sloan Foundation is launching a series of distinguished books—at once authoritative and engrossing—for the general reader. The first three follow.

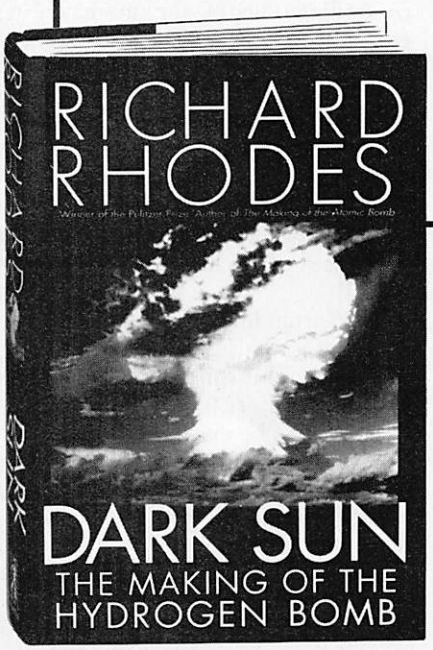
RICHARD RHODES
Winner of the Pulitzer Prize: Author of The Making of the Atomic Bomb
DARK SUN
THE MAKING OF THE HYDROGEN BOMB

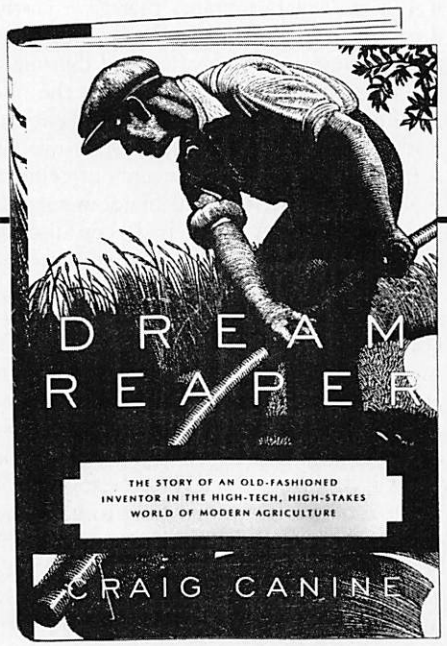
DREAM REAPER
THE STORY OF AN OLD-FASHIONED INVENTOR IN THE HIGH-TECH, HIGH-STAKES WORLD OF MODERN AGRICULTURE
CRAIG CANINE

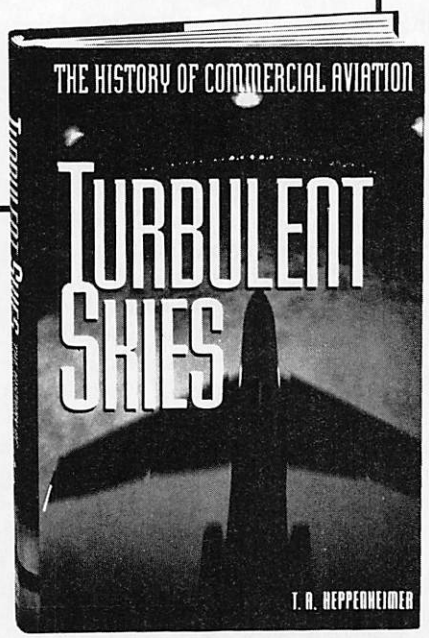

Richard Rhodes tells the secret story—scientific, technological and political—behind the hydrogen bomb.

The Pulitzer Prize-winning author of *The Making of the Atomic Bomb* tells an essential story—a cautionary tale of mythic proportions—of the technological era.

"A book of formidable range...melding previous scholarship with an abundance of fresh material...written with a sharp eye for anecdote, character and political context... brilliantly rich and vivid."
—New York Times Book Review

SIMON & SCHUSTER

Craig Canine lets us share the savvy and the suspense—through 13 years—of a contemporary American inventor.

His story—of a Kansas farmer whose invention may someday change the way grain is harvested throughout the world—illuminates America's agricultural history.

"Can a farm machine seem as vivid as a character in a story? The Bi-Rotor reaper does, as we follow two Kansas cousins and their dream of creating the perfect harvesting machine...A remarkable story of modern farming." —Tony Hiss

KNOPF

T.A. Heppenheimer shows us how America's $200 billion aviation industry was born and took flight.

The fascinating story—from the end of World I to the present—of daredevils and innovators, of the power of big business, and the awe-inspiring achievements of modern technology.

"An important addition to the history of technology as well as business. [The author] is as gifted at explaining the development of the jet engine as he is at tracing the rise and triumph of the aircraft industry over ground transport."–Publishers Weekly

WILEY

"The launch of the Sloan Series is an important and exciting event."
—Richard Preston, author of *The Hot Zone*

Circle No. 40 on Readers' Service Card

be that this statement alone guaranteed the successful cloning of the AT gene which occurred just a few months after the publication of the book (K. Savitsky *et al.*, *Science* **268**, 1749 [1995]). Studies on DNA repair and mutation are indeed proceeding rapidly. What is impressive is how well Friedberg, Walker, and Siede have done in presenting an overall point of view that will remain useful even as new details are added.

Bernard S. Strauss
Department of Molecular Genetics and Cell Biology, University of Chicago, Chicago, IL 60637, USA

■

Geocrystallography

Physics and Chemistry of Earth Materials. ALEXANDRA NAVROTSKY. Cambridge University Press, New York, 1994. xiv, 417 pp., illus. $79.95 or £55; paper, $34.95 or £22.95. Cambridge Topics in Mineral Physics and Chemistry, 6.

As new technological materials become increasingly complex in structure and bonding, they are beginning to resemble the materials that make up our planet. Perovskite-type crystals are a case in point, defining the structures of both the high-temperature superconductors and the predominant mineral of the Earth. Such novel materials as fullerenes and chemical-vapor-deposition diamond have even been found in rocks and meteorites millions of years old. Thus materials scientists have more in common with geologists than ever before.

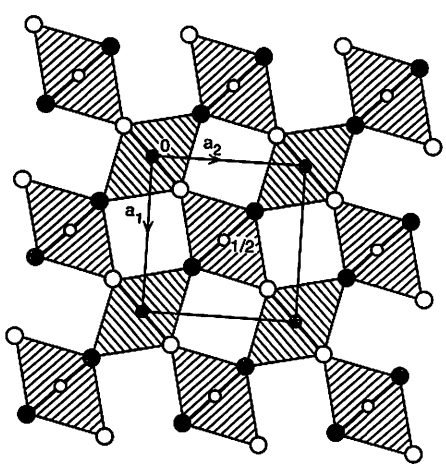

"The structure of rutile, TiO_2. The tetragonal structure consists of edge-sharing chains of TiO_6 octahedra running parallel to the *c*-axis. Octahedra in adjacent chains are joined at their corners. This polyhedral representation is a projection down the *c*-axis, parallel to the chains. The shaded symbols are atoms at a *z*-coordinate of 0, and the open circles are at $z = 1/2$. The unit cell is outlined." [From *Physics and Chemistry of Earth Materials*]

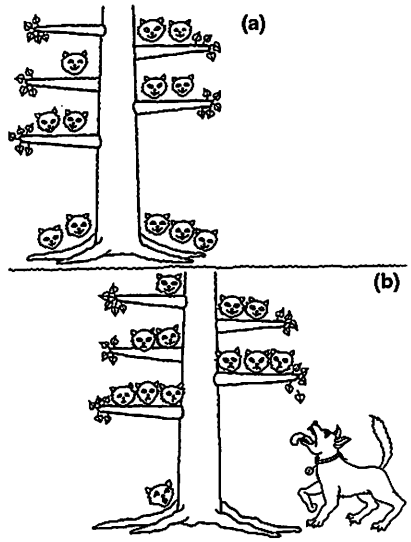

"Schematic of a population inversion. (a) Without an external driving force, the particles (cats) are distributed in the lower-lying energy levels (branches) according to the Boltzmann distributions. (b) With external pumping of energy (dog), the particles populate higher energy states (higher branches) more than lower ones. Lasing action may be likened to an upper branch breaking, returning its occupants to their ground state in a coherent pulse." [*From Physics and Chemistry of Earth Materials*]

Physics and Chemistry of Earth Materials is a unique monograph at the interface between the disciplines. Written by one of the leaders in combining mineralogical and materials research, it illustrates how basic approaches of materials science, solid-state chemistry, and condensed-matter physics can be used to understand what makes up our planet, and maybe even how it works on the inside. One might characterize the book as "elementary" in that it contains few equations, derivations, or details of the underlying physics. Yet it touches on many of the key concepts, as well as the experimental and theoretical methods used in current materials research.

One of the high points of the book is the extensive chapter on crystal chemistry, which contains a superb discussion of how complex crystal structures are related. The rich diversity of both earthly and superconducting perovskite-like crystals is described, as are defect, modulated, and biopyribole-type structures. Insights attained through years of research are incorporated into these pages, and it is vintage Navrotsky to use spinel as a recurring theme throughout the book: this deceptively simple (cubic) crystal structure accommodates a great variety of complexity, including crystallographic disorder, nonstoichiometry, and variable valences.

The overview of chemical bonding is pleasing in the comparisons made between the "chemist's" (molecular, real space) and "physicist's" (infinite crystal, reciprocal space) traditional approaches, but the discussion of theoretical methods now available is less satisfying; though it is useful to have short definitions of the numerous acronyms plaguing theorists, the underlying approximations are not really clarified. Still, the point is well made that simple geometrical models of crystals, such as ionic radii and Pauling rules, remain useful, even in this day of sophisticated "first-principles" calculations.

I have found that the book can work well with two very different audiences: geology or materials students being introduced to modern methods and concepts of materials science, and the more experienced materials researchers, who can enjoy seeing revealed the close analogies between their work and current studies of our planet.

Raymond Jeanloz
Department of Geology and Geophysics, University of California, Berkeley, CA 94720–4767, USA

■

Books Received

Advanced Engineering Dynamics. Jerry H. Ginsberg. 2nd ed. Cambridge University Press, New York, 1995. xvi, 462 pp., illus. $74.95.

Advanced Methods of Pharmacokinetic and Pharmacodynamic Systems Analysis. Vol. 2. David Z. D'Argenio, Ed. Plenum, New York, 1995. x, 217 pp., illus. $75. From a workshop, Los Angeles, May 1993.

Beyond Prejudice. The Moral Significance of Human and Nonhuman Animals. Evelyn B. Pluhar. Duke University Press, Durham, NC, 1995. xxi, 371 pp. $49.95; paper, $19.95.

Biochemistry and Molecular Biology of Fishes. Vol. 4, Metabolic Biochemistry. P. W. Hochachka and T. P. Mommsen, Eds. Elsevier, New York, 1995. xiv, 515 pp., illus. $232.25 or Dfl. 395.

Chemists' Views of Imaging Centers. Ali M. Emran, Ed. Plenum, New York, 1995. xiv, 537 pp., illus. $129.50. From a symposium, Chicago, Aug. 1993.

Chernobyl. The Forbidden Truth. Alla Yaroshinskaya. University of Nebraska Press, Lincoln, 1995. xxii, 136 pp., illus. $25; paper, $10. Translated from the Russian by Michèle Kahn and Julia Sallabank. Reprint, 1994 ed.

The Day Before America. William H. MacLeish. Houghton Mifflin, Boston, MA, 1995. x, 277 pp., illus. Paper, $11.95. Reprint, 1994 ed.

Democracy, Dialogue, and Environmental Disputes. The Contested Languages of Social Regulation. Bruce A. Williams and Albert R. Matheny. Yale University Press, New Haven, CT, 1995. xii, 256 pp., illus. $32.50.

The Ecology of the Chernobyl Catastrophe. Scientific Outlines of an International Programme of Collaborative Research. V. K. Savchenko. UNESCO, Paris, and Parthenon, New York, 1995. xx, 200 pp., illus. $85 or £48. Man and the Biosphere, vol. 16.

The Ecology of Tropical Food Crops. M. J. T. Norman, C. J. Pearson, and P. G. E. Searle. 2nd ed. Cambridge University Press, New York, 1995. x, 430 pp., illus. $69.95; paper, $29.95.

Field Penetration and Magnetization of High Temperature Superconductors. Anant Narlikar, Ed. Nova, Commack, NY, 1995. xviii, 445 pp., illus. $97. Studies in High Temperature Superconductors, vol. 14.

Final Report. Advisory Committee on Human Radiation Experiments. U.S. Government Printing Office,

Vignettes: Interpretative Seismology

In southern Chile a legend describes how earthquakes are due to the fights between two big snakes, Cai-cay, mistress of the waters, and Tre-treg, who fills with stones the hole Cai-cay digs to store her waters. Snakes responsible for earth tremors appear in the Greco-Roman tradition and in early medieval Italian palimpsests. In ancient China the winged dragon-snake Lung shook the earth and in India an elephant was believed to be the cause of seismic tremor. A giant bull shook the earth on its horns in the Caucasus and the Hebrews made a bull responsible for their seismic catastrophes, just as the bull of Knossos shook the island of Crete. In Kamchatka, a peninsula off the Siberian coast, earthquakes were believed to be caused by a subterranean dog and in Mexico by a jaguar. A subterranean frog or fish caused the local earthquakes in central Asia and an underworld goddess was the originator of earthquakes in Babylon.

—*Matthys Levy* and *Mario Salvadori*, in *Why the Earth Quakes* (Norton)

Every time there is an earthquake in California, I stare at my fingernails. It is about the only time I have anything like a deep communion with those hardened hunks of clear, dead tissue. As the television shows pictures of bridges collapsed and cars crushed into slabs, I regard those keratin-filled first cousins of hair and silently intone to myself a science writer's mantra:

SanFranciscoismovingnorthwardatthespeedfingernailsgrowinayear.
SanFranciscoismovingnorthwardatthespeedfingernailsgrowinayear.

—*Stephen Strauss*, in *The Sizesaurus* (Kodansha)

Washington, DC, 1995. xii, 925 pp. Paper, $44.

The Gamma Ray Sky with Compton GRO and SIGMA. M. Signore, P. Salati, and G. Vedrenne, Eds. Kluwer, Norwell, MA, 1995. xiv, 421 pp., illus. $192 or £124 or Dfl. 295. NATO ASI Series C, vol. 461. From an institute, Les Houches, France, Jan.–Feb. 1994.

Genes, Blood, and Courage. A Boy Called Immortal Sword. David G. Nathan. Belknap Press of Harvard University Press, Cambridge, MA, 1995. xii, 276 pp., illus. $24.95.

Haemophilus, Actinobacillus*, and *Pasteurella. W. Donachie, F. A. Lainson, and J. C. Hodgson, Eds. Plenum, New York, 1995. viii, 245 pp., illus. $85. From a conference, Edinburgh, July-Aug. 1994.

The Handbook of Brain Theory and Neural Networks. Michael A. Arbib, Ed. MIT Press, Cambridge, MA, 1995. xvi, 1118 pp., illus. $175; until 30 Sept., $150.

The Immortal Fire Within. The Life and Work of Edward Emerson Barnard. William Sheehan. Cambridge University Press, New York, 1995. xiv, 429 pp., illus. $49.95.

The Immune Functions of Epidermal Langerhans Cells. Heidrun Moll. Springer-Verlag, New York, and Landes, Austin, TX, 1995 (distributor, CRC Press, Boca Raton, FL). xvi, 193 pp., illus. $89. Medical Intelligence Unit.

Inside the Tornado. Marketing Strategies from Silicon Valley's Cutting Edge. Geoffrey A. Moore. HarperBusiness, New York, 1995. xii, 244 pp., illus. $25 or $C35.

Keys to Infinity. Clifford A. Pickover. Wiley, New York, 1995. xviii, 332 pp., illus., + plates. $24.95.

Kimberlites, Orangeites, and Related Rocks. Roger Howard Mitchell. Plenum, New York, 1995. xiv, 410 pp., illus. $89.50.

Land Ecology. An Introduction to Landscape Ecology as a Base for Land Evaluation, Land Management and Conservation. Isaak S. Zonneveld. SPB Academic, Amsterdam, 1995. xii, 199 pp., illus. Paper, $43.75.

Leasing the Ivory Tower. The Corporate Takeover of Academia. Lawrence C. Soley. South End Press, Boston, 1995. vi, 204 pp. $40; paper, $13.

Making the Russian Bomb. From Stalin to Yeltsin. Thomas B. Cochran, Robert S. Norris, and Oleg A. Bukharin. Westview, Boulder, CO, 1995. xvi, 318 pp., illus. $55.

Managing Habitats for Conservation. William J. Sutherland and David A. Hill, Eds. Cambridge University Press, New York, 1995. xii, 399 pp., illus., + plates. $84.95; paper, $29.95.

Mantle and Lower Crust Exposed in Oceanic Ridges and in Ophiolites. R. L. M. Vissers and A. Nicolas, Eds. Kluwer, Norwell, MA, 1995. vi, 214 pp., illus. $115 or £72 or Dfl. 155. Petrology and Structural Geology, vol. 6. From a symposium, Strasbourg, Spring 1993.

Naturally-Produced Organohalogens. Anders Grimvall and Ed W. B. de Leer, Eds. Kluwer, Norwell, MA, 1995. xiv, 437 pp., illus. $177.50 or £112.50 or Dfl. 250. Environment and Chemistry, vol. 1. From a conference, Delft, The Netherlands.

The Nature of the Outer Banks. Environmental Processes, Field Sites, and Development Issues, Corolla to Ocracoke. Dirk Frankenberg. University of North Carolina Press, Chapel Hill, 1995. xvi, 157 pp., illus. Paper, $14.95.

Neurobiological and Clinical Consequences of Stress. From Normal Adaptation to Post-Traumatic Stress Disorder. Matthew J. Friedman, Dennis S. Charney, and Ariel Y. Deutch, Eds. Lippincott-Raven, Philadelphia, 1995. xxiv, 551 pp., illus. $129.

Oncogene Techniques. Peter K. Vogt and Inder M. Verma, Eds. Academic Press, San Diego, 1995. xxxii, 703 pp., illus. $99. Methods in Enzymology, vol. 254.

1001 Questions Answered About the Mineral Kingdom. Richard M. Pearl. Dover, New York, 1995. x, 326 pp., illus. Paper, $8.95. Reprint, 1968 ed.

PCR Strategies. Michael A. Innis, David H. Gelfand, and John J. Sninsky, Eds. Academic Press, San Diego, 1995. xvi, 373 pp., illus. $79.95; spiralbound, $39.95.

The Penguins. Spheniscidae. Tony D. Williams. Oxford University Press, New York, 1995. xiv, 295 pp., illus., + plates. $60. Bird Families of the World, 2.

Quantum Communications and Measurement. V. P. Belavkin, O. Hirota, and R. L. Hudson, Eds. Plenum, New York, 1995. xii, 532 pp., illus. $135. From a workshop, Nottingham, UK, July 1994.

Quantum Electrodynamics with Unstable Vacuum. V. L. Ginzburg, Ed. Nova, Commack, NY, 1995. x, 247 pp., illus. $89. Proceedings of the Lebedev Physics Institute, Academy of Sciences of Russia, vol. 220.

Radiation in Our Environment. Walter Lee. Faun, Baltimore, 1995. xvi, 172 pp., illus. Paper, $9.95.

Radiobiological Disasters. Consequences of Accidents at Nuclear Power Stations. E. B. Burlakova, Ed. Nova, Commack, NY, 1995. x, 267 pp., illus. $89. From a conference, Moscow, June 1991.

Satellite Meteorology. An Introduction. Stanley Q. Kidder and Thomas H. Vonder Haar. Academic Press, San Diego, 1995. x, 466 pp., illus. $54.95.

Schneider on Schneider. The Conversion of the Jews and Other Anthropological Stories. David M. Schneider as told to Richard Handler. Duke University Press, Durham, NC, 1995. x, 242 pp. + plates. $44.95; paper, $14.95.

Science and Culture. Popular and Philosophical Essays. Hermann von Helmholtz. David Cahan, Ed. University of Chicago Press, Chicago, 1995. xviii, 418 pp., illus. $52 or £41.50; paper, $17.95 or £14.25.

The Synergy Between Dynamics and Reactivity at Clusters and Surfaces. Louis J. Farrugia, Eds. Kluwer, Norwell, MA, 1995. viii, 368 pp., illus. $184 or £114 or Dfl. 255. NATO ASI Series C, vol. 465. From a workshop, Drymen, UK, July 1994.

T-Cell Receptor Use in Human Autoimmune Diseases. Mark M. Davis and Joel Buxbaum, Eds. New York Academy of Sciences, New York, 1995. xiv, 464 pp., illus. $175. Annals of the New York Academy of Sciences, vol. 756. From a conference, San Diego, April 1994.

Thrips Biology and Management. Bruce L. Parker and Margaret Skinner, Eds. Plenum, New York, 1995. xvi, 636 pp., illus. $145. NATO ASI Series A, vol. 276. From a workshop, Burlington, VT, Sept. 1993.

Understanding Enzymes. Trevor Palmer. 4th ed. Prentice Hall/Ellis Horwood, New York, 1995. xx, 398 pp., illus. Paper, $65.33.

The Universal Turing Machine. A Half-Century Survey. Rolf Herken, Ed. 2nd ed. Springer-Verlag, New York, 1995. xvi, 611 pp., illus. Paper, $49.

Vaccines 95. Molecular Approaches to the Control of Infectious Diseases. Robert M. Chanock *et al.*, Eds. Cold Spring Harbor Laboratory Press, Cold Spring Harbor, NY, 1995. xxii, 441 pp., illus. Paper, $100. From a meeting, Oct. 1994.

Viral Vectors. Gene Therapy and Neuroscience Applications. Michael G. Kaplitt and Arthur D. Loewy, Eds. Academic Press, San Diego, 1995. xxviii, 486 pp., illus. $90; spiralbound, $49.95.

What Is Life? Lynn Margulis and Dorion Sagan. Simon and Schuster, New York, 1995. 208 pp., illus. $40.

Who Will Feed China? Wake-Up Call for a Small Planet. Lester R. Brown. Norton, New York, 1995. 165 pp., illus. $19.95 or $C25.99; paper, $8.95. Worldwatch Environmental Alert.

Why the Earth Quakes. Matthys Levy and Mario Salvadori. Norton, New York, 1995. 215 pp., illus. $25.

"You Do Teach Atoms, Don't You?" A Case Study in Breaking Science Curriculum Gridlock. Lyman Lyons and Susan Bolyard Millar. LEAD Center, Madison, WI, 1995. xii, 79 pp., illus. Paper, $10.

Publishers' Addresses

Below is information about how to direct orders for books reviewed in this issue. A fuller list of addresses of publishers represented in *Science* appears in the issue of 26 May 1995, page 1220.

ASM (American Society for Microbiology) Press, 1325 Massachusetts Ave., NW, Washington, DC 20005. Phone: 202-737-3600. Fax: 202-942-9342.

Cambridge University Press, 110 Midland Ave., Port Chester, NY 10573–4930. Phone: 800-872-7423; 914-937-9600. Fax: 914-937-4712.

PRODUCTS & MATERIALS

Graphing Software

GraphPad Prism is software that plots, graphs, and helps analyze data. Analysis methods include nonlinear regression (curve fitting), spline curves, area under the curve, frequency distribution, statistics by row or column, and survival curves. There are also commands for manipulating data. The plots, graphs, analysis, and page layouts are all kept in a single file and displayed in a single window. The program runs under Microsoft Windows. **SoftShell. Circle 137.**

Embedding Kits

A new line of embedding media for microscopy and histology includes cold curing kits for materials science; ultraviolet low temperature kits for immunolabeling, in situ hybridization, and histochemistry; and high resolution microscopy kits. **Electron Microscopy Sciences. Circle 138.**

Nonenzymatic Cell Recovery

MatriSperse Cell Recovery Solution is a nonenzymatic method to recover cells cultured on Matrigel Matrix. Matrigel Matrix has widespread use to enhance differentiated functions of many cell types in vitro. With the new solution, a matrix-free suspension can be easily obtained by depolymerizing the Matrigel Matrix for 1 hour at 4°C. The short incubation period at a low temperature minimizes intracellular biochemical changes during cell recovery, and the nonenzymatic polymerization process avoids digestion of extracellular portions of cell surface receptors and adhesion molecules. The solution can be used to recover cells for subsequent biochemical analyses, particularly of short-lived mRNAs or polypeptides and cell surface molecules. It can also be used to replate cells onto a different matrix or to determine cell numbers. **Becton Dickinson Labware. Circle 139.**

Tissue Fixative

Histochoice MB Tissue Fixative, designed for the molecular biologist, is formulated to preserve antigenic sites for antibody probes and nucleic acid sites for molecular probes. Most fixed sections do not require predigestion or other recovery procedures to make important sites available. It is also a preservative that leaves antigens and nucleic acids in their native state, allowing binding for specific probes. Primary antibodies can often be diluted severalfold due to the increased number of preserved antigenic sites. It can replace formaldehyde-based, alcohol-based, Zenkers, B-5, B-3, Bouin's, and other fixatives. **Amresco. Circle 140.**

Fast Cameras for Calcium Ratio Imaging

The fast readout Capella family of cooled charge-coupled device camera systems are suited to use in calcium ratio imaging experiments. The family offers a wide dynamic range of 4096 to 16,386 gray levels, which is of particular relevance in the neurosciences, where it is important to observe the relationship between calcium fluxes throughout the neuron in order to understand cell signaling and its response to various agonists. In these

Newly offered instrumentation, apparatus, and laboratory materials of interest to researchers in all disciplines in academic, industrial, and government organizations are featured in this space. Emphasis is given to purpose, chief characteristics, and availability of products and materials. Endorsement by *Science* or AAAS is not implied. Additional information may be obtained from the manufacturers or suppliers named by circling the appropriate number on the Readers' Service Card and placing it in a mailbox. Postage is free.

The transcription source

Only Ambion offers five different transcription kits for specific applications

Whether your *in vitro* transcription demands are for high specific activity RNA probes, large mass amounts of RNA, non-radioisotopic RNA probes, end-labeled RNA or large mass amounts of capped RNA, Ambion offers an *in vitro* transcription kit specifically designed to meet your research needs.

Easily prepare high specific activity RNA probes

•

Ultra high yield technology for 10 to 50 times the yield of conventional reactions

•

Produce 5′-Hydroxyl-terminated transcripts

•

Efficiently transcribe small templates with consistent results

•

Easily obtain high yields of capped RNA

Contact us today for information on our full range of transcription kits for specific applications.

(512) 445-6979 (512) 445-7139 FAX

(800) 888-8804

Ambion

Innovative Products for RNA Analysis

Circle No. 34 on Readers' Service Card

TiterMax®

Worldwide Adjuvant of Choice

- High, long-lasting titers
- Reliable alternative to Freunds
- Animal safe
- Antibody specific

In response to our customers' requests, TiterMax is now packaged in 1.0 and 5.0 ml vials, in addition to our 0.5 and 10 ml vials currently sold.

CytRx® CORPORATION
154 Technology Parkway
Norcross, GA 30092
1-800-345-2987 • 1-770-368-9500
Fax: 1-770-447-8875
http://www.cytrx.com/titermax/

For more information or to purchase TiterMax contact one of the following TiterMax Distributors:

- **Canada:** CedarLane Laboratories Ltd., Tel: 800-268-5058, Fax: 905-878-7800
- **Germany:** Serva Feinbiochemica GmbH & Co. KG, Tel: 6221-502-134, Fax: 6221-502-143
- **Italy:** Charles River Italia S.p.A., Tel: 039-509-915, Fax: 039-508-219
- **Japan:** Funakoshi Co., Ltd., Tel: 3-5684-1627, Fax: 3-5684-1775
- **United Kingdom:** Stratech Scientific Ltd., Tel: 0582-481884, Fax: 0582-481895
- **United States:** CytRx Corporation, Tel: 1-800-345-2987, 770-368-9500, Fax: 770-447-8875
  Sigma Immunochemicals, Tel: 800-262-9141, Fax: 314-664-3143

Circle No. 32 on Readers' Service Card

cases the wide dynamic range of the Capella family enables the processes and cell body to be studied simultaneously without the camera being saturated by larger signals from the cell body. **AstroCam. Circle 141.**

■

Protein Modeling Software

The ChemProtein module of Chem-X features powerful homology building of three-dimensional protein models. The software enables the user to build models of partially known proteins using other proteins as templates. Now available for all Chem-X supported platforms, including Windows and Power Macintosh, it is the only desktop homology building software, according to the manufacturer. **Chemical Design. Circle 142.**

■

Two New Polymerases

TaKaRa Ex Taq Polymerase and LA Taq Polymerase are new reagents for polymerase chain reaction (PCR). TaKaRa Ex Taq has an incorporation fidelity four times greater than Taq polymerase. Depending upon the complexity of the DNA target, Ex Taq can produce from 10 to 100 times more product than Taq. It has a processivity rate that allows it to extend normal PCR capability to 10 kilobases or longer without sacrificing yield. LA Taq Polymerase and its buffer are optimized for long PCR from complex genomic targets, such as human genomic DNA. It has a sixfold higher incorporation fidelity than Taq polymerase, making it a good choice for genomic cloning, gene expression, and mutagenesis analysis. It is available in several PCR kits. **Oncor. Circle 143.**

■

Prestained Electrophoresis Standards

Kaleidoscope Prestained Standards are protein standards for electrophoresis and protein immunoblotting. They consist of seven individually colored proteins (6.5 to 200 kD). Every vial includes a lot-specific molecular weight calibration of each protein. They are supplied in a stable sample buffer, so no dilution or aliquoting is necessary when stored at –20°C for up to 1 year. **Bio-Rad Laboratories. Circle 144.**

■

Vacuum Concentrator

Concentrator 5301 is for gentle concentration of DNA, RNA, nucleotides, and proteins as well as for preparing for gel electrophoresis. The user can choose between the basic concentrator model, which can be operated with the user's pump, and the complete system, which is equipped with a maintenance-free, chemical-resistant diaphragm pump. The standard delivery package includes a fixed-angle rotor for 48 2-ml test tubes. The complete system also features an

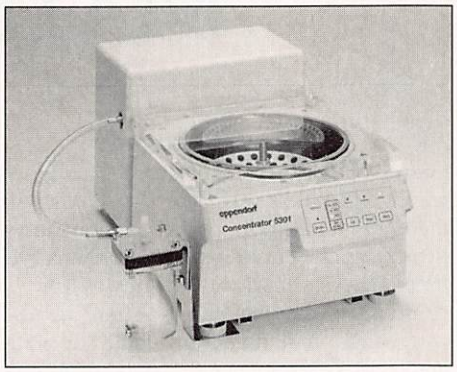

emission condensator that cleans outgoing air up to 85%. For larger numbers of samples, a 72-place rotor is available for 0.5-ml tubes or a 70-place rotor for 2-ml tubes. **Eppendorf. Circle 145.**

■

Literature

The Binding Site 1995/1996 Catalogue contains more than 3000 kits and reagents and describes many new products including human Immunoglobulin G subclass kits for use on various nephelometric/turbidimetric analyzers, isoelectric focusing kits, new antibodies, and more. **The Binding Site. Circle 146.**

Endogen Product Catalog 1995/1996 features more than 200 enzyme-linked immunosorbent assay (ELISA) kits and reagents for immunological research, including 75 new products. New products include human, mouse, and pig cytokine ELISA kits; mouse cytokine MiniKits; human, mouse, rat, and pig cytokines; antibodies to cytokines; and antibodies to human, mouse, and rat cell adhesion markers. **Endogen. Circle 147.**

Integrated GPC/SEC Systems describes new gel permeation chromatography systems. The PL-GPC210 is for ultrahigh temperatures up to 210°C. The PL-GPC110 operates at temperatures up to 110°C. **Polymer Laboratories. Circle 148.**

Electrophoresis 95: Power Supplies and Apparatus Catalog features systems for vertical mini gels and blots, horizontal submarine gels, isoelectric focusing, tube gels, and immunoelectrophoresis and immunodiffusion. **E-C Apparatus. Circle 149.**

Prospekt describes an on-line solid-phase extraction system. It outlines the configurations of the system to fit individual applications. **Spark Holland. Circle 150.**

Whatever the source: Proteinase K will get you to the DNA!

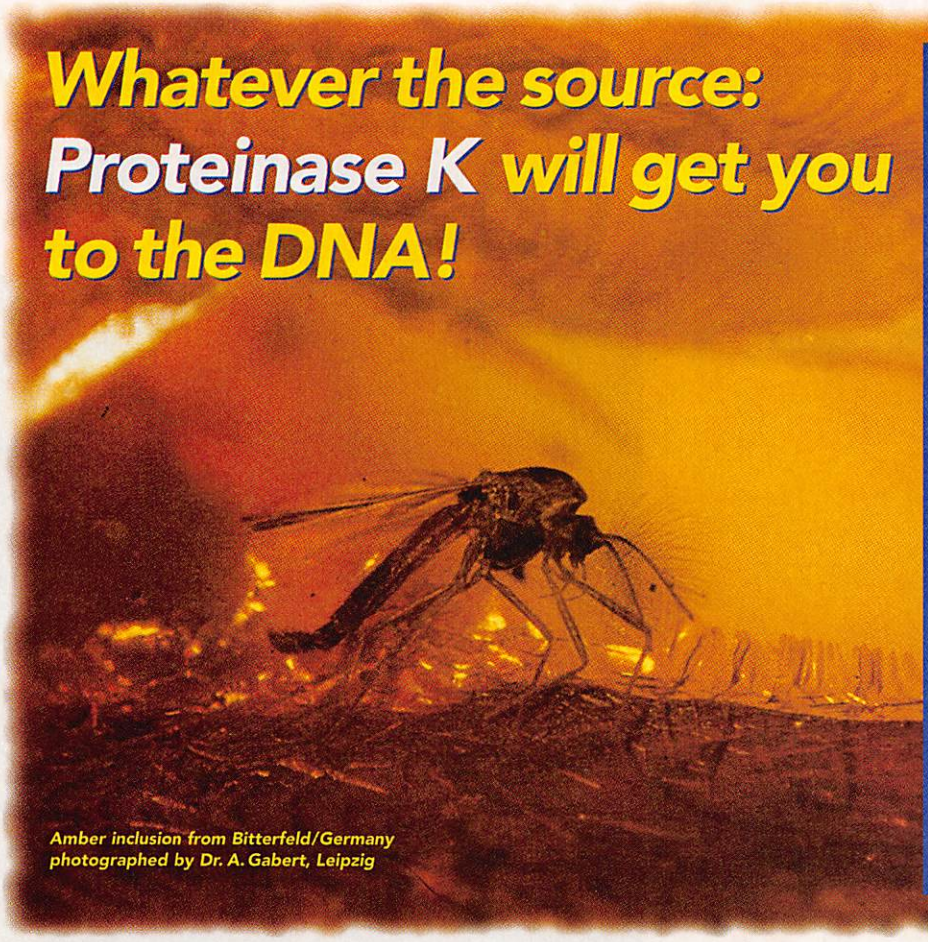

Amber inclusion from Bitterfeld/Germany photographed by Dr. A. Gabert, Leipzig

Since more than 20 years we are the world's largest producer of Proteinase K.

For further information, please call us:

USA:
EM Science
Phone: 1-800-222-0342
Fax: (609) 423-4389

Rest of the World:
Merck KGaA, Darmstadt/Germany
Phone (+49) 6151-72 75 93
Fax: (+49) 6151-72 68 59

Circle No. 23 on Readers' Service Card

AAAS with Pride!

Buy 2 or more sets and receive a 10% Discount

Tree rings and optical tweezers. Circadian rhythms and magnetic fields. The mysteries of science come to life with these colorful, glossy notecards featuring four recent covers of *Science* magazine. Twelve to a set.

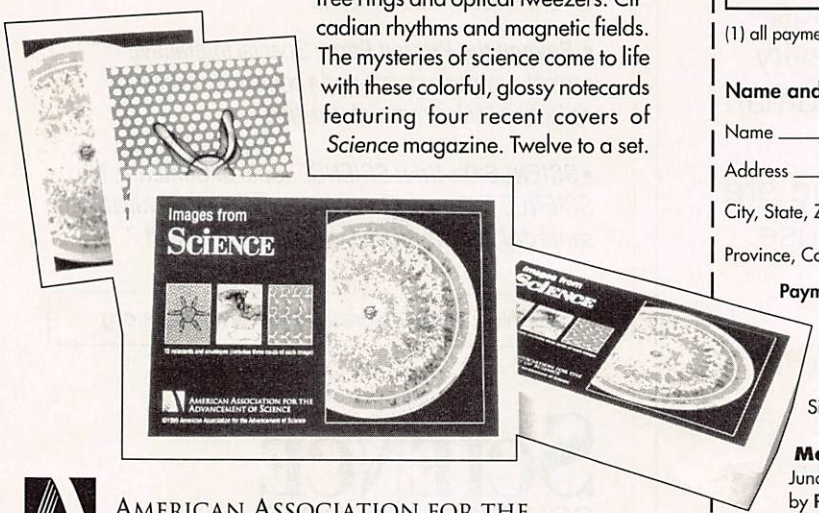

Quantity	Non-Member	Member	Discount	Total
	$13.50	$10.80		
			Subtotal	
			Shipping and handling	$4.00
			DC and California add applicable sales tax	
			For shipments to Canada, add 7% GST tax	
			For foreign air mail, add 25% of subtotal	
			(1) **Total**	

(1) all payments must be made in U.S. dollars

Name and Address *(please print)*

Name _____

Address _____

City, State, Zip Code _____

Province, Country, Postal Code _____

Payment information ☐ Check/Money Order enclosed
☐ MC/Visa Exp. date _____

Credit card number _____

Signature _____

Mail To: AAAS Distribution Center, P.O. Box 521, Annapolis Junction, MD 20701 or **FAX** 301-206-9789, **Credit Card orders** by **Phone** 1-800-222-7809

AMERICAN ASSOCIATION FOR THE ADVANCEMENT OF SCIENCE

UNDERSTANDING ALZHEIMER'S DISEASE

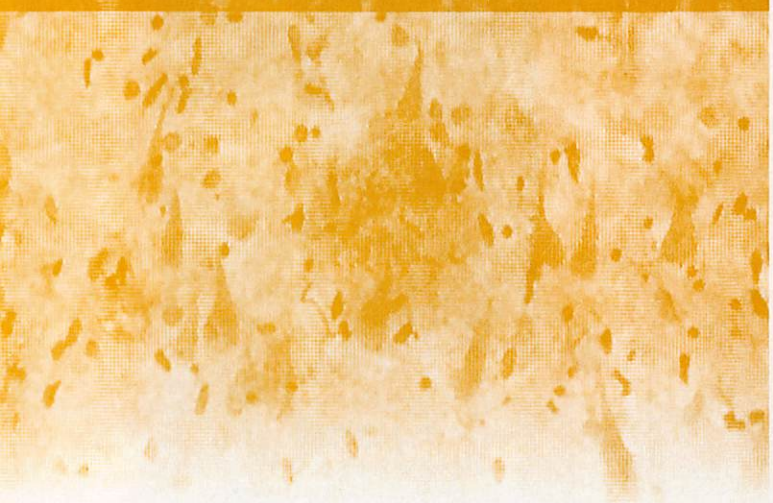

with

Human rApo E2, E3, & E4

From

PanVera Corporation

PanVera's recombinant human apolipoprotein E isoforms are useful biochemical tools for studying the role of Apo E in the progression of Alzheimer's Disease. Recently, Apo E proteins were also suggested to play a role in human longevity and aging. PanVera's recombinant human Apo E2, E3, & E4 are highly purified, retain excellent biological activity, and are individually available for convenient use.

PANVERA

800-791-1400

608-233-5050
Fax: 608-233-3007
E-Mail: info@panvera.com
Home page: http://www.panvera.com/

PanVera Corporation
545 Science Drive
Madison, WI 53711 USA

photo courtesy of Chemicon International, Inc.

Circle No. 30 on Readers' Service Card

SCIENCE ENTERS CYBERSPACE!

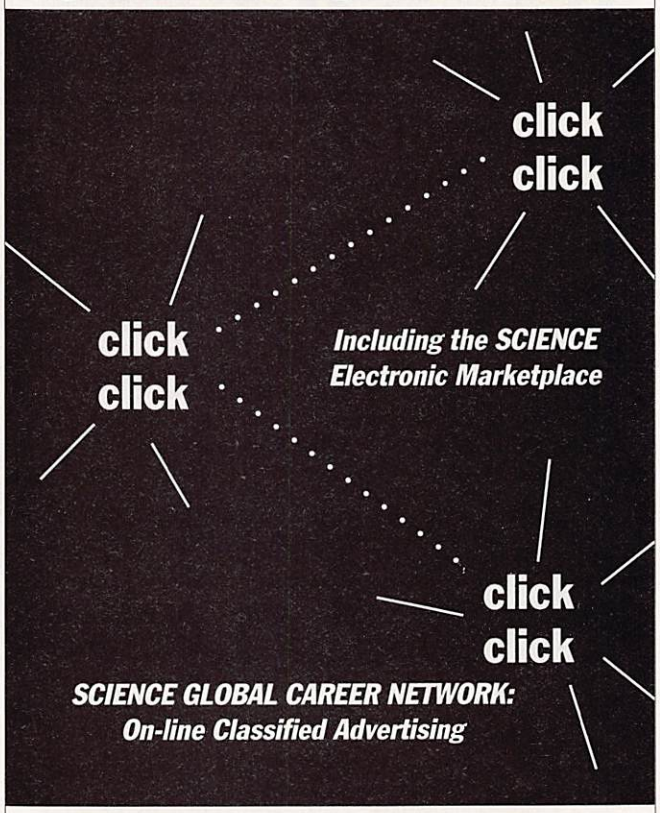

The world of SCIENCE On-line: *Now you can access these exclusive features on the SCIENCE World Wide Web home page with just a click of your mouse:*

- ***SCIENCE Electronic Marketplace:*** *The latest scientific product information from top companies.*
- ***SCIENCE GLOBAL CAREER NETWORK:*** *On-line classified advertising.*
- ***Beyond the Printed Page:*** *Special interactive projects, important data and a constantly evolving collection of electronic information.*
- ***SCIENCE On-line:*** *SCIENCE Table of Contents, the SCIENCE Editorial, This Week in SCIENCE available the same day that the printed version is published!*

SCIENCE WWW Address: ***http://www.aaas.org***

SCIENCE
COVERS THE WORLD

SCIENCE
PERSONNEL PLACEMENT

LINE CLASSIFIED ADVERTISEMENTS

Deadlines: Ads are due by Thursday, 10 a.m., 2 weeks prior to the issue date. *Science* is published each Friday, except the last Friday of the year. Call for holiday deadlines. Ads must be submitted in writing.

How to Submit a Classified Ad:
Prepare double-spaced typewritten copy. Do not include any abbreviations. *Science* will edit and typeset ads according to *Science* guidelines. Include billing information, and desired publication date. Available categories: Positions Open, Meetings, Announcements, Courses and Training, Search Firms. *Science* cannot provide proofs of typeset line ads.

Mail, FAX or Email materials to:
Science Classified Advertising
1333 H Street, N.W., Room 814
Washington, DC 20005
Telephone: 202-326-6555 or 202-326-6534
FAX: 202-682-0816
Internet Email: science_classifieds@aaas.org
(please include telephone number in email correspondences)

Rates: Ads are $43 per line; $430 minimum. One line equals 52 characters and spaces; centered headings equal 32 characters and spaces. A 3% cash discount is granted to all prepaid ads. Line advertisements are not commissionable.

Estimates: *Science* will provide a cost estimate for line ads. This is an approximate cost only. Allow for variation between estimated lines and actual typeset lines and resulting final cost. Purchase orders must allow for some degree of flexibility and/or adjustment.

Ads from Outside the U.S.: A discount of $30 will be offered to advertisers making payment in U.S. dollars by checks drawn on U.S. banks. Contact Debbie Cummings at telephone: +44(0) 1223 302067 or fax: +44(0) 1223 576208.

Credit Cards: *Science* accepts American Express, MasterCard and VISA. Discount does not apply to credit cards.

Cancellations: Deadline for cancellation is 10 a.m., Tuesday,10 days prior to issue date.

DISPLAY PERSONNEL ADVERTISEMENTS

For rates and info. for fractional display ads call:

Bethany Ritchey
Recruitment Display Advertising
Telephone: 202-326-6541
FAX: 202-682-0816

Janis Crowley
Recruitment Advertising Manager
Telephone: 212-496-7704
FAX: 202-682-0816

Debbie Cummings
European Recruitment Advertising
Telephone: +44 (0) 1223 302067
FAX: +44 (0) 1223 576208

Science Global Career Network: Unless otherwise instructed, every classified advertisement submitted for publication in *Science* is automatically posted on *Science*'s on-line classified advertising service, Science Global Career Network, at no additional charge. Science Global Career Network address:
WWW: http://www.aaas.org
Gopher: gopher.aaas.org
Science reserves the right, at its discretion, to edit or decline to publish advertisements submitted to it.

POSITIONS OPEN

FACULTY POSITION
Scripps Institution of Oceanography
Observational Marine Physics

The Scripps Institution of Oceanography (SIO) of the University of California, San Diego (UCSD) invites applications for an **ASSISTANT** or **ASSOCIATE PROFESSOR** (tenure-track or tenured) in observational marine physics. Applicants with an interest in conducting innovative observational work in the marine environment will be given strongest consideration. Fields of interest include, but are not limited to: marine electromagnetics, ocean optics, and the ocean-atmosphere boundary layer. Applicants must hold a Ph.D. degree or equivalent and will be expected to teach and supervise students, primarily at the graduate level, conduct an extramurally funded research program, and participate in the administrative functions of SIO and UCSD. The level and salary will depend upon the experience of the successful applicant and will be based on the UC pay scale. Assistant-level candidates will be expected to show evidence of their potential through letters of recommendation and a publication record appropriate for their experience. Associatel-level candidates must show evidence of a strong research record in their specialization. Closing date for applications: February 15, 1996. Please send a letter of application, curriculum vitae including teaching experience, and the names and addresses of five referees to: **Chair-OMP, SIO Graduate Department, University of California, San Diego, 9500 Gilman Drive, La Jolla, CA 92093-0208.** *UCSD is an Equal Opportunity/Affirmative Action Employer.*

TUFTS UNIVERSITY
JOINT APPOINTMENT
DIRECTOR
Community Health Program
AND ASSISTANT OR ASSOCIATE PROFESSOR
Department of Economics

The Community Health Program and the Department of Economics seek a health economist or a health policy specialist. The position will involve a joint appointment, half time with the Department of Economics and half time as **DIRECTOR** of the Community Health Program, an interdisciplinary course of study for undergraduates. Candidates should have a Ph.D. or equivalent degree in economics or a related discipline and should be tenurable in the Department of Economics. Economics will be the person's disciplinary department. Evidence of successful teaching and research in the economics of health and/or health policy analysis is required, and experience in academic administration is desirable. Appointment will be at an **ASSISTANT PROFESSOR OR ASSOCIATE PROFESSOR** level, depending on the qualifications of the candidate. Applicants should send curriculum vitae and samples of written work and names and addresses of three references to: **Dr. Margery Davies, Administrator, Community Health Program, Tufts University, 112 Packard Avenue, Medford, MA 02155.** The search will continue until the position is filled.

Tufts University is committed to an aggressive program of Equal Opportunity and Affirmative Action. Candidates are encouraged to identify their status in their cover letters.

INVERTEBRATE ZOOLOGIST

Wabash College seeks an invertebrate zoologist with a strong field and ecological orientation. **TENURE-TRACK POSITION** in accord with College's guidelines and review procedures. Ph.D. required and teaching experience is desirable. The Biology Department, with seven full-time faculty positions, encompasses molecular biology, organismal biology, and population biology. We seek a person with abilities and interests at the ecological level. Responsibilities include teaching a modern course in invertebrate zoology, participating in general biology courses, and periodic contributions to all-college interdisciplinary courses. Development of a research program involving undergraduates is expected. An endowed fund provides a summer research stipend during the first two years, and start-up funds for research are available. Send letter of application, curriculum vitae, brief statement of research and teaching interests, and three letters of recommendation by January 8, 1996, to: **David T. Krohne, Chair, Biology Department, Wabash College, P.O. Box 352, Crawfordsville, IN 47933.** Questions may be directed to: **Krohned@Wabash.edu.** *Wabash College, a liberal arts college for men, encourages women and minorities to apply. Equal Opportunity Employer.*

POSITIONS OPEN

UNIVERSITY OF Miami
SCHOOL OF MEDICINE

FACULTY POSITIONS in Molecular Immunology. The Department of Microbiology and University of Miami has tenure-track faculty positions at the Assistant or Associate Professor level open for molecular immunologists. We are particularly interested in individuals that examine cellular signaling, transcriptional regulation or molecular mechanisms related to lymphocyte activation, development, or apoptosis. The chief criteria for a candidate is proven excellence in research and the potential to develop an externally funded research program. Quality research facilities, generous start-up funds, and salary will be made available to the successful candidates. Interested individuals are invited to write a letter of intent and enclose a curriculum vitae, list of publications, description of future research plans, and names of three references to: **Chairman, Molecular Immunology Search Committee, Department of Microbiology and Immunology, University of Miami School of Medicine, P.O. Box 016960 (R-138), Miami, FL 33101.** *Equal Opportunity/Affirmative Action Employer.*

ENVIRONMENTAL RISK ANALYSIS AND POLICY

The Yale University School of Forestry and Environmental Studies seeks to make a **TENURED** appointment in the field of Environmental Risk Analysis and Policy. This individual will be expected to develop and maintain an active teaching and research program in the policy dimensions of environmental health risk. Research interests in complex mixtures of environmental contaminants, risk distribution and its policy implications, susceptible populations, and other policy-relevant aspects of exposure and risk assessment would be especially welcome. An ability to teach in an interdisciplinary, professional training program and to participate in interdisciplinary research is essential.

The deadline for receipt of application materials is January 8, 1996. Please send a statement of research and teaching interests, a curriculum vitae, and the names and addresses of three references to: **Jared L. Cohon, Dean, Yale University, School of Forestry and Environmental Studies, 205 Prospect Street, New Haven, CT 06511.**

Yale University is an Equal Opportunity/Affirmative Action Employer. Women and minority group members are encouraged to apply.

BIOCHEMIST

The James Madison University Chemistry Department is committed to excellence in undergraduate instruction and research and seeks a **TENURE-TRACK ASSISTANT PROFESSOR** starting fall 1996, pending state funding. Ph.D. in biochemistry, chemistry, or related area required; postdoctoral experience desirable. Teaching responsibilities in introductory and upper-division biochemistry courses and the department's service courses and laboratories. Research with undergraduates required; collaboration with other departments encouraged. Résumé, statements of teaching philosophy and research interests, and three letters of recommendation to: **Search Committee, Department of Chemistry, James Madison University, Harrisonburg, VA 22807.** Complete application should be received by January 15, 1996 to ensure consideration. *James Madison University is an Affirmative Action/Equal Employment Opportunity Employer and especially encourages applications from minorities, women and persons with disabilities.*

ECOLOGY AND DEVELOPMENTAL BIOLOGY

Two **TENURE-TRACK POSITIONS** to begin September, 1996. 1) Ecologist: including teaching in evolution and systematics; marine biology background advantageous. 2) Developmental biologist: including teaching capabilities in comparative anatomy and embryology. Small liberal arts college with broad range of undergraduate courses and specialized courses through M.S. level. 300-acre campus on the North Shore of Long Island presents a rural setting, within an hour of Manhattan. Please send curriculum vitae, supporting material, and names of at least three references to: **Dr. M. Shodell, Department of Biology, Long Island University, C.W. Post Center, Brookville, NY 11548.** Closing date: January 26, 1996. *Equal Opportunity Employer.*

THINGS TO COME: THE YEAR AHEAD IN CALIFORNIA BIOTECHNOLOGY AND PHARMACEUTICALS

BY JOHN TIMPANE

"It's going to be a year when we have the chance to run again." That's Duane Roth, CEO of Alliance Pharmaceutical Corp. in San Diego, California. Like many watchers of California biopharma, Roth sees 1996 as a good year for investment, innovation and employment.

Californian biotechnology employs 108,000 people, which will grow to 160,000 or more by the turn of the century. After a year and a half in a holding pattern—reflecting the national health care debate and a few high-profile failures in biotech clinical trials—biomoney started to flow about halfway through 1995. "The gates are definitely open again," says Gina Kollin, director of human resources for Shaman Pharmaceuticals, Inc., of South San Francisco. "That's going to give a lot of companies the chance to stay up and running while they get a product to market."

Twenty-seven biotech products are now on the shelves, with over 290 in clinical development, and more than three times that number in preclinical. Those facts are suggestive. To be sure, the excellent discovery scientist will always be in demand. But the real need is going to be downstream—the PhDs, MSs, and BSs in clinical research, synthetic chemistry, regulatory affairs, validation, process development, manufacturing, and marketing who will help develop new drugs and speed them to market. Job-seekers dreaming of California need to retool their conceptions of the scientific career. Below we take a closer look at some of the hot fields.

Antisense, Gene Therapy, Genomics. "Antisense is one of the fields that people are very excited about," says Lester Kaplan, corporate vice president of research and development for Allergan in Irvine. "And with gene therapy, you'll see the excitement continue as well. There the big challenge lies in finding the right delivery system." And the Human Genome Project is still the mother of all collaborative efforts—but, as Kaplan points out, "there's a lot of uncertainty about how all this new knowledge is going to be applied."

Manufacturing. "All our indicators suggest a significant preparation throughout California for manufacturing," according to A. Stephen Dahms, director of the 22-campus California State University system Biotechnology Research and Education Program. He points to Vacaville, a northern California town that now hosts manufacturing centers for both Chiron and Genentech. "The Bay Area is well ahead of Southern California in moving from a research boutique phase to true manufacturing," he says, "and that should affect the number and kind of jobs these companies will be advertising for."

Pharmacokinetics, Medicinal and Synthetic Chemistry, and Beyond. "There don't seem to be enough qualified people in these areas," says Kollin. "I keep seeing a big need for people with expertise in metabolism and formulation—really well-paid, important areas." Chemists who can actually make the salable compounds of the future—and help test them—will be key (and much sought-after) players in the future of California biopharma. Kaplan says that "combinatorial chemistry seems to offer a lot of promise as a way of speeding up drug discovery."

Regulatory Savoir-Faire. From two-thirds to three-quarters of all new biotech job listings require some knowledge of regulatory codes and procedures, according to Dahms. Every future job-seeker should learn three words, according to Roth: GCP (good clinical practice), GMP (good manufacturing practice), and GLP (good laboratory practice). "If your résumé says, 'I have a basic understanding of regulatory laws,'" Roth says, "it's a plus."

Clinical Research Associate (CRA). "The CRA is definitely the hottest job in town," says Roth. "Already you see companies competing hard for good people. Nurses are very important, but so is anyone with a BS in chemistry or biology and experience in clinical research." Pay in many cases exceeds that for PhD discovery researchers. But is the job rewarding? "There's nothing more powerful than visiting the patient who has benefitted from your product," says Roth. "Knowing you've helped save lives—that's the most powerful reward you can get."

Validation/QA/QC. A new manufacturing facility will cost a company an average of $35 million to establish—and fully 17% of that money is devoted to validation. "The word validation just isn't in the lexicon of most educators and scientists yet," says Dahms. "That's a shame, because these can be very rewarding careers. You get to conduct very focused research aimed at answering concrete questions, and your results contribute directly—and rapidly—to the development effort." As for quality control and quality assurance, Dahms says, "I'm seeing many job ads looking for a BS in chemistry with experience in QA."

The Experienced MS and BS. Kollin says that "whereas we're seeing a flood of molecular biology and chemistry PhDs on the market, there is probably an even greater need for the MS and BS scientist who has good lab experience." Everyone urges these useful scientists to get that experience as they get their degree. As Roth puts it, "We don't have time to train people. We need some familiarity with what we do—get that while you're getting your degree or while you work."

Creativity. Academia, industry, and individuals have to think without blinders about future careers. Dahms sees it from the university perspective: "What we need is a curriculum that produces students whose background is interesting to the industry," he says, "and we can do this largely with existing labs and lectures. We just have to think differently." Job-seekers should simply think with as wide a horizon as they can. "The more cross-trained you are, the better," Roth says. "If you work with us, you'll be asked to do a lot of things. We'll say, 'Here's a problem. What can you contribute?'"

In the meantime, companies are innovating in as many new ways as they can find. Shaman pursues what it calls an "ethnomedical research process," in which western-trained scientists collaborate with healers from indigenous tribes in the tropical rain forest to study plants and compounds that treat disease. Kollin says, "There are new platforms, new products, new kinds of work. That's what California has always been about."

TOXICOLOGIST

Genentech is a pace-setting company, internationally known for discovering, developing, manufacturing and marketing pharmaceuticals for significant unmet medical needs. We are currently seeking a Ph.D. Toxicologist to join our Toxicology Department.

You will design, conduct and scientifically evaluate Safety Assessment studies conducted in animals or appropriate alternate test systems in support of U.S. and international marketing applications. Candidates will be expected to independently prepare comprehensive preclinical safety assessments in the support of these applications and to present and defend this data to regulatory authorities. The position involves working closely with project development teams to provide expertise on all investigational and regulatory safety issues involving protein and chemical therapeutics.

Qualified candidates will have a Ph.D. or equivalent in Toxicology and a minimum of 3 years' experience in the Pharmaceutical/Biotechnology industry working with a wide variety of pharmaceutical agents and classes of compounds. Experience with protein therapeutics is highly desirable. Individuals with experience in the areas of endocrinology, cardiovascular pharmacology, oncology, neuro sciences, or immunology are encouraged to apply. Board certification in Toxicology is desirable.

Join us and enjoy our progressive culture, exciting success, and excellent benefits package that includes fully paid medical/dental/vision coverage, free health club membership, and Company stock purchase opportunities. For immediate consideration, please send your resume to Genentech, Inc., Human Resources Dept. NSDT, 460 Pt. San Bruno Blvd., South San Francisco, CA 94080. Genentech is an Equal Opportunity Employer. We value the contributions of our diverse workforce.

Genentech, Inc.

Ph.D. Mass Spectrometrist

Arris Pharmaceutical Corporation is an innovative biopharmaceutical company using an integrated approach to drug discovery in an environment that promotes team work and rewards creativity. Arris is seeking a highly motivated scientist to lead our Mass Spectrometry effort. You will become a member of an interdisciplinary team supported by state-of-the-art instrumentation to discover drugs which interact with protease and cytokine receptor targets of major therapeutic value.

You will work closely with synthetic chemists, molecular biologists and pharmacologists to assist in the discovery of novel therapeutics. You would be expected to maintain a diverse group of spectrometric instrumentation and to design, develop and implement mass spectrometric screening protocols. Specific research responsibilities include technology development for affinity screening, protein analytical biochemistry and support for pharmacokinetics investigations. A Ph.D. in Mass Spectrometry or other protein Bioanalytical experience with particular emphasis in protein mass spectrometry, macromolecular and protein-ligand interactions, as well as familiarity with automated data handling is required. Candidates should have experience with ESI, MALDI, FAB, EI, CI mass spectrometry and HPLC, SDS/PAGE, electroblotting and CE separation techniques.

Headquartered in Northern California, Arris offers an excellent salary, attractive benefits, equity participation and career advancement opportunities in a growing company. Please forward your resume to:

Arris Pharmaceutical

Arris Pharmaceutical Corp.
Human Resources Department
Attention: Job# SMV125
385 Oyster Point Blvd., Suite 3
South San Francisco, CA 94080

Equal Opportunity Employer

BIOLOGY and BIOTECHNOLOGY RESEARCH PROGRAM

Join us in developing the next generation of research that leverages our genomic studies and expands our growing effort in protein structure analysis. Our goals are identification of the genes and analysis of the structure & function of normal and variant proteins of DNA repair and metabolism that affect **susceptibility to disease, especially cancer**, and application of **microbial genomics** to industrial and environmental processes.

BBRP encourages collaboration among investigators with expertise in different disciplines through formation of teams that address **complex, multidisciplinary research objectives.**

We seek applicants with expertise in several areas including molecular biology, protein biochemistry, computational biology, protein structure analysis, biology and biochemistry of DNA repair and metabolism, genomics, genetic variation, sequence analysis, microbial genetics, bioinstrumentation, analytical chemistry, cytogenetics, genetic toxicology.

Excellent support facilities and infrastructure include the DOE Human Genome Center, Program for Protein Structure Analysis, Center for Accelerator Mass Spectrometry, the resources of the Computations, Engineering and Chemistry Departments.

Appointments will be made (6-10) at the **postdoctoral or tenure-track** positions depending upon accomplishments, career goals and leadership potential or demonstrated ability. Candidates should have a PhD or MD and experience in relevant field.

Interested individuals should send resumes, including publication list, statement of research accomplishments and future research goals, names of three references, and e-mail addres to: **Ms. Mary Anne Holman, Recruiting & Employment Division, Dept. AJSCC15MH, Lawrence Livermore National Laboratory, P.O. Box 5510, Livermore, CA 94551-5510.** LLNL offers an attractive salary/benefits package. We are proud to be an Equal Opportunity Employer. M/F/D/V.

University of California
Lawrence Livermore National Laboratory

Worldwide Product Manager

Radiochemicals/ Molecular Biology

ICN Pharmaceuticals, Inc., a major international pharmaceutical firm with over one-half billion dollars in revenue is seeking a Product Manager for our worldwide research radiochemicals business.

The qualified candidate we seek will have 7 or more years experience developing and implementing marketing plans for radiochemicals. The ideal candidate will have experience interacting with production, technical services and customers resulting in sales increases, upgraded products and new products.

We offer a very competitive compensation package including bonus potential, stock options and relocation assistance. Please send your resume to: **Corporate Human Resources,**

ICN Pharmaceuticals, Inc.
3300 Hyland Avenue
Costa Mesa, CA 92626
Or FAX your resume to:
(714) 641-7256
EO/AA Employer M/F/H

PRODUCT MANAGERS
Genetic & Instrument Systems

■

STRATAGENE, a leader in the development and manufacture of molecular biology research products, has two immediate openings for qualified Product Managers. Responsibilities include the generation, implementation, tracking and reporting of tactical sales and marketing programs worldwide for genetic and instrument systems products. BS/BA degree in Molecular Biology or related field (or equivalent) and at least 3-5 years' experience marketing molecular biology products are required, along with laboratory experience and a strong understanding of the molecular biology market.

Interested candidates should send a resume to: **Stratagene, 11011 N. Torrey Pines Rd., La Jolla, CA 92037, Attn: Professional Staffing.** Please indicate position of interest by code: Genetic 22054-95A, or Instrument 22055-95A. AA/EOE.

STRATAGENE®

UNIVERSITY OF CALIFORNIA

FACULTY POSITION
TENURE TRACK
Developmental Biology
Department of Biology
University of California, San Diego

The Department of Biology at the University of California, San Diego invites applications for a tenure-track faculty position at the Assistant Professor level. We are seeking exceptional candidates pursuing imaginative approaches to any basic problem in Developmental Biology. The successful candidate is expected to develop a vigorous research program and participate in undergraduate and graduate teaching.

A Ph.D. degree and two or more years of productive postdoctoral research experience are required. Salary (based on the UC pay scale) will be commensurate with qualifications and experience. This position is contingent on availability of funds.

Applicants should send curriculum vitae, statement of research interests, bibliography, and the names, fax numbers, and e-mail addresses of three referees by February 15, 1996, to:

Developmental Biology Search Committee
University of California, San Diego
Department of Biology 0346
9500 Gilman Drive
La Jolla, CA 92093-0346

To apply by e-mail: **devbio@ucsd.edu**

The University of California is an Equal Opportunity/Affirmative Action Employer.

Assistant Professor of Genetics

The Department of Botany and Plant Sciences, University of California, Riverside, announces a position available July 1, 1996. The position is an 11-month, tenure-track appointment in the College of Natural and Agricultural Sciences and in the Agricultural Experiment Station. The successful candidate will be expected to develop a vigorous, innovative, independent research program in plant developmental genetics using genetics, molecular, cellular, and other techniques to elucidate fundamental mechanisms underlying plant development. Opportunities are available for interacting with researchers in plant cell, molecular, and developmental biology, plant physiology, and other disciplines. The successful candidate will be expected to become involved in undergraduate and graduate teaching as well as serve as major professor of graduate students in the Department of Botany and Plant Sciences and in the interdepartmental Genetics Program. A Ph.D. in genetics or related field is required. The candidate must possess a strong commitment to teaching excellence and a high research potential. Send letter of application, curriculum vitae, statement of research interest, and arrange to have at least three confidential letters of reference sent to: Dr. W.W. Thomson, Search Committee Chair, Botany and Plant Sciences Department, University of California, Riverside, CA 92521-0124. Phone: (909) 787-4619; Fax: (909) 787-4437; email: susanm@ucrac1.ucr.edu; WWW:http://cnas.ucr.edu/~bps/homepage.html. The application deadline is January 26, 1996. *The University of California is an Affirmative Action/Equal Opportunity Employer.*

TENURE-TRACK FACULTY POSITION
ASSISTANT PROFESSOR

Crump Institute for Biological Imaging
Department of Molecular and Medical Pharmacology
UCLA School of Medicine

The Crump Institute for Biological Imaging is a new Institute at UCLA that is committed to the merger of imaging and modern biology to examine systems ranging from cellular subassemblies up to human subjects. The Institute and the Department of Molecular and Medical Pharmacology at UCLA are seeking a junior faculty member with interests in both synthesis and protein chemistry. The successful applicant will be expected to develop an independent research program with emphasis in radiolabeled proteins and other biochemical imaging probes for positron emission tomography and confocal fluorescence microscopy. The individual we seek will also act as a member of a research consortium and should have the ability to interact with scientists of diverse interests who have come together to advance biology and medicine through the use of novel probes and bio-medical imaging modalities. The faculty includes scientists with strengths in chemistry, biochemistry, molecular biology, pharmacology, nuclear medicine, biophysics, and biomathematics.

Candidates should have a Ph.D. in Chemistry, Biochemistry, or a closely related field. Teaching of graduate and M.D./Ph.D. students is expected. Send curriculum vitae, a description of research plans, and three letters of recommendation to: **Theresa Sama, Search Coordinator, Crump Institute for Biological Imaging, JLNRC, UCLA School of Medicine, 10833 Le Conte Avenue, Los Angeles, CA 90095-1770.**

ASSISTANT PROFESSOR of CHEMISTRY

University of California, Riverside

The Department of Chemistry invites applications for a tenure-track faculty position at the Assistant Professor rank starting July 1, 1996. The position requires a Ph.D. in analytical, inorganic, organic, physical, or other areas of chemistry, an ability to conduct an innovative and vigorous research program in fundamental aspects of atmospheric chemistry or related chemical/environmental areas, and excellent prospects for teaching chemistry at the graduate and undergraduate levels. Postdoctoral experience will be helpful. The successful candidate for this position will complement the ongoing research in the Department of Chemistry and the UC Riverside Statewide Air Pollution Research Center (SAPRC). The successful candidate will be a joint appointment in the Department of Chemistry and SAPRC. The SAPRC mission includes fundamental chemical studies of atmospheric processes as viewed in the broadest sense. Applicants should send a complete resume and statement of research interests, and should have three original letters of reference sent to Professor Steven R. Angle, Chemistry Faculty Search Committee Chair, Department of Chemistry, University of California, Riverside, CA 92521-0403. Evaluation of applications will begin on 15 January 1996, but the position will be open until filled. The University of California is an Affirmative Action, Equal Opportunity Employer. Additional local campus information is available at http://cnas.ucr.edu/ and http://www.chem.ucr.edu/

Research Scientist

VICAL INCORPORATED, a leader in the development of gene-based pharmaceutical products for human gene therapy is currently seeking a Research Scientist. The incumbent will be responsible for carrying out original and applied research in the area of Cancer Gene Therapy. The incumbent will be expected to provide experimental and intellectual contributions to Vical's primary direct DNA injection technology in the area of cancer therapy with an emphasis on the immunotherapy of cancer. The ideal candidate will possess the following:

- A Ph.D. with a minimum of 2-3 years postdoctoral experience;
- A strong background in tumor biology and cancer immunotherapy;
- Excellent communication skills and team skills;
- Strong publication record in journals reporting original cancer research.

Please send your resume to **Vical, Inc. Human Resources, 9373 Towne Centre Drive, Suite 100, San Diego, CA 92121 or fax to (619) 453-3452.**

EOE

OPPORTUNITIES IN CELLULAR AND MOLECULAR DIAGNOSTICS

We are seeking multiple individuals to join an expanding research group focusing on rare cell isolation and differentiation. The goal of this aggressive program is the development of methods that allow the isolation, enrichment and positive identification of rare cells for diagnostic purposes. PhD applicants with at least 5 years' related research experience and MS/BS applicants with preferably up to 5 years' related experience are encouraged to apply for positions within this group. Post-doctoral positions are also available for individuals with at least 2 years' related research experience. Knowledge and experience with one or more of the following technologies is a necessity: isolation, purification and labeling of mammalian RNAs, cDNA cloning methodologies, construction, analysis and maintenance of cDNA libraries, subtraction hybridization strategies, RT-PCR, DD-PCR, *in-situ* hybridization and M13 based sequencing. Knowledge of cell biology and bioinformatics is desirable. These individuals will be part of an exciting multidisciplinary project with an on-going world-class industrial and academic collaboration. (Ref: CMD)

Other Opportunities Available in R&D

Amplification and Detection Technology
We also seek PhD and post-doctoral applicants with prior experience in nonisotopic nucleic acid labeling and detection. Candidates with experience in target amplification and/or novel signal amplification systems are encouraged to apply. (Ref: ADT)

Development
We also seek BS/MS/PhD applicants with a minimum of 3+ years' assay development experience in the diagnostics or pharmaceutical industry. (Ref: DMT)

Competitive salary, benefits and relocation allowance provided.

For consideration, please forward your CV to the **Human Resources Department at Boehringer Mannheim Corporation, 2400 Bisso Lane, P.O. Box 4117, Concord, CA 94524-4117 or fax your resume to (510) 674-1680.** Please include the reference code. Principals only please. EOE.

Terrapin a dynamic young organization with proprietary targets in intracellular signaling and a unique drug discovery technology located at 750 Gateway Blvd., South San Francisco, CA 94080, Fax (415) 244-9388, has the following openings:

Computational Chemist - This position is available in our Chemistry Department. The ideal candidate should have a Ph.D. and 3-5 years postdoc experience with strong background in computer aided drug design & excellent command of multivariate statistics. Knowledge of chemical databases, proteins structure & function or pharmacophore development is a plus. If you are independent & have excellent communication skills, please send your resume and references to Dr. Hugo Villar at the above address.

Senior Scientist - Hematopoesis Cell Biology - The ideal candidate should have a Ph.D. with in-depth knowledge and extensive hands-on experience in human bone marrow biology as well as a proven track record with bone marrow cultures and multi-myeloid lineage assays. Candidates with lymphoid lineages experience in a pharmaceutical company environment and the ability to lead research project will be given preference. Please send your resume and references to Dr. Deborah Higgins at the above address.

Research Assistant position available for exploring T cell mediated signal transduction. The successful candidate will have a BS/MS with 2-4 years experience in immunology or signal transduction. This position requires strong tissue culture skills and expertise in signal transduction techniques. Experience with establishment and maintenance of T cell clones is highly desirable. Please send your resume and references to Dr. Nicki Vasquez at the above address.

Research Assistant position available to run biochemical screening assays, a variety of biomedical procedures and laboratory robotics. The ideal candidate will have a BS/MS with biology and chemical science training as well as demonstrated laboratory experience in biochemical assay development or procedures. Applicant should be meticulous & capable of maintaining highly accurate record keeping as well as responsible and thorough. Please send resume and references to Dr. Richard Sportsman at the above address.

Research Assistant position available in Molecular Biology for an individual skilled in automated fluorescence DNA sequencing. The ideal candidate will have basic skills in molecular biology (PCR, cloning, plasmid preparation, RNA work a plus). This position requires a BA/BS with 1-2 years experience. Please send resume and references to Dr. Gene Napolitano at the above address.

Research Assistant position available in Hematopoesis Cell Biology. *In vitro* cell culture and *in vivo* experience are essential. The ideal candidate must have a basic knowledge of hematopoesis. Candidates with the ability to do bone marrow cultures & multi lineage assays will be given preference. This position requires a BS/MS in biological science and some post graduate experience. Please send resume and references to Dr. Deborah Higgins at the above address.

Terrapin
TECHNOLOGIES, INC.

Terrapin is an Equal Opportunity Employer.

Detector Instrumentation Department Head

The Ernest Orlando Lawrence Berkeley National Laboratory (EOLBNL) is seeking a nationally or internationally recognized authority and leader in the field of instrumentation for radiation detection and measurement to serve as Head of the Detector Instrumentation Department. This individual should have a broad interest in instrumentation development including significant experience and demonstrated competency and achievements in one or more of the following technical areas: analog signal processing, state-of-the-art microelectronics technology, solid-state detector research and development, or large systems for radiation detection. An extensive publication record, a demonstrated ability to provide effective technical leadership to large groups and complex technical projects, and good management and communication skills are required.

The department, consisting of a staff of 25 engineers, scientists, and technicians collaborates with scientists in Berkeley Lab programs in High Energy and Nuclear Physics, Astrophysics, Materials, and Biosciences. The staff have competency in application-specific integrated circuits design, high bandwidth, low noise analog and digital systems, high speed data acquisition, and filtering systems and advanced solid-state detectors.

Reporting to the Engineering Division Director, the Head will provide overall technical leadership to the department, manage staff, determine and/or establish programmatic goals and requirements, assemble engineering and technical teams to meet those goals and requirements, and contribute technically to one or more of the detector R&D or instrumentation projects underway at the Laboratory. The Head is also expected to develop new technical initiatives within or from outside the Laboratory and carry out his/her own research activities either within the Engineering Division or one of the Berkeley Lab's programmatic divisions (e.g. Physics, Nuclear Science, Materials, Life Sciences).

L•B•N•L

Berkeley Lab provides excellent benefits and compensation packages, and the opportunity for career growth. Please mail your resume to: **Ernest Orlando Lawrence Berkeley National Laboratory, Attn: Human Resources Dept., Bldg. 938A, JSCI3520, One Cyclotron Road, Berkeley, CA 94720.** Or fax: **(510) 486-5870.** E-mail: **jamagee@lbl.gov**. Equal opportunity employer. Women and minorities are encouraged to apply.

POSITION ANNOUNCEMENT

Position: Assistant Professor of Atmospheric Science, Department of Soil and Environmental Sciences, and Assistant Research Scientist, Statewide Air Pollution Research Center (SAPRC). Salary and compensation shall be determined within allowable University parameters.

Date Available: July 1, 1996

Responsibilities: This 9 month tenure-track position is 60% teaching (Soil and Env. Sci.) and 40% research (SAPRC). The individual is to carry out research in atmospheric science that will complement current research being conducted at the University of California, Riverside. A particular research area of interest is that involving atmospheric particulate matter, including research into the formation, transport and transformations of particles and particle-associated chemicals in the atmosphere. The individual will teach undergraduate course(s) in environmental science and have the opportunity to teach a graduate course in their area of specialty.

Qualifications: Candidates must have met all requirements of Ph.D. within one year of appointment in a relevant discipline, and a background in atmospheric science. Candidates must possess a strong commitment to teaching excellence, and have the ability to conduct an innovative and vigorous research program.

Application Procedures: Candidates for this position are requested to submit a curriculum vita, a statement of research interests and teaching interests, transcripts and any supporting information to Roger Atkinson, Department of Soil and Environmental Sciences, University of California, Riverside, CA 92521. Applicants must also request at least three individuals to write letters of recommendation on their behalf. Applications will be accepted until January 15, 1996.

The University of California, Riverside, is an Affirmative Action/ Equal Opportunity Employer.

CHIEF
LABORATORY FOR ASTRONOMY AND SOLAR PHYSICS

The NASA/Goddard Space Flight Center invites applications and nominations for this position, located in Greenbelt, Maryland. The vacancy may be filled as either a permanent Senior Executive Service position or on a time limited basis through an appropriate university or intergovernmental arrangement.

The Chief of the Laboratory for Astronomy and Solar Physics is responsible for developing and conducting a broad program of experimental and theoretical research, in specific areas of space science. These areas include: highly advanced state of the art studies of the properties of astrophysical sources with emphases on the Sun, comets, stars, the interstellar medium, stellar clusters, galaxies, galaxy clusters and the early universe; the development of space astronomy instruments; and laboratory and theoretical investigations in support of astrophysical studies from space. The incumbent participates in the overall development and implementation of the Center-wide space science objectives.

The Chief performs individual research and may act as a principal investigator, co-investigator, or a project scientist on NASA missions. Participation on Agency-wide panels and committees is also required of the incumbent.

Desirable qualifications include a Ph.D. degree with extensive post-graduate research experience as well as experience in the scientific and administrative management of research programs which has established the candidate as an authority in astronomy, astrophysics, and/or solar physics. The candidate should also possess demonstrated executive management abilities commensurate with the high level management responsibilities of this position.

Compensation is range is currently $107,300 to $122,040 per annum, including locality pay. Submit OF 612, "Optional Application for Federal Employment" or any other written format you choose and a supplemental statement addressing the SES Executive Core Qualifications and the Technical Qualifications of the position. Mail applications to:

Keith P. Lowe
Human Resources Operations Office, Code 113.8
Office of Human Resources
NASA/Goddard Space Flight Center
Greenbelt, MD 20771

For more information about position requirements and application procedures, please call Mr. Lowe at (301) 286-9951 or (301) 286-7918 (TDD).

Complete application must be postmarked by January 23, 1996

Equal Opportunity Employer *U.S. citizenship required.*

MARINE BIOLOGICAL LABORATORY
1996 Summer Research Fellowships

FULL FELLOWSHIP This fellowship covers most costs of conducting summer research, plus living and travel expenses:
Nikon Fellowship- Any area of biological sciences requiring the use of advanced microscopy.

PARTIAL FELLOWSHIPS These fellowship funds may be available individually or in concert to cover many of the costs of conducting summer research, including living and travel expenses, in the following areas:

Robert Day Allen Fellowship - cell motility and cytoarchitecture
Frederik B. Bang Fellowship Fund - for research using marine models in molecular biology or biomedicine
Frank A. Brown, Jr. Memorial Readership - covers fees for desk rental and full privileges in the MBL/WHOI Library
Charles R. Crane Fellowship Fund - independent research in any area
John O. Crane Fellowship Fund - independent research in any area
Jean and Katsuma Dan Fellowship Fund - supports scientific visits to Japan by junior American investigators
Bernard Davis Fund - microbiology and evolution
Erik B. Fries Fellowship - covers laboratory or library expenses
M.G.F. Fuortes Fellowship - neuroscience
Daniel S. Grosch Fellowship and Scholarship Fund - environmental toxicology
Ann E. Kammer Fellowship Fund - for women researchers, with a preference for neuroscience
Esther A. and Joseph Klingenstein Fund - supports laboratory space expenses for research in neurobiology
Stephen W. Kuffler Fellowship - neurobiology
Lucy B. Lemann Fellowship - research in any area
Frank R. Lillie Fellowship - provides a research laboratory and funds for travel and supplies
MBL Associates Fellowships - research in any area
James A. and Faith Miller Memorial Fund - any area, with developmental biology preferred
William Townsend Porter Fellowship for Minority Investigators - collaborative research in any area of physiology
Herbert W. Rand Fellowship - research in any area
The Evelyn and Melvin Spiegel Fellowship Fund - any area, developmental biology preferred
H. B. Steinbach Fellowship - cell biology and physiology

Application Deadline for fellowships and laboratory space rental is **January 15, 1996**

Applications are reviewed by the MBL Fellowship Committee. Notification of decisions will be mailed by March 15.

For application forms and additional information, please contact:

Fellowship Coordinator, Office of Research Administration Marine Biological Laboratory,
7MBL Street, Woods Hole, MA 02543-1015
Tel: (508) 289-7441/Fax: (508) 457-1924/
E-mail: skaufman@mbl.edu Or download information off the Internet/World-Wide-Web at
http://www.mbl.edu

MARINE BIOLOGICAL LABORATORY

MBL *is an* EEO/*Affirmative Action Institution*

FACULTY POSITIONS
Immunogenetics/ Molecular Genetics

The newly reorganized Department of Microbiology and Immunology at Vanderbilt University is continuing to expand its research base in molecular biology of the immune system with a special emphasis on immunogenetics and molecular genetics. Tenure-track positions at the assistant professor level are available. In exceptional cases faculty positions at the associate professor and professor levels will be considered. The candidates should have experience in applying molecular biology approaches to the problems within the area specified above. Start-up funds and newly renovated space are available. Faculty members holding PhD and/or MD degrees will have academic appointments in the School of Medicine and in the Graduate School of Vanderbilt University. Send applications with curriculum vitae, present and future research plans, and at least three names of references to:

Jack J. Hawiger, Professor and Chairman
Department of
Microbiology and Immunology
Vanderbilt University School of Medicine
A-5321 Medical Center North
Nashville, TN 37232-2363.

Women and minorities are encouraged to apply. Vanderbilt University is an Equal Opportunity/ Affirmative Action University. Review of applications will begin immediately and continue until positions are filled.

VANDERBILT UNIVERSITY

POSTDOCTORAL POSITION

A position is available immediately to study regulation of the mammalian nervous system. The research will focus on isolation of factors which regulate alternative splicing of neuronal-specific genes. Candidates should have a Ph.D. with experience in molecular and cellular biology; some knowledge of protein purification techniques is desirable.

The Shriver Center is an affiliate of Massachusetts General Hospital and Harvard Medical School. The Department of Biomedical Sciences provides extensive core facilities and many opportunities for scientific interactions.

Please send C.V. and the names/phone numbers of three references to:

Athena Andreadis, Ph.D., E. K. Shriver Center, Biomedical Sciences, Room 205, 200 Trapelo Road, Waltham, MA 02254,
Fax: (617) 893-4824,
email: aandreadis@shriver.org

EUNICE KENNEDY SHRIVER CENTER

An Equal Opportunity Employer

SENIOR RESEARCH IMMUNOLOGIST

Merck Research Laboratories in West Point, Pennsylvania, a world leader in biological and pharmaceutical research, has an immediate opening for a Senior Research Immunologist in the department of Virus and Cell Biology.

The successful candidate must have experience in the immunology of multiple virus systems with knowledge of medical or biochemical virology or immunology. The focus of this position will be to develop methods to assess the immune response to viral vaccines and apply novel assays to characterize vaccine viruses and measure immunity to viruses. Experience in molecular, biochemical or biophysical characterization of viruses is also desired.

A Ph.D. in Immunology, Virology or related field, or equivalent with postdoctoral experience in the growth and characterization of viruses is required.

Excellent salary and benefit programs accompany this position at our modern research facilities located 25 miles northwest of Philadelphia. Please send curriculum vitae with cover letter to: **Personnel Manager, Ad#B-42, MRL Human Resources, WP42-2, Merck Research Laboratories, P.O. Box 4, West Point, PA 19486.** EEO/AA/V/Employer.

MERCK
Research Laboratories

POSITIONS OPEN

PHYSICAL OCEANOGRAPHER

The University of Southern Mississippi (USM) invites applications for a nine-month, tenure-track faculty position in physical oceanography in the Center for Marine Sciences. The appointment will be made at the **ASSISTANT** or **ASSOCIATE PROFESSOR** level depending upon the applicant's previous teaching and research experience. The successful applicant must hold a Ph.D. in physical oceanography or a closely related field and have a strong research interest in coastal oceanographic processes. Applicants with interests in interdisciplinary research problems are particularly encouraged to apply. The appointee is expected to maintain a strong externally funded research program, to supervise graduate students, and to develop and teach courses at the graduate level. The Center for Marine Sciences is a multidisciplinary academic unit with research and teaching programs in biological, chemical, geological, and physical oceanography, including numerical ocean modeling. The USM Center for Marine Sciences is located at NASA's John C. Stennis Space Center on the Mississippi-Louisiana border. Besides NASA research activities, the Stennis Space Center is also the home of the U.S. Naval Oceanographic Office, NOAA's National Data Buoy Center, the Naval Research Laboratory-SSC, and the Maury Oceanographic Library. Ample opportunities are available for research collaboration with oceanographers at these federal agencies. More information about our program is available at **http://www.coam.usm.edu/cms/** on the Internet. The starting date is August 14, 1996. Qualified applicants should mail a complete curriculum vitae, a statement of teaching and research interests, and names of four references to: **Dr. Denis A. Wiesenburg, The University of Southern Mississippi, Center for Marine Sciences, Building 1103, Room 102, Stennis Space Center, MS 39529.** Application deadline is January 12, 1996. *Affirmative Action/Equal Employment Opportunity/ADA Institution.*

CONSERVATION BIOLOGY AND WILDLIFE ECOLOGY

The Yale University School of Forestry and Environmental Studies seeks to make a **TENURED** appointment in the field of Conservation Biology and Wildlife Ecology. Responsibilities of the position will include development of a research program, presentation of graduate courses/seminars, and advising Master's and doctoral students. Individuals with research interests in population biology and related areas and in the policy implications of conservation biology would be especially attractive. The ability to thrive in an interdisciplinary, professional program is essential.

The deadline for receipt of application materials is January 8, 1996. Please send a statement of research and teaching interests, a curriculum vitae, and the names and addresses of three references to: **Jared L. Cohon, Dean, Yale University, School of Forestry and Environmental Studies, 205 Prospect Street, New Haven, CT 06511.**

Yale University is an Equal Opportunity/Affirmative Action Employer. Women and minority group members are encouraged to apply.

QUANTITATIVE POPULATION ECOLOGIST
University of California, Berkeley

Applications are invited for a tenure-track position in quantitative population ecology at the **ASSISTANT PROFESSOR** level in the Department of Integrative Biology. Area of organismal interest is open, but preference will be given to a person with special skills in experimental design, quantitative analysis and/or modelling. The successful applicant will participate in teaching our upper-division course in population and community ecology and will be expected to develop an advanced undergraduate and graduate-level course in quantitative and experimental methods in ecology. He or she will also offer seminars in the area of specialty.

Applications must be posted by January 19, 1996; the appointment will begin on July 1, 1996. Submit a curriculum vitae, three letters of recommendation, a statement of research and teaching goals, and reprints of your three most significant publications to: **Chair, Population Ecology Search Committee, Department of Integrative Biology, 3060 Valley Life Sciences Building, University of California, Berkeley, CA 94720-3140.** *The University of California is an Affirmative Action/Equal Opportunity Employer.*

POSITIONS OPEN

THE CLEVELAND CLINIC FOUNDATION
OPTHALMIC RESEARCH PROGRAM IN MACULAR DEGENERATION AND INHERITED RETINAL DISEASES
Division of Ophthalmology
The Cleveland Clinic Foundation (CCF)

Two positions, at the level of Assistant, Associate or Full Professor, are immediately available in Opthalmic Research in the newly expanding Eye Institute. Three additional positions will be filled in the fall of 1997. Basic investigators with training in molecular biology, cell biology, biochemistry, human genetics, or epidemiology, with research interests that impact the clinical areas of macular degeneration and inherited retinal diseases, will be seriously considered. Applicants should send curriculum vitae; names of three references; and a statement of past research activities, current interests, and career goals to: **Joe G. Hollyfield, Ph.D., Director of Ophthalmic Research, Research Institute FFb, The Cleveland Clinic Foundation, Cleveland, OH 44195-5245. FAX: 216-445-3670. Email: <hollyfj@cesmtp.ccf.org>.** *CCF is an Equal Opportunity/Affirmative Action Employer.*

PROFESSOR AND CHAIR OF PHARMACOLOGY AND CELL BIOPHYSICS

The University of Cincinnati College of Medicine invites applications and nominations for **CHAIR** of this department, which has a history of academic and research excellence. Current faculty support includes two training grants and two NIH Merit awards. The College receives approximately $60 million in sponsored program awards and has significant interdisciplinary programs of distinction in cardiology, neuroscience, and oncology. Faculty have been internationally recognized for expertise in the generation/evaluation of transgenic mice. The college is developing an interdisciplinary Structural Biology program with 750, 600, and 500 MHz NMRs.

We seek qualified candidates with distinguished records in research, teaching, and service, and demonstrated excellence in leadership and administration. Individuals with nationally and internationally recognized and funded research programs in molecular approaches to pharmacology or related disciplines are particularly encouraged to apply. The Chair is responsible for medical and graduate instruction in pharmacology as well as for maintaining and developing outstanding, externally supported research programs within the department. Review of candidates will begin in late 1995. Send nominations and applications (include letter of interest, curriculum vitae, and three references) to: **Jerry B. Lingrel, Ph.D., Pharmacology Search Committee Chair, University of Cincinnati College of Medicine, 231 Bethesda Avenue, Cincinnati, OH 45267-0524.** *University of Cincinnati is an Affirmative Action/Equal Opportunity Employer. Women, Minorities, Disabled, Veterans encouraged to apply.*

HUMBOLDT STATE UNIVERSITY
Department of Biological Sciences
Two Positions: Animal Development and Phycology

TENURE-TRACK FACULTY POSITIONS starting August 21, 1996. Animal Development: requires Ph.D. in zoology or biology, with emphasis in animal development. Primary responsibilities will be to teach courses in animal development and general zoology; candidate should possess sufficient breadth in vertebrate zoology to teach a course in herpetology or vertebrate natural history. Phycology: requires Ph.D. in the biological sciences with an emphasis in freshwater and marine phycology. Primary responsibilities will be to teach courses in marine phycology, freshwater algae, and general botany. Both: other duties will include advising undergraduates and Master's students and serving on faculty committees. Research is expected. Send résumé, three letters of recommendation, and academic transcripts to: **Animal Development Search Committee or Phycology Search Committee, Department of Biological Sciences, Humboldt State University, Arcata, CA 95521. Telephone: 707-826-3245; FAX: 707-826-3201.** Completed application materials must be postmarked by February 15, 1996. *Equal Opportunity/Affirmative Action Employer. Women, persons with disabilities, and minorities are encouraged to apply.*

POSITIONS OPEN

BIOLOGIST

The University of Minnesota, Morris seeks an individual who combines broad intellectual interests with a strong commitment to undergraduate teaching and research involving undergraduates, to fill a **TENURE-TRACK** position in microbiology and biochemistry beginning September 16, 1996. The selected candidate will teach a broad range of undergraduate biology courses including lower-level courses for both majors and nonmajors and upper-level courses in microbiology, biochemistry, and another area such as immunology, virology, mycology, or plant or animal pathology. The selected candidate will also participate periodically in the teaching of a one-quarter interdisciplinary course required of all freshmen. The selected candidate will share in the governance and development of the biology program as well as the campus at large. Candidates must expect a Ph.D. in microbiology or a related field by September 16, 1996. Preference will be given to candidates with a broad liberal arts background. Two years of teaching experience at the undergraduate level is required. (Graduate TA experience is acceptable.) The University of Minnesota, Morris is a small, selective, residential, undergraduate liberal arts college of the University of Minnesota. Salary range: $32,000 to $40,000 depending on qualifications. Applications must include a letter of application, résumé, graduate transcript(s), three reference letters, and two statements: (1) a teaching statement in which approaches to teaching are described and past teaching experiences are evaluated, and (2) a research proposal in which the applicant proposes a research program that is viable and accessible to advanced students at a small liberal arts institution. Send applications to: **Biology Search Chair, Division of Science and Mathematics, University of Minnesota, Morris, MN 56267-2128.** Applications must be received by January 31, 1996. *The University of Minnesota is an Equal Opportunity Educator and Employer.*

NEUROBIOLOGIST

The Department of Cell Biology, Developmental Biology and Neurobiology at Rutgers University, New Brunswick invites applications for one or possibly two **TENURE-TRACK POSITIONS** from individuals with postdoctoral experience and a record of significant research achievement in cellular and molecular analysis of synaptic function and plasticity. Successful candidates will be expected to develop an active research program, participate in the ongoing expansion of neurobiological research at Rutgers, and contribute to graduate and undergraduate education. The appointment will begin in September 1996 in the newly organized Department of Cell Biology, Developmental Biology and Neurobiology. Applicants should send a curriculum vitae, a statement of research interest, and three letters of recommendation to: **Dr. Richard E. Triemer, Chair, Department of Biological Sciences, Nelson Biological Laboratories, Rutgers University, Piscataway, NJ 08855-1059** by February 15, 1996. *Rutgers University is an Equal Opportunity/Affirmative Action Employer.*

FACULTY POSITIONS IN MEMBRANE/CELL PHYSIOLOGY

The Department of Physiology of the Medical College of Pennsylvania and Hahnemann University invites applications for full-time, tenure-track faculty positions at the rank of **ASSISTANT PROFESSOR, ASSOCIATE PROFESSOR** or **PROFESSOR.** Applicants must have a record of independent research in an area of membrane or cell physiology. Future areas targeted for expansion include epithelial and cardiovascular membrane structure/function. Appointees will join a Department that was initiated in 1992 and is built around the theme of membrane and cell physiology. Such a cohesive Departmental theme ensures excellent opportunities for interactions and collaboration. The Department occupies space in a recently renovated building located in a very pleasant residential area of Philadelphia. Salaries and start-up packages are competitive. In addition to establishing and maintaining a competitive research program, successful candidates will be expected to participate in teaching in a medical physiology course. Applications will be accepted until March 1, 1996. Send a curriculum vitae, a brief description of research interests and plans, and the names, addresses, and telephone numbers of at least three references to: **Dr. John M. Russell, Department of Physiology, Medical College of Pennsylvania and Hahnemann University, 2900 Queen Lane, Philadelphia, PA 19129. Email: russell@medcolpa.edu.**

S C I E N T I S T S

Challenging infectious and cardiovascular diseases, allergies, cancer and central nervous system disorders...

That's Schering-Plough

From molecules to medicines. At Schering-Plough, scientists are discovering and developing the novel therapeutics that challenge mankind's most debilitating diseases. To continue this important work, we seek talented scientists with knowledge and dedication.

SCIENTIST
Immunology

We seek an independent self-starter to play an important role on a professional research team. To qualify, you will need a BS in Biology or related field and 7-10 years of experience or an MS and 5-8 years of experience. Background must include training and experience conducting in vivo experiments as well as knowledge of in vitro cell culture and molecular biology techniques. Expertise in lymphocyte isolation and fractionation, DNA sequencing and gene expression evaluation is desirable. Experience in FACS analysis is helpful. To be considered for this position, please respond to Dept. DD95-48.

SCIENTIST
Allergy

We seek a talented scientist to assume major responsibilities for conducting ongoing studies of T cell activation and cytokine production at the molecular level. To qualify, you will need a BS in Cell or Molecular Biology or Immunology and 7-10 years of experience or an MS and 5-8 years of experience. Background must include experience in lymphocyte isolation and cell culture. Experience in a variety of recombinant DNA techniques is highly desirable. A high degree of organization and independence is a must. To be considered for this position, please respond to Dept. DD95-43.

We offer an excellent compensation package including a competitive salary and comprehensive benefits. For prompt, confidential consideration, we invite you to forward a resume indicating the Dept. Code for your position of interest and salary requirements to: Human Resources-BG, Schering-Plough Research Institute, MS #1255, 2015 Galloping Hill Road, Kenilworth, NJ 07033-0539. We are an equal opportunity employer. *We regret we are unable to respond to each resume. Only those selected for an interview will be contacted.*

Schering-Plough Research Institute

Using Science For Human Advantage

DIRECTOR, AHERF CARDIOVASCULAR INSTITUTE

Allegheny Health, Education and Research Foundation (AHERF), parent corporation of Allegheny General Hospital and Allegheny-Singer Research Institute in Pittsburgh, PA, The Medical College of Pennsylvania and Hahnemann University Hospitals and St. Christopher's Hospital for Children in Philadelphia invite applications for a newly created position.

Successful candidate will have an M.D., Ph.D. or equivalent doctoral degree, experience working in a cardiovascular/pulmonary surgical or medical environment, appropriate experience directing and administering research programs in cardiovascular specialties, including clinical and basic research and a demonstrated record of excellence in research. Demonstrated leadership capabilities to collaborate among clinical and basic science faculty in a variety of cardiovascular and other disciplines, plus the ability to function in an interdisciplinary setting needed.

Attractive recruitment package includes research laboratory space, the ability to recruit new faculty, and a research endowment. Interested individuals please submit curriculum vitae and references to: **James H. McMaster, M.D., President and CEO, Allegheny-Singer Research Institute, 320 E. North Avenue, Pittsburgh, PA 15212.** EOE. M/F/H/V.

ASRI
ALLEGHENY-SINGER RESEARCH INSTITUTE

PROCESS/ANALYTICAL BIOCHEMIST

Merck Research Laboratories is considered by many to be the premier research organization in the pharmaceutical industry based on its unparalleled success at creating important new pharmaceuticals and vaccines, which have been used to improve human health worldwide.

The Bioprocess R&D group is responsible for the development of processes and analytical techniques to be used for manufacture and release of all biologically-made new vaccine and drug candidates. We are looking for talented Ph.D. Biochemists, Molecular Biologists and Molecular Immunologists at various levels of experience to join our group. The successful candidate would have the objective of gaining a more fundamental understanding of our processes, our analytical methods and our products, and of applying that knowledge to improve productivity and reproducibility.

The work is varied with the opportunity to work in a team which moves product candidates from Basic Research through process scale-up and Clinical evaluation to start-up in manufacturing. Current product candidates require the development of purification processes and analytical methods for polysaccharides, proteins, purified viruses, conjugates and plasmid DNA.

Merck offers excellent salary and benefits programs for this position located in our research facilities 25 miles northwest of Philadelphia. Please send curriculum vitae with cover letter and the names of three references to: **Personnel Manager, Ad#B-43, MRL Human Resources, WP42-2, Merck Research Laboratories, P.O. Box 4, West Point, PA 19486.** EEO/AA/V/Employer.

MERCK
Research Laboratories

POSITIONS OPEN

ASSISTANT PROFESSOR
Department of Microbiology and Cell Science
University of Florida at Gainesville

The Department of Microbiology and Cell Science, University of Florida, is expanding and invites applications for a new **TENURE-TRACK POSITION**, available August 1, 1996. This position is equally divided between teaching and research and includes start-up funds. The successful candidate will be expected to develop an externally funded research program in the area of microbial genetics/physiology, microbial ecology, or host/bacterial interactions (human, animal, or plant). Teaching responsibilities will include participation in undergraduate and graduate courses, training of graduate students, and other University-related activities. Candidates should have a Ph.D. in microbiology, biochemistry, or related science and at least two years of postdoctoral experience. The closing date for this position is January 1, 1996. Applicants should submit a curriculum vitae, summary of research interests, and three letters of reference to: **Lonnie O. Ingram, Department of Microbiology and Cell Science, Museum Road, P.O. Box 110700, University of Florida, Gainesville, FL 32611-0700.** *The University of Florida is an Affirmative Action/Equal Employment Opportunity Employer.*

ASSISTANT/ASSOCIATE/FULL PROFESSOR
Microbiology and Immunology/Cancer Research

The Department of Microbiology and Immunology and the Center of Excellence in Cancer Treatment, Research, and Education at Louisiana State University Medical Center invite applications for a tenure-track **FACULTY** position. Applicants should have a doctoral degree, postdoctoral research experience, and a commitment to excellence in teaching and cancer research. Special consideration will be given to established investigators with national funding in an area of research that directly concerns clinical cancer. Responsibilities include teaching medical students and the training of the 30 departmental doctoral students. Excellent facilities, start-up funds, and competitive salary are offered. Curriculum vitae, future research plans, status of funding, and three letters of reference should be sent to: **Dr. Dennis J. O'Callaghan, Professor and Head, Department of Microbiology and Immunology, LSUMC, 1501 Kings Highway, Shreveport, LA 71130-3932.** *An Equal Opportunity Employer.*

BIOLOGY FACULTY POSITION

The Department of Biology of Saint Joseph's University invites applications for a tenure-track faculty position at the **ASSISTANT PROFESSOR** level. We are seeking a broadly trained eukaryotic cell biologist. Successful applicants will be expected to participate in non-major courses, teach a freshman cell biology course, and develop an upper-division/graduate-level course in advanced cell biology. Development of an active independent research program involving undergraduate/M.S. students is expected. Ph.D. required; postdoctoral and teaching experience are assets. Please send curriculum vitae, copies of all transcripts, an outline of teaching and research goals (including a list of needed equipment), and names and telephone numbers of three references to: **Dr. John J. Tudor, Chair, Department of Biology, Saint Joseph's University, 5600 City Avenue, Philadelphia, PA 19131.** Review of applicants will begin in mid-January 1996. *St. Joseph's University is a four-year liberal arts university in the Jesuit tradition. Equal Opportunity/Affirmative Action Employer.*

MEDICAL SCIENTIST

A **TENURE-TRACK** position is available at Indiana University for a medical scientist to take part in the School of Optometry's scientific and clinical contribution to the teaching, treatment, and research on the eye. We seek a candidate enthusiastic to join our professional and graduate-level didactic and research programs, particularly to teach medical school–level biochemistry and in other appropriate areas, and to take advantage of opportunities for collaborative research. Minimum requirements include an earned doctorate and additional postdoctoral experience. Send curriculum vitae, three letters of reference, and statement of teaching and research interests to: **Dr. David Goss, Chair, Search and Screen Committee, School of Optometry, Indiana University, 800 East Atwater, Bloomington, IN 47405.** Deadline for applications is January 15, 1996. *An Affirmative Action/Equal Opportunity Employer.*

STROKE NEUROSCIENTIST
DEPARTMENTS OF CELLULAR BIOLOGY, NEUROLOGY AND NEUROSURGERY
Schumpert Chair in Neurobiology

Full-time tenure-track, joint faculty position available January 1, 1996. Applicants should have a Ph.D. or M.D., postdoctoral experience, and a record of excellent research accomplishments in cell/molecular biology of stroke or related diseases. Candidates should have an established record of extramurally funded research support and be willing to participate in the Neuroscience graduate program. Faculty rank will be commensurate with level of experience. A very attractive package including Schumpert Chair, research facilities and start-up funds is available. Send curriculum vitae and description of current and future research plans to:

Leonard L. Seelig, Ph.D.
Department of Cellular Biology and Anatomy
P.O. Box 33932
Shreveport, LA 71130

Louisiana State University Medical College is an Affirmative Action Employer.

ECOLOGIST
DEPARTMENT OF BIOLOGY

The Department of Biology at Central Michigan University invites applications for a ten-month tenure-track **FACULTY POSITION** in aquatic or terrestrial ecology at the **ASSISTANT PROFESSOR** level to begin August 1996. A Ph.D. is required. Postdoctoral research experience and ability to teach biological statistics is preferred. The successful candidate will be expected to teach undergraduate and graduate (M.S.) courses, establish an active research program, and seek extramural funding. Preference will be given to applications received prior to January 26, 1996. Send curriculum vitae, statement of teaching interests, research objectives, graduate and undergraduate transcripts, and three letters of reference to: **Ecology Search Committee, Department of Biology, Central Michigan University, Mt. Pleasant, MI 48859. FAX: 517-774-3462.**

Central Michigan University (Affirmative Action/Equal Opportunity Institution) encourages diversity and resolves to provide equal opportunity regardless of race, sex, disability, sexual orientation or other irrelevant criteria.

FACULTY POSITIONS
Developmental and Cell Biologists

The Department of Molecular Genetics and Cell Biology invites applications for new faculty positions in the field of mammalian developmental genetics at the **ASSISTANT PROFESSOR** level, although exceptional candidates at any level will be considered. The quality of the research program and its relationship to existing strengths in the Department will be the most important considerations. Complete applications with three letters of recommendation should be sent by January 15, 1996 to: **Dr. Elaine Fuchs, Chair, Search Committee, Department of Molecular Genetics and Cell Biology, The University of Chicago, 920 East 58th Street, Chicago, IL 60637.** *An Affirmative Action/Equal Opportunity Employer. Women and members of minority groups are strongly encouraged to apply.*

PHYTOPLANKTON CURATOR

The Provasoli-Guillard National Center for Culture of Marine Phytoplankton (CCMP) at Bigelow Laboratory is seeking a **CURATOR**. Experience in culturing phytoplankton, algal taxonomy, and light microscopy required. Experience in electron microscopy, molecular biology, or computer science is desirable but not necessary. M.S. or equivalent is minimal requirement. The position requires some heavy lifting (ca 15 kg) and good eyesight for microscopy. The CCMP provides marine phytoplankton cultures to the scientific and aquaculture communities (see our Home Page–http://ccmp.bigelow.org). Please send curriculum vitae and three letters of reference by January 15, 1996 to: **Dr. Robert A. Andersen, Bigelow Laboratory for Ocean Sciences, West Boothbay Harbor, ME 04575 USA.** *Equal Employment Opportunity.*

ASSISTANT PROFESSOR
CHEMICAL ENGINEERING
Massachusetts Institute of Technology

Applicants are invited for a junior-level, **TENURE-TRACK FACULTY POSITION** in the Department of Chemical Engineering at the Massachusetts Institute of Technology. Applicants should have a Ph.D. in chemical engineering or a closely related field, should have demonstrated excellence in academic research, and should have a strong interest in teaching graduate and undergraduate chemical engineering. Send résumé including the names of at least three references, graduate transcripts, and a description of research interests to: **Dr. Robert A. Brown, Head, Department of Chemical Engineering, Massachusetts Institute of Technology, Cambridge, MA 02139.** Material should be received by January 1, 1996. *MIT is an Equal Opportunity/Affirmative Action Employer.*

FACULTY POSITION
BIOLOGICAL CHEMISTRY

The Department of Chemistry at the University of North Carolina at Chapel Hill invites applications for a tenure-track position in biological chemistry. The successful applicant must have a Ph.D., postdoctoral experience, a strong record of research, and the ability to teach biological chemistry effectively at the undergraduate and graduate levels. Preference will be given to individuals who can establish a strong research program in biological chemistry and interact enthusiastically with other chemists, and whose appointment would be at the rank of **ASSISTANT PROFESSOR.** Review of the applications will begin December 15, 1995. Send a curriculum vitae, a brief research plan, a statement of teaching interests, and four letters of recommendation to: **Dr. Nancy L. Thompson, Department of Chemistry, CB 3290 University of North Carolina, Chapel Hill, NC 27599-3290.** *The University of North Carolina is an Equal Opportunity/Affirmative Action Employer.*

Tulane University is seeking to fill a vacant faculty position at the **TENURE-TRACK ASSISTANT PROFESSOR** level. It is possible that a candidate with exceptional qualifications may be considered for a position at a higher level. We are seeking a person with a Ph.D. at the time of appointment that can demonstrate high standards of both teaching and research, and who emphasizes applications of geology to environmental problems. Such a person may have a research field in any specialty, however, strong consideration will be given to those candidates that specialize in fields such as sedimentary geology, geohydrology, geomorphology, remote sensing, geochemistry, or geophysics, and can interact with researchers and students in a developing interdisciplinary environmental science program at Tulane. Applicants should send a letter of application, statement of research and teaching interests, current curriculum vitae, and the names, addresses, and telephone numbers of three references to: **Stephen A. Nelson, Department of Geology, Tulane University, New Orleans, LA 70118. Email: snelson@mailhost.tcs.tulane.edu.** The search will remain open until a qualified applicant is found. *Tulane University is an Affirmative Action/Equal Opportunity Employer. Women and minorities are encouraged to apply.*

DEVELOPMENTAL BIOLOGIST/GENETICIST
ASSISTANT PROFESSOR

TENURE-TRACK POSITION opens fall 1996. Requires teaching genetics, developmental biology, team teaching introductory biology, and advising seniors in thesis research. Ph.D., familiarity with mammalian development and embryology, and previous teaching experience required. Send letter of application, three letters of reference, curriculum vitae and list of references by February 1, 1996 to: **Dr. Donald Toczek, Director, Biology Department, Hillsdale College, Hillsdale, MI 49242.** *Equal Opportunity Employer.*

UNIVERSIDAD DE CHILE ASTRONOMY

Open position for **ASSISTANT/ASSOCIATE PROFESSOR,** tenure-track. Candidate must be a Ph.D., with interest in theoretical astrophysics. Teaching duties include graduate courses in astronomy and undergraduate courses in physics. Please send curriculum vitae and two reference letters before December 31, 1995, to: **Departamento de Astronomia, Casilla 36-D, Santiago, Chile. FAX: 562-229-4101; Email: oficina@das.uchile.cl.**

Roche

Our Preclinical Research Department in Basel is looking for a new member for its

Computational Chemistry

team, to work in the development of new methods in the area of molecular modeling and biostructure-based de-novo design tools.

Candidates are expected to have a strong background in chemical and biostructural research and experience in the algorithmic implementation of methods and tools in this field.

We expect you to have a PhD in chemistry, biochemistry or biophysics, combined with extensive informatics experience, or, alternatively, solid informatics qualifications plus several years' professional experience in the chemistry/biostructure area.

We have strong preferences for platform-independent, modular and eventually object-oriented implementations. Currently our in-house systems are developed in C and run on SGI hardware.

Located in Switzerland we offer a dynamic multidisciplinary international research environment and encourage collaboration with academic groups.

Please apply in writing to our personnel department, Mrs. M. Waespe, quoting reference Science 13/95/Wa.

F. Hoffmann-La Roche Ltd.
P.O. Box, CH-4002 Basel

Greenland's Home Rule

The Danish Research Academy

Greenland Ph.D.-Fellowships

With the purpose af strengthening the research infrastructure of Greenland, the Greenland Home Rule, The Danish Research Academy, and the Danish Ministry of Research with its associated Research Councils announce 2-3 Ph.D.- fellowships.

Applications may cover research training in any discipline within Humanities, Social Sciences, Health Sciences, Natural Sciences and Technology.

Successful candidates are expected to enroll at a Danish University, alternatively another University of relevance to the chosen object.

Fellowships are open to individuals permanently associated with the Greenland society, preferentially people with greenlandic educational background.

Candidates not fully qualifying for a Ph.D.-enrolment at the time of application may be supported for a maximum of 1 year prior to ordinary enrolment.

The application should include a project proposal and indicate at which institute/faculty/university the candidate would prefer to enrol. It is therefore recommended that applicants seek contact to relevant academic advisors prior to developing the application.

Fellowships are granted according to Danish University guidelines, which include a maximum of 149 payments of D.kr. 3.551 during the study period of 3 years. Additional 4.580 D.kr. per month may be obtained from teaching activities or other study-related work.

The application should be submitted in 4 copies to the Danish Research Academy which will ensure a peer review prior to selection of the candidates.

Additional information can be obtained from the Research Academy, att: Rector Ole Fejerskov, phone + 45 8614 4899, fax: + 45 8614 4871, e-mail: academy@inet,unic.dk.; Director Torben Cordtz, the Greenland Home Rule, phone: 00299 230 00; or Director Ove Poulsen, Ministry of Research and Technology, phone + 45 3392 9880, e-mail: OPO@fsk.dk.

Application forms can be obtained from the Danish Research Academy. Deadline for application: **January 15, 1996.**

Greenland covers 2.175.600 sq. km of which 85 pct. is icecovered. The Greenlandic population is 56.000 with 13.000 living in the capital of Nuuk in Westgreenland.

Research in Greenland by Greenlandic research institutes are carried out by Greenland University, the Greenland Nature Institute and the National Museum of Greenland.

Danish research institutes and universities have facilities in Godhavn at the Disco Island, in Kangerlussuaq Airport and at Zackenberg in the North East of Greenland. More than 200 research projects are carried out of Greenland every year partly with logistic support from Danish Polar Center.

POSITIONS OPEN

ASSISTANT PROFESSOR

The Department of Biological Sciences, University of Iowa, invites applications from highly qualified candidates for a **TENURE-TRACK POSITION** in developmental biology or developmental neurobiology, especially from candidates whose research makes use of cellular imaging or molecular genetic techniques. Postdoctoral experience and evidence of strong potential as an independent scholar are required. Teaching duties in both undergraduate and graduate courses will be negotiated based on the candidate's interests and experience. Applicants should ask three referees to send letters of recommendation and should themselves send a curriculum vitae, selected reprints, statement of future research plans, and description of teaching interests by January 15, 1996 to: **Neuro/Development Search Committee, Department of Biological Sciences, Univesity of Iowa, Iowa City, IA 52246.** *Women and minority candidates are encouraged to apply. The University of Iowa is an Affirmative Action/Equal Opportunity Employer.*

BIOLOGIST

Saint Vincent College invites applications for a tenure-track, **ASSISTANT PROFESSOR** level position in cell and molecular biology, beginning in the fall of 1996. Requirements include a Ph.D. and some teaching or post-doctoral experience. Teaching responsibilities will include courses and labs in molecular genetics and advanced cell biology. Supervision of senior research projects (required of all biology majors) and participation in team-taught general biology are also expected.

Saint Vincent College is a Catholic, Benedictine, liberal arts institution that serves 1200 undergraduates. The Biology Department consists of five faculty members and 120 students and emphasizes preparation for graduate and professional school studies.

Please submit a curriculum vitae, three letters of recommendation, transcripts, and a statement of teaching and research interests by December 22, 1995 to: **Director of Personnel, Saint Vincent College, 300 Fraser Purchase Road, Latrobe, PA 15650-2690.** *We are an Equal Opportunity/Affirmative Action Employer.*

DEPARTMENT OF BIOCHEMISTRY
EAST TENNESSEE STATE UNIVERSITY
James H. Quillen College of Medicine

We are seeking an individual at the level of **ASSISTANT** or **ASSOCIATE PROFESSOR** (tenure-track) to develop a research program in the area of cholesterol metabolism as it relates to cardiovascular disease. A secondary interest in the role of lipid metabolism in the regulation of cell growth would also be desirable. The primary appointment will be in the Department of Biochemistry with a joint appointment in the Department of Internal Medicine. Competitive start-up and salary support will be provided.

Interested candidates should send a curriculum vitae and the names, addresses, and telephone numbers of three references by January 31, 1996 to: **Dr. Michael Sinensky, Chairman, Department of Biochemistry, East Tennessee State University, James H. Quillen College of Medicine, Box 70581, Johnson City, TN 37614-0581.** *Affirmative Action/Equal Opportunity Employer.*

TENURE-TRACK POSITION
STROKE AND AGING

The University of Kansas Medical Center (KUMC) is seeking applications for a new **FACULTY POSITION** in the Center on Aging and an appropriate basic science department. The successful candidate will be a cellular, molecular, or integrative neuroscientist with a Ph.D., M.D., or equivalent degree and an established research program relating to ischemic neuronal injury and/or functional recovery from stroke. This individual will hold a position of scientific leadership and facilitate the integration of pre-existing Center on Aging clinical research programs in rehabilitation with a strong neuroscience group whose interests include neuronal death, plasticity, pathogenesis, motor control and development. Send curriculum vitae, a statement of research interest, and names and addresses of three references to: **Stephanie Studenski, M.D., M.P.H., Director, Center on Aging, University of Kansas Medical Center, 3901 Rainbow Boulevard, Kansas City, KS 66160-7117.** *KUMC is an Affirmative Action/Equal Opportunity Employer and encourages applications from women and minorities.*

TENURE-TRACK FACULTY POSITION
VETERINARY SCIENCE

The Department of Veterinary Science, University of Arizona, seeks an outstanding individual with an active research program in the field of vector-borne infectious diseases for a **TENURE-TRACK FACULTY POSITION.** Of particular interest are broadly trained scientists focusing on veterinary molecular virology and/or the biology of vector-borne infectious diseases of veterinary or zoonotic importance. The successful applicant will participate in the research and teaching missions of the university by developing an extramurally funded research program of sufficient scope and caliber to support high quality training opportunities for graduate students, and by teaching in discipline-related courses in the department's undergraduate and graduate programs. Excellent opportunities also exist for interdisciplinary research collaboration with faculty such as those comprising the Vector Biology Program, Center for Insect Science at The University of Arizona. The Vector Biology Program will soon be recruiting an additional tenure-track faculty member who is working at the vector-parasite interface to add to its growing emphasis in public health and medical entomology. Applicants for the position in Veterinary Science must hold the Ph.D. degree; applications from those also holding the D.V.M. or M.D. degree are encouraged. Rank and salary will be commensurate with the successful applicant's qualifications. The starting date is July 1, 1996. Applicants should send a letter of intent describing long-term career goals, and qualifications, interests and accomplishments in research and teaching, curriculum vitae, and the names and addresses of four references to: **Dr. Michael W. Riggs, Chair-Search Committee, Department of Veterinary Science, Veterinary Science/Microbiology Building, University of Arizona, Tucson, AZ 85721.** Review of applications will begin February 15, 1996; applications will be accepted until a suitable candidate is identified. *The University of Arizona is an Equal Opportunity/Affirmative Action Employer.*

THEORETICAL ECOLOGIST
Arizona State University

We invite applications for a reopened and broadened search for a tenure-track position at the **ASSISTANT PROFESSOR** level beginning in fall 1996. Candidates must have a primary research interest and record of accomplishment in the development and testing of broad ecological theory. We welcome applicants from all of the many disciplines relevant to ecology. The successful candidate will be expected to establish an active research program, to participate in undergraduate and graduate-level teaching, and to develop a course in ecological modelling.

Candidates must have demonstrated a strong commitment to teaching and research and must have a Ph.D. in an appropriate area by August 1996. Applicants should forward a curriculum vitae, selected reprints, statements of teaching and research goals, and arrange for three letters of reference to be sent directly to: **Ecologist Search Committee, Department of Zoology, Arizona State University, Box 871501, Tempe, AZ 85287-1501.** Review of applications will begin February 1, 1996 and the 1st of each month until position is filled. Applications from two individuals for a single shared appointment will be considered. *Arizona State University is an Affirmative Action/Equal Opportunity Employer.*

The Department of Biology, Tennessee Technological University, invites applications for a tenure-track appointment at the **ASSISTANT PROFESSOR** level in field botany/vascular plant systematics, beginning August 1996. Applicants must have a Ph.D. in botany and be broadly trained in biology. Teaching responsibilities include regional vascular plant systematics, environmental botany, and introductory biology. The successful applicant will be expected to develop an active research program, direct graduate student research, and serve as curator of the herbarium. Send letter of application, curriculum vitae, and names, addresses, and telephone numbers of three references to:

Chair, Search Committee
Department of Biology
Tennessee Technological University
Cookeville, TN 38505

Closing Date: January 15, 1996 or until filled.

An Affirmative Action/Equal Employment Opportunity Employer.

MOLECULAR BIOLOGIST

Tenure-track **ASSISTANT PROFESSOR** position starting July 1996. Ph.D. required. Teaching and post-doctoral research experience desirable. The successful candidate will participate in undergraduate courses in Developmental Biology, Cellular Biology, Recombinant DNA Techniques, and in University-wide programs. The appointee will join a biology faculty deeply involved in creating a strong research-oriented program for undergraduate students, and will contribute to this effort. Applications are especially encouraged from candidates whose research focuses on developmental biology using molecular techniques. Please forward a letter of application with curriculum vitae, transcripts, statement of teaching and research interests, and representative publications by January 3, 1996, and arrange to have three letters of recommendation sent as quickly as possible to: **Dr. Randall Fuller, Chair, Department of Biology, Colgate University, Hamilton, NY 13346-1398.** *Women and minorities are especially encouraged to apply. Colgate University is an Equal Opportunity/Affirmative Action Employer.*

ASSISTANT/ASSOCIATE PROFESSOR of Audiology and Hearing Sciences (Psychoacoustics), Department of Communication Sciences and Disorders, Northwestern University. Full-time (academic year), tenure-track position. Ph.D. required. Conduct research, direct graduate seminars, and teach upper-division courses in psychoacoustics. Start fall 1996; application deadline February 15, 1996. Send letter and curriculum vitae to: **Chair, Audiology and Hearing Sciences Program, Northwestern University, 2299 North Campus Drive, Evanston, IL 60208-3550. Telephone: 708-491-3164; FAX: 708-491-2523; Email: dcg679@nwu.edu.** *Northwestern University is an Affirmative Action/Equal Opportunity Employer. Hiring contingent upon eligibility to work in the United States of America.*

COGNITIVE NEUROSCIENTIST

The Department of Psychology at the University of Missouri-Columbia (UMC) invites applications for a tenure-track appointment at the **ASSISTANT** or **ASSOCIATE PROFESSOR** level, with research specialization in the neural basis of human information processing (e.g., ERPs, lesion analysis). Please submit curriculum vitae, reprints, a cover letter stating research and teaching interests, and three letters of reference to: **Dr. Steven Hackley, Department of Psychology, 210 McAlester Hall, UMC, Columbia, MO 65211. (Email: shackley@MIZZOU1.missouri.edu; Telephone: 314-882-3277.)** We anticipate interviewing in February 1996; start date August 1996. *Affirmative Action Employer.*

POSTDOCTORAL POSITION immediately available in **Dr. Susan E. Kane's** lab, to study mechanisms of multidrug resistance in human cancers and the application of drug resistance to gene therapy. Requires a Ph.D. in biology or related field; experience in molecular biology, virology, or hematopiesis strongly preferred. Send curriculum vitae and three reference letters to: **City of Hope National Medical Center, Human Resources, Attn: SK, 1500 East Duarte Road, Duarte, CA 91010. FAX: 818-301-8448; Email: jyasminch@smtplink.coh.org.** Other research opportunities are also available. Call our Jobline at **818-301-8200.** *Equal Opportunity Employer.*

POSTDOCTORAL POSITIONS available immediately to develop new DNA fluorescence labeling and analysis methods and apply them to the Human Genome Project. Experience with organic synthesis and nucleic acid enzymology preferred for the bioorganic position. Experience with microfabrication, capillary electrophoresis, DNA sequencing, and biophysical spectroscopy preferred for the biophysical position. Send résumé to: **Dr. Richard A. Mathies, Chemistry Department, University of California, Berkeley, CA 94720.** *The University of California is an Equal Opportunity/Affirmative Action Employer.*

POSTDOCTORAL POSITION to study mechanisms involved in interactions between testicular macrophages and Leydig cells. Experience in several of the following areas desired: lipid chemistry, cell adhesion molecules, HPLC, mass spectroscopy, cell culture, molecular biology, and electron microscopy. Applicant must possess enthusiasm for science. Send curriculum vitae to: **James C. Hutson, Department of Cell Biology and Biochemistry, Texas Tech University HSC, Lubbock, TX 79430.** *Equal Opportunity Employer.*

MACROMOLECULAR SCIENCES

Investigator/Sr. Investigator

SmithKline Beecham Pharmaceuticals, a world leader in pharmaceutical research, has an opportunity for an Investigator to join the Department of Macromolecular Sciences.

The selected candidate will provide leadership in the following areas: the discovery of new enzyme targets; the design and implementation of novel enzyme screening assays and identification of optimal substrates, including the design and testing of novel substrates from phage display or combinatorial libraries; and the characterization and activation of enzymes. This individual will also participate with crystallography, biophysical and protein biochemistry groups in characterization of proteins.

Qualifications include a Ph.D. in Biochemistry, Chemistry or a related field with at least 2 years of postdoctoral experience, plus demonstrated creativity and productivity as evidenced in a strong publication record. Thorough knowledge of protein structure/ function relationships and enzymology, and experience in the application of biophysical techniques are required. Excellent oral and written communication skills and the ability to interact in a multidisciplinary environment are key.

Located in our state-of-the-art research facility in suburban Philadelphia, SmithKline Beecham offers an excellent compensation/benefits/relocation package. Interested candidates should send C.V. with salary requirements to: SmithKline Beecham Pharmaceuticals, Job Code H5-0488, P.O. Box 2645, Bala Cynwyd, PA 19004. We are an Equal Opportunity Employer, M/F/D/V.

SB
SmithKline Beecham
Pharmaceuticals

Challenging the natural limits.

DISCOVER SUGEN:

A LEADER IN SIGNAL TRANSDUCTION RESEARCH

SUGEN, Inc., a dynamic biopharmaceutical company in the San Francisco Bay Area, is focused on the discovery and development of drugs for the treatment of cancer, immunological disorders and diabetes. Our research teams identify novel kinases and phosphatases, and elucidate signaling pathways in disease relevant models. We currently have the following opportunities.

Immunology

GROUP LEADER: This group will focus on immunosuppression and inflammation. The position requires a Ph.D. and several years of experience in immunological research. Experience in signal transduction pathways essential.

Gene Expression

SCIENTIST: This Ph.D.-level position requires an individual experienced in vector construction and eukaryotic and prokaryotic expression systems.

Please send *c.v.*, along with the names, addresses and telephone/fax numbers of three references, to: **SUGEN, Inc., Human Resources Dept. SC, 515 Galveston Drive, Redwood City, CA 94063.** A competitive salary and benefits, including stock options, support these positions. Equal Opportunity Employer.

SUGEN, Inc.

Chair, Department of Chemistry
Ohio University

Applications are invited for the position of Chair of the Department of Chemistry in the College of Arts and Sciences at Ohio University. Ohio University, located in the city of Athens (population 30,000), is a state university with Carnegie Research II status and has undergraduate and graduate student enrollments of 16,000 and 2,500 respectively. The Department of Chemistry has 22 full-time tenure-track faculty with approximately 300 undergraduate majors in traditional chemistry, forensic chemistry, biochemistry, and pre-professional programs, and 50 Ph.D. and M.S. students. The research strengths of the Department are in analytical chemistry and the chemistry of biological systems, and candidates for the Chair should have their research interests in one of these areas. The successful applicant will be expected to lead a reorganization of the Department which will include focusing the Ph.D. program in the areas of current strength. Candidates should have an international reputation in their research area, an established record of external funding and publication in quality journals, current substantial external funding and qualifications which merit tenure and rank of Professor. Candidates should also have administrative skills and/or experience which will enable them to maintain an active research program in addition to assuming the administrative responsibilities as Chair of the Department. Salary and research support for the position are competitive. This position is contingent on final budgetary approval by Ohio University. Letters of application containing a curriculum vitae, a description of research interests and current areas of activity, names of three references, and a statement describing administrative experience and philosophies should be addressed to: **Dr. P. Johnson, Search Committee Chair, Department of Chemistry, Clippinger Laboratories, Ohio University, Athens, Ohio 45701.** Completed applications will be reviewed beginning January 15, 1996, with July 1, 1996 as the negotiable staring date for the position. *Ohio University is an Equal Opportunity/Affirmative Action Employer.*

IDEXX. Nothing Short of Brilliant.

IDEXX, a leader in the development of advanced biotechnology-based detection systems for animal health and food and environmental applications, currently has the following opportunity available:

Research Scientist

You will be responsible for the development of ATP-bioluminescence test kits. The ideal candidate will have experience in enzymology (preferably with luciferase), lyphilization and basic microbiology skills. A Ph.D. and 2+ years' post-doctoral experience required. Communication and management skills important.

Please send a cover letter and resume with references to: **IDEXX Laboratories, Inc., Human Resources, Code EERS, One IDEXX Drive, Westbrook, ME 04092.** No phone calls please. We are an Equal Opportunity Employer M/F/D/V.

IDEXX

CALIFORNIA CAREER OPPORTUNITIES

PATHOLOGY: The University of California, Davis, School of Medicine seeks a full-time academic Chairperson of Pathology. Candidates must possess an M.D. degree and be Board Certified in Anatomic/Clinical Pathology, be eligible for licensure in California and be academically qualified for appointment at the professorial level. Demonstrated evidence of excellence in academic and clinical service administration, teaching, and research is required. Please forward the following: (1) letter describing administrative, teaching, and research background; (2) curriculum vitae; (3) names and addresses of five references to Chair, Search Committee for Chair of Pathology, c/o Karen Eilers, Office of the Dean, School of Medicine, East Health Sciences Drive, University of California, Davis, California 95616. This position will be "Open Until Filled"; for full consideration, applications should be received by March 31, 1996. *The University of California is an Affirmative Action/ Equal Opportunity Employer.*

POSITIONS OPEN

POSTDOCTORAL POSITIONS
Roswell Park Cancer Institute
Department of Human Genetics
with Thomas B. Shows, Ph.D. and
Pieter J. de Jong, Ph.D.

Positions available for Ph.D./M.D. in human genome research including projects involving: efficient construction of sequence ready clone sets; analysis of conserved repetitive DNA; application of recombination-based cleavage methods for chromosome analysis and genome manipulation; transcript mapping; positional cloning of disease loci; sequencing the genome; and improvements in large-insert cloning technology.

Experience in molecular genetic and genome technology is required. Please send curriculum vitae, a description of your research experience and future interests, and names and telephone numbers of three references to: **Chair, Department of Human Genetics, Roswell Park Cancer Institute, Buffalo, NY 14263.** *Roswell Park is a Minority/Female/Disabled/Veteran Affirmative Action Employer.*

SCIENTIST/POSTDOCTORAL POSITIONS
Molecular Characterization of Ion Transport Proteins

SCIENTIST (RESEARCH ASSISTANT PROFESSOR) and **POSTDOCTORAL POSITIONS** are available immediately at the University of Rochester to investigate the molecular physiology of secretion in exocrine gland cells. Structure/function studies will include the cloning and *in vitro* expression of ion transport proteins. Ph.D. with a background in molecular and cellular biology required. Send curriculum vitae and the names of three references to: **Dr. James E. Melvin, School of Medicine and Dentistry, Box 611, University of Rochester, 601 Elmwood Avenue, Rochester, NY 14642. FAX: 716-473-2679; Email: melvin@medinfo.rochester.edu.** *Equal Opportunity/Affirmative Action Employer.*

POSTDOCTORAL POSITION available immediately to study molecular cardiovascular physiology. Candidates must have an M.D., D.V.M. or Ph.D. with training in physiology, pharmacology, or related area, and a firm commitment to research. Background in molecular biology desired but not necessary. Projects include: (1) studies involving *in vivo* hemodynamic (macro- and microcirculatory) analysis of transgenic animals, and/or (2) gene therapy involving the arterial wall and/or heart. Send curriculum vitae, summary of research interests, and names of three references to: **Dr. R. Wayne Barbee, Division of Research, Alton Ochsner Medical Foundation, 1520 Jefferson Highway, New Orleans, LA 70121.** *Ochsner is an Affirmative Action/Equal Opportunity Employer.*

POSTDOCTORAL POSITION is available immediately to study the regulation of activation of matrix metalloproteinases in cancer. Applicants should have a strong background and experience in enzymology, protein chemistry, and molecular biology. Research involves structure-function studies of enzyme domains, enzyme-inhibitor interactions, kinetic analysis, site directed mutagenesis, and recombinant protein expression. Send curriculum vitae and names of three references to: **Dr. Rafael Fridman, Department of Pathology, Wayne State University, 540 East Canfield Avenue, Detroit, MI 48201.**

POSTDOCTORAL ASSOCIATE

A **POSTDOCTORAL ASSOCIATE** is sought for ongoing studies on the posttranscriptional control of development in *Xenopus* and mouse. These involve the analysis of RNA-protein interactions and translational control, oocyte microinjection, and the generation of transgenic mice. Please submit a curriculum vitae and the names and addresses of three persons who may act as references to: **Dr. Joel Richter, c/o Human Resources, Worcester Foundation for Biomedical Research, 222 Maple Avenue, Shrewsbury, MA 01545.** *Affirmative Action/Equal Opportunity Employer.*

POSTDOCTORAL POSITION available to study transcriptional regulation in the bacterial flagellar regulon. Applicants should have background in molecular biology. Please send curriculum vitae and a list of references to: **Dr. Philip Matsumura, University of Illinois at Chicago, Department of Microbiology and Immunology, M/C 790, 835 South Wolcott Avenue, Chicago, IL 60612-7344.** *UIC is an Affirmative Action/Equal Opportunity Employer.*

POSTDOCTORAL POSITIONS

Two grant-funded **POSTDOCTORAL RESEARCH ASSOCIATE** positions are available immediately to participate in an epidemiological study of body composition and cardiovascular disease risk factors. The primary focus of the work is to assist in analyzing data collected in the ongoing Fels Longitudinal Study and to collaborate in writing manuscripts describing specific findings from these data. Opportunities exist for participating in the expansion of the scope of the research into new related areas. A doctoral degree in one of the following areas is required; epidemiology, sports medicine, biostatistics, exercise physiology, human biology, nutrition, genetic epidemiology or a related field. Ability to work independently and cooperatively within a team of established investigators is essential. Current research interests within this team center on the role of changes in body composition over the life span in the development of cardiovascular and other age-related diseases, biostatistical methods for serial analyses, genetic epidemiology, and aging. Applicants with statistical and analytical background and compatible research interests are preferred. Positions are open until filled. Send curriculum vitae, a short statement of research interests, and names of three references to: **Chair, Postdoctoral Search Committee, Division of Human Biology, Department of Community Health, Wright State University School of Medicine, 1005 Xenia Avenue, Yellow Springs, OH 45387-1695. FAX: 513-767-6922.** *Equal Opportunity Employer/Affirmative Action.*

POSTDOCTORAL POSITION
Joslin Diabetes Center/Harvard Medical School

Applications are invited for a **POSTDOCTORAL POSITION** available immediately for NIH-funded studies of polyendocrine autoimmune diseases (diabetes, thyroiditis, and adrenalitis) and diabetic kidney complications in mice. Candidates should have a Ph.D. or M.D./Ph.D. with zero to two years of postdoctoral experience in molecular biology or immunogenetics and possess expertise in breeding studies, gene mapping, cloning, sequencing, and expression. Please send curriculum vitae and the names, addresses, and telephone numbers of three references to: **Dr. Masakazu Hattori, Section on Immunology and Immunogenetics, Joslin Diabetes Center, One Joslin Place, Boston, MA 02215. Email: hattorim@joslab.harvard.edu; FAX: 617-732-2589.**

POSTDOCTORAL RESEARCH ASSOCIATE
NEUROCHEMISTRY/MOLECULAR BIOLOGY

NIH RO1-funded position, salary commensurate with qualifications. Individual will perform HPLC analysis of novel neurotransmitters, and molecular cloning of receptors and ion channels in the auditory/vestibular periphery. Send curriculum vitae, previous publications, and names of three references to: **Dr. Dennis Drescher, Laboratory of Bio-otology, Wayne State University School of Medicine, 540 East Canfield Avenue, 259 Lande Medical Research Building, Detroit, MI 48201.** *Wayne State University is an Equal Opportunity/Affirmative Action Employer.*

POSTDOCTORAL POSITION
Biological Mass Spectrometry

Position available early 1996, projects involve structural studies of protein toxins and microcapillary HPLC methods development. Submit curriculum vitae and names of three references to: **Dr. Murray Hackett, Department of Medicinal Chemistry, University of Washington, Box 357610, Seattle, WA 98195-7610.** Address inquiries for further information to: **mhackett@u.washington.edu.** *The University of Washington is an Equal Opportunity/Affirmative Action Employer.*

POSTDOCTORAL OPPORTUNITY available now in the Markey Center for Cell Signaling for biochemist with background and interest in protein kinases, phosphatases or G-proteins in cellular signaling. Candidates must have published first-author peer-reviewed papers in good journals. Preference may be given to individuals who are available by February 1, 1996, but all interested persons are urged to provide a letter of inquiry, curriculum vitae, and three references to: **Dr. Thomas W. Sturgill, University of Virginia Health Sciences Center, Markey Center for Cell Signaling, Box 577, Charlottesville, VA 22908. FAX: 804-924-9659.** *An Equal Opportunity/Affirmative Action Employer.*

RESEARCH ASSOCIATE
MOLECULAR VIROLOGY
University of Southern California

POSTDOCTORAL POSITIONS are available to study the molecular biology of gene expression and RNA synthesis of several viruses, including mouse hepatitis virus, human hepatitis delta virus, and hepatitis C virus. Background in molecular biology, virology, or biochemistry is desirable. Please send curriculum vitae to: **Dr. Michael Lai, Department of Molecular Microbiology and Immunology, University of Southern California, 2011 Zonal Avenue, HMR-401, Los Angeles, CA 90033. FAX: 213-342-9555.** *University of Southern California is an Equal Opportunity Employer.*

POSTDOCTORAL POSITION
Cellular Neurobiology

POSTDOCTORAL POSITION available immediately to investigate the function of transmembrane heparan sulfate proteoglycans in the developing nervous system. A broad range of cell biological, molecular, and biochemical techniques will be utilized. Experience with cell culture and molecular biology techniques (cloning, mammalian expression, site directed mutagenesis) and protein purification and characterization are desirable. Interested candidates should send a curriculum vitae, names of three references, and a brief summary of research experience to: **Geisinger Human Resources (DJC), 100 North Academy Avenue, Danville, PA 17822-1529.** *Equal Opportunity Employer. Minority/Female/Disabled/Veteran.*

POSTDOCTORAL/RESEARCH ASSOCIATE

Available for the study of human molecular genetics of inherited ophthalmic diseases. Current research includes: Linkage mapping, mutation analysis, SSCP, DGGE, Cosmid Contig maps, selective hybridization cloning, library screening, apoptosis research, gene transfer studies. Send curriculum vitae and names, telephone and Email addresses of three references to: **Kent W. Small, M.D., Associate Professor, Doris Stein Eye Research Center, 200 Stein Plaza—UCLA, Los Angeles, CA 90024-7007.** *An Equal Opportunity/Affirmative Action Employer.*

POSTDOCTORAL FELLOWSHIP: excellent opportunity to participate in research program to utilize protein chemistry and molecular biological techniques in reproductive endocrinology among a diverse group of scientists. Send letter of application to:

Dr. Robert E. Canfield
Columbia University
College of Physicians & Surgeons
630 West 168th Street (PH10-305)
New York, NY 10032

Columbia University is an Equal Opportunity/Affirmative Action Employer.

POSTDOCTORAL RESEARCH
Transcriptional Regulation and Virology

Shelley L. Berger, Ph.D.: Analysis of human and yeast adaptors in transcriptional activation and in HSV-1 reactivation from latency. **Paul M. Lieberman, Ph.D.:** Function of TF11A and TF11D recruitment by activators that disrupt viral latency. **The Wistar Institute, 3601 Spruce Street, Philadelphia, PA 19104.** *Equal Opportunity Employer.*

RESEARCH ASSOCIATE

RESEARCH ASSOCIATE position available immediately to clone transcription factors regulating expression of the chemoattractant cytokine RANTES. Requirements: Ph.D. in relevant biology with at least three years of post-degree laboratory experience. Experience in cloning transcription factors desired. Send curriculum vitae with three references to: **Dr. Alan Krensky, Department of Pediatrics, Stanford University, Stanford, CA 94305-5119.**

ENDOCRINOLOGY FELLOWSHIP

Unexpectedly available, starting July 1996 in multidisciplinary clinical/research division. Will accept transfer from other program. Contact: **Maria Grant, Chief, Division of Endocrinology, Department of Medicine, University of Florida, Gainesville, FL. Telephone: 904-392-2726; FAX: 904-846-2231.** Must be able to commit by December 31, 1995.

DNX Transgenics, *a subsidiary of DNX Corporation, is a leading transgenic animal development company providing custom transgenic animal model development capabilities and Biodigm® transgenic animals to the biomedical research community.*

PRINCIPAL SCIENTIST TRANSGENIC ANIMAL SCIENCE

An opportunity exists for a Ph.D. Scientist to direct commercial transgenic animal projects, develop new transgenic animal technologies and evaluate the utility of transgenic animal models for drug discovery.

Qualified candidates will have a Ph.D. in molecular biology or related field and 2-5 years postdoctoral experience developing transgenic animal models. Experience developing animal models by homologous recombination is highly desirable. Animal science experience and 2-3 years of industry experience in a supervisory role are also preferred. Excellent oral and written communication skills and the ability to work in a team environment are essential.

DNX Transgenics offers an excellent compensation package including competitive salary, stock option program and comprehensive benefits. For the opportunity to be an integral part of this expanding organization, send curriculum vitae and references to:

Human Resources
DNX Corporation
575 Route 28, Raritan, NJ 08869

Equal Opportunity Employer

Florida State University
Vice President for Research

The Florida State University, a member of the State University System of Florida, is seeking a vice president for research. The university is located in Tallahassee, the state capital.

The Florida State University, founded in 1857, is a comprehensive Research I university with extensive research facilities and a faculty of 1100. The university awards approximately 300 doctoral, 1400 master's, and 5,000 baccalaureate degrees annually. Its 30,000 students, of whom 5,600 are graduate students, are enrolled in sixteen schools and colleges. Expenditures in contracts and grants for 1995-96 will total $100 million.

The vice president for research is the senior administrative officer in the university responsible for research policy and the administration of sponsored research. The vice president represents the university to local, state, and national public and private entities in all matters related to research. The vice president reports to the president of the university. The following units report to the vice president for research: National High Magnetic Field Laboratory, Supercomputer Computations Research Institute, Marine Laboratory, Laboratory Animal Resources, and the Institute for Science and Public Affairs. Technology transfer, the Research Foundation, and Innovation Park are responsibilities of this office.

The University is searching for a scholar of national prominence who has had university-based research experience. Candidates should have successfully achieved significant funding from federal or other sources. National experience involving university representation with federal agencies, or service with a national agency or professional advocacy organization is highly desirable. Candidates should have administrative experience within a complex academic or related organization and strong communication skills.

Nominations or applications for the position should be sent to the **Chair of the Search Committee, Dean Alan Mabe, Office of Graduate Studies, 408 Westcott, Florida State University, Tallahassee, FL 32306-1047.** Dean Mabe can be reached at (904) 644-3500 or vpsearch@westcott.wes.fsu.edu. Information about the university can be found at its web site, http://www.fsu.edu/

A completed candidate folder will include a curriculum vitae, a list of five references, and a statement of candidacy. The closing date for the receipt of nominations is January 12, 1996 and the closing date for the receipt of all materials is January 19, 1996.

The Florida State University is an Equal Opportunity/Affirmative Action employer that encourages applications from minorities and women and complies with the Americans with Disabilities Act. It is a public-record agency pursuant to Chapter 119, Florida Statutes.

CANCER PREVENTION RESEARCHER

The H. Lee Moffitt Cancer & Research Institute and the College of Medicine at the University of South Florida are seeking applicants for a tenure-earning Associate or Full Professor faculty position for a laboratory based independent researcher with expertise in translational research. This position will be in the Cancer Prevention Program.

The successful candidate will be a doctoral level (MD or Ph.D.) investigator who will have responsibility for conducting laboratory research in the area of molecular and immunohistochemical markers for the early detection of preneoplastic conditions and early cancer. This research should lead to the design of interventions to target these markers with chemopreventive agents. The successful candidate will also have an established track record of obtaining external funding and five years academic or research experience at, or comparable to, the Assistant Professor level. The position will include heading up the Molecular Core Laboratory designed to support marker studies initiated by clinical researchers at the Cancer Center.

H. Lee Moffitt Cancer Center & Research Institute, adjacent to the Health Sciences Center on the University of South Florida's Tampa Campus includes a modern, 162-bed inpatient and ambulatory facility for children and adults, a 25-bed bone marrow transplantation program, a recently established high volume screening program including a fixed site and mobile unit and a new basic research facility.

Send inquiries and current curriculum vitae to Gail Shaw, M.D., Program Leader, Office of Faculty Recruitment, 12902 Magnolia Drive, Tampa, Florida 33612. Applicants must be postmarked by deadline date of January 31, 1996.

H. LEE MOFFITT CANCER CENTER
& RESEARCH INSTITUTE
University of South Florida College of Medicine

Moffitt Cancer Center is an Equal Opportunity Employer. The University of South Florida is an Equal Opportunity/Equal Access/Affirmative Action Employer. For disability accommodations please contact Jody Swanson at (813) 975-7894 a minimum of five working days in advance.

Department of Earth and Atmospheric Sciences
University of Alberta

Tenure Track Position in Resource/Environmental Management

The University of Alberta recently established the Department of Earth and Atmospheric Sciences through the merger of the Departments of Geology and Geography. Detailed information about the department can be found on the World Wide Web at: http://www.ualberta.ca/~eas/home.html. The new department wishes to further strengthen its teaching and research in the area of Resource/Environmental Management. We are particularly interested in an individual with expertise in the social dimensions of environmental earth science and geological activity.

The appointment will be at the Assistant Professor level (salary range of $39,230-$55,526). Applicants must hold a Ph.D. degree and have a proven research record. Previous teaching experience would be a significant asset.

Two Tenure Track Positions in Geoprocessing

The University of Alberta recently established the Department of Earth and Atmospheric Sciences through the merger of the Departments of Geology and Geography. Detailed information about the department can be found on the World Wide Web at: http://www.ualberta.ca/~eas/home.html. The new department wishes to strengthen its research programs in geoprocessing through the appointment of two new faculty members. Appointees will have responsibility for teaching and research in the areas of Geographic Information Systems (GIS), Cartography, Remote Sensing, and Quantitative Methods (with emphasis on spatial applications). Experience with application of these methods to an area of research such as biogeography, human geography, terrain analysis, geological exploration, geological mapping, and/or atmospheric sciences would be an advantage.

One position will be at the Assistant Professor level and the second position may be at a higher level if the candidate has a proven track record in teaching and research.

Salary ranges are: Assistant Professor - $39,230-$55,526; Associate Professor- $48,736-$69,664; and Professor- starting at $60,567. Applicants must hold a Ph.D. degree and have a proven research record. Previous teaching experience would be a significant asset. Applications, including a resume, a statement of research interests, and the names and addresses of three referees, should be addressed to Dr. Brian Jones, Chair, Department of Earth and Atmospheric Sciences, University of Alberta, Edmonton, Alberta, Canada, T6G 2E3. (Fax: 403-492-2030; e-mail: bjones@gpu.srv.ualberta.ca). Deadline for receipt of applications is January 15, 1996. The appointments will commence on July 1, 1996 providing suitable candidates can be found.

In accordance with Canadian Immigration requirements, priority will be given to Canadian citizens and permanent residents of Canada.

The University of Alberta is committed to the principle of equity in employment. As an employer we welcome diversity in the workplace and encourage applications from all qualified women and men, including Aboriginal peoples, persons with disabilities, and members of visible minorities.

POST DOCTORAL RESEARCH POSITION
UNIVERSITY OF ARIZONA
DEPARTMENT OF ASTRONOMY
STEWARD OBSERVATORY
CENTER FOR ASTRONOMICAL ADAPTIVE OPTICS

Applications are invited for a research associate position with the Center for Astronomical Adaptive Optics. The Center is building a powerful adaptive optics system for operation with the new 6.5 m telescope which will replace the MMT in 1997. The system will routinely achieve the diffraction limit of the 6.5 m aperture at 1.6 and 2.2 microns. Very low thermal background is projected since correction will be done with an adaptive secondary. The sodium laser guide star system to be used with the 6.5 m is already installed at the present MMT, allowing 0.3 arcsec images over the whole sky by rapid correction of image motion.

Applicants must have a recent PhD in astronomy, and will be expected to concentrate on scientific observations with adaptive optics at wavelengths from 1 to 2.5 microns. Preference will be given to the candidate who brings expertise in areas of extragalactic astronomy, complementing current research on the solar system, stellar companions and the Galactic center. Previous experience with adaptive optics and an interest in the physics and technology underlying adaptive correction will be taken into consideration.

The position is funded for two years at a salary beginning at $38,000, with the possibility of extension. Interested applicants should send curriculum vitae and names and addresses of three referees to **Dr. Roger Angel at Steward Observatory, University of Arizona, Tucson, Arizona 85721, (520) 621-4409, fax (520) 621-9843.** Application review will begin January 2, 1996. *The University of Arizona specifically encourages applications from women and minorities. AA/EEO/ADA.*

The University of **Montana**

VICE PRESIDENT FOR RESEARCH AND DEVELOPMENT

The University of Montana-Missoula invites applications and nominations for the position of Vice President for Research & Development. The Vice President will provide leadership and direction for all research programs at the University in Missoula and will coordinate research and creative activities at the University's three other campuses. The Vice President reports directly to the President of the University, acts on the President's behalf for research activities and is responsible for research planning, program development and developing new opportunities for research. The Vice President develops relationships with government agencies and the private sector, strengthens research infrastructure and nurtures ideas and research initiatives.

The University of Montana includes campuses in Missoula, Butte, Dillon and Helena. The University of Montana-Missoula is a comprehensive, doctoral-granting institution committed to excellence in teaching, research and service. The University maintains nine doctoral and 43 masters' programs, having a combined graduate enrollment of over 1,700 students, and has rapidly growing research and creative activities.

Candidates must have an earned doctorate and a strong record of research and other achievements, a clear understanding of the role of research and creative activities and their relationship to graduate education, demonstrated experience in research administration, the developed ability to communicate effectively, and the capacity to provide leadership essential to the continued development of research and creative activity at the University.

Salary will be commensurate with experience and qualifications. The position is available 1 July 1996. Nominations must be received no later than 16 January 1996 and applications, including vitae and the names of five references, by 16 February 1996.

Address all inquires, applications and nominations to:

Mr. Robert Frazier, Executive Assistant to the President
Chair, Vice Presidential Search Committee
The University of Montana
Missoula, MT 59812-1291
Telephone: (406) 243-2311; FAX: (406) 243-2797
e-mail: frazier@lewis.umt.edu

The University of Montana is an equal opportunity employer.

VASCULAR BIOLOGIST/ PHARMACOLOGIST

The Pharmacology Department of Merck Research Laboratories, a world leader in the discovery and development of pharmaceutical and biological products, has a career opportunity for a Vascular Biologist/Pharmacologist. The successful candidate will be responsible for the development of new, quantitative animal models of vascular growth and repair such as re-endothelialization, angiogenesis, vascular reactivity, proliferation and restenosis. Candidate will also participate in ongoing antithrombotic/anticoagulant projects by conducting and/or supervising *in vivo* experiments.

The position requires an M.D., Ph.D. or equivalent in physiology, pharmacology or related field with a minimum of 2 years postdoctoral experience.

Excellent salary and benefit programs accompany this position at our modern research facilities located 25 miles northwest of Philadelphia.

Please send curriculum vitae with cover letter to: **Personnel Manager, Ad#B-41, MRL Human Resources, WP 42-2, Merck Research Laboratories, P.O. Box 4, West Point, PA 19486.** EEO/AA/V/Employer.

MERCK
Research Laboratories

TOXICOLOGIST

Rohm and Haas Company, a leading chemical company serving global markets, has an immediate opening for a Toxicologist with expertise in *in vitro* methodology. This position is at our Corporate Research Center in Spring House, PA, near Philadelphia.

We are looking for a scientist to assume the leadership of a laboratory conducting assays in genetic toxicology, as well as research in toxicology using *in vitro* methods. The assays and research are primarily directed toward the expeditious development of new products for regulatory acceptance.

The successful candidate will have a Ph.D. degree in a relevant discipline, with demonstrated technical expertise in *in vitro* toxicology methods: e.g., genetic toxicology, cytotoxicity, receptor-mediated toxicity. This scientist will also have a substantive publication record in the peer-reviewed literature.

Our position requires a broad perspective of toxicology, as well as outstanding oral and written communication skills to interact effectively with regulatory scientists and our company's scientific staff. Candidates must be skilled in project management and have the drive, aptitude and motivation to work effectively in multidisciplinary teams.

Rohm and Haas offers a highly competitive salary and benefits program, including relocation assistance. We invest heavily in research and in resources to develop our Research staff. Candidates must be legally qualified to hold regular employment in the U.S. For consideration, please forward your resume or C.V., including publication list and references, to: **Corporate Staffing #295, Rohm and Haas Research Laboratory B-70, 727 Norristown Road, Spring House, PA 19477-0904.**

ROHM AND HAAS

An Equal Opportunity Employer M/F/H.

SIUE

MOLECULAR PLANT SYSTEMATIST. The Department of Biological Sciences, Southern Illinois University at Edwardsville, invites applications for a tenure-track position in molecular plant systematics at the Assistant Professor level. We seek applicants with extensive training in botany and expertise in evolutionary biology. We are particularly interested in candidates who take a broad view of plant systematics, but who apply molecular techniques to problems in evolution, conservation biology or other related fields. The successful candidate will teach a course in modern plant systematics and share responsibility for teaching general botany for biology majors and a general education course in biology for nonmajors. Candidates should exhibit potential for independent and innovative research involving undergraduate and graduate students and a willingness to support the Ecology, Evolution and Environment specialization in Biology and the Environmental Studies Program. Qualifications: Ph.D., preferably in botany, with teaching experience; post-doctoral experience strongly preferred. To apply, send a letter of application with a statement of your teaching and research interests, curriculum vitae, university transcripts, names and addresses of three persons who will serve as references, and reprints of no more than three publications to: **Chair, Molecular Plant Systematist Search Committee, Southern Illinois University at Edwardsville, Department of Biological Sciences, Box 1651, Edwardsville, IL 62026-1651.** Review of applications will begin on Feb. 15, 1996 and continue until position is filled. SIUE is a comprehensive regional university located in the St. Louis Metropolitan Region, and is dedicated to excellence in undergraduate education. *SIUE is an affirmative action/equal opportunity employer.*

WEST VIRGINIA UNIVERSITY

Two Tenure-Track Faculty Positions

The Departments of Physiology and Otolaryngology at West Virginia University Health Sciences Center invite applications for two state-funded tenure-track faculty positions available Spring 1996. We seek scholars to establish vigorous and independent research programs and to participate in departmental teaching and service missions. Qualified applicants with established records of research productivity are invited to apply for either position or for both, as appropriate. **Applicants should send a letter of application, a curriculum vitae, reprints of publications, a statement of research interests and professional goals, and arrange to have three letters of recommendation sent by January 15. Applications received by the deadline will be given first consideration.**

The PHYSIOLOGY DEPARTMENT seeks a scientist to apply molecular and cellular approaches to fundamental mechanisms of development, plasticity or remodeling. The department is building an integrative group to investigate physiological mechanisms at the molecular and cellular level. Address application to: **Dr. David L. Kreulen, E.J. van Liere Professor and Chair, Department of Physiology, Box 9229, West Virginia University, Morgantown, WV 26506.**

The OTOLARYNGOLOGY DEPARTMENT seeks an individual to join a growing group of scientists and to apply molecular approaches to fundamental questions in the auditory or vestibular systems. Candidates with interests in development, regeneration, signal transduction, cell biology and/or molecular genetics are encouraged to apply. A joint appointment in the appropriate basic science department is available. Address application to: **Dr. Stephen J. Wetmore, Chair, Department of Otolaryngology, Box 9200, West Virginia University, Morgantown, WV 26506.**

West Virginia University is an Affirmative Action/Equal Opportunity Employer.

CARING TOGETHER

POST-DOCTORAL FELLOW

Bone/Cell/Molecular Biology

Saint Francis Hospital & Medical Center is seeking candidates who have completed a doctoral degree to join our NIH-supported Bone Biology Laboratory.

Interested candidates should send a resume and references to:

Dr. Ernesto Canalis, Director, Department of Research, Saint Francis Hospital & Medical Center, 114 Woodland Street, Hartford, CT 06105-1299.

SAINT FRANCIS | MOUNT SINAI

EEO/AA - M/F/D/V Pre-Employment Drug Testing

REQUEST FOR PROPOSALS
MOLECULAR GENETIC STUDIES
INHERITED RETINAL DEGENERATIONS

Proposals are invited for molecular genetic analysis of inherited retinal degenerations such as retinitis pigmentosa and allied disorders, Usher syndrome, and inherited macular degenerations. Proposals must focus on the genetic etiology of retinal degeneration, definition of the mechanisms related to known genetic etiologies, and/or therapeutic approaches based on known etiology and mechanisms. Innovative approaches to causes of the understudied genetic types, especially recessive RP, are encouraged.

New and renewal applications will be reviewed together by a special panel of consultants to The Foundation's Scientific Advisory Board, solely on the basis of scientific merit and program relevance. Awards will average $100,000 annually for three years.

Interested individuals should submit a letter of intent which briefly summarizes the proposed research, provides background of the laboratory, includes curricula vitae of the principal investigators and gives an approximate budget. Following a preliminary review, complete applications will be invited from a limited number of applicants. Deadline for letter of intent is January 22, 1996, for application is May 3, 1996, and funding is expected to begin September 1, 1996.

Address letters of intent to: **Department of Science, The Foundation Fighting Blindness, Executive Plaza One, Suite 800, 11350 McCormick Road, Hunt Valley, MD 21031-1014. Telephone: 410-785-1414, FAX: 410-771-9470.** *(Formerly: RP Foundation Fighting Blindness, Baltimore, MD)*

The Chinese University of Hong Kong Faculty of Medicine

The University (founded 1963) offers comprehensive programmes up to PhD level. Student enrollment in 1995–96 is around 11,500 full-time equivalent. The Faculty of Medicine offers undergraduate and postgraduate programmes in Medicine, Nursing and Pharmacy. The MBChB programme admits 160 students annually and is fully recognized by the General Medical Council of the United Kingdom. Clinical courses are taught at the Medical Faculty's 1,450-bed teaching hospital, the Prince of Wales Hospital, which is one of the regional hospitals in Hong Kong and at the Lek Yuen Health Centre. English is used in teaching and administration in the Faculty of Medicine.

Applications are invited for the following post:

Department of Physiology (Ref. 95/129(665)/2)
Lecturer (carrying the title of **Assistant Professor** or **Associate Professor**, as appropriate)
Applicants should have a Ph.D. degree or a medical qualification and some teaching and research experience in the field of Physiology. The Department offers courses to medical, nursing and pharmacy students of the Faculty and students majoring in Human Biology. The Department specialises in research in the areas of ion channels and epithelial transport, sensory and central nervous system physiology, vascular physiology, muscle physiology, molecular endocrinology and reproductive physiology. The appointee is expected to assume duty in August 1996 or as soon as possible thereafter.

Annual Salary and Fringe Benefits
HK$454,200–758,700 by 10 increments
(approx. exchange rate in November 1995 : £1=HK$12.2, US$1=HK$7.8)
Starting salary will be commensurate with qualifications and experience.

Benefits include leave with full-pay, medical and dental care, education allowance for children, housing benefit for eligible appointee (with appointee contributing 7.5% of salary towards the provision of housing). Appointment may be made either on regular or contract terms. Under regular contract, retirement benefits are provided by the University. Fixed term contract also carries where appropriate a contract-end gratuity (15% of basic salary).

Application Procedure
Send full resume in duplicate and names and addresses of three referees, with copies of academic credentials (in duplicate) and recent publications, to the Personnel Office, The Chinese University of Hong Kong, Shatin, N.T., Hong Kong (Fax: (852)2603 6852) before December 31, 1995. Please quote the ref. no and mark "Recruitment" on cover. [Note: The University reserves the right not to fill the post or to fill the post by invitation.]

UNIVERSITY OF COLORADO AT BOULDER

Molecular, Cellular, and Developmental Biology

We seek tenure-track faculty working on developmental biology of multicellular eucaryotes, particularly mammals. Preference will be given to candidates at the assistant professor level. Appointments could begin as early as August 1996. Successful candidates must have demonstrated outstanding research ability and teaching skills. Send résumé, representative reprints, an outline of future research directions, and three letters of recommendation to: **New Faculty Search, MCD Biology, University of Colorado, Boulder, CO 80309-0347.** Dossiers considered upon receipt. Latest possible receipt of all application materials: 2/1/96.

The University of Colorado is an equal opportunity/ affirmative action employer.

GLOBAL CAREER OPPORTUNITIES

AUSTRALIAN NATIONAL CENTRE IN HIV VIROLOGY VACANCY FOR SENIOR SCIENTIST

The Australian National Centre in HIV Virology Research laboratories at the Macfarlane Burnet Centre for Medical Research, in Melbourne, is seeking a highly-qualified, independent HIV virologist.

The National Centre laboratories at Macfarlane Burnet Centre have a staff of approximately 30 scientists, and are conducting work in a variety of areas of HIV virology, including control of transcription, function of HIV accessory proteins, mechanisms of drug resistance, characterization of virus strains from long-term non-progressors, ascertaining the role of macrophages and dendritic cells in HIV pathogenesis, and development of novel therapeutics (including gene therapy) and vaccines for HIV infection. The Centre is part of the Macfarlane Burnet Centre, Australia's premier virology research institute which has a staff of 120, with major research programs in epidemiology, international health, hepatitis viruses and respiratory viruses, in addition to the HIV research being conducted by the National Centre units. The academic environment, space, and technical facilities are excellent. Melbourne is one of the most livable cities in the world, and is also he centre of Australia's first-rate biomedical research community.

The Centre is seeking an independent scientist with a clearly defined research program on HIV, or in a closely related area, to join one of the three National Centre laboratories at Macfarlane Burnet Centre. The areas of research that the applicant pursues is flexible; the main criterion is that it complement the existing research programs of the Centre. Applicants should have substantial research experience, a strong publication record in high-quality, peer-reviewed journals, and should show evidence of scientific creativity and independence.

Further information from: **Professor John Mills—Director**
Phone: 61 3 9280 2823 Fax: 61 3 9280 2926

Salary is negotiable and will be in accordance with current NH&MRC levels in the range of Senior Research Fellow (From Aust. $56,440) to Principal Research Fellow (Aust. $68,571).

Applications with complete resume and three work related referees should be addressed to:

Mr Derrick Harvie,
Administrator, NCHVR
C/o Macfarlane Burnet Centre,
P.O. Box 254,
Fairfield
Victoria 3078
Australia

NCHVR

POSITIONS OPEN

RESEARCH ASSOCIATE IN ECOLOGY
Mountain Research Center
Montana State University, Bozeman

One-year position, beginning February 1996 (possible renewal for two more years). Research on biodiversity in montane environments (herpetological expertise preferred but not required); contribute to and facilitate interdisciplinary research on integration of human activities with natural ecosystem processes; help implement a multi-user biosystematics lab; mentor student research. Ph.D. in ecology or related field and record of publication in ecosystem processes required. The successful candidate will be able to integrate ecological and biosystematic techniques, attract extramural funds, and communicate effectively with other ecologists, biosystematists, GIS technical staff, land managers, economists, and sociologists. Submit curriculum vitae, three letters of recommendation, reprints of relevant publications, and a letter explaining relevant research interests to: **Research Ecologist Search Committee, Mountain Research Center, 408 Traphagen Hall, Montana State University, Bozeman, MT 59717.** Screening of applications begins on January 2, 1996, and continues until a suitable candidate has been chosen. Access **http://www.montana.edu/~wwwmrc/** for a detailed job listing.

ADA/Equal Opportunity/Affirmative Action/Veterans Preference.

RESEARCH ASSOCIATE

A world leading biotechnology company seeks the following professional to work in California.

You will participate in a neurobiology research project using your expertise in laboratory procedures and extensive laboratory animal handling. A B.A./B.S. in psychology, neurobiology, or biology is required, as is four plus years of laboratory experience, preferably in the pharmaceutical industry. Will use DOS software to compile and analyze data. Prefer experience with HPLC-ECD, lipid biochemistry, basic neurohistology, and neuropharmacological assays.

For immediate consideration, please mail your résumé to: **Personnel Department, Job Code: LAB, 1524G Cloverfield Boulevard, Santa Monica, CA 90404.** Principals only, please.

Equal Opportunity Employer.

NMR FACILITY MANAGER

For six Varian spectrometers (200-500 MHz) and a 4.7T imager/spectrometer. Responsible for calibration, maintenance, and cryogen service. Must be familiar with SUN computers and UNIX. Additional duties include operator training network and accounting management, implementation of new pulse sequences, and design and construction of specialized items such as surface coils. Experience with molecular modeling desirable. Ability to interact collaboratively with a variety of investigators is important. Ph.D. or equivalent experience desired. Send résumé and three letters of reference to: **Dr. Stanford Smith, Chemistry Department, University of Kentucky, Lexington, KY 40506-0055.** *The University of Kentucky is an Equal Opportunity Employer.*

MOLECULAR MICROBIOLOGIST

Panlabs, a leading drug discovery and process development service company, is seeking a **MOLECULAR BIOLOGIST** to genetically engineer industrial production strains of fungi and actinomycetes. A Ph.D. and several years of pertinent experience is desirable, but we will consider anyone with a demonstrated ability to solve difficult problems in molecular microbiology. The successful candidate will work at the bench, both independently and with the team. Strong communication and interpersonal skills are essential. Send a curriculum vitae or résumé and names of three references to: **Panlabs, Inc., Human Resources S12, 11804 North Creek Parkway South, Bothell, WA 98011.** *An Equal Opportunity Employer.*

BEHAVIORAL NEUROSCIENTIST. The University of California, San Francisco. The Gallo Center is seeking an experienced behavioral neuroscientist to collaborate with Gallo scientists to study behavioral responses to alcohol in animal models and transgenic mice. Experience in neuropharmacology is desirable. Salary and appointment commensurate with experience. Send curriculum vitae and three letters of reference to: **Ivan Diamond, M.D., Ph.D., Director, Gallo Center, Building 1, Room 101, San Francisco General Hospital, San Francisco, CA 94110.** *The Gallo Center is an Equal Opportunity/Affirmative Action Employer. Women, minority groups and disabled individuals are encouraged to apply.*

POSITIONS OPEN

MOLECULAR BIOLOGIST (INSECTS)

USDA, Agricultural Research Service (ARS) announces a position for a Research Molecular Biologist (Insects), GS-14/15 for the Red River Valley Agricultural Research Center at Fargo, North Dakota. The successful applicant will lead a research unit in the development of biological and biochemical approaches for suppressing pest insect populations. Incumbent will utilize molecular biology techniques for genome characterization, DNA sequencing, hybrid gene construction, and the development of gene transfer technology. Applicants must meet minimum education requirement, plus have at least one year of research experience at the postdoctoral level equivalent to the next lower grade. Salary ($57,760 to $88,326 per annum plus 3.74% locality pay) is commensurate with qualifications. For vacancy announcement ARS-D-6-W-022 and application forms, call **Ms. Melanie Nyquist, Telephone: 701-239-1203** and for information on research, contact **Dr. Don Zimmerman, Telephone: 701-239-1370.** *U.S. citizenship is required.* Application must be postmarked on or before December 26, 1995. *ARS is an Equal Opportunity Employer. Women and minorities are encouraged to apply.*

COURSES AND TRAINING

1996 COURSE ANNOUNCEMENT
GENETIC ANALYSIS METHODS FOR MEDICAL RESEARCHERS

This intensive four-day course centers on mapping human genetic diseases with emphasis on the mapping of complex common disease phenotypes. The concentration is on the entire disease mapping process, integrating clinical classification, pedigree collection, molecular genetic analysis, statistical analysis, and gene characterization. The course emphasizes the global decision-making process and overall study design. A residential conference center setting promotes extensive interaction between the students and the internationally recognized faculty.

Date and location: April 14–17, 1996, The Center for Executive Education at Babson College, Boston, Massachusetts.

Deadline for completed application: January 15, 1996. For information, write: **Dr. Margaret Pericak-Vance, Box 2900, Duke University Medical Center, Durham, NC 27710**; or contact: **Ms. Nadine Powers, Course Administrator. Telephone: 919-684-6274; FAX: 919-684-6514; Email: genclass@genemap.mc.duke.edu. WWW: http://www.mc.duke.edu/depts/genetics/courses/index.html.**

Computational Science Graduate Fellowship Program

The U.S. Department of Energy is offering a Graduate Fellowship in Computational Science. The award benefits of the program are: 1) Stipends ($1,500 per month for the first year). 2) Full payment of tuition and fees. 3) Open to students entering first year graduate school with uninterrupted study toward a Ph.D. degree. 4) Renewable up to 48 months. 5) Practicum at DOE laboratories.

For an application booklet contact: **Computational Science Graduate Fellowship Program, Ames Laboratory, 126 Wilhelm Hall, Ames, IA 50011. Telephone: 515-294-7900; Email: petersen@ameslab.gov.** Application deadline: January 24, 1996. *Must be a U.S. citizen or permanent resident,* GRE required.

The Fellowship is administered by the Ames Laboratory. *This is an Equal Opportunity program and is open to all qualified persons without regard to race, sex, creed, color, age, physical disability or national origin.*

NASA PLANETARY BIOLOGY INTERNSHIPS

The Marine Biological Laboratory, Woods Hole, Massachusetts, invites applications from graduate students and seniors accepted to graduate programs. Interns will receive awards of $2,200 plus travel to participate in research at NASA centers and collaborating institutions for approximately eight weeks. Typical intern programs include: global ecology, remote sensing, microbial ecology, biomineralization, origin and early evolution of life. Application deadline: March 1, 1996. For information/applications contact: **Michael Dolan, Planetary Biology Internship, Department of Biology, Box 3-5810, University of Massachusetts, Amherst, MA 01003-5810. Email: pbi@bio.umass.edu; Telephone: 413-545-3223.** *An Equal Opportunity/Affirmative Action Institution.*

COMPUTER MARKETPLACE

For *Mac Lovers*
The best bibliography software
-only for the Mac-
bookends pro ver. 3.2
e-mail: westing3@aol.com
http://www.westinginc.com/westing
Phone: 1-800-325-1862
Circle No. 25 on Readers' Service Card

MARKETPLACE

Commonwealth Biotechnologies, Inc.

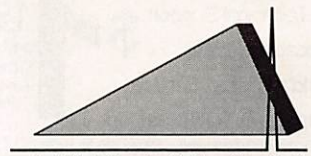

Specializing in Research and Development Support for the Life Science Investigator

- Automated DNA sequence analysis < $0.50 per base
- Custom DNA/RNA synthesis
- Protein/peptide synthesis and sequence analysis
- Spectroscopy/calorimetry experiments
- Mass spec services; MALDI-TOF, ES/MS

LET US QUOTE YOUR SPECIAL PROJECTS

Fax: 804-648-2641 Phone: 800-RELY-CBI
E-mail address: CBI@richnet.com 800-735-9224

Circle No. 16 on Readers' Service Card

SURGICAL INSTRUMENTS FOR RESEARCH
A 100-page catalog of specially selected surgical instruments and accessories for the research professional. Please contact us for your FREE copy today.
FST FINE SCIENCE TOOLS INC.
415-349-1636 · Fax 415-349-3729
REPRESENTATIVES WORLDWIDE
e-mail: 73633.260@compuserve.com
VANCOUVER SAN FRANCISCO HEIDELBERG

Circle No. 39 on Readers' Service Card

CustomPeptides
Need! Quality peptides at competitive prices.
Want to deal with an experienced company offering:
- Special amino acid containing peptides
- Synthesis of difficult sequences
- Phosphopeptides
- Biotinylated peptides
- Fluorescent labeling
- Peptide conjugation
- Large scale synthesis

Welcome to American Peptide. We can satisfy your peptide needs from small to large quantities at a ***considerably reduced prices.*** We offer different purity levels to match your exact needs, either for screening, antibodies production or drug development.

New 1996-97 Catalog
Comprehensive selection of bioactive peptides - Many new peptides - Highest quality - Amyloids & other peptides for neuroscience. Fax/call for a free copy!

62-0-72	β-Amyloid (25-35)	98%	0.5 mg	50.00
62-0-74	β-Amyloid (1-28)	98%	0.5 mg	85.00
62-0-78	β-Amyloid (1-40)	98%	0.5 mg	150.00
62-0-80	β-Amyloid (1-42)	98%	0.5 mg	225.00

AMERICAN PEPTIDE COMPANY
777 E Evelyn Ave. Sunnyvale, CA 94086 USA
Toll Free: 800-926-8272 Tel: 408-733-7604 Fax: 408-733-7603

Circle No. 29 on Readers' Service Card

Marketplace ads continue on page 1538

Continued from page 1537

MARKETPLACE

CUSTOM ANTIBODIES TO PEPTIDES & PROTEINS
Purification, Conjugation and ELISA Titration Available
HTI
HTI BIO-PRODUCTS, INC.
1 (800) 481-9737 OR (619) 788-9691 Fax (619) 788-9694

Circle No. 22 on Readers' Service Card

CUSTOM **DNA** SYNTHESIS
PURE & SIMPLE
- Superb Technical Support
- Impeccable Quality
- World's Fastest Service
- Cap Gel & TOF Mass Spec

$1 19* per base
$10 setup
50 nmole scale

* Some restrictions apply. Please call for details.

MIDLAND
STILL THE UNDISPUTED #1 CUSTOM DNA SYNTHESIS SERVICE
THE MIDLAND CERTIFIED REAGENT COMPANY
Phone 1-800-247-8766 FAX 915-694-2387
email mcrc@oligos.com

Circle No. 2 on Readers' Service Card

CHARLES EVANS & ASSOCIATES®
SPECIALISTS IN MATERIALS CHARACTERIZATION
MALDI Analytical Service
Mass Spectrometry of:
Peptides Oligonucleotides Proteins
Synthetic Polymers
Call 415-369-4567 Fax 415-369-7921

Circle No. 27 on Readers' Service Card

The premium antibody for phosphotyrosine detection is available from the laboratory where it originated, for the low price of
PY20 from **TRANSDUCTION LABORATORIES**
1-800-227-4063
only **$100/mg!**
Quality Antibodies for Signal Transduction Research

Circle No. 18 on Readers' Service Card

DAKO CORPORATION
Product and price lists available for:
- Apoptosis & Cell Cycle antibodies
- Cell Adhesion Molecules & Integrin antibodies
- Multi-Drug Resistance antibodies

For Research Use Only.
Call for FREE catalog
800/424-0021
Fax: 805/566-6688
DAKO

Circle No. 47 on Readers' Service Card

MARKETPLACE

FLUORESCENT MICROSPHERES
Distinctive colors for biology, diagnostics, physiology, aerosol, and filter testing applications.
- Diameters from 0.025 µm to 10 µm in red, green, blue fluorescence
- Assorted surface properties for protein coupling
- Free catalog available

Call 800-334-3883 Toll Free or in Calif. 415-424-1177, FAX 415-424-1158
Duke Scientific Corporation
P.O. BOX 50005
2463 FABER PLACE
PALO ALTO, CA 94303

Circle No. 8 on Readers' Service Card

MOLECULAR BIOLOGY
The Midland Certified Reagent Co. Molecular Biology Group
"We Clone Around the Clock!"
GENE SYNTHESIS *We built the world's largest synthetic gene!*
CUSTOM MUTAGENESIS *Only the changes you want*
DNA SEQUENCING *As fast as 24 hours*
-Guaranteed and Confidential-
Ph (800)247-8766 Fx (915)694-2387 **MIDLAND** Web Site: http://www.mcrc.com

Circle No. 9 on Readers' Service Card

IDT®
INTEGRATED DNA TECHNOLOGIES, INC.
Custom DNA Synthesis
$1.65 / Base
200 nmole Scale
No Set-up Fee
Column Purified
24 Hour Shipping
Q.C. by PAGE on *Every* Oligo
Call today, join over 200 institutions already on our discount programs!
E-mail: orders@idtdna.com
Web Site: http://www.idtdna.com
Fax: 1-319-645-2921
Phone: 1-800-328-2661

Circle No. 1 on Readers' Service Card

Custom **PEPTIDES**
Purity >70%, $20/Res. (offer thro. May)
1st order disc., no setup fee, free HPLC/A.A. analy.
PEPTIDE ANTIBODY: $250/Rabbit
UNBEATABLY: NO CHARGE IF NO ANTIBODY PRODUCTION
PEPTIDE LIBRARY: from $150/library
TANA LAB., LC. 1-800-400-0070 (Tel) +1-713-663-7163 (Fax)

Circle No. 13 on Readers' Service Card

The Peptide Engineering Specialist
PeptidoGenic
e mail: pkim@ecnet.com
Fax: 510-371-1156
Voice: 1-800-597-7873
No Setup Fee, Free HPLC, IonSpray Mass.
Custom Peptide : **$20**/residue/crude/5days
IonSpray MS Service :MS ($30), LC/MS ($250)

Circle No. 15 on Readers' Service Card

MARKETPLACE

CUSTOM DNA as low as $1.19 base UP TO 30 BASES
150 nmol scale (>10 ODU)
Deprotected • No set-up charges
Synthesis report • 24-48 hours shipping

CUSTOM PEPTIDES as low as $20 residue 8-30 RESIDUES
15-40 mg • No set-up charges
Free mass spec & HPLC tracing
Desalted • 5-8 days shipping

1-800-227-0627
FAX 214-420-0442
BIO•SYNTHESIS INCORPORATED
E-Mail: biosyn@onramp.net
Internet: http://www.biosyn.com
FDA#001235 • NIH BPA#263-00038171-04-BPA/G

Circle No. 19 on Readers' Service Card

SFM-Human Endothelial Cell System
More Cells / Lowest Price / Highest Quality
Start up a 75 cm Flask / Recombinant Mitogen
CSC Certificate™ #30566
cell systems
1-800-697-1211

Circle No. 38 on Readers' Service Card

SCIENTIST®
Fits Equations To Data
- *nonlinear algebraic equations*
- *implicit algebraic equations*
- *Laplace transforms*
- *ordinary differential equations*
- *various splines/polynomials*

1-800-942-6284
MICROMATH®

Circle No. 11 on Readers' Service Card

Custom DNA from $1.00/base
ransom hill bioscience, inc.
no setup, no minimum, no baloney!
internet: visla@delphi.com fax: (800) 597-8509

Circle No. 21 on Readers' Service Card

Custom DNA
Purified & Delivered in 48 hours
$5.00 per base • Purified
Guaranteed minimum 100µg
Research Genetics, Inc.
1-800-533-4363

Circle No. 3 on Readers' Service Card

Sigma has been earning the confidence of scientific researchers for over fifty years. The reason? Our total commitment to customer satisfaction. Nowhere is this dedication more evident than in our electrophoresis product line. Use-tested and strictly assayed to ensure lot-to-lot consistency,

Confidence

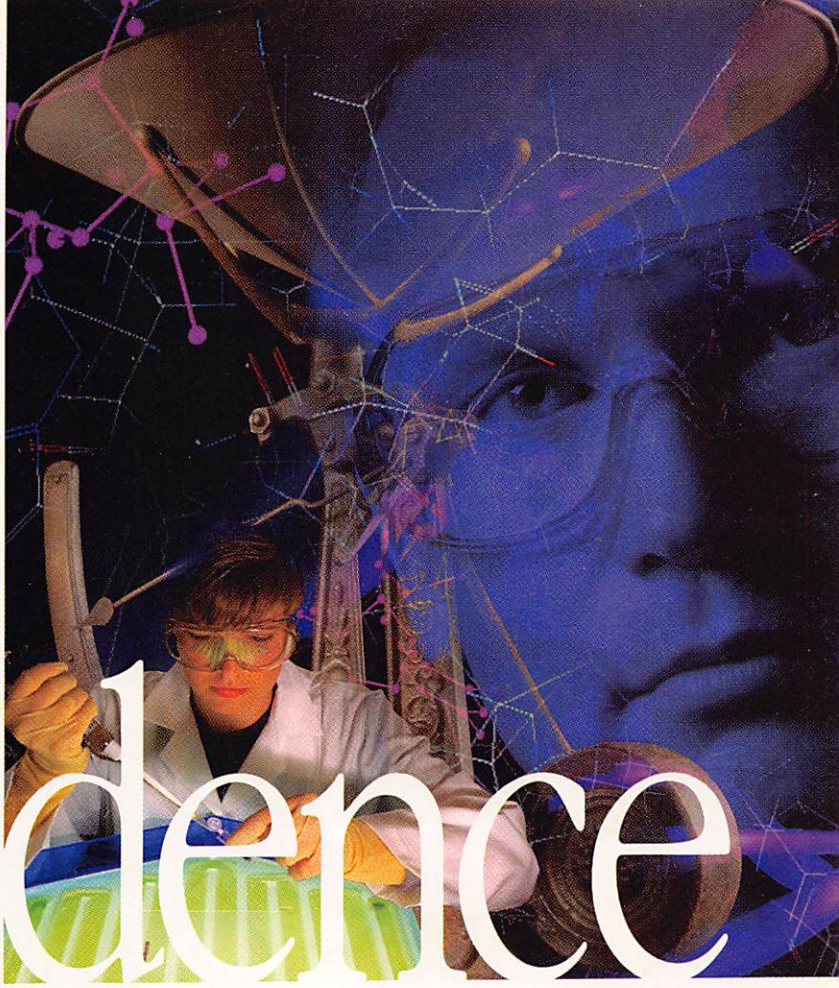

Sigma electrophoresis products provide reliable and consistent results in even the most demanding research environments. And as with all Sigma products, a technical support representative is available to offer reliable assistance when questions arise concerning uses and applications.

Electrophoresis Reagents and Markers

Sigma's complete line of electrophoresis reagents includes gel reagents and precast gels, stains, buffers and molecular weight markers. To receive a free copy of our brochure highlighting these products, use the Reader Service Number.

Circle No. 43 on Readers' Service Card

Capillary Electrophoresis

Sigma's capillary electrophoresis products include standards and buffers which optimize the separation of many biological molecules including proteins, water soluble vitamins, peptides, dsDNA and oligonucleotides. Our protocols reduce the time required to calibrate your system prior to analyzing unknown samples.

Circle No. 44 on Readers' Service Card

Imaging Products and Equipment

Sigma provides researchers with a single, comprehensive source for Electrophoresis and Imaging equipment and supplies. Highlighted products in this brochure include film, autoradiography supplies, and products for photodocumentation.

Circle No. 45 on Readers' Service Card

SIGMA CHEMICAL COMPANY

Address	P.O. Box 14508, St. Louis, Missouri 63178
Phone	800-325-3010 Collect Outside USA/Canada: 314-771-5750
Fax	800-325-5052 Collect Outside USA/Canada: 314-771-5750
Internet	*http://www.sigma.sial.com*

AUSTRALIA AUSTRIA BELGIUM BRAZIL CZECH REPUBLIC FRANCE GERMANY HUNGARY INDIA ITALY JAPAN
KOREA MEXICO NETHERLANDS POLAND SPAIN SWEDEN SWITZERLAND UNITED KINGDOM UNITED STATES

Introducing the new ABI PRISM™ 377 DNA Sequencer.

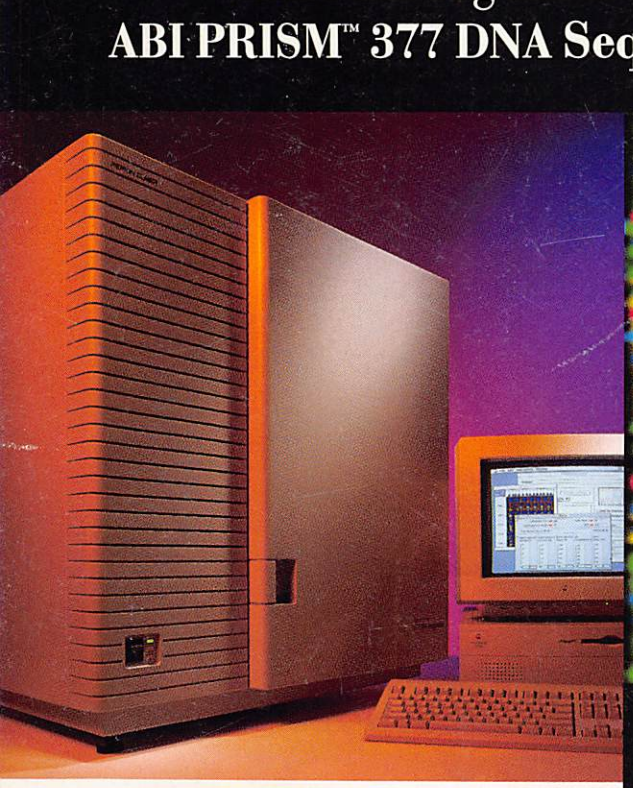

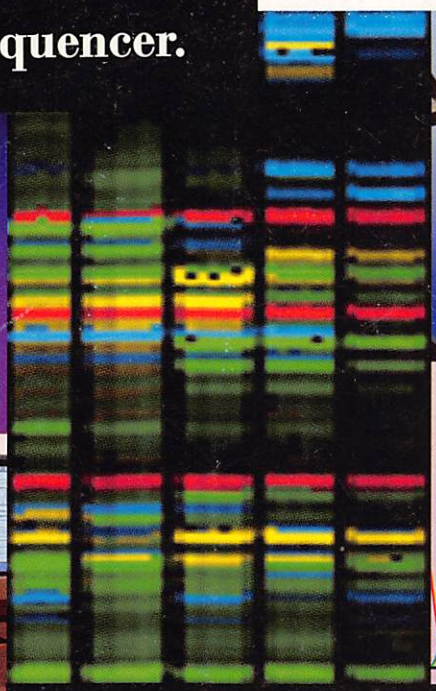

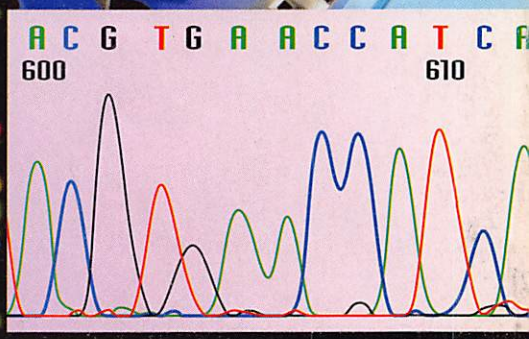

Greater productivity, no matter how you measure it.

The ABI PRISM™ 377 DNA Sequencer goes beyond previous technology to bring you unprecedented productivity for all your DNA sequencing and fragment analysis applications.

The ABI 373 set the standard for accuracy and throughput with automated four-dye, one-lane detection. Now the ABI PRISM 377 raises that standard with powerful new hardware and software capabilities that take performance and reliability to new levels.

You've never seen a system this fast. Using simultaneous multicolor detection and advanced electrophoresis technology, the ABI PRISM 377 generates data four times faster than the ABI 373.

You'll also find that the 377's versatile vertical gel format offers even greater precision and more control for fine-tuning electrophoresis parameters.

And the ABI PRISM 377 is so easy to use, you'll be running samples with complete confidence in no time. A Macintosh Power PC interface streamlines data collection and analysis with your choice of DNA Sequencing or GeneScan™ software.

Of course, the ABI PRISM 377 is backed by Perkin-Elmer's worldwide technical support organization. With over eight years of experience in genetic analysis, our Applied Biosystems Division offers you the most comprehensive range of systems, technologies, and applications expertise in the industry.

So if you're looking for greater DNA sequencing and fragment analysis productivity, find out how the ABI PRISM 377 measures up. For more information, call 1-800-345-5224. Outside the U.S. and Canada, contact your Perkin-Elmer representative.

PERKIN ELMER

Europe Langen, Germany Tel: 49 (0) 6103 708 301 Fax: 49 (0) 6103 708 310
Japan Tokyo, Japan Tel: (0473) 80-8500 Fax: (0473) 80-8505
Latin America Mexico City, Mexico Tel: 52-5-651-7077 Fax: 52-5-593-6223
Australia Melbourne, Australia Tel: (03) 9212-8585 Fax: (03) 9212-8502

Perkin-Elmer is a registered trademark and ABI PRISM and GeneScan are trademarks of The Perkin-Elmer Corporation. All other trademarks and product names are the property of their respective owners.